

METALLURGY IN THE GLOAMING: NON-FERROUS METALWORK FROM THREE EARLY ANGLO-SAXON CEMETERIES AT RAF LAKENHEATH, SUFFOLK

Matthew Nicholas

ORCID ID: <http://orcid.org/0000-0003-0018-835X>

A thesis submitted in partial fulfilment of the requirements for the degree of
Doctor of Philosophy

Department of Archaeology and Conservation
Cardiff University

*Submitted September 2015
Viva January 2016
Corrected thesis submitted April 2016*

File Name: *Nicholas – 2015 – Eriswell non-ferrous metallurgy.pdf*
File status: *Final*

This thesis and associated data are available under an Attribution-NonCommercial-ShareAlike
4.0 International licence (CC BY-NC-SA 4.0)



<http://creativecommons.org/licenses/by-nc-sa/4.0/>

This licence excludes all third party content (quotes, maps, data etc.) which should be
considered © Copyright the named creator or organisation unless explicitly stated otherwise.

Reliving the past, that is the most fantastic adventure of all.

The event, relived, grows more and more enigmatic, and richer and richer in meaning. Turning to the past, I reach the future, I recall people I never knew. In the time/space continuum of consciousness, Was and Will Be occupy the same point.

(Konrád 1992, 7)

Summary

In the late 1990s Suffolk County Council Archaeology Service (now Suffolk Archaeology) began a series of excavations in advance of construction work at the US Air Force base RAF Lakenheath (Eriswell, Suffolk). During the course of this work three substantial Early Anglo-Saxon cemeteries (dated from 475 to 650 CE) were excavated.

These sites are some of the largest and best preserved Anglo-Saxon cemeteries excavated in modern times. Many of the inhumations were furnished. Amongst the host of grave goods were approximately 800 non-ferrous metal objects. This presented a significant opportunity to examine Early Anglo-Saxon non-ferrous metallurgy.

Previous studies of Early Anglo-Saxon non-ferrous artefacts have tended to focus on acquiring quantitative data using invasive sampling on specific (predominantly cast) object types. The data from these small subsets of objects were then extrapolated to create an interpretation of the technological and metallurgical skills of the era. As this tended to exclude sheet metal objects and the more utilitarian metalwork it is suggested by the author here that this approach is not representative and leaves something to be desired.

In this study it was decided to focus on producing a broad data set that, whilst being qualitative, would allow broad trends in alloy composition to be assessed (if present) against a variety of variables. Data was predominantly acquired using handheld portable X-ray fluorescence (HHpXRF).

The results showed that the usage of copper and silver alloys in the Early Anglo-Saxon period is more complex than has previously been suggested. It is thought that this is predominantly linked to decisions regarding an object's manufacturing technique, but there is also evidence to suggest that elements of cultural identity may have also had a role to play. There is also evidence for continuity of practice between the late Romano-British and Early Anglo-Saxon periods.

Acknowledgements

You don't realise it at the beginning (when excitement is in order) but PhDs are strange beasts and PhDs in archaeology even more so. And then, as time goes on, you begin to worry: have you undertaken a mission with unnerving parallels to Nikolaï Fyodorov's *Philosophy of the Common Task* (1990)? You wonder if, like the 19th Century Russian librarian, you are attempting something as endless and esoteric as the resurrection of the dead through memory, scientific endeavour and self-imposed social and moral purgatory. But then finally — suddenly even — the end is in sight. That it is so, however, is nothing to do with yourself and everything to do with those around you. And so it is here. That this thesis is completed and does not lay unfinished amongst digital dust is nothing to do with myself and everything to do with a host of wonderful people.

Firstly thanks must go to my supervisors: Professor John Hines (2010-15), Dr Panagiota (Yiota) Manti (2011-15) and Professor Ian Freestone (2010-11). I'd like to thank Professor Freestone for starting me off on this project and Dr Manti for providing supervision (despite being donated a PhD student at short notice whilst completing her own thesis) and her rigorous approach to science (which hopefully I've picked up a bit of). Professor Hines merits special thanks for his willingness to put up with my flights of fancy, his tireless work trying to catch all my errors and being a constant guiding and supporting presence throughout this project.

The project was funded by Ministry of Defence Estates and managed by Suffolk Archaeology (formerly Suffolk County Council Archaeology Service). Particular thanks must go to the project manager Jo Caruth who provided access to the objects and background information about the sites.

Many people have provided advice, guidance or acted as sounding boards throughout this project. Dr Mary Davis (National Museum Wales), Dr Tim Young (Cardiff University & Geoarch), Phil Parkes (Cardiff University) and Dr Lesley Frame all provided invaluable advice on analysis and metallurgy. Further thanks should go to Dr David Dungworth (Historic England) for providing a spreadsheet of the Blades data (and lots of other help and advice over the years), the brilliant staff at Bruker for HHpXRF advice (Mike Dobby, Dr Robert Shannon and Dr Bruce Kaiser), Tom

Cotterell (National Museum of Wales) for assistance using the XRD, Louise Mumford (National Museum of Wales) for searching out equipment at short notice for me (and enjoyable chats) and Professor Annemie Adriaens (Ghent University) for access to the IMMACO alloys. Finally (but by no means least) thanks to Dr Jocelyn Baker, Dr Alice Stevenson and Nick Wells for advice, hints, tips and tricks.

This thesis wouldn't have been possible without the help of a number of members of Cardiff University staff who went out of their way to provide assistance. Thanks to Rob Thomas and Aled Cooke for sorting me out with a monitor in the final stages of writing (and other assorted IT help), Sue Virgo for general assistance and Helen Szewczyk for putting up with me and prodding me through assorted admin. I'd also like to thank Kirsty Harding and Ian Dennis for regular sanity saving conversations. Finally, particular thanks must go to Keith and Paul (the John Percival building porters) who were always happy to help me lock up equipment late in the evening (despite me often disturbing their dinner night after night).

Huge thanks to colleagues past and present from the PGR office who, not only put up with me moan about the godawful state of Cardiff University management (not, it must be stressed, at the departmental level), but also provided friendship *and* advice on my work. So, in no particular order, *danke* to: Susan Stratton, Dr Lara Hogg, Eric Nordgren, Dr Jennifer Jones, Dr Julia Best, Dr Heather Giddens, Dr Chris Timmins, Dr Nicola Emmerson, Chris Wilkins, Heather Crowley, Dr Jimmy Peake, Dr Ros Warden, and Dr Caroline Pudney. It's a shame we never got around to publishing that study on Jaffa Cakes. Or balancing more stuff on Susan's head. Or eating more marshmallows.

Right, I feel like I'm going on a bit now, so I'll cut to the chase. Apologies to everyone I have missed, I valued your help enormously (but I'm running out of space).

A huge thanks to my mum, dad and brother (and Charlotte and Ben) for their love and support. And the biggest thanks of all to my amazing wife, Dr Alice Forward. I couldn't have done it without you.

It goes without saying that all mistakes are my own.

Right, I'm going to pop the kettle on and listen to the new Lovely Eggs album.

Hnyl fawr am nawr!

Acknowledgements

(slight return)

As a postscript to the acknowledgments I'd like, now the viva is over and done with (I think: I'd be lying if I said I could remember much of it), to take the time to thank Professor Keir Waddington for chairing the examination and Dr Alan Lane and Professor Martín-Torres for taking the time to examine my thesis. I'm hugely grateful for the time given up by all and the comments I received.

CONTENTS

<i>List of Figures</i>	XII
<i>List of Tables</i>	XXIII
<i>List of Equations</i>	XXXI
Chapter 1: Primer	32
1.1 Introduction.....	32
1.2 Site location and context.....	32
1.2.1 Geology	34
1.3 Site Archaeological overview	35
1.3.1 ERL 046	40
1.3.2 ERL 104	40
1.3.3 ERL 114	42
1.4 Dates and Phasing	43
1.5 How objects are defined.....	45
1.5.1 Numbering objects.....	45
1.5.2 Object categories.....	46
Chapter 2: Beginnings.....	49
2.1 A theoretical background to Anglo-Saxon non-ferrous metalwork studies.....	49
2.1.1 ‘The overcrowded nature of things’	52
2.1.2 Archaeometric cul-de-sacs	54
2.1.3 Individualism	55
2.1.4 Year Zero	58

2.1.5	We're all communitarians now	60
2.2	The Chemical Canvas	63
2.2.1	Alloy production and usage in the early middle ages	66
2.2.2	Alloys through the Ages	78
2.3	Research Questions	80
2.3.1	Attitudes to Alloys	81
2.3.2	Research Objectives	91
Chapter 3:	Analytical Methodology	95
3.1	Introduction	95
3.1.1	Methodological Approaches	95
3.2	Background to X-ray fluorescence	100
3.2.1	The Spectra	102
3.2.2	Repetition, Hesitation, and Deviation: Limits of detection and Determination	112
3.2.3	Correction overkill? Reasoning a methodology	113
3.3	HHpXRF methodology	128
3.3.1	Equipment, software and workflow	128
3.3.2	Voltage and Currents	129
3.3.3	Limits and Standards	145
3.4	Further issues	162
3.4.1	Copper alloy penetration Depth	162
3.4.2	Silver alloy thickness and penetration depth	167
3.4.3	Distance	172
3.4.4	Ambient temperature and detection sensitivity stability	175
3.4.5	Detector Drift	177
3.5	Conclusion	178

3.5.1	Workflow.....	179
Chapter 4:	Data Exploration.....	181
4.1	Introduction.....	181
4.1.1	Descartes Vs The Simplex: Analysis of Compositional Data	182
4.1.2	Software.....	185
4.1.3	Centring.....	185
4.2	Classical statistical summary.....	186
4.3	Principal Components.....	191
4.3.1	Untransformed PCA.....	191
4.3.2	Log-ratio transformed PCA.....	200
4.4	Comparison of untransformed and clr transformed PCA	214
4.4.1	Hierarchical Clusters.....	214
4.5	Conclusion	230
Chapter 5:	Silver Results.....	232
5.1	Introduction.....	232
5.2	Identification of silver objects.....	232
5.3	Object Breakdown.....	233
5.3.1	Silver objects by cemetery and grave.....	233
5.3.2	Silver objects by typology.....	235
5.3.3	Silver objects by sex, gender and phase	237
5.3.4	Silver objects by fabrication technique.....	242
5.4	Archaeological interpretation of clusters.....	244
5.5	Discussion.....	263
5.5.1	Recycling models.....	266
5.6	Conclusion	267
Chapter 6:	Gilt objects.....	268

6.1	Introduction.....	268
6.1.1	Diffusion	269
6.1.2	Hot or Not?	270
6.1.3	Analysis depth.....	272
6.2	Interpretation	274
6.2.1	Site and graves	274
6.2.2	Object typologies	275
6.2.3	Gender and Phasing.....	276
6.3	Discussion.....	278
6.3.1	Mercury Sources.....	278
6.4	Conclusion	284
Chapter 7: Filler, lead and tin alloys		286
7.1	Introduction.....	286
7.2	Filler alloys in context	286
7.2.1	Eriswell filler alloys	288
7.2.2	Filler alloys: Net Peak Area results	290
7.3	Lead rich alloys.....	299
7.3.1	Lead and tin rich alloys: object overview.....	302
7.4	Conclusion	306
Chapter 8: Copper Alloys		308
8.1	Introduction.....	308
8.2	How ‘objects’ are defined	309
8.3	Corrosion	309
8.4	Excluded objects.....	311
8.5	Categorical variables	312
8.5.1	Distribution across cemeteries	312

8.5.2	Objects by typology	313
8.5.3	Manufacture method	315
8.5.4	Sex, gender and phase.....	319
8.6	Exploratory data analysis	324
8.6.1	Normality	324
8.6.2	Outliers	330
8.6.3	Classical statistical summary and distributions.....	348
8.6.4	Principal Components	362
8.6.5	Hierarchical Clustering	371
8.7	Clusters in context	378
8.7.1	Clusters in a major context	378
8.7.2	Clusters in a minor context.....	388
8.7.3	Clusters and typologies.....	390
8.7.4	Clusters and graves	406
8.7.5	Clusters and phases.....	427
8.8	Conclusion.....	429
Chapter 9: Endings.....		434
9.1	Morphing into the future.....	437
9.2	Discussion.....	439
9.2.1	Patterns of alloy usage	439
9.2.2	Distribution and site variation.....	447
9.2.3	Primary metal production and the nature of trade in metals	449
9.2.4	Continuity?.....	452
9.3	The End of the Affair	454
Bibliography.....		458
Digital Appendices.....		494

Appendix I. MBH Standards	495
Appendix II. Silver alloy clusters	496
Appendix III. Silver alloy categorical variables.....	500
Appendix IV. Silver alloy NPA data	504
Appendix VI: Gilt XRD peak list	511
Appendix VII: Gilt object categorical variables.....	514
Appendix VIII: Gilt object NPA data.....	516
Appendix IX: Filler alloys on non-ferrous objects: categorical variables	520
Appendix X: Filler alloys on non-ferrous objects: NPA data.....	526
Appendix XI: Base and filler alloys on copper alloy objects: NPA data.....	534
Appendix XII: Lead alloy object categorical variables.....	545
Appendix XIII: Lead alloy object NPA data.....	547
Appendix XIV. Summary of copper alloy objects.....	549
Appendix XV. Copper alloy net peak area data.....	584
Appendix XVI. Copper alloy outliers.....	652
Appendix XVII. Copper alloy cluster groups.....	663
Appendix XVIII. Blades copper alloy groups.....	696

List of Figures

Figure 1-1: Location of the modern county of Suffolk (left) and Eriswell within (right). UK and Suffolk maps created by Nilfanion (2010a; 2010b) under a Creative Commons Attribution-Share Alike 3.0 Unported licence.	32
Figure 1-2: Showing known Anglo-Saxon sites near Eriswell. After Caruth and Anderson (2005, 3, Figure 3). OS map © Crown Copyright 2005. All rights reserved. (2005). Suffolk HER data © Suffolk County Council.....	34
Figure 1-3: Geological map showing the approximate locations of the three cemeteries. Geological Map Data © NERC 2015. Underlying map © Crown Copyright (2015), Ordnance Survey (Digimap Licence).	35
Figure 1-4: The 1958 National Grid 1:10560 map of Eriswell (tile TL78SW) with the approximate location of cemetery ERL 008 highlighted. Note that the airfield was not shown on OS maps until the 1960s. © Crown Copyright and Landmark Information Group Limited 2015. All rights reserved. (1958).....	36
Figure 1-5: Hutchinson’s plan of ERL 008 (1966, 4, Figure 2).....	37
Figure 1-6: Location of the cemetery excavation areas. After Caruth and Anderson (2005, 1, Figure 1). OS map © Crown Copyright 2005. All rights reserved. (2005).....	38
Figure 1-7. Showing the location of all excavation areas (cemeteries individually identified) and areas where grubenhouses / sunken featured buildings (SFBs) have been identified, indicating early Anglo-Saxon occupation After Caruth and Anderson (2005, 4, Figure 4). OS map © Crown Copyright 2005. All rights reserved. (2005).	39
Figure 1-8: Plan of graves in ERL 046 (Caruth and Anderson 2005, 10, Figure 8).	40
Figure 1-9: Plan of graves in ERL 10 (Caruth and Anderson 2005, 7, Figure 6).	41
Figure 1-10: The horse and warrior burial in G323, ERL 104. Photo from Caruth and Anderson (2005, 8, Figure 7).	42
Figure 1-11: Plan of graves in ERL 114(Caruth and Anderson 2005, 11, Figure 9).	43
Figure 1-12: Schematic diagram of the phasing used in this study (courtesy of Professor John Hines).	44
Figure 2-1: Academic publications containing ‘community’ and ‘Archaeology’ measured as a percentage of the yearly total number of publications containing ‘archaeology’. It is notable that, despite the considerable decrease in the number of publications containing archaeology since 2006 (27900 down to 22000 in 2010), the use of community is still increasing. Data from Google Scholar (excludes patents and legal opinions).	61
Figure 2-2:Ternary diagram of copper alloy types (after Blades, 1995, p. 127).....	65
Figure 2-3: Graph showing the number of ‘Early Saxon’ copper alloy objects analysed by Blades (1995).....	72
Figure 2-4: Graph showing a breakdown of copper alloy artefacts from Eriswell by object class.....	73

Figure 2-5: Ternary diagram of Roman brooches from Richborough (data from Bayley and Butcher 2004, Table 23 (digital appendix)) and early Saxon brooches (data from Blades 1995, 87–97). There are too many types of brooch in the Bayley and Butcher study to identify them all effectively here by colour. 74

Figure 2-6: Ternary Diagram showing non-ferrous artefacts from Cadbury and Longbury. The points are numbered as follows: 1 - Ring/annular brooch ; 2 - Brooch pin; 3 -binding strip; 4 - button brooch; 5- small bar; 6 - Ring/annular brooch; 7 brooch pin; 8 - binding strip; 9 - button brooch; 10- Anglo-Saxon brooch; 11- Anglo-Saxon brooch pin; 12 – droplet; 13 - droplet. Data from Northover 1995, 74 (no table number) and Campbell and Lane (1994, 34, Table 1). Points 1-4 are presented as a mean of 3 results from each object. 78

Figure 2-7: Copper alloy usage through time. Roman data was taken from Dungworth (1995), early Saxon, late Saxon and medieval data is from Blades (1995), post medieval data is from Dungworth (2000). Mid Saxon data is combined from Nicholas (2003). After Nicholas (2003) and Bayley et. al. (2008, 50, Figure 65). With additional data from Wilthew (1984) and Brownsword and Hines (1993). 79

Figure 3-1: X-ray fluorescence in action with the ejection of an electron (left) and the release of a characteristic x-ray (right). 101

Figure 3-2: HHPXRF schematic showing 1) cathode (surrounding the tube as a ring); 2) Rhodium anode target; 3) electron beam between cathode and anode; 4) filter 5) Beryllium window; 6) object; 7) x-ray path and 8) detector. The thick dashed line shows the beam path (after Nazaroff 2009, p.891, fig. 4 and Kaiser & Wright 2009, p.6 fig. 4). 102

Figure 3-3: Rayleigh (top) and Compton (bottom) scattering. 103

Figure 3-4: Objects analysed with approximate areas targeted highlighted. 134

Figure 3-5: Spectra for silver disc 046-1087 normalised to the $K\alpha$ Rhodium peak (20.0740 E/keV). Spectra are presented on logarithmic scale with each individual spectrum colour coded to settings and areas as follows: Test setting A (Area A – green; Area B – blue), B (Area A – red; Area B; yellow), D (Area A – Pink; Area B – Purple) and E (Area A – Black; Area B – Grey). 137

Figure 3-6: Spectra for copper alloy sheet 046-1603 normalised to the $K\alpha$ Rhodium peak (20.0740 E/keV). Spectra are presented on logarithmic scale with each individual spectrum colour coded to settings and areas as follows: Test setting A (Area A – green; Area B – blue), B (Area A – red; Area B - yellow), D (Area A – Pink; Area B – Purple) and E (Area A – Black; Area B – Grey). 138

Figure 3-7: Spectra for 046-1812 focussing on the gold and mercury peaks. The spectrum on the left was acquired in an SEM under environmental conditions (using INCA software), the spectra on the right was acquired using an HHPXRF. As can be seen the XRF provides superior resolution in distinguishing between the gold and mercury peaks. 140

Figure 3-8: Bar charts of the major elements in spangle 046-1603 1087 by test setting (in alphabetical order) with error bars calculated according to Rousseau's (2001) Limit of Determination of a Method (see Equation 5 on page 111 for more details). 143

Figure 3-9: Bar charts of the major elements in silver sheet 046-1087 by test setting (in alphabetical order) with error bars calculated according to Rousseau's (2001) Limit of Determination of a Method (see Equation 5 on page 111 for more details). The low lead peak in setting F is due to the analysis being retaken at a later date (due to a memory stick corruption issue) in a slightly different area (i.e. lead segregation).....	144
Figure 3-10: Scatter plot of measured mean (n=10) quantitative results on reference alloys at two settings against certified values. The R2 values in the top left are for 40 kV - 7.9 μ A, bottom right for 40 kV - 9.6 μ A.....	151
Figure 3-11: Qualitative analyses of the MBH alloys (net peak area). Empirically calibrated measured data (Cal. Measured), Standard Deviation (SD), Coefficient of Variation (Cv) and Limit of Determination of a Method (LDM) are presented.	154
Figure 3-12: Qualitative analyses of IMMACO alloys. Standard Deviation (SD), Coefficient of Variation (Cv) and Limit of Determination of a Method (LDM) are presented. The results acquired at 40kV and 9.6 μ A. were previously published in Nicholas and Manti (2014) in Table 3.....	156
Figure 3-13: Scatter plot of the measured mean (n=10) qualitative results on reference alloys at two settings against certified values. The R ² values in the top left are for 40 kV - 7.9 μ A, bottom right for 40 kV - 9.6 μ A.....	157
Figure 3-14: SEM-BSE images (acquired by Dr Panagiota Manti.) of experimentally corroded IMMACO alloys showing the corroded surface of the alloys in polished section. Images taken at \times 500 magnification; detail on IMMACO C at \times 1000 magnification. From Nicholas and Manti (2014, Figure 1).....	165
Figure 3-15: Elemental map (captured using an SEM) showing decuprification as seen on a Cu-Sn-Ag pin from a Kentish Nydam style brooch pin. The pin had suffered a break during excavation, allowing the cross section to be analysed. The image in the top left is a backscatter image, the remaining three show maps for the elements labelled.....	168
Figure 3-16: Graph of % reductions in signal strength (see Table 3-20)	173
Figure 3-17: An example of drift in from a screenshot of the S1PXRF software.....	177
Figure 4-1: Cu-Sn-Zn ternary diagram. The diagram on the left presents the original diagram, that on the right the centred version.....	186
Figure 4-2: Scatter plot matrix of major elements from silver objects NPA. The diagonal shows a histogram of the element distribution. Minor elements are excluded for ease of viewing. Created using R package GGally (Schloerke et al. 2014). The correlations are reproduced in Table 4-3 without the scatterplots for easier reading.	190
Figure 4-3: Scree plot of principal components	193
Figure 4-4: Scree plot of the results of Horn's Parallel Analysis for component retention (2010 iterations, using the 95 th percentile estimate). See Table 4-6 for further details.	194
Figure 4-5: Factor plot of PC1 and PC2.....	195

Figure 4-6: Individual PCA biplots plots showing the first two principal components with points illustrated by site (A), grave number (B), object category (C) and object class (D).	196
Figure 4-7: Results of Horn's Parallel Analysis for component retention 1770 iterations (30 x n), using the 95 th percentile estimate. See Table 4-8 for associated data.	198
Figure 4-8: Factor plot (left) and biplot (right) of the 'high' silver PCA.	200
Figure 4-9: clr ternary diagram scatter plot matrix of major elements from silver objects. The * at the apex of each diagram is the third component and represents the geometric mean of the remaining components (van den Boogaart and Tolosana-Delgado 2006). Created using the R package 'compositions' (van den Boogaart, Tolosana, and Bren 2014).	206
Figure 4-10: Scree plot of clr PCA.	208
Figure 4-11: 3D symmetrically scaled centred log-ratio (clr) biplots of silver data showing variables and observations. Three biplots (A-C) show the same data set in an XY orientation with observation points identified by categorical variables as follows: site (top left); object class (top right) and grave number (bottom left). The fourth biplot (d) shows the rays without the observations in an YZ orientation to better display the Cu, Ag and Pb rays.	209
Figure 4-12: Scree plot of 'high' silver clr PCA.	211
Figure 4-13: Symmetrically scaled centred log-ratio (clr) biplots of 'high' silver data showing variables and observations. Three biplots (A-C) show the same data set in an XY orientation with observation points identified by categorical variables as follows: site (top left); object class (top right) and grave number (bottom left). The fourth biplot (d) shows the rays without the observations in an YZ orientation to better display the Cu, Ag and Pb rays.	213
Figure 4-14: 'High' silver biplots with natural groups (identified visually) delimited by dashed lines: A - Euclidean PCA biplot (note that the group of three individuals is defined simply as 'not the other two'). B - 3D symmetrically scaled clr biplot showing in XY orientation.	214
Figure 4-15: Hierarchical Clustering on untransformed PCA results using Ward's method for agglomerating clusters produced using the R package 'FactoMiner' and base R function 'hclust'. The clusters are illustrated in two ways: A – balance dendrogram of clusters (the dashed lines indicate where the tree was cut and are colour coded), B – 2D biplot and C – biplot with dendrogram.	216
Figure 4-16: Hierarchical Clustering on compositional data using Ward's method for agglomerating clusters produced using the R package 'compositions' and base R function 'hclust'. The clusters are illustrated in two ways: A – balance dendrogram of clusters (the dashed lines indicate where the tree was cut and are colour coded), B – 2D clr biplot and C - 3D symmetrically scaled biplot with individuals colour coded by cluster.	217
Figure 4-17: Centred clr ternary diagram scatter plot matrix of major elements from silver objects with individuals identified using clusters defined using hierarchical clustering, The * at the apex of each diagram is the third component and represents the geometric mean of the	

remaining components (Boogaart and Tolosana-Delgado 2006). Created using the R package ‘compositions’ (Boogaart, Tolosana, and Bren 2014).....	221
Figure 4-18: untransformed scatter plot matrix showing clusters.....	222
Figure 4-19: Au-Sn-Zn Au ternary diagrams. The top two (A & B) show the untransformed clusters un-centred (A) and centred (B). The bottom two (C&D) show the clr clusters un-centred (C) and centred (D).....	225
Figure 4-20: Ag-Sn-Zn ternary diagrams. The top two (A & B) show the untransformed clusters un- centred (A) and centred (B). The bottom two (C&D) show the clr clusters un-centred (C) and centred (D).....	226
Figure 4-21: 3D ternary diagrams of Ag-Au-Sn-Zn with Ag at the apex of the pyramid. The top two (A & B) show the untransformed clusters un-centred (A) and centred (B). The bottom two (C&D) show the clr clusters un-centred (C) and centred (D).....	227
Figure 4-22: 3D ternary diagrams of Cu-Pb-Sn-Zn with Ag at the apex of the pyramid. The top two (A & B) show the untransformed clusters un-centred (A) and centred (B). The bottom two (C&D) show the clr clusters un-centred (C) and centred (D).....	229
Figure 5-1: Bar chart of the number of silver objects by site.....	233
Figure 5-2: Bar chart showing the number of silver objects by cemetery and object category.	236
Figure 5-3: Silver objects by category (left) and class (right). The colour coding in the class graph is taken from the categories.	236
Figure 5-4: Bar chart showing the number of silver objects by cemetery with biological sex on the X axis and object category as the stratum variable.	238
Figure 5-5: Bar charts of showing the number of silver objects by cemetery with assigned gender on the X axis and object category as the stratum variable.....	239
Figure 5-6: Bar charts of object classes with biological sex on the X axis and cemetery as the stratum variable	240
Figure 5-7: Bar charts of object classes with assigned gender on the X axis and cemetery as the stratum variable.	241
Figure 5-8: Bar charts showing the number of silver objects according female inhumation phasing (left) and male phasing (right). The cemetery is the stratum variable in both.....	242
Figure 5-9: Bar chart of fabrication techniques and object class. It should be noted that the ‘unknowns’ in the cast category are predominantly formed of ‘melted blobs’ that are assumed to be associated with cremations, i.e. these could have represented sheet, wire or cast objects that were melted in the cremation process.	243
Figure 5-10: Ternary diagrams with individuals colour coded according to clr clusters. A & B show Au- Sn-Zn diagrams un-centred and centred respectively, C & D Ag-Sn-Zn diagrams centred and centred respectively.	246

Figure 5-11: 3D ternary diagrams with individuals colour coded according to clr clusters. The top two (A & B) show Au-Ag-Sn-Zn un-centred (A) and centred (B). The top two (C & D) show Cu-Pb-Sn-Zn un-centred (C) and centred (D).....	247
Figure 5-12: Bar chart showing the percentage of silver objects with cluster as the stratum variable and cemetery on the X axis.	249
Figure 5-13: Pie charts showing the silver clusters present within each grave. The number of objects in each grave is presented adjacent to the right of the grave number.	250
Figure 5-14: Centred ternary diagram showing silver wrist clasps colour coded according to clusters.	255
Figure 5-15: Un-centred ternary diagram showing the silver equestrian objects from grave 323.	256
Figure 5-16: Bar chart showing the number of objects by object category with cluster as the stratum variable.	257
Figure 5-17: Bar chart showing the percentage of objects by object sub class with cluster type as the stratum variable. See Table 5-8 for the relevant data.....	258
Figure 5-18: Bar chart showing the percentage of objects by object fabrication technique with cluster type as the stratum variable. The cast objects consisted solely of a few ‘melted blobs’ and so are not indicative of any particular object type. See Table 5-9 for the relevant data.....	259
Figure 5-19: Bar chart showing object class with clusters in the stratum variable and fabrication as the facet available in the rows. The ‘cast’ objects have not been included here as they solely consisted of ‘melted blobs’.....	260
Figure 5-20: Bar chart showing grave phases (top row female, bottom row male) with clusters in the stratum variable and cemetery as the facet available in the rows.....	261
Figure 6-1: XRD spectra for gilding on wrist clasp 046 – 1811. Analysis was undertaken on a PANalytical X’pert PRO at the National Museum Wales. The full data for the analysis are available in Appendix 1.....	270
Figure 6-2: Phase diagram for the Cu-Hg system from Chakrabarti and Laughlin 1985, 522, Figure 1.	272
Figure 6-3: Modern political map of Europe showing cinnabar deposits known to have been exploited in the Roman and /or medieval (red stars) and Eriswell (blue circle). The locations are: Almadén (Spain), Avala (Serbia), Carnia (Austria), Ephesus (Turkey), Idrija (Slovenia), Moschellandsberg (Germany), Rosenau (Romania), Sicily (Italy), Sizma (Turkey) and Tuscany (Italy). See Table 6-7 for details and references of the antiquity of mining activities at each location. Data from Rapp (2009, 180) and Maras et al. (2013, 686), base vector map by Erind (2010).....	280
Figure 6-4: Amalgam mortars from Hamwic (left) and Clausentum (right). From (Bayley and Russel 2008).....	284

Figure 7-1: A schematic sketch cross section and plan illustrating how the break in great square head brooch 104-1704 was repaired with the use of a filler alloy and copper alloy plate. Not to scale.	289
Figure 7-2: Ternary diagram showing solders and non-solder areas on silver objects. See Table 7-3 for Net Peak Area data.	291
Figure 7-3: Ternary diagram showing solders and non-solder areas on copper alloy objects. The Net Peak Area data can be found in Appendix XI:.....	293
Figure 7-4: Lead-tin phase diagram from ASM International (1992, 1300) after Karakaya and Thompson (1988).....	294
Figure 7-5: Silver-gold-copper phase diagram. From ASM International (1992, 1494) after Prince, Raynor, and Evans (1990, 65)	295
Figure 7-6; Ag-Pb-Sn phase diagram from ASM International (1992, 1503) after Petzow and Effenberg (1988).	298
Figure 7-7: Silver – copper phase diagram. From Subramanian and Perepezko (1993, 63, Fig. 1)....	299
Figure 7-8: Ternary diagrams of ‘lead’ alloy NPA. See Table 7-6 for the NPA data.....	302
Figure 7-9: Sketch profile and plan of 114-1039. Studs 114-1037 and 114-1044 share the same form. Not to scale.....	305
Figure 8-1: Example of the impact of corrosion on two objects that had areas of uncorroded and significantly corroded alloy available for analysis.	311
Figure 8-2: Bar chart of manufacture by site.	316
Figure 8-3: Bar chart showing a breakdown of cast objects and further degrees of working.	319
Figure 8-4: Bar charts showing object categories as the row variable, cemetery on the x-axis and sex and gender as the stratum variables. The data for the graphs can be found in Table 8-11.....	320
Figure 8-5: Density plots showing the distribution of the data for major elements.....	326
Figure 8-6: Q-Q plots for normal distribution. The black dots show the individuals and the straight line the theoretical normal distribution.	327
Figure 8-7: Q-Q plots for lognormal distribution. The black dots show the individuals and the straight line the theoretical lognormal distribution.	328
Figure 8-8: Density plots of clr transformed copper alloy data.	329
Figure 8-9: Univariate scatterplots for the (untransformed) elements. The top plot includes silver, the bottom excludes it. Circles indicate individuals that are within the main distribution, crosses outlying individuals. The colour scheme is based on a heat map (i.e. a cooler colour indicates the degree of how much an outlier outlies). Created using the R package ‘mvoutlier’ (Filzmoser and Gschwandtner 2015).....	332
Figure 8-10: Biplot of ilr transformed data both including and excluding arsenic (left and right respectively) showing individuals within the main distribution outliers (circles) and outliers (crosses). The colour scheme is heat map based (i.e. the warmer the colour the more outlying it is). Created using the R package ‘mvoutlier’ (Filzmoser and Gschwandtner 2015).	333

Figure 8-11: Univariate scatter plots of ilr transformed outliers. Circles indicate individuals that are within the main distribution, crosses outlying individuals. Created using the R package 'mvoutlier' (Filzmoser and Gschwandtner 2015).	334
Figure 8-12: Two parallel coordinate plots, the top shows all data, the bottom outliers only. The colour scheme is based on a heat map (i.e. a warmer colour indicates the degree of how much an outlier outliers). The minimum of the variables is zero and the maximum is one. Created using the R package 'mvoutlier' (Filzmoser and Gschwandtner 2015).....	335
Figure 8-13: Parallel coordinate plot of untransformed data. Outliers are in red, non-outliers in grey. The minimum of the variables is zero and the maximum is one. Created using the R package 'ggally' (Schloerke et al. 2014).	336
Figure 8-14: Ternary diagram showing Roman copper alloy objects from Eriswell (excluding coins) over analyses of Roman dress accessories from other sites in the UK. The comparable data are drawn from analyses by Bayley and Butcher (2004) and Blades (1995). The site codes are as follows: RICH – Richborough; LINC – Lincoln; BALD – Baldock, Hertfordshire; NORN - Nornour, Isles of Scilly; STAL - St Albans, Hertfordshire. Blades analysis was undertaken using ICP-MS, Bayley and Butcher's AAS. Each data set was closed as a sub composition before being combined with the others for the purposes of plotting the diagram.....	338
Figure 8-15: Extract from Figure 3-10 and Figure 3-13 showing scatter plots of measured mean (n=10) arsenic quantitative (left) and qualitative (right) results on reference alloys at 40 kV - 7.9 μ A against certified values.....	353
Figure 8-16: Scatterplot matrix of Eriswell untransformed data using the R package 'PerformanceAnalytics' (Peterson and Carl 2014). Pairwise complete observations only. Data has been scaled.	355
Figure 8-17: Scatterplot matrix for Blades (1995, 86–97) early Saxon copper alloy data set (excluding two non-copper alloy results, analysis numbers 762 & 766). No zero replacement used, pairwise observations only.	356
Figure 8-18: Scatterplot matrix of Eriswell untransformed data excluding arsenic using the R package 'PerformanceAnalytics' (Peterson and Carl 2014). Pairwise complete observations only. Data have been scaled.	358
Figure 8-19: Scatterplot matrix of clr transformed data. The * at the apex of each diagram is the third component and represents the geometric mean of the remaining components.	359
Figure 8-20: Scatterplot matrix of clr transformed data with zinc as a constant at the apex of the pyramid.....	362
Figure 8-21: Scree plot of the results of Horn's Parallel Analysis for component retention with 23430 (30 x n) iterations, using the 95 th percentile estimate. See Table 8-33 for further details.....	369
Figure 8-22: untransformed Principal Components Analysis. On the left are a biplot (top) and scree plot (bottom) showing the results of robust PCA (see also Table 8-35). On the right are a biplot (top) and scree plot (bottom) showing the results of non-robust PCA (see also Table 8-34). The	

robust PCA was undertaken using the R package ‘pcaPP (Filzmoser, Fritz, and Kalcher 2014)’, the non-robust using the R package ‘FactoMineR’	369
Figure 8-23: clr transformed Principal Components Analysis. On the left are a biplot (top) and screplot (bottom) showing the results of robust PCA (see also Table 8-37). On the right are a biplot (top) and screplot (bottom) showing the results of non-robust PCA (see also Table 8-36). All plots produced using the R pacakage ‘compositions’	370
Figure 8-24:Biplots showing individuals coloured according to cluster membership. Please note that the group numbers do not mean that the clusters are directly comparable, i.e. U1 and UR1 are not exactly the same. For a summary of the clusters see Table 8-38. For details on each individual’s group membership see Appendix XVII on page 671.....	372
Figure 8-25: Parallel co-ordinate plots showing the variables scaled and centred with individuals colour coordinated according to cluster membership. The colours used are the same as in Figure 8-24. The top plot shows the clusters defined from the untransformed robust PCA, the bottom plot shows the transformed robust PCA clusters. Missing values are plotted at 10% below the minimum of the variable for the missing value and the variables are ordered by skewness (i.e. the most skewed variables are first in the plots). The variables have been scaled univariately with a maximum of 1 and centred. Created using the ‘ggparcoord’ function from the R package ‘GGally’ (Schloerke et al. 2014).	374
Figure 8-26: Scaled scatterplots with pairwise complete observations only (hence cluster group TR 1 being missing from the Zn – Sn transformed plot). Individuals are coloured according to cluster membership.....	375
Figure 8-27: Ternary diagrams showing tin – lead – zinc (top) and the apex of a copper – tin – zinc diagram (bottom). Individuals are coloured according to cluster membership.....	376
Figure 8-28: Comparison of alloy classification systems in tin – zinc scatterplots. The top plot (Mortimer 1991, 105, Figure 1) shows Mortimer’s classification system (reproduced in Table 8-39) based on her analysis of cruciform brooches (Mortimer 1990). The middle left, right and bottom left all show Blades’ Early Saxon data (1995, 86–97) classified according to his alloy types (reproduced in Table 8-40), Pollard et al.’s alloy types (reproduced in Table 8-41) and the hierarchical clustering used in this study respectively. On the bottom left is Eriswell (scaled and using the zero replaced data) with classification derived from the hierarchical clustering.	381
Figure 8-29: Tin – zinc – lead ternary diagrams. On the top left is Blades’ Early Saxon data (1995, 86– 97) classified according to his alloy types (reproduced here in Table 8-40) and on the top right is the same data but with individuals identified classified according to Pollard et al.’s (2015, 700, Table 2) definitions (reproduced here in Table 8-41). The bottom left diagram shows individuals identified by clusters produced after robust transformed PCA and HC was performed on Blades data (using the processes outlined earlier). On the bottom right the Eriswell data is provided for comparison, again with individuals identified by clusters derived from the HC.	383

Figure 8-30: Parallel co-ordinate plots of Blades' Early Saxon data (1995, 86–97) showing the variables scaled and centred with individuals colour coordinated according to group membership as follows: top - Blades groups, middle - Pollard et al.'s (2015) groups, bottom – hierarchical clusters . Missing values are plotted at 10% below the minimum of the variable for the missing value and the variables are ordered from left to right by skewness. The variables have been scaled univariately with a maximum of 1 and centred.	386
Figure 8-31: MCA biplot of clusters and minor element presence ('yes') or absence ('no'). A jitter has been added to make the individuals more visible, otherwise the majority overlap and appear singular	389
Figure 8-32: Results of a correspondence analysis between manufacture method and hierarchical clusters on the Eriswell data set.	391
Figure 8-33: Bar chart of clusters and manufacturing method. For the raw figures see Table 8-45.	392
Figure 8-34: Results of a correspondence analysis between hierarchical clusters and object sub class on the Eriswell data set.	393
Figure 8-35: Results of a correspondence analysis between hierarchical clusters and object sub class on the Eriswell data set excluding wrist clasp forms Form C 1, Form B and Form B 18. The object categories are colour coded according to object class membership.....	395
Figure 8-36: Results of a correspondence analysis between manufacture method and hierarchical clusters on the Eriswell data set with all beads excluded. See Figure 8-32 for the same plot with beads included.....	398
Figure 8-37: Schematic diagram of a bucket bead.....	399
Figure 8-38: Ternary diagram of grave 005 from ERL 046.....	408
Figure 8-39: Ternary diagram of grave 015 from ERL 046.....	409
Figure 8-40: Ternary diagram of grave 024 from ERL 046.....	410
Figure 8-41: Ternary diagram of grave 025 from ERL 046.....	411
Figure 8-42: Ternary diagram of grave 038 from ERL 046.....	412
Figure 8-43: Ternary diagram of grave 172 from ERL 104.....	413
Figure 8-44 Ternary diagram of grave 231 from ERL 104.....	414
Figure 8-45: Ternary diagram of grave 242 from ERL 104.....	415
Figure 8-46: Ternary diagram of grave 255 from ERL 104.....	416
Figure 8-47: Ternary diagram of grave 315 from ERL 104.....	417
Figure 8-48: Ternary diagram of grave 323 from ERL 104.....	418
Figure 8-49: Ternary diagram of grave 350 from ERL 104.....	420
Figure 8-50: Ternary diagram of grave 362 from ERL 104.....	421
Figure 8-51: Ternary diagram of grave 405 from ERL 114.....	422
Figure 8-52: Ternary diagram of grave 422 from ERL 114.....	423
Figure 8-53: Ternary diagram of grave 447 from ERL 114.....	424
Figure 8-54: Ternary diagram of grave 458 from ERL 114.....	426

Figure 8-55: Bar chart showing the percentage of cluster type by male and female grave phase (top and bottom respectively). See Table 8-62 for the actual number of objects. 427

Figure 8-56: Extract from Figure 8-28. The left plot shows Blades' Early Saxon data (1995, 86–97) classified according to the HC used in this study, on the right is Eriswell (scaled and using the zero replaced data) with classification derived from the HC. It can be seen that there is similarity in the distribution of the clusters, supporting the decision to treat the Eriswell NPA data compositionally. 429

Figure 8-57: Parallel co-ordinate plot of Blades' Early Saxon data (1995, 86–97) (top) and Eriswell (bottom) showing the variables scaled and centred with individuals colour coordinated according to cluster membership. Missing values are plotted at 10% below the minimum of the variable for the missing value. The variables have been scaled univariately with a maximum of 1 and centred..... 432

List of Tables

Table 1-1: Object categories, classes and sub classes used in this thesis.	48
Table 2-1: Niello compositions and approximate dates of use in Western Europe (from La Niece 1983).....	67
Table 3-1: Energies of X-ray peaks of interest (organised in atomic number order) and potential overlaps.	105
Table 3-2: Summary of recent HHPXRF studies (excludes exclusive studies of non-bulk methods i.e. Papadopoulou et al. 2006 study of micro-XRF) featuring summaries from the cited studies..	124
Table 3-3: Bruker HHPXRF software used in this study.....	128
Table 3-4: Full range of filters available. Thickness is provided in both Mil (0.001 inch / thousandths of an inch) and micrometres (μm).....	129
Table 3-5: Summary of the five objects from Eriswell cemetery 046 selected for analysis.....	130
Table 3-6: Detailed description and Corrosion assessment of Eriswell non-ferrous objects.....	133
Table 3-7: Tube settings used	135
Table 3-8: Mean Net Peak Area data (n=10), coefficient of variation (C_v) and limit of determination (\pm) for major elements on each object (see Figure 3-4 and Table 3-6 for object details) under four different test settings (see Table 3-7, excluding settings A, C and D). The LDM is calculated according Rousseau's (2001) Limit of Determination of a Method (see Equation 5 on page 111 for more details). A full set of data including the minor and trace elements can be found in the relevant Net Peak Area data appendices.	142
Table 3-9: Showing the mean Net Peak Area (data from Table 3-8) and the percentage increase in peak area.	143
Table 3-10: Given values for major elements in the MBH Analytical and IMMACO reference materials used in this study, In Appendix I a table with minor and trace elements along with uncertainty is provided.	146
Table 3-11: Given and empirically calibrated measured analyses of the MBH alloys (wt%). Empirically calibrated measured data (Cal. Measured), Standard Deviation (SD), Coefficient of Variation (C_v) and Limit of Determination of a Method (LDM) are presented. The results acquired at 40kV and 9.6 μA . were previously published in Nicholas and Manti (2014) in Table 1.....	148
Table 3-12: Given and empirically calibrated analyses of IMMACO alloys. Standard Deviation (SD), Coefficient of Variation (C_v) and Limit of Determination of a Method (LDM) are presented. The results acquired at 40kV and 9.6 μA . were previously published in Nicholas and Manti (2014) in Table 2.	150
Table 3-13: Maximum LDM (\pm) values across all MBH and IMMACO reference alloys as analysed at 40 kV - 7.9 μA	161
Table 3-14: MBH reference alloy compositions with density.	163

Table 3-15: Depth (μm) from which the stated percentage for the relevant peak energy originates within the sample with a 40 keV incident x-ray. Calculated using the formula from Potts, Williams-Thorpe, and Webb (1997, 32, Equation 2) with mass attenuation coefficient data from Berger et al. (2010).	164
Table 3-16: Corrosion products and densities.	166
Table 3-17: Depth (μm) from which the stated percentage for the relevant peak energy originates within the sample with a 40 keV incident x-ray. Calculated using the formula from Potts, Williams-Thorpe, and Webb (1997, 32, Equation 2) with mass attenuation coefficient data from Berger et al. (2010).	166
Table 3-18: Un-normalised compositions for six silver alloys chosen to represent a variety of silver compositions: the great square-headed brooches (Brownsword and Hines 1993) are early medieval in date and represent a low Ag compositions; the Faversham and Winchester objects (Mortimer 1986) are relatively high Ag roman objects that also contain Zn; and the CNR alloys are an Ag-Cu reference alloy (Casaletto et al. 2010).	169
Table 3-19: Depth (μm) from which the stated percentage for the relevant peak energy originates within the sample with a 40 keV incident x-ray. Calculated using the formula from Potts, Williams-Thorpe, and Webb (1997, 32, Equation 2) with mass attenuation coefficient data from Berger et al. (2010). See section 3.4.1, page 159 for a detailed description of this process.	170
Table 3-20: Summary of results from the distance test on reference material 32X SN6. The table shows the percentage decrease in signal received by the HHpXRF detector taking position 0 as 100%.	172
Table 3-21: Net peak areas for Cu, Sn and Zn with percentage values for each peak normalised to the total of all three peaks.	173
Table 3-22: Net peak areas for Pb, Sn and Zn with percentage values for each peak normalised to the total of all three peaks.	174
Table 3-23: Peak counts at differing temperature. The bold values represent the maximum value reached and the percentage difference the variation between the value above and the max value.	176
Table 3-24: Net peak areas and ratios for three elements at differing temperatures.	176
Table 3-25: Analysis settings for the analysis of the non-ferrous assemblage from Eriswell.	179
Table 4-1: Classical statistical summary for the silver data set.	189
Table 4-2: Pairwise linear correlations both including and excluding minor elements.	189
Table 4-3: Correlation matrix for major elements.	191
Table 4-4: Principal component data. Figures in bold are judged to be significant values (those making at least a 10% contribution).	192

Table 4-5: Variance of each component. Those components that should be retained according the Guttman-Kaiser Criterion are italicised. Only those components with a value above 1 (i.e. greater than the weight of an individual) should be retained according to the criterion.....	193
Table 4-6: Results of Horn's Parallel Analysis for component retention 2010 iterations (30 x n), using the 95 th percentile estimate. Only those elements that should be retained are presented. See Figure 4-4 for graphical representation.....	195
Table 4-7: Objects removed from the second round of PCA.	197
Table 4-8: Results of Horn's Parallel Analysis for component retention 1320 iterations (30 x n), using the 95 th percentile estimate. Only those elements that should be retained are presented. See below for scree plot.....	197
Table 4-9: Principal component data for the trimmed 'high' silver set. Figures in bold are judged to be significant values (those making at least a 10% contribution).	199
Table 4-10: Example of Multiplicative Replacement on two Eriswell Silver objects.	203
Table 4-11: Variation array for Eriswell silver. Upper triangle: log-ratio variances; lower triangle: log-ratio means. Bold values are those that have the largest variance.....	205
Table 4-12: clr Principal Component data. Figures in bold italics are significant values (those making at least a 10% contribution).	207
Table 4-13: Component eigenvalues for clr PCA. Those components that should be retained according the Guttman-Kaiser Criterion are italicised. Only those components with a value above 1 (i.e. greater than the weight of an individual) should be retained according to the criterion.	208
Table 4-14: Variation array for Eriswell silver. Upper triangle: log-ratio variances; lower triangle: log-ratio means. Bold values are those that have the largest variance.....	211
Table 4-15: Component eigenvalues for the 'high' silver clr PCA. Those components that should be retained according the Guttman-Kaiser Criterion are italicised. Only those components with a value above 1 (i.e. greater than the weight of an individual) should be retained according to the criterion.	212
Table 4-16: clr 'high' silver Principal Component data. Figures in bold italics are significant values (those making at least a 10% contribution).....	212
Table 4-17: Comparison between cluster groups showing the number of individuals within corresponding groups.....	218
Table 4-18: Cluster results. A full table with categorical variables included can be found in Appendix III.....	220
Table 5-1: Number of silver objects by site and grave number.	234
Table 5-2: Number of inhumations that contain silver objects in cemeteries ERL 046, 104 and 114.	235
Table 5-3: Table showing the number of silver objects by cemetery, object category, class and sub class.	237

Table 5-4: No of silver objects by fabrication technique and site.....	243
Table 5-5: No of silver objects by fabrication technique, site, object category and class.....	244
Table 5-6: Silver wrist clasps. Those from the same grave (i.e. a hook and eye piece) which fall in the same cluster are highlighted.	254
Table 5-7: Silver equestrian objects from grave 323.....	256
Table 5-8: Object categories, classes and sub classes with the number of objects by cluster.	258
Table 5-9: Showing showing the number of objects by object fabrication technique and cluster type. The cast objects consisted solely of a few melted drops (predominantly associated with cremations and so are not indicative of any particular object type. See Figure 5-18 for a bar chart of the results.	260
Table 6-1: Attenuation coefficients for fluorescent Cu–K α (8.05 KeV) and Sn–K α (25.27 KeV) x-rays in gold amalgam and gold matrices. The t_{crit} shows the maximum from which Cu and Sn K α x-rays would be able to escape from the respective matrices with an incident x-ray of 40 KeV). Calculated using the formula from Potts, Williams-Thorpe, and Webb 1997, 32 , Equation 2.For a detailed discussion on calculating the critical penetration depth see page 159.	273
Table 6-2: Number of gilt and non-gilt graves for cemeteries ERL 046, 104 and 114.....	274
Table 6-3: Showing graves containing objects, the gilt object categories and the number of gilt objects.	275
Table 6-4: showing gilt objects by site, category, class and sub class.....	276
Table 6-5: Number of gilt objects by site and assigned gender.	277
Table 6-6: Number of objects by phase.	277
Table 6-7: Cinnabar mining areas shown in Figure 6-3 with dates for the earliest documented extraction activities. Those that are noted as medieval have sites as.....	281
Table 7-1: Areas of filler alloy associated with joining (i.e. soldering / brazing) by site and object category.	289
Table 7-2: Areas of filler alloy on silver objects. See Appendix X: for full Net Peak Area data (including coefficient of variation where applicable).	290
Table 7-3: Net peak areas for solders and non-solders. The full solder data (including the coefficients of variation) are in Appendix X.; non-solder silver data are available in Appendix V.....	292
Table 7-4: Net peak area data for necklace and pendants 104-2317. For data with the coefficient of variant (where applicable) see Appendix X: and Appendix XI:.	297
Table 7-5: ‘Lead’ objects. A full table of the categorical variables can be found in Appendix XII:. See Table 7-6 for the net peak area data.	300
Table 7-6: Mean net peak area data for the ‘lead’ objects. A full version of the data, including coefficients of variation, is available in Appendix XIII:. See.....	301
Table 8-1: Copper alloy objects excluded from statistical interpretation in this chapter.....	312
Table 8-2: Number of copper alloy objects by site.	312

Table 8-3: Number of inhumations that contain copper alloy objects in cemeteries ERL 046, 104 and 114.....	313
Table 8-4: The number of copper alloy objects analysed by site, object category and object class..	314
It should be noted that there is a large amount of utilitarian ('miscellaneous') metalwork analysed here (84 objects, 10.39% of the assemblage), including a number of nails and bolts. At this juncture it should be remembered that the number of objects used here refers to the different fabricated parts that make up a composite object (as discussed on page 305). Consequently there are not seven buckets listed in Table 8-5 but seven different parts to one bucket (small find 1306 from grave 031 in ERL 046).....	
Table 8-6: The number and type of brooches analysed by cemetery. It should be remembered that the number of objects refers to the different fabricated parts that make up a composite object (as discussed on page 305). Consequently the number presented here may differ from how Anglo-Saxon brooch scholar would normally consider or count.....	315
Table 8-7: Number of copper alloy objects by manufacture method.....	316
Table 8-8: Showing the number of copper alloy objects by working type and object category.....	317
Table 8-9: Number of sheet objects within the miscellaneous fittings category from ERL 104.	318
Table 8-10: A breakdown of cast objects showing further degrees of working.....	318
Table 8-11: Number of copper alloy objects by site, object category, biological sex and assigned gender.....	321
Table 8-12: Copper alloy dress accessories associated with male gendered burials.....	321
Table 8-13: Copper alloy dress accessories associated with female gendered burials.....	322
Table 8-14: Number of copper alloy objects by female (top) and male (bottom), grave phase, site and manufacturing method.....	323
Table 8-15: results of a Shapiro-Wilks test for normality on untransformed copper results with a decreasing sample size. The individuals in the reduced samples were randomly selected using the base R function 'sample'. It should be noted that although these samples were randomly selected there is a chance that if replicated multiple times the results would not follow the same pattern of an increasing p-value.	325
Table 8-16: Non early medieval outliers and categorical variable. See Table 8-17 for associated Net Peak Area data.....	339
Table 8-17: Non early medieval outliers. The unshaded row shows the net peak areas (mean if more than one analysis taken) for each element, the second (shaded) row shows the coefficient of variation. The final column shows the number of analyses. See Table 8-16for associated categorical variables.	341
Table 8-18: Contaminated measurements identified during outlier analysis with categorical variables.	344
Table 8-19: Net Peak Area data for contaminated analyses. The unshaded row shows the net peak areas (mean if more than one analysis taken) for each element, the second (shaded) row	

shows the coefficient of variation. The final column shows the number of analyses. See Table 8-18 for associated categorical variable.	345
Table 8-20: Full list of the objects excluded from further analysis after outlier analysis. The final column details the reason: UP – unphased non-Anglo-Saxon object; C – contaminated analysis.	347
Table 8-21: Showing elements and the number of missing values for the Eriswell data and Blades Early Saxon data (1995, 86–97) (two non-copper alloy objects have been excluded from Blades results here, these are Blades analysis numbers 762 & 766).	348
Table 8-22: Maximum LDM (\pm) values for arsenic across all MBH and IMMACO reference alloys as analysed at 40 kV - 7.9 μ A. For the full table with all elements see Table 3-13, page 158. The NPA result should be considered valid only for flat uncorroded alloys that completely cover the HHpXRF window	349
Table 8-23: Classical statistical summary for the copper alloy data set.....	351
Table 8-24: Correlation matrix for the copper alloy data set including arsenic.....	351
Table 8-25: Top ten most highly correlated pairs for the copper alloy data set including arsenic....	352
Table 8-26: Correlation matrix for Blades (1995, 86–97) early Saxon copper alloy data set (excluding two non-copper alloy results, Blades analysis numbers 762 & 766).	353
Table 8-27: Summary showing number of objects and the identification of arsenic by site.	357
Table 8-28: Correlation matrix for the Eriswell copper alloy data set excluding arsenic.....	357
Table 8-29: Top ten most highly correlated pairs for the copper alloy data set excluding arsenic. ..	358
Table 8-30: Variation array for Eriswell copper alloys including arsenic. Upper triangle: log-ratio variances; lower triangle: log-ratio means. Bold values are those that have the largest variance.	360
Table 8-31: Variation array for Eriswell copper alloys excluding arsenic. Upper triangle: log-ratio variances; lower triangle: log-ratio means. Bold values are those that have the largest variance.	360
Table 8-32: Variance of each component. Those components that should be retained according the Guttman-Kaiser Criterion are italicised. Only those components with a value above 1 (i.e. greater than the weight of an individual) should be retained according to the criterion.....	366
Table 8-33: Results of Horn's Parallel Analysis for component retention with 23430 (30 x n) iterations, using the 95 th percentile estimate. Only those elements that should be retained are presented. See Figure 8-21 for the scree plot.	366
Table 8-34: untransformed principal components. Figures in bold are judged to be significant values (those making at least a 10% contribution).....	366
Table 8-35: untransformed robust principal components. Figures in bold are judged to be significant values (those making at least a 10% contribution).....	367

Table 8-36: clr transformed non-robust principal components. Figures in bold are judged to be significant values (those making at least a 10% contribution). For scree plot and biplot see Figure 8-23.	367
Table 8-37: clr transformed robust principal components. Figures in bold are judged to be significant values (those making at least a 10% contribution). For scree plot and biplot see Figure 8-23.	368
Table 8-38: Cluster groups showing the number of objects by cluster and site. Please note that the group numbers do not mean that the clusters are directly comparable, i.e. U1 and UR1 are not exactly the same. For details on each individuals group membership see Appendix XVII on page 671.	371
Table 8-39: Mortimer’s (1991, 106) description of her copper alloy definitions.	378
Table 8-40: Blades (1995, 126) description of his copper alloy definitions.	379
Table 8-41: Pollard et al.’s description of their copper alloy definitions (2015, 700, Table 2).	379
Table 8-42: Results of robust transformed PCA on Blades Early Saxon data set (1995, 86–97). Significant figures (those explaining over 10% of variance are in bold). Antimony and silver have been included to enable comparability with the Eriswell results.	380
Table 8-43: Showing the reported and normalised results (weight percent) from Blades’ analysis (Blades analysis number 351) on a wrist clasp from Morning Thorpe (1995, 91). Note that normalised the lead crosses the 4% threshold set by Blades for distinguishing between leaded and unleaded alloys.	387
Table 8-44: Pollard et al.’s (2015, 708–9, Tables 5 & 6) trace element groups and the percentage of Early Saxon objects they found in Blades (1995) data. The final two columns show the number and percentage of objects from Eriswell that fall into the same categories. The Eriswell details are provided for interest only and should not be considered valid.	390
Table 8-45: Manufacture method and cluster membership. For a bar chart of the data see Figure 8-33.	392
Table 8-46: Number of wrist clasps by hierarchical cluster type.	394
Table 8-47: The number of alloy cluster types used for the production of wrist clasps analysed by Blades (1995). Eriswell is provided for comparison at the bottom of the table.	394
Table 8-48: Number of brooches by hierarchical cluster type.	396
Table 8-49: Showing the percentage of annular brooches by manufacture method in each cluster. The final column shows the actual number of objects.	396
Table 8-50: The percentage of the alloy types used for the production of annular brooches analysed by Blades (1995). Eriswell is provided as a comparison at the bottom of the table. Blades did not provide any details of the manufacturing processes used on the objects he analysed so it is not possible to provide a breakdown by cast and sheet.	397
Table 8-51: Showing number beads by manufacture and cluster type.	397

Table 8-52: Showing the percentage of objects by category and their cluster membership. The final column shows the actual number of objects. Only those object classes with 10 or more objects are displayed here.	398
Table 8-53: The percentage of bucket pendants and other bead types by cluster.....	399
Table 8-54: Analysis of bucket SF 1306 from ERL 046. The coefficient of variation provided is across the amalgamated analyses presented above. Major elements only. For full results see Appendix V on page 512.	401
Table 8-55: Showing the percentage of equestrian object from grave 323 (ERL 104) by object sub class, manufacturing method and cluster membership. The final column shows the actual number of objects.	402
Table 8-56: Showing the percentage of suspension related belt fitting objects by object sub class, manufacturing method and cluster membership. The final column shows the actual number of objects. The latch-lifters are 104-3313-A, 104-2787-A-A and 104-2787-C-A.	402
Table 8-57: NPA data for composite girdle-hanger 1061 from ER 114.	403
Table 8-58: The percentage of the alloy types used for the production of girdle-hangers analysed by Blades (1995). Eriswell is provided as a comparison at the bottom of the table. Blades did not provide any details of the manufacturing processes used on the objects he analysed so it is not possible to provide a breakdown.	403
Table 8-59: Girdle-hangers from Eriswell with cluster memberships. The column 'Hines Description' is an amalgamation of information provided to the author in two batches in 2010 and 2013 by Professor John Hines.	405
Table 8-60: Graves at Eriswell that contain more than 10 copper alloy objects.	406
Table 8-61: Objects from grave 422.....	423
Table 8-62: Number of objects per cluster in each phase. The final column shows the actual number of objects in each phase.	428

List of Equations

Equation 1: Formulae to compare reference material with an unknown to quantify the concentration of an element (where C_{unk} and C_{std} are the unknown and standard concentration and I_{unk} and I_{std} the corrected background intensity for the unknown and standard) (Frame, 2009: 106, equation 5.2). 107

Equation 2: Formula devised by Potts et al. (1997: 770) for the correction of sample geometry where $I_{measured}$ is the intensity of characteristic X-rays from a sample or object with an irregular surface and $B_{measured}$ is the resulting intensity of the scattered radiation (i.e. Compton and Rayleigh). $B_{reference}$ is the intensity of scattered radiation from a flat reference sample of similar (or the same) composition. 111

Equation 3: Formulae developed by Maia et al. (1997) and Bos & Vrieling (1998) for the correction of sample geometry (where R_{ik} is the relative instrument calibration factor; I_i the intensity of the characteristic X-rays of the sample and I_k and the intensity of the characteristic X-rays of a selected reference material)..... 112

Equation 4: Equation for calculating the Lower Limit of Detection (ILD) in XRF spectra where I_b equals the average background intensity and σ_b the counting errors (Gullayanon 2011, 22 equation 5). 113

Equation 5: Formula for calculating the Limit of Determination of a Method. The mean concentration for an element (C) is derived from ten analyses of the same material taken under the same analytical conditions. C_m is the measured concentration, n the repetition number. From Rousseau (2001, 41, Equation 12). 113

Equation 6: Equation from Potts, Williams-Thorpe, and Webb (1997, 32, Equation 2) for calculating the critical penetration depth where p is the density of the sample, Ψ_1 is the incident angle, Ψ_2 the take-off angle, $\mu(E_0)$ the mass attenuation coefficient primary radiation (cm^2/g) and $\mu(E_i)$ the mass attenuation coefficient characteristic radiation (cm^2/g)..... 162

Equation 7: Formulae for Multiplicative Replacement Strategy for zeroes from Martin-Fernandez et al. (2003, 262, Equation 6): r^j is the modified non-zero value, δ_j is the small value which replaces the zero, x_j is the original unmodified non-zero and c is the constant of the sum constraint..... 202

CHAPTER 1: PRIMER

“Overhead the arch of heaven spread more ample than elsewhere...such cloudlands, such sunrises, such sunsets...”

(Kingsley 1866, 15)

1.1 INTRODUCTION

This chapter provides a brief overview of the three cemeteries the artefacts analysed in this study were excavated from alongside a brief introduction to some of the terminology used throughout.

It should be noted that the names used for the Eriswell cemeteries in this thesis (ERL 046, ERL 104 and ERL 114) are the Suffolk Historic Environment Record’s (HER) permanent record numbers for the sites.

1.2 SITE LOCATION AND CONTEXT



Figure 1-1: Location of the modern county of Suffolk (left) and Eriswell within (right). UK and Suffolk maps created by Nilfanion (2010a; 2010b) under a Creative Commons Attribution-Share Alike 3.0 Unported licence.

This study focuses on the analysis of the non-ferrous metalwork from three cemeteries at RAF Lakenheath, Suffolk (Figure 1-1). The cemeteries are thought to date from 475 to 650 CE (Caruth and Anderson 2005, viii).

RAF Lakenheath (NGR: TL 7305 8035) is located within Eriswell and Lakenheath parishes (Forest Heath district) in the north-west corner of the county of Suffolk. The site is located in a transitional fen edge zone (Sussams 1996) with the Brecks (a sandy gorse covered landscape) to the east. Although the border between the two zones can shift (due to climatic changes and human activity) the nearby presence of Caudle Head spring would have ensured a continued fen like environ. (Anonymous 2013, 98). To the west lay the Fens proper, thought to have been largely uninhabitable marshland during the Anglo-Saxon times (Caruth and Anderson 2005, 2). This position of the Eriswell cemeteries is not unusual for an early Anglo-Saxon site (see West 1998), with numerous others being known in the vicinity (Figure 1-2) and on other fen edge zones in other counties. Some of these nearby sites include cemeteries with non-ferrous artefacts that have been previously published such as Holywell Row (Suffolk SHER No. MNL 084). The previously published data will be used as comparative material during this study.

It used to be thought — due to the similarity of finds found in cemeteries and settlements across the Fen basin edges (Fox 1923, 315–316) — that this resulted from invading Saxons sailing across the sea and into the Fens, settling where boats landed (Darby 1934, 185). Nowadays this rather simplistic explanation has been replaced by a much more complex and nuanced picture of movement, trade and exchange of ideas, identities, material goods and people across the Fens and the North Sea (Hines 2013a).

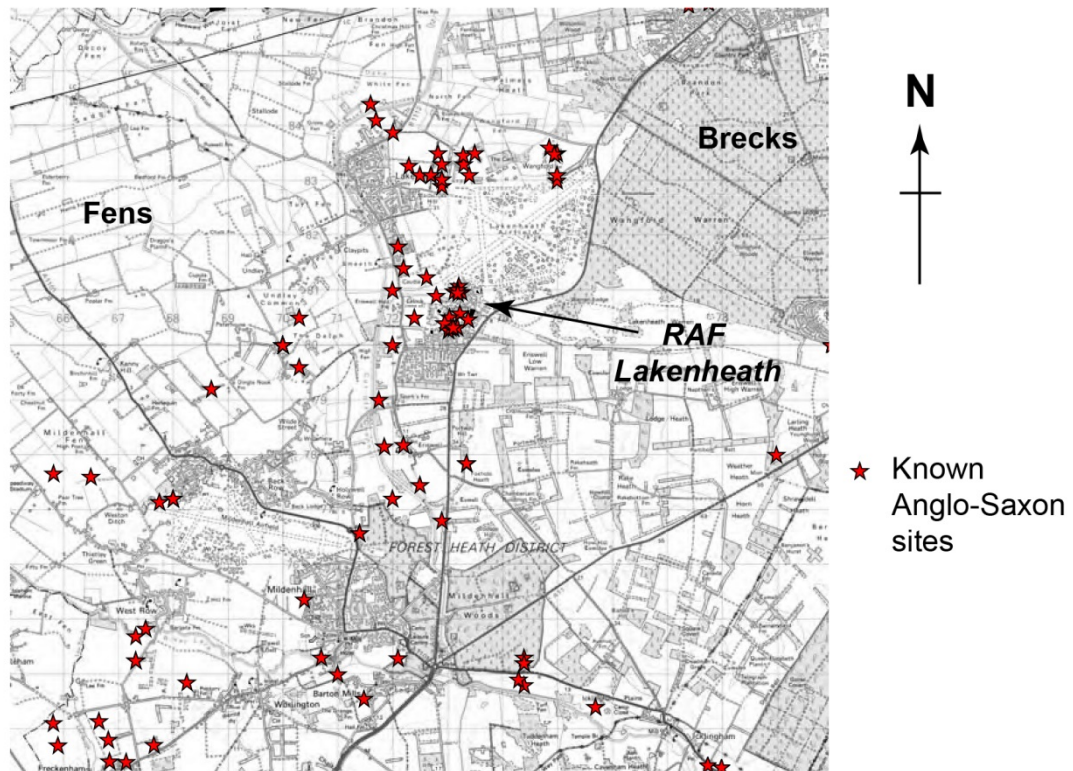


Figure 1-2: Showing known Anglo-Saxon sites near Eriswell. After Caruth and Anderson (2005, 3, Figure 3). OS map © Crown Copyright 2005. All rights reserved. (2005). Suffolk HER data © Suffolk County Council.

The post-Roman and Anglo-Saxon activity does not sit in isolation and there is extensive evidence for activity from prehistory onwards in the surrounding area. Many sites were first recorded by Grace Briscoe, the first excavator of Eriswell (see page 35). Of particular interest for this study are the nearby Romano-British settlements such as Roman Field (NGR TL 728 833, see Suffolk SHER No. LKH 029 and Briscoe 1953) and Caudle Head (NGR approx. TL 731 808, see Suffolk SHER No's. ERL 009, ERL 015, ERL 023, ERL 024, LKH 030, LKH 031 and LKH 032).

1.2.1 GEOLOGY

Both the Brecks and the Fens sit on chalk bedrock. The transitional border zone means the cemeteries are on the edge of different superficial geologies (Figure 1-3). The Brecks sit on a chalk plateau with occasional overlying superficial cover sands. The Fens are covered with superficial deposits of peats, alluvial deposits and river terrace gravels. The varied superficial geology leads to variable preservation states (Caruth and Anderson 2005, 8).

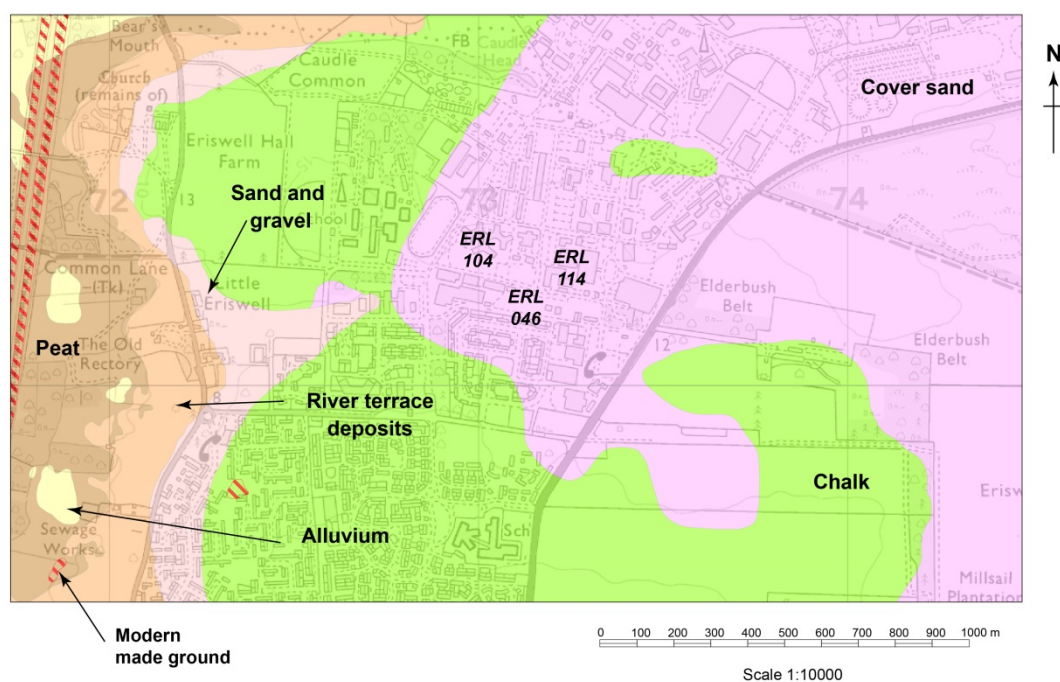


Figure 1-3: Geological map showing the approximate locations of the three cemeteries. Geological Map Data © NERC 2015. Underlying map © Crown Copyright (2015), Ordnance Survey (Digimap Licence).

1.3 SITE ARCHAEOLOGICAL OVERVIEW

This thesis does not start one and a half millennia ago with a founder burial, but summer 1947: one of the hottest in modern times. In that sweltering year a quiet fen edge corner was wrought to life. The atmosphere, normally soporific with Breckland dust and the scent of meadowsweet, was rendered new as a perfume of tarmacadam and diesel permeated the air: Lakenheath, a Royal Air Force (RAF) base mothballed in 1944, was being bought back to life (Law 2014, 12).¹

Increased cold war tensions had led to the reactivation of the airbase. Initially it was for use by the RAF, but new geopolitical realities meant new tenants and the next year the US Air Force (USAF) moved in. In the late 1950s the imminent arrival of the USAF 48th Fighter Wing required a major upgrading of facilities and construction began on housing, medical centres and assorted infrastructure (Law 2014, 14). During the course of these works an inhumation of an elderly individual (thought to be male) was discovered. Alongside the burial were a selection of grave goods (including a knife, pin, two annular brooches and a pair

¹ The airfield itself is recorded on the Suffolk Historic Environment Record under the SHER number LKH 339.

of tweezers) that suggested an Anglo-Saxon date (Wilson and Hurst 1958, 189). This burial (located at NGR: TL 7311 8029, see Figure 1-4) was augmented in 1959 with further discoveries made by workmen excavating a trench. With the agreement of the Ministry of Works and the USAF, excavations were undertaken on a limited area (Figure 1-5) and 33 graves were excavated (Briscoe and Le Bard 1960). The graves in this cemetery (also known as Little Eriswell or ERL 008) contained a variety of non-ferrous metal grave goods including cruciform brooches (five), small-long brooches (four) annular brooches (18), square-headed brooches (two), wrist clasps (12 individual hook and eye pieces), girdle hangers (five), silver rings (two) and hair fasteners (two). The assemblage suggested that the cemetery was a “*very typical East Anglian one*” (Hutchinson 1966, 16), although the quality of the workmanship apparently left something to be desired in the eyes of the excavators: “*...there are no outstanding brooches, indeed they give an impression of degeneracy and poor workmanship...*” (1966, 16).

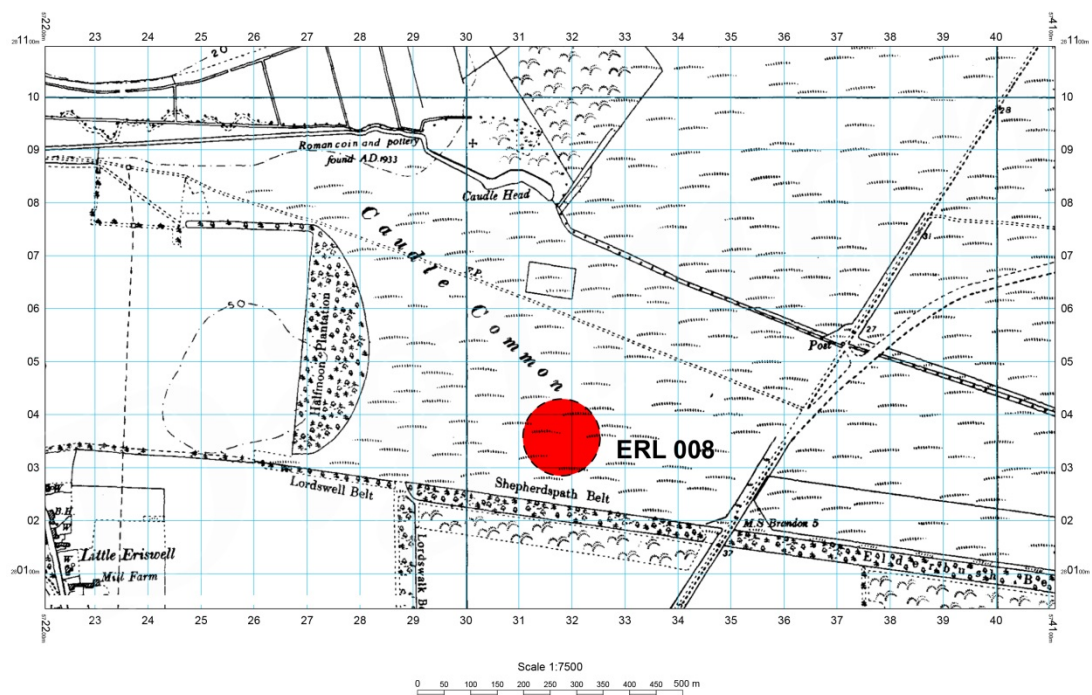


Figure 1-4: The 1958 National Grid 1:10560 map of Eriswell (tile TL78SW) with the approximate location of cemetery ERL 008 highlighted. Note that the airfield was not shown on OS maps until the 1960s. © Crown Copyright and Landmark Information Group Limited 2015. All rights reserved. (1958).

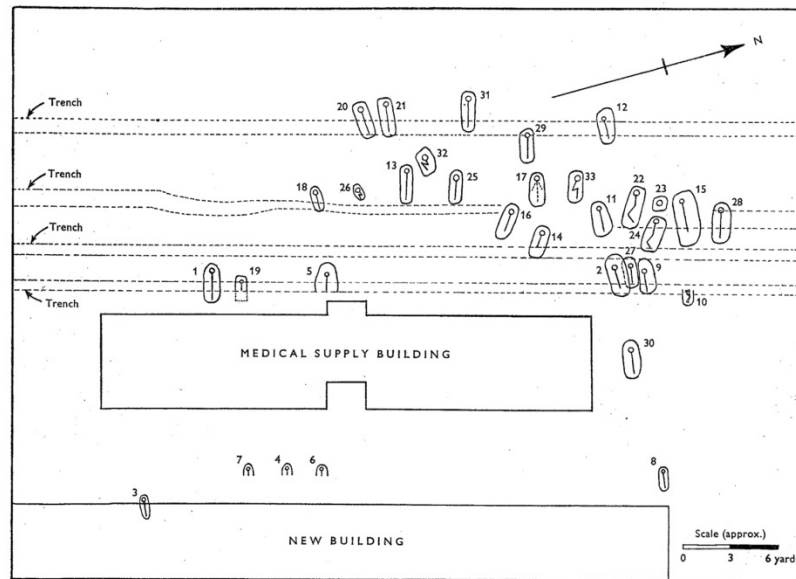


Figure 1-5: Hutchinson's plan of ERL 008 (1966, 4, Figure 2).

There was no further archaeological investigation at the site for several decades beyond occasional finds, the reporting of human remains and finds during the construction of a swimming pool in 1972/3 (Suffolk County Council Archaeological Service 2009; West 1998), and the recovery of grave goods from the spoil of a sewer pipe trench in 1980s (Martin, Plouviez, and Ross 1982, 160; West 1998).^{2,3}

In the 1990s it became apparent that much of the infrastructure, particularly housing and recreational facilities, were significantly outdated (many being post-war prefab construction) and that a program of development and renewal was required (Law 2014, 14). This led to a program of substantial archaeological investigations on several sites, three of which feature in this study (see Figure 1-6):

- ERL 046: an Anglo-Saxon cemetery with approximately 59 graves. Excavated during the summer of 1999 in advance of a new skills development centre.

² For spot finds from Eriswell see the Suffolk HER catchall SHER number "ERL Misc" at <https://heritage.suffolk.gov.uk>

³ No finds or remains appear to have been preserved from the swimming pool site and no report is readily available. The site is documented as ERL 058 on the Suffolk HER and is thought to be part of ERL 046.

- ERL 104: an Anglo-Saxon cemetery with approximately 261 graves. Excavated July – November 1997 in advance of a new dormitory development.
- ERL 114: an Anglo-Saxon cemetery with approximately 65 graves and is the same site as ERL 008. Excavated between March and June 2001 in advance of a new hospital annex and associated car-parking development. Material excavated in the 1950s as ERL 008 does not feature in this study.

These three cemeteries are believed to be the “*largest and best preserved Anglo-Saxon cemetery group available for analysis*” with 80% of all three cemetery areas excavated (Caruth and Anderson 2005, viii). Found with the burials was a host of grave goods including ceramics, glass beads (analysed by Peake 2013), preserved textiles, ironwork and non-ferrous metalwork.

There were approximately 800 non-ferrous objects recovered during the above phases of excavation and the analysis in this study focuses exclusively upon them. The non-ferrous artefacts were originally assessed by Catherine Mortimer in 2000 (Freestone and Mortimer 2005, 119).

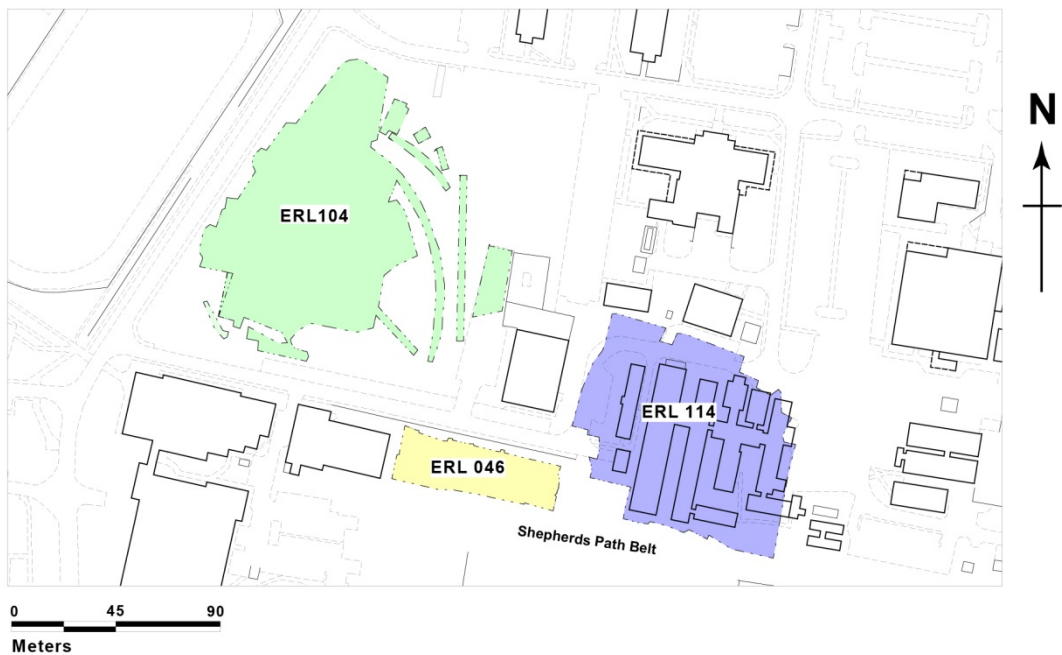


Figure 1-6: Location of the cemetery excavation areas. After Caruth and Anderson (2005, 1, Figure 1). OS map © Crown Copyright 2005. All rights reserved. (2005).

There are other post-Roman and early Anglo-Saxon sites that were excavated as part of RAF Lakenheath development, but these do not feature in this study. To the north of the cemeteries two settlement loci were investigated (Figure 1-7). The first is to the immediate north of the cemeteries (ERL 101), the second was noted in a number of excavations and watching briefs to the north-east of Caudle Head. Both were primarily identified by the presence of grubenhause (or sunken featured buildings).

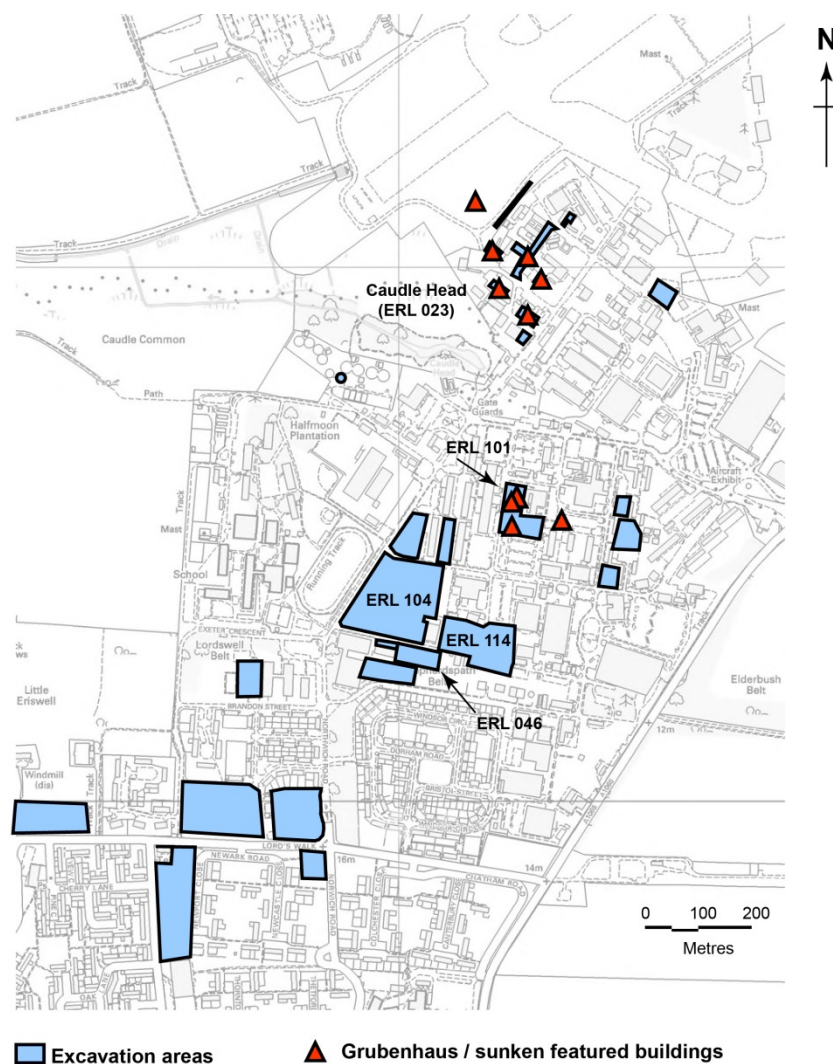


Figure 1-7. Showing the location of all excavation areas (cemeteries individually identified) and areas where grubenhause / sunken featured buildings (SFBs) have been identified, indicating early Anglo-Saxon occupation After Caruth and Anderson (2005, 4, Figure 4). OS map © Crown Copyright 2005. All rights reserved. (2005).

These settlement sites do not feature as part of this project. A brief summary of each of the three cemeteries now follows.

1.3.1 ERL 046

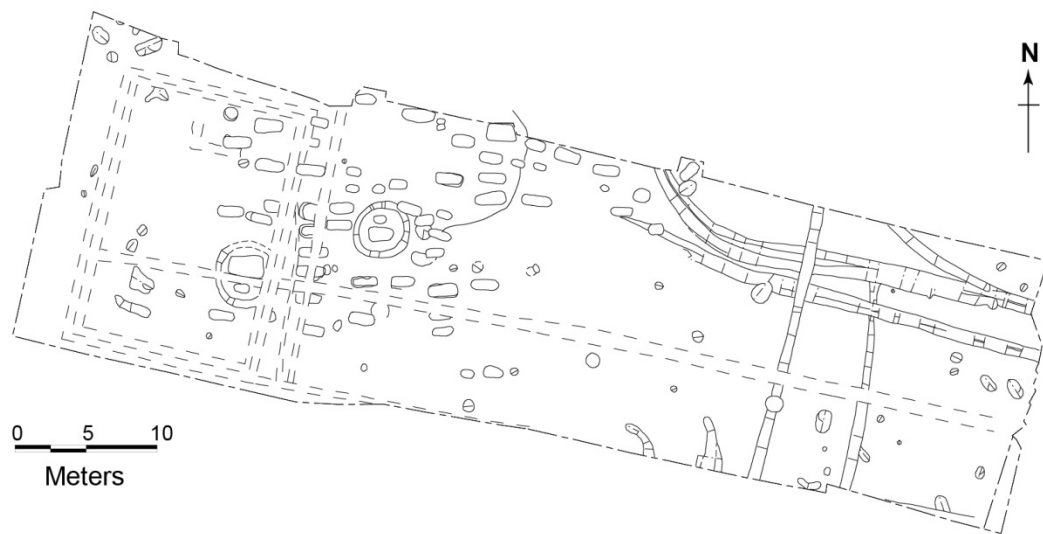


Figure 1-8: Plan of graves in ERL 046 (Caruth and Anderson 2005, 10, Figure 8).

ERL 046 is a small cemetery of 59 graves (Figure 1-8). It is not certain if the site is definitely a separate cemetery from ERL 114, but the excavators believe that the latter's focus around a Bronze Age mound suggest that they are indeed so (Caruth and Anderson 2005, 9).

Two pairs of burials appeared particularly significant, each pair (both being an adult male and child) being surrounded by a ring ditch. One of the adult male burials also contained a horse burial (Caruth and Anderson 2005, 10).

In contrast to the other two cemeteries the excavators noted that there was a distinct row like alignment to the burials. There is also a suggestion that wealthier burials were more tightly grouped than in ERL 104 (Caruth and Anderson 2005, 10).

1.3.2 ERL 104

ERL 104 (Figure 1-9) is the largest of the three cemeteries with 267 graves recorded. The site had previously been a baseball field, but a significant depth of windblown sand had protected the cemetery from disturbance during levelling work in the 1980s. The only significant truncation to any burials was caused by a sewer pipe trench constructed in the 1970s (Caruth and Anderson 2005, 7–8).

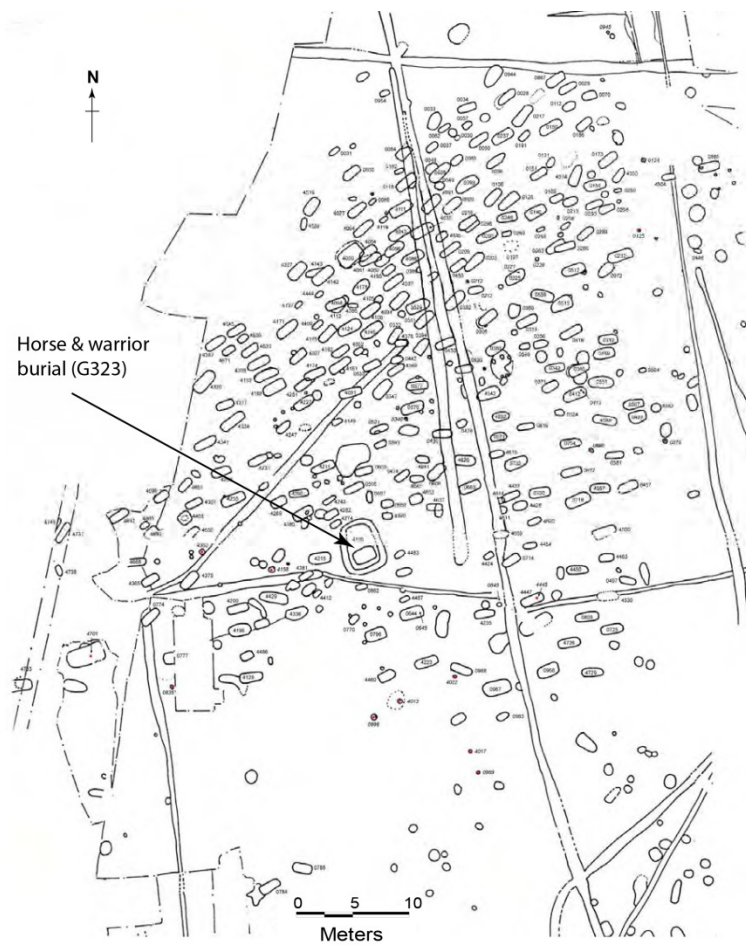


Figure 1-9: Plan of graves in ERL 10 (Caruth and Anderson 2005, 7, Figure 6).

The most unique burial in the cemetery was the horse and warrior inhumation (G323). This spectacular grave (Figure 1-10) — possibly familiar to readers from the BBC TV program ‘Meet The Ancestors’ (Richards 1999; Richards 2013) — contained a male horse of about 5 years age (O’Connor 2005, 86) buried alongside an adult male. The associated tack had numerous copper alloy, silver alloy and gilt fittings (analysed in this study).

There were a small number of cremations found in the cemetery (Caruth and Anderson 2005, 9). There were some non-ferrous objects associated with the cremations. These are often melted and amorphous (i.e. they were subject to the cremation process).



Figure 1-10: The horse and warrior burial in G323, ERL 104. Photo from Caruth and Anderson (2005, 8, Figure 7).

1.3.3 ERL 114

ERL 114 (Figure 1-11) is a continuation of ERL 008. There were 65 graves excavated. The burials excavated in the 1950s (i.e. ERL 008) are not featured in this study. In the centre of the cemetery was a circular area devoid of any post-Roman burials. In the centre of this circular area were two Bronze Age burials. It is thought that this represents a round barrow — presumably still extant in the post-Roman period — which has subsequently been removed. The barrow appears to have acted as a focus for the Anglo-Saxon cemetery (Caruth and Anderson 2005, 10–11).

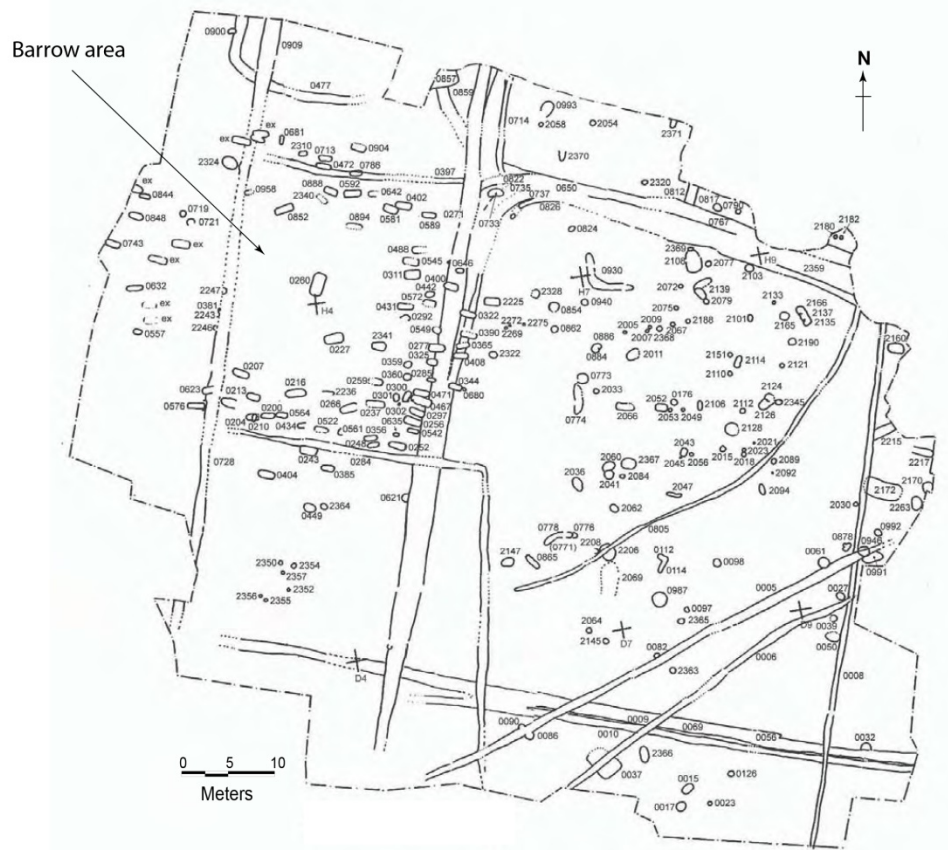


Figure 1-11: Plan of graves in ERL 114 (Caruth and Anderson 2005, 11, Figure 9).

1.4 DATES AND PHASING

The three cemeteries are believed to date from approximately 475 to 650 CE (Caruth and Anderson 2005, viii). The flatness of the C14 calibration curve for this period makes the production of accurate dates difficult (McCormac et al. 2004). Consequently radiocarbon dating, archaeology’s most patronized scientific dating technique, is difficult in this early post-Roman period (although refinements have been made, see McCormac et al. 2008). The recent Bayesian based chronological framework for Anglo-Saxon burials (Hines et al. 2013) has significantly improved our understanding and the potential for placing burials in a calendrical context. However, the paucity of relatively detailed studies of very early cemeteries (like those at Eriswell) meant that the study had to leave the earliest phases relatively un-fleshed out (pers. comm. Professor John Hines). Consequently, with no ready-made chronology available, there was a need to develop a detailed phasing for the Eriswell cemeteries. This was undertaken by Professor John Hines. His phasing is used in this study and a brief overview of it

is provided here. A full discussion on the phasing will be found in the forthcoming Eriswell publication.

The phasing was produced using the grave goods and it was sought to ensure that maximum compatibility with existing schemes was maintained. Graves were assigned to a chronological phase, using correspondence analysis, where they contained a requisite quantity of diagnostic grave goods. Because of the reliance on grave goods there was a need to produce separate gendered male and female (as opposed to osteo-archaeology defined) phasing series. As can be seen in Figure 1-12 there is relatively good comparability between the phasing boundaries between the two genders.

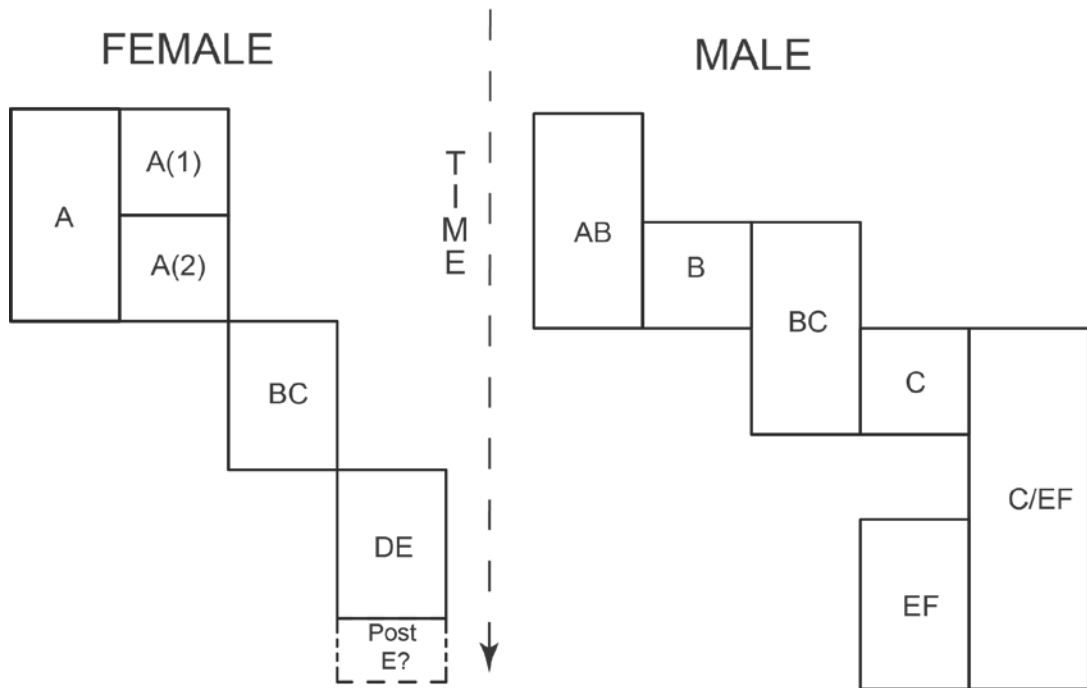


Figure 1-12: Schematic diagram of the phasing used in this study (courtesy of Professor John Hines).

Hines found that there were 97 female graves that could be phased. A majority of these (81 in total) contained a similar suite of goods as used by Penn and Brugmann (2007) in the phasing of early (i.e. A(1) and A(2) in Figure 1-12) female graves from other nearby cemeteries in East Anglia (pers. comm. Professor John Hines). The later graves were phased primarily based on the presence of polychrome beads in line with Hines et al. (2013). The male graves

are primarily phased on the basis of shield boss and spearhead typologies (pers. comm. Professor John Hines).

1.5 HOW OBJECTS ARE DEFINED

1.5.1 NUMBERING OBJECTS

The small find numbering for each of the three Eriswell cemeteries starts at the same point, i.e. some small find numbers are duplicated (or even tripled) across the three cemeteries. Consequently each object is always presented with its cemetery code either in the context of the sentence (if discussing many objects) or numerically is association with the small find number (e.g. ‘104-1487-A’).

Many of the Eriswell non-ferrous objects are composite; composed of different parts fabricated in different ways. A necklace can be composed of a copper alloy wire suspension hoop holding silver sheet spangles and a cast silver pendant. Likewise a silver wrist clasp will be composed of two separately fabricated hook and eye pieces.⁴ As part of the same object — excavated from the same context and, if not attached, then in close physical proximity to one another — these will be documented under one small find number.

From an analytical viewpoint it is obviously nonsensical to amalgamate and average all readings for a composite object under its small find number. This means that the count of objects provided here is different from that found in the small finds catalogue; e.g. brooch 1737 from cemetery ERL 046 is composed of the main (cast) body, a wire spring and a pin. Their recording as one number in the small finds catalogue is based on the physical proximity of the three components rather than any known chemical relationship between the individual components themselves (i.e. one or more could be a later additions or repairs). Therefore each of these components is counted separately, with each distinct area defined with a letter provided as a suffix after the small find number, i.e. ‘*site—small find number—analysis area*’ (or ‘046-1737-A’, ‘046-1737-B’ and ‘046-

⁴ It should be noted at this juncture that a recent metal detecting discovery in Suffolk suggests that wrist clasp eye and hook pieces may have been produced in the same mould and in the same casting operation. See Booth (2015) for further details (PAS no. SF-66EDD6).

1737-C’). Occasionally a small find number was sub-divided during post-excavation processing and conservation. In these cases the small find sub-division is provided after the small find number, i.e. ‘*site—small find number—small find sub-division—analysis area*’ or ‘114-2540-B-A’.

1.5.2 OBJECT CATEGORIES

In this thesis each object is categorised in a series of hierarchical variables with three different levels for object types. These different levels were assigned by the author based on the descriptions provided by Suffolk County Council Archaeology Service and Professor John Hines. Wrist clasps are described according to the typology set out in Hines (1993).

A summary of the object levels for the non-ferrous artefacts can be found in Table 1-1 below.

Object Category	Object Class	Object Sub Class
Coins, Tokens and Jettons	Coin	Undefined Coin
	Token	Undefined Token
Dress Accessories	Bead	Undefined Bead
	Bead	Undefined Buckle
	Belt Fitting	Belt ring
	Belt Fitting	Girdle-hanger
	Belt Fitting	Latch-lifter
	Belt Fitting	Strap-end
	Belt Fitting	Strap-mount
	Brooch	Annular
	Brooch	Applied disc
	Brooch	Applied saucer
	Brooch	Bar
	Brooch	Bird
	Brooch	Colchester
	Brooch	Cruciform
	Brooch	Fish
	Brooch	Great square-headed
	Brooch	Penannular
	Brooch	Radiate-head
	Brooch	Roman
	Brooch	Small-Long
Brooch	Square/cross	
Brooch	Undefined Brooch	
Buckle	Buckle Pin	

Object Category	Object Class	Object Sub Class
	Buckle	Buckle Plate
	Buckle	Undefined Buckle
	Miscellaneous	Chain
	Necklace	Necklace Ring
	Necklace	Pendant
	Pin	Undefined Pin
	Ring	Bracelet
	Ring	Ear Ring
	Ring	Finger ring
	Wrist Clasp	Form A
	Wrist Clasp	Form B
	Wrist Clasp	Form B 12
	Wrist Clasp	Form B 13 a
	Wrist Clasp	Form B 13 c
	Wrist Clasp	Form B 17 a
	Wrist Clasp	Form B 18
	Wrist Clasp	Form B 20
	Wrist Clasp	Form B 7
	Wrist Clasp	Form C 1
	Wrist Clasp	Undefined Wrist Clasp
Equestrian objects	Tack	Bit
	Tack	Bridle Fitting
	Tack	Bridle mount
	Tack	Mount Strip
	Tack	Strap-mount
	Tack	Undefined Equestrian
	Bucket	Bucket
Military and weaponry	Shield	Misc. Shield Fragment
	Shield	Shield Mount
	Spear	Spear Ring
Miscellaneous Fittings	Belt Fitting	Strap-end
	Buckle	Buckle Plate
	Fragment	Bracket
	Fragment	Sheet
	Fragment	Strip
	Fragment	Wire
	Miscellaneous	Binding Ring
	Miscellaneous	Box Fitting
	Miscellaneous	Clip
	Miscellaneous	Ring
	Miscellaneous	Rove
	Miscellaneous	Sheet
	Nails and Bolts	Rivet
	Nails and Bolts	Stud
Personal equipment	Implement	Awl

Object Category	Object Class	Object Sub Class
	Purse	Purse Fitting
Toilet and surgical objects	Cosmetic Implements	Brush fittings
	Cosmetic Implements	Tweezers
	Cosmetic Implements	Undefined Cosmetic Implement
Unknown	Unknown	Unknown

Table 1-1: Object categories, classes and sub classes used in this thesis.

CHAPTER 2: BEGINNINGS

“The iniquity of oblivion blindly scatters her poppyseed and when wretchedness falls upon us one summer’s day like snow, all we wish for is to be forgotten”

(Sebald 2002, 24)

This chapter seeks to explore some of the broader background milieu in which the study takes. It is organised in three sections. The first takes a general look at the theoretical and historical development of early medieval studies and the context within which previous non-ferrous metallurgical studies took place. The second section discusses the metallurgical background (page 63). The third section combines the lessons from the previous two sections to develop and focus the research priorities for this study (page 80).

2.1 A THEORETICAL BACKGROUND TO ANGLO-SAXON NON-FERROUS METALWORK STUDIES

In the very early history of medieval archaeology (best summarised in Gerrard 2003, 5–29 and Hines 2013b) little interest was shown in the monuments, sites and finds of the post Romano-British period; Anglo-Saxons were the preserve of historians. This began to change in the mid-19th century with the work of antiquarians — such as Charles Roach Smith (Roach Smith 1848; Roach Smith 1871), John Yonge Akerman (Akerman 1855; Akerman 1853a; Akerman 1853b; Akerman 1857; Akerman 1863), and John Mitchell Kemble (Kemble 1863) — whose studies of pre-Christian Anglo-Saxons were pivotal in popularising the study period. ⁵ As the 19th Century wore on the importance of Medieval archaeology was increasingly recognised and sites were subject to the latest scientific excavation techniques (see Pitt-Rivers 1883). The early medieval, however, was left behind, with objects, particularly non-ferrous dress accessories,

⁵ Akerman (1806–1873) was a numismatist who published widely on the Anglo-Saxons including a populist book on the subject, the *Remains of Pagan Saxondom* (1855) which did much to illuminate the importance of the period to the public (and the growing number of amateur archaeological societies, see Levine, 2003). Akerman did not limit his interest to archaeology, collecting many ethnographic objects, some of which ended up in the possession of Arthur John Evans before being donated to museums (see the Melanesian sling shot in the Pitt Rivers Museum — accession number 1928.68.10 — for example)

viewed as more art than artefact (although it should be remembered that this focus was not purely for aesthetic reasons but driven by a desire to understand the chronology of the period through stylistic changes).⁶

As the Victorian era faded a new generation began to study early medieval archaeology, and, by the early to mid-twentieth Century, were publishing studies that focussed less on art, more on “*the everyday rubbish*” (Standley, Hicks, and Forward 2013).⁷ These studies (see Ward Perkins 1937; Jope 1947; V. Evison, Hodges, and Hurst 1974; Myres 1969; Myres 1977) for ceramic focussed studies; Leeds, 1913 and 1945 for landscape/distribution articles and Leeds 1949 for investigation of non-ferrous brooches), marking a significant advance from studies of prestige, were heavily typological. In itself not an issue (we need typologies so *we* can understand the data), the studies often had a heavy art historical approach. Leeds’ study of great square-headed brooches falls into this category, with little study of the technology behind the object (somewhat surprising given his love of post-medieval technologies).⁸ This is not unexpected, for, whilst metallurgists and some archaeologists had begun to start showing an interest in the past of their science (i.e. Gowland 1912; Wang 1919), most archaeologists were slow to appreciate the story hidden within the crystal structure of a metallic artefact. This is understandable, for archaeologists at the time were working within a philosophical framework that equated people with objects; if a whole object can tell you about a person or community, then why look deeper into its constituent parts?

⁶ It could be argued that Pitt-Rivers’ excavation at Caesars Camp was something of a false start for later Medieval Archaeology, the methodological lessons the General imparted not being picked up by those studying the period for several decades.

⁷ It can, with some plausibility, be argued that the Victorian period did not end until as late as the 1930s; many scholars who had their formative training in the 19th century continuing to work until their deaths in the early to mid-20th Century.

⁸ Leeds, although best remembered today as an early medievalist, was as interested in post-medieval artefacts and their production. He studied post medieval wine bottles and taverns (Leeds 1914 and 1941) and examined construction works in Oxford, collecting objects he found interesting (including 39 post medieval pins and pieces of wire used for pin production, now in the Pitt Rivers Museum: 1910.15.1 .1–4, 1910.15.2 .1–30, 1910.15.3 .1–5, see Nicholas & Hicks, 2013 for details). For a detailed website (including full bibliography) dedicated Leeds’ life, see http://www.ashmolean.org/ash/amps/leeds/archive/leeds_life.html

This did not begin to change until 1946 with the formation of the Royal Anthropological Institute's (RAI) Ancient Mining and Metallurgy Committee (AMMC).⁹ This group sought to:

“...collate the researches done by scientists in various departments such as pure Metallurgy, Geology, and field archaeology, and also promote co-operation with scholars in other countries. The Committee hopes to arrange for the scientific examination of metal objects with a view to determining their constituents and technique of manufacture”, and urged “Field archaeologists...to collaborate by supplying specimens of metal, especially copper”

(Anonymous 1946, 99)

The group initially had a distinctly prehistoric flavour; this did not, however, stop the committee from investigating early medieval objects (for example see Collins & Beeny, 1950). The broad impact of the AMMC was considerable, and, as it fell into inaction during the late 1960s (perhaps symptomatic of the growing professional divide between archaeology and anthropology that reached its peak in Clarke’s pronouncement “archaeology, is archaeology, is archaeology”, 1968, p. 13), the Historical Metallurgy Society was formed to replace it and meet the growing need for archaeometallurgical interventions presented by the increased volume of rescue archaeology being undertaken. The improved profile both groups brought to archaeometallurgy, powered by individuals such as Herbert Henry Coghlan (1896-1981), Leo Biek (1922-2002) and Ronald F. Tylecote (1916 - 1990), had little impact on Anglo-Saxon studies. In 1976 Tylecote could muster no more than a paragraph on early medieval copper alloys, stating “*We know very little of the immediate post-Roman period of non-ferrous metallurgy*” (1976, 69).

Parallel to this, stylistic studies of Anglo-Saxon non-ferrous metalwork were gathering pace. Few, however, contained scientific investigations (metallographic or compositional) of the objects (for examples see Evison, 1968, 1977, 1978). This began to change in the late 1970s and early 1980s, as the increased availability and lower cost of less destructive analytical equipment opened up the

⁹ For a brief history of the RAI Ancient Mining and Metallurgy Committee see <http://www.therai.org.uk/archives-and-manuscripts/archive-contents/ancient-mining-and-metallurgy-committee-a89/>

potential to study a much broader range objects and assemblages (Bayley and Watson 2009, 363–364). This was matched with a concerted attempt by archaeological scientists to make archaeologists aware of the range of techniques available and their applicability to archaeological materials (Phillips 1985). Many of those undertaking analysis were heavily influenced by the approach of Peter Northover in the 1970s and early 1980 to the study of Bronze Age material (see for example Northover 1977).

The impact of processualist methodologies – although slow to reach Anglo-Saxon archaeology – made a significant impact. Studies, such as that by David Leigh (1980) took a systematic approach that incorporated not just typologies, but all aspects of production. This approach snowballed, and the results can now be seen in a host of works focussing on Cruciform brooches (Mortimer 1990), great square-headed brooches (Hines 1997), Quoit brooches (Suzuki 2000) and Button brooches (Suzuki 2007) and These works, and others like them, provided in-depth typologies tied in with chronologies, technologies and social impacts of specific object classes. These studies were all focussed on specific categories of highly decorative non-ferrous metalwork. Consequently there may as a result have been something of a distortion in our understanding of non-ferrous metal usage.

2.1.1 ‘THE OVERCROWDED NATURE OF THINGS’

(Wire 2011)

No neutral “scratch line” exists from which to jump to a self-sustaining tradition-free intellectual system. All the cultural situations from which we pursue our practical and intellectual inquiries are historically conditioned.

(Toulmin 1992, 179)

One of the greatest legacies of post-modernist thought was an awareness that there is no absolute truth in humanity; a subject expounded on in detail by the late, great, Stephen Toulmin in his seminal *Cosmopolis* (1992). Focussing specifically on the Enlightenment legacy, Toulmin recounts, as an example, how

Descartes viewed Euclidean geometry as a distinct idea that was equally available to all cultures and epochs (Toulmin 1992, 177). Western thought only began to challenge these assumptions in the mid twentieth century when scholars such as Whorf (1956) with studies on the Hopi Native Americans (“*Are our own concepts of 'time,' 'space,' and 'matter' given in substantially the same form by experience to all men, or are they in part by the structure of particular languages?*” p. 200-1) and White (1947) with anthropologies of mathematics (“*The square root of minus one is real....The question at issue, however, is not, Are these things real?, but Where is the locus of their reality?...Nothing is more real than an hallucination*” p. 290-1) began to question this Enlightenment inheritance.

The questioning threaded and quickened its way through scholarly studies of many disciplines. There was a growing realisation that the enlightenment had not marked a year zero. As Toulmin put it (1992, p. 179):

*The idea that handling problems rationally means taking a totally fresh start had been a mistake all along. All we can be called upon to do is to take a start **from where we are at the time we are there...**There is no way of cutting ourselves free of our conceptual inheritance: all we are required to do is use our experience critically and discriminantly, **refining and improving** our inherited ideas...¹⁰*

The world of letters and science had not been wrought anew in the 18th Century, it was a refinement built atop what had been, as was post modernism itself. Sadly, the latter half of the message was lost as the new ways threaded their way through the humanities; by the time they reached archaeology being critical, more often than not, became more important than ‘discriminantly’, ‘refining’ and ‘improving’.

The times were a-changin’ and, as Alcock produced a mournful preface to the 2nd edition of Arthur’s Britain (1989, p. xvii), Flannery’s iconic old timer (1982) hoiked his hat, holstered his trowel, cracked open a beer and wandered into the

¹⁰ A surprisingly positivist statement.

sunset.¹¹ Archaeology was left a world in which, as summarised by Trigger (2006, p. 468), “*any individuals or groups had the right to use archaeological data to create the pasts they wanted... [a position] hailed by its supporters as democratizing archaeology and purging it...of elitist pretensions*”. Post-processualism was more punk than post-modern; an attitude perfectly at home in the newly dominant neoliberal political paradigm of the 1980s that replaced post war embedded liberalism (Harvey 2007, 11).¹²

2.1.2 ARCHAEOLOGICAL CUL-DE-SACS

The transition from processualist to post-processualist world left archaeological science in something of a cul-de-sac; practitioners were often viewed as uninterpretive operators whose position was to present data to archaeological synthesisers/theorists. The problem, as noted by Wylie (1992, pp. 27–28), was that synthesisers would often subjugate data to predetermined theories, failing to investigate how data had become theory-laden.

The theory-laden nature of data was recognised by scientists in the late 19th Century (see Worthington, 1895, pp. 64–66, 75; described in detail by Daston & Galison, 2010, pp. 11–16) who realised that the scientific observer’s perceptual experience of an experiment was a critical component of how theories and ideas were constructed, i.e. “*things don't look the same to observers with different conceptual resources*” (Bogen, 2010; see also Kuhn, 1962). This realisation is incorporated within the laws of qualitative structure under which science operates; laws which state that “*all sciences characterize the essential nature of the systems they study. These characterizations are invariably qualitative in nature, for they set the terms within which more detailed knowledge can be developed*” (Pylyshyn and Bannon 1989, 111).¹³ The archaeological theorists of the 1980s and 90s tended to ignore this nuanced conceptual inheritance from the Modern era, instead focussing on constructing

¹¹ With apologies to Bob Dylan.

¹² This is not meant to denigrate true punks, but rather those who believed Punk to be about chord sequences and the right haircut before settling into a middle age life as buy-to-let landlords and Lib Dem voters.

¹³ A concept developed by Newell and Simon (1976).

grand critical theories which saw data through a cloud of theory (see Johnson, 2007, p. 102). In ignoring that the framework archaeological scientists were working in already accounted for theory-laden data, it became possible to marginalise the scientists and their data as too simplistic to be involved in the creation of new archaeological ideas. The net result was that archaeometric data became marginalised; reduced to fiche or archive, rarely fully integrated into reports. In its place was obfuscation, as post-processualists adopted the appearance of scientific presentation (even as they were ignoring science itself) to dress up personal viewpoints as facts that had precedence in data (see Bintliff's [2011, p. 16] deconstruction of Kristiansen's [2004, fig. 2] graph of cultural evolution). An issue not solely limited to archaeology, it has been criticised in recent years:

“It's plausible that philosophers...could do better by examining and developing techniques and results from logic, probability theory, statistics, machine learning, and computer modelling, etc. than by trying to construct highly general theories of observation and its role in science” (Bogen 2010)

In post-Roman and early-medieval archaeologies post-processualism was slow to take off (when compared with prehistoric archaeology). A greater focus on landscape context brought focus to the issue (Hinton 1987, 2) and studies that understood materiality through ‘textual’ interpretations began to appear (Halsall 1995, 4), ethnographic approaches made a return (Hines 2003) and finds were investigated in more complex and ways (Williams 2004). Having said this it should be noted that, as Gilchrist states (2009, 388), engagement with theory tended to be selective and explicit theoretical approaches to early-medieval archaeology rare. In material studies much of the theoretical advancement was in the area of ceramic studies and, starting with Pader’s study of mortuary remains (1982) and Richards’ study of cremation urns (1987), data and the subjective began to be married (in the words of Karkov 1999, 16).

2.1.3 INDIVIDUALISM

The individualistic theology of much post-processualist thought led to a sidelining of analytical data. Deigned ‘methodological individualism’ (Dobres and Robb 2000, 11), it is an affliction which particularly affected agency-based interpretations (Souvatzi 2008, 38–39). In some sense methodological individualism was an issue of scale, reflecting archaeologists’ choosing to follow the thin thread of an individual (object or person) vertically through the temporal plane, rather than attempting to examine a greater ‘horizontal’ spread of how individuals completed the pattern of the social collective (Whittle 2003, 12; Derevenski 2000). It can also be seen to represent a deep-rooted conceptual problem; the post-processual fetishizing of the individual. Representative of the 1980s neoliberal fire in which the theoretical framework was forged, it required archaeologists to abstract themselves from “*all those particularities of social relationship in terms of which we have been accustomed to understand our responsibilities and interests [to] arrive at a genuinely neutral, impartial, and, in this way, universal point of view*” (MacIntyre 1988, 3). The problem is, of course, how one can arrive at a genuinely neutral, impartial, universal point of view whilst, at the same time, believing in a post-modernity which insists there is no such thing as a genuinely neutral, impartial, universal point of view.

Echoing the Latourian approach to scientific data (Latour and Woolgar 1979) the 80s generation of archaeologists were rejecting the specialist; objects were ideological (Parker-Pearson 1984, 61), data produced from them were subjective and existed to be subjugated to theory.

The methodological individualism had a peculiar effect in the study of non-ferrous Anglo-Saxon dress accessories. Whilst broader theoretical developments meant that there was a renewed and re-invigorated attempt to distil the relevance of any similarities and / or differences between objects (i.e. brooches) and understand the social implications of an object’s materiality there was also a simultaneous narrowing of focus. A dominating research objective became to discover workshop or artisan groups or to see if objects could be matched as pairs. A not unworthy objective, this was been hampered by the lack of rigorous conceptual frameworks of what a workshop actually *is* in this period. Identified

by Brooks (1994, 166) as a significant issue, this is an area that has still not been fully tackled, and has often resulted in reducing scientific data interpretation to a predominantly functionalist approach. There has also been a renewed focus on the publication of individual pieces of non-ferrous metalwork; an odd brooch from here or a unique wrist clasp from there (perhaps a response to the wealth of discoveries produced by the Portable Antiquities Scheme).¹⁴ Whilst oddity, aberration and uniqueness have their place — and indeed are themes that have seen a certain level of resurgence in recent critiques of post-modern materiality studies (Olsen 2003, 93; Daston and Galison 2010, 63) — there are issues, perhaps best expressed by Ralph Marett who deplored the study of aberrations at the expense of ‘normal’ culture:

...we go about collecting odd bits of contemporary culture which seem to us to be more or less out of place in a so-called civilized world. (Marett 1914, 21)

Aberration is a cultural spatial variable itself influenced by vectors of discovery and recognition. Geographical scale versus aberration functions not only at regional magnitudes, but also microscopic and elemental levels. An object may appear unique in form, but the material utilised, the technological choices made etc. may be ‘common’ or ‘banal’.

This is not to say that aberration does not exist, merely that one should be aware that, as a construct, it does not apply at all scales equally.¹⁵ Consequently it is not a contradiction to say that an object is both an aberration and common at the same time, merely that we should be aware and ensure our research is reflexive and adaptable to this factor: outliers and interesting different individuals should not outbalance the study of the broader community.

To counter such a fate, interpretation should be reflexive and adaptive. It is still sought to consider the potential for shared origins, however this should not

¹⁴ Also possibly a response to the modern ‘publish or perish’ culture. One academic mentioned to me they called these papers the ‘shitty-quickie’; rare objects and examples are quick to write articles about and their oddity makes publication relatively straight forward, easily bulking out a publication record.

¹⁵ There is a flaw here in that I have ignored any Deetz (1968) style social scale.

subsume investigation of how non-ferrous object materiality affected the social function these objects played in early medieval society (*à la* Jones 2004, 355). Such approaches have shown considerable benefits; producing richer, more pluralistic, interpretations (for an example with particular reference to early medieval non-ferrous metal work see Inker 2000).

2.1.4 YEAR ZERO

At the start of a new millennium, as the dust from 9/11 settled and the levees of Mississippi groaned, an anguished Bruno Latour cried out “*was I wrong to participate in the invention of this field known as science studies?*” (2004, 227). Latour’s remorse was in response to a world where, when every narrative is equal, deniers of global warming, jihadists and anti-Islamists had equality of voice with the climate specialist, the moderate and the peaceful.

Within archaeology similar concerns were being voiced over the nature of science, theory-laden data and critical theoretical practice.¹⁶ Whilst some took a practical approach to tackling these issues, designing projects that incorporated specialists at the very core (such as the Old Scatness project, Dockrill et al. 2010), a greater number took a specifically theoretical approach. Gosden (2005), aware of the dangers of sacrificing the macro for the micro, strove to avoid the narrowing of focus that is inherent in the individualistic nature of post-processualism. Musing on agency and objects and focusing on the Romanisation of Britain, Gosden sought to create a narrative that, whilst focussing on the idea of agency within objects themselves, covered a whole land of communities. Elsewhere, Boivin (2004) and Jones (2002; 2004), engaged with theory from a scientific perspective, seeking to argue for a materials-based framework which, whilst accepting that textually based analysis (i.e. Tilley, 1990) is now a component of our understanding, placed the “*material qualities of material culture as central*” (Jones 2004, 331). This approach has some similarities with the Surface Reading approach developed by critical theorists and linguists (Best and Marcus

¹⁶ These concerns had been voiced in the wider sciences nearly ten years earlier, see Sokal (1996).

2009).¹⁷ These papers marked a significant advance from earlier interventions by scientists which, whilst identifying weaknesses in the post-processual approach, were themselves weak in finding/proposing rapprochement (i.e. O'Connor, 1991).

Jones' article stimulated considerable, predominantly supportive, debate in the subsequent issue of *Archaeometry* (Bray and Pollard 2005; Gosden 2005a; Killick 2005; Mithen 2005; Taylor 2005; Thomas 2005). Particularly noteworthy was Taylor's criticism, not for the nature of the piece, but for the narrow view taken of post-modernism (Taylor 2005, 196). Indeed, this is a criticism that can also be laid at the feet of the most vocal post-processual archaeologists, who themselves acted as if their theories presented something of a year zero (Bintliff 1991, 274): a direct contradiction of Toulmin's belief that post-modernism should refine and improve our inherited ideas.

Archaeology has moved on from the battles of 20-30 years ago; one need only compare TAG 1990 (see Bintliff, 1991) with TAG 2010 to see the considerable increase in people debating *things* and *data* rather than theory alone.¹⁸ The post-modern epoch is not over; however, the neoliberal settlement — which infused economics, politics and thought since the end of embedded liberalism in Britain — *is* possibly at an end. We must not at this juncture throw out the very real benefits post-modernism has provided us with. By enabling us to understand that there is no pre-ordained truth or rationality, it enables us to get closer to people who once were. We should continue to recognise the duality of the nature of our existence and the resulting tension that is created, or, as Searle (1995, Introduction, no page number) put it:

We live in exactly one world, not two or three or seventeen. As far as we currently know, the most fundamental features of that world are as described by physics, chemistry and other natural sciences....[but] How does a mental reality, a world of consciousness, intentionality, and other mental phenomena, fit into a world consisting entirely of physical particles in fields of force?

¹⁷ Surface reading takes an empirical approach to studying texts, recognising that there is a truth to 'which a text bears witness' and that not all meaning is hidden (Best and Marcus 2009, 1).

¹⁸ See the Bristol TAG program at <http://www.bristol.ac.uk/archanth/tag/index.html>

We live in a world bound by chemical bonds and physical forces, yet the patterns we perceive and the rationalities we deduce are our own; or, to reverse engineer George Orwell (1975, 69), each mind is another world.¹⁹ These worlds, the one and the many, are not contradictory. So, whilst “*there are facts, and they do matter*” (Sokal 1996, 63), the locus of reality and rationality we construct from them is not fixed; an outlook entirely cognisant with the qualitative laws of structure (Pylyshyn and Bannon 1989, 111–112).²⁰ This is not to suggest that we should ignore physical realities and try to bind copper and zinc ions with cognition rather than electrochemical bonds (to paraphrase Olsen, 2003, p. 88), but we must continue to recognise that, in deciding to interpret something, we have already formed an idea of what it is and chosen its most important facets (see Taylor, 2005, p. 197 summarising Wylie, 1989). It is consequently no contradiction to say there are facts and that we can be objective about them, but that we must be aware that *our* objectivity is constructed from *our* rationality (based on *our* normative culture) and therefore we cannot guarantee that we are correct or that others perceive as us.

2.1.5 WE'RE ALL COMMUNITARIANS NOW²¹

The economic events of the 1970s undermined the embedded liberalism that had governed much of the Western world since 1945 (Helleiner 1996, 15–16). Likewise there is a suggestion that economic events since 2007/8 are challenging the neoliberal model (Etzioni 2009; Etzioni 2011a). The outcome of what happens next is uncertain; it is likely only hindsight and history can offer an answer. There are, however, trends that one can identify that indicate a general shift in thought; perhaps the most significant of these being the re-emergence of community (be it communitarianism or the recent mainstream re-emergence of nationalist ideologies and politics) as central to any paradigm alteration. The

¹⁹ Referring to George Orwell's observations in *A Hanging* (originally published in the *Adelphi*, August 1931) “one of us would be gone--one mind less, one world less”.

²⁰The way in which sciences will characterise the systems they study by creating a set of qualitative laws to act as a framework within which further knowledge can be developed. First proposed by Newell and Simon (1976).

²¹ With apologies to Milton Friedman and Richard Nixon (“*We're all Keynesians now*”).

increasing communitarian aspect offers an opportunity to develop the post-modernist archaeologies of recent decades and escape the methodological individualism. We must realise that an individual's personal preferences and deliberations are not wholly autonomous, but “*reflective of and affected by communal processes*” (Etzioni 2011b, 108); crucially important when recent research has argued that community-forming traits as generosity to be evolutionary predetermined (Delton et al. 2011). A direct challenge to the individualism of neoliberalism (archaeologically expressed in the methodological individualism of the 1980s & 90s), it is perhaps evident in archaeology from archaeologists' response to the age of austerity (i.e. the Southport Group, 2011) and the greater awareness of the importance of community archaeology projects. This can be crudely measured in an academic archaeological context using article databases and keywords (echoing the methodology of Marriner, 2009). The results show an increasing usage of community in archaeological publications with a rapid uptake apparently emerging after 2007 (see Figure 2-1).

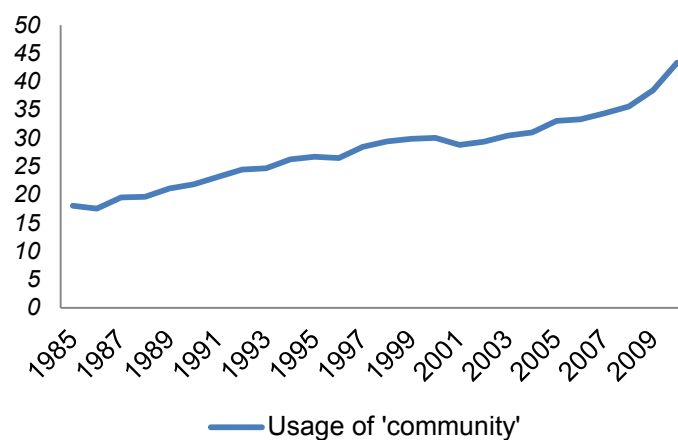


Figure 2-1: Academic publications containing 'community' and 'Archaeology' measured as a percentage of the yearly total number of publications containing 'archaeology'. It is notable that, despite the considerable decrease in the number of publications containing archaeology since 2006 (27900 down to 22000 in 2010), the use of community is still increasing. Data from Google Scholar (excludes patents and legal opinions).

In post-Roman and early medieval studies the emergence of new ways of thinking is most visible in James Gerrard's recent book (2013). Here he critiques existing perceptions for basing themselves in a framework where the decline of Rome is to be mourned for the loss of financial complexity and international trade. Consequently the post-Roman period is viewed predominantly as a

stopgap; a brief uncivilised interlude (civilisation being intrinsically linked to the existence of currency) on our way to develop fiat monies and capitalism (2013, 76). Instead Gerrard argues that we should see it as a period where personal power, local relationships and local structures came to the fore when there was no need to sublimate them to an imperial state (2013, 274–276).

This is also relevant in this study because it acts as a useful reminder of the importance of communal practices and values when interpreting the composition of the objects. It is all too easy when (metaphorically) drilling down to the elemental level to focus on individual actors and agents and forget that the metallurgical practice and the associated choices made by an individual craftsman are very much undertaken within a framework of their societies shared cultural and social values.

We will now move on to discuss the metallurgical context for this study before returning to some of these theoretical concepts when developing the research objectives for the study (from page 80 onwards).

2.2 THE CHEMICAL CANVAS

The worlds that humans construct are composed of patterns. These patterns — learned, taught, developed — form “*the opposite of a chaos...an entity which could be named*” (Watanabe 1985, 2). Out of the bedlam, these building blocks of organisation coalesce, forming the bounds of cognitive rationality (Ohlsohn 1990, 501) (it need not be a rationality we understand from our own mind-set).

Artefacts are composed of patterns. Some are visually discernible: volume, mass, shape/dimensions, materials, colours, textures. From these attributes we identify patterns that construct our perception of objects (patterns being an intrinsic component of knowledge, Pawlak, 1991, p. 2); as photons reflected from the play of light across an Anglo-Saxon brooch hit our visual cortex, we marvel and imagine that we too are perceiving as another once did. Although a valid emotional response, it is highly subjective. For whilst we may view photons and the visual element of the electromagnetic spectrum as facts or constants, the perception (the patterns we construct) from them are subjective; a point forcefully driven home by Baker (2013) in her discussion on the interpretation of non-ferrous object colour in the Anglo-Saxon period.

The presence of a non-ferrous object is in part defined by the chemical composition which, at the atomic level, is one of the key determinants of the potential of the material to be worked. Metal gives designs form, it gives flight to variations in artistic composition, it also fetters. The melting point, mechanical properties (tenacity, hardness) and colour are constrained by chemistry which places micro- and macroscopic crystalline limits on our visual world. All are factors affected by the delicate interplay of metallic and metalloid elements: for example pure copper has a melting point of 1084.62°C, the addition of lead lowers this yet also alters the physical properties of the metal produced; it is a new alloy.

The different metals used to produce an object are at the core of our understanding of artefacts. Whilst visually identifiable similarities in form, material and style may suggest a relationship between the two objects, what this

relationship may mean (real or imagined? skin deep or with chemical integrity?) can only be answered by understanding the composition. To this end, a brief summary of non-ferrous metal sources and usages in the early medieval period is provided here.

The increasing quantity of sites excavated in a rescue and (post-PPG16) commercial context, combined with an increased recognition of the importance of prompt post-excavation analysis and publication, has significantly increased the quantity of early medieval metallurgical material analysed. Luckily for us there is a heavy bias towards material from the south-east of England (predominantly the result of the amount of development in this region); although there are notable exceptions (York for example, see Bayley 1992).

Before continuing, it is worth considering what to call the alloys used. Long an issue of contention for archaeologists (Rickard 1932), alloys are, culturally, infinitely divisible; the smallest variations can be named differently.²² What is more, there is no guarantee that the names we assign based on chemical composition were part of the rationality that composed the worlds of those who made and used the objects (Mortimer 1990, 354), as can be seen in the changing textual usage of copper and brass in the medieval period (Rickard 1932, 284).

Variability over time is also an issue and, in choosing our terms, we have to be aware that the more detailed chemical typology we produce the less comparability with later and earlier periods there will be (Mortimer 1990, 347). The decision on what to call the alloys here is not a simple one. The statistical approach used in this study (see Chapter 4 on page 181) uses hierarchical clustering to determine alloy groups. This, however, does not necessarily lead to a terminology that is easily understood or relatable to other studies. Consequently a broad group of textual classifications for copper alloys based upon those used in Bayley (1991, pp. 13–17), with subdivisions (such as leaded) may also be applied. These broad divisions are bronze (copper and tin), brasses (copper and zinc), gunmetals (copper, zinc and tin) and copper (see Figure 2-2).

²² Pewters and gunmetals in the 17th and 18th centuries are a good example of this, where slight variations were regularly patented and given trade names, see Tutania for an example (Nicholas 2008, 234).

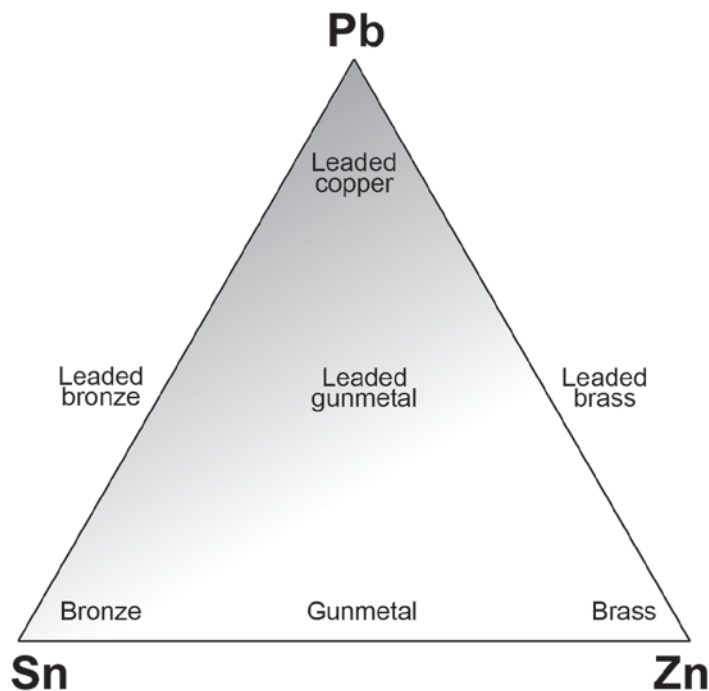


Figure 2-2: Ternary diagram of copper alloy types (after Blades, 1995, p. 127).

These are modern definitions; nonetheless the usage is accepted as relatively standard (see Blades 1995, 31–32; Blair and Blair 1991, 81; Dungworth 1995) and need not be an issue as long as it is remembered that they are only a tool to aid our interpretation.

It should be remembered that different studies, although often using the same terminology, use different element thresholds to define that terminology and that one person's bronze can be another's gunmetal. Consequently one should be mindful that linguistic terminology — although common — is not always directly comparable for specific objects. This is particularly relevant when examining data sets that have been reassessed in other studies. In this study this specifically applies to Blades' (1995) early Saxon data, which will be used as a comparison to the results acquired here. A substantial comparison of copper alloy nomenclature previously used can be found in Chapter 8 on page 378.

2.2.1 ALLOY PRODUCTION AND USAGE IN THE EARLY MIDDLE AGES

The increase in the number of sites excavated and the increasing quantity of medieval non-ferrous alloys analysed has dramatically increased understanding of our metallurgical past. This section provides a brief overview of our current knowledge and understanding of non-ferrous metallurgy from the 5th-7th centuries.

2.2.1.1 PRIMARY METALLURGY AND THE SOURCE OF METALS IN THE MIDDLE AGES

Whilst a significant amount is known about Late Romano-British ferrous and non-ferrous mining and smelting activities (Edmondson 1989; Hirt 2010; Hodginson 1999), there is a relative paucity in our knowledge of early medieval extractive and primary metallurgy. This is partially the result of a historical bias in sites excavated (with a heavy focus on easily recognisable sites such as cemeteries: Bayley, Crossley, and Ponting 2008, 49) compounded by the geographical focus of modern commercial archaeology (most development being in the South-East of Britain, an area not particularly noted for its non-ferrous metalliferous mineral wealth).²³ In the west, particularly modern day Cornwall and Devon, there is a slight improvement in our understanding with possible 6th-8th Century CE tin ingots, discovered at Praa Sands, Beagrie (Biek 1994) and Bigbury Bay (Fox 1995).²⁴ Further evidence of possible early medieval extractive tin metallurgy has come from geoarchaeological analysis. In the Erme Valley (Devon) radiocarbon dating of peat deposits associated with high tin levels in alluvial silt fractions has suggested a peak in tin streaming between CE. 245–386 and CE 460–730 (Thorndycraft, Pirrie, and Brown 2004, 233). The presence of Mediterranean imports in the region has also been used to suggest that extractive metallurgy was continuing (Campbell 2007, 130) and Gerrard states that there is currently no evidence that suggests any reason why mining should have ceased in

²³ A rare case where absence of evidence is probably evidence of absence.

²⁴ Rather than modern administrative units, Ceremonial Counties are used in this document, as these tend to be less prone to alterations.

the post-Roman period (2013, 111). If mining did continue, whether any of the tin (assuming it definitely is early medieval) made its way to the East of Britain is currently unknown.

2.2.1.2 COPPER, NIELLO AND ABDUCTIVE REASONING

The evidence for early medieval extractive copper (Cu) metallurgy in the British Isles is currently slim. It should be noted, however, that there is some evidence that may suggest a supply of pure copper was available to craftspeople in the East of England from the 6th Century onwards: Niello.

Niello is a traditional decorative technique that utilises the application of silver or copper (combined, leaded or neither depending on date) sulphide ground up into a powder and applied with a quill or as a bar rubbed across the surface (Presbyter 2000, 104–105,108). Utilised across Eurasia between the 1st to the 18th Century CE, the technique was occasionally, in the late 19th and early 20th centuries, confused with glass-based treatments (enamels etc.) (Moss 1953). Analysis by Susan La Niece at the British Museum in the 1980s produced a broad chronological framework of niello compositions in the British Isles (1983, see Table 2-1 below).

Composition	Century (CE)
Silver sulphide (Ag, S)	1 st - 6 th
Silver copper (not necessarily in that order) sulphide (Ag, Cu, S)	6 th – 12 th
Leaded silver copper sulphide (Ag, Cu, S, Pb)	12 th – 18 th ²⁵

Table 2-1: Niello compositions and approximate dates of use in Western Europe (from La Niece 1983)

Detailed quantitative analytical results of niello are rarely published, qualitative characterization being sufficient to place the mixture in La Niece’s chronological framework. Nevertheless, it should be noted that no analyses report early medieval niellos containing zinc, tin or lead (La Niece 1983; Oddy et al. 1983; Newman, Dennis, and Farrell 2007); metals whose presence is used to suggest

²⁵ These dates are approximate and for Western Europe only. Niello continues to be used outside of Europe to the present day. For more details see La Niece (1983).

the recycling of copper alloys for the early medieval period. Therefore it seems reasonable to deduce that sources of pure copper and sulphur (or copper sulphide) were both available to and utilised by some (niello tends to be restricted to Kent in the sixth century, see Brugmann 1999) Anglo-Saxon craftspeople for niello, contrasting the standard view that there were no supplies of fresh metals available (Mortimer 1990, 22).²⁶ Where these materials were extracted (there is currently no physical evidence for copper mining between the end of the Romano-British period and the High Medieval in Britain, (Bayley, Crossley, and Ponting 2008, 51) and/or processed, and the networks formed around them is currently unknown.²⁷

2.2.1.3 ZINC AND BRASS

Zinc (Zn) is the crucial element in the production of brass. Yet, unlike many of the other metals and metalloids we will be dealing with in this study, the production of metallic zinc for trade and production was not possible in Britain (until the early post-medieval period: Day 1998) due to a very specific thermal property: its boiling point.

In the British Isles and mainland Europe there are two main zinc minerals which are of particular interest for their historical usage, smithsonite ($ZnCO_3$) and hemimorphite ($Zn_4Si_2O_7(OH)_2 \cdot H_2O$). These two minerals occur in the upper oxidised zones of an ore body, are frequently found in concert, are similar in colour (white, stained brown, blue or green), lustre (vitreous) and physical appearance (botryoidal, i.e. a rounded globular form). As such they are visually indistinguishable, and until the mid-19th century were referred to as one with the name, *calamine*. This term is no longer used to refer to these minerals (instead it describes a mixture of zinc oxide and ferric oxide) except in an archaeological or historical context.

²⁶ It is unlikely that copper sulphide mineral deposits were being exploited in the early medieval period, oxidised copper ore bodies still being plentiful until the high medieval period (see Dungworth and Nicholas 2004, 29).

²⁷ Whilst today it is possible to refine copper from alloys using electrolysis the Anglo-Saxons had no equivalently 'easy' technique. Consequently if the copper were from recycled sources it would suggest an extraordinary degree of 'quality control', with only pure copper objects selected, recycled and subsequently used for specific purposes.

Due to its low boiling point, it proved difficult to develop a process of smelting zinc minerals to a pure metallic state. Zinc oxide needs to be heated in contact with charcoal above 1000°C to reduce it. At this point, however, zinc is a gas and would quickly react with oxygen to form zinc oxide. A process of producing the pure metal (distillation) was not discovered until the 13th (India) or 16th Centuries CE (Europe) (Day 1998).

As with copper, there is currently little positive evidence for the exploitation of zinc ore bodies in Britain during the early medieval period (the majority are located in the South West of Britain). If its ores were being extracted they were likely traded/exchanged in combination with copper (as brass) rather than in unprocessed mineral form; the assumption being there is little economic benefit to the expense of transporting gangue minerals.²⁸ Therefore a brief introduction to the brass production process is presented below.

With the production of metallic zinc for alloying purposes not possible, an alternative process was required, cementation. Brass cementation, different from iron or gold/silver cementation, is widely used to describe a process in usage in Britain from the Roman British period until the 18th Century in the production of brass.²⁹

The calamine may have first been calcined; a process of heating the ores in an open hearth to a temperature of no more than 500°C. This would remove carbonates from smithsonite ($\text{ZnCO}_3 \rightarrow \text{ZnO} + \text{CO}_2$) or dehydrate hemimorphite ($\text{Zn}_4\text{Si}_2\text{O}_7(\text{OH})_2 \cdot \text{H}_2\text{O} \rightarrow \text{Zn}_4\text{Si}_2\text{O}_7(\text{OH})_2 + \text{H}_2\text{O}$). The calamine could also be placed directly in the crucible for the cementation process; however, the oxidising gases released would affect the reducing atmosphere and the effectiveness of the cementation process.

²⁸ There is an intriguing suggestion in Pollard et al. (2015, 711) that there is an injection of new 'brass' in the middle Anglo-Saxon period. A recent PhD thesis by Unn Pedersen has identified a similar injection in Norway from circa. 800 CE (pers. comm. Professor John Hines).

²⁹ Cementation is a term with varied usages dependant on the metal involved (and who you ask). Iron cementation refers to a process used to increase the carbon content of iron by heating the metal in contact with a carbon-rich source (i.e. charcoal).

Copper would be broken into small pieces (to maximise surface area) and placed in a crucible along with the calamine and charcoal. The crucible would be sealed and heated to approximately 950-1000°C. The charcoal in the heated crucible results in a reducing atmosphere. At 750°C hemimorphite decomposes to willemite (Zn_2SiO_4) (Taylor 1962), and above 950°C the zinc oxide decomposed from smithsonite reacts with the carbon monoxide produced by the charcoal to produce a zinc vapour ($ZnO + CO \rightleftharpoons Zn + CO_2$). Any zinc silicates (i.e. willemite) would remain unreduced and take no further part in the reaction.³⁰ The zinc, being in a gaseous state, then diffuses into the copper, forming brass. When diffusion is complete the temperature is raised above 1000°C, melting the brass granules (the addition of zinc lowers the melting point of copper) and enabling casting (Bayley 1998).

2.2.1.4 GILDING

Beyond the 'base' alloy out of which the object was cast, further metals or metalloids were utilised to alter the appearance of selected objects. Whilst some processes, such as tinning, used materials whose source we have already discussed (see page 67), one process - gilding - used a metal whose source has seen a surprising lack of discussion in early medieval studies: mercury.

The transformative properties of gilding, the act of adding a thin layer of gold atop another material, were well known from prehistory. A variety of techniques can be utilised dependent on material to be gilded, technological knowledge and resources available. These have been neatly summarised in Oddy (1991) who provides an overview of foil gilding, gold leaf, diffusion bonding and fire gilding. Analysis has suggested that, from the 3rd Century AD, the dominant technique was fire gilding (Oddy 1980, 129; Oddy 1991, 33). Fire gilding involves the dissolving of gold in mercury, the amalgam being painted on to a cleaned and pre-treated surface. When the application is complete the object is heated to volatilize off the mercury (it boils at 356.73°C) leaving a thin (thickness to be measured in micrometres) film of gold attached. Crucially for analytical purposes,

³⁰ Zinc silicates require a very high temperature to reduce and were not routinely exploited until the mid to late 19th Century (Percy 1861, 596).

not all mercury is volatilized, and detectable levels are expected to remain after the gilding process (Lins and Oddy 1975, 370). As was detailed by Patterson (1971, 302), however, gold-mercury mineralisation is known to have been exploited in antiquity and it cannot be ruled out that detectable mercury may occasionally result from the gold ore body (for a detailed examination on the formation and distribution of gold-mercury combined ore formations see Nekrasov 1996). It should also be noted that mercury can be used to gild objects in a cold process (i.e. requiring no application of heat). This is explored more in Chapter 6 (on page 270).

The mercury gilding of post Roman/early medieval objects raises an important question that has, so far, received little attention in early medieval scholarship; where was the mercury coming from? Deposits of cinnabar (HgS) are known across Europe from Tuscany, Austria, Serbia and Spain (Rapp 2009, 180). The largest of these, the Almadén mine in Spain (containing one third of the world's total supply of mercury: Hernández et al. 1999, 539), was exploited from the Roman period onwards (Edmondson 1989, 94) with production only ceasing in 2000. With links between west Britain and the Iberian Peninsula in the early medieval period being well attested (Fulford 1989) the Almadén mine may perhaps be considered the most likely source of mercury.³¹ This is discussed in further detail on page 278.

³¹ Evidence for this in the Late Anglo-Saxon period may potentially be found in Bald's *Leechbook* (a mid-ninth century medical textbook); where analysis of the text has suggested that quicksilver for medical purposes may have been imported from the Iberian Peninsula (Cameron 1993, 104).

2.2.1.5 SECONDARY METALLURGY: ALLOY USAGE IN THE PRODUCTION OF EARLY MEDIEVAL NON-FERROUS OBJECTS IN MAINLAND SOUTHERN BRITAIN

East Anglia is not particularly noted for its non-ferrous mineral wealth. Consequently, craftspeople producing non-ferrous objects (if produced locally) would presumably have had to utilise imported materials (either ‘new’ or scrap) or locally sourced scrap (Fleming 2012). With a perceived lack of post-Roman/early Anglo-Saxon settlement excavated in the area (Wade 2000, 23; Taylor 1984, 116–117), analytical work has tended to focus on funerary assemblages (Bayley, Crossley, and Ponting 2008, 49). This leads to a heavy bias on cast dress accessories, particularly brooches, as these are some of the highest profile grave goods (in terms of perceived potential for understanding culture and ethnicity). The impact of this can be seen in metallurgical studies that often focus exclusively on brooches (such as Mortimer 1990; Baker 2013) and even those that take a broader approach. In Blades’ (1995) broader non-object specific study of copper alloy metallurgy brooches over-dominate the analysed assemblages (see Figure 2-3 below). A comparison with Eriswell (Figure 2-4 below) shows that, whilst brooches do dominate the excavated assemblage, there are other significant classes of objects that are not analysed to any great extent in Blades’ study. This is despite them being present in the excavated assemblages (beads are a particularly good example and this is explored more in Chapter 8).

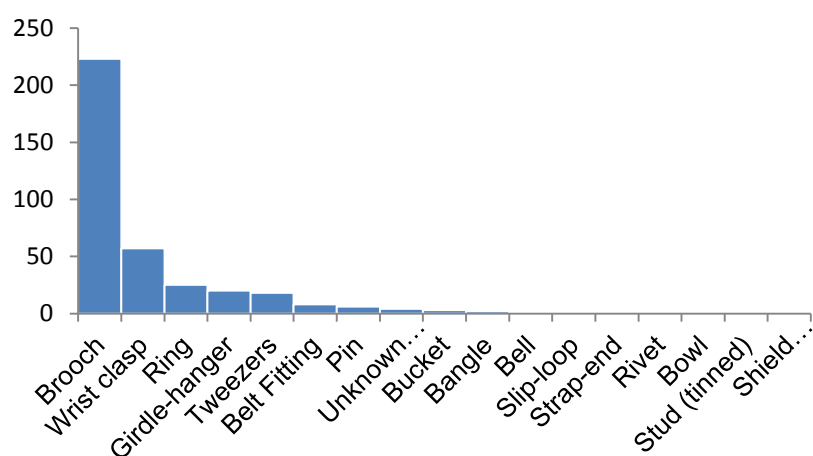


Figure 2-3: Graph showing the number of ‘Early Saxon’ copper alloy objects analysed by Blades (1995).

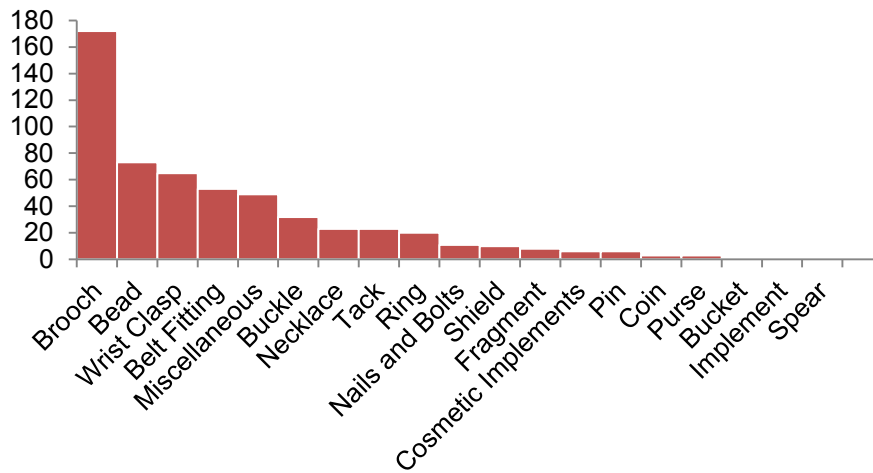


Figure 2-4: Graph showing a breakdown of copper alloy artefacts from Eriswell by object class.

This focus on brooches means that sheet objects often get ignored, despite making up a significant component of copper alloy assemblages. At Eriswell sheet objects account for nearly half of all copper alloy objects (See Chapter 8, page 312). Consequently one has to wonder how secure our extrapolated interpretations are when they exclude a significant volume of the metallurgical technology of the era. It should also be noted that the object typologies on which analysis traditionally focusses (cruciform brooches and wrist clasps particularly) tend to be those that appear to express significant Scandinavian influence (Hines 1984). Isotopic analysis of individuals from the cemetery at West Heslerton (Montgomery et al. 2005, 136) suggested a potential link between non-local individuals and objects like cruciform brooches in the cemetery's early phases. Therefore we must be aware that extrapolations — especially where analysis is from very early objects — may be based on a metallurgical culture that is not necessarily representative of the cemeteries immediate geographical hinterland or the 'blended' population interred there.

Analyses (i.e. Mortimer 1990; Campbell and Lane 1994; Blades 1995; Northover 1995; Wilthew 1984) of cast objects have generally suggested bronzes and gunmetals (both predominantly leaded) to be the most common copper alloys in usage during the early Anglo-Saxon period, with occasional brasses represented.

In Figure 2-5 ternary diagrams show Romano-British brooches from Richborough (as analysed by Bayley and Butcher 2004) and early Anglo-Saxon brooches (as analysed by Blades 1995). It can be seen in the Richborough diagram that, whilst there are mixed alloys, there are distinct brass and leaded bronze clusters. In contrast the Anglo-Saxon brooches appear much more mixed and there is a very clear reduction in the number of brass brooches. In both diagrams many objects contain a significant amount of lead. The addition of lead lowers the melting point of copper alloys and increases the fluidity (Dungworth 2001) making the copper alloy easier and more economical to work with when casting. Lead also affects the malleability when the alloy has solidified; consequently leaded copper alloys are less suited to drawing, rolling and hammering. Many of these brooches are cast objects (with exceptions such as some annular brooches) and so the lead content would be beneficial.

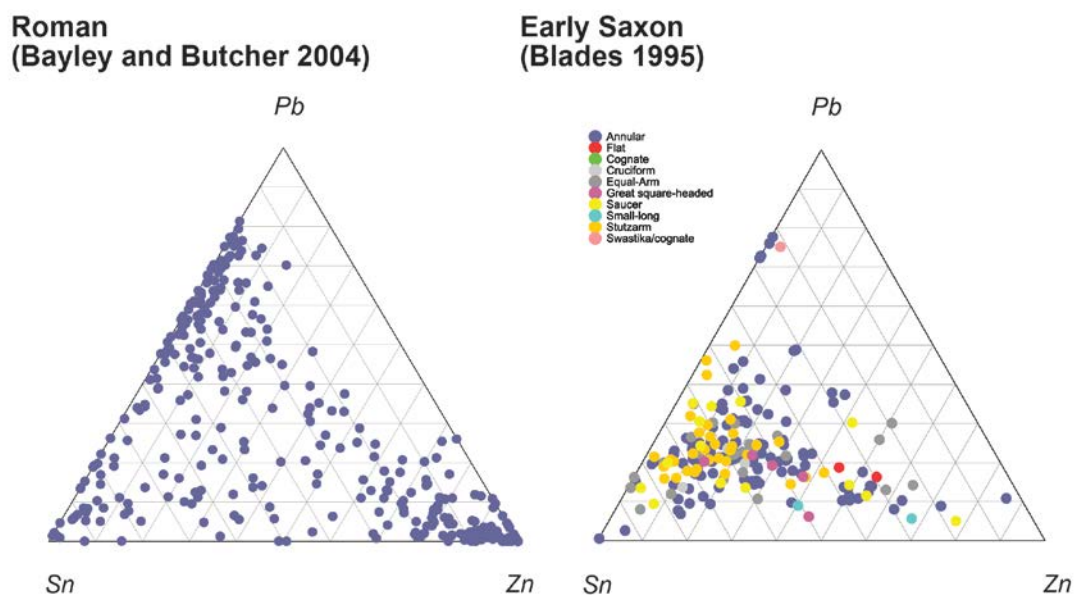


Figure 2-5: Ternary diagram of Roman brooches from Richborough (data from Bayley and Butcher 2004, Table 23 (digital appendix)) and early Saxon brooches (data from Blades 1995, 87–97). There are too many types of brooch in the Bayley and Butcher study to identify them all effectively here by colour.³²

The use of tin rich (i.e. bronzes) over zinc rich alloys (i.e. brasses) in the early Anglo-Saxon period forms part of a long term trend. As has been noted in studies of Roman brooches (Bayley and Butcher 2004; Bayley, Crossley, and

³² The Bayley and Butcher digital appendix is also available on the Archaeology Data Service website at <http://dx.doi.org/10.5284/1000191>

Ponting 2008, 49) there is an increasing tendency from the 1st Century CE for mixed copper alloys to be used, rather than pure brasses. This shift in alloy usage has been linked to changing production practices, with objects requiring less post-casting forging; it is unknown if this is the result of a restricted supply of brass (Bayley, Crossley, and Ponting 2008, 49). This is discussed in further detail on page 78.

Beyond the triumvirate of zinc, tin and lead which control our understanding of copper alloys are a host of other elements — antimony (Sb), arsenic (As), bismuth (Bi), cobalt (Co), nickel (Ni), manganese (Mn), silver (Ag), gold (Au) and others — which influence the properties of the metal and our interpretation. Many were likely unconsciously added (some not being known as individual elements until the post-medieval period), becoming included as a result of co-smelting (where metal elements present in the ore body are inadvertently smelted along with the main metal) or during recycling. Whether consciously added or not they do help us to define the purpose for which an alloy is used.³³ Antimony, for instance, increases the tenacity and hardness of copper, but if there is more than 0.2% present the metal may crack when rolled or worked (Gowland 1912). Arsenic meanwhile can increase the tenacity and hardness whilst not affecting the ductility or malleability of pure copper when present at a maximum of 0.8%; above this figure the malleability will, however, be affected (Gowland 1912). Ninety-three of the 380 objects analysed by Blades (1995) contained 0.2%+ antimony (the maximum was 0.95%, mean 0.16, sd 0.08), Mortimer (1990, 369) found lower levels of antimony in cruciform brooches with a mean of 0.07% and sd of 0.03). A high proportion of both Blades' and Mortimer's artefacts also contained arsenic, (Blades [1995]: maximum 0.26%, mean 0.05%, sd 0.04%; Mortimer [1990, 370]: 0.17% mean, sd 0.12), suggesting that, as indicated by the lack of brasses and the objects themselves, these were alloys best suited for casting.

³³ Whilst people may not have been directly aware of such elements they may well have been aware of the different properties afforded to a metal by using a certain ore, or adding a certain type of object to a melt.

Attempts had been made in the late 1980s to examine the distribution of trace elements in early Anglo-Saxon alloys (i.e. Mortimer 1990, 370–371); however, the low level of concentrations made the discovery of patterns difficult when combined with the minimum detection limits (MDL) available on the analytical equipment of the period. The increasing availability of higher sensitivity equipment, particularly inductively coupled plasma spectroscopy, did allow a slightly later generation to have some success in this area. Blades in particular made a significant advance investigating nickel and arsenic (1995, 194–197), discovering differing levels across types and sites. This, he suggested, indicated that metal was not being repeatedly recycled from the same pool (levels not showing temporal variation), but that it must come from a fairly ‘fresh’ source (again because the levels showed little sign of dilution) (1995, 194–197). Recently, a substantial reinvestigation of Blades data by Pollard et al. (2015) using a novel technique based on groups of trace elements presence / absence (this is discussed in more detail in Chapter 8) also suggested an injection of fresh metal, most notably in the Middle Anglo-Saxon period.

Perhaps one of the most interesting impurities previously identified is gold. Both Mortimer (1990, 366) and Blades (1995, 197–198) detected trace quantities of gold in early Anglo-Saxon copper alloys.³⁴ Blades also noted that the quantity of gold present decreased in the later Anglo-Saxon period. Interpreted as evidence of recycling (gold levels resulting from the melting of gilded objects), there has as yet been little in depth study of the phenomenon, and serious geological and cultural questions need to be answered before we can be certain of our explanation.

In Britain tin was most frequently obtained from cassiterite (SnO₂), an ore obtained predominantly not by mining, but from deposits in water courses during this period (a process often called streaming). As has been recently noted (Dube 2006, 108) both gold and cassiterite can, despite different specific gravities,

³⁴ The greater sensitivity of Blades’ analytical technique and the uniformity with which he applied it (Mortimer used a mixture of XRF, Microprobe and AAS, but not all on every brooch investigated) allows for such conclusions to be drawn easier from the entire dataset. Blades’ gold levels across all Early Anglo-Saxon objects had a mean value of 0.02%, sd 0.05%.

become deposited in the same auriferous alluvial placer.³⁵ Consequently we should not rule out the possibility that the source of trace gold detected by Mortimer and Blades is not gilded objects, but tin (either new or recycled in the form of bronze). In tandem, consideration should continue to be given to the gilded object recycling theory. We need to investigate the number of gilded objects required to produce these compositions, and, if thought correct, consider if a pecuniary decision (was copper more valuable or scarce than gold?) or a cultural choice with little economic consideration.

The quantity of analysis in the east has not been matched in the west of Britain, and sadly many important early medieval assemblages (such as Dinas Powys) await full in depth scientific investigation. Nevertheless, a small number of analyses on assemblages from sites such as Longbury Bank (Dyfed) and Cadbury Castle (Somerset) have thrown some light on the situation. Analysis (see Figure 2-6) showed that, whilst some objects were produced from quaternary alloys, others (particularly casting droplets from Longbury) were pure high tin bronzes. This has been interpreted as reflecting “*the availability of pure copper and tin ingots in the Celtic West and are rather different from the ternary or quaternary alloys found in Anglo-Saxon metalwork which tend to contain zinc, being derived from Roman scrap*” (Campbell and Lane 1994, 35). It should be noted, however, that high tin bronzes are also present in Anglo-Saxon assemblages (see Figure 2-5). There is also the problem of the small number of alloys analysed: we simply cannot realistically compare distributions of alloy types with the paucity of evidence currently available. Consequently, although it may be a reasonable assumption, we should not take it as a given that different resources were being exploited and different alloys were being produced in the west and east of southern Britain.

³⁵ Deposits of heavy mineral particles (i.e. those with high specific gravities) separated from lighter sands by gravity during sedimentation (Selley 2000: 10-12).

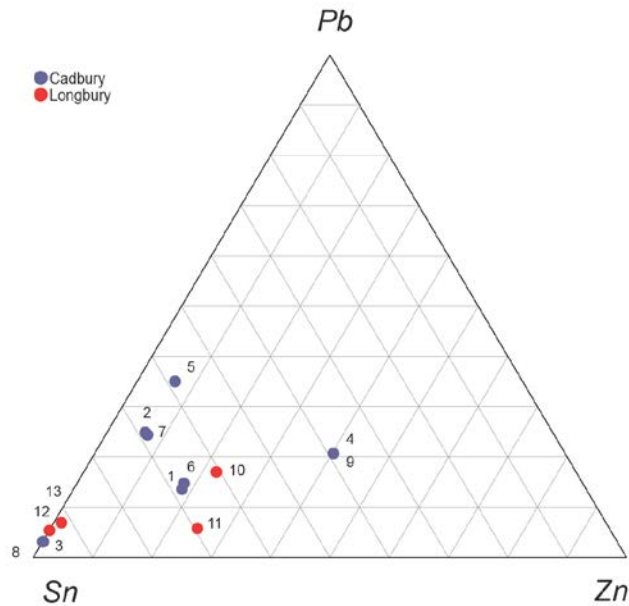


Figure 2-6: Ternary Diagram showing non-ferrous artefacts from Cadbury and Longbury. The points are numbered as follows: 1 - Ring/annular brooch; 2 - Brooch pin; 3 - binding strip; 4 - button brooch; 5 - small bar; 6 - Ring/annular brooch; 7 brooch pin; 8 - binding strip; 9 - button brooch; 10- Anglo-Saxon brooch; 11- Anglo-Saxon brooch pin; 12 – droplet; 13 - droplet. Data from Northover 1995, 74 (no table number) and Campbell and Lane (1994, 34, Table 1). Points 1-4 are presented as a mean of 3 results from each object.

2.2.2 ALLOYS THROUGH THE AGES

The placing of alloy usage in a long view temporal context illuminates aspects of technology and society that would otherwise be lost (such as the potential continuity between Roman and early Anglo-Saxon cast alloys mentioned on page 78).

In Figure 2-7 a range of quantitative and qualitative data is combined from a variety of sources and covers a period spanning the 1st to the 17th century CE. When combined with the data from Figure 1 we can see a trend in the increasing use of bronze from approximately the 3rd century CE which reaches its peak in the Late Saxon period, before declining as brass becomes the dominant copper alloy. It is not the place here to discuss near 2000 years of copper alloy usage, but it is interesting that early Anglo-Saxon copper alloy usage appears to fit into of a long term trend. The alloys utilised are not an aberration, but form a continuation of a late Roman trends (specifically the zinc decline). This

continuity has been noticed by a number of scholars (Caple 1986, 543; Baker 2013, 88; Pollard et al. 2015, 706).

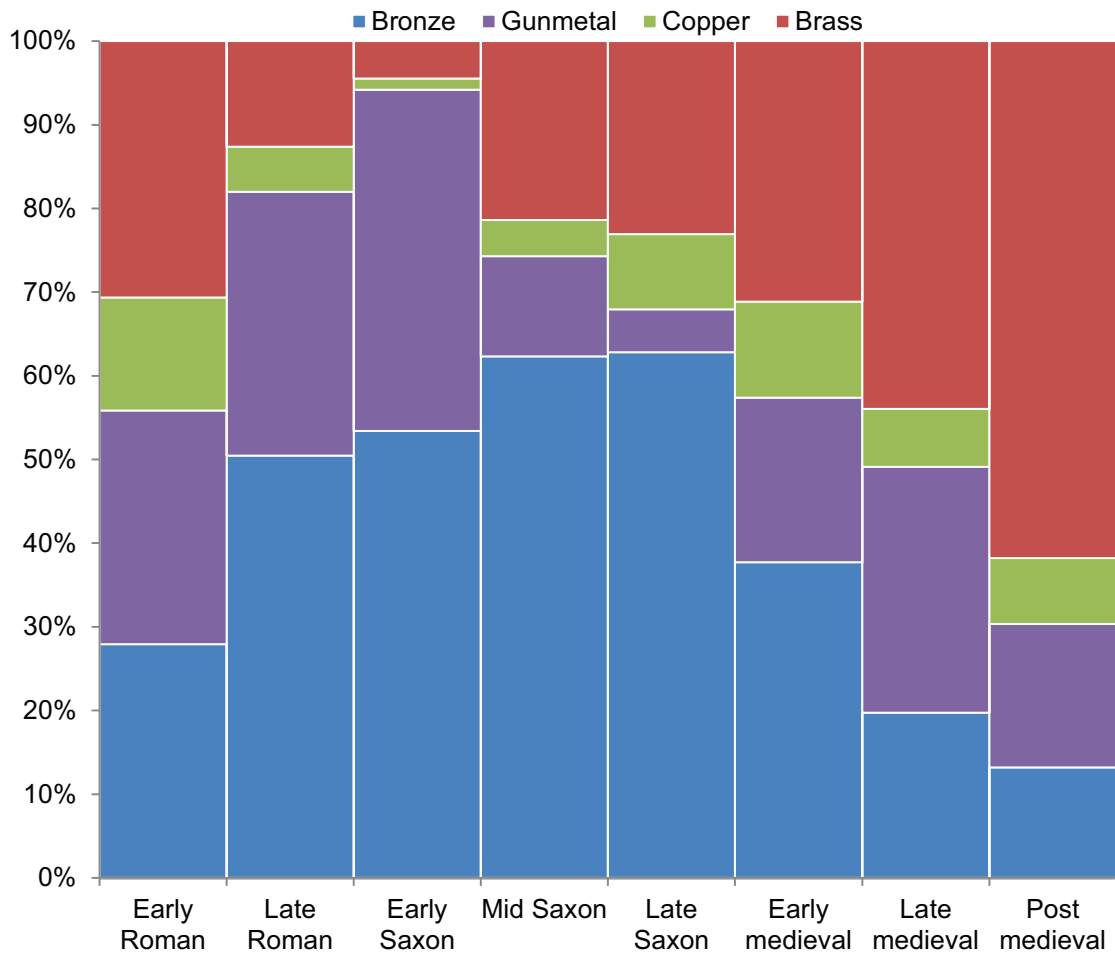


Figure 2-7: Copper alloy usage through time. Roman data was taken from Dungworth (1995), early Saxon, late Saxon and medieval data is from Blades (1995), post medieval data is from Dungworth (2000). Mid Saxon data is combined from Nicholas (2003). After Nicholas (2003) and Bayley et. al. (2008, 50, Figure 65). With additional data from Wiltbew (1984) and Brownsword and Hines (1993).

It is currently unknown if the zinc decline is linked to volatilisation of zinc during re-melting of brasses (and therefore is evidence of recycling), changes in alloy preference or bias because of the types of objects analysed. The first is most frequently thought to be the root cause of the zinc decline (Dungworth 1997a); recent research however has suggested that the volatilisation might not be the cause, instead the mixing of alloys is resulting in zinc dilution across the entire alloy supply (Pollard et al. 2015, 706).

2.3 RESEARCH QUESTIONS

The preceding pages have aimed to set out some of the philosophical, historical, technological and methodological context for the work in this study. It is aimed here to briefly bring together some of the disparate strands so far mentioned along with an outline of research questions that will be investigated.

This study is part of a larger, MAP2 (English Heritage 2006) and MoRPHE compliant (Lee 2006), post-excavation project. Before the post-excavation started a substantial post-excavation assessment was produced (Caruth and Anderson 2005). This contained a short assessment and list of research priorities for the non-ferrous assemblages by Freestone and Mortimer (2005). Before the research objectives of this study are outlined there will be a brief restatement of the non-ferrous research objectives. These are presented below:

1. How potential recycling was organized remains unexplored. Could sufficient material simply be collected locally, or was it imported from continental Europe or even further afield?
2. To what extent artefacts were produced locally, in regional centres, or imported?
3. In the case of indigenous production, were the craftsmen peripatetic or attached to specific communities?
4. Were there specialist producers of different types of artefact in the same material?

The completion of these tasks would require some specific approaches. The first two points are heavily reliant on trace elements and isotopes and the last two points are envisaged in the post-excavation assessment as being particularly reliant on studies of tool and stamp marks to identify individual craftspeople. These questions are very much framed within the context of previous research. Yet, as discussed, there may be a heavy bias in the results of previous research due to the type of objects selected for analysis. Because of this the viability of these objectives will be discussed alongside a short discussion. At the end of this updated research priorities will be presented.

2.3.1 ATTITUDES TO ALLOYS

“If there is a Dark Ages in British history, this is it”

(James 2001, 99)

“And if a thing is not in God’s mind, then what chance of it remaining in those of mortal men?”

(Ishiguro 2015, 69)

The results of analyses from previous studies on Anglo-Saxon copper alloys show the alloys to be mixed. They do not display the same clear divisions between different alloy types (i.e. bronze and brasses) that can be found in early Romano-British alloys (Figure 2-5, page 74) and there appears to be a significant decline in the use of brass (Figure 2-7 on page 79). Although there is a decrease in the number of objects made from alloys that could be described as brasses, Anglo-Saxon alloys do contain a noticeable amount of zinc; suggesting that the primary source of material for the production of copper alloys in post-Roman and early medieval period was recycled Roman alloys. The decline of brass appears to be a continuation of a trend that starts in the mid-late Romano-British period. That this continued in the post-Roman and early medieval period suggests a considerable degree of oft overlooked continuity (Caple 1986, 543; Baker 2013, 71). This continuity is also marked by the use of mercury to gild, no sources of which lay within several hundred miles of Britain’s south coast. The brass decline appears to cease from the mid-Saxon period onwards, with brasses becoming increasingly popular (a trend also noted in Scandinavia: Arrhenius 1982, 16).

The decline in brass, the more mixed nature of the alloys and the subsequent re-emergence of brass has led to the development of a narrative focussing on a total collapse of the Roman metal economy (Fleming 2012, 23) leading to a “*metallurgy of survival — adequate but not technically fastidious*” (Mortimer 1990, 397).

Too much of our interpretation of Early Anglo-Saxon non-ferrous alloys is clouded by Dark Age thinking. It is not our place to judge what is fastidious or

not. We can use our scientific knowledge to understand the physical limitations of a particular alloy, but we must be wary of judging it by our own standards. To base assumptions on the technological level of a culture based on the purity of alloys is to base them on our own ideas of what a ‘good’ alloy is and to misunderstand the nature of technology (a point forcefully driven home by Dungworth in relation to differences in trace impurities between Iron Age and ‘clean’ Roman alloys in the British Isles: 1997a, Section 6.6). That alloy usage could be described as ‘metallurgy of survival’ is indicative of the political and social mind-set of the period when much initial analytical work was done. The trouble is — however pithy, however much a grain of truth may lie at the heart — it is a subjective attitude (without necessarily being aware of it). It is as nonsensical as today saying that early medieval recycling is ‘metallurgy of the carbon foot print conscious’ or ‘metallurgy of austerity’.

Objects are a complex coalescence of a multitude of patterns (physical and intangible) into social matter. In reducing materials solely to simple issues such as access to resources we deny them their vital materiality. We should not ignore these requirements; if we do we risk re-working the already exhaustive art-historical studies of Bakka (1958), Haseloff (1974) and Dickinson (2002).³⁶ Instead we should incorporate the insights that scientific analysis allows; that the sensory and symbolic implementation of the designs did not take place in a state of incorporeal cognitive bliss, but were very much rooted in the material/physical world from which they are fashioned.

We should not pose our questions within the frameworks of yesterday; we should build upon and refine them. Rather than examining recycling purely as an economic necessity we should broaden ourselves. Is not there something very powerful in the act of reusing the material culture of a previous society and forging it anew, might there not be hidden symbolism in the metallic crystalline matrix itself? Recent analysis of Romano-British copper alloy Horse and Rider brooches showed bronze (as opposed to brass) compositions (Fillery-Travis 2010), perhaps suggesting that, as brass is identified with Roman culture (Ponting

³⁶ This should not be read as a critique of these studies per se. They are invaluable.

2002) the use of bronze may have been a statement of non-Roman identity. Looking again at the differences between the Longbury Bank bronze droplets (see page 83) and the more mixed Anglo-Saxon alloys, perhaps one could see statements of identity or cultural choice (something previously identified by Oddy 1983 and Blades 1995, 149) in alloy choice (one adopting an element of Roman identity, another refuting) rather than a story of resource access. Unfortunately the small quantity of analysis undertaken on Western British post-Roman non-ferrous metals prevents this going beyond speculation at the moment. It should also be noted that attempts to see if a brass divide existed as an indicator of Romanisation in the early Romano-British period immediately ran into problems with the nature of the objects available for analysis; specifically the ‘non-Roman’ bronzes which were both small in number and from very different depositional contexts to chronologically similar Romano-British artefacts available for analysis (Dungworth 1997b, 908).

2.3.1.1 CASTING A WIDER NET

Much analysis of early Anglo-Saxon non-ferrous metalwork has focussed on specific classes of dress accessories. These objects, predominantly brooches, are often cast. Partially this is the result of the dominance of funerary assemblages in the excavated archaeological record. The problem is that broad assumptions of alloy use in life have been drawn from these assemblages of death. Whilst it is not doubted that the brooches were utilised in life as well the grave (as evidenced by the high degree of wear found on many: Leigh 1980, 484–493; Martin 2015, 136–140), there is no escaping that they represent a particular form of usage.

The varied, often leaded, copper alloys used in cast dress accessories are appropriate for the form of the objects and their production, requiring no or little post casting forging. Sheet and wrought objects are different; the physical demands placed upon the crystalline structure of being hammered and bent, annealed and worked again, make it uncertain how well the ‘standard’ compositions for cast objects could have withstood these processes. Blades (1995, 151–152) found little difference between wrought and cast objects in the objects he analysed, but he had no comparable data against which to test his theories.

Consequently any copper-alloy object from the Eriswell assemblage that appears to have been significantly worked post-casting must be investigated in detail to provide comparable data and it should be considered a key priority to discover that nature of the metal used in these objects. The eventual results of the crystallographic texture analysis on two probable wrought hoops (ERL046, small find numbers 1094 and 1367) will assist us in this, giving a statistically valid (Artioli 2007) understanding of the crystal structure and enabling us to understand how the alloys worked in more detail.³⁷

The big question here is about any potential difference in the composition of cast and (the so far relatively ignored) sheet objects. Previous studies have — as discussed earlier — been heavily skewed towards cast objects. This is despite sheet metals making up a considerable quantity of copper alloys from post-Roman grave good assemblages. At Eriswell approximately half the copper alloy objects are sheet metal (see Chapter 8). Determining if there is any difference in the alloy composition of these in comparison to cast objects such as cruciform brooches is a key area of enquiry for this study. Unfortunately it is not financially viable to subject all Eriswell objects to neutron diffraction.

2.3.1.2 RECYCLING AND RESOURCE MANAGEMENT

It is thought that recycled Roman scrap provided the source for the majority of copper alloys. However, some analysis of trace elements, such as nickel and arsenic, has suggested that there was not a repeated recycling of metalwork (Caple 1986, 530; Blades 1995, 194–197; Pollard et al. 2015, 712–713). It has also been noted that there is a lack of re-recycling, with Martin (2015, 142) suggests that the number of heavily repaired and worn brooches found in graves suggests a certain reticence to melt and recast ‘Anglo-Saxon’ non-ferrous material culture. This raises a significant question: if this is metallurgy of survival, then why is the community so willing to dispose of a valuable resource by burying metalwork with the dead when it could be recycled?

³⁷ Analysis to be undertaken by Dr Winfried Kockelmann at the ISIS pulsed neutron and muon source, Rutherford Appleton Laboratory.

2.3.1.3 STAMPED DECORATION

Stamped decoration is one of a number of decorative techniques that are applied to the surface of a non-ferrous object after casting (i.e. the decoration is not imparted via impressing a stamp into a mould). The technique results in the impression of a small design, frequently geometric, on the surface. The stamping is frequently repeated, each discrete impression forming a textural (Leigh 1990, 107) stylistic interplay with surrounding elements.³⁸

Stamped decoration is not repoussé. Although similar in technique, each imparting design with a percussive impact, repoussé is undertaken from the back, stamped decoration on the front.

The impartation of the design requires a metallic bar with a clearly defined design with sharp edges etched on to one longitudinal end, the opposing end being flat to take the impact of the hammer. This punch will most frequently be produced of iron, although conceivably non-ferrous alloys could have been stamped with punches of non-ferrous alloys with a higher hardness value (Leigh 1980, 276). No early medieval punches for non-ferrous metalwork have been conclusively identified in the archaeological record (Mortimer and Stoney 1996, 6), whereas ferrous punches have been conclusively identified at the Helgö workshop (Tomtlund 1978, 17–18). It may perhaps be considered therefore that non-ferrous punches, although possible, are unlikely.

The object to be stamped would be placed on a solid hard bed that would not absorb the force of the impact, ensuring a clear and precise conduction of the design (Untracht 2005, 85). Ideally the punch should be used only once in each location to ensure the design remains clear and defined. In Anglo-Saxon non-ferrous alloys the presence of antimony and other alloying components (such as lead or arsenic), which affect the mechanical properties of the metal, may have

³⁸ Zoomorphic Anglo-Saxon punch marks are not completely unknown, see Inker (2000, 41, Figure 14).

imparted extra importance to the use of a single blow, multiple impacts potentially weakening the integrity of the brooch.³⁹

2.3.1.3.1 HISTORIOGRAPHY OF STAMPS

Stamped decoration has long been recognised as an element of artistic composition, considered in detail from the earliest studies of non-ferrous metalwork. They were not, however, considered from a technical viewpoint until the later decades of the 20th century.

In his 1980 thesis Leigh devoted considerable attention to stamped decoration, macroscopically photographing (at x2 magnification) and tracing individual stamps. In undertaking this Leigh was able to produce three groups of brooches which possibly displayed use of same/similar circular stamps (Leigh 1980, 270) and a single group which shared a triangular stamp with central dot (1980, 269).^{40, 41} Beyond this subset of brooches Leigh was unable to make any correlations with previously published examples, noting with disappointment that images were not detailed enough to make meaningful comparisons (1980, 268).

Leigh returned to the theme in 1990, examining in greater detail the lack of correlations. A discussion of potential reasons included survival and discovery rates (including recycling due to a non-ferrous metal shortage, punch life, punch anthropology (taboos against reuse? taboos about how used?) before concluding that small sample size may be the real issue (Leigh 1990, 114). Inveighing against the lack of high quality published macro images and attendant lack of analysis,

³⁹ Antimony especially can affect the cold working properties of a copper alloy, with anything >0.04% potentially resulting in cracks forming (Gowland 1921, 53).

⁴⁰ Group A: one from Sarre, Kent (Maidstone Museum, no accession number provided); one from Dover, Kent (British Museum, registration number 1963,1108.770).
Group B: two from Howletts, Kent (British Museum, registration numbers 1936,0511.83-84); two from High Down, Sussex (Worthing Museum, accession numbers 3427 & 3428); one from Sarre, Kent (British Museum, registration number 1893,0601.230); one from Finglesham (private collection, Northbourne) and two from Herpes, Charante, France (British Museum, registration numbers 1905,0520.231-232).
Group C: one from Bifrons, Kent (Maidstone Museum, no accession number provided); one from Mersham, Kent (Canterbury Museum, accession number RM 2636) and one from Howletts, Kent (British Museum, 1936,0511.82).

⁴¹ Group formed of three brooches excavated in 1855 from Chessell Down (British Museum, registration numbers 1867,0729.14-16) and one from Stowting, Kent (British Museum, registration number OA.274)

Leigh proposed that his system of macro photographs, whilst allowing for a certain level of analysis, should be replaced with the use of silicon rubber casts.

The use of a silicon rubber cast to investigate archaeological tool marks was first undertaken on a study of lines in insular late Iron Age metalwork (Lowery, Savage, and Williams 1971). Silicon is un-reactive with non-ferrous metals and has a fairly negative coefficient of thermal expansion (does not expand when heated) (Bullis 1990, 431). It therefore presents little risk to the object, whilst creating a mirror image of the design. As incursions becoming extrusions, the incisions of the punch become clearer, revealing the micro geometry (or characteristics / personalities / flaws) of the tool of used. The mould also makes it easier to examine the stamp, stripping away distracting tones of corrosion and elemental variation and reducing all to grey.

The casting technique was used with some success to investigate stamped decoration in the study of the Gundestrup Cauldron (Larsen 1987). Larsen visually examined all stamped decoration on each of the individual panels which make the piece, selecting individual stamps for further study. Those selected were cast, with the cast being examined in an electron microscope (1987, 397–399). There is unfortunately no mention of the detector type used in the SEM.

The technique showed some success in distinguishing groups of punches used, suggesting at least three silversmiths each with a different set of punches (1987, 399, Table 2 & Figures 17-20). The discovery of correlations between impact marks relied on the investigator's cognition (to form new classifications) and recognition (to identify known classes), i.e. a supervised classification system. No detail was provided on the determiners (hereafter *d* features) in dimensional space that were selected to form the basis of identification, but it is assumed the basic measurements (diameters, thickness etc.) were found to be sufficient.

2.3.1.3.1.1 EDIX HILL

In 1996 a large assemblage of metalwork from the early 6th-to mid-7th century Edix Hill cemetery in Cambridgeshire (TL 373 495) was analysed in the English

Heritage Ancient Monuments Laboratory.⁴² The cemetery, first discovered in the 1840's, was comprehensively excavated between 1989 and 1991 (Malim and Hines 1998), and is a comparable assemblage to Lakenheath. As part of the post-excavation analysis an extensive assessment and investigation was undertaken into punched decoration on the non-ferrous metalwork (Mortimer and Stoney 1996). This study is perhaps the most exhaustive investigation of punched decoration so far undertaken. Mortimer's classification scheme sorted punched decoration into five categories (1996, 7):

- Solid geometric
- Solid, adapted from geometric
- With punched additions
- With filled/engraved internal grooves
- With punched and filed additions

The scheme was specifically designed to move away from the purely typological groupings utilised by Leigh and Larsen and produce a technically based classification that could be undertaken in a post-excavation environment without the need for access to expensive analytical equipment (Mortimer and Stoney 1996, 8). This classification system is essentially a form of fuzzy set theory (see Zimmermann 2001 for a general introduction), grouping the simplest elements of the patterns (primitives) into a structured syntactic approach whilst allowing room for 'unsupervised' classification.

2.3.1.3.1.2 WOOD FOR THE TREES? PATTERN THEORY AND STAMPS

Recent decades have seen significant advancement in computational power matched with consistent falls in price (Moore's Law, see (Schaller 1997), triggering a rush in more affordable techniques of analysis and investigation (many familiar to archaeologists). One area that has, as of yet, received very little

⁴² See the Historic England National Monuments Record PastScape website for further details http://www.pastscape.org.uk/hob.aspx?hob_id=368376

recognition in the archaeological world is pattern recognition and the classification of patterns (an intrinsic component of knowledge, Pawlak 1991, 2).

Particulars of a class are bound together by concept rather than exact similarities (Watanabe 1985, 57). By searching for exact similarities we are therefore traversing the definitions of class; ‘no problem’ some may muse. There is, however, a sizable issue; the *why* is ill defined. Matching exact punches may suggest that the same hand has created the same object, perhaps allowing us to understand how craftspeople moved across landscapes and ideas with them (assuming people are their objects). Alternatively, however, it may be that the same punch was handed around or forgotten, picked up, used by another. Conceptual studies of what a workshop is (person or a place) have been sadly lacking in early medieval archaeology. Within current data sets and theorising on concepts on Anglo-Saxon workshops *we simply do not know*.

Recent advances in technology and forensic sciences have allowed the development of techniques that enable tools and their marks to be linked together (see Demoli et al. 2004 for instance). Whilst not of direct interest, studies such as this show particular potential for us in overcoming the issue that has caused so many problems; despite significant variations visible between wires cut consecutively with the same pair of pliers it was still possible to account for the variation and produce statistically valid links (Demoli et al. 2004, 489). This approach, using an Optoelectronic Correlator Device and Fourier transform analysis of the images, has been expanded to archaeological artefacts (cuneiform tablets specifically, Demoli et al. 2002). Utilising these techniques and approaching punch and tool marks with rigorous theoretical reasoning (particularly focussing on what questions to ask and why) we may be rewarded with greater insight than the narrow perspective of past studies has allowed us.

The potential limitations are evident. The search for exact matches has rarely been tried on full site assemblages (with honourable exception for the Mortimer study). Further full studies may provide illumination for work practises in the early medieval period. We should, however, be aware that punch marks were

only one of a litany of styles and techniques available to the craftsperson and that stamps form an integral part of the ‘universe of discourse’ (Pawlak 1991, 2) that composes the symbolism of metalwork form.

Unfortunately, though the potential is great, this is too big an area to be integrated into this study. The requisite equipment and software are not available in the Department of Archaeology and Conservation at Cardiff University and nor is there the money to buy them. Even if it were then the scale of work required leads one to conclude that this would be best investigated as a separate study. This, unfortunately, means that points three and four in the original research agenda (were craftsmen peripatetic or attached to specific communities and were there specialist producers of different types of artefact in the same material?) have to be dropped as these were very much based on the idea of being able to identify individual craftspeople through tool marks and stamps.

2.3.1.4 NO BROOCH IS AN ISLAND

In the past research on Anglo-Saxon copper alloys has focussed exclusively on the mixed nature of the alloys analysed and likely recycled source materials. The narrative developed from this has focussed exclusively on resource management within the context of an assumed total collapse of economies, trade links and cultural identities in the post-Roman era. In doing so, it has isolated the copper alloys and complex composite objects are reduced to a singular facet of their identity. This is despite the fact that they may be composed of many different metals (i.e. gilt surfaces, silver sheets, filler alloys, niellos) that may tell a very different story about resource acquisition.

Recent ethnographic and geographic research has illustrated how the exchange of material goods – even raw fruit – can have significant social and cultural impact on the communities they travel through and end up in (Cook 2004). This is not to suggest that early medieval exchange of mercury occurred in a late 20th century market framework, but that ethnographic and anthropological studies of these systems do have something to teach us; no ‘thing’ is an island.

Mercury for gilding was likely acquired indirectly; it is highly improbable that early Anglo-Saxon craftspeople were dealing direct with Iberian (or Central/South Eastern European/Apennine Peninsula based) miners. Yet there is a continuous thread that winds its way across the Continent, a thread that goes beyond the Germanic North Sea sphere within which early Anglo-Saxon metalwork is frequently considered. The thread is temporal as well as geographic; mercury trade routes in the early medieval period may well have been the same as (or similar to) their Roman predecessors.

The symbolism inherent in the Eriswell metalwork is not solely based on the conceptual artistic realisations of a particular community, but embodies aspects inherent in the materials themselves; aspects they will have acquired on their journey. Investigating the relationship between community and mercury is therefore crucial to understanding any social impact of the production process and of the objects themselves. Similar things can be said of all the materials used in the production of the Eriswell assemblage, down to the clay used in crucibles and the fuel that burns and transforms the copper alloys. As we construct our chaîne opératoire and create context, as we study the actors and the networks formed we should strive to remember that these objects do not exist in isolation, but that their materiality is constrained by the normative culture of those involved and that they are “*reflective of and affected by communal processes*” (Etzioni 2011b, 108). Then perhaps we may be able to understand a little more how symbols and materials combine and, to paraphrase de Waal (2011, 16), displace small parts of the world around them. After all no *thing* is an island.

2.3.2 RESEARCH OBJECTIVES

The points originally identified as the main research thrust of this study (summarised at the start of this section on page 80) have been reconsidered with additional context from the current document. It has been sought to ensure that these objectives tie in with points identified in the research frameworks for East Anglia (Brown et al. 2000, 52) and the Historical Metallurgy Society (Bayley, Crossley, and Ponting 2008, 68) for the period. It is not believed that it will be possible to answer all these completely, but given the extent of the assemblage it

should be possible at the very least to pose questions for future research in a data rich context.

1. Understand the range of compositions used for different manufacturing techniques

The nature of the alloys used for cast objects may not be suitable for wrought and sheet metalwork. The Eriswell assemblage will provide valuable comparable data to the existing research on this matter (i.e. Mortimer 1990; Brownsword and Hines 1993; Blades 1995; Baker 2013), enabling us to better understand what was physically and culturally expected of the objects. Examining this will also illuminate any possible bias in previous studies, generalising on results from cast broaches only.

2. Investigate the case for continuity

There is considerable scope to develop our understanding of any continuity (or lack thereof) between Roman and early Anglo-Saxon non-ferrous metallurgy. This includes trends in alloy compositions (i.e. the decline of brass) and the potential continuation of Roman trade routes (i.e. for mercury). Evidence for this last point can be indirect only. The presence of mercury in the gilding layers will indicate its use and it is known that there are no suitable mineral resources within the British Isles. Therefore the presence of mercury will indicate that trade must have taken place, but the source will remain somewhat elusive.

3. Investigate the nature (if any) of primary metal production

There are indications that tin may have continued to be produced in the South West of Britain. Analysis of the Eriswell assemblage will allow us to better understand if these resources were accessible to those in the South East. This will be achieved by examining the range of compositions for examples of relatively 'clean' alloys when compared to the majority of the dataset. Undertaking further work (such as sourcing through isotope analysis) is considered beyond the scope of this project. If not, was this a

choice relating to cultural identity, or did enmities between East and West prevent trade or exchange occurring?

4. Is there any cultural identity expressed in the non-ferrous compositions

It is hoped that it may be possible to investigate the potential for identity that may be encoded in the alloy choices made. This will primarily be achieved by comparing compositional groups against object types (particularly those objects — such as brooches and bucket pendants — that are strongly linked by archaeologists with cultural identity). There may also be scope to examine if this is also linked to resource management (i.e. were recycled metals collected locally, imported from continental Europe or further afield?), however identification of this may be difficult.

5. The nature of distribution and intra-site(s) variation

The reconstruction of the Eriswell small finds databases (including structured, controlled language and a full set of relationships) will allow the placing of alloy compositions into the wider Eriswell context. This includes areas such as investigating the distribution of alloy types between artefact categories and the distribution of alloys in relation to the spatial patterning of artefact distribution between the three cemeteries. This last point links to the previous research objective in investigating expressions of cultural identity through compositions.

Achieving these objectives requires a large scale of analysis to compensate for the object bias in previous studies. Essentially this involves analysing the whole assemblage of approximately 800 objects, requiring careful selection of the major analytical technique. As is discussed in the next chapter there were numerous instances where invasive sampling was not an option. Therefore a further research objective is added relating to the methodological approach:

6. Investigate the production of a reliable non-destructive compositional method of analysis.

This approach, whilst sacrificing some precision, will create the context currently missing from narrower focussed studies. Questions relating to sourcing based on minor and trace elements need to wait until we have a better understanding of the basic range of alloys in use.

CHAPTER 3: ANALYTICAL METHODOLOGY

“...learning does not consist only of knowing what we must or we can do, but also of knowing what we could do and perhaps should not do.”

(Eco 1984, 97)

3.1 INTRODUCTION

This chapter is in three sections. The first provides a brief overview of the range of analytical techniques available, the second an overview of X-ray fluorescence and the third a development of a practical analytical methodology (including assessments of instrumental and sampling uncertainty) to analyse the Eriswell assemblage.

3.1.1 METHODOLOGICAL APPROACHES

There already exists a body of high quality analyses (particularly Blades 1995 study, which is used in this thesis) which can act as comparable data. From the previous data a narrative of post-Roman and early Anglo-Saxon non-ferrous metallurgy has been created. A fundamental question then is how should the Eriswell material be analysed to either build upon or question this? Previous analytical studies have had a biased focus on brooches (which are predominantly cast) and so there is, as identified earlier, a need to analyse a large body of sheet objects to see if the same alloy is being used. This also requires us to analyse a large body of the cast objects from Eriswell to ensure that any site (and intra site) difference is accounted for (crucial if Gerrard’s hypothesis about local networks coming to the fore is correct: 2013, 274–276).

These questions, at least in the first instance, rely on a characterisation of the major alloying elements (tin, zinc and lead). Questions relating to sourcing based on minor and trace elements need to wait until we have a better understanding of the basic range of alloys in use.

To achieve the research aims of this study it is envisaged that the majority of the assemblage will have to be analysed. Furthermore many of these objects are composite with gilded surfaces and silver sheets that will also require investigation. The demands of the scale of analysis mean there is a need to make a careful choice of the major analytical technique to be used. There is a need for rapidity, repeatability and the ability to non-destructively analyse a range of (sometimes) very delicate objects that cannot be readily moved from their mounts. Within the range of analytical equipment at the Department of Archaeology and Conservation in Cardiff University this leaves two choices: hand-held portable x-ray fluorescence (HHpXRF) and scanning electron microscopy (SEM).⁴³ There are, of course, advantages and disadvantages to both.

The depth to which different analytical techniques can penetrate (dependent on current, density of material, vacuum states etc.) is crucial in understanding what we are analysing. The electron microscope is primarily a surface analysis technique, in contrast HHpXRF can excite the sample up to a maximum depth of a couple hundred μm in a copper alloy and nearly a millimetre in corrosion products (depending on the density of the corrosion product, the strength of the beam and characteristic energy of the element peak one is interested in, see page 162 for further details).⁴⁴ Electron microscopy can be particularly useful for characterising thin surface deposits (such as gilding, for an example see Chamón et al. 2010), where HHpXRF would also analyse the alloy beneath. In contrast the SEM is less likely to provide good bulk characterization of the alloy, its spectrum disproportionately reflecting surface corrosion processes (such as de-cuprification) which alter the ratios of metals present. Results provided by XRF will still be affected by this, but less so than the SEM.

To gain quantitative data a program of invasive sampling has to be undertaken. Cutting small sections from some of the whole decorative pieces is unacceptable from the view of long term curation, display and study potential. Drilling the

⁴³ Access to an ICP-MS is possible in the Earth Sciences department at Cardiff, but there are cost implications, especially for the analysis of circa. 800 objects. Interdisciplinary goodwill does not stretch that far yet.

⁴⁴ For a comparative study of analytical depth and technique see Aucouturier and Darque-Ceretti (2007).

reverse of brooches (as in Mortimer 1990, Appendix 1.3) will allow the gathering of corrosion free quantitative data but is only suitable where there is a relatively thick cast structure (as is the bow of cruciform brooches where Mortimer drilled). There are a large number of objects where preservation and uniqueness mean that *any form* of invasive sampling is insupportable. This includes a whole bucket from grave 031 in ERL 046 and the tack from grave 323 in ERL 104.⁴⁵

The limitations on sampling raise issues. Whilst statistical approaches can be used to randomise choice, we would still be dealing with an artificial set (i.e. not all objects can be sampled) and we would (to some extent) have already formed an idea of what the objects are and what their most important facets are; we have decided that some are too well preserved, unique or of aesthetic value to sample.⁴⁶ Unfortunately that decision means (if following a quantitative sample based strategy) we cannot know if there is an aspect of the metallurgy that is leading us to make those decisions (different alloys corroding at different rates etc.). There is also the issue that process of sampling and sample preparation will place time constraints on the number of objects and analyses it is possible to achieve. Even more significantly still there is also the question of how necessary quantitative data is to meet the research objectives set out here: will an extra decimal point of accuracy and precision really assist us in our understanding? To restate: we are seeking to characterise the alloys based on their major elements and it could be argued that knowing there is 11.23 % tin and 4.38% zinc in an object is of no more use than knowing there is 11% and 4% respectively, or even simply that there is more tin than zinc. This leads one to the conclusion that — given the demands of the study — HHPXRF is likely the best choice.

This is not a common choice. Although bench-top XRF is readily employed (Bayley and Butcher 2004; Dungworth 1997a), and the physicochemical matrix effects are understood, comparatively little study has been undertaken on the challenges and opportunities presented by HHPXRF employed on the surface of

⁴⁵ The tack and bucket underwent full conservation at the British Museum and were only made available for analysis in a fully conserved state shortly before they were to go on display.

⁴⁶ Any excavated assemblage is, of course, an artificial set anyway. But it seems foolish to make it more artificial still.

archaeological copper alloys. Inter-laboratory assessment of calibrated XRF results has demonstrated the erroneous impact calibrations can have on the data (Heginbotham et al. 2011). Qualitative analyses using the ratio of the fluorescent lines intensities of selected elements (Shalev, Shilstein, and Yekutieli 2006) as an indication of mass (Shilstein and Shalev 2011), have successfully been used for certain applications, but discarded for others (Shackley 2010). Classification of the EDXRF results can be undertaken with a visual assessment of the relative heights of the characteristic peaks (as in Dennis 1999; Dungworth 2000; Nicholas 2003b). Whilst peak heights are proportional to the abundance of the elements present in the objects, they are also dependent on a number of variables such as absorption of secondary X-rays, the shape of the object and the effects of burial conditions (Bayley 1992, 817–819). Alternatively net peak areas (NPA), produces numerical data which can be statistically explored, could be useful for a qualitative assessment of major elemental ratios in alloys.

Net peak areas (generally synonymous with net peak intensity) are the area of the peaks of interest with the background spectrum removed following a background modelling and deconvolution routines (details of the software used to achieve this are discussed on page 128). They are used here as opposed to peak heights (i.e. counts per second at the apex of a peak) as they reduce statistical uncertainty when dealing with small peaks and a solid detector with a relatively low (and changing) resolution (Janssens 2003, 406; Janssens 2013, 104; Gao 2010, 72).

When dealing with a small number of objects there may be issues about the reliability of any conclusions drawn from the data set, but the larger the set from which the data is extracted the more reliable the data becomes. Due to significant inter-laboratory reproducibility problems, resulting from many issues including software used (empirical calculations versus fundamental parameters), detection limits and filters (Heginbotham et al. 2011) the HHpXRF results will at no point be processed or presented as quantitative. The usage of HHpXRF will require the development of a rigorous methodology (see page 128). Before that, however, a brief description of some of the other analytical techniques that will be used in this study.

3.1.1.1 OPTICAL MICROSCOPY

Non-ferrous metalwork was initially categorised and assessed with a Nikon SMZ1000 microscope with Digital Sight DS-01 camera attached. The microscope was calibrated prior to use with a stage micrometer.

Microscopic examination prior to analysis will allow the extent of corrosion and the limit of original surface to be examined; crucial as corrosion can have a significant impact on analytical results (see pages 110 and 162). Optical examination is also desirable on gilt objects, as searching for diagnostic features such as joins or overlaps (which may be expected with foil) or ‘splashes’ of gilding (as would be expected with the use of an amalgam) can be crucial in discovering erroneous mercury identifications (Lins and Oddy 1975, 370) or confirming amalgam usage (Leigh 1980, 280–281).

3.1.1.2 X-RADIOGRAPHY

X-radiography on the Eriswell non-ferrous material was undertaken by conservators employed by SCCAS prior to the start of this project. Multiple objects (ferrous and non-ferrous) were x-rayed together; therefore there were occasional incidences where detailed x-rays were required to examine specific areas and features. The work was carried out on a Faxitron 43855E x-ray system. The system is not digital, therefore, images were digitally scanned and edited for contrast and brightness in Photoshop CS6.⁴⁷

3.1.1.3 X-RAY DIFFRACTION (XRD)

Analytical techniques like X-ray fluorescence (XRF) and scanning electron microscopy (SEM) can identify the inorganic elements present in a sample. They cannot, however, tell us what compounds are present. So, in the case of gilding, both XRF and SEM will detect the presence of mercury and gold in a mercury gilt surface but cannot tell us which intermetallic compounds are present. Understanding these compounds is crucial in understanding if a hot or cold gilding process was used (see Chapter 6, page 270 for a description of the two

⁴⁷ Previous experience suggests that two voltages (100 Kv and 110 Kv) for both one and two minutes should suffice for most objects.

processes). X-ray Diffraction (XRD) can inform us of this, and so will be used to characterise surface treatments where required. The XRD unit used in this study is an XPERT-PRO PAN analytical diffractometer. Objects are placed on a fixed stage and analysed with a divergent beam with a footprint of 200 mm² for 11 sec/step (7-100°2 θ) acquisition time. Data was analysed with X'Pert HighScore V2.1.2 and PDF-02 database.

3.1.1.4 SCANNING ELECTRON MICROSCOPY (SEM)

Where Scanning Electron Microscopy is undertaken it is done so with a CamScan MaXim 2040 Scanning Electron Microscope (SEM) fitted with an Oxford Instruments INCA energy dispersive analysis system (EDS). Any analysis was undertaken in backscatter mode, the visual investigation of surface layers (such as gilding) occurred secondary electron mode.

3.2 BACKGROUND TO X-RAY FLUORESCENCE

All Eriswell non-ferrous objects are to be characterised using energy dispersive X-ray fluorescence (ED-XRF), providing a non-destructive, relatively quick, qualitative method of identifying the alloys represented. This section is provided for Anglo-Saxon archaeologists who wish to know more about the background to the method.

XRF is a technique that works by bombarding a material with x-rays generated in an x-ray tube. These, upon hitting the material to be analysed, cause inner orbital electrons to be ejected from the atoms which compose the material (ionization). As the atom re-stabilises (with outer shell electrons replacing those lost in the inner) a characteristic x-ray for that element is released (see Figure 3-1). The XRF counts these, displaying the results in the form of a spectrum, enabling us to determine the composition of the material.

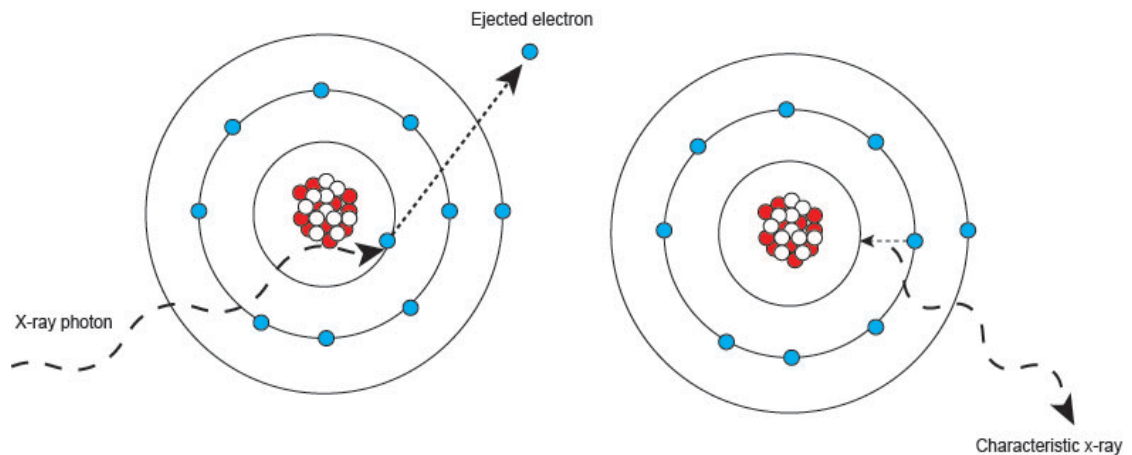


Figure 3-1: X-ray fluorescence in action with the ejection of an electron (left) and the release of a characteristic x-ray (right).

The X-ray tube (see Figure 3-2 for a simplified schematic diagram) consists of a cathode (the negative terminal) emitting electrons; these are accelerated towards an anode target (the positive terminal) mounted in a vacuum chamber. On striking the anode (composed of a pure metal such as rhodium) 99% of kinetic energy is lost as heat (Beutel, Kundel, and Van Metter 2000, 11). The remaining 1% interacts with the target atoms, creating Bremsstrahlung radiation (also known as continuous or continuum radiation) or characteristic x-rays (Frame 2009, 111), before passing through a beryllium window and, bombarding the sample. Both have specific qualities resulting from their creation that are crucial to understanding the spectrum:

- Bremsstrahlung radiation is created when electrons decelerate on reaching the anode, being repelled by the electrons of the target atoms and releasing radiation (photons) in the process (Drobny 2010, 13; Snyder 2009, 6). The energy of these photons varies from zero to the maximum Kv applied to the X-ray tube (hence the alternate name of continuous or continuum radiation) (Frame 2009, 111). This makes them crucial for the analysis for the analysis of higher Z elements above the energy of the characteristic radiation.
- Characteristic radiation is created when the beam electrons eject an inner shell electron from the target material and a characteristic x-ray is released. This x-ray will have the energy of the target material (in our case

Rhodium, 20.07 keV), and therefore will not fluoresce any element requiring higher energy.

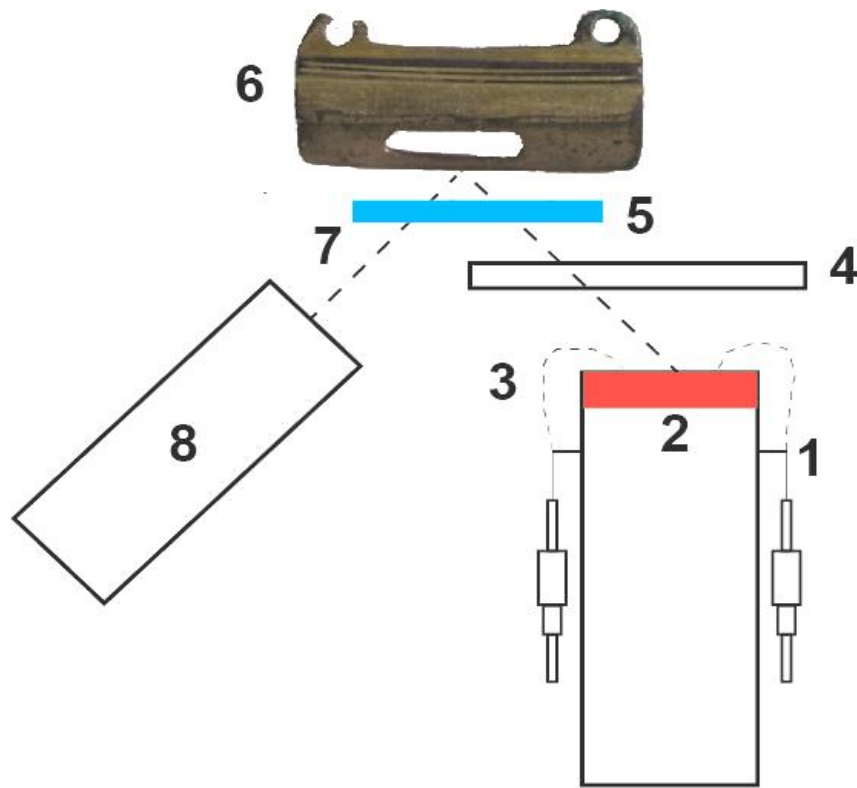


Figure 3-2: HHpXRF schematic showing 1) cathode (surrounding the tube as a ring); 2) Rhodium anode target; 3) electron beam between cathode and anode; 4) filter 5) Beryllium window; 6) object; 7) x-ray path and 8) detector. The thick dashed line shows the beam path (after Nazarov 2009, p.891, fig. 4 and Kaiser & Wright 2009, p.6 fig. 4).

3.2.1 THE SPECTRA

The spectrum produced by the XRF does not wholly reflect the materials fluoresced in the material analysed, but also on a number of effects and phenomena that produce their own peaks and affect the veracity of results. Some of these result from the nature of the equipment and the materials used (i.e. rhodium peaks from the anode material and filter fluorescence) or from environmental factors (including cosmic radiation: Helsen and Kuczumow 2009, 150). Others meanwhile result from the physics of x-ray photons and their interactions with the atomic and sub-atomic particles present in the sample. Of this latter group those whose effect on the interpretation of the Eriswell material the most are discussed below.

3.2.1.1 ELASTIC AND INELASTIC SCATTERING

Scattering occurs when an X-ray photon interacts with an electron in the object under analysis, but does not eject it. There are two types: elastic (also known Rayleigh or Thompson) and inelastic (Compton) scattering (see Figure 3-3). The first occurs when an X-ray photon changes direction after interaction with an electron (which is not excited or ionised) or whole atom whilst conserving its original energy (Markowicz 2002, 25), the latter when a photon collides with an electron — transferring some energy to the recoil electron — and is deflected from its original direction (Markowicz 2008).

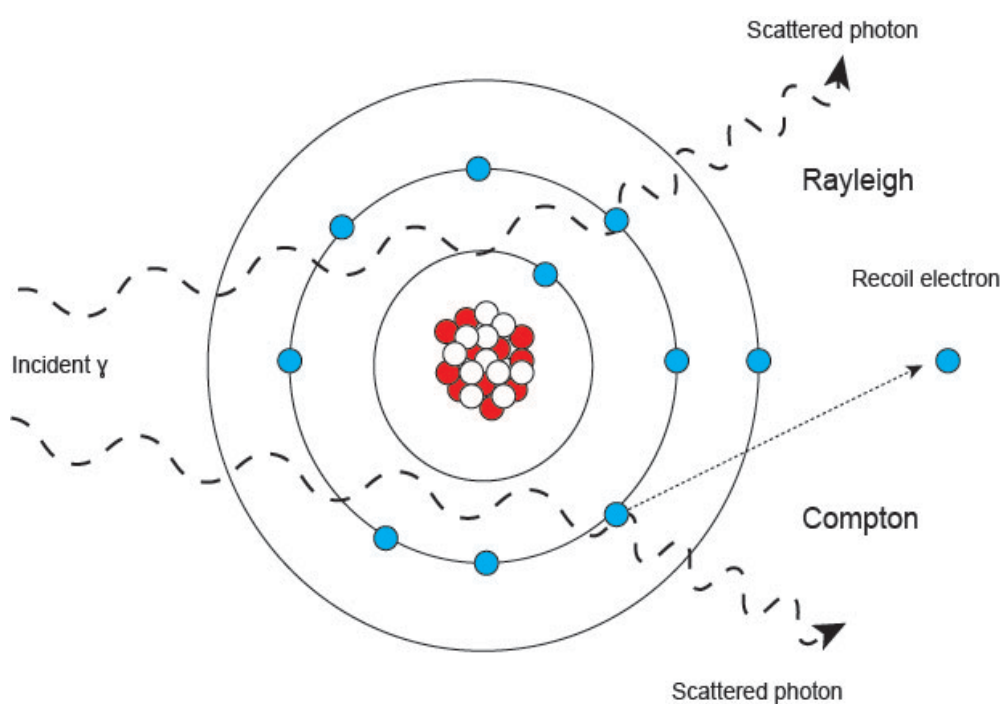


Figure 3-3: Rayleigh (top) and Compton (bottom) scattering.

Both Compton and Rayleigh scattering contribute to the background and other features of the spectra. Rayleigh scattering creates the Rhodium peak in the spectra, i.e. characteristic radiation is deflected, retains the energy of Rhodium and is detected as such. Compton scattering meanwhile results after the collision of photon and electron (resulting in the excitation of an electron) does not lead to energy from the photon being passed to the ejected electron (Kaiser and Wright 2009, 22) but instead being released as a lower energy photon that has no relationship to the incident x-ray (Snyder 2009, 11). This lower energy photon is then detected by the HHpXRF.

This effect is frequently visible in the Eriswell assemblages with broad peaks occurring at 21.17 keV (the energy of palladium $K\alpha$). It is unfortunately all too easy to mistake peaks such as this as an indication that this or that rare element is really present; however, as quick investigations often show (combined with a lack of L or M peaks) it is the result of Compton scatter. ⁴⁸

3.2.1.2 BRAGG SCATTERING

Bragg's Law (Bragg 1913) forms the basis for our understanding of the interaction of X-rays and crystal structures, theorizing on how parallel planes of atoms (the crystal lattice) diffract X-rays, producing a diffraction peak (He 2009, 13–14). The potential issue with the analysis of archaeological materials is the use of a single crystal model on a polycrystalline metal with lattice planes orientated in different directions (a common issue in other areas of X-ray analysis, see Ice and Larson, 2000: 644); the non-uniform crystal structure causing interference with the diffraction (Kaiser and Wright 2009, 24) leading to 'particle size broadening' (Snyder 2009, 38), i.e. broader peaks. Bragg scattering can therefore (to some extent) prove useful in XRF by informing broadly on the structure of the material. It also presents a problem; the broadening of peaks can obscure the identification of elements where there is an overlap in energies (see Table 3-1 for a list of potential overlaps).

⁴⁸ Palladium itself is often found with platinum. There are deposits of gold-platinum-palladium mineralisation in Russia and Mongolia (Sotnikov 2001), Greece (Economou-Eliopoulos 2000) and Poland (Piestrzyński, Pieczonka, and Gluszek 2002) but these there is no sign of platinum in the objects. Palladium does occur with some gold deposits in SW Britain without platinum (Colman 2010; Shepherd et al. 2005). These, however, are not readily available deposits, and, consequently, it seems unlikely that they were being exploited until recent times.

Peaks of interest		Potential overlapping peaks					
Element	keV	Element	keV	Element	keV	Element	keV
Ni K α	7.47	Co K β	7.65				
Ni K β	8.3	Cu K α	8.04	Zn K α	8.63		
Cu K α	8.04	Ni K β	8.3				
Cu K β	8.94	Zn K α	8.63				
Zn K α	8.63	Cu K β	8.94				
Zn K β	9.61	Pt K α	9.43	Au K α	9.7		
As K α	10.5	Pb L α	10.5				
As K β	11.8	Pt K β	11.2				
Ag K α	22.1						
Ag K β	25.2	Sn K α	25.2				
Ag L α	2.98	S K β	2.46				
Ag L β	3.28	K K α	3.31	Sb L α	3.6	Ca K α	3.69
Ag L γ	3.52	Sb L α	3.6	Ca K α	3.69	K K α	3.31
Sn K α	25.2	Ag K β	25.2				
Sn K β	28.8						
Sn L α	3.44	Ca K α	3.69	K K α	3.31		
Sn L β	3.82	Sb L α	3.6	Ca K α	3.69		
Sn L γ	4.13	Ca K β	4.01	Ti K α	4.51		
Sb K α	26.2	Cd K β	26.4				
Sb K β	30.1						
Sb L α	3.6	K K α	3.31	Sb L α	3.6	Ca K α	3.69
Sb L β	4.01	Ca K β	4.01	Ca K α	3.69		
Sb L γ	4.35	Ti K α	4.51				
Au K α	9.7	Hg K α	9.98				
Au K β	11.5	Hg K β	11.9				
Au L α	13.4	Hg L α	13.8				
Hg K α	9.98	Au L α	9.7	Pb L α	10.5		
Hg K β	11.9	Au L β	11.5				
Hg L α	13.8	Au L α	13.4				
Pb K α	10.5	As K α	10.5	Hg K α	9.98		
Pb K β	12.6	Kr K α	12.6				
Pb L α	14.8	Kr K β	14.2				
Bi K α	10.8	As K α	10.5	Pb L α	10.5		
Bi K β	13.0	Rb K α	13.4				
Bi L α	15.2	Rb K β	15.1				

Table 3-1: Energies of X-ray peaks of interest (organised in atomic number order) and potential overlaps.

The presence of Bragg scattering in the XRF spectra can be determined using a three step process outlined in Nagel and Herschbach (2009: 21439):

- Determine the energies of peaks suspected to result/suffer from Bragg scattering.

- Shift the angle at which the sample is placed (altering the angle at which the X-ray hit the lattice) to see if the location or breadth of a peak alters.
- Add a filter that blocks the incident X-ray energy required to produce that peak (if an entire erroneous peak is suspected to result from Bragg scattering).

3.2.1.3 CHEMICAL MATRIX EFFECTS

Chemical matrix effects refer to a suite of issues that can attenuate the signal, including (but not exclusively) the reabsorption of characteristic x-rays by adjacent atoms (reducing the amplitude of x-rays emitted) and the secondary fluorescence of x-rays (characteristic x-rays produced by other higher energy characteristic x-rays) (Markowicz 2008).

These effects concern us in XRF when samples are of sufficient volume to attenuate the signal (Nielson 1977, 641), i.e. when a sample is of intermediate or infinite thickness.⁴⁹ In some cases — where a sample is ‘thin’ (such as particulates on a film) or (in infinitely thick samples) the background is constant between samples — matrix effects can safely be ignored (Sitko 2009, 1162; De Vries and Vrebos 2002, 340). Neither of these applies to the Eriswell assemblage with all material being infinitely thick (discussed in more detail in section 3.4.1 on page 162) and heterogeneous (affecting the background).⁵⁰

The effects can be corrected by analysing and calibrating a range of reference materials of known compositions (see page 145 for full details of reference materials used in this study). As outlined in De Vries and Vrebos (2002, 341) this procedure has remained little changed for ED-XRF since its inception in the post-war period; reference materials are analysed, calibration curves are

⁴⁹ Infinite thickness refers to a sample of enough mass to absorb all the incident radiation (Cesareo and Gigante 2008, 207), i.e. they exceed saturation mass. Thin samples (such as particulates on a film) are less susceptible to matrix effects simply because the smaller sample size means there is less material to attenuate the signal.

⁵⁰ The exact point at which an object becomes infinitely thick depends on its composition and the mass absorption coefficient of the elements. Even thin (to us) sheet metal objects (such as 046-1603, see Figure 3-4) in the Eriswell assemblage are thick enough that they will completely attenuate the signal and therefore will not fall into this boundary zone. This is discussed in more detail on page 141.

constructed for elements of interest (with correction for matrix effects) and these are applied to samples of unknown (but assumed) composition (see Equation 1 below).⁵¹

$$\frac{C_{\text{unk}}}{C_{\text{std}}} = \frac{I_{\text{unk}}}{I_{\text{std}}}$$

Equation 1: Formulae to compare reference material with an unknown to quantify the concentration of an element (where C_{unk} and C_{std} are the unknown and standard concentration and I_{unk} and I_{std} the corrected background intensity for the unknown and standard) (Frame, 2009: 106, equation 5.2).

Further to this a range of empirical mathematical corrections — developed since the late 1970s as computing power increased (see Nielson 1977 for an early example) — have been developed to enable semi-quantitative results even where no reference material has been used.⁵² These methods, including Monte Carlo simulations and Fundamental Parameter (FP) methods, allow for a significant increase in the precision and accuracy of results, especially when combined with reference materials and calibration curves. FP methods (summarised in detail by Markowicz, 2008: 31–32) work by comparing the fluorescent radiation intensities of known pure elements to the intensities of those in the unknown sample. A significant advantage is the methods ability to correct for secondary fluorescence of x-rays, an option not available when using Equation 1 above (Frame 2009, 106).

In a recent study (Heginbotham et al. 2011) the comparative reproducibility of results between 17 different laboratories working with archaeological copper alloys were studied. The results showed considerable variations, with greatest accuracy (particularly for minor and trace elements) being achieved being achieved when FP methods were combined with standards (Heginbotham et al. 2011, 187). This reinforces the results of an investigation into HHpXRF by Zwicky and Lienemann (2004: 300) who found that “*these instruments are very handy but the spectral resolution and counting statistics are poor... the investigations show clearly that*

⁵¹ See page 57 for a brief discussion on presumptive assumption in science with reference to Taylor (2005) and Wylie (1989).

⁵² Please note that the term semi-quantitative can be problematic, see Zwicky and Lienemann (2004) for a discussion.

the results obtained with the portable ED-XRF spectrometer do not meet the quality requirements of laboratory analysis, but they are good enough for field investigations”.

The HHPXRF software set up at Cardiff University (see page 128 for full equipment and software details) does not currently include the ability to apply fundamental parameter corrections to spectra (for a background to fundamental parameters see Kitov 2000).⁵³ All results will nevertheless be compared with a range of known reference materials which will provide some level of quality control. The non-availability of FP will affect the reproducibility of the results, however, it should be remembered that – with consistent application and maintenance of standards – all results of this programme of work will maintain a consistent internal logic that should not affect the validity of the empirical conclusions on the nature of the assemblage.

3.2.1.4 SPECTRUM ARTEFACTS

Beyond scattering, physical and chemical matrix effects there are further interactions with x-rays and the equipment that can convolute attempts at spectrum interpretation. These include sum peaks, silicon escape peaks, edge effects, contamination peaks and the influence of ambient instrument temperature.

Sum peaks occur when two photons of the same energy hit the detector at the same time and are counted as double the individual energies (i.e. a sum peak for Cu $K\alpha$ 8.047 will have an energy of 16.094 keV). These peaks can usually be easily identified, as they superficially resemble a $K\alpha$ and $K\beta$ doublet, but their closeness disabuses one of this notion (Ellis 2002, 225). Sum peaks are particularly prevalent in copper alloys (Frame 2009, 115); the most significant issue this presents is their potential to obscure peaks of elements genuinely present in the sample (this may be an issue with minor and trace elements above 10 keV such as lead and bismuth).

Escape peaks are an artefact of the detector material. In the Bruker instrument used on the Eriswell assemblage (see page 128) the detector is made of silicon.

⁵³ FP software is available as an optional extra from Bruker, but was beyond the budget of this project.

An escape peak occurs when the returning characteristic x-rays generate silicon x-rays on striking the detector. The majority of these are reabsorbed and count towards the energy of the characteristic photon; those that do not, however, result in the energy of the photon being counted at 1.74keV less (Frame 2009, 116).

Edge effects are the final artefact that concern us; here a characteristic photon, striking the detector at the edge and at a certain angle, will pass through ensuring its full charge is not collected (Ellis 2002, 229). In experimental work on archaeological copper alloys (Frame 2009, 116) the energy of the resultant peak was found to be around 0.6 times less than it's true energy.

Contamination peaks result from a failure to clean the HHPXRF window. If qualitatively characterizing the major components of a sample this is not necessarily an issue, but when examining minor and trace elements the effect can potentially be considerable. As the Eriswell assemblage (many of the objects in which are coated with pulverulent corrosion products) is to be analysed by placing the object atop the analytical window this may be an issue. To avoid this the window is cleaned with between objects. The effectiveness of this cleaning can be checked by regularly running blank tests and checking for contamination.

In the introduction to this section (page 100) it was mentioned that 99% of kinetic energy is lost as heat. This can have a significant effect on the performance of the instrument and the results gathered (Mahuteau 2008, 18); for whilst the detector is maintained at a -15°C the air between it and the sample are not, and this ambient temperature will increase steadily during continued use of the equipment and/or in warm environments (McNeil and Cecil 2009, 4) On an earlier model of the machine used in this study (a KeyMaster Tracer II) Mahuteau noted that above temperatures of 35.6°C the spectra rapidly decrease in intensity (2008, 18–19). This change in gain results from the increased ambient temperature affecting the performance of the amplifiers (as noted in the U.S. Environmental Protection Agency test method 6200, 2007: 7). It is unknown if the Tracer III HHPXRF used in this study suffers in the same way as the Tracer

II to increased temperatures. Consequently a study will be undertaken to examine optimal ambient temperature ranges for analysis (see page 175).

3.2.1.5 ARCHAEOLOGICAL ARTEFACTS

Archaeological metals (in comparison to the homogeneous pellets XRF was developed to analyse) are often non-uniform (with varying crystal sizes), heterogeneous in nature with corrosion layers (creating an uneven surface and further affecting the uniformity and homogeneity with zones of de-cuprification etc.). The impact of these physical and chemical matrix effects on the analysis of archaeological metals are well attested (see Bayley 1992, 817–819). Yet these difficulties need not prevent relatively precise and accurate data being gathered as long as an awareness of the difficulties an archaeological assemblage may present are discovered through the development of a rigorous methodology and incorporated into correction procedures (see Milazzo & Cicardi 1997 for an example).

Previous analysis of early-medieval non-ferrous metals has shown that, like their late Roman predecessors (Bayley and Butcher 2004; Bayley, Crossley, and Ponting 2008, 49), the copper alloys used tend to be leaded alloys. Lead does not typically alloy with cast copper alloys (Scott 1991, 27) instead forming separate crystals. Whilst these may be evenly distributed throughout the structure this cannot be guaranteed (lead crystals may for instance gather at the base of the object during cooling in the mould etc.), especially when one is working with a complete object and is unable to examine the microstructure. Consequently there is a risk that the areas chosen for analysis are not representative of the alloy composition, something which can affect the reliability of results.

There is no magic bullet for avoiding the issue of lead segregation when non-destructively analysing whole objects. One must simply keep a constant eye on results as they are gathered, identify objects where this appears to be an issue and take further analyses in different areas until a level of agreement and consistency is achieved in the data.

One issue of particular concern to us here is the inconsistent positioning of objects over the analytical window.⁵⁴ When analysing complete archaeological objects this is somewhat unavoidable, it being rarely possible to position a brooch with corroded ferrous pin so the metal is in complete contact with the XRF window. The greater distance between the object and the HHpXRF window will result less accurate results (from scattering angles, attenuation of signal in air etc.) and higher background (from environmental factors, see section 3.2.1.3 above). Even when an archaeological object appears flat against the window it rarely truly is; the surface geometry at the macroscopic and microscopic level being a traverse of corrosion pitting, pulvarecent compounds and yawning canyons of fissures. These factors can be corrected for gaps of up to 3mm (for higher Z elements) using a correction formula developed by Potts et al. (1997: 770) following work by (Giauque et al. (1993) (see Equation 2 below).

$$I_{corrected} = I_{measured} \times B_{reference} / B_{measured}$$

Equation 2: Formula devised by Potts et al. (1997: 770) for the correction of sample geometry where $I_{measured}$ is the intensity of characteristic X-rays from a sample or object with an irregular surface and $B_{measured}$ is the resulting intensity of the scattered radiation (i.e. Compton and Rayleigh). $B_{reference}$ is the intensity of scattered radiation from a flat reference sample of similar (or the same) composition.

Before deciding if a correction formula such as Potts et al. (1997) is required it was first decided to undertake a series of experiments on the impact of increasing source-to-sample distance. The details and results of this can be read on page 166.

A second issue is width of objects in the Eriswell assemblage; for whilst many finger and suspension rings are infinitely thick they are distinctly not infinitely wide, often failing to cover the entirety of the HHpXRF window (see ring 046-1812 on page 134 as a good example). Where only qualitative analysis is desired simply placing the sample so the widest, thickest part is in the centre of the window is acceptable. For quantitative or semi-quantitative analysis (especially where the sample is both too narrow to cover the window and with a non-flat

⁵⁴ Only the most relevant procedures are outlined here, for a full summary please see Markowicz (2008: 22, 25–26).

profile) refinements become desirable. One such method was developed by Maia et al. (1997) who, following the work of Bos & Vrielink (1998), developed a system that utilises an opaque mask (the thickness of the mask does not adversely affect results in this method as long as it is <2mm thick) and a Monte Carlo simulation of photon interactions in the sample (see Equation 3 below).⁵⁵ The mask reduces the area of the sample that is accessible to the incident photons to its least geometric, allowing for results consistent intensities of $\pm 5\%$ for a range of distances from 3 to 12 mm (but decreasing in effectiveness as distance increases).

$$R_{ik} = I_i \div I_k$$

Equation 3: Formulae developed by Maia et al. (1997) and Bos & Vrielink (1998) for the correction of sample geometry (where R_{ik} is the relative instrument calibration factor; I_i the intensity of the characteristic X-rays of the sample and I_k and the intensity of the characteristic X-rays of a selected reference material).

Because of the greater distance allowed by the correction factor and its proven application to archaeological metals it is tempting to see the Maia et al. (1997) approach as applicable in this study. The construction of an appropriate mask, however, was beyond the budget and scope of this study.

3.2.2 REPETITION, HESITATION, AND DEVIATION: LIMITS OF DETECTION AND DETERMINATION

The results from each sample under each set of conditions were averaged (mean) and the standard deviation (SD) and Coefficient of Variation (C_v) calculated. As well as these the production of a further set of figures was considered to provide information of the accuracy and repeatability of the measurements. These are briefly introduced below and considered in further detail with analysis of the reference alloys.

⁵⁵ As part of this study Monte Carlo simulations were undertaken using the XMI-MSIM software package (available from <http://github.com/tschoonj>). There was not the time or support to develop these into useful applications for use in the thesis however. For more details on the XMI-MSIM software see Schoonjans et al. (2012).

$$LoD = \bar{I}_b + 3.0\sigma_b$$

Equation 4: Equation for calculating the Lower Limit of Detection (LLD) in XRF spectra where \bar{I}_b equals the average background intensity and σ_b the counting errors (Gullayanon 2011, 22 equation 5).

Following the methodology of Gullayanon (2011: 64) the lower limit of detection can be calculated using Equation 4, allowing the calculation of the lowest net peak intensity that can be detected. It was decided not use this approach as, whilst useful to understand the theoretical limits of the instrument, it can provide a false sense of accuracy. More on this can be read on page 160.

The uncertainty was evaluated using the Limit of Determination of a Method (LDM) developed by Rousseau (2001: 41, equation 12). This formula (see Equation 5 below) does not provide a limit of detection but allows us to calculate with 95.4% confidence level how well the analytical method (in this case HHpXRF) can repeat the given result under the same conditions (Rousseau 2001: 41).

$$LDM = 2. \sqrt{\frac{\sum_{m=1}^n (C_m - \bar{C})^2}{n - 1}}$$

Equation 5: Formula for calculating the Limit of Determination of a Method. The mean concentration for an element (\bar{C}) is derived from ten analyses of the same material taken under the same analytical conditions. C_m is the measured concentration, n the repetition number. From Rousseau (2001, 41, Equation 12).

3.2.3 CORRECTION OVERKILL? REASONING A METHODOLOGY

During the previous pages it may have crossed the mind of the reader that to concern ourselves to such a degree with x-ray physics and geometry of samples is (perhaps) overkill when analysing the surface of a corroded archaeological object. After all, when over one thousand years of corrosion can penetrate deeper than an incident photon, why bother? Certainly, previous studies on whole objects have shown that a simple visual assessment of the spectrum (as in Dennis 1999; Dungworth 2001; Nicholas 2012) — assessing the relative heights of the characteristic peaks — can allow us to interrogate the technology of an assemblage and draw valid (if broad) conclusions. There are problems with this, however; for whilst peak heights are proportional to the abundance of the

elements present in the objects, they are also dependent upon the physical and chemical matrix variables discussed earlier. When considering the size of the Eriswell assemblage (approximately 800 non-ferrous artefacts), these may be considered acceptable compromises, so why differ?

As part of the rationale behind this study is an attempt to produce a full survey of the non-ferrous technology of Eriswell — one not biased towards particular forms — then it may be reasonably suggested that we should attempt to gain the highest quality of data for every object within the limits of the equipment and time available. After all, it is possible to downscale a data set to make comparisons with earlier works, but difficult (if not impossible) to upscale it.

3.2.3.1 THE IMPORTANCE OF ELSEWHERE

“These are my customs and establishment ...

Here no elsewhere underwrites my existence.”

(Larkin 2003, 105)

The development of a methodology is an evolutionary affair based on the customs and technology of colleagues near and far, predecessors, superiors, laboratory, discipline and near disciplines: it is a process of elsewhere influence. It is a process in which self-opinion is sublated into a rationale developed from previous studies; a sublation simultaneously balanced with an increasing restriction in rhetoric as the study scope narrows from broad science to subject and/or material specific areas. This is OK. It is the way science works and it allows us to stand on the shoulder of giants whilst not losing ourselves in a maze of unnecessary detail on photon physics. There is, however, a problem. For whilst XRF has a long and proud history in the analysis of archaeological artefacts (it was not nicknamed the “*the curator's dream*” for nothing, British Museum n.d.) it appears that there are surprisingly few detailed published archaeological applications on HHPXRF (Phillips and Speakman 2009). This has become an issue of some contention in North American archaeology, with one leading archaeological scientist stating: “*it became clear that there were many pXRF*

instruments out there being used for any number of applications by a discipline not necessarily prepared for it intellectually” (Shackley 2010).

To avoid this study being intellectually unprepared a survey of available published and grey literature was undertaken in order to assess the settings and methods most frequently used (see Table 3-2 below).

Publication	Mat.	HHpXRF type	Software package(s)	Settings	Correction or calibration procedures described?
Frahm et al. (2014b)	Obsidian	Two instruments used: NITON XL3t (Si-PIN detector) (Silver anode) NITON XL3t GOLDD+ (SDD detector) (Silver anode)	Niton software packaged with instrument.	Two built in modes used with both instruments ('mining' and 'soils') 50 kV, μA automatically adjusted by instrument NITON XL3t specific settings: specimens analysed for 300 seconds. Max 40 μA . Helium purge used for lighter elements. NITON XL3t GOLDD+ specific settings: Max 200 μA .	Compton normalization of spectra followed by Fundamental parameters used on both systems.
Frahm et al. (2014a)	Obsidian	Thermo Scientific Niton XL3t GOLDD+ (SDD detector) (Silver anode)	Niton software packaged with instrument.	50 kV, μA automatically adjusted by instrument (to a max of 200 μA). Analyses taken for 10 seconds. Instrument used handheld.	Initially used a factory-set calibration factors, then subsequently linear-regression calibrations based on 24 obsidians analysed by NAA and XRF at the University of Missouri's Research Reactor (MURR) and by electron microprobe analysis (EMPA) at the University of Minnesota. Full detail of these not included in publication as due to be published in a forthcoming paper by the authors.
Orfanou and Rehren (2014)	Copper alloys	A custom built portable (but not handheld) XRF developed at the Institute of Nuclear Physics, NCSR Demokritos	Readers referred to Karydas (2007).	40 kV, 30 μA and 300 seconds live time. Two readings per sample.	Four certified reference materials (BCR-691). Further details not provided in the paper, but study follows the protocols and settings presented in Karydas (2007).

Publication	Mat.	HHpXRF type	Software package(s)	Settings	Correction or calibration procedures described?
Simsek et al. (2014)	Ceramics	Bruker Tracer III-V (Si-PIN detector) (Rhodium anode)	No mention of software used for acquisition. Data processed as net peak areas using Bruker Artax software. Results normalised to silicon peak. Statistica used for biplots etc.	40 kV, 4 μ A for trace elements analysis and 15 kV, 18 μ A for major elements detection. Each spectra taken for 360 seconds with the instrument on a tripod. Three to six measurements taken from each objects at both settings.	Qualitative analysis so no calibration. No mention of the use of any reference materials to check instrument performance. Unglazed samples analysed to act as comparison with glazed along. A number of other samples also analysed to act as comparators. One particular sample, Brongniart white porcelain, used as a 'benchmark of 18th century high potassium feldspatic, pure mullite white paste, and it was used as reference for bodies produced at Meissen with feldspars as flux'. Standards used for bench top XRF, but appears no standards used to directly check performance of the Tracer.
Bonizzoni et al. (2013)	Bricks	Bruker Tracer III SD (SDD detector) (Rhodium anode)	No mention of software used in spectra acquisition, Spectra smoothed using LabVIEW. MATLAB used for principal components analysis and graphs produced using Statistica.	40 kV, 20 μ A, spot size of 4-mm radius and time of 100 seconds	Standards used for bench top XRF, but appears no standards used to directly check performance of the Tracer.
Fernandes et al. (2013)	Copper alloys	Thermo Scientific Niton XL3t GOLDD (SDD detector)	No detail.	Max of 50 kV and 40 μ A. Setting called "mining mode" used with a helium purge in a bench-top stand. No mention of any filters or the length of analysis	Stated that factory calibrations used and additional standards measured. No mention of what the standards were.
Gauss et al. (2013)	Sediment cores	Thermo Scientific Niton XL3t 900-series GOLDD + (SDD detector)	No specific reference but appears to be the software packaged with the instrument.	Instrument fixed to a tripod. Each sample analysed for a total of 150 seconds under four different excitation settings: (1) main filter, 30 s; (2) low filter, 30 s; high filter, 30 s; and light filter, 60 s. There is no mention of what the filters are composed of (presumed to be the built in filters).	Niton Fundamental Parameters. Soil standards GBW 7411 and NCS 73308 analysed.

Publication	Mat.	HHpXRF type	Software package(s)	Settings	Correction or calibration procedures described?
Liu et al. (2013)	Glass	OURSTEX 100FA (SDD detector) (Palladium anode)	Spectra processing (inc. production of net peak area) done using software supplied by OURSTEX.	40 kV for monochromatic and filter modes & 15 kV for direct mode, and with a current of 0.5–1.0 mA. Spot size of 2.5 mm. Three readings of 100 seconds taken from each area under each of the three settings. No mention of filter composition or thickness	Twenty-nine glass standards from Breitlander Eichproben und Labomaterial GmbH and NIST (NIST 1411, 1412, 610, 612) used
Forouzan et al. (2012)	Ceramics	InnovX α -4000 (Si-Pin detector) (Tungsten anode)	No detail.	40 kV and 50 μ A.	Fundamental parameters with standards.
Forster and Grave (2012)	Obsidian	Bruker Tracer III-V (Si-PIN detector) (Rhodium anode)	KTIS1CalProcess for calibration construction. No further details.	40 kV, 13 μ A with a 0.152 mm Cu, 0.025 mm Ti, 0.305 mm Al filter. Ten analyses at 180, 240 and 300 seconds on each object.	Calibration constructed with standards with Compton normalisation and matrix correction factors.
Johnson (2012)	Ceramics	Bruker Tracer III-V (Si-PIN detector) (Rhodium anode)	Bruker S1PXRF software (version 3.8.22). R (version 2.13.1) used for calibrated results.	15 keV and 20 μ A with a 25 μ m Ti filter and vacuum attachment. Analysis time of 60 seconds. Instrument turned on for at least 30 minutes prior to initial measurement to allow the detector temperature to fully cool and stabilize.	Extremely detailed discussion of using the statistical programming program language R for producing calibrations.
Liu et al. (2012)	Glass	OURSTEX 100FA (SDD detector) (Palladium anode)	Spectra processing (inc. production of net peak area) done using software supplied by OURSTEX.	40 kV for monochromatic and filter modes & 15 kV for direct mode, and with a current of 0.5–1.0 mA. Spot size of 2.5 mm. Three readings of 100 seconds taken from each area under each of the three settings. No mention of filter composition or thickness	Twenty-two glass standards produced by Breitlander Eichproben und Labomaterial GmbH used to construct a calibration. Calibration checked against two standards not used in its construction (NIST 1411 and SVF2)

Publication	Mat.	HHpXRF type	Software package(s)	Settings	Correction or calibration procedures described?
Burley, Sheppard, and Simonin (2011)	Volcanic glass	InnovX α -4000 (Si-Pin detector) (Tungsten or silver anode – does not specify which)	No details.	Instrument mounted in stand. Analyses run under two manufacturer settings: the standard analysis package and Light Element Analysis Package (LEAP). Average live-time of 117 seconds. No further details.	NIST 2709 powdered soil standard analysed at the start of every run to monitor instrument performance. Powdered obsidian reference materials used to construct calibration. Readers referred to Sheppard et al. (2011) for further details (see below).
Goren, Mommsen, and Klinger (2011)	Ceramics	Thermo Scientific Niton XLt-900 GOLDD (SDD detector)	Niton NDT _r 6.5.2	Niton pre-set ‘mining matrix’ used with four different settings (using different voltages, filters etc.) for main, low, high, and light ranges. In total each area was analysed for 180 seconds live-time. Each object analysed in three different areas. No further detail on tube or anode current or filters provided.	Calibrated with standards. Data subjected to a best relative fit for each case with respect to the average values using the standard Bonn statistical procedure. Detailed description provided on pages 688-89.
Millhauser, Rodríguez-Alegría, and Glascock (2011)	Obsidian	InnovX α -4000 (Si-Pin detector)	Software supplied by manufacturer. No further details.	40 kV & 20 μ A (InnovX Light Element Analysis Package).	Standardless calibration (fundamental parameters?)
Sheppard et al. (2011)	Volcanic glass	InnovX α -4000 (Si-Pin detector) (Tungsten or silver anode – does not specify which)	No details.	Instrument mounted in stand. Analyses run under two manufacturer settings: the standard analysis package and Light Element Analysis Package (LEAP). Average live-time of 117 seconds. No further details.	NIST 2709 powdered soil standard analysed at the start of every run to monitor instrument performance. Powdered obsidian reference materials used to construct calibration.

Publication	Mat.	HHpXRF type	Software package(s)	Settings	Correction or calibration procedures described?
Speakman et al. (2011)	Ceramics	Bruker Tracer III-V (Si-Pin detector) (Rhodium anode)	No detail.	Two settings used: <ul style="list-style-type: none"> 40 kV, 15 μA, with a 0.076-mm copper filter and 0.0305-mm aluminium filter placed in the X-ray path for a 200-second live-time count. 12 kV, 15 μA, for a 200-second live-time count. 	Different processes used for the two settings. For setting 1 peak intensities were calculated as ratios to the Compton peak of rhodium, converted to parts-per-million (ppm) using linear regressions derived from the analysis of 15 obsidian reference samples. For setting 2 peak intensities for peaks were converted to parts-per-million (ppm) using a quadratic regression model based on the analyses of reference materials. Reference materials named and cited.
Frame (2009)	Non-ferrous slags	Bruker Tracer III-V (Si-Pin detector) (Rhodium anode)	S1PXRF, S1CALPROCESS, ARTAX	40keV with a 1mil Ti, 12mil Al filter and 42keV using 12mil Al, 1mil Ti, 12mil Cu filter.	Concentration calculated using Equation 1 (see page 8)
Kato, Nakai, and Shindo (2009)	Glass	Developed in house at the Tokyo University of Science with OURSTEX Co. Ltd. System has a palladium tube with a silicon drift detector (SDD) and utilises a Moxtek AP3.3 polymer window.	ANALYZER' program, part of the OURSTEX Co. Ltd. analytical suite. Stat-Partner 2.0 used for statistical analysis.	Spectra acquired for 300 seconds live-time with a beam current of 0.25 mA (white X-rays mode)/1.00 mA (monochromatic mode). all at voltage of 40 kV.	Equipment tested on NIST standard materials (SRM 621, 1412, 1830, 1831) to create calibration curve.

Publication	Mat.	HHpXRF type	Software package(s)	Settings	Correction or calibration procedures described?
Nazaroff and Shackley (2009)	Obsidian	Bruker AXS Tracer 3-V (Si-Pin detector) (Rhodium anode)	S1PXRF, S1CALPROCESS (Bruker packages)	40keV, 9.0 μ A. 300 seconds live-time with a 6mil Cu, 1 mil Ti and 12 mil Al filter.	<p>Archaeological obsidian samples with composition determined by non-portable EDXRF used as reference materials.</p> <p>A further standard obsidian reference material was used daily to ascertain equipment stability.</p> <p>Sample T tests to determine variance from control groups. Examination of effect object size had on results.</p>
Phillips and Speakman (2009b)	Obsidian	Bruker AXS Tracer III-V	Not mentioned (presumably S1PXRF and possibly ARTAX?).	40 keV current and 15 mA on anode. 0.076 mm copper - 0.0305 mm aluminium filter used. 200 seconds live-time.	Peak intensities calculated as ratios to the Compton peak of rhodium, converted to (ppm) using linear regressions derived from analysis of 15 well characterized obsidian samples previously analysed by NAA and/or XRF.
Craig et al. (2007)	Obsidian	X-ray source: Amptek Eclipse II, silver anode). Detector: Amptek XR-100CR and aluminum collimator detector.	XRF-FP (Amptek and CrossRoads Scientific).	25 keV, 20 μ A. 200 seconds live-time.	Obsidian from known sources used at the beginning and end of daily sample collection to assure stability of the system and monitor instrument drift .
Emery and Morgenstein (2007)	Mud bricks	Thermo Scientific NITON XLt-793W	DeltaGraph used for plotting measurements. No further detail.	No tube or anode settings mentioned. All analysis counted for at least 240 seconds live-time.	No detail

Publication	Mat.	HHpXRF type	Software package(s)	Settings	Correction or calibration procedures described?
Ferretti et al. (2007)	Non-ferrous metals	In house system constructed at the Institute for Technologies Applied to Cultural Heritage of the Italian National Research Council with a water cooled X-ray tube and a Peltier-cooled Si-Drift detector produced by Ketek.	No detail	45 kV current on tube, 120 seconds live-time.	Used systems developed in Ferretti (2004).
Morgenstein and Redmount (2005)	Ceramic sherds	Thermo Scientific NITON XLt-793W	SPSS-11 used for statistical analysis. No further detail.	No tube or anode settings mentioned. Operated in bulk sample mode using the complete list of element concentration and detection limits available on the system. Length of live-time determined by plotting detection-limit data against time of exposure to determine where detection-limit curves changed slope.	No detail
(Ferretti 2004)	Non-ferrous metals	X-ray tube – 60 kV, 1.6 mA with two detectors Si-PIN mod XR100T (Amptek) and Si-drift type (Ketek)	No detail.	Amptek detector: 60 kV, 4 mA. 0.5 mm Cu - 0.13mm Al filter. Ketek detector: 60 kV, 1.6 mA. . 0.5 mm Cu filter.	Study is on the process of developing method and corrections for higher Z elements.

Publication	Mat.	HHpXRF type	Software package(s)	Settings	Correction or calibration procedures described?
Karydas et al. (2004)	Non-ferrous metals	Rh-anode side-window, low power X-ray tube, PIN X-ray detector with 240 eV FWHM at MnK α and a 300 μ m nominal crystal thickness and battery operated MCA card.	MI-NUIT program used for non-linear least square minimization procedure. No further detail.	Ni, V and Kapton filter. Operational voltage of 40 kV used on all objects.	FPA. Detailed procedure provided on pages 20-22.
Pappalardo et al. (2004)	Ceramic glaze	X-rays generated by ^{109}Cd excitation source. Detector is a Ge (IGLET-ORTEC)	Guelph PIXE and AXIL QXAS	No detail	Calibrated using pure elements. PIXE data used as matrix input to XRF calculation.
Pantazis et al. (2002)	Gold	Amptek, Inc., XR-100CR X-ray Detector, PRS400 transmission Au anode X-ray tube and Amptek MCA8000A card for data acquisition.	No detail	No detail	No detail
Williams-Thorpe et al. (1999) & Williams-Thorpe et al. (2003)	Stone	Spectrace TN9000 (^{55}Fe ^{109}Cd & ^{241}Am excitation source) (solid state mercury iodide detector)	No detail	As in Potts et al. (1997).	Fundamental Parameters and surface irregularity correction (see section 3.2.1.5).

Publication	Mat.	HHpXRF type	Software package(s)	Settings	Correction or calibration procedures described?
(Potts, Webb, and Williams-Thorpe (1997))	Stone	Spectrace TN9000 (⁵⁵ Fe ¹⁰⁹ Cd & ²⁴¹ Am excitation source) (solid state mercury iodide detector)	No detail	Use three excitation sources ⁵⁵ Fe (emits Mn K _a /K _b radiation at 5.9 and 6.5 keV) ¹⁰⁹ Cd (emits 22,1-24.9keV and ²⁴¹ AM (emits 59.9 keV gamma line). Samples prepared as pressed pellets. Samples counted at 20, 50 and 100 seconds live-time.	Surface irregularity correction (the approach used for this is discussed in this thesis on page 111).

Table 3-2: Summary of recent HHpXRF studies (excludes exclusive studies of non-bulk methods i.e. Papadopoulou et al. 2006 study of micro-XRF) featuring summaries from the cited studies.

Examining Table 3-2 it becomes clear that Phillips and Speakman (2009a) and Shackley's (2010) concerns over the strength of HHPXRF methodologies were completely justified, with surprisingly few studies prior to 2009 including adequate details on their setups in publications. Post-2009 there appears to be an improvement with significantly more detail being included (i.e. Frame 2009). There is, however, a continuing unwillingness to include tube and current settings (i.e. Goren et al. 2011). Sometimes this is because the HHPXRF model automatically adjusts current settings to ensure optimal counts, as is the case with the NITON XL3t GOLDD+ (Frahm et al. 2014) (although this is not always stated in the article, Frahm's publications being a notable exception). It is crucial that these data are included as the tube voltage indicates what range of elements is being excited and the anode current the flux of the x-rays (see page 140 for further detail).

A number of studies (i.e. Pantazis et al. 2002; Morgenstein and Redmount 2005; Fernandes, van Os, and Huisman 2013) provide no detail on the software packages used to perform analysis, calibrations or interpretation of spectra. This appears to be a widespread issue as indicated using a Google Scholar search where the search string 'Bruker Tracer XRF' produces approximately 1550 results compared to 3 with the inclusion of 'CalProcess' (the Bruker calibration software) or 'X-RAY OPS' (the control program).⁵⁶ This is disappointing as access to this information is extremely important; many programs are proprietary and do not necessarily perform corrections and calibrations in the same manner (even within iterations of the same software as noted by (Frahm, Doonan, and Kilikoglou 2014)). At the time of writing there does not appear to be a standardised test and assessment of the major platforms, with existing comparative studies having focussed on the primarily on analytical methods (i.e. Heginbotham et al. 2011; Goodale et al. 2012). Consequently it appears that we are labouring under the assumption that different software packages perform equally and that precision and accuracy are purely factors of instrumentation. This is dangerous and it would be desirable for a comprehensive program of

⁵⁶ Search carried out on 16/08/2012.

comparative software benchmarking (the benefits of this to a discipline can be tremendous, see Sim et al. 2003) to be included in subsequent comparative HHpXRF studies.

It is notable that the majority of studies focus on homogeneous materials (such as obsidian) and that there are relatively few studies on inhomogeneous materials such as non-ferrous alloys. Although bench-top XRF is readily employed (Bayley and Butcher 2004; Dungworth 1997b) and the physicochemical matrix effects are understood, comparatively little study has been undertaken on the challenges and opportunities presented by HHpXRF employed on the surface of archaeological non-ferrous alloys. There is little in the way of established practice on which to base the methodology here.

3.2.3.2 GREAT EXPECTATIONS

“WE CANNOT ESTABLISH VALIDITY IF WE DON’T PROVIDE THE PROTOCOLS USED IN ANALYSES AND THE ANALYSIS OF STANDARDS”

(Shackley 2010, 19; capitalisation original emphasis)

A significant investment has been made by both scientists and archaeologists in the success of HHpXRF as a technique on archaeological assemblages. As seen above, however, significant questions have been raised as to the quality of the data it is possible to gather with this method. With this in mind an immediate question may occur to the reader; why continue to use this technique on the Eriswell assemblage? There are two primary reasons for this:

- HHpXRF is a fast technique. Its limitations may be significant, but within the aims of the study (to assess the chemistry of the whole of the assemblage) it becomes the most appropriate. This has been backed up by previous studies which demonstrate that the use of HHpXRF on large assemblages has been shown to have validity (Tykot 2010).
- It is the best technique available in the Department of Archaeology at Cardiff University to achieve the above.

To ensure that the data in this study are both of the highest possible quality and fully open to interrogation a list of guiding principles for data collection and reporting have been drawn up. These are based on Shackley's '*Preliminary Protocol for PXRF Analysis of Archaeological Materials*' (Shackley 2010) and conclusions drawn from assessing the studies presented in Table 3-4:

- Standardisation. A series of relevant reference materials to be analysed. A sub-section of the standards will be run each morning and evening to check the stability of the equipment. Further to this a single standard may be run between each object to check validity.
- Further to the above, all standards used should be included in the report. If not possible to have a detailed summary in the main text then they must *at least* be noted by recognisable name/code.
- Corrosion state of the object should be noted and recorded. If possible areas that have suffered substantial corrosion (visually and at microscopic level) should be avoided. If it is not possible to avoid these areas then this should be noted.
- Geometry of the object in relation to the window should be noted (i.e. what is the state of the surface? Does it sit flat on the window?)
- The HHpXRF window should be regularly cleaned (or protected) to avoid contamination.
- Blank runs should (as judged appropriate) be undertaken to test for window contamination.
- All settings, including tube voltage, anode current and filters to be reported.
- The software used to gather and process the spectrum should be noted. Any correction process used within the software should be declared.
- If quantitative analysis is undertaken any and all corrections (i.e. slope and background) should be reported to assist with reproducibility.

3.3 HHPXRF METHODOLOGY

This section presents the development of the HHPXRF methodology used on the Eriswell non-ferrous assemblage.

3.3.1 EQUIPMENT, SOFTWARE AND WORKFLOW

Analysis was undertaken with a Bruker AXS Tracer III-SD portable XRF equipped with a rhodium tube and silicon drift detector (SDD). The instrument has a 10×8 mm ellipse spot size as determined by exposure to x-ray film. Four filters (listed in Table 3-4) were provided with the system to reduce scatter and background. Settings were optimised using Bruker XRayOps software and analysis undertaken with the Bruker S1PXRF package. Qualitative analysis is undertaken using Bruker ARTAX software, quantitative with S1CalProcess (either in S1PXRF or independently in CalProcess). Quantitative analysis was not attempted in this thesis beyond this methodology due to problems relating to quantitative calibrations (documented below and in Nicholas and Manti 2014)) and for fear of presenting a false degree of accuracy. A list of the Bruker software along with the versions used can be found in Table 3-3.

<i>Software</i>	<i>Version</i>	<i>Description</i>
XRayOps	1.2.15	Allows granular control of the tube settings to be used in S1PXRF..
S1PXRF	3.8.30	The software through which spectra are acquired. Can be used to produce quantitative data in collaboration with S1CalProcess.
ARTAX	7.3.50	Software for interpretation and qualitative analysis of spectra.
S1CalProcess	2.2.32	Excel plugin for creating calibrations for use in S1PXRF.

Table 3-3: Bruker HHPXRF software used in this study.

In qualitative analysis spectra are exported from S1PXRF as .txt files (unfortunately this entails a slight loss of resolution as the data is reduced from 2048 channels to 1024) and imported into ARTAX (another Bruker program). Here spectra are de-convoluted and evaluated (this includes background and escape corrections and de-convolution using Bayesian statistics). This produces data on the net peak areas for all chosen elements (pers. comm. Dr Lesley Frame).

Filter Number	Filter Colour	Filter elements and thickness			Notes
		Al	Ti	Cu	
1	Yellow	12 mil / 300 μm	1 mil / 25 μm	N/A	
2	N/A	N/A	N/A	N/A	No filter present
3	Green	12 mil / 300 μm	1 mil / 25 μm	6 mil / 150 μm	
4	Blue	N/A	1 mil / 25 μm	N/A	
5	Red	12 mil / 300 μm	1 mil / 25 μm	1 mil / 25 μm	

Table 3-4: Full range of filters available. Thickness is provided in both Mil (0.001 inch / thousandths of an inch) and micrometres (μm).

In this study each spectra was individually examined in both S1PXRF and Artax for the presence of peaks before processing.

3.3.2 VOLTAGE AND CURRENTS

In order to determine the most appropriate settings with which to analyse the assemblage it was decided to evaluate a range voltages, currents and filters. To achieve this an approach was devised that saw a selection of archaeological finds analysed in order to assess relative HHpXRF performance under the following criteria:

- Levels of background noise
- Trace and minor element peak visibility
- Stability
- Precision

In this study the qualitative analysis and testing focussed on un-quantified materials. Consequently measurement accuracy — whilst being recognised as an important issue — was deemed of not to be of immediate concern during this initial assessment (being best assessed against reference materials). Archaeological objects were selected as the issues encountered (corrosion, sample geometry etc.) were more representative of real world scenarios than would be found solely in reference materials. That there was no known value was not a concern when assessment focussed on relative performance via spectra interpretation.

3.3.2.1 OBJECTS ANALYSED

Five objects were selected for inclusion in this series of test to act as a representative of the issues that are expected to be encountered across the Eriswell assemblage; this included cast copper alloys, hammered silver and copper sheet, objects with varying states of corrosion and one gilded object. An explicit decision was made to choose only objects excavated from securely dated Early Anglo-Saxon deposits to minimise the risk of analysing intrusive later materials with unrepresentative compositions. All objects were from cemetery ERL 046. In Table 3-5 below a brief summary of each of the objects selected is provided:

Site	Small Find No.	Context	Grave No.	Material	Description
046	1812	415	018	Copper alloy, gold	Wrist clasp
046	1813	415	018	Copper alloy	Suspension ring
046	1362	245	007	Copper alloy	Belt ring
046	1087	146	042	Silver	Pendant
046	1603	263	021	Copper alloy	?Spangle

Table 3-5: Summary of the five objects from Eriswell cemetery 046 selected for analysis.

A visual classification focussed on the ascertaining the nature and extent of the corrosion on both brooches and the resulting implications for analytical analysis. The extent of corrosion was recorded using the pro-forma vocabulary outlined in (Robbiola, Blengino, and Fiaud 1998, 2091). The results of the assessment are presented in Table 3-6 below along with a detailed description of the object. The Eriswell objects are not homogeneous constructions, different areas having components created from a selection of different materials in different combinations; consequently, where different materials are present (as with the wrist clasp 1812), a separate assessment is provided for each area. Prior to analysis the objects were not cleaned beyond their current conserved level.

Each object was analysed in two areas, with the exception of the gilded wrist clasp 1812 which was analysed in four areas (two on the copper-alloy reverse, two on the gilded face). The number of areas of analysis was chosen as the maximum possible on the smallest object (spangle 1603). An attempt was made to ensure that the same areas on each object were analysed under each test setting. A brief summary of each object is presented below along with the

rationale for selection. Figure 3-4 (below) shows an image of the front and reverse of each object with the areas analysed highlighted.

Site	Small Find No.	Description	Appearance	Corrosion type	Hardness / Compactly	Limit of Surface
046	1812	<p>Cast copper alloy wrist clasp, gilded on the both hook and eye sides. Possible parallel Hines form B18g? Fully cleaned and conserved, some patina but no pulveresent corrosion.</p> <p>Four areas were analysed in total; two on the un-gilded reverse (areas A & B), 2 on the gilded front (areas C & D, see figure 1).</p> <p>The object was selected because of both its gilded front and the as cast copper-alloy structure. The explicit aims of in selecting this object were to:</p> <ul style="list-style-type: none"> • Test the gilded area to examine the abilities of the HHPXRF to determine mercury levels and to assess the level of substrate detected. • The un-gilded reverse does not sit flat on the window of the HHPXRF (approx. maximum gap of 1 mm), an explicit choice made to assess effectiveness when material is not in full contact with the window. 	Smooth and Shiny (reverse and gilded face)	Uniform (reverse and gilded face)	Very hard (reverse and gilded face)	<p>Untouched at the microscopic scale (reverse).</p> <p>Untouched at the microscopic scale. Gilding remains uncorroded, exposed Cu alloy has some patina (gilded face)</p>
046	1813	<i>A suspension ring (possibly from a necklace) with a 21.09 mm diameter. The ring appears to have been subject to some post casting working. The object was selected because its width did not completely cover the HHPXRF window, offering an opportunity to examine the effect of low count rates on the viability of the data gathered. Two areas were analysed (A & B, see figure 1).</i>	<i>Smooth and Shiny</i>	<i>Uniform</i>	<i>Hard to nearly hard</i>	<i>Untouched at the microscopic scale</i>
046	1362	Cast, wrought, belt ring with a 38.33 mm diameter, round-section and 7.26 mm thickness. Very similar to 1813 but the hoop completely covers HHPXRF window. Selected to act as a comparative to hoop 1813. Two areas were analysed (A & B, see figure 1).	Rough	Uniform	Hard to pulveresent	Deformed
046	1087	<i>Sheet silver disc-shaped pendant (31mm diameter) with zoomorphic raised decoration and form A punched decoration (solid triangular punch) forming a single ring around the outer edge. There is an associated (not analysed) loop of folded copper-alloy sheet that appears to have been attached but weld mark visible on disc. It was attempted to avoid the solder when analysing the disc. The object was selected as being representative of the silver objects from Eriswell, the majority of which are sheet metal. Two areas were analysed (A & B, see figure 1)</i>	<i>Smooth</i>	<i>Uniform</i>	<i>Hard to nearly hard</i>	<i>Untouched at the microscopic scale</i>

Site	Small Find No.	Description	Appearance	Corrosion type	Hardness / Compactly	Limit of Surface
046	1603	Fragment of copper-alloy sheet with 2 small holes and larger hole. Recorded as 'diamond-shaped' on-site, so possibly a spangle (or mount, wrist clasp etc.). Completely covers HHPXRF window. Excavation or post-excavation break shows un-corroded metal remaining in the core of the sheet. Chosen to examine copper alloy sheet metal and the potential effect of pulvaresent corrosion. Two areas were analysed (A & B, see figure 1).	Rough	Uniform	Pulvaresent	Destroyed

Table 3-6: Detailed description and Corrosion assessment of Eriswell non-ferrous objects.

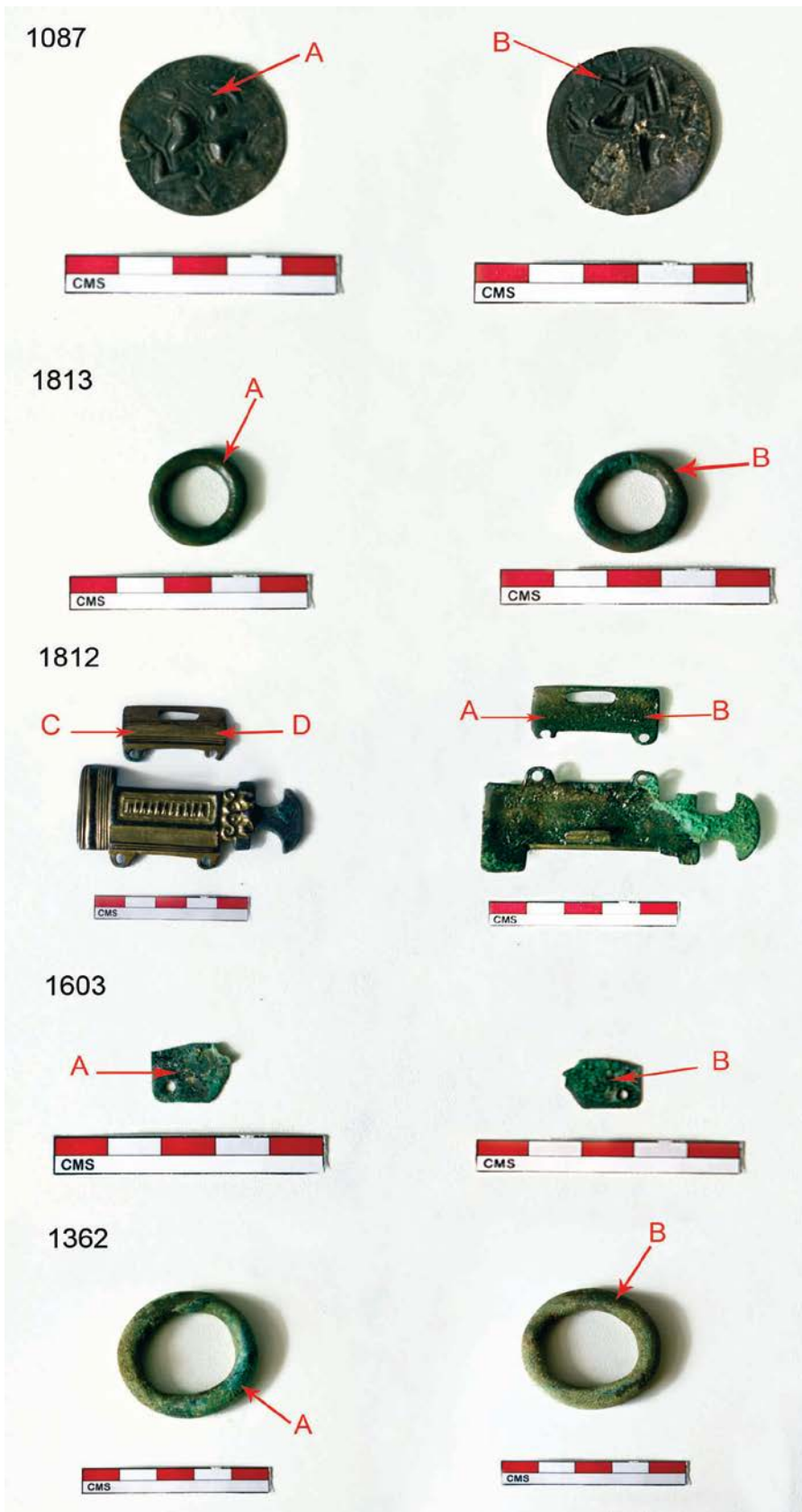


Figure 3-4: Objects analysed with approximate areas targeted highlighted.

3.3.2.2 SETTINGS

The five test objects were analysed under a series of seven settings (listed in Table 3-7). These seven were arrived at by starting with the voltage and current from two settings recommended in the Bruker HHPXRF user manual (Kaiser and Wright 2009, 45–48); ‘lab rat mode’ for general detection of all metallic elements (40 Kv and 0.6 to 1.4 μ A) and ‘Poisons mode’ for higher Z elements (40 Kv and 3.4 to 8 μ A). The suggested micro amperes were increased based on experience of the HHPXRF within Cardiff (pers. comm. Dr Lesley Frame), allowing the opportunity to take advantage of the higher count rates the SDD is capable of compared with Si(PIN) detector available in previous models (100,000 versus 15,000) to arrive at 40 kV / 2.6 μ A and 40 kV / 9.6 μ A. Both of these were applied with a filter (25 μ m titanium - 300 μ m aluminium; setting B & E in Table 3-7) and without (A & D). These two voltage and current settings were augmented by a further two, reached by taking the median current between 2.6 - 9.6 (6.1, setting F in Table 3-7) and 6.1 – 9.6 (7.9, setting G).

Setting Name	High Voltage	Filament Current	High Voltage ADC (Kv)	Anode Current (μ A)	Anode Scaler?	Pulse Length	Filter Setting	Vacuum?
A	164	190	40	2.6	Yes	201	2	No
B	164	190	40	2.6	Yes	201	1	No
C	177	190	40	9.6	No	201	5	No
D	178	190	40	9.6	No	201	2	No
E	178	190	40	9.6	No	201	1	No
F	173	190	40	6.1	No	201	1	No
G	174	190	40	7.9	No	201	1	No

Table 3-7: Tube settings used

As can be seen the voltage applied to the x-ray tube remains consistent at 40 Kv across all settings. This high energy allows for the effective excitation of higher Z elements⁵⁷ above Zinc ($K\alpha$ energy 8.63 keV) such as silver, tin, gold, antimony and mercury. The increase in the current on the x-ray tube does not affect the energy of the x-rays emitted, but will increase the flux (rate of flow). This higher flux leads to higher count rates and higher peaks, but also higher background. Consequently it is important to examine the spectra produced and determine

⁵⁷ Z number refers to the atomic number / the number of protons in a nucleus.

which of the stepped increases (2.6, 6.1, 7.9, 9.6 μA) offers the best peak resolution in the regions of interest.

The 40Kv / 9.6 μA setting was also used with a 25 μm copper - 25 μm titanium - 300 μm aluminium filter (setting C in Table 3-7). The presence of copper in the filter negates its use for the study of copper in the copper alloys, but it does reduce scatter and background in the region of interest for higher Z elements. This area of the spectrum is of particular interest in determining the method used for gilding the Eriswell objects (i.e. is mercury present or not?). This filter was therefore included as a comparison to determine if settings A, B, D and E were adequate for this purpose.

None of the settings were applied with a vacuum, vacuum settings being best suited for lower Z elements (such as silicon, sodium, phosphorus, sulphur, potassium, calcium etc.) which are of little interest in this study of non-ferrous alloys.

Settings were optimised using the Bruker XRayOps software and analysis was undertaken using the Bruker S1PXRF package. All analyses were run for 100 seconds livetime.

Each object was analysed ten times under the setting outlined above, with five analyses being carried out in each area. The decision to analyse two areas was taken because the objects were not large enough to be analysed in more than this. Five analyses were taken in each area to assess the stability of the settings and investigate any possible ionization that might affect the lower Z elements.

Peaks were identified in S1PXRF and double checked in ARTAX. The data was then processed and exported as net peak areas as laid out on page 128. The mean of the ten readings per sample/per condition was taken and the Coefficient of Variation (Cv) calculated.

3.3.2.3 RESULTS

3.3.2.3.1 FILTER VERSUS NONE

The first set in evaluating the results of the different tube settings was to examine the impact of having a filter or not. To do this the four test settings were selected for a visual comparison of the spectra (with a particular focus on the background). These were settings A and B (40Kv and 2.6 μ A without a filter and with filter 1)⁵⁸ and settings D and E (40Kv and 9.6 μ A without a filter and with filter 1). These were chosen as being the high and low extremes of the anode currents chosen for this assessment. The results for two objects, silver sheet 046-1087 (Figure 3-5) and copper alloy sheet 046-1603 (Figure 3-6), are shown over the page.

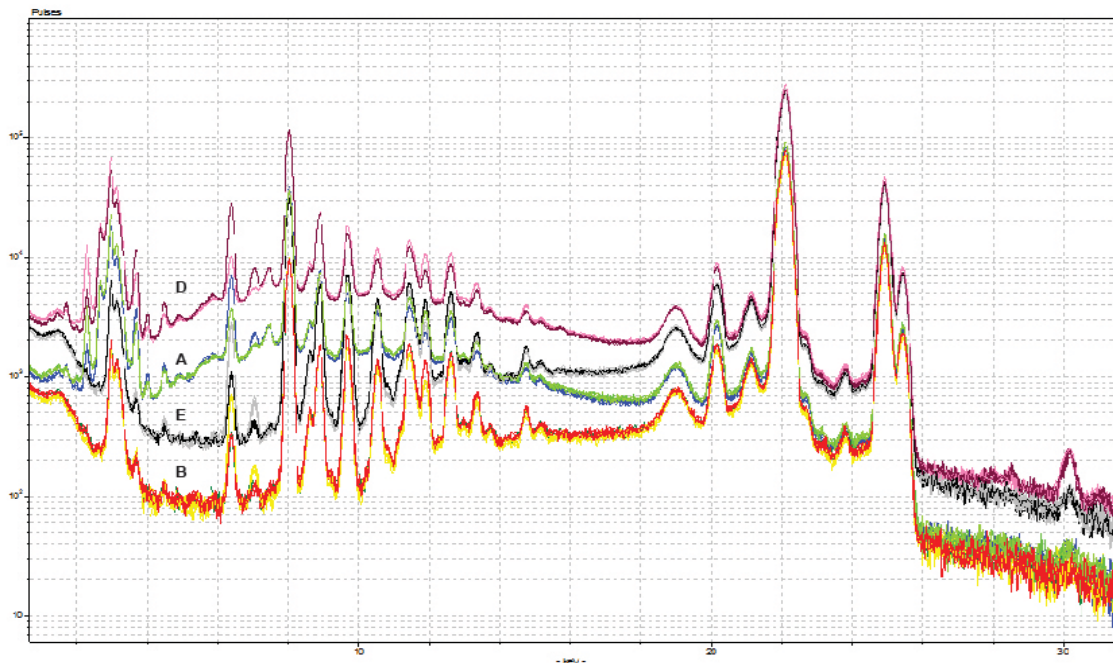


Figure 3-5: Spectra for silver disc 046-1087 normalised to the $K\alpha$ Rhodium peak (20.0740 E/keV). Spectra are presented on logarithmic scale with each individual spectrum colour coded to settings and areas as follows: Test setting A (Area A – green; Area B – blue), B (Area A – red; Area B; yellow), D (Area A – Pink; Area B – Purple) and E (Area A – Black; Area B – Grey).

⁵⁸ The 12 mil / 300 μ m Ti and 1 mil / 25 μ m Al filter.

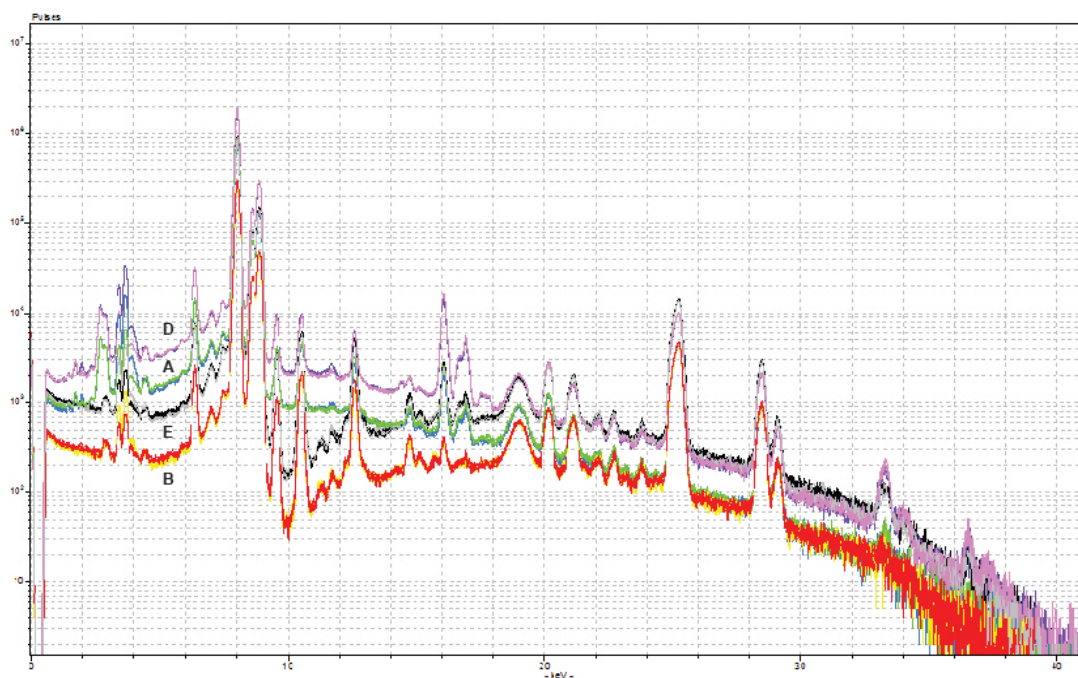


Figure 3-6: Spectra for copper alloy sheet 046-1603 normalised to the $K\alpha$ Rhodium peak (20.0740 E/keV). Spectra are presented on logarithmic scale with each individual spectrum colour coded to settings and areas as follows: Test setting A (Area A – green; Area B – blue), B (Area A – red; Area B – yellow), D (Area A – Pink; Area B – Purple) and E (Area A – Black; Area B – Grey)

The graphs show the spectra normalised to the K-Alpha Rhodium peak (20.0740 keV) and presented on a logarithmic scale with each individual spectrum colour coded to settings and analysis area. It can be seen in both figures that, as expected, the analyses without filters (settings A & D) have substantially higher background than those using filter 1 (settings B & E), particularly in the crucial 10-15 keV range (where peaks for gold, lead, arsenic and mercury are seen). Consequently the HHPXRF will not be used without filters in this study.

3.3.2.3.2 MERCURY DETECTION

The transformative properties of gilding — the act of adding a thin layer of gold atop another material — have been well known from prehistory to the modern day. A variety of techniques can be utilised dependent on material to be gilded, technological knowledge and resources available. These have been neatly summarised in Oddy (1991) who provides an overview of foil gilding, gold leaf, diffusion bonding and fire gilding.

It is generally considered that mercury gilding is the technique most commonly used to gild early medieval non-ferrous objects (Oddy 1980, 129). The mercury

gilding processes (either hot or cold, discussed in more detail in Chapter 6 on page 270) involves the application of mercury to the surface of the non-ferrous object to be gilded. Crucially for analytical purposes some mercury remains after the completion of the gilding process and detectable levels are expected to remain (Lins and Oddy 1975).

In this study it was decided that methodologically, in the first instance, HHPXRF analysis would be undertaken to see if mercury (Hg) and gold (Au) peaks were present (indicating mercury gilding). If not, then optical and electron microscopy would be undertaken to investigate the method further.

Detecting mercury can prove problematic as the gold $L\alpha$ peak at 9.71 keV can obscure the mercury L alpha peak at 9.98 keV. Therefore it was decided to test the impact of different tube and filter settings on mercury detection. As part of this a setting with a different filter (filter 5) was used (setting C).⁵⁹ The results from this setting are not presented here as it quickly became apparent readings using filter 1 were adequately detecting both gold and mercury peaks (the aim here being simple identification). This can be seen below in Figure 3-7, a series of spectra from settings B, E, F and G on object 046-1812. As can be seen, clear gold and mercury peaks are visible. As a comparison the same object was also analysed in a CamScam 2040 SEM. The SEM has a max 20 kV operating range, consequently the peaks examined are the Au $M\alpha$ (2.0450 keV) and Hg $M\alpha$ (2.195 keV). As can be seen in the SEM spectra in Figure 3-16 this peak range offers poor resolution compared with the $L\alpha$ peaks it is possible to examine with the HHPXRF.

⁵⁹ Filter 5: Al 12 mil / 300 μm ; Ti 1 mil / 25 μm ; Cu 1 mil / 25 μm

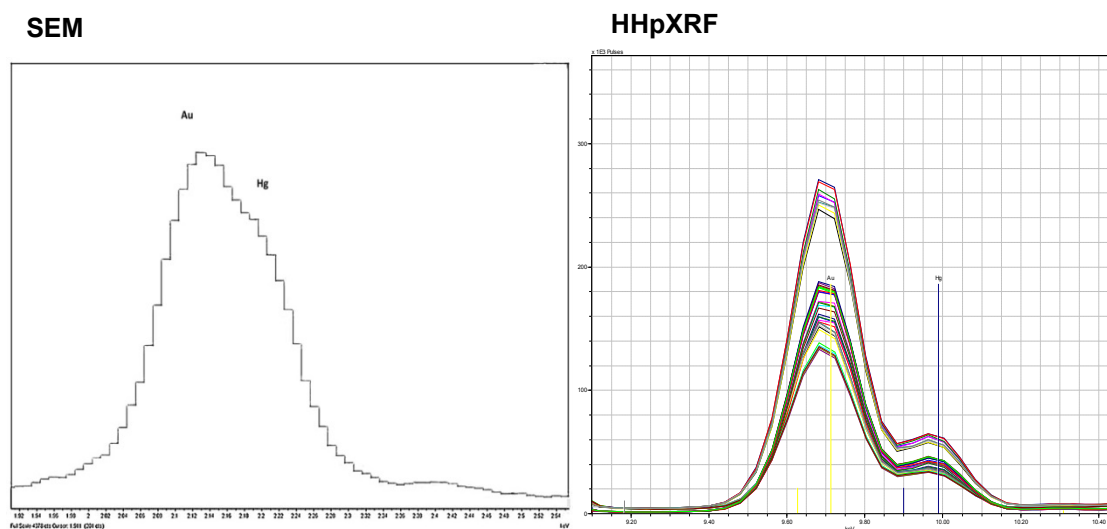


Figure 3-7: Spectra for 046-1812 focussing on the gold and mercury peaks. The spectrum on the left was acquired in an SEM under environmental conditions (using INCA software), the spectra on the right was acquired using an HHpXRF. As can be seen the XRF provides superior resolution in distinguishing between the gold and mercury peaks.

3.3.2.3.3 PEAK AREA AND ANODE CURRENT

It has already been determined in section 3.3.2.3.1 that using filter 1 improves the sensitivity in the mid region of the spectrum (the 10-15 keV range). This eliminated settings A and B (which used no filter, see Table 3-7) from consideration. The use of a copper containing filter (filter 5) was also considered for the identification of higher Z elements (particularly gold and mercury). This was discarded because the copper in the filter would interfere with results and the improved identification offered no improvement for identification purposes than using filter 1. This leaves four remaining settings to be evaluated: B (40 Kv and 2.6 μ A), E (40 kV and 9.6 μ A), F (40 kV and 6.1 μ A) and G (40 kV and 7.9 μ A). The purpose of this section is briefly to examine these four settings and begin to assess which should be examined further for use in this project (minor and trace elements are examined in more detail with the reference materials after this section).

Increasing the anode current is generally seen as being of most use when one wishes to compensate for the loss of intensity when using a lower voltage (Bezur and Casadio 2012, 275). Across all settings the tube voltage is kept at steady 40 kV here, so it may seem that this is a moot point. However, object size and geometries vary greatly and (without a collimator to focus the beam) the peak

intensities from a pin will be considerably lower than a spangle which covers the entirety of the window. This is particularly relevant as the instrument used in this study does not automatically adjust the anode current to attain optimal counts (unlike the NITON XL3t GOLDD+). Table 3-8 (below) shows the net peak areas and coefficient of variation of for the major elements.

Object	Test Setting	Ag K α	Cu K α	Pb L α	Sn K α	Zn K α
1087						
B	Net Peak Area (NPA) mean (n=10)	648219	43408	6239	182	1587
	<i>Coefficient of Variation (C_V)</i>	0.05	0.02	0.1	0.32	0.06
	<i>LDM (\pm)</i>	67278	1468	1195	116	193
E	NPA	2151741	149895	21004	606	5075
	<i>C_V</i>	0.03	0.07	0.08	0.28	0.05
	\pm	143743	22445	3437	335	533
F	NPA	1141616	75955	5331	380	3903
	<i>C_V</i>	0.1	0.05	0.13	0.25	0.14
	\pm	220238	7892	1364	190	1128
G	NPA	1759509	118895	18233	496	5815
	<i>C_V</i>	0.1	0.01	0.08	0.22	0.11
	\pm	359673	1480	2909	216	1254
1362						
B	NPA	1291	532314	260621	50057	4684
	<i>C_V</i>	0.07	0.62	0.69	0.003	0.64
	\pm	186	656477	358066	332	5978
E	NPA	3680	2174177	489911	157866	18441
	<i>C_V</i>	0.06	0.23	0.43	0.03	0.32
	\pm	432	1011566	423528	8846	11802
F	NPA	2235	955419	440981	88225	8667
	<i>C_V</i>	0.07	0.67	0.68	0.06	0.67
	\pm	293	1275995	596914	10416	11665
G	NPA	3812	1611221	740758	149426	14926
	<i>C_V</i>	0.1	0.66	0.66	0.07	0.66
	\pm	763	2118542	971054	21148	19740
1603						
B	NPA	1192	1248741	9620	43157	115660
	<i>C_V</i>	0.08	0.06	0.08	0.04	0.04
	\pm	200	150018	1549	3759	10103
E	NPA	3940	4160050	27159	140596	389101
	<i>C_V</i>	0.09	0.05	0.09	0.03	0.03
	\pm	734	388731	4623	8329	22217
F	NPA	2546	2357980	15703	80116	221729
	<i>C_V</i>	0.05	0.06	0.11	0.05	0.02
	\pm	244	301226	3583	7292	7915

Object	Test Setting	Ag K α	Cu K α	Pb L α	Sn K α	Zn K α	
	G	NPA	3915	3640006	23421	123673	335950
		C_V	0.04	0.04	0.08	0.03	0.03
		\pm	305	295908	3566	7303	18789
1812							
	B	NPA	1161	1315349	10304	43820	8047
		C_V	0.08	0.03	0.06	0.01	0.04
		\pm	191	81718	1271	1210	636
	E	NPA	3356	4042671	29573	127850	24489
		C_V	0.08	0.03	0.08	0.01	0.04
		\pm	559	268796	4582	2389	1926
	F	NPA	2309	2337598	14756	73280	14426
		C_V	0.11	0.03	0.09	0.03	0.04
		\pm	501	140656	2753	4336	1094
	G	NPA	3227	3337964	23969	111022	21601
		C_V	0.07	0.03	0.09	0.03	0.04
		\pm	460	232894	4233	7422	1867
1813							
	B	NPA	1291	532314	260621	50057	4684
		C_V	0.07	0.62	0.69	0.003	0.64
		\pm	186	656477	358066	332	5978
	E	NPA	3680	2174177	489911	157866	18441
		C_V	0.06	0.23	0.43	0.03	0.32
		\pm	432	1011566	423528	8846	11802
	F	NPA	2118	1088356	79481	59028	143083
		C_V	0.14	0.45	0.3	0.23	0.58
		\pm	621	713035	23526	27483	150955
	G	NPA	2944	1764986	135820	74041	299793
		C_V	0.04	0.1	0.13	0.04	0.03
		\pm	225	347605	34755	5542	15515

Table 3-8: Mean net peak area data ($n=10$), coefficient of variation (C_V) and limit of determination (\pm) for major elements on each object (see Figure 3-4 and Table 3-6 for object details) under four different test settings (see Table 3-7, excluding settings A, C and D). The LDM is calculated according Rousseau's (2001) Limit of Determination of a Method (see Equation 5 on page 113 for more details). A full set of data including the minor and trace elements can be found in the relevant net peak area data appendices.

The mean results show an increase in peak area as the anode current (μA) is increased. As illustrated in Table 3-9 the first step (between 2.6 μA and 6.1 μA) tends to show the largest percentage increase in peak area, the second (between 6.7 μA and 7.9 μA) a smaller increase and the third between setting G (7.9 μA) and E (9.6 μA) the smallest. This is reinforced by presenting the figures in bar charts (copper alloy spangle 046-1603 in Figure 3-8 and silver sheet 046-1087 in Figure 3-9).

Object	Test Setting	Ag K α	%	Cu K α	%	Pb L α	%	Sn K α	%	Zn K α	%
1603	B	1192		1248741		9620		43157		115660	
	F	2546	114	2357980	88.83	15703	63	80116	86	221729	92
	G	3915	54	3640006	54.37	23421	49	123673	54.37	335950	52
	E	3940	0.65	4160050	14.29	27159	15	140596	14	389101	16
1812	B	1161		1315349		10304		43820		8047	
	F	2309	99	2337598	77.72	14756	43	73280	67	14426	79
	G	3227	40	3337964	42.79	23969	62	111022	52	21601	50
	E	3356	4	4042671	21.11	29573	23	127850	15	24489	13

Table 3-9: Showing the mean net peak area (data from Table 3-8) and the percentage increase in peak area.

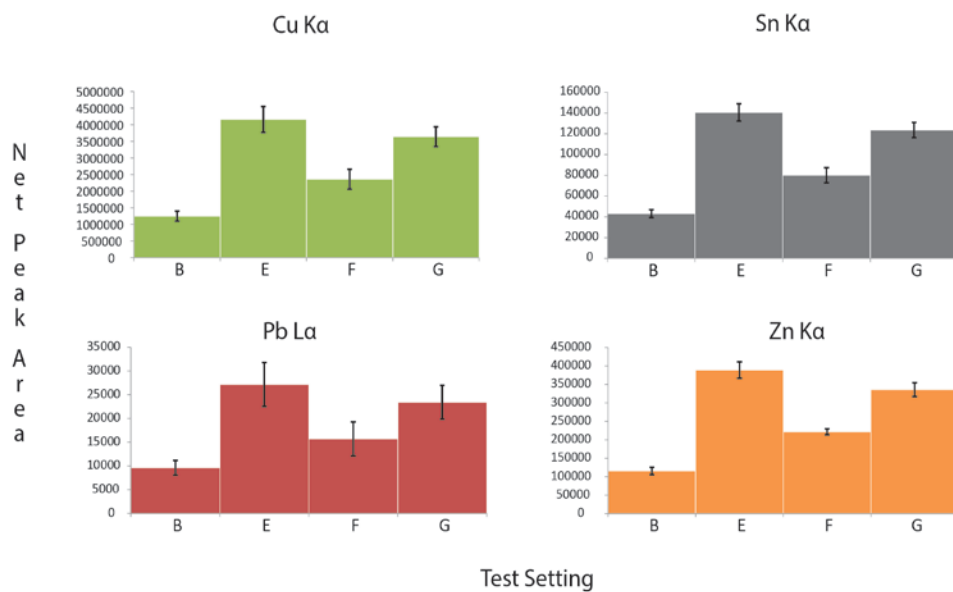


Figure 3-8: Bar charts of the major elements in spangle 046-1603 1087 by test setting (in alphabetical order) with error bars calculated according to Rousseau's (2001) Limit of Determination of a Method (see Equation 5 on page 113 for more details).

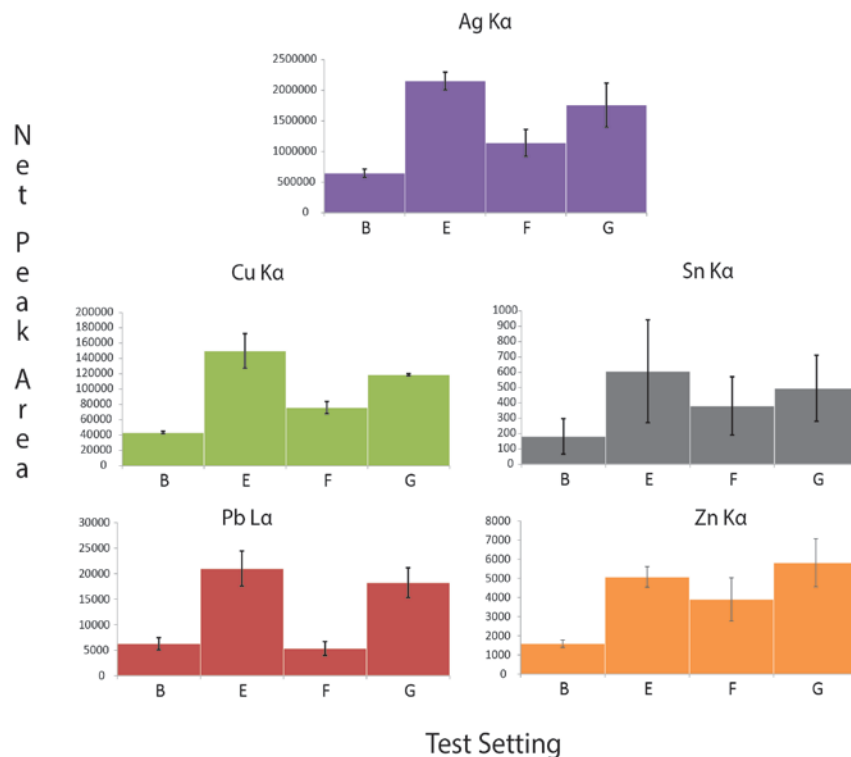


Figure 3-9: Bar charts of the major elements in silver sheet 046-1087 by test setting (in alphabetical order) with error bars calculated according to Rousseau's (2001) Limit of Determination of a Method (see Equation 5 on page 113 for more details). The low lead peak in setting F is due to the analysis being retaken at a later date (due to a memory stick corruption issue) in a slightly different area (i.e. lead segregation).

The error bars in the charts are the Limit of Determination of a Method (LDM) provided in Table 3-8. As can be seen the error tends to increase as the level of the element decreases (Pb in Figure 3-8 and Sn in Figure 3-9 for instance). For the detection of trace and minor elements this could prove an issue, particularly for some of the 'lighter' metallic elements such as Co ($K\alpha$ 6.92); if the error is greater than the peak how secure can we be that it is really there at all? In contrast higher currents increase peak intensities and the security of peak identification (although obviously this is but one factor affecting peak intensity). Consequently it is suggested that, with variable object sizes, a higher current (of either 7.9 or 9.6 μA) is used to ensure effective peak intensities. A filter will reduce the background offers an effective compromise and should ensure optimal analytical performance (following the principles laid out in Shackley 2011, 25) in the analysis of the Eriswell objects.

These two settings will be investigated in more detail in the next section on the analysis of the reference materials.

3.3.3 LIMITS AND STANDARDS

“The nicest thing about standards is that there are so many of them to choose from.”

(Tanenbaum 1988, 254)

The preliminary assessment of five Eriswell objects in the previous section was used along with data from previous analytical studies of early medieval alloys (Mortimer 1991; Blades 1995; Bayley 1991) to select a range of appropriate reference materials to allow an assessment of the sampling uncertainty. As there were no non-ferrous reference materials suitable for use with the HHpXRF in Cardiff University Department of Archaeology and Conservation a total of six (the maximum affordable under the budget available) were chosen and purchased from MBH Analytical.⁶⁰ These were subsequently augmented with a further five certified copper alloys designed to meet ancient alloy compositions produced from the IMMACO project (Wadsak et al. 2000; Beldjoudi et al. 2001) with As, Pb, Sn and Zn certified values valid for an analyses spot diameter 5mm (Ingelbrecht, Adriaens, and Maier 2001). A summary of both the MBH and IMMACO compositions is provided below in Table 3-10. In Appendix I the full set of MBH values (including minor and trace elements) are given along with their certified values and uncertainty.⁶¹

⁶⁰ Holland House, Queens Road, Barnet, EN5 4DJ, England

⁶¹ The IMMACO reference alloys were kindly supplied by Professor Annemie Adriaens, Ghent University.

	Mn	Fe	Co	Ni	Cu	Zn	As	Bi	Pb	Ag	Sn	Sb
31X B5		0.06	0.01	0.01	76.22	23.6	0.01	0.01			0.05	0.01
32X LB10		0.01	0.05	0.69	77.98	0.57		0.06	11.74		8.16	0.59
32X PB10		0.01		0.05	87.85	0.05	0.01	0.01	0.07		11.87	0.02
32x SN6		0.1	0.66	0.2	86.39	1.17	0.77	0.16	1.56	1.16	7.31	0.32
33X GM29		0.01		0.03	89.36	4.23			0.05		6.12	
74X CA7					0.33		0.01	0.01	0.1	4.21	95.26	0.01
IMMACO A	0.2	0.2		0.1	76.5	6	0.2		9		7	0.5
IMMACO B	0.4	0.5		0.2	81.1	15	0.1		0.4		2	
IMMACO C	0.2	0.2			93.4	0.06	5		0.2		0.2	0.5
IMMACO D	0.1	0.1		0.3	78.8	0.1	0.3		10		10	0.3
IMMACO E	0.3	0.3		0.5	90.2	0.1	0.2		0.2		7	0.7

Table 3-10: Given values for major elements in the MBH Analytical and IMMACO reference materials used in this study, In Appendix I a table with minor and trace elements along with uncertainty is provided.

These reference materials were analysed under two settings from Table 3-7: E (40 kV and 9.6 μ A) and G (40 kV and 7.9 μ A) and processed two ways. It should be noted that some of the work here was previously published in a study (Nicholas and Manti 2014) that developed out of the methodology presented here. Data previously published will be referenced back to that article.

As in the previous section ten analyses were taken from each reference material, each from a different area. This permitted assessment of alloy homogeneity and enabled statistical evaluation of the measurements. The Bruker ARTAX software was used for qualitative data analysis with NPA for all elements present calculated (see Table 3-3 on page 128 for software details). Empirical calibrations were constructed using analyses on the MBH and IMMACO alloys. Data were normalised in S1CalProcess using the Region of Interest (ROI). Appropriate slope and background corrections were made for overlapping elements (e.g. lead and arsenic). It should be noted that the performance of calibrations was assessed by treating reference materials as ‘unknowns’. This use of the same alloys constrains calculation of the global uncertainty.

3.3.3.1 CALIBRATED RESULTS

The NPA and wt% concentrations from each analysed sample were averaged (mean, n=10) and the standard deviation (SD), Coefficient of Variation (C_v) and Limit of Determination of a Method (LDM) calculated. The results are presented in Table 3-11 (MBH alloys) and Table 3-12 (IMMACO alloys).

Sample & Description	Fe K α	Co K α	Ni K α	Cu K α	Zn K α	As K α	Bi L α	Pb L β	Ag K α	Sn K α	Sb K α
31X B5											
Given values	0.06	0.01	0.01	76.22	23.6	0.01	0.01			0.05	0.01
40 kV 9.6 μA											
Measured Mean (n=10)	0.05	0.04	0.02	76.63	23.45	0.05	0.03			0.25	nd
SD	0.00 3	0.004	0.002	0.01	0.02	0.00 2	0.001			0.00 3	
C _v	0.05	0.11	0.09	0	0	0.03	0.02			0.01	
LDM (\pm)	0.00 5	0.01	0.004	0.02	0.03	0.00 3	0.001			0.01	
40 kV 7.9 μA											
Measured Mean (n=10)	0.04	0.02	0.04	76.49	23.49	nd	0.02			0.07	nd
SD	0.00 2	0.005	0.002	0.01	0.02		0.000			0.01	
C _v	0.05	0.21	0.05	0.000	0.001		0.005			0.08	
LDM (\pm)	0.00 4	0.01	0.004	0.03	0.04		0.000 2			0.01	
32X LB10											
Given values	0.01	0.05	0.69	77.98	0.57		0.06	11.74		8.16	0.59
40 kV 9.6 μA											
Measured M _i	0.04	0.04	0.69	77.58	0.32		0.02	11.44		8.39	0.58
SD	0.00 3	0.004	0.01	0.13	0.01		0.005	0.1		0.04	0.02
C _v	0.06	0.08	0.01	0.002	0.02		0.3	0.01		0.01	0.03
LDM (\pm)	0.01	0.01	0.01	0.26	0.02		0.01	0.2		0.09	0.03
40 kV 7.9 μA											
Measured Mean (n=10)	0.03	0.03	0.71	78.44	0.36		0.06	11.60		8.16	0.56
SD	0.00 2	0.01	0.01	0.13	0.02		0.001	0.05		0.04	0.01
C _v	0.07	0.19	0.01	0.002	0.04		0.02	0.004		0.01	0.02
LDM (\pm)	0.00 4	0.01	0.02	0.26	0.04		0.002	0.12		0.08 3	0.02
32X PB10											
Given values	0.01		0.05	87.85	0.05	0.01	0.01	0.07		11.8 7	0.02
40 kV 9.6 μA											
Measured M _i	0.05		0.05	87.45	0.01	0.05	0.04	0.09		12.1 1	0.03
SD	0.00 2		0.001	0.04	0.01	0.00 2	0.001	0.01		0.04	0.01
C _v	0.05		0.03	0	0.47	0.04	0.02	0.08		0.00 3	0.27
LDM (\pm)	0.00 4		0.003	0.08	0.01	0.0	0	0.01		0.08	0.01
40 kV 7.9 μA											
Measured Mean (n=10)	0.04		0.04	87.57	0.18	0.01	0.02	0.06		11.9 3	0.04
SD	0.00 2		0.003	0.05	0.01	0.00	0.000	0.01		0.05	0.01
C _v	0.06		0.06	0.001	0.06	0.28	0.01	0.11		0.00	0.19
LDM (\pm)	0.00		0.01	0.10	0.02	0.00 4	0.000 3	0.01		0.10	0.01
32x SN6											
Given values	0.1	0.66	0.2	86.39	1.17	0.77	0.16	1.56	1.16	7.31	0.32
40 kV 9.6 μA											

Sample & Description	Fe K α	Co K α	Ni K α	Cu K α	Zn K α	As K α	Bi L α	Pb L β	Ag K α	Sn K α	Sb K α
Measured M,	0.07	0.66	0.24	86.32	0.95	0.95	0.14	2.78	1.15	7.44	0.34
SD	0.00 2	0.01	0.003	0.03	0.02	0.01	0.004	0.04	0.01	0.03	0.01
C _v	0.03	0.01	0.01	0	0.02	0.01	0.03	0.01	0.01	0.00 4	0.02
LDM (\pm)	0.00 4	0.01	0.01	0.05	0.03	0.02	0.01	0.07	0.01	0.05	0.01
40 kV 7.9 μA											
Measured Mean (n=10)	0.10	0.66	0.23	86.59	1.27	0.99	0.05	2.65	1.15	7.12	0.33
SD	0.00 3	0.01	0.005	0.05	0.02	0.01	0.000	0.03	0.01	0.04	0.01
C _v	0.03	0.01	0.02	0.001	0.02	0.01	0.01	0.01	0.01	0.01	0.03
LDM (\pm)	0.01	0.02	0.01	0.09	0.05	0.02	0.00	0.05	0.01	0.08	0.02
33X GM29											
Given values	0.01		0.03	89.36	4.23			0.05		6.12	
40 kV 9.6 μA											
Measured M,	0.04		0.03	88.8	3.91			nd		5.68	
SD	0.00 2		0.002	0.08	0.01					0.09	
C _v	0.05		0.07	0.001	0.003					0.02	
LDM (\pm)	0.00 4		0.005	0.16	0.02					0.18	
40 kV 7.9 μA											
Measured Mean (n=10)	0.04		0.03	88.60	3.93			nd		6.03	
SD	0.00 2		0.003	0.06	0.02					0.06	
C _v	0.05		0.08	0.001	0.01					0.01	
LDM (\pm)	0.00 4		0.01	0.12	0.05					0.12	
74X CA7											
Given values				0.33		0.01	0.01	0.1	4.21	95.2 6	0.01
40 kV 9.6 μA											
Measured M,				0.33		nd	0.23	0.1	4.23	95.4 1	0.03
SD				0.05			0.005	0.01	0.02	0.17	0.04
C _v				0.14			0.02	0.09	0.005	0.00 2	1.42
LDM (\pm)				0.09			0.49	0.02	0.04	0.34	0.07
40 kV 7.9 μA											
Measured Mean (n=10)				0.34		nd	0.07	0.10	4.24	95.3 4	0.02
SD				0.08			0.002	0.01	0.05	0.13	0.05
C _v				0.22			0.02	0.12	0.01	0.00	2.31
LDM (\pm)				0.15			0.003	0.02	0.11	0.26	0.11

Table 3-11: Given and empirically calibrated measured analyses of the MBH alloys (wt%). Empirically calibrated measured data (Cal. Measured), Standard Deviation (SD), Coefficient of Variation (Cv) and Limit of Determination of a Method (LDM) are presented. The results acquired at 40kV and 9.6 μ A, were previously published in Nicholas and Manti (2014) in Table 1.

Sample & Description	Mn Kα	Fe Kα	Ni Kα	Cu Kα	Zn Kα	As Kα	Pb Lβ	Sn Kα	Sb Kα
IMMACO A									
Given values	0.2	0.2	0.1	76.5	6	0.2	9	7	0.5
40 kV 9.6 μA									
<i>Measured M.</i>	0.2	0.2	0.1	77.2	6.1	0.1	10.5	7.1	0.5
SD	0.01	0.01	0.03	0.46	0.29	0.16	0.52	0.44	0.03
C _v	0.04	0.03	0.39	0.01	0.05	1.9	0.05	0.06	0.06
LDM (\pm)	0.01	0.01	0.05	0.93	0.58	0.31	1.04	0.89	0.05
40 kV 7.9 μA									
<i>Measured M.</i>	0.15	0.17	0.09	77.24	5.97	0.28	9.27	7.13	0.50
SD	0.04	0.03	0.002	0.52	0.20	0.17	0.50	0.08	0.01
C _v	0.28	0.15	0.02	0.01	0.03	0.59	0.05	0.01	0.01
LDM (\pm)	0.09	0.05	0.00	1.05	0.40	0.33	1.56	0.15	0.01
IMMACO B									
Given values	0.4	0.5	0.2	81.1	15	0.1	0.4	2	
40 kV 9.6 μA									
<i>Measured M.</i>	0.4	0.5	0.2	79.6	15.3	0.1	0.7	1.9	
SD	0.01	0.01	0.01	0.11	0.15	0.01	0.04	0.04	
C _v	0.02	0.03	0.04	0.001	0.01	0.08	0.06	0.02	
LDM (\pm)	0.018	0.027	0.02	0.23	0.31	0.02	0.08	0.09	
40 kV 7.9 μA									
<i>Measured M.</i>	0.39	0.49	0.19	79.64	15.35	0.09	0.65	1.95	
SD	0.02	0.01	0.00	0.07	0.12	0.01	0.04	0.02	
C _v	0.05	0.01	0.02	0.00	0.01	0.06	0.05	0.01	
LDM (\pm)	0.15	0.02	0.01	0.48	0.29	0.07	0.10	0.07	0.01
IMMACO C									
Given values	0.2	0.2		93.4	0.06	5	0.2	0.2	0.5
40 kV 9.6 μA									
<i>Measured M.</i>	0.2	0.2		93.6	nd	4.9	nd	0.4	0.4
SD	0.01	0.02		0.41		0.42		0.01	0.01
C _v	0.06	0.11		0.004		0.09		0.01	0.03
LDM (\pm)	0.02	0.05		0.82		0.85		0.01	0.03
40 kV 7.9 μA									
<i>Measured M.</i>	0.21	0.20		93.53	nd	4.92	nd	0.31	0.46
SD	0.02	0.02		0.45		0.38		0.05	0.01
C _v	0.11	0.10		0.005		0.08		0.17	0.02
LDM (\pm)	0.05	0.04		0.91		0.75		0.10	0.02
IMMACO D									
Given values	0.1	0.1	0.3	78.8	0.1	0.3	10	10	0.3
40 kV 9.6 μA									
<i>Measured M.</i>	0.11	0.1	0.38	78.78	0.29	0.31	9.39	9.89	0.24
SD	0.01	0.01	0.06	0.45	0.06	0.07	0.15	0.22	0.06
C _v	0.05	0.14	0.14	0.01	0.20	0.22	0.02	0.02	0.23
LDM (\pm)	0.01	0.03	0.11	0.91	0.12	0.14	0.31	0.45	0.11
40 kV 7.9 μA									

Sample & Description	Mn K α	Fe K α	Ni K α	Cu K α	Zn K α	As K α	Pb L β	Sn K α	Sb K α
<i>Measured M.</i>	0.06	0.05	0.25	79.11	0.28	0.18	10.31	9.90	0.34
SD	0.01	0.00	0.01	0.39	0.07	0.11	0.49	0.14	0.01
C _v	0.21	0.10	0.04	0.00	0.27	0.64	0.05	0.01	0.02
LDM (\pm)	0.03	0.01	0.02	0.77	0.15	0.23	0.98	0.28	0.02
IMMACO E									
Given values	0.3	0.3	0.5	90.2	0.1	0.2	0.2	7	0.7
40 kV 9.6 μA									
<i>Measured M.</i>	0.29	0.33	0.49	89.95	0.62	0.22	0.38	6.83	0.72
SD	0.01	0.02	0.01	0.10	0.02	0.01	0.017	0.09	0.02
C _v	0.04	0.07	0.02	0.001	0.04	0.04	0.04	0.01	0.02
LDM (\pm)	0.02	0.04	0.02	0.19	0.04	0.02	0.03	0.18	0.03
40 kV 7.9 μA									
<i>Measured M.</i>	0.33	0.33	0.48	89.76	0.17	0.19	0.34	6.96	0.71
SD	0.02	0.01	0.01	0.10	0.02	0.01	0.01	0.08	0.02
C _v	0.07	0.04	0.01	0.00	0.11	0.06	0.04	0.01	0.02
LDM (\pm)	0.04	0.02	0.01	0.19	0.04	0.02	0.03	0.16	0.03

Table 3-12: Given and empirically calibrated analyses of IMMACO alloys. Standard Deviation (SD), Coefficient of Variation (C_v) and Limit of Determination of a Method (LDM) are presented. The results acquired at 40kV and 9.6 μ A. were previously published in Nicholas and Manti (2014) in Table 2.

The results show good reproducibility (standard deviation and Limit of Determination) and accuracy for major elements (Cu, Sn, Zn, Pb) at both 7.9 and 9.6 μ A. This decreases for lower concentrations of Pb (32X SN6) and low As content in all alloys.

Reproducibility and accuracy are slightly decreased for the IMMACO metals but mean concentrations lie within certified uncertainty for low arsenic concentrations (IMMACO A, B, D, E), Pb and Sn (IMMACO D). 32X LB10 is very similar to IMMACO D used for calibration. Lead and tin are slightly higher for IMMACO A demonstrating the need for alloys similar in composition used for empirical calibrations. Some variation of lead and tin in leaded bronzes may be due to inhomogeneity and a larger analysis spot size used compared to certification (IMMACO alloys certified values valid for an analysis spot diameter 5mm, Bruker Tracer III-SD spot size of 10 x 8mm ellipse).

To visualise the performance of the calibrations the results are plotted against the given values in a scatter plot and the R² calculated (Figure 3-10 below). As can be

see both settings perform well with the exception of bismuth (Bi) and there is little to choose between them.

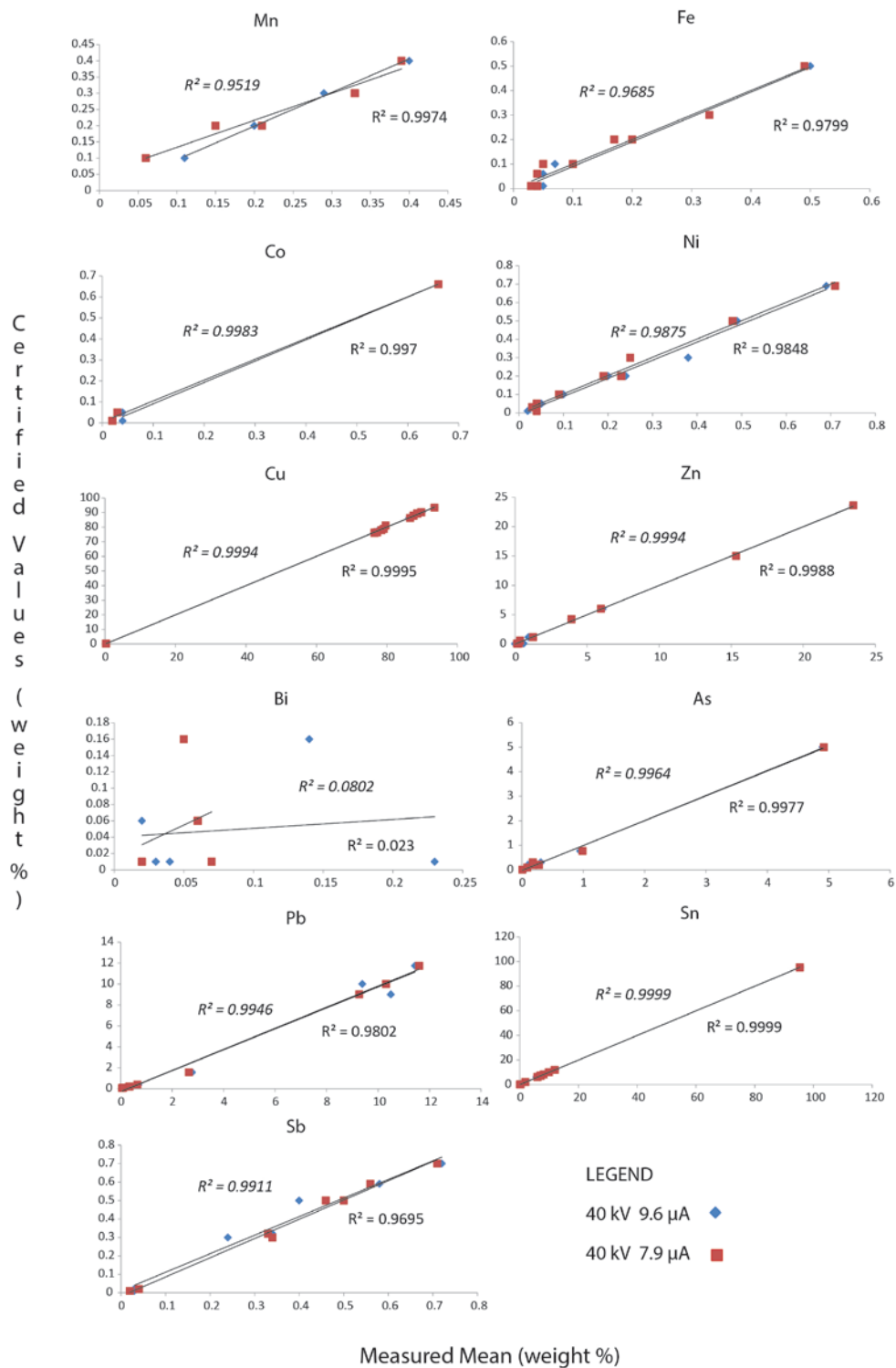


Figure 3-10: Scatter plot of measured mean ($n=10$) quantitative results on reference alloys at two settings against certified values. The R^2 values in the top left are for 40 kV - 7.9 μ A, bottom right for 40 kV - 9.6 μ A.

3.3.3.2 NET PEAK AREA RESULTS

The same spectra as used in the quantitative results were produced using Bruker's Artax software to produce Net Peak Areas. The results (MBH reference materials in Table 3-11 and IMMAGO in Table 3-12) show that the 7.9 μA setting tends to be associated with lower peak areas than the 9.6 μA setting (no surprise). The 7.9 μA setting appears to show good reproducibility for copper, tin and zinc, but significant spread for arsenic and lead. The 9.6 μA setting shows similar results except for copper, where it failed to produce a peak area for MBH reference alloy 74X CA7 (given value 0.33%, see previous tables).

It is interesting to note that where small peaks were visually confirmed in spectra (such as arsenic in IMMAGO A and zinc in IMMAGO E) qualitative processing was more successful than the calibration at identifying them. This may indicate that a better selection of reference materials is required to improve performance, however, it should be noted that previous studies are contradictory in whether an increased number of reference materials improves accuracy previous work suggests increasing the number of standards improves accuracy.⁶²

High lead (as with 32X LB10, IMMAGO A and D) appears to decrease the reproducibility of the major element present (in this case copper) when compared with lower lead alloys with the same major element (see for instance 31X B5). This is no great surprise given that lead does not typically alloy with cast copper alloys (Scott 1991: 27) instead forming separate crystals (although this increased error may also be due to the use of a larger spot size than those used in the certification).

⁶² Heginbotham et al. (2011, 186) suggest that (generally) it does not, whilst Johnson (2014, 584) both notes and demonstrates that the Bruker S1CalProcess software is designed to work with a large number of reference materials.

Sample & Description	Fe K α	Co K α	Ni K α	Cu K α	Zn K α	As K α	Bi L α	Pb L α	Ag K α	Sn K α	Sb K α
31X B5											
40 kV 9.6 μA											
Measured Mean (n=10)	7176	1310	528	5138163	2081478	1145	351			1174	220
SD	288	187	191	8791	4610	61	48			203	105
C _v	0.04	0.14	0.36	0.00	0.002	0.05	0.14			0.17	0.48
LDM (\pm)	601	379	399	16230	8310	114	90			382	187
40 kV 7.9 μA											
Measured M.. (n=10)	6113	1214	712	4506236	1869032	595	855		1051	835	94
SD	254	237	132	16293	7256	72	123		163	76	26
C _v	0.04	0.20	0.19	0.004	0.004	0.12	0.14		0.15	0.09	0.28
LDM (\pm)	508	474	264	32587	14513	933	1299		326	151	52
32X LB10											
40 kV 9.6 μA											
MM	3652	3085	34717	4577112	50948		7879	27782 8		116082	612 7
SD	236	288	346	22193	359		133	5860		652	247
C _v	0.06	0.09	0.01	0.005	0.01		0.02	0.02		0.01	0.04
LDM (\pm)	529	600	719	44634	1845		268	11720		1309	494
40 kV 7.9 μA											
Measured M.	3021	2775	30451	3968756	50969	559	24015 6	24015 5	1353	98782	477 8
SD	155	136	372	15164	605	46	3678	95	106	517	169
C _v	0.05	0.05	0.01	0.004	0.01	0.08	0.02	0.04	0.08	0.01	0.04
LDM (\pm)	314	301	753	31673	4986	488	50099 4	50104 8	218	1035	339
32X PB10											
40 kV 9.6 μA											
Measured M,	3936		7546	5313567	18454	756	736	2093		195611	192
SD	344		209	7291	345	110	67	119		876	124
C _v	0.09		0.03	0.001	0.02	0.15	0.09	0.06		0.004	0.65
LDM (\pm)	689		418	14582	690	220	134	237		1753	248
40 kV 7.9 μA											
Measured M.	3146	521	3826	4580459	21851	587	1973	1973	1169	165016	42
SD	188	211	226	12376	265	62	153	48	125	1213	40
C _v	0.06	0.41	0.06	0.003	0.01	0.11	0.08	0.14	0.11	0.01	0.95
LDM (\pm)	376	423	452	24753	530	354	3416	3428	251	2427	79
32x SN6											
40 kV 9.6 μA											
Measured M,	8364	51219	10141	5394683	113999	30654	5411	48970	37672	119022	388 6
SD	348	1338	260	129594	2615	760	244	1310	1105	2496	145
C _v	0.04	0.03	0.03	0.02	0.02	0.02	0.05	0.03	0.03	0.02	0.04
LDM (\pm)	9281	107979	7685	693736	562400	64624	11407	98980	79420	41938	819 3

Sample & Description	Fe K α	Co K α	Ni K α	Cu K α	Zn K α	As K α	Bi L α	Pb L α	Ag K α	Sn K α	Sb K α
40 kV 7.9 μA											
Measured M.	6624	43290	9294	4548447	107390	606	40352	40352	31792	97137	269 2
SD	173	352	291	13225	681	38	597	76	246	856	133
C _v	0.03	0.01	0.03	0.003	0.01	0.06	0.01	0.02	0.01	0.01	0.05
LDM (\pm)	345	704	583	26451	1363	56569	77275	77284	492	1712	267
33X GM29											
40 kV 9.6 μA											
Measured M.	3977		6502	5722269	380760			2019		99210	
SD	397		224	32887	2168			96		1878	
C _v	0.1		0.03	0.006	0.006			0.05		0.02	
LDM (\pm)	8385		13707	1206360 2	802713			3794		213659 8	
40 kV 7.9 μA											
Measured M.	3313	385	2712	4943599	349116	590	1478	1478	1109	84675	35
SD	159	181	157	22000	1716	40	156	48	143	1106	26
C _v	0.05	0.47	0.06	0.004	0.005	0.07	0.11	0.23	0.13	0.01	0.73
LDM (\pm)	318	362	315	44000	3431	1048	2680	2697	287	2212	51
74X CA7											
40 kV 9.6 μA											
Measured M.		2684				3869	348	3814	18255 8	111267 7	nd
SD		413				119	77	144	668	4835	23
C _v		0.15				0.03	0.22	0.04	0.004	0.004	1.33
LDM (\pm)		101763					10604	94841	30592 5	209581 6	815 9
40 kV 7.9 μA											
Measured M.	2015	71	140	13173	431	818	5262	5262	15459 8	933941	11
SD	247	50	49	148	52	36	146	77	1964	13527	31
C _v	0.12	0.71	0.35	0.01	0.12	0.04	0.03	0.29	0.01	0.01	2.80
LDM (\pm)	494	101	98	297	104	1541	10546	10549	3928	27054	63

Figure 3-11: Qualitative analyses of the MBH alloys (net peak area). Empirically calibrated measured data (Cal. Measured), Standard Deviation (SD), Coefficient of Variation (C_v) and Limit of Determination of a Method (LDM) are presented.

Sample & Description	Mn K α	Fe K α	Ni K α	Cu K α	Zn K α	As K α	Pb L α	Sn K α	Sb K α
IMMACO A									
40 kV 9.6 μA									
Measured Mean (n=10)	5268	10530	9075	4403332	524931	11586	156270	102880	5214
SD	324	342	456	66666	26648	2541	12400	1336	117
C _v	0.06	0.03	0.05	0.02	0.05	0.22	0.08	0.01	0.02
LDM) (\pm)	648	685	912	133332	53297	5082	24800	2671	234
40 kV 7.9 μA									
Measured Mean (n=10)	2775	8099	8468	3838241	431288	6760	87875	89508	4588
SD	1357	938	417	126941	21812	2944	41399	1454	218
C _v	0.49	0.12	0.05	0.03	0.05	0.44	0.47	0.02	0.05
LDM) (\pm)	2714	1876	834	253881	43625	5888	82799	2909	436
IMMACO B									
40 kV 9.6 μA									
Measured M.	12956	30466	14914	4834170	1256514	2807	9643	31047	
SD	792	567	317	61163	19956	506	407	666	
C _v	0.06	0.02	0.02	0.01	0.02	0.18	0.04	0.02	
LDM) (\pm)	1583	1134	635	122327	39912	1012	815	1333	
40 kV 7.9 μA									
Measured M.	10968	26720	13526	4167562	1107308	2609	8051	26903	
SD	433	391	362	57227	16501	301	370	444	
C _v	0.04	0.01	0.03	0.01	0.01	0.12	0.05	0.02	
LDM) (\pm)	1260	939	751	161776	33847	2262	32434	1753	
IMMACO C									
40 kV 9.6 μA									
Measured M.	<i>6225</i>	<i>12281</i>		<i>5879435</i>	nd	<i>240729</i>	<i>8076</i>	<i>3646</i>	<i>6255</i>
SD	963	1100		85142		21190	1282	156	291
C _v	0.15	0.09		0.01		0.09	0.16	0.04	0.05
LDM) (\pm)	1926	2201		170285		42381	2565	312	582
40 kV 7.9 μA									
Measured M.	5364	11150		5062741	nd	207468	6715	3159	5514
SD	654	947		53108		16534	803	96	83
C _v	0.12	0.08		0.01		0.08	0.12	0.03	0.02
LDM) (\pm)	1308	1894		106216		33067	1606	192	167
IMMACO D									
40 kV 9.6 μA									
Measured M.	<i>1254</i>	<i>3901</i>	<i>18172</i>	<i>4362832</i>	<i>33055</i>	<i>18718</i>	<i>268101</i>	<i>137945</i>	<i>2862</i>
SD	296	212	322	80094	2121	2415	35092	2818	150
C _v	0.24	0.05	0.02	0.02	0.06	0.13	0.13	0.02	0.05
LDM) (\pm)	592	424	644	160188	4242	4830	70184	5637	300
40 kV 7.9 μA									
Measured M.	1361	3238	16047	3720113	32032	14989	191065	117565	2558
SD	415	240	496	85206	946	4016	43931	2195	172
C _v	0.31	0.07	0.03	0.02	0.03	0.27	0.23	0.02	0.07
LDM) (\pm)	831	481	992	170412	1891	8033	87862	4390	343
IMMACO E									

Sample & Description	Mn K α	Fe K α	Ni K α	Cu K α	Zn K α	As K α	Pb L α	Sn K α	Sb K α
40 kV 9.6 μA									
Measured M.	8854	16140	28490	5082641	38244	7111	6352	108087	7818
SD	1057	527	562	59263	1774	365	259	1858	237
C _v	0.12	0.03	0.02	0.01	0.05	0.05	0.04	0.02	0.03
LDM (\pm)	2114	1054	1124	118526	3548	731	518	3717	475
40 kV 7.9 μA									
Measured M.	7609	14241	24855	4389192	38693	6288	5302	93623	6771
SD	696	722	563	81968	1389	438	196	2692	275
C _v	0.09	0.05	0.02	0.02	0.04	0.07	0.04	0.03	0.04
LDM (\pm)	1392	1444	1127	163936	2779	875	392	5384	550

Figure 3-12: Qualitative analyses of IMMACO alloys. Standard Deviation (SD), Coefficient of Variation (C_v) and Limit of Determination of a Method (LDM) are presented. The results acquired at 40kV and 9.6 μ A. were previously published in Nicholas and Manti (2014) in Table 3.

To visualise the performance of the net peak area results they are plotted against the given values in a scatter plot and the R² calculated (Figure 3-13 below). The results have not undergone the same corrections as the calibrated results, so naturally they are not numerically correct as the weight percent version of the same graph (Figure 3-10). Having said that, both settings are still performing reasonably well (again with the exception of bismuth) with the exception of the 9.6 μ A setting on copper, where the failure to produce a peak area for MNH reference alloy 31X B5 has a considerable impact on the R² score.

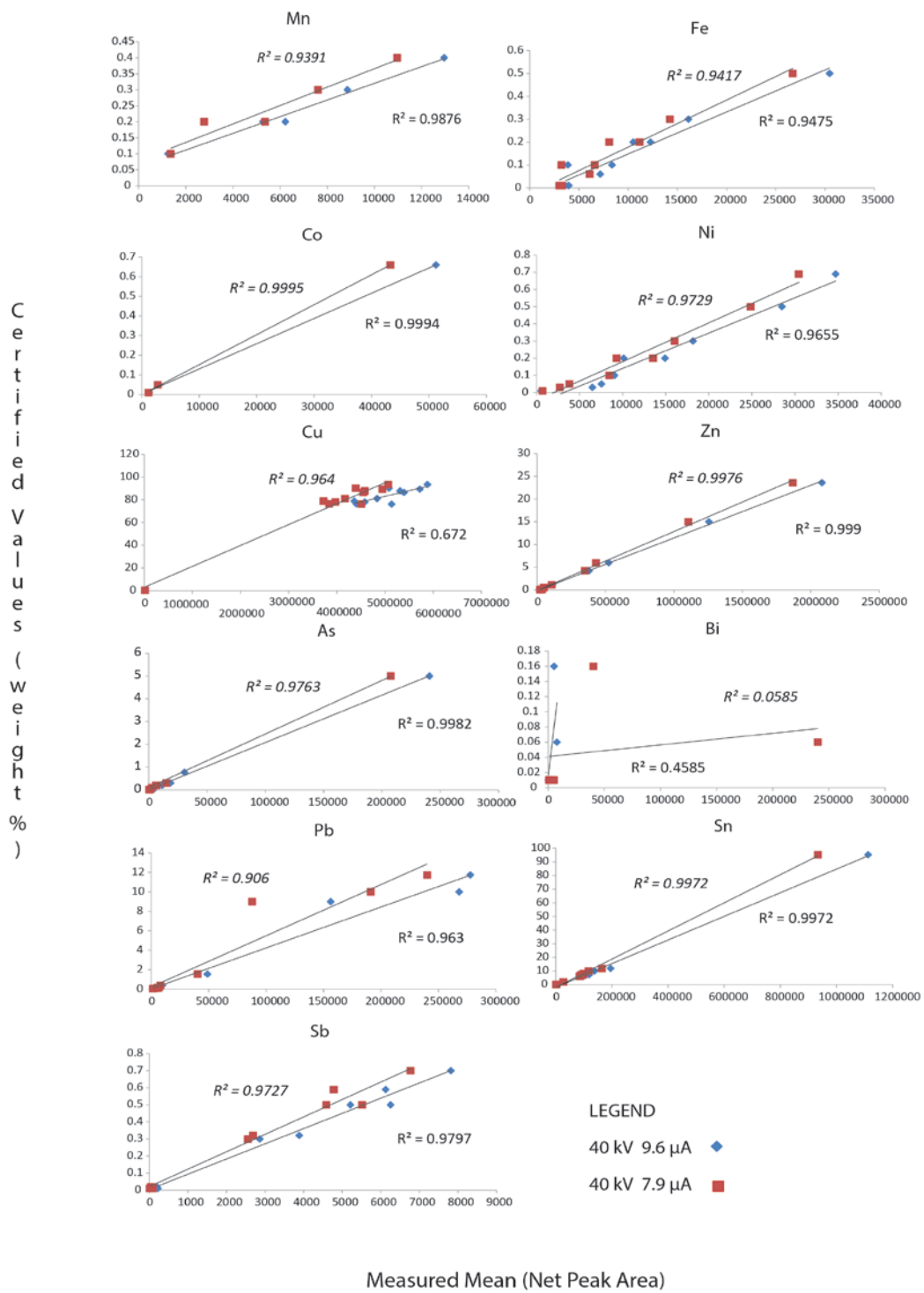


Figure 3-13: Scatter plot of the measured mean ($n=10$) qualitative results on reference alloys at two settings against certified values. The R^2 values in the top left are for 40 kV - 7.9 μ A, bottom right for 40 kV - 9.6 μ A.

3.3.3.3 7.9 OR 9.6 μ A

The purpose of section 3.3.2 (page 129) was to evaluate a range of tube settings and decide on one that would offer the best performance. Of the initial settings two were retained for assessment with the reference alloys. Both had the same kV (40) and filter (filter 1: 25 μ m titanium and 300 μ m aluminium) with variation occurring in the anode current: 7.9 and 9.6 μ A.

Calibrations were produced for both settings using a set of reference alloys and tested on those same reference alloys. The calibrations at both settings performed well. The same spectra were also processed as net peak areas (i.e. qualitatively). For the most part the results show a relatively good degree of reproducibility and a reasonable degree of correlation with the given values. There was an exception with the bismuth values (where the results are admittedly terrible) and the performance of the 9.6 μ A at detecting a low copper peak (in sample 31X B5).

With relatively little between them choosing a setting with which to progress is not obvious. The poor performance of the 9.6 μ A setting on a small copper value is a worry, especially if reproduced in reference alloys with similar matrices. Unfortunately there was not the budget within the Department of Archaeology at Cardiff to buy more samples and assess this. As a result — whilst being aware that this may have been a one off — it is thought that it perhaps best to choose 7.9 μ A.

3.3.3.4 NET PEAK AREA OR WEIGHT PERCENT

In this section the spectra have been processed two ways: as net peak areas and using a calibration (producing results in weight percent). Which one of these should be used in this study?

The calibrated results are in closer agreement with the given values than the net peak areas. Yet these results were gained on a cleaned and uncorroded surface. The Eriswell objects will be analysed on their corroded surface (sampling or cleaning a large enough area to analyse with the Bruker Tracer III-SD would risk damaging the aesthetic integrity of the artefacts), affecting the results and leading

them to deviate from the ‘true’ compositions. This was demonstrated in a separate study by experimentally corroding the IMMACO alloys used here (Nicholas and Manti 2014). The results showed a significant increase in LDM (the \pm) as a result of the corrosion processes and the increased inhomogeneity of the sample introduced by the corrosion layer. This increase in LDM suggests that treating the data produced using the empirical calibration as quantitative would be an error. In contrast the reproducibility in the corroded alloys (however processed) is within an acceptable range for most qualitative archaeological interpretations.

The work here has shown that processing data as net peak areas can result in data that are less numerically accurate than those produced using an empirical calibration. This is not to suggest that the use of a calibration (produced empirically or otherwise) should be the preferred choice for data processing, but that there is a case for processing corroded copper alloy data in the following order:⁶³

- Data processed using net peak areas (or similar): allows a presence / absence assessment to be combined with the production of numerical data that can be statistically interpreted. Unknown samples can be assessed and broadly classified.
- Where appropriate calibrations (and/or appropriate standards to create an appropriate calibration) exist the data can be reprocessed using these to provide figures that take into account element energy overlaps (slope corrections) etc. Although processed using a calibration it should be remembered that these data are still qualitative.

The latter point presents a significant issue: how one can provide numerical data processed in this manner (i.e. weight percent or ppm) with enough caveats that they will not be subsequently mistaken for quantitative.

⁶³ XRF calibrations – on portable instruments or otherwise – are best suited when the unknown is relatively known. Given the highly mixed nature of Anglo-Saxon alloys it is doubtful that Cardiff University currently has enough reference materials to make the unknown known.

There is nothing inherently quantitative in the use of a calibration in the production of weight percent data (to some extent the difference between quantitative and qualitative data is a matter of scale) and it is possible to produce qualitative data using a calibration (see Davis 2014, 173–174).⁶⁴ Despite this in archaeology weight percent data are often viewed as quantitative and it is a significant concern here that, no matter the error margins presented and qualifications made, a figure of 2% \pm 1.5% for an element will be taken by many non-archaeometrists as simply 2%. Net peak areas in contrast have a certain usefulness in this area, being obscure enough a format to avoid misuse. This obscure format does of course present its own challenges: how to interpret the data. This will be the subject of the next chapter.

Subsequent to the production of this methodology, a study (Johnson 2014) has backed up (to some extent) the decision not to use calibrated results. This study examined the performance of the Bruker S1CalProcess calibration construction software against a custom built calibration tool (using the statistical programming language R). The results showed that S1CalProcess performed poorly especially when there were only a limited range of reference alloys. As financial constraints mean only a small number of reference alloys were affordable for this project it seems that it was retrospectively prudent to avoid using the software.

3.3.3.4.1 LIMITS

Using the formula from Equation 4 (page 113) the lower limit of detection was calculated for the MBH reference alloys. This illustrates the lowest net peak intensity that can be detected. In practical terms it is of limited use (and so will not be reported here) as the Eriswell materials are corroded and the standards are not (leading to very different backgrounds). Nevertheless it was found to be a useful exercise to this HHPXRF operator in the early stages in corroborating visual identifications in assisting in illuminating when a peak can genuinely be said to be present or not.

⁶⁴ Of course in pursuit of smaller scales one must be careful not to end up a modern day version of Zeno's Achilles and the Tortoise paradox.

The Limit of Determination of a Method (LDM) was calculated for each reference alloy. Taking the maximum values across all alloys for each element presents the lowest level of the element that can be detected in matrices similar to the reference alloys (Table 3-13). Whilst some may think of the LDM as fundamentally different from an Instrumental Limit of Detection, in practical terms the LDM performs the same function and is superior (as ILDs are much lower than the real world limit of detection, see Rousseau (2001) for a discussion) and the \pm becomes an indicator of the minimum amount that can be identified (i.e. with an LDM of 0.75% an arsenic result of 0.6% has an error margin between existence or not).

	Mn	Fe	Co	Ni	Cu	Zn	As	Bi	Pb	Ag	Sn	Sb
Weight %	0.15	0.05	0.02	0.02	1.05	0.4	0.75	0.003	1.56	0.11	0.28	0.11
NPA	2714	1894	704	1127	253881	43625	56569	500994	501048	3928	27054	550

Table 3-13: Maximum LDM (\pm) values across all MBH and IMMACO reference alloys as analysed at 40 keV - 7.9 μ A.

Of course the spectra are not being processed quantitatively here so this should be viewed merely as an indicator of potential performance under optimum conditions of a flat uncorroded sample.

3.4 FURTHER ISSUES

There are a number of further issues that impact on HHPXRF practice and the quality of the results. These will be briefly examined here.

3.4.1 COPPER ALLOY PENETRATION DEPTH

Understanding how deep the x-rays are penetrating into the sample and from where the signal is derived is crucial. If the object being analysed is too thin then it may not attenuate the entire signal and will therefore not be infinitely thick (this has an impact on how you process the data, particularly with calibrations). To prevent this critical penetration depth can be calculated using the formula in Equation 6.

$$t_{\text{crit}} = -\text{LN}\left(\frac{I}{I_0}\right)/p\mu_{\text{tot}}$$

Where:

$$\mu_{\text{tot}} = \mu(E_0)\text{csc}\Psi_1 + \mu(E_i)\text{csc}\Psi_2$$

Equation 6: Equation from Potts, Williams-Thorpe, and Webb (1997, 32, Equation 2) for calculating the critical penetration depth where p is the density of the sample, Ψ_1 is the incident angle, Ψ_2 the take-off angle, $\mu(E_0)$ the mass attenuation coefficient primary radiation (cm^2/g) and $\mu(E_i)$ the mass attenuation coefficient characteristic radiation (cm^2/g).

This equation (from Potts, Williams-Thorpe, and Webb 1997) calculates the depth from which a certain percentage of the signal is derived depending on the alloy density and the incident photon energy. At 99% penetration this is known as the critical penetration depth or t_{crit} , above this thickness the signal is attenuated by the sample. If the sample is thinner than the t_{crit} for a peak of interest then it is not infinitely thick for that peak.

This is calculated on a selection of the MBH reference materials analysed earlier. First the compositions are normalised and the density calculated (see Table 3-14). The mass attenuation coefficients were derived from the NIST XCOM database (Berger et al. 2010) and the critical penetration depths calculated for each element of interest using an incident angle (from the tube to the sample) of 52°

and take-off (from sample to detector) angle of 63° (converted into radians for the calculation) and an incident energy of 40 keV.

	Reference Material					
	31X B5	32X LB10	32X PB10	32x SN6	33X GM29	74X CA7
<i>Fe</i>	0.06	0.01	0.01	0.1	0.01	
<i>Co</i>	0.01	0.05		0.66		
<i>Ni</i>	0.01	0.69	0.05	0.2	0.03	
<i>Cu</i>	76.22	77.98	87.85	86.39	89.36	0.33
<i>Zn</i>	23.6	0.57	0.05	1.17	4.23	
<i>As</i>	0.01		0.01	0.77		0.01
<i>Bi</i>	0.01	0.06	0.01	0.16		0.01
<i>Pb</i>		11.74	0.07	1.56	0.05	0.1
<i>Ag</i>				1.16		4.21
<i>Sn</i>	0.05	8.16	11.87	7.31	6.12	95.26
<i>Sb</i>	0.01	0.59	0.02	0.32		0.01
ρ (g•cm ⁻³)	8.449296	8.996476	8.735127	8.802318	8.750045	7.466169

Table 3-14: MBH reference alloy compositions with density.

The results (Table 3-15) show the critical penetration depth along with the depths that would provide 90, 80 and 50% of the signal for that element’s energy. Those peaks with high characteristic photon energies — such as Ag K α (22.16 keV), Sn K α (25.27 keV) and Sb K α (26.4 keV) — have, not surprisingly, the thickest t_{crit} values. The thickest t_{crit} value across all the MBH alloys is 207 μ m (0.2 mm) for the Sb K α peak in 31X B5. This is still thinner than any sheet in the Eriswell assemblage (where possible — i.e. the sheet was not still soldered to a larger object — the thickness of sheets was measured using a calibrated Mitutoyo digital Vernier calliper).

If one overly focusses on the t_{crit} value then there is a danger of overlooking another significant fact: the contribution is not uniform as depth increases and 50% of the signal originates from near the surface of the object. As the Eriswell objects are being analysed on the corroded surface the contribution of corrosion product needs to be taken into account.

Element	Fe	Co	Ni	Cu	Zn	As	Bi	Pb	Ag	Sn	Sb
Peak	$K\alpha$	$K\alpha$	$K\alpha$	$K\alpha$	$K\alpha$	$K\alpha$	$L\alpha$	$L\alpha$	$K\alpha$	$K\alpha$	$K\alpha$
Photon energy (KeV)	6.40	6.93	7.48	8.05	8.64	10.54	10.84	10.55	22.16	25.27	26.36
T_{crit} (μm)											
31X B5	46.09	56.60	68.51	82.23	97.80	24.20	25.92		30.87	205.11	224.24
32X LB10	26.59	32.44	39.14	46.70	54.20		25.27	25.27		158.61	172.14
32X PB10	32.12		47.58	57.00	67.61	24.65	26.40	25.22	32.18	192.87	209.10
32x SN6	33.36	40.85	49.26	57.68	68.02	24.57	26.30	25.14	143.91	188.63	200.56
33X GM29	37.38		55.48	66.54	79.00			24.69		196.65	
74X CA7				20.68		38.51	41.07	39.37	144.78	165.69	174.29
90% signal (μm)											
31X B5	23.05	28.30	34.25	41.12	48.90	12.10	12.96		102.55	102.55	112.12
32X LB10	13.30	16.22	19.57	23.35	27.10		12.63	12.63		79.30	86.07
32X PB10	16.06		23.79	28.50	33.81	12.32	13.20	12.61	16.09	96.44	104.55
32x SN6	16.68	20.42	24.63	28.84	34.01	12.29	13.15	12.57	71.95	94.32	100.28
33X GM29	18.69		27.74	33.27	39.50			12.34		98.32	
74X CA7				10.34		19.26	20.54	19.68	72.39	82.84	87.14
80% signal (μm)											
31X B5	16.11	19.78	23.94	28.74	34.18	8.46	9.06		71.68	71.68	78.37
32X LB10	9.29	11.34	13.68	16.32	18.94		8.83	8.83		55.43	60.16
32X PB10	11.22		16.63	19.92	23.63	8.61	9.22	8.81	11.25	67.41	73.08
32x SN6	11.66	14.28	17.22	20.16	23.77	8.59	9.19	8.79	50.29	65.92	70.09
33X GM29	13.07		19.39	23.25	27.61			8.63		68.73	
74X CA7				7.23		13.46	14.35	13.76	50.60	57.90	60.91
50% signal (μm)											
31X B5	6.94	8.52	10.31	12.38	14.72	3.64	3.90		30.87	30.87	33.75
32X LB10	4.00	4.88	5.89	7.03	8.16		3.80	3.80		23.87	25.91
32X PB10	4.83		7.16	8.58	10.18	3.71	3.97	3.80	4.84	29.03	31.47
32x SN6	5.02	6.15	7.42	8.68	10.24	3.70	3.96	3.78	21.66	28.39	30.19
33X GM29	5.63		8.35	10.02	11.89			3.72		29.60	
74X CA7				3.11		5.80	6.18	5.93	21.79	24.94	26.23

Table 3-15: Depth (μm) from which the stated percentage for the relevant peak energy originates within the sample with a 40 keV incident x-ray. Calculated using the formula from Potts, Williams-Thorpe, and Webb (1997, 32, Equation 2) with mass attenuation coefficient data from Berger et al. (2010).

In Figure 3-14 SEM-BSE images of experimentally corroded IMMACO alloys are shown (image originally published in Nicholas and Manti 2014, Figure 1). The corrosion layers vary between 10–150 μm in depth. As part of understanding how it will affect the results there is a need to understand how deep the x-rays are penetrating and from whence the signal returned is coming from. Are we solely analysing the corrosion or do the results included uncorroded metal?

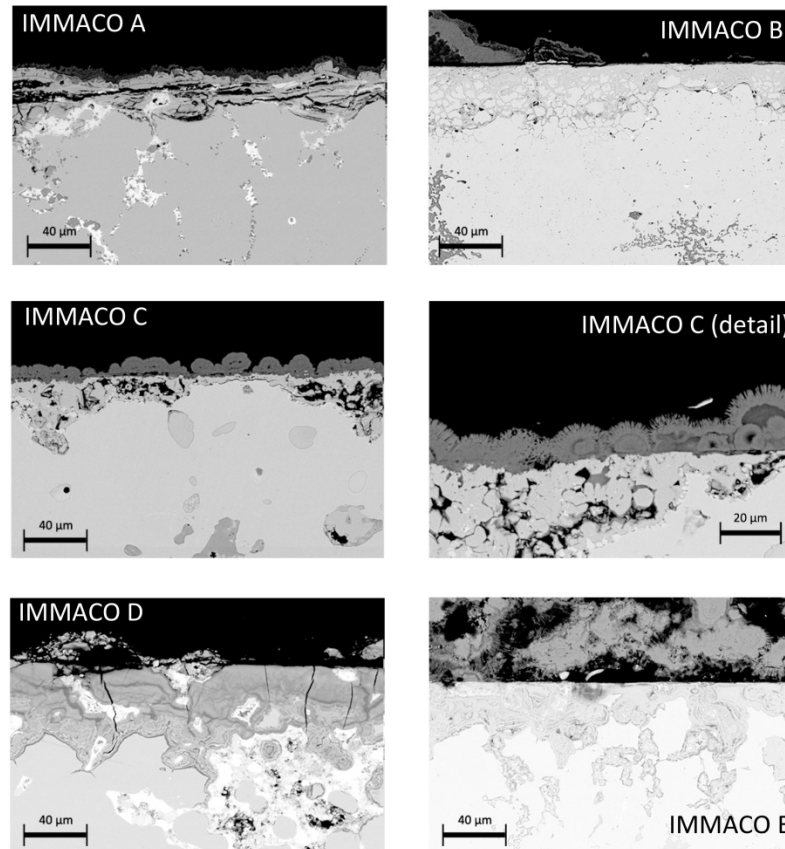


Figure 3-14: SEM-BSE images (acquired by Dr Panagiota Manti.) of experimentally corroded IMMACO alloys showing the corroded surface of the alloys in polished section. Images taken at $\times 500$ magnification; detail on IMMACO C at $\times 1000$ magnification. From Nicholas and Manti (2014, Figure 1).

X-Ray Diffraction analysis on the corroded IMMACO alloys (undertaken by Dr Panagiota Manti, see Nicholas and Manti 2014 for details) identified a range of corrosion products on the alloys including (but not limited to) nantokite, malachite, cuprite, zinc oxide and zinc sulphide. The t_{crit} values for these can be calculated to see what thickness would completely attenuate the signal and prevent any uncorroded alloy being analysed. The same process is used as before. Table 3-16 shows the corrosion products considered and their densities.

Corrosion product	Formula	ρ (g·cm ⁻³)
<i>Malachite</i>	Cu ₂ CO ₃ (OH) ₂	3.8
<i>Cuprite</i>	Cu ₂ O	6.14
<i>Nantokite</i>	CuCl	4.22
<i>Zinc sulphide</i>	ZnS	4.09
<i>Zinc oxide</i>	ZnO	5.61

Table 3-16: Corrosion products and densities.

The results (Table 3-17) show the t_{crit} depths for characteristic energies of the major elements in the MBH alloys in a matrix of the listed corrosion product. If a corrosion layer is thicker than the listed depth then it will completely attenuate the characteristic energy of the peak of interest from the uncorroded substrate.

Element	Fe	Co	Ni	Cu	Zn	As	Bi	Pb	Ag	Sn	Sb
Peak	$K\alpha$	$K\alpha$	$K\alpha$	$K\alpha$	$K\alpha$	$K\alpha$	$L\alpha$	$L\alpha$	$K\alpha$	$K\alpha$	$K\alpha$
Photon energy (KeV)	6.40	6.93	7.48	8.05	8.64	10.54	10.84	10.55	22.16	25.27	26.36
T_{crit} (μm)											
<i>Malachite</i>	159.57	196.72	239.74	289.09	345.30	93.59	100.28	95.74	596.20	793.31	867.01
<i>Cuprite</i>	71.51	87.88	106.76	128.33	152.80	38.05	40.77	38.94	243.05	324.33	354.62
<i>Nantokite</i>	70.62	87.30	106.91	129.69	156.07	67.16	72.03	68.73	436.00	582.54	637.13
<i>Zinc sulphide</i>	74.23	91.66	112.18	135.96	163.42	63.72	68.32	100.65	404.34	539.33	589.39
<i>Zinc oxide</i>	75.97	93.39	113.50	136.51	162.65	42.54	45.56	43.52	265.88	354.04	387.01

Table 3-17: Depth (μm) from which the stated percentage for the relevant peak energy originates within the sample with a 40 keV incident x-ray. Calculated using the formula from Potts, Williams-Thorpe, and Webb (1997, 32, Equation 2) with mass attenuation coefficient data from Berger et al. (2010).

This is of course somewhat simplistic. It assumes a uniform homogeneous monoculture of corrosion whereas the experimentally corroded alloys in Figure 3-14 clearly show inhomogeneous pitted layers. Nevertheless it is still a useful exercise in illustrating the impact corrosion and sampling volume will have (especially on those elements whose keV is lower or occurs at an absorption edge). Unfortunately that includes key elements such as copper and zinc and there is a chance (dependent on the thickness of the products) that the majority of the signal may derive from the corrosion layers. However this does not prevent the extraction of useful numerical information from spectra acquired from the surface of corroded objects (see Nicholas and Manti 2014).

3.4.2 SILVER ALLOY THICKNESS AND PENETRATION DEPTH

The surface analysis of silver alloys has been the subject of detailed study. Research has shown that the surface analysis of silver objects often shows elevated levels of silver (Hughes and Hall 1979; Klockenkämper, Bubert, and Hasler 1999; Condamin and Picon 1964; Beck et al. 2004; Leigh, Cowell, and Turgoose 1984; Mortimer and Draper 1997, 4–5) compared to analysis on the interior (accessed by sampling). One study of high medieval Austrian coinage found a difference of up to 50% in the silver content between the surface and the interior (Linke et al. 2003).⁶⁵

The effects of this can be visually seen in the elemental map in Figure 3-15. This shows the cross section of a pin from a Kentish Nydam style brooch acquired in a CamScam 2040 SEM (20 kV) by the author. The pin was broken during excavation, allowing the cross section to be analysed. The maps show the proportion of each element present in relation to the density of the colour. As can be seen, the proportion of copper present in the corrosion zone is significantly less than in the interior of the object. In contrast the silver and tin remain present at roughly the same levels. The corrosion layer varies in depth from approximately 50-150µm.

⁶⁵ These differences can be the result of corrosion or deliberate attempts to enrich the silver content at the surface.

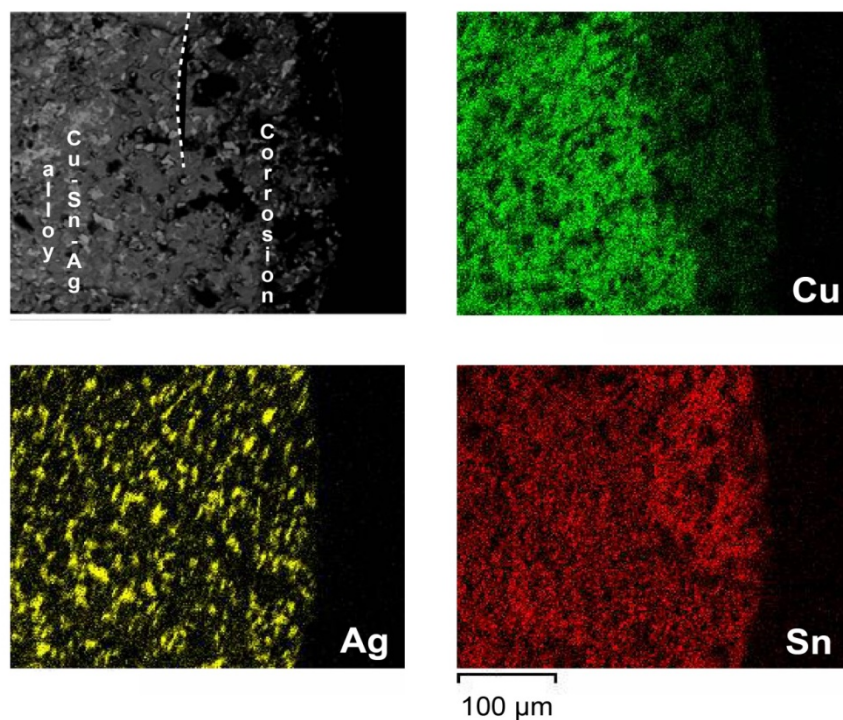


Figure 3-15: Elemental map (captured using an SEM) showing decuprification as seen on a Cu-Sn-Ag pin from a Kentish Nydam style brooch pin. The pin had suffered a break during excavation, allowing the cross section to be analysed. The image in the top left is a backscatter image, the remaining three show maps for the elements labelled.

What impact do these corrosion layers have on the HHpXRF results for the silver alloys? Budgetary constraints meant there were no silver reference alloys available during this study with which to compare. Despite this it is still possible build an impression of the impact corrosion will have on the results here by calculating critical penetration depth (t_{crit} , calculated using the Equation 6) To enable this a selection of six period appropriate silver alloys were selected from the literature (un-normalised compositions in Table 3-18): two low silver Anglo-Saxon great square-headed brooches (object ID's: Holywell Row 11 & Suffolk [IV], Brownsword and Hines 1993); two late Romano-British silver alloys containing zinc (object ID's: 746-Winchester and 750-Faversham, Mortimer 1986) and two copper-silver reference materials created for an investigation into the corrosion of silver archaeological objects (object ID's: CNR Alloy C & D, Casaletto et al. 2010). The compositions of these were normalised (if not already) and the density calculated. The mass attenuation coefficients were derived from the NIST XCOM database (Berger et al. 2010) and the critical penetration

depths calculated for each element of interest using the incident and take-off angles stated on page 162 and an incident energy of 40 keV.

ID	Type	Composition (weight %)										Density
		Sb	Sn	Ag	Pb	As	Zn	Cu	Ni	Fe	Au	$\frac{\rho}{(\text{g}\cdot\text{cm}^{-3})}$
Holywell Row 11	Great square-headed brooch	0.14	5.81	30.6	1.29	0.1	3.22	57.5	0.01	1.36		9.177
Suffolk [IV]	Great square-headed brooch	0.15	5.82	31.9	1.68	0.07	4.8	55.5	0.01	0.08		9.182
750 - Faversham	Inscription			82	0.6		4.4	12.6			0.4	10.088
746 - Winchester	Plain Stone			92.3	0.5		3.5	3.3			0.4	10.286
CNR Alloy C	Reference alloy			92.5				7.5				10.357
CNR Alloy D	Reference alloy			96.5				3.5				10.428

Table 3-18: Un-normalised compositions for six silver alloys chosen to represent a variety of silver compositions: the great square-headed brooches (Bronnswold and Hines 1993) are early medieval in date and represent a low Ag compositions; the Faversham and Winchester objects (Mortimer 1986) are relatively high Ag roman objects that also contain Zn; and the CNR alloys are an Ag-Cu reference alloy (Casaletto et al. 2010).

The results (Table 3-19) show the critical penetration depth along with the depths that would provide 90, 80 and 50% of the signal for that element's energy. Those peaks with high characteristic photon energies — such as Ag $K\alpha$ (22.16 keV), Sn $K\alpha$ (25.27 keV) and Sb $K\alpha$ (26.4 keV) — have, not surprisingly, the thickest t_{crit} values. Deep enough in fact to penetrate beneath a corrosion layer like the one seen in the pin in Figure 3-15 (although the majority of the signal will come from the corrosion layers). Meanwhile the elements most subject to the corrosion processes — Cu $K\alpha$ (8.05 keV), and Zn $K\alpha$ (8.64 keV) — have relatively shallow t_{crit} depths in comparison.

Obviously one should not read too much into the t_{crit} depths. In both cases the depth which provides 50% of the spectrum for Cu $K\alpha$ and Ag $K\alpha$ is, on average, 84.95% less than the t_{crit} . Still, it can be seen that corrosion and sampling volume will impact most on those elements whose keV is lower. Unfortunately that includes Cu and Zn: elements that can be of interest (depending on the research questions) in understanding the silver alloy compositions.

Element	Fe	Ni	Cu	Zn	Au	As	Pb	Ag	Sn	Sb
Peak	K α	K α	K α	K α	L α	K α	L α	K α	K α	K α
Photon energy (keV)	6.40	7.48	8.05	8.64	9.71	10.51	10.55	22.16	25.27	26.40
t_{crit} depth (μm)										
Holywell Row 11	20.20	28.89	34.56	41.06		26.24	26.84	136.79	171.33	119.88
Suffolk [IV]	19.62	28.90	34.58	41.05		26.28	26.28	135.13	168.96	117.02
750 Faversham			20.06	23.82	24.75		30.34	121.56		
746 Winchester			18.09	21.47	25.71		31.49	118.60		
CNR Alloy C			18.08					119.70		
CNR Alloy D			17.40					118.56		
90% signal depth (μm)										
Holywell Row 11	10.10	14.44	17.28	20.53		13.12	13.42	68.40	85.67	59.94
Suffolk [IV]	9.81	14.45	17.29	20.53		13.14	13.14	67.57	84.48	58.51
750 Faversham			10.03	11.91	12.37		15.17	60.78		
746 Winchester			9.04	10.74	12.85		15.75	59.30		
CNR Alloy C			9.04					59.85		
CNR Alloy D			8.70					59.28		
80% signal depth (μm)										
Holywell Row 11	7.06	10.10	12.08	14.35		9.17	9.38	47.81	59.88	41.90
Suffolk [IV]	6.86	10.10	12.08	14.35		9.18	9.18	47.23	59.05	40.90
750 Faversham			7.01	8.32	8.65		10.60	42.48		
746 Winchester			6.32	7.50	8.98		11.01	41.45		
CNR Alloy C			6.32					41.83		
CNR Alloy D			6.08					41.43		
50% signal depth (μm)										
Holywell Row 11	3.04	4.35	5.20	6.18		3.95	4.04	20.59	25.79	18.04
Suffolk [IV]	2.95	4.35	5.20	6.18		3.96	3.96	20.34	25.43	17.61
750 Faversham			3.02	3.59	3.72		4.57	18.30		
746 Winchester			2.72	3.23	3.87		4.74	17.85		
CNR Alloy C			2.72					18.02		
CNR Alloy D			2.62					17.84		

Table 3-19: Depth (μm) from which the stated percentage for the relevant peak energy originates within the sample with a 40 keV incident x-ray. Calculated using the formula from Potts, Williams-Thorpe, and Webb (1997, 32, Equation 2) with mass attenuation coefficient data from Berger et al. (2010). See section 3.4.1, page 162 for a detailed description of this process.

What does this mean for the metallurgical and archaeological interpretation of the results? Primarily it means that (as noted Beck et al. 2004, 161) the data here cannot be used to assess the fineness of the alloy. Traditionally an assessment of fineness has been the objective of the small number of analytical studies undertaken on early medieval Anglo-Saxon silver alloys (see Brownsword and Hines 1993; Mortimer and Draper 1997 for example). These studies had limited amounts of material available (two objects each in the two examples cited),

impacting on the overall conclusions that could be drawn. In these circumstances focussing on the fineness of the silver alloys is entirely sensible; without a larger body of material from which to gain context there is not much more to say other than to try and present as accurate a representation of the ‘true’ alloy as is possible.

The methodology and data set here require a different approach; the emphasis has been on breadth rather than depth. Studying fineness is not an option and the silver levels cannot and should not be used to deduce any conclusions from the results here. What can be done is to look at broad patterns in alloy composition (i.e. the clusters defined in Chapter 4) and attempt to abductively identify broad behavioural patterns from the qualitative data.

The Eriswell silver alloys included a number of sheet pieces, many still soldered to the panels of Cu alloy objects. None of these sheets, where measuring was possible, was thinner than 0.7 mm (measured using a calibrated Mitutoyo digital Vernier calliper). The maximum t_{crit} depth in the examples above (Table 3-19) was 149.49 μm (or 0.149 mm) for Ag $K\alpha$ on brooch Holywell Row 11. Consequently the silver objects here are most likely infinitely thick. Of course one must be aware of the possibility of thinner pieces (i.e. those impossible to measure accurately because they are still soldered to the front of a brooch) which may be only of intermediate thickness for higher energy peaks, whilst bearing in mind that it is unlikely that any of the sheets were as thin as the t_{crit} values for Cu $K\alpha$ (a maximum of 13.98 μm or 0.013 mm) or other lower energy peaks.

Therefore, although there is always a danger of contamination in the results, it is unlikely to come from intermediately thick samples. Instead it will be human error: the (despite best efforts) incorrect positioning of an object over the window or stray particles of loose corrosion products transferred by gloved hands. Thus a degree of care must still be taken when viewing the results with an awareness that the results will not be precise.

3.4.3 DISTANCE

To determine the effect on the signal detected a test was designed in which a reference material, chosen for closely representing an alloy of the type expected to be encountered, was raised by a set amount between readings. Analysis was started with the reference material (32X SN6) placed directly on the XRF window. Between each run a single wooden lollypop stick (width 1.66 mm) was placed on each side of the window to raise the material before analysis continued. The reference material was raised a total of eight times up to a maximum height of 13.28 mm.

The results (see Table 3-20) showed that for the first two height increases (1.66 and 3.32 mm) the average decrease in signal across Cu, Zn, Sn, Sb and Pb was 20%. Thereafter the steps in reduction began to decrease, but not in a linear fashion as previously. When the maximum height of 13.28 mm was reached 94% of the signal strength had been lost. Examining the figures in detail it is no surprise to see that higher Z elements (such as Sn and Pb) – with their shorter wavelengths - are decreasing at a slower rate than lower Z elements (Cu and Zn).

Distance from Window (mm)	Zn %	Cu %	Pb %	Sn %	Avg. Step % reduction	Avg. total % reduction
0	100	100	100	100	0	0
1.66	79	79	81	81	20	20
3.32	58	58	62	61	20	41
4.98	40	39	43	44	17	58
6.64	25	24	28	30	15	73
8.3	18	17	21	22	9	82
9.96	11	11	14	15	6	87
11.62	7	7	9	10	3	91
13.28	5	4	7	7	4	94

Table 3-20: Summary of results from the distance test on reference material 32X SN6. The table shows the percentage decrease in signal received by the HHPXRF detector taking position 0 as 100%.

These results, when plotted as a line graph, appear stark (see Figure 3-16 below). Consequently the immediate conclusion one may be tempted to draw is that, unless an object is directly placed upon the window, the figures retrieved will be unreliable.

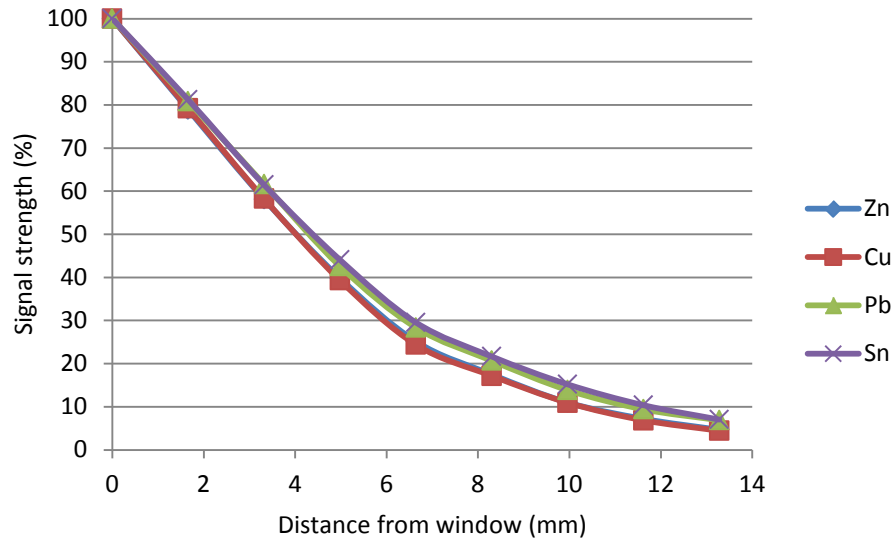


Figure 3-16: Graph of % reductions in signal strength (see Table 3-20)

This is indeed the true if taking result values (net peak areas) and interpreting them as final values. If, however, we treat the relationship between the values as being of true significance a different picture emerges (see Table 3-21 and Table 3-22). Here, the relationship between the net peak areas remains relatively stable (although reflecting the increased predominance of higher Z elements as distance increases, see also Figure 3-16).

Distance from window (mm)	Cu NPA	Cu %	Sn NPA	Sn %	Zn NPA	Zn %
0	4557177	95.69	97464	2.05	107681	2.26
1.66	3601839	95.65	78887	2.10	84740	2.25
3.32	2650336	95.60	59693	2.15	62418	2.25
4.98	1788813	95.43	42814	2.28	42759	2.28
6.64	1110275	95.22	28708	2.46	27014	2.32
8.3	781391	95.15	21039	2.56	18795	2.29
9.96	497858	94.93	14766	2.82	11809	2.25
11.62	312133	94.60	10072	3.05	7736	2.34
13.28	201889	94.47	6823	3.19	4998	2.34

Table 3-21: Net peak areas for Cu, Sn and Zn with percentage values for each peak normalised to the total of all three peaks.

Distance from Window (mm)	Pb NPA	Pb %	Sn NPA	Sn %	Zn NPA	Zn %
0	39651	16.20	97464	39.81	107681	43.99
1.66	32762	16.68	78887	40.17	84740	43.15
3.32	24957	16.97	59693	40.59	62418	42.44
4.98	17254	16.78	42814	41.64	42759	41.58
6.64	11492	17.10	28708	42.71	27014	40.19
8.3	8379	17.38	21039	43.64	18795	38.98
9.96	5615	17.44	14766	45.87	11809	36.69
11.62	3807	17.61	10072	46.60	7736	35.79
13.28	2785	19.07	6823	46.71	4998	34.22

Table 3-22: Net peak areas for Pb, Sn and Zn with percentage values for each peak normalised to the total of all three peaks.

In Nicholas and Manti (2014, Figure 6) the experiment was repeated using uncorroded and experimentally corroded IMMACO reference alloys. The outcome showed a similar result to that from the uncorroded sample here for both uncorroded and corroded.

The results in Table 3-21, Table 3-22 and demonstrate just how little the variations in signal strength can affect interpretations *assuming that the ratios being compared remain relatively stable*. When the elements of interest all have relatively high atomic numbers (such as in non-ferrous alloys) within a relatively limited range then this may be a reasonable assumption to make.

There will be slight differences as higher Z elements lose less strength as height increases. Considering the atomic number ranges of the major, minor and trace elements of primary interest in the Eriswell assemblage we can place them into three groups:

- Group 1 - Co (atomic number: 27), Ni (28), Cu (29), Zn (30) and As (33).
- Group 2 - Ag (47), Sn (50), Sb (51).
- Group 3 - Au (79), Hg (80), Pb (82) and Bi (83).

We can therefore expect Groups 2 and 3 to be slightly over-represented in readings where distance gaps between window and object exist. It would appear, however, that within a distance of <5mm the near linear decrease ensures that ratios are relatively stable and differences are tolerable. Consequently qualitative

statistical interpretations of the Eriswell assemblage should be fairly secure (as discussed in the next chapter).

3.4.4 AMBIENT TEMPERATURE AND DETECTION SENSITIVITY STABILITY

The S1PXRF software provides two readings from the Tracer III-SD instrument on detector and ambient temperature (the latter reported in Centigrade the former in Fahrenheit). The detector temperature — maintained at -15.0° — is of little immediate concern to us (excluding the fact that any change suggests the instrument is broken). In contrast the ambient temperature and its effects on stability of the resulting spectra are. The ambient temperature is measured in the exit/entrance chamber (i.e. the space between the beryllium window and the anode and detector). This space is not cooled and the temperature is consequently subject to fluctuation due to changes in the environmental surroundings and the conversion of kinetic energy to heat as electrons strike the anode. Anecdotal evidence gathered during the use of the instrument at Cardiff indicates that ambient temperature can increase by as much as 20°C during two hours near continuous use (dependent on environmental conditions such as the vagaries of the Welsh climate, number of people in the room etc.). Whilst this increase has never resulted in the instrument reaching the top end of the ambient temperature operating parameters for the Tracer III-SD as documented by Bruker ($-10^{\circ}\text{C}/14^{\circ}\text{F}$ - $+50^{\circ}\text{C}/122^{\circ}\text{F}$, Bruker Elemental 2010, 22) the fact that it is regularly operating within 6°C of the maximum suggests it is worth checking for any impact on the results, especially as previous studies (admittedly with different HHpXRF models) have shown that the ambient temperature can significantly affect instrument performance (McNeil and Cecil 2009; Mahuteau 2008; U.S. Environmental Protection Agency 2007).

	Ambient Temperature (°C)							RSD
	31.94	33.56	35.94	37.22	40.94	42.33	43.56	
Fe K α	1615	1705	1741	1811	1675	1663	1643	3.61
% diff. from max	11	6	4		8	8	9	
Cu K α	484498	486636	500968	503247	494670	495031	496399	1.29
% diff. from max	4	3	0		2	2	1	
Zn K α	10940	10694	11057	11156	10881	11039	11005	1.26
% diff. from max	2	4	1		2	1	1	
Compton peak	855	899	721	729	707	685	703	10.29
% diff. from max	5		20	19	21	24	22	
Ag K α	1867	1904	1888	2001	1819	1936	1974	3.04
% diff. from max	7	5	6		9	3	1	

Table 3-23: Peak counts at differing temperature. The bold values represent the maximum value reached and the percentage difference the variation between the value above and the max value.

Ambient Temperature (°C)	Cu NPA	%	Sn NPA	%	Zn NPA	%
31.94	4462795	96	97469	2	111082	2
33.56	4453193	96	97717	2	111098	2
35.94	4534829	96	95326	2	106275	2
37.22	4557177	96	97464	2	107681	2
40.94	4542109	96	96252	2	110395	2
42.33	4567388	96	97388	2	111901	2
43.56	4555164	96	97115	2	110758	2

Table 3-24: Net peak areas and ratios for three elements at differing temperatures.

The results, reported as raw peak heights (Table 3-23) and net peak areas (Table 3-24) show little difference at the normal range of temperatures experienced at Cardiff University.

3.4.5 DETECTOR DRIFT

Experience has shown the Silicon Drift Detector in the Bruker Tracer III-SD has a tendency to drift, causing peaks to not line up correctly (see Figure 3-17 for an example).

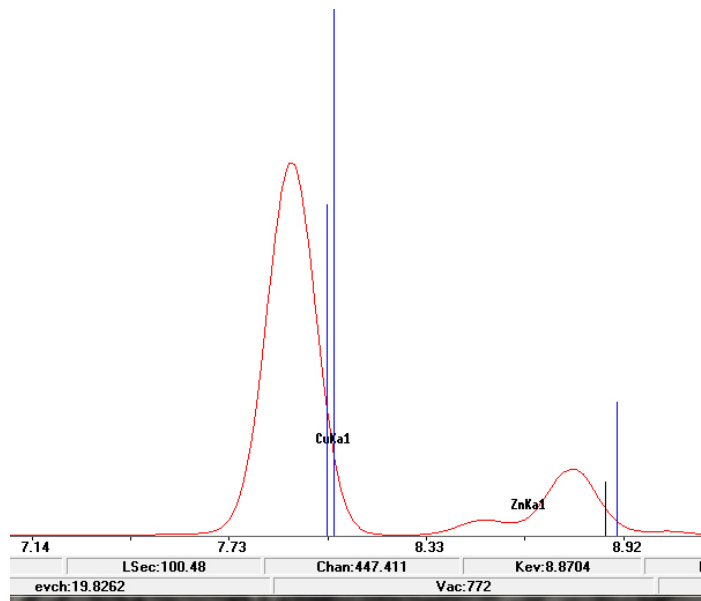


Figure 3-17: An example of drift in from a screenshot of the S1PXRF software.

There are three reasons this may be occurring: the instrument has been on for a long time (with an X-flash Silicon Drift Detector the eV per channel [*evch* in Figure 3-17] increases the longer the instrument is on); the unit is drifting more than it should; the unit has a setting which makes it start at too high an eV per channel when first turned on.⁶⁶

This can easily be corrected, but if missed can have a significant impact on the processed net peak areas (as the peak area outputted will not reflect the true peak area). Consequently each spectra will be examined for drift and corrected before exporting to Artax.

⁶⁶ Pers comm. Dr Robert Shannon (calibration physicist Bruker AXS).

3.5 CONCLUSION

When analysing heterogeneous non-ferrous alloys what does the HHpXRF analyst need to consider in meeting the challenges and issues covered here? The results of this chapter (along with those from Nicholas and Manti 2014) have suggested that HHpXRF is not capable of producing quantitative data on corroded surfaces with tight precision, but it is capable of producing numerical data which can be interrogated with appropriate statistical methods (to be discussed in the next chapter). It has also highlighted a number of basic practical issues that, incorporating previous suggestions by Heginbotham et al. (2011) and Shackley (2010), can help construct basic operational protocols for HHpXRF and surface analysis of copper alloys that will be adhered to throughout this study:

- Results from the surface analysis of corroded heterogeneous materials such as a copper alloy's surface should always be presented as qualitative no matter how processed. The production of qualitative data does not preclude the production of numerical data and appropriate compositional statistics can create descriptive alloy classifications that have scientific and cultural validity.
- Producing qualitative data requires the same rigour as would be applied if the intention was to produce quantitative data, including:
 - Appropriate standards analysed to assess the internal consistency of the instrument's performance and the reproducibility assessed and reported.
 - The spectra from the standards processed and reported using every process used to process the 'unknown' data.
 - All settings, including tube voltage, anode current and filters documented and reported.
- The method of converting peak intensities into interpretable data can have as significant effect as corrosion layers on the accuracy of analysis. Consequently the programs used (including version numbers) to process

the spectra (in every step) are noted as the implementation of algorithms can change rapidly. This is crucial given the surprising diversity in software packages currently in use (as noted in Heginbotham et al., 2011, p. 185).

3.5.1 WORKFLOW

Considering these points an HHPXRF workflow was developed using the settings outlined in Table 3-25 below.

Tube voltage	40 kV
Anode current	7.9 μ A
Filter	Bruker filter 1 (Al 12 mil / 300 μ m, Ti 1 mil / 25 μ m)
Time	100 seconds

Table 3-25: Analysis settings for the analysis of the non-ferrous assemblage from Eriswell.

1. Analysis to be undertaken in a Bruker bench top stand with a laptop running XRayOps (version 1.2.15) and S1PXRF (version 3.8.30).⁶⁷
2. Before analysis the stability of the settings (pulse length etc.) is checked in XRayOps.
3. On loading S1PXRF reference alloys are first run to check on instrument performance and allow monitoring of stability over time.
4. Objects to be analysed the maximum number of times that the surface area will allow (to check for lead segregation and allow the results to be averaged).
5. The window is regularly checked for contamination.
6. At the end of the session reference alloys are analysed again (for the same reasons as in step 3).
7. Each spectra is individually examined and the presence of all peaks are noted.
8. Spectra are exported from S1PXRF as txt files for processing in Artax (version 7.3.50). This compresses 2048 channels to 1024.

⁶⁷ Cardiff University Health and Safety policy, with no exceptions, explicitly states that no student can use the HHPXRF outside of one designated room in the Department (i.e. no site visits) and requires the examination window to always be in a completely shielded chamber (i.e. no use of the Bruker tripod is allowed).

9. The presence of peaks is double checked again in Artax and compared with the list compiled in step 7. Only spectra with exactly the same peaks are processed together (i.e. if one spectrum from an object has an arsenic peak whilst another does not they will not be processed together).
10. Spectra processed to produce net peak areas in Artax.

The processing and interpretation of the net peak area results is the subject of the next chapter, where the silver alloy data set is used to develop a methodology.

CHAPTER 4: DATA EXPLORATION

“Yes, yes I know...you can multiply and divide almost anything by something else — the length of canes by the width of hats — and come up with all kinds of constants and variables”

(Lem 1976, 25–26)

4.1 INTRODUCTION

This chapter performs the function of presenting the development of a methodology for exploring and interpreting the net peak area HHpXRF results. The archaeological interpretation of the result can be found in Chapter 5 (page 232).

With large multivariate data sets there is a need to reduce dimensionality to help us to reveal and understand the significance behind the results. With non-ferrous archaeometallurgical studies this can take the form of plotting the results in ternary diagrams to aid interpretation (see for instance the use of ternary diagrams to differentiate between brass, bronze and leaded alloys in Bayley & Butcher 2004, pp.23–25). This relies on a good understanding of the system behind the production, on expectations that the elements (and alloy definitions) chosen were of the same importance in the past as in the present and on the three or four elements chosen being an effective expression of the variance within the data.

To avoid bias or ineffective element selection we can use multivariate statistics to reduce dimensionality, discover relationships and determine what is of genuine significance. With multivariate data perhaps one of the most popular approaches to achieve this is principal components analysis (PCA), and this shall be used in this study.

The application of PCA on HHPXRF net peak area data has been examined in respect of archaeological ceramics and stone tools (Forster et al. 2011; Grave et al. 2012; Forster and Grave 2012; Mitchell et al. 2012). Undertaking PCA on data is not, however, straightforward and there is a crucial decision to be made: what transformations should be used?

4.1.1 DESCARTES VS THE SIMPLEX: ANALYSIS OF COMPOSITIONAL DATA

Statistics is a form of logic taking place in geometrical planes. For centuries this took place in a Euclidean space (R^D) until, in 1896 (Pearson & Lee), it was observed that compositional data — having a definitive end point — did not suit this geometrical space and treating them as such could lead to false correlations. This remained a problem until, in 1982, Aitchison discovered that compositions were about ratios **not** absolute values, as the end (say 100%) is a forced sum and not a natural endpoint (Bacon-Shone 2011, 3). In practical terms we can understand this by considering a hypothetical metallurgical example. A copper alloy is analysed and found to have a composition of 86% copper, 12% tin and 1.5% zinc (weight percent). The components do not add up to 100% as there are other elements not reported that were either below the hypothetical analysis technique's limit of detection or not analysed for. To get around this the results are closed as a sub-composition. The closing operation does not affect the statistical interpretation because we are interpreting the ratios / relationships and not the values themselves. When a composition is closed as a sub-composition the ratios between the elements are preserved and we retain compositional coherence (van den Boogaart and Tolosana-Delgado 2013, 15). Where doubts in the reader's mind remain on considering ratios between alloying elements of more importance than their values it should be remembered that we conceptually interpret alloy compositions in much the same way. We do not take each element separately and focus purely on the abundance of an individual but take the whole as a pattern; we recognise that there is more copper than any other element and

that, despite the presence of zinc, tin is the major alloying element. From this we then categorise as a bronze (i.e. knowing the tin content does not tell us much unless we also know the other components, enabling us to linguistically categorise it).

As Pawlowsky-Glahn and Egozcue note (2006, 2) most statistical techniques were created for use on unconstrained random variables, which (as we have seen in the previous paragraph) compositional data are not. Consequently compositional data is best interrogated not in Euclidean space (\mathbb{R}^D) but a constrained space (the Simplex or S^D , see Tolosana-Delgado, Otero, and Pawlowsky-Glahn 2005 for an introduction). The constrained working space is achieved by applying an appropriate logarithmic transformation (See page 203 for details of the transformation used in this study) to the data whereupon the variances between the log ratios are examined rather than original values themselves. The log ratio approach has some considerable advantages to directly using the ratios themselves: once transformed the data can be analysed using standard techniques such as PCA (as used here, see page 200) and the transformed values can be mapped directly back to the original data allowing the interpretations to be translatable to the 'real world' (Aitchison and Egozcue 2005, 830). Since Aitchison's seminal studies a considerable body of work (summarised in Bacon-Shone 2011) has developed, enabling substantial advances to be made on the interpretation of compositional data.

The application of compositional statistical approaches is relatively common in geosciences (see Tolosana-Delgado 2012 for some uses and misuses) and its usage in archaeometry has been subject to some debate over the years (see for instance Baxter 1993; Tangri and Wright 1993; Baxter and Freestone 2006; Charlton et al. 2012). Consequently deciding whether to perform log-ratio transformations on data sets is not necessarily a clear cut decision.

A key question for us here is do net peak area (NPA) data meet the requirements to be approached in a compositional manner? The standard definition of compositional data is that all the vectors are positive and sum to unity (Bacon-Shone 2011, 3). The data here are all positive and (although the figures stretch into the tens or hundreds of thousands) can be normalized and recent research has shown that units of measurement — such as units of concentration — can be considered compositional (Buccianti and Pawlowsky-Glahn 2005; Pawlowsky-Glahn, Egozcue, and Delgado 2007, 5). As Otero et al. (2005, 1405) have shown the form of the units are not important, what is are that the results provide information on the relative abundance of a part within the extent of what is being measured or, in other words, relative data can be compositional. Nevertheless the question is the appropriateness of treating it as such here; the data are not quantitative, they have not been processed using appropriate calibrations and the ratios between any normalised figures will carry information not only about composition but also the analysis time, beam strength, object geometry and surface texture. Consequently there is a risk that analysing the data in a compositional manner presents both a false semblance of accuracy and false confidence in the results (as discussed in the previous chapter). Yet to some extent we do exactly this when we choose three elements as a sub-composition, sum them to a constant endpoint, place them in a ternary plot and use the graphical representation of the ratios to deduce patterns and groups. It should also be remembered that previous studies (and experimental work here in the previous chapter) have shown that surface analyses with XRF can reasonably and relatively accurately (if not quotable to the n^{th} decimal) characterize alloy types (Craddock, Wallis, and Merkel 2001, 120). Therefore the issue is not as clear cut as one might assume.

It is crucial that geometry is not chosen arbitrarily for the data analysis of the Eriswell objects. With this in mind the analysis of the silver objects here is undertaken using principal components using both untransformed data (i.e. in a

Euclidean geometry) and constrained logarithmically transformed data (i.e. in a Simplex geometry) with an aim of not only presenting the results of the analysis but also providing a reasonably thorough evaluation of the approaches. This can be found in section 4.3 (page 191) below. The approach is subsequently further evaluated on copper alloys by comparing the results of statistical interpretations on Eriswell NPA results and Blades (1995) early Anglo-Saxon data (both logarithmically transformed). This can be found in Chapter 8.

4.1.2 SOFTWARE

Statistical analysis in this chapter utilised two different statistical programs. Untransformed PCA was conducted using R (R Core Team 2014), the GUI RStudio (RStudio 2014) and the package FactoMineR (Francois Husson et al. 2014). Compositional data (in the statistical sense) were analysed using the standalone program CoDaPack (Comas-Cufi and Thió-Henestrosa 2011) and the R package compositions (van den Boogaart, Tolosana, and Bren 2014). Where other R packages were used these are cited in the text.

Before being imported into both software packages the relevant NPA data was extracted from the spreadsheet using array formulas in Excel 2010 and saved as a .csv file.

4.1.3 CENTRING

In the examination of the data a number of ternary diagrams are presented. In some of these centring will be utilised instead of magnifying highly populated areas of a diagram.

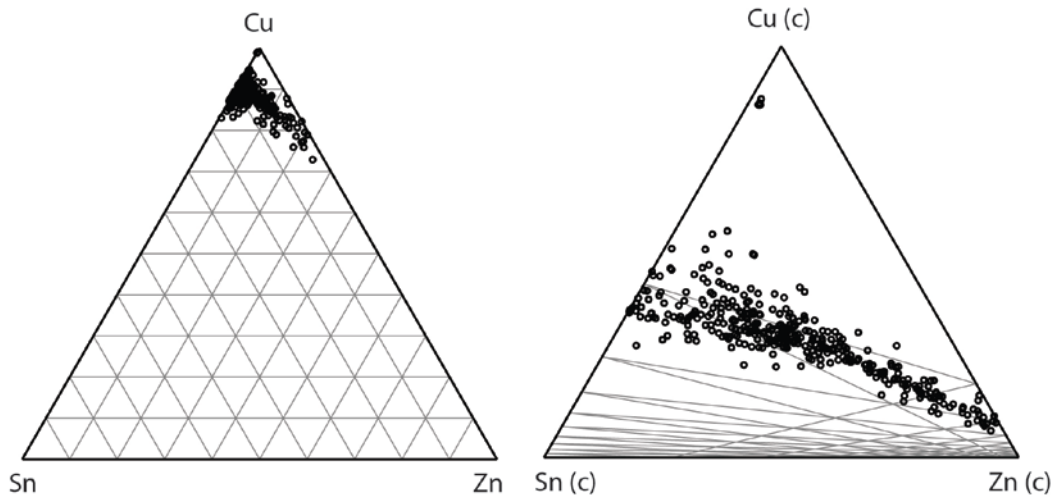


Figure 4-1: Cu-Sn-Zn ternary diagram. The diagram on the left presents the original diagram, that on the right the centred version.

Centring involves the perturbation of the data set to better illustrate those individuals near the edges of the diagram. This is an alternative to simply magnifying the diagram to focus on the detail of a small area, a method which has the disadvantage of excluding some individuals if they are significantly outlying from the main body of the data. An example of this is shown in Figure 4-1, where a copper-tin-zinc ternary diagram is presented as both original and centred). As can be seen the perturbation rescales the data to its barycentre (i.e. the centre of the mass of the individuals), allowing easier visualization of the individuals whilst maintaining the straight lines of the internal divisions (von Eynatten, Pawlowsky-Glahn, and Egozcue 2002). It is sought to keep this form of presentation to a minimum as it is recognised that it is not to everyone's taste. Where it is used the un-centred diagram is always presented as a companion for context to help the reader understand the degree of rescaling.

4.2 CLASSICAL STATISTICAL SUMMARY

A number of areas of solder on silver objects have been excluded from this statistical analysis and are considered separately in Chapter 7 (page 286). For a description of how objects are defined in this study see page 45. In the analysis

of one object (shield mount 104-3675-2-A) it proved impossible to avoid areas of gilding (as evidenced by a mercury peak, see the NPA data in Appendix IV). As gold appears to be an important element (as discussed later in this chapter) in understanding silver artefact composition it was decided to excluded this object from the analysis as some of the gold detected will likely have been contributed by the gilding. Consequently **n=67** for all initial statistical analysis presented here unless explicitly stated otherwise.

Besides silver the other major constituents are lead, gold and copper. Tin and zinc are also present in the majority of the assemblage. Arsenic, antimony, bismuth and nickel are minor elements only occasionally present.

Other elements identified in the analysis include calcium, iron, titanium, manganese and zirconium. It was considered that, as only the surface of the objects was analysed, these were likely contributed by traces of remaining soil and corrosion. The iron, often particularly high, is frequently contributed by the corrosion products from nearby (in the burial context) objects. Although not included here these elements are included in the full set of net peak area silver data available in Appendix IV.

As stated silver is the major constituent; however several objects from ERL 104 have a significantly lower silver content than the majority, with large contributions from copper, lead and zinc (small finds 1061, 1336, 1176, 2950 and 3674, see Appendix IV).

As highlighted above the compositions of the alloys are relatively variable, as one would perhaps expect if the main source for the raw material was recycled objects (the predominant main hypothesis for the production of Anglo-Saxon metalwork as highlighted earlier in Chapter 2). Because of this we have a poor understanding of the system and the human choices which are contributing to the final composition; we do not understand how objects were chosen for recycling, the choices that went into the recycled objects and contributed to their

chemistry (ore body choice, processing methods etc.). We do not even understand if choice was, at any stage, a genuine option in the decision making process. Furthermore we are working with qualitative data from the corroded surface, likely leading to some altered levels from the 'true' composition. This leads to a significant degree of fuzziness in our understanding; we do not have the same kind of depth of knowledge of variables, dependents and contributory factors that an archaeometallurgist exploring a smelting landscape has when undertaking similar exploratory statistics. Therefore one must expect a higher degree of variance in the analysis and execute an extra degree of care when interpreting the results. Nevertheless it is hoped the following will demonstrate it is possible, with qualifications, to identify patterns and relationships within the data set.

Before exploratory statistical investigation, the data (Cu, Pb, Sn, Ag, As, Sb, Au, Bi and Zn) were assessed for normality by examining the histograms of distribution (visible in the diagonal of Figure 4-2) and applying the Shapiro-Wilk normality test. No element had a normal distribution (visually demonstrated in the diagonal of Figure 4-2), with many having a heavy-tailed distribution. As principle components are being used descriptively to assess the data this does not unduly concern us as the technique does not make assumptions about data structure (Abdi and Williams 2010). The silver NPA was assessed for outliers using Analysis of Variance (ANOVA). None were identified. In Table 4-1, below, a classical statistical summary for the net peak area for the major elements in the silver objects is presented for information.

	Percentile						
	<i>Mean</i>	<i>Std.Dev</i>	<i>Min</i>	<i>25</i>	<i>50</i>	<i>75</i>	<i>Max</i>
Cu	225783	296475	15276	58053	118790	210277	1302209
Pb	30068	34063	2655	11269	15968	33824	146103
Sn	14785	28587	0	0	879	19161	148379
Ag	1262378	371022	446149	1001812	1275694	1574156	2009713
Au	23663	21113	0	12518	19782	28778	93407
Cu	225783	296475	15276	58053	118790	210277	1302209

Table 4-1: Classical statistical summary for the silver data set

The data exploration begins by looking for correlations between pairs of variables. Table 4-2 shows the correlation coefficients for the top ten pairwise linear correlations both including and excluding the minor elements.

	First Variable	Second Variable	Correlation
Including As, Bi, Sb & Ni	Pb	Sn	0.728
	Cu	Zn	0.609
	Sn	Zn	0.564
	Cu	As	0.538
	Pb	Zn	0.530
	Cu	Sn	0.323
	Ag	Au	0.295
	Cu	Pb	0.256
	Au	Bi	0.188
	Ag	Bi	0.168
Excluding As, Bi, Sb, Ni	Pb	Sn	0.728
	Cu	Zn	0.609
	Sn	Zn	0.564
	Pb	Zn	0.530
	Cu	Sn	0.323
	Ag	Au	0.295
	Cu	Pb	0.256
	Sn	Ag	-0.121
	Pb	Au	-0.079

Table 4-2: Pairwise linear correlations both including and excluding minor elements.

The scatterplot matrix of major elements in Figure 4-2 (the correlations are also available in Table 4-3), whilst not particularly clean, does show some pairs of elements that may be correlated. Lead / tin, silver / gold and copper / zinc (although the latter does not have a particularly good spread of points across the plot). It is interesting to note that copper does not correlate particularly highly with any other major element.

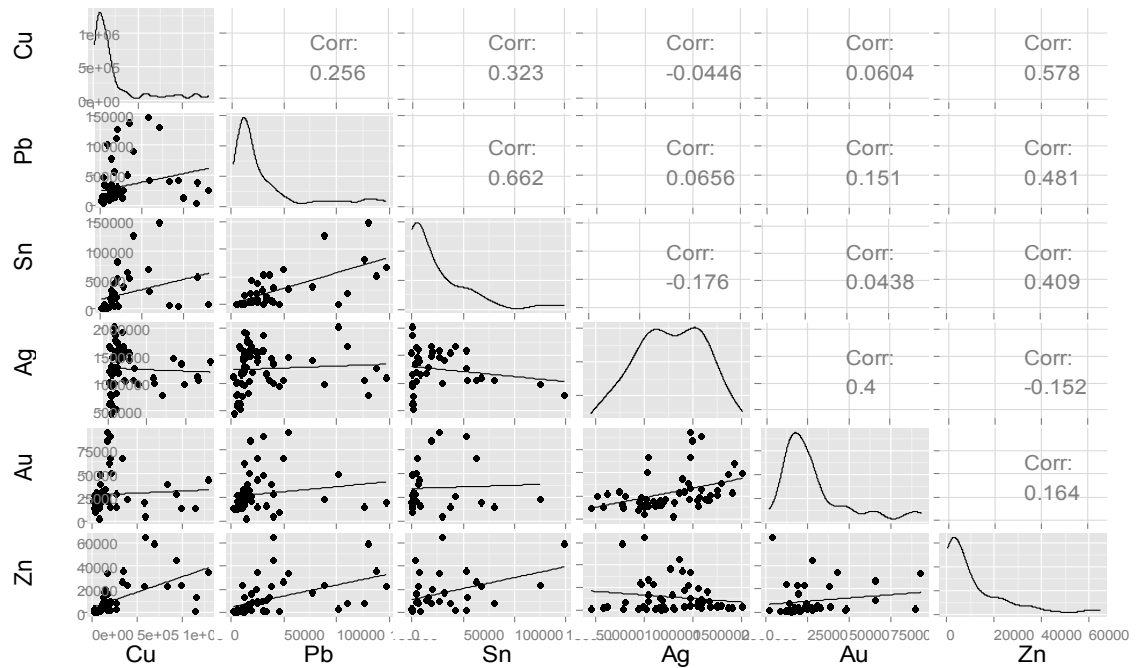


Figure 4-2: Scatter plot matrix of major elements from silver objects NPA. The diagonal shows a histogram of the element distribution. Minor elements are excluded for ease of viewing. Created using R package GGally (Schloerke et al. 2014). The correlations are reproduced in Table 4-3 without the scatterplots for easier reading.

This is confirmed by calculating the correlation coefficients, presented in Table 4-2 where the top ten pairwise linear correlations sorted by greatest correlation are presented (the table presents the correlations calculated with all elements and with only major elements for comparison). In the major elements the highest correlation is between lead / tin (0.728), thereafter the coefficients rapidly fall and by copper / tin (fifth in the list) it is a relatively poor 0.323.

The relatively low scores in the major elements may be of slightly less concern than feared if we consider the contributing factors (particularly the impact of

analysing the surface) that may complicate the data (see page 167 of Chapter 3 and Chapter 4 for more details).

There is no attempt as of yet to try and examine covariance between groups as the only groups available at this point are our archaeological categorical variables (site, grave number, object category) and these will be investigated in due course after geometries and PCA have been fully considered.

	Cu	Pb	Sn	Ag	Au	Zn
Cu	1	0.2557	0.323	-0.0446	-0.0136	0.6093
Pb	0.2557	1	0.7282	0.0656	-0.0791	0.5301
Sn	0.323	0.7282	1	-0.1209	-0.0396	0.5644
Ag	-0.0446	0.0656	-0.1209	1	0.2951	-0.0562
Au	-0.0136	-0.0791	-0.0396	0.2951	1	-0.0607
Zn	0.6093	0.5301	0.5644	-0.0562	-0.0607	1

Table 4-3: Correlation matrix for major elements.

4.3 PRINCIPAL COMPONENTS

As stated in the introduction the principal components analysis is being conducted in two geometries, Euclidean (i.e. ‘traditional’) and the Simplex (involving a log-ratio transformation of the data).

In both processes the analysis will only focus on the major elements (i.e. minor and trace elements such as bismuth are excluded).

4.3.1 UNTRANSFORMED PCA

4.3.1.1 ZEROS

A method of handling missing values is required to conduct PCA and different approaches are required for the untransformed and transformed PCA. As already mentioned the R package ‘FactoMineR’ is used to conduct PCA on the untransformed data. At the time this data processing methodology was written the package automatically handled missing values by replacing them with the column mean. This is the process used in this chapter. Subsequently the team behind ‘FactoMineR’ produced a new package, ‘missMDA’ (Francois Husson

and Josse 2014), that uses a leave-one-out cross-validation method to calculate and impute missing values. This is not used here, but is implemented in the copper alloys chapter. It should be borne in mind that both methods do not alter the existing non-zero data meaning that the ratios between the figures will not be maintained. As the ratios are crucial in understanding the transformed data a different zero replacement strategy will be used for transformed PCA (see page 200).

4.3.1.2 RESULTS

		PC 1	PC 2	PC 3	PC 4	PC 5	PC 6
Cu	Loading (L)	0.6680	-0.0328	0.6071	0.2522	0.2830	-0.2009
	Contribution (%)	19.6200	0.0764	39.6909	10.2673	17.9497	12.3957
Pb	L	0.7724	0.1262	-0.4397	0.0953	-0.2792	-0.3272
	%	26.2296	1.1325	20.8215	1.4645	17.4725	32.8794
Sn	L	0.7366	-0.1254	-0.4880	-0.0409	0.3939	0.2162
	%	23.8563	1.1181	25.6427	0.2702	34.7614	14.3512
Ag	L	-0.0921	0.8420	-0.0753	0.5001	-0.0112	0.1631
	%	0.3727	50.4517	0.6105	40.3711	0.0280	8.1660
Au	L	0.1510	0.8139	0.1098	-0.5329	0.1119	-0.0792
	%	1.0025	47.1329	1.2972	45.8373	2.8046	1.9254
Zn	L	0.8110	-0.0352	0.3329	-0.1053	-0.3470	0.3140
	%	28.9189	0.0884	11.9372	1.7896	26.9837	30.2822
Percentage of Variance		37.9098	23.4216	15.4765	10.3266	7.4377	5.4277
Cumulative Proportion		37.9098	61.3314	76.8079	87.1346	94.5723	100

Table 4-4: Principal component data. Figures in bold are judged to be significant values (those making at least a 10% contribution).

The principal component results (Table 4-4) show the cumulative proportion to rises quickly in the first two components with a much more gradual increase thereafter to 100% of the variance. The first decision is to decide where to ‘stop’, i.e. how many components should be retained for investigation and further analysis. A traditional method of doing this is to look for the ‘elbow’ on the screen plot of the eigenvalues or variance. However, the scree plot (Figure 4-3) of the results in Table 4-4 shows no such obvious cutting point.

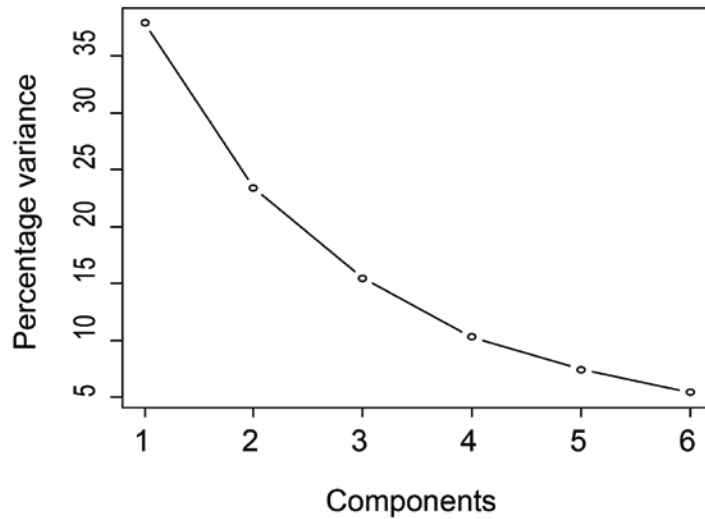


Figure 4-3: Scree plot of principal components

Therefore there is a need to check further. For this the Guttman-Kaiser Criterion (Guttman 1954; Kaiser 1960) can be used. This method states that only components with eigenvalues greater than one (i.e. greater than the weight of an individual) should be considered. In Table 4-5 (below) the eigenvalues for the components are presented. As can be seen only the first two have values greater than one, suggesting that all components from here on should be discarded.

PC 1	PC 2	PC 3	PC 4	PC 5	PC 6
<i>2.2746</i>	<i>1.4053</i>	0.9286	0.6196	0.4463	0.3257

Table 4-5: Variance of each component. Those components that should be retained according the Guttman-Kaiser Criterion are italicised. Only those components with a value above 1 (i.e. greater than the weight of an individual) should be retained according to the criterion.

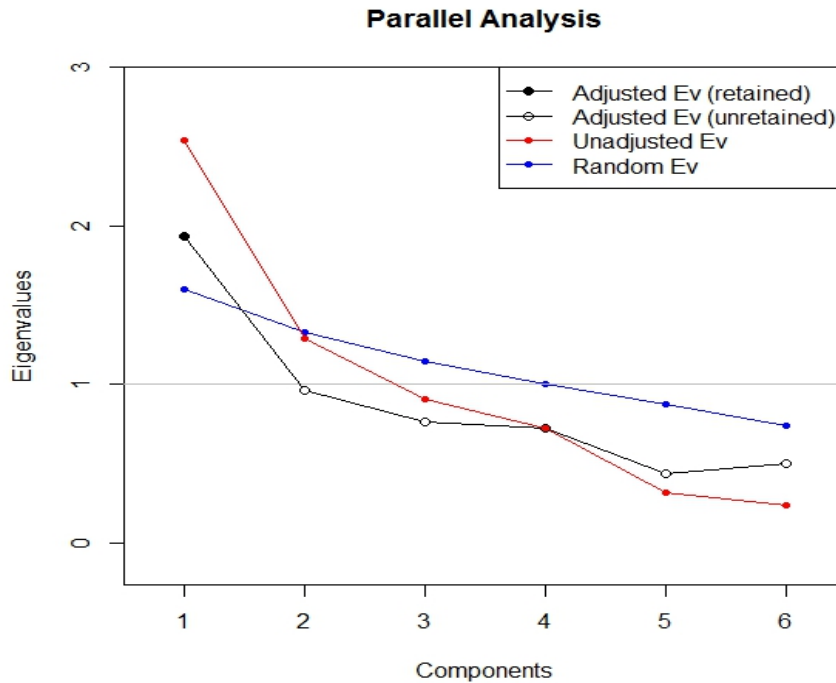


Figure 4-4: Scree plot of the results of Horn's Parallel Analysis for component retention (2010 iterations, using the 95th percentile estimate). See Table 4-6 for further details.

It should be noted that the Guttman-Kaiser Criterion has come in for some significant and legitimate criticism (Yeomans and Golder 1982; Wilson and Cooper 2008) due to its rule of thumb nature and presumptions of near infinite sample size. For extra security we can instead use Horn's Parallel Analysis (Horn J.L. 1965). The results of parallel analysis (Table 4-6 and Figure 4-4, implemented using the R package 'paran', Alexis Dinno, 2012) indicate that only the first component should be considered. This is a significantly different result to that suggested by the visual examination of the scree plot and the Guttman-Kaiser Criterion. However Parallel Analysis has been demonstrated to perform significantly better than either of the previous two methods (Zwick and Velicer 1986). Consequently only one component will be retained here for interpretation.

Component	Adjusted Eigenvalue	Unadjusted Eigenvalue	Estimated Bias
1	1.935774	2.537797	0.602022

Table 4-6: Results of Horn's Parallel Analysis for component retention 2010 iterations ($30 \times n$), using the 95th percentile estimate. Only those elements that should be retained are presented. See Figure 4-4 for graphical representation.

4.3.1.3 INTERPRETATION

In interpreting the PCA results a minimum 10% contribution was used as the rule of thumb in assessing which elements to consider as significant within the component. Although Parallel Analysis indicates the second component should be discarded it is briefly considered here as it is needed to provide something to plot against in factor plots and biplots. These tally with the correlations seen in the scatterplot matrix (Figure 4-2) and correlation matrix (Table 4-2 and Table 4-3).

On the first component copper, lead, tin and zinc load heavily and all loadings are positive except silver. The second component consists of silver and gold loading very heavily (accounting for nearly all the variance) they, along with lead, also load positively whilst copper, tin and zinc load negatively. The factor plot (Figure 4-5) displays these loadings on the two components graphically.

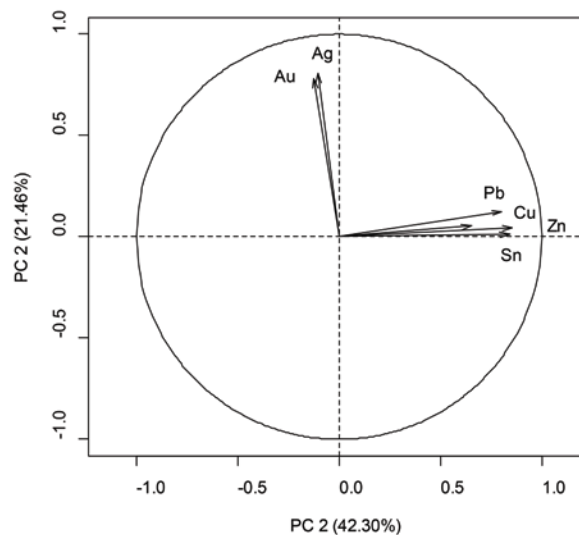


Figure 4-5: Factor plot of PC1 and PC2.

Examining the results in a biplot (Figure 4-6) we can see the majority of individuals distributed in an relatively tight linear distribution across the lower and upper left quadrants along the length of PC 2 (the Y axis). This distribution represents the variances in the silver and gold content. Scattering out from this along the X axis of PC 1 is a less coherent distribution that represents variances in the non-precious-metal elements, It is also interesting to note that in all the categoroidal variables (site, grave number, object category and object class) colour coded on the biplots there appears to be no obvious coherent grouping.

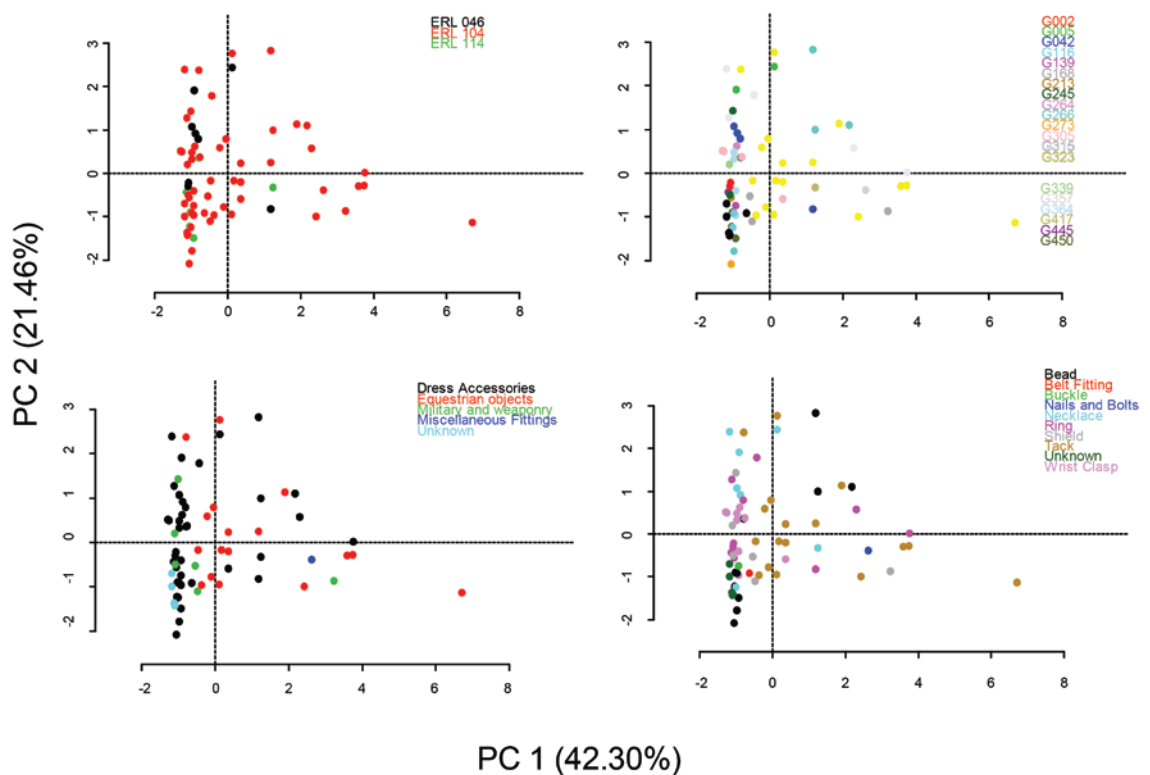


Figure 4-6: Individual PCA biplots plots showing the first two principal components with points illustrated by site (A), grave number (B), object category (C) and object class (D).

The first component only accounts for 37.9% of total variance, indicating that the biplot is a poor quality projection of the data. Considering this it seems prudent to repeat the analysis excluding those objects where – as an approximate rule of thumb – silver accounts for less than two-thirds silver of the NPA

presence.⁶⁸ This removes eight objects from the data set (See Table 4-12), leaving us with 59 objects.

Site	SF No	Analysis Area	Grave No.	Category	Class	Sub Class
104	1336	A	G266	Dress Accessories	Bead	Undefined Bead
104	BM18	B	G323	Equestrian	Tack	Bridle Fitting
104	BM1	C	G323	Equestrian	Tack	Bridle Fitting
104	1583	A	G266	Dress Accessories	Bead	Undefined Bead
104	1779	A	G305	Dress Accessories	Wrist Clasp	Form A
104	2317	D	G315	Dress Accessories	Ring	Ear Ring
104	3675-3	A	G168	Military and weaponry	Shield	Shield Mount
46	1144	A	G42	Dress Accessories	Ring	Finger ring

Table 4-7: Objects removed from the second round of PCA.

4.3.1.4 HIGH SILVER UNTRANSFORMED PCA

The Parallel Analysis is repeated on the trimmed data set. The results (Table 4-8 and

Figure 4-7) show that only the first component should be retained for further analysis (as earlier PC2 shall be used for biplots).

Component	Adjusted Eigenvalue	Unadjusted Eigenvalue	Estimated Bias
1	2.057590	2.704968	0.647378

Table 4-8: Results of Horn's Parallel Analysis for component retention 1320 iterations ($30 \times n$), using the 95th percentile estimate. Only those elements that should be retained are presented. See below for scree plot.

⁶⁸ Surface analysis of silver alloys can lead to overestimations of the 'true' alloy content. Consequently there is a chance that the objects in Table 4-7 may have very low Ag contents indeed. For further details see page 224 in Chapter 5.

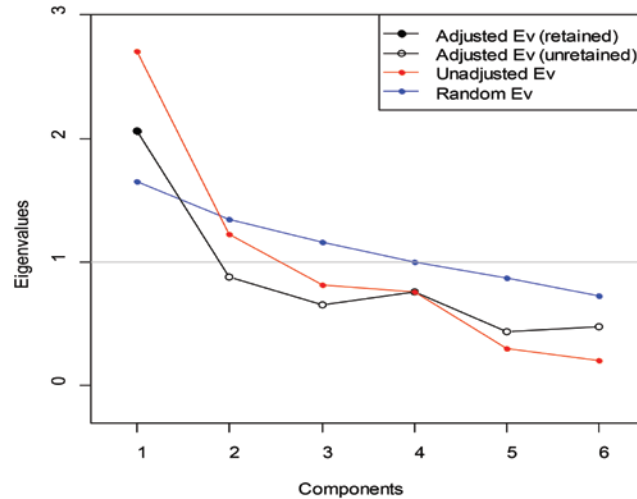


Figure 4-7: Results of Horn's Parallel Analysis for component retention 1770 iterations ($30 \times n$), using the 95th percentile estimate. See Table 4-8 for associated data.

The retained component accounts for a total of 45.08% of the variation in the data set. As with the previous example a minimum 10% contribution was used as starting point for determining which elements were to be considered of significance.

Although the loadings for the individual elements have changed the overall results and conclusions are very similar. On the first component copper, lead, tin and zinc make the largest contributions (all loadings are positive). The second component consists of silver and gold loading very heavily (accounting for nearly all the variance) they, along with lead, also load positively whilst copper, tin and zinc load negatively.

		PC 1	PC 2	PC 3	PC 4	PC 5	PC 6
Ag	<i>Loading (L)</i>	0.2435	0.7312	0.6085	-0.1353	0.1266	0.0384
	<i>Contribution (%)</i>	2.1917	43.8117	45.5423	2.4061	5.3058	0.7424
Au	<i>L</i>	0.1865	0.7709	-0.4909	0.3371	-0.1274	0.0111
	<i>%</i>	1.2852	48.6930	29.6473	14.9367	5.3759	0.0620
Cu	<i>L</i>	0.8152	0.0719	-0.2447	-0.4223	0.1102	-0.2828
	<i>%</i>	24.5662	0.4240	7.3658	23.4462	4.0195	40.1782
Pb	<i>L</i>	0.7838	-0.1845	0.3511	0.3080	-0.3437	-0.1244
	<i>%</i>	22.7097	2.7878	15.1636	12.4705	39.0963	7.7721
Sn	<i>L</i>	0.7680	-0.2125	-0.0214	0.4846	0.3550	0.0604
	<i>%</i>	21.8046	3.7013	0.0565	30.8803	41.7253	1.8320
Zn	<i>L</i>	0.8616	-0.0843	-0.1345	-0.3473	-0.1163	0.3136
	<i>%</i>	27.4425	0.5822	2.2245	15.8602	4.4772	49.4133
Percentage of Variance		45.0828	20.3401	13.5489	12.6768	5.0345	3.3169
Cumulative Proportion		45.0828	65.4229	78.9718	91.6486	96.6831	100

Table 4-9: Principal component data for the trimmed 'high' silver set. Figures in bold are judged to be significant values (those making at least a 10% contribution).

In the untrimmed factor map (Figure 4-5) there was close correlation between silver and gold on the one hand with the other elements tightly grouped. The factor plot here (Figure 4-8) is similar but does show a little more variation.

The biplot of the individuals (Figure 4-8) show that the majority of the individuals are still distributed in an approximate linear distribution, although this now runs in a diagonal fashion from the lower left to upper right quadrants. Again, this distribution may represent variations in the silver and gold content within the individuals. The first component now accounts for 45.08 % of the variation, and this is reflected in the superior (when compared to previous) projection of individuals on the biplot with the variances in the copper, lead, tin and zinc content seen in the raw data (Appendix IV) now possibly being visible. Several outliers (visually identified, not statistically) from the distribution can be identified, particularly the individuals in the lower right quadrant (representing higher variance in tin and lead from the main body) and the individual from grave 266 in the upper right quadrant.

Visually examining the individuals (Figure 4-8) it appears that there may be approximately three natural groups suggesting discrete compositional categories;

two within the main distribution and a third composed of outliers. This will be investigated along with an archaeological interpretation of the Euclidean PCA on page 214.

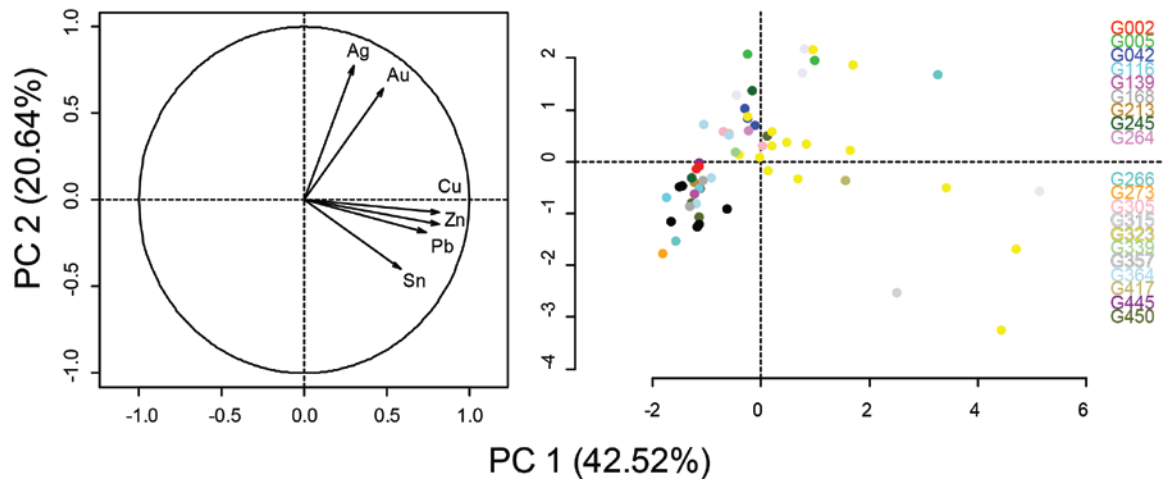


Figure 4-8: Factor plot (left) and biplot (right) of the 'high' silver PCA.

4.3.2 LOG-RATIO TRANSFORMED PCA

4.3.2.1 ZEROES

Processing data in a compositional manner involves working with data which has undergone a logarithmic transformation. As there is no logarithm of zero, approaching data compositionally therefore requires us first to deal with zero values. There are three options; accepting that values are truly zero (essential zeroes), amalgamation or rounded zeroes. Essential zeroes are those that are genuinely not present and whose zero value is not a function of equipment sensitivity, experimental design etc. (Aitchison and Kay 2003). With the data here, analysed using HHpXRF on the corroded surface, determining essential zeroes versus those that are simply below detection limit is not an easy or obvious task. To some extent this has been dealt with by restricting multivariate analysis to significant elements (those that are near consistently present) and excluding minor or trace elements only occasionally present.

To deal with the remaining zeroes (particularly an issue for zinc and tin) there is a choice of amalgamation or rounded zeroes. The latter involves the amalgamation of similar variables with zeroes into broader categories (see for example the household survey and hunter vs prey examples in Aitchison and Kay 2003). While this approach can be applicable to scientific compositional data it requires a good understanding of the chemical system and formation processes behind the samples analysed: appropriate in geochemistry (see the alkalis example in Alvarez 2007) and associated archaeometric analyses (such as smelting slags), it is not valid here. We may understand the chemistry behind silver alloys, but we currently do not have a good enough understanding or models of the human choices that went into producing Early Anglo-Saxon silver objects from the presumed recycled source materials to effectively amalgamate variables.

Rounding zeroes involves the replacement of zero values with minimal values. Although the idea of replacing values may sound extreme it is a fairly common activity in the reporting of scientific and archaeometric data. This often manifests itself as data tables with values being reported in the form of a statement of an element being below the minimum detection limit or presented as '<0.1', 'tr' etc. Accepting the zeroes in the major elements as absolute zeroes was ruled out above (because of equipment sensitivity and the nature of surface analysis we cannot be certain) as was the use of amalgamation.⁶⁹ Consequently rounded zeroes will be used here.

Replacing a zero is not as simple as inserting a minimal value in its place and the method (there are several different methods of replacing zeroes) has to be chosen carefully; the wrong approach can lead to false distributions and

⁶⁹ For the four major elements (copper, tin, zinc and lead) 6.53% (51 in total) of the Eriswell copper alloy data set is composed of zeros. In Blades (1995) analysis of Early Anglo-Saxon objects (acquired using ICP-AES on uncorroded invasively acquired samples) the number of zeros present in the same set of elements is 0.02% (three in total). This suggests that — assuming that the alloys are relatively comparable — the majority of the zero values recorded in the Eriswell data are indeed rounded zeros, but that we should be open to the possibility of the presence of a small number of absolute zeros. Blades' data is examined in more detail in Chapter 8 in consort with the copper alloy results. That chapter also contains a more detailed breakdown of the frequency of zero values, see Table 8-21 on page 346.

correlations (for an overview of zero replacement methods and issues see Martín-Fernández, Palarea-Albaladejo, and Olea 2011). To minimise this risk a method called Multiplicative Replacement Strategy will be used here. A Multiplicative Replacement Strategy involves the replacement of a zero value with a small value and multiplicatively modifying non-zeroes with a sum-constraint (see Equation 7). This approach, proposed by Martín-Fernandez et al. in 2000, has been demonstrated (Martín-Fernández, Barceló-Vidal, and Pawlowsky-Glahn 2003) to perform significantly better than alternative methods in retaining coherence in the ratios and distribution.

$$r^j = \begin{cases} \delta_j, & \text{if } x_j = 0, \\ \left(1 - \frac{\sum_{k|x_k=0} \delta_k}{c}\right) x_j, & \text{if } x_j > 0, \end{cases}$$

Equation 7: Formulae for Multiplicative Replacement Strategy for zeroes from Martín-Fernández et al. (2003, 262, Equation 6): r is the modified non-zero value, δ_j is the small value which replaces the zero, x_j is the original unmodified non-zero and c is the constant of the sum constraint.

The CoDaPack software used here implements the approach of Martín-Fernandez et al. (2003) to replace zeroes with a value 65% of the detection limit. In replacing zeroes in the Eriswell NPA data the first choice is what the detection limit should be; not an easy choice due to the qualitative nature of the data. On page 161 a series of net peak area limits of determination on experimentally corroded reference alloys were produced. The use of these was considered, but there were a couple of reasons why it was initially felt that these were still too unrepresentative of reality. Firstly, whilst they are corroded, the reference alloys have (when compared with the archaeological examples) a relatively flat geometry and complete coverage of the instrument window (in a way that a pin or curved brooch catch will not) and this will impact on the results. Secondly it is felt that there may be a false degree of accuracy in using these figures. For, in reality, the limit of detection was not based on a mathematically derived integer, but something less quantifiable: the author's

eyes.⁷⁰ As discussed on page 179 in the previous chapter each peak in each spectrum was subject to two separate visual examinations to decide if the peak was genuinely present (and not the result of matrix effects or the beta peak of another element). The second of these steps was undertaken in the Bruker Artax software immediately before the peak areas were calculated. For the net peak area data produced by this software one is the minimum peak area that can be outputted. Consequently — as the easiest way to quantify the identification of a peak is as a binary choice (i.e. one has identified it as being present or not) — it seemed sensible to choose one as the detection limit in this dataset and therefore 0.65 as the replacement zero value (see Table 4-10 for an example).

Site	Small Find No.		Cu	Pb	Sn	Ag	Au	Zn
104	1007 A	<i>Original</i>	22510	5638	588	1002421	12930	0
		<i>Replaced Zero</i>	22509.99	5637.996	587.9996	1002420.38	12929.99	0.65
046	1086 A	<i>Original</i>	111134	15968	0	1743259	30588	3107
		<i>Replaced Zero</i>	111133.96	15967.99	0.65	1743258.40	30587.99	3106.999

Table 4-10: Example of Multiplicative Replacement on two Eriswell silver objects.

This was the choice made going forwards in this thesis. However, it may be noted that 0.65 is a very small value when compared with the peak heights and therefore there may be a risk that this value is unrealistically low and will distort the ratios, introducing false correlations. Consequently it may, with the benefit of hindsight, be better to use the limits of determination that were initially ruled out a few paragraphs earlier.⁷¹ This is not the only potential problem with the approach used here. Subsequent to the production of this thesis the author became aware of the work of Sanford et al. (1993) who noted that the imputation of replacement values in a data set where more than 10% of the values are zero can result in artificial correlations. This is an issue here for the silver alloy data set, where the percentage of zeros present in the main elements of interest

⁷⁰ This — and other user behaviour — can be built into the model to some extent by having a number of different individuals repeating the process of analysing the reference alloys and producing the LDM. Unfortunately this does require you to have at least two other people with the desire and / or time to undertake this process in the building.

⁷¹ Many thanks to Professor Marcos Martín-Torres for his highlighting of this issue.

(copper, lead, tin, silver, gold and zinc) is 14.3% (43 zeros in total). It is thought to be less of an issue in the copper alloy data set where the percentage of zeros for the four major elements (copper, tin, zinc and lead) is 6.53% (51 in total). Strategies for avoiding possible false correlations in this situation — such as the use of a parametric approach — are proposed in Palarea-Albaladejo et al. (2007). Consequently it has been decided that further investigation into the zero replacement strategy for the data sets here is required (including a sensitivity analysis of differing zero replacement strategies). It is intended to undertake and publish this as part of a further study into the overall analytical and interpretive approach used here. In the interim the reader must be aware that there is a real risk of false correlations in the results discussed in both the silver and copper alloy chapter where the zero replacement method discussed here is utilised.

4.3.2.2 TRANSFORMATIONS

For the following analysis and interpretation data will be transformed using a centred log-ratio (clr) approach (for a detailed introduction and background to the clr transformation see Aitchison 2003, 30; Pawlowsky-Glahn and Egozcue 2006 and Filzmoser et al. 2009, 622). A centred log-ratio transformation is one of three possible choices, the other two being additive log-ratio (alr) and isometric log-ratio (ilr). Each has its benefits and drawbacks as discussed Bacon-Shone (2011, 5–6) and Agterberg (2014, 474); alr can be arbitrary, the singular matrix of clr can cause problems with other statistical tests and ilr requires transformation based on an orthonormal partition (Egozcue et al. 2003). As there is no canonical basis for the partition when undertaking an ilr transformation (Bacon-Shone 2011, 6) and as this is a rather tentative exploration of the applicability of the concept of working in a constrained space to NPA data it is perhaps considered best that the ilr transformation is avoided for now. Instead a clr transformation (for details of the mathematics behind this transformation see Aitchison (2003, 30) and Filzmoser et al. (2009, 622)) will be used. Although this limits potential

for some statistical tests, this is of little concern here: the data are predominantly non-normally distributed and analysis is limited to a descriptive inferences.

The clr data transformation is undertaken in the CoDaPack software once zeroes have been replaced and the compositions closed as a sub-composition.

4.3.2.3 CENTRED LOG-RATIO PCA

As with the untransformed PCA we start with the full data set (excluding solders and the mercury contaminated result) used in section 4.3.1 (n=67).

The variation array in Table 4-11 below shows the log-ratio mean and variances (for a classical summary of the same data see Table 4-1).

Xi\Xj	Zn	Cu	Pb	Sn	Ag	Au	clr variances
Zn		11.605	11.9585	27.7937	14.3183	40.2749	9.9414
Cu	5.0625		0.938	20.0892	1.0796	18.2056	0.936
Pb	3.1984	-1.8641		18.4092	0.7244	18.6648	0.7322
Sn	-1.5776	-6.6401	-4.776		23.665	54.4457	16.3502
Ag	7.329	2.2665	4.1307	8.9066		15.6379	1.5206
Au	1.6493	-3.4132	-1.549	3.2269	-5.6797		16.8212
					Total Variance		46.3016

Table 4-11: Variation array for Eriswell silver. Upper triangle: log-ratio variances; lower triangle: log-ratio means. Bold values are those that have the largest variance.

Examining the log-ratio means and the centred log-ratio (clr) variances in Table 4-11 we can see that tin-zinc, tin-gold and zinc-gold have the largest variability. This is no surprise. The NPA figures in Appendix IV show significant variation visible with the naked eye before any statistical manipulation; the small subset of objects with apparent lower Ag content tend to contain higher quantities of other metals. Not surprisingly these tend to be other white metals such as zinc (for example in shield mount 1176) and tin (shield mount 1191). What's more tin and zinc show the greatest variability in presence / absence. Of the silver alloys analysed here only 44% definitely contain tin, and 72% definitely contain zinc. Of the tin silver alloys 32% contained zinc and only 19% of zinc silver alloys also contained tin. The least variation in the dataset is between copper-silver and lead-silver.

The variances can be visually displayed in a scatterplot matrix. As the data are being processed compositionally then a different form of scatterplot matrix is required to that used earlier. The result (Figure 4-9) is similar to Figure 4-2 in that it shows pairs of elements, however, this is in the form of clr transformed ternary diagram with the third component (three components being needed for a ternary diagram) representing the geometric mean of the remaining components (van den Boogaart and Tolosana-Delgado 2006) .

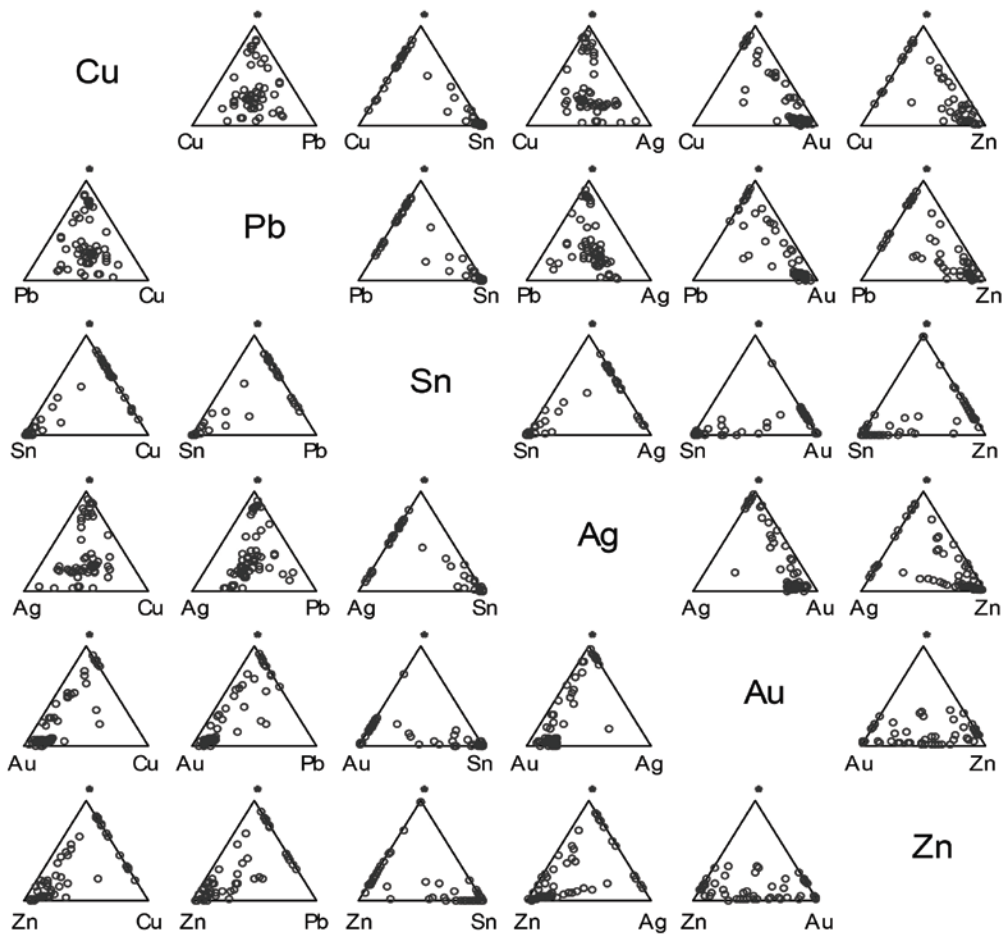


Figure 4-9: clr ternary diagram scatter plot matrix of major elements from silver objects. The * at the apex of each diagram is the third component and represents the geometric mean of the remaining components (van den Boogaart and Tolosana-Delgado 2006). Created using the R package 'compositions' (van den Boogaart, Tolosana, and Bren 2014).

The PCA results (Table 4-12) show the first component explaining 62.017% of the total variance and the second 27.6% (89.61% in total). This immediately seems to indicate that the first two components should be retained.

		PC 1	PC 2	PC 3	PC 4	PC 5
Ag	Loading (L)	-0.1176	-0.0253	-0.4878	-0.3224	0.6906
	Contribution (%)	1.3829	0.0640	23.7959	10.3946	47.6960
Au	L	-0.7208	0.2647	0.4936	-0.0039	-0.0076
	%	51.9523	7.0065	24.3652	0.0015	0.0058
Cu	L	-0.0326	-0.0524	-0.3521	0.8329	-0.1086
	%	0.1063	0.2746	12.3980	69.3749	1.1795
Pb	L	-0.0100	-0.0068	-0.3631	-0.4468	-0.7083
	%	0.0100	0.0046	13.1847	19.9638	50.1722
Sn	L	0.6372	0.5846	0.2805	-0.0090	0.0826
	%	40.6001	34.1750	7.8684	0.0081	0.6823
Zn	L	0.2439	-0.7647	0.4288	-0.0507	0.0514
	%	5.9484	58.4754	18.3878	0.2571	0.2642
Percentage of Variance		62.01	27.6	8.94	1.1	0.35
Cumulative Proportion		62.01	89.61	98.55	99.65	100

Table 4-12: *clr* Principal Component data. Figures in bold italics are significant values (those making at least a 10% contribution).

Unfortunately the ‘paran’ package cannot be used to undertake Parallel Analysis on compositional data in R, the process only being valid when PCA is performed using correlation not covariance matrices (Dinno 2014). Consequently a scree plot and the Guttman-Kaiser Criterion have to be used in deciding how many components to retain.

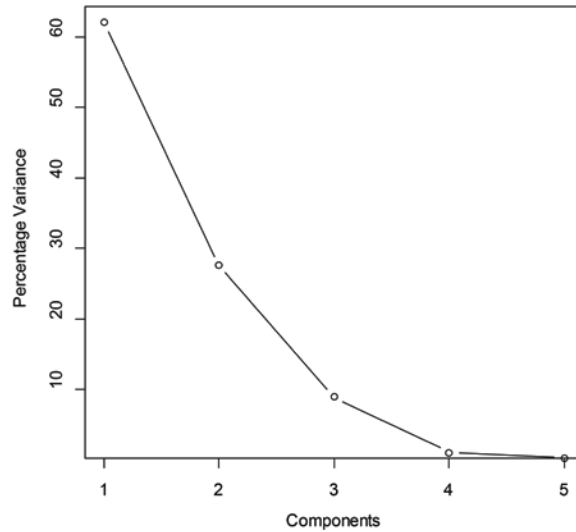


Figure 4-10: Scree plot of clr PCA.

The scree plot (Figure 4-10) shows the ‘elbow’ at PC 3. This, however, may be somewhat misleading as the first two components explain 89.61 % of the variance suggesting that only these two should be retained. Examining the eigenvalues (Table 4-13) according to the Guttman-Kaiser Criterion supports this with only PC 1 & 2 having values over one. Therefore only the first two components will be examined here.

PC 1	PC 2	PC 3	PC 4	PC 5
<i>3.1005</i>	<i>1.38</i>	0.447	0.055	0.0175

Table 4-13: Component eigenvalues for clr PCA. Those components that should be retained according to the Guttman-Kaiser Criterion are italicised. Only those components with a value above 1 (i.e. greater than the weight of an individual) should be retained according to the criterion.

On the first component gold and tin load heavily (negatively and positively respectively). On the second component zinc (negatively) and tin (positively) load heavily.

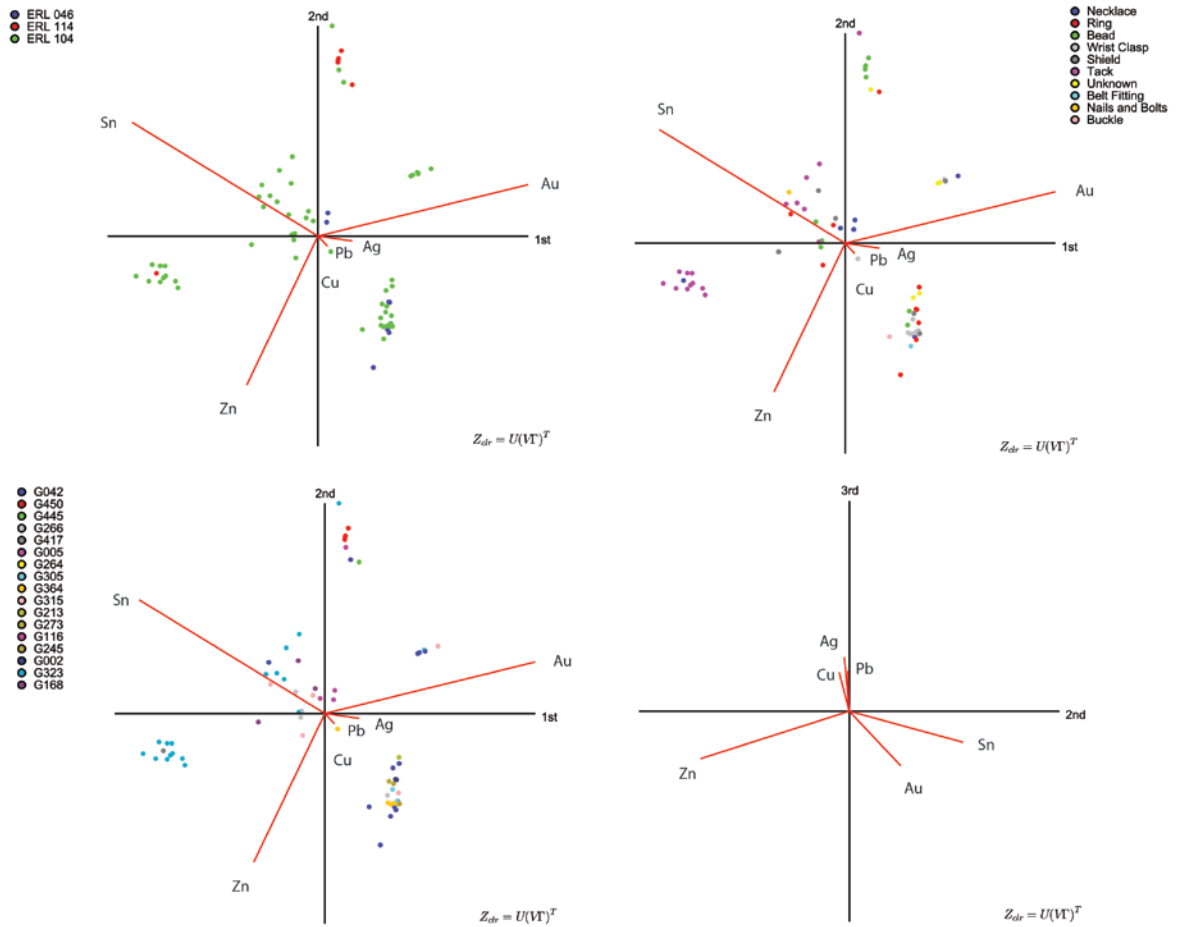


Figure 4-11: 3D symmetrically scaled centred log-ratio (clr) biplots of silver data showing variables and observations. Three biplots (A-C) show the same data set in an XY orientation with observation points identified by categorical variables as follows: site (top left); object class (top right) and grave number (bottom left). The fourth biplot (d) shows the rays without the observations in an YZ orientation to better display the Cu, Ag and Pb rays.

Plotting the data in a clr biplot reinforces this (Figure 4-11), with categorical rays (representing the variation) for zinc, tin and gold being the largest. The angle between the rays relates to their correlation (K.G van den Boogaart and Tolosana-Delgado 2013). The gold, tin and zinc rays are the most dispersed, accounting for the majority of the variance (as one would expect from the variance array in Table 4-11 and PCA results in Table 4-12). The closeness of the relatively short silver, copper and lead rays suggests these may be low-variance sub compositions (again matching the results in the variation array).

It is noticeable how different the clr PCA projection of variance is from the untransformed PCA; clr explains PC1 variance as being between gold and tin, untransformed between everything except silver and gold. There is similar variation with PC2; untransformed PCA explains variance between silver and gold whilst clr as tin and zinc. Examining the raw data (Appendix IV) it may be suggested that the clr PCA is producing a better projection of the data than the untransformed PCA as it reflects the presence / absence of zinc and tin in the data set.

It is also interesting to note that the clr PCA biplot suggests the presence of five natural groups within the data. One significant similarity between the two approaches is that, apart from the equestrian objects in the bottom left quadrant of the biplots, there appears to be little correlation between the distribution of individuals and the archaeological categorical variables.

To ensure a full and equal comparison between techniques (and because corrosion may mean the silver level is minimal in these objects, see footnote 68 above) the analysis is rerun excluding the objects listed in Table 4-7.

4.3.2.4 HIGH SILVER PCA

Reproducing the variation array (Table 4-14) we can see that, whilst the figures are slightly different from the full silver set in Table 4-11, the interpretation of the centred log-ratio (clr) variances remains essentially the same: tin-zinc, tin-gold, tin-silver and copper-tin have the largest variability, copper-silver and lead-silver have the least.

Xi\Xj	Cu	Pb	Sn	Ag	Au	Zn	clr variances
Cu		0.4537	19.4972	0.5673	16.5305	12.6735	0.7627
Pb	-1.6636		18.3552	0.5546	17.3827	12.3208	0.6535
Sn	-6.7207	-5.0571		22.7072	51.507	29.234	16.0258
Ag	2.5446	4.2083	9.2654		15.0514	14.3449	1.3466
Au	-2.9981	-1.3344	3.7227	-5.5427		39.6956	15.8369
Zn	-5.2352	-3.5716	1.4855	-7.7798	-2.2371		10.5205
						Total Variance	45.1459

Table 4-14: Variation array for Eriswell silver. Upper triangle: log-ratio variances; lower triangle: log-ratio means. Bold values are those that have the largest variance.

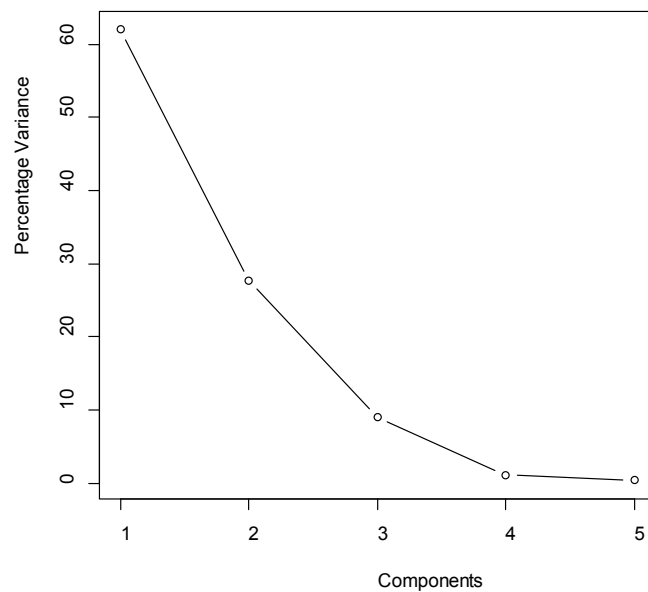


Figure 4-12: Scree plot of 'high' silver clr PCA.

As previous the scree plot (Figure 4-12) shows the 'elbow' at PC 3. This, however, may be somewhat misleading as the first two components explain a majority of the variance (See Table 4-16), suggesting that only these two should be retained. Examining the eigenvalues (Table 4-15) according to the Guttman-Kaiser Criterion supports this with only PC 1 & 2 having values over 1. Therefore only the first two components shall be examined here.

PC 1	PC 2	PC 3	PC 4	PC 5
2.998	1.514	0.447	0.026	0.015

Table 4-15: Component eigenvalues for the ‘high’ silver clr PCA. Those components that should be retained according the Guttman-Kaiser Criterion are italicised. Only those components with a value above 1 (i.e. greater than the weight of an individual) should be retained according to the criterion.

The principal component results (Table 4-16) show remarkable similarity to the previous clr PCA. On the first component tin and zinc load heavily (negatively and positively respectively), but with the inertia more equitably distributed between the two. PC2 shows some variation from previous with tin now also loading heavily (positively) alongside gold (negatively) zinc (positively).

		PC 1	PC 2	PC 3	PC 4	PC 5
Ag	Loading (L)	0.0440	-0.0206	0.3664	-0.8274	0.1103
	Contribution (%)	0.1936	0.0424	13.4246	68.4593	1.2167
Au	L	0.0174	-0.0143	0.3613	0.4564	0.7028
	%	0.0303	0.0204	13.0535	20.8302	49.3948
Cu	L	-0.6406	0.5791	-0.2863	0.0164	-0.0730
	%	41.0415	33.5351	8.1966	0.0269	0.5329
Pb	L	0.1099	-0.0276	0.4770	0.3262	-0.6975
	%	1.2079	0.0762	22.7524	10.6407	48.6526
Sn	L	0.7169	0.2564	-0.5035	0.0106	0.0023
	%	51.4004	6.5740	25.3507	0.0112	0.0005
Zn	L	-0.2475	-0.7730	-0.4150	0.0178	-0.0450
	%	6.1263	59.7519	17.2221	0.0317	0.2025
Percentage of Variance		59.96	30.28	8.94	0.52	0.3
Cumulative Proportion		59.96	90.24	99.18	99.7	100

Table 4-16: clr ‘high’ silver Principal Component data. Figures in bold italics are significant values (those making at least a 10% contribution).

The ‘high’ silver PCA results are relatively similar to the ‘low’ silver PCA results; therefore it is no surprise to discover that the ‘high’ silver clr biplot (Figure 4-14) is also similar to the ‘low’ silver clr biplot (Figure 4-11). Categorical rays (representing the variation) for zinc, tin and gold are the largest. The zinc, tin and gold rays are the most dispersed, accounting for the majority of the variance (as one would expect from the variance array in Table 4-14 and PCA results in Table 4-16). The closeness of the relatively short silver, copper and lead rays suggests

these may be low-variance sub-compositions (again matching the results in the variation array).

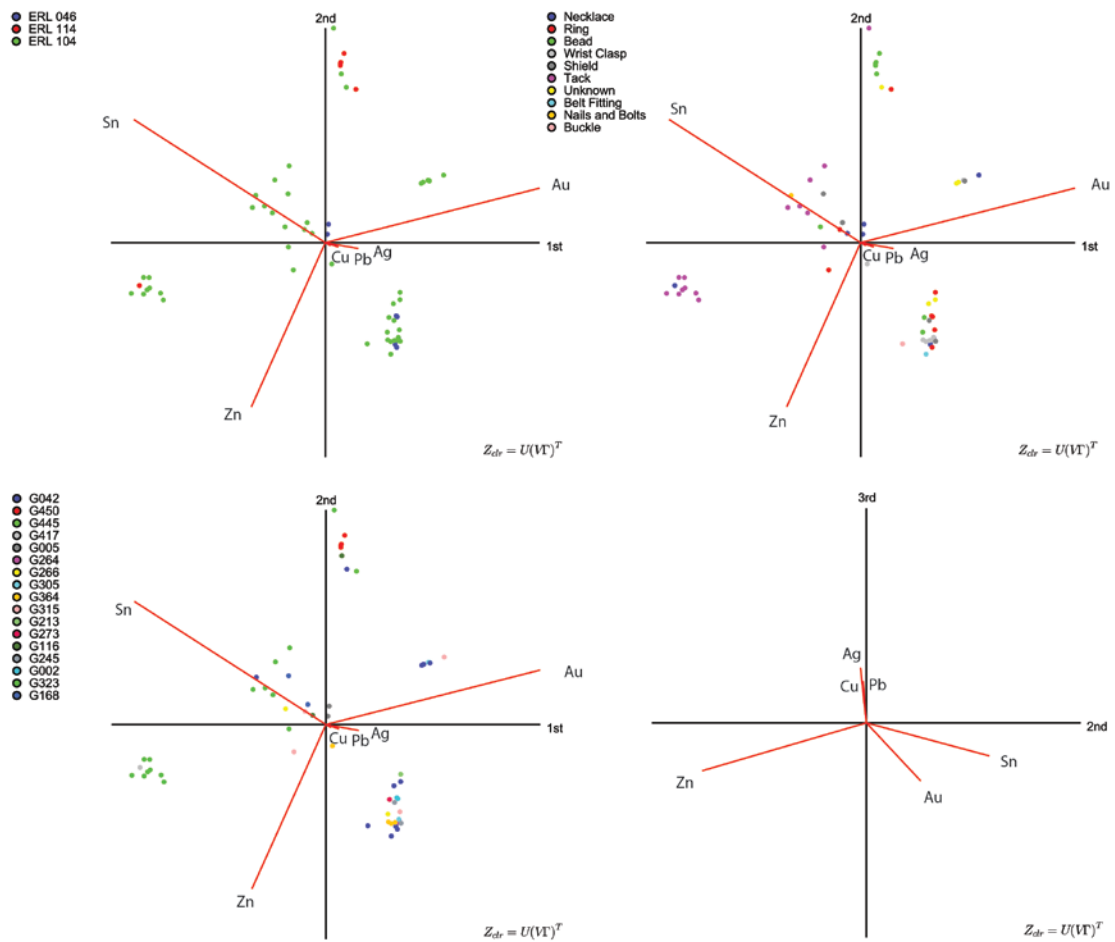


Figure 4-13: Symmetrically scaled centred log-ratio (clr) biplots of ‘high’ silver data showing variables and observations. Three biplots (A-C) show the same data set in an XY orientation with observation points identified by categorical variables as follows: site (top left); object class (top right) and grave number (bottom left). The fourth biplot (d) shows the rays without the observations in an YZ orientation to better display the Cu, Ag and Pb rays.

Examining the individuals in the biplots it can be seen that the distribution is similar between the current and previous plots and it is interesting to note that the distribution of individuals in untransformed PCA was affected more than clr PCA by the inclusion of analyses which included objects with lower silver compositions. In both clr biplots approximately five natural groups of individuals can be seen, suggesting discrete compositional categories. This is one more group

than suggested by the untransformed PCA and, as can be seen from the grave number biplots in Figure 4-8 and Figure 4-14, there is little in common in the way the individuals are distributed within the groups. A full assessment of this is undertaken below.

4.4 COMPARISON OF UNTRANSFORMED AND CLR TRANSFORMED PCA

In both the untransformed and clr PCA there have been indications of coherent natural groups within the data (see Figure 4-14). These groups do not conform to any of our archaeological categorical variables and there is little (archaeologically) in common between the groupings suggested. Consequently these will be examined in detail here as a way of assessing the performance of the dimensional reduction and correlations against metallurgical considerations.

4.4.1 HIERARCHICAL CLUSTERS

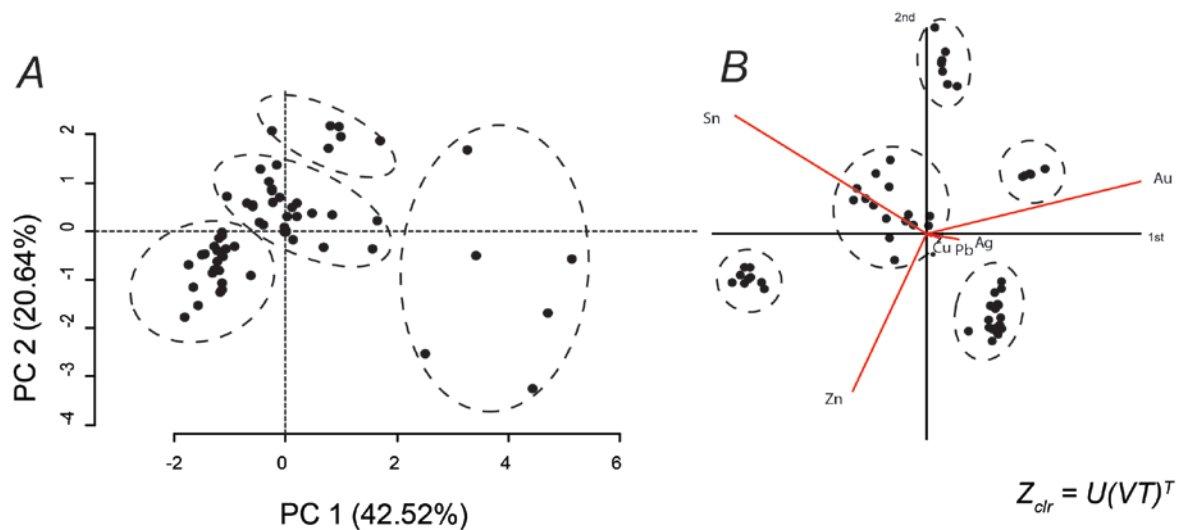


Figure 4-14: 'High' silver biplots with natural groups (identified visually) delimited by dashed lines: A - Euclidean PCA biplot (note that the group of three individuals is defined simply as 'not the other two'). B - 3D symmetrically scaled clr biplot showing in XY orientation.

The first step is to assess if the natural groups seen in the biplots are valid and not an unsatisfactory simulacrum from a fevered PhD student's imagination. For

this hierarchical clustering is used. On the untransformed PCA the Hierarchical Clustering on Principal Components (HCPC) function of the R package ‘Factominer’ was used. On the transformed data the R package ‘compositions’ (van den Boogaart, Tolosana, and Bren 2014) and the base package ‘hclust’ function was used. In both, Ward’s method (Ward 1963) is used to agglomerate the clusters. As the method is sensitive to outliers (Milligan 1980) this initial examination will only be applied to the trimmed silver data set (see Table 4-7 for the analyses excluded).

Ward’s method seeks to minimize within-cluster variance using the squared Euclidean distance. Although this sounds like it may present a problem for compositional data any problem is avoided by applying the hclust base R function to a transformed dataset in the ‘compositions’ package (van den Boogaart and Tolosana-Delgado 2006; van den Boogaart and Tolosana-Delgado 2013).

The results of both (Figure 4-15 and Figure 4-16) show balance dendrograms and biplots with colour coded individuals according to the clusters identified by the partition of the data in the dendrograms. These partitions are defined by cutting the dendrogram at an appropriate point and treating all branches beneath this height as one cluster. Deciding where to cut is a subjective matter, and following (Boogaart and Tolosana-Delgado 2013), the decision was based on long height intervals with minimal agglomeration.

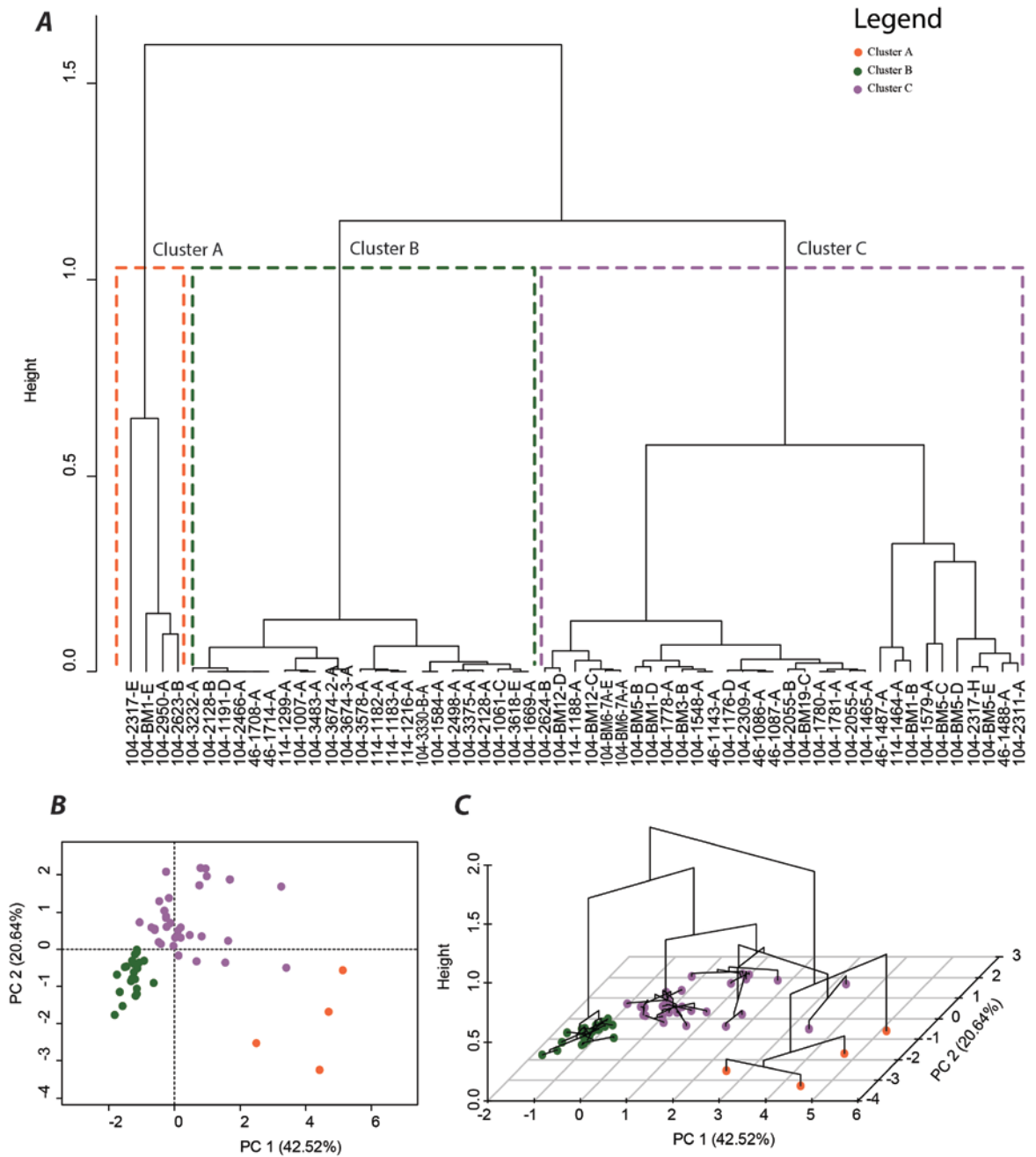


Figure 4-15: Hierarchical Clustering on untransformed PCA results using Ward's method for agglomerating clusters produced using the R package 'FactoMiner' and base R function 'hclust'. The clusters are illustrated in two ways: A – balance dendrogram of clusters (the dashed lines indicate where the tree was cut and are colour coded), B – 2D biplot and C – biplot with dendrogram.

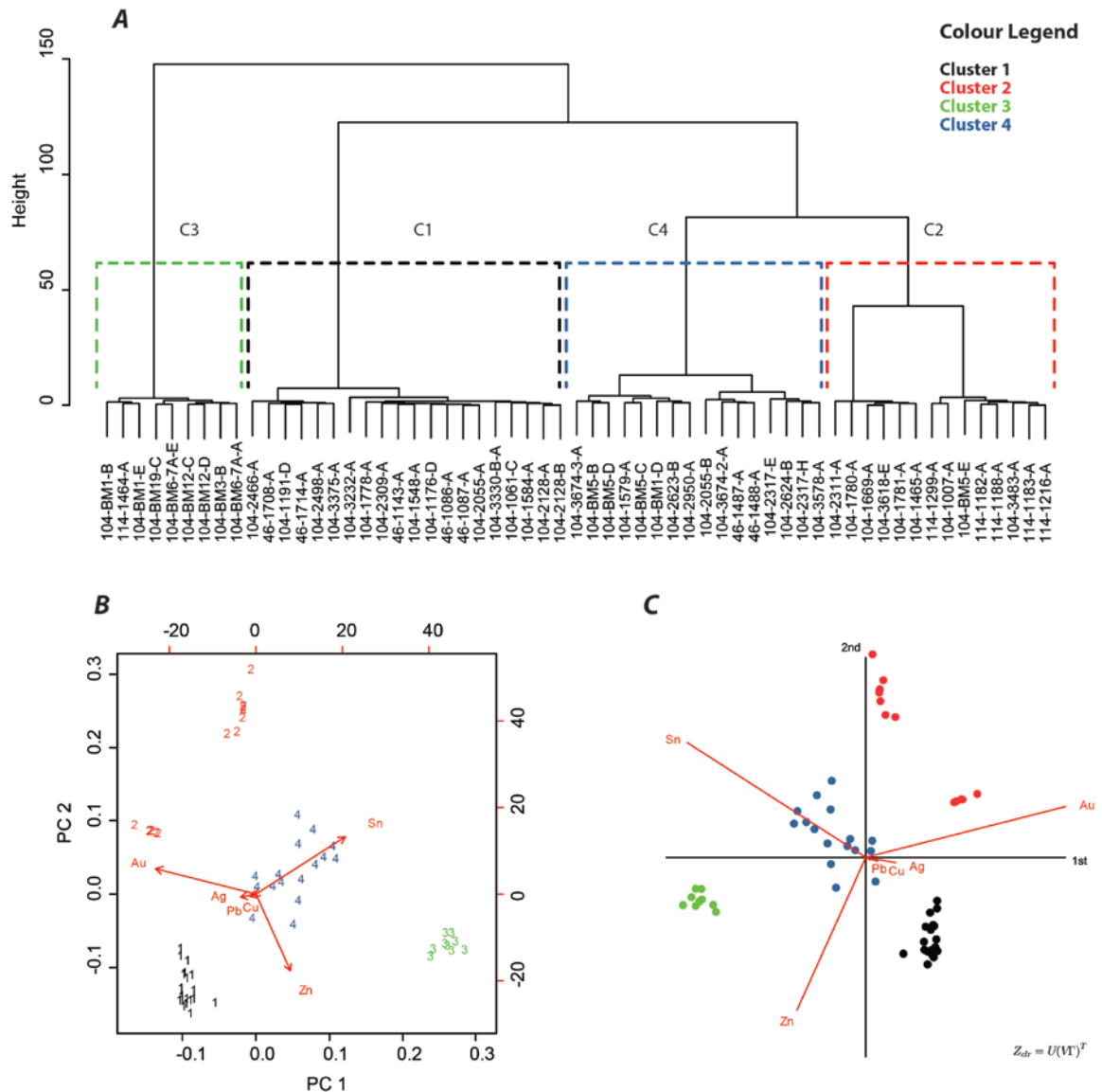


Figure 4-16: Hierarchical Clustering on compositional data using Ward's method for agglomerating clusters produced using the R package 'compositions' and base R function 'hclust'. The clusters are illustrated in two ways: A – balance dendrogram of clusters (the dashed lines indicate where the tree was cut and are colour coded), B – 2D clr biplot and C - 3D symmetrically scaled biplot with individuals colour coded by cluster.

It may be argued that the positions chosen for cutting are not ideal as they create groups out of outliers (cluster A in Figure 4-15) or incorporate two possible disparate groups within a cluster (cluster 2 in Figure 4-16). This is inevitable given the variations from the 'true' composition we can expect from analysing the corroded surface (as discussed on page 167); to cut at lower heights would present a false degree of accuracy. It should be noted that the clusters defined by

Hierarchical Clustering are relatively similar to the natural groups visually identified in the biplots in Figure 4-14.

Examining the clusters (Table 4-18, the same table with full categorical variable context can be found in Appendix II) shows that there is a certain degree of comparability between them. The analyses which form cluster A in the untransformed set (the ‘outlier’ cluster in Figure 4-15) fall within clusters 4 in the clr transformed set (Table 4-17). The transformed clr cluster 2 set also contains analyses that are clustered in untransformed clusters B and C and clr cluster 4 is present in all three untransformed cluster groups. If the earlier biplots and PCA results hadn’t already made it clear then this does; different geometries are producing different results.

Transformed cluster group	Untransformed cluster group		
	A	B	C
1		12	8
2		8	6
3	1		8
4	3	3	10

Table 4-17: Comparison between cluster groups showing the number of individuals within corresponding groups

Object ID	Untransformed cluster group	Transformed cluster group
046-1086-A	C	1
046-1087-A	C	1
046-1143-A	C	1
114-1182-A	B	2
114-1183-A	B	2
114-1188-A	C	2
114-1216-A	B	2
114-1299-A	B	2
114-1464-A	C	3
046-1487-A	C	4
046-1488-A	C	4
104-1548-A	C	1
104-1579-A	C	4
104-1584-A	B	1
104-1778-A	C	1
104-1780-A	C	2
104-1781-A	C	2
104-2055-A	C	1
104-2055-B	C	4
104-2128-A	B	1
104-2128-B	B	1
104-2309-A	C	1
104-2311-A	C	2
104-2317-E	A	4
104-2317-H	C	4
104-2466-A	B	1
104-3330-B-A	B	1
104-3483-A	B	2
104-3578-A	B	4
104-1176-D	C	1
104-1191-D	B	1
046-1708-A	B	1
046-1714-A	B	1
104-2623-B	A	4
104-2624-B	C	4
104-3674-2-A	B	4
104-3674-3-A	B	4
104-BM1-B	C	3
104-BM1-D	C	4
104-BM1-E	A	3
104-BM12-C	C	3
104-BM12-D	C	3

Object ID	Untransformed cluster group	Transformed cluster group
104-BM19-C	C	3
104-BM3-B	C	3
104-BM5-B	C	4
104-BM5-C	C	4
104-BM5-D	C	4
104-BM5-E	C	2
104-BM6-7A-A	C	3
104-BM6-7A-E	C	3
104-1007-A	B	2
104-1061-C	B	1
104-1465-A	C	2
104-1669-A	B	2
104-2498-A	B	1
104-2950-A	A	4
104-3232-A	B	1
104-3375-A	B	1
104-3618-E	B	2

Table 4-18: Cluster results. A full table with categorical variables included can be found in Appendix II.

4.4.1.1 CLUSTERING AND SCATTER PLOT MATRICES

To evaluate these disparate cluster results there needs to be an examination of how these clusters actually represent themselves on the alloy compositions. To do this they each are briefly examined in scatter plots matrices.

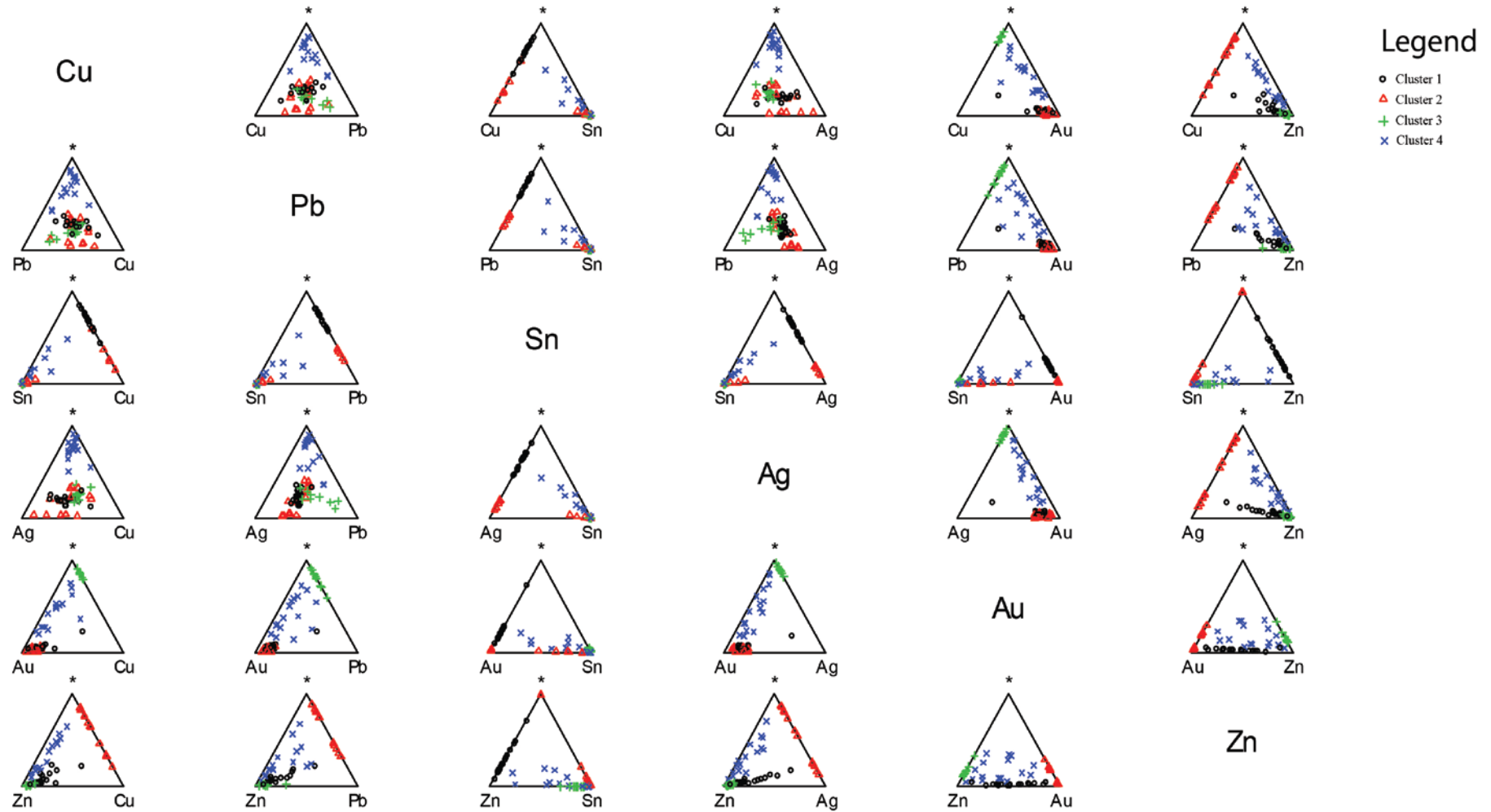


Figure 4-17: Centred clr ternary diagram scatter plot matrix of major elements from silver objects with individuals identified using clusters defined using hierarchical clustering. The * at the apex of each diagram is the third component and represents the geometric mean of the remaining components (Boogaart and Tolosana-Delgado 2006). Created using the R package 'compositions' (Boogaart, Tolosana, and Bren 2014).

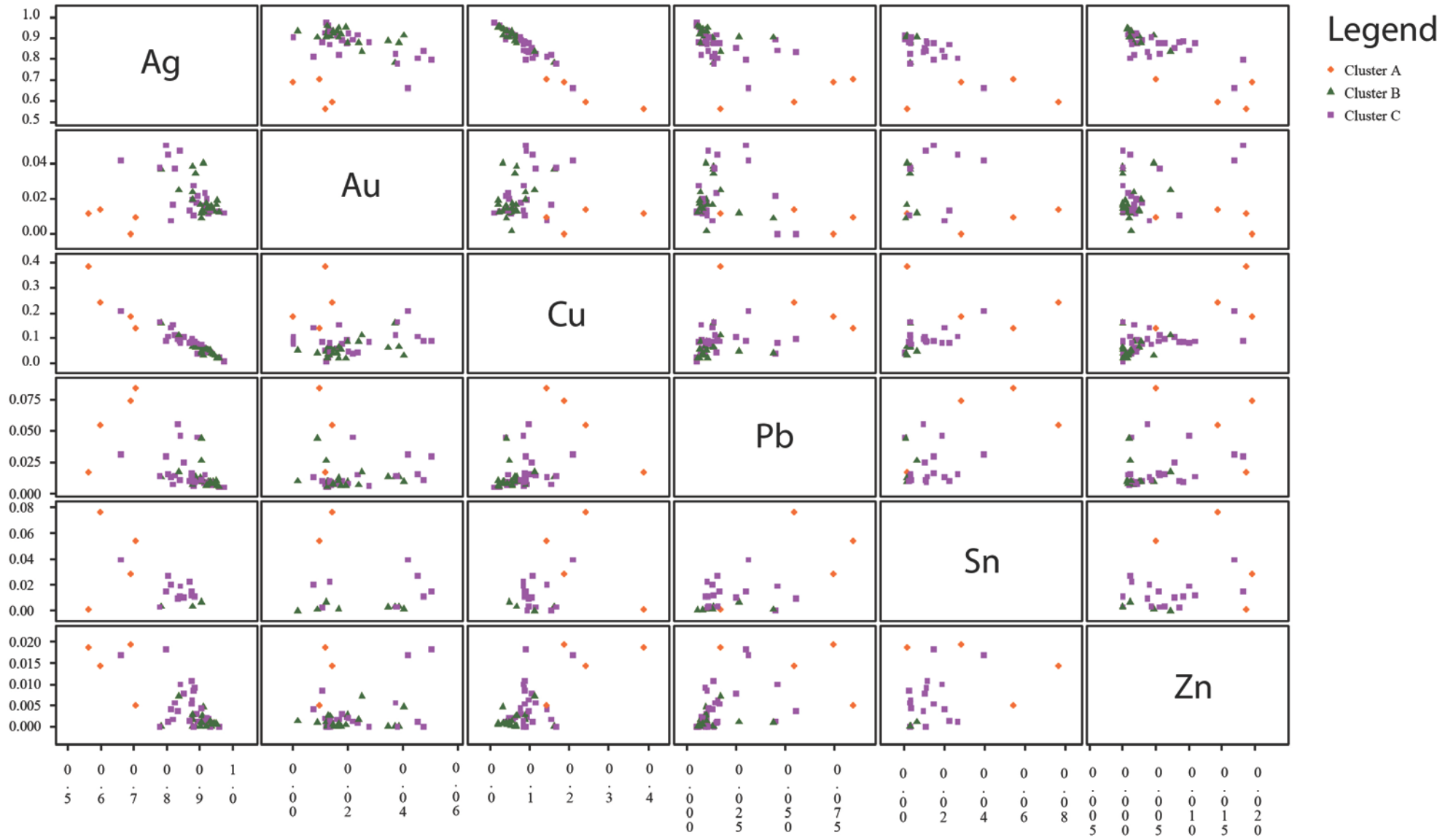


Figure 4-18: untransformed scatter plot matrix showing clusters.

In the clr biplots it appeared as if there were five groups. Hierarchical clustering, however, only identified four (at the level the tree was cut). This led to two possible groups in the upper right quadrant of the XY orientated biplot being grouped together as cluster 2. In some of the scatter plots (Figure 4-17), such as tin-lead, cluster 2 is clearly split into two groups. Is this a problem? Only if you ignore the context of the PCA results. The clr PCA had two significant components; the first was explained as the variance between gold and tin and the second as between zinc and tin. Lead did not feature as making a significant contribution to the variance in either of these two components. This is clearly represented in the centred clr ternary diagram scatter plot matrix and in the gold-tin and tin zinc plots cluster 2 can be seen to be relatively tightly grouped.

In the untransformed scatterplot matrix (Figure 4-18) the cluster results look less clear than in the clr example. Cluster A (the outlier cluster) is consistently, well, outlying. Clusters B & C tend to be more closely grouped and overlapping. There is, however, some distinction and cluster B is often more tightly grouped than cluster C. For example in silver-copper it can be seen that cluster B tends to contain more Ag whilst individuals in cluster C appear to contain more Cu. The same relationship can be seen in silver-lead, silver-tin and silver-zinc. Consequently it appears that cluster B tends to contain a higher silver content than cluster C and cluster A is more mixed than either of them. Despite this there is still significant overlap and difficulty in drawing any firm conclusions. In no plot do the clusters appear tightly or well defined. This is no surprise as the only significant component in the PCA results was composed of everything *except* silver and gold.

4.4.1.2 COMPARATIVE TERNARY DIAGRAMS

There is a need to directly compare the cluster results. To achieve this ternary diagrams will be used with data that has not been transformed in any way.

Ternary diagram requires us to choose three or four elements from the six used in the analysis here. There are twenty possible permutations of these six elements, so to ensure that they are not chosen at random the selection is based on the variance in the appropriate PCA results (Table 4-9 and Table 4-16).⁷²

The first principal component of the untransformed PCA proved difficult to interpret with all elements excluding silver and gold loading heavily. The second principal component focussed on the relationship between silver and gold; meanwhile the factor plot (Figure 4-8) suggested close correlations between silver and gold, copper and zinc, and lead and tin. On the first component of the clr PCA gold and tin loaded heavily. On the second tin and zinc loaded heavily. In the variable rays tin, zinc and gold were the most dispersed with the remaining three (copper, lead and silver) relatively tightly grouped. Whilst the loadings appear different there are some similarities between the two; in both untransformed and the clr results tin and zinc load heavily. The results for the remainder differ, however there is one similarity; silver is not associated with tin and zinc, and gold is not associated with zinc in both (see the rays in the both the untransformed and clr plots). Selecting silver-tin-zinc and gold-tin-zinc as sub-compositions in a ternary diagram should therefore provide an opportunity to examine cluster performance with elements that express the maximum variance in the data under both geometries.

⁷² These are: Cu,Pb,Sn; Cu,Pb,Ag; Cu,Pb,Au; Cu,Pb,Zn; Cu,Sn,Ag; Cu,Sn,Au; Cu,Sn,Zn; Cu,Ag,Au; Cu,Ag,Zn; Cu,Au,Zn; Pb,Sn,Ag; Pb,Sn,Au; Pb,Sn,Zn; Pb,Ag,Au; Pb,Ag,Zn; Pb,Au,Zn; Sn,Ag,Au; Sn,Ag,Zn; Sn,Au,Zn; Ag,Au,Zn;

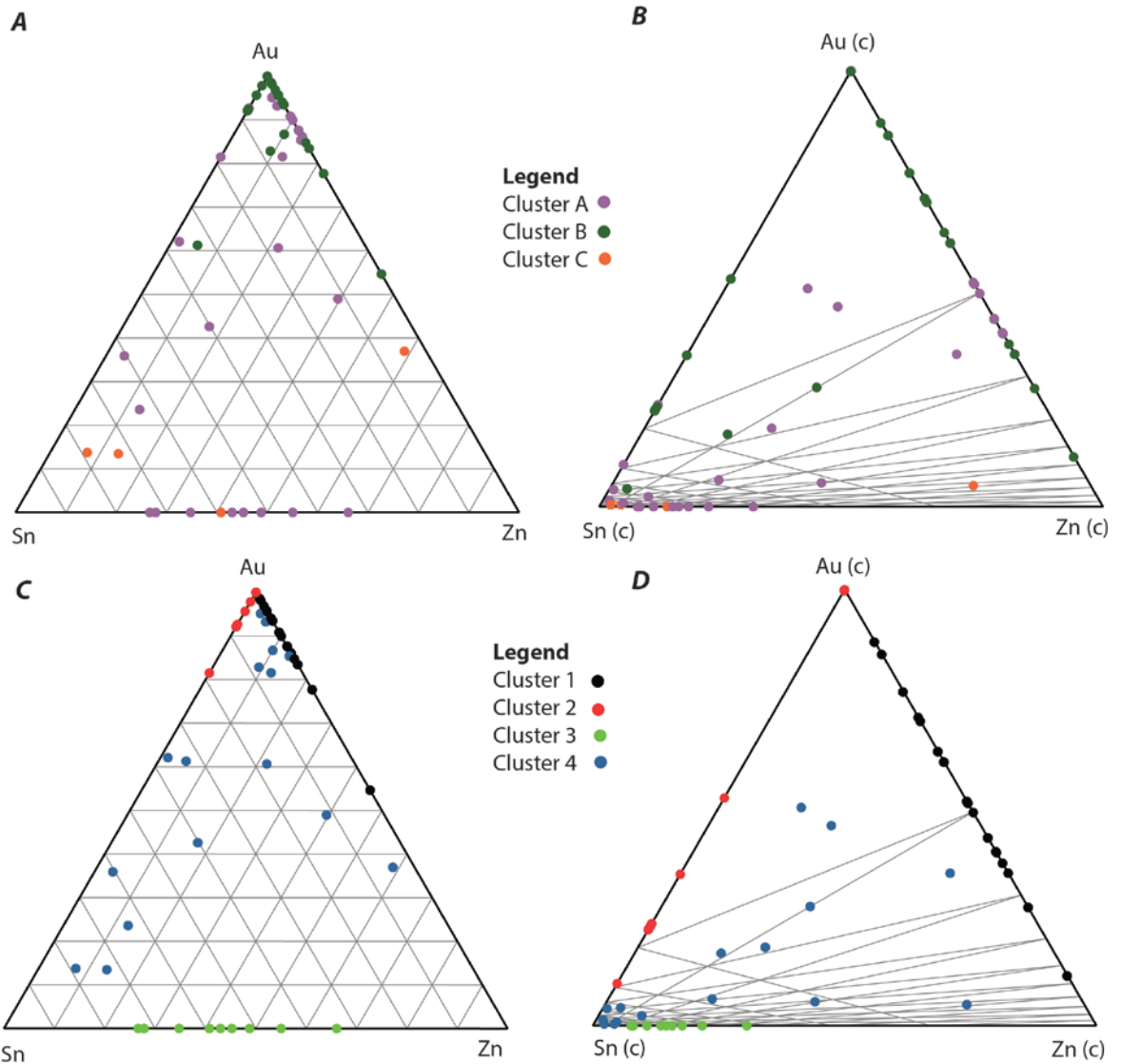


Figure 4-19: Au-Sn-Zn Au ternary diagrams. The top two (A & B) show the untransformed clusters un-centred (A) and centred (B). The bottom two (C & D) show the clr clusters un-centred (C) and centred (D).

The gold-tin-zinc ternary diagram (Figure 4-19) shows the different clusters defined by the two geometries. In the untransformed diagrams (diagrams A & B in Figure 4-19) Cluster B tends to be higher in gold than clusters A & C and cluster C tends to be lower in Au than clusters A & B. There is, however, considerable overlap and there appears to be very poor boundary definition between the groups. In contrast the clr clusters (diagrams C & D in Figure 4-19) show much better delimitation as follows:

- Cluster 1 contains zinc and minimal tin.
- Cluster 2 contains tin and minimal zinc
- Cluster 3 contains both tin and zinc and minimal gold.
- Cluster 4 is more mixed and contains all three elements.

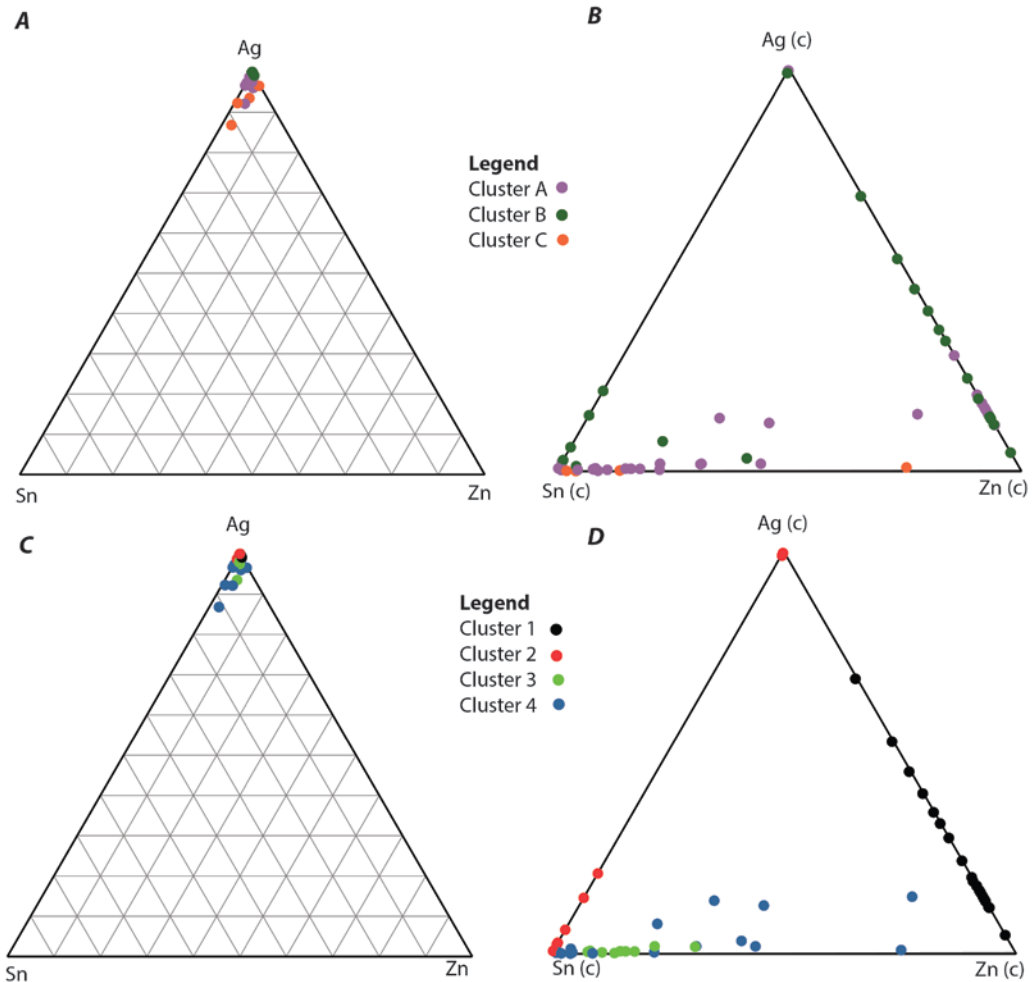


Figure 4-20: Ag-Sn-Zn ternary diagrams. The top two (A & B) show the untransformed clusters un-centred (A) and centred (B). The bottom two (C & D) show the *clr* clusters un-centred (C) and centred (D).

A repetition of the test with a silver-tin-zinc ternary diagram (Figure 4-20) shows similar results. The untransformed clusters (diagrams A & B in Figure 4-20) show that cluster B tends to contain a higher Ag content than clusters A & C and that cluster C tends to contain less silver than clusters B & A (a distribution best visible in A, the un-centred ternary diagram). Once again there is, however, considerable overlap and there appears to be very poor boundary definition

between the groups. In the centred ternary diagram (diagram B) it becomes apparent that there is particularly poor delimitation in the clusters in relation to the tin and zinc contents.

The clr clusters (diagrams C & D in Figure 4-20) again show much better delimitation with clusters 1 and 2 show the same distribution trends in regards to tin and zinc as previous. There is poorer boundary definition with regards to clusters 3 & 4, but cluster 4 does tend to contain more Ag than cluster 3.

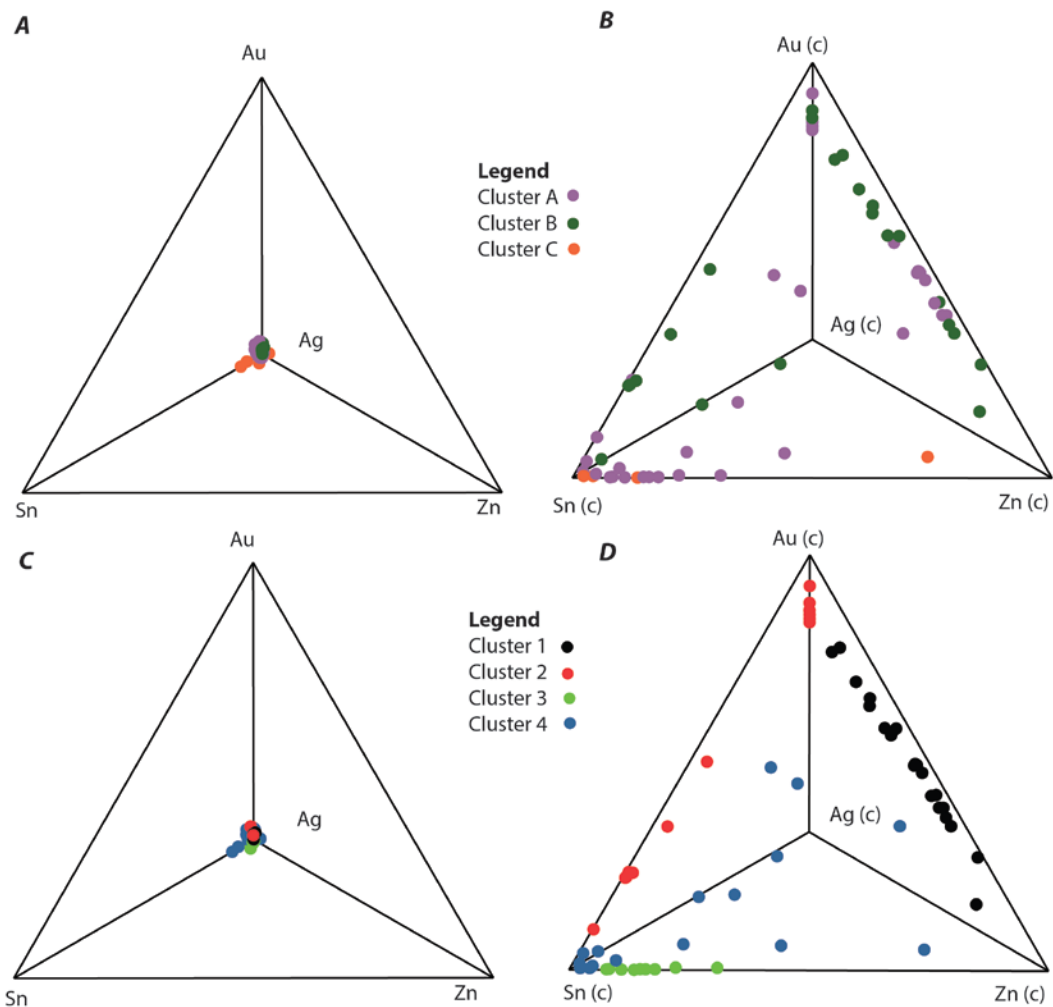


Figure 4-21: 3D ternary diagrams of Ag-Au-Sn-Zn with Ag at the apex of the pyramid. The top two (A & B) show the untransformed clusters un-centred (A) and centred (B). The bottom two (C & D) show the clr clusters un-centred (C) and centred (D).

The four elements from the previous two diagrams can be combined to create a 3D ternary diagram for silver-gold-tin-zinc. The results (Figure 4-21) are, not

surprisingly, similar to the conclusions drawn from Figure 4-19 and Figure 4-20. The untransformed clusters (diagrams *A* & *B* in Figure 4-21) are again poorly defined, indeed in combining all four elements it becomes difficult to see much in the way of a logical distribution at all. The *clr* clusters (diagrams *C* & *D* in Figure 4-21) again perform relatively well with clusters 1, 2 and 3 being defined as follows:

- Cluster 1 contains zinc and minimal tin.
- Cluster 2 contains tin and minimal zinc. The two natural sub groups previously identified within cluster 2 are clearly visible and are separated by gold content.
- Cluster 3 contains tin and zinc and minimal gold.
- Cluster 4, as seen in the un-centred diagram in Figure 4-19, contains a mixture of gold, tin and zinc.

In the previous three figures it has been sought to maximise variance by using elements suggested in both sets of PCA results. There is a risk, however, that in trying to interpret the two sets of PCA a bias has been introduced that means the untransformed clusters are not effectively or fairly represented. To reduce this risk the exploration is continued but focussing exclusively on the untransformed PCA results to decide which elements to include in the ternary diagram. Whilst the first PCA (Table 4-9) was mixed (with all elements except Ag and Au loading heavily) four elements did load heavily: copper, lead, tin and zinc. These four will be used in the next set of ternary diagrams.

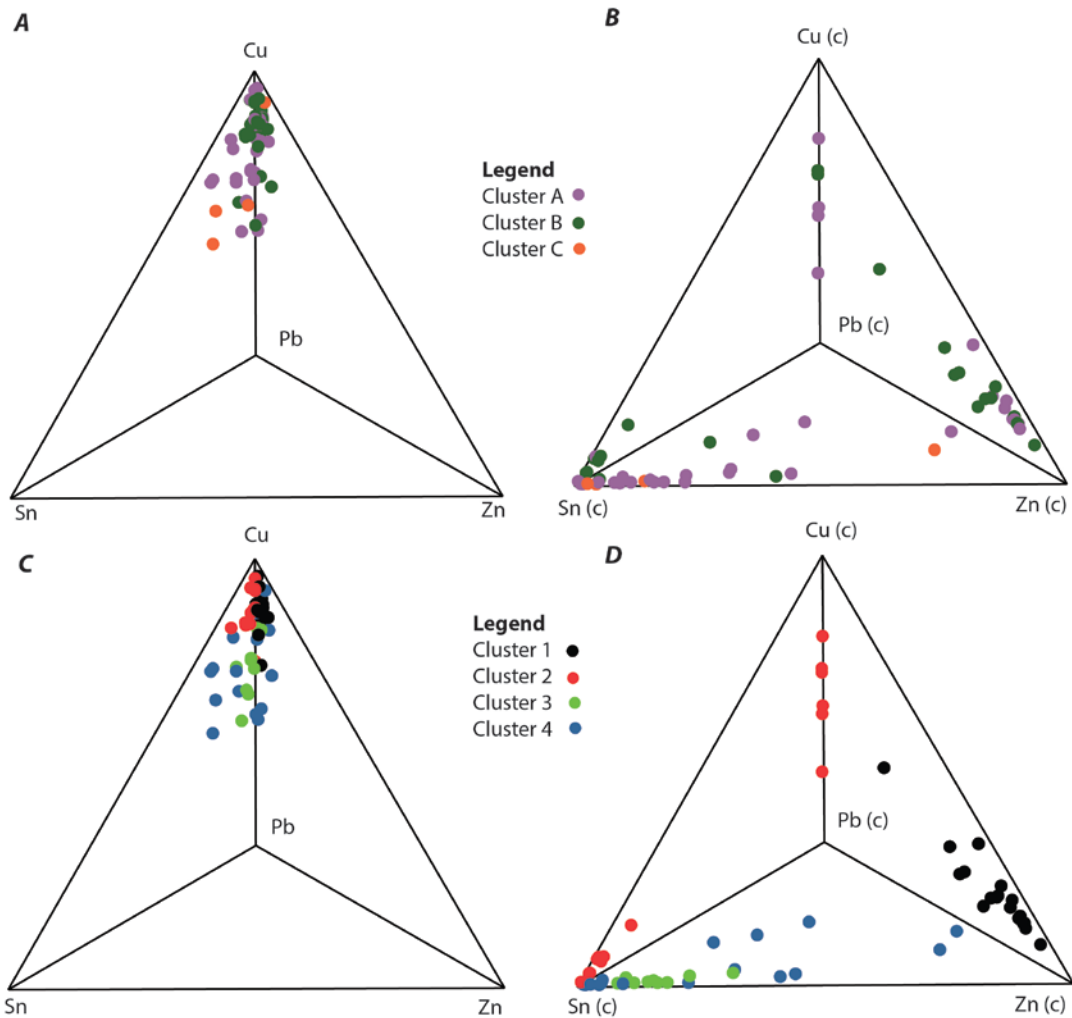


Figure 4-22: 3D ternary diagrams of Cu-Pb-Sn-Zn with Ag at the apex of the pyramid. The top two (A & B) show the untransformed clusters un-centred (A) and centred (B). The bottom two (C & D) show the clr clusters un-centred (C) and centred (D).

The results (Figure 4-22) again appear to show the clr clusters performing better than the untransformed clusters at representing the compositions of the individuals with little coherence to the untransformed cluster distribution (diagrams A & B in Figure 4-22). In contrast the clr clusters (diagrams C & D in Figure 4-22) do show clear separation between clusters 1 and 2 (as earlier based on Sn and Zn content). Clusters 3 and 4 are mixed and it is hard to see any differentiation; however this is not a surprise as neither copper nor lead were considered by the clr PCA to explain a significant proportion of the variance. Consequently it appears that, even when choosing only those elements suggested

by the untransformed PCA results, the untransformed hierarchical clustering is performing poorly.

4.5 CONCLUSION

The results of the previous section show both untransformed and clr transformed PCA and clustering producing workable results. In the untransformed data cluster B tended to contain a higher silver content than cluster C and cluster A was more mixed than either of them. Despite this there was still significant overlap and difficulty in drawing any firm conclusions. In no plot do the clusters appear tightly or well defined and the results are extremely noisy. In contrast the clusters derived from the clr transformed data were relatively well defined in the ternary diagrams and some clear results based on the compositions could be drawn (particularly in relation to tin and zinc content).

Compositional data techniques focus on the relationships between the log-ratios rather than the figures themselves, but NPA data are not purely representative of the composition. There is no calibration and no correction. Consequently the ratios between the net peak areas are not purely representative of the composition; they will also carry some information about the surface geometry and texture, about beam and detector performance. They are not purely compositional. Thus one might expect statistical analysis on untransformed data to be more appropriate.

This might make the results here appear somewhat surprising. The assessment appears unambiguous; working with the data in a compositional manner produces more comprehensible dimensionality reduction than untransformed data. Clearly those experimental and archaeological data artefacts carried in the ratios are exerting less of an influence than one might presume. This was noted in the work of Bonizzoni et al. (2013); the spectra (and consequently the net peak areas) are influenced by the size of peak intensity and background. This will therefore lead to lower peak areas for those analyses where there is a higher

background. Likewise larger, flat objects which completely cover the HHpXRF window will have higher peak intensities than a smaller object (such as a pin) which does not. Standardising the data without any logarithmic transformations will lead to the undue influence of background noise in a correlation matrix whilst the variables with the highest values (due to object size etc.) will dominate the first component in PCA irrespective of if these values express any real underlying variance (as seen in the untransformed PCA here). Performing logarithmic transformations on the dataset reduces wide-ranging peak areas to a smaller scale which enables comparison to be effectively undertaken (Bonizzoni et al. 2013, 264–265).

To be clear, caution must still be exercised. Because of corrosion, care still has to be taken when interpreting the results. These clusters are not exact representations of the compositions and will likely shift if the uncorroded alloy was analysed. Nevertheless, it is still reasonable to assume that there is an internal referential logic to their organisation. Even if there is less silver and more copper or zinc than indicated here groups will still remain groups even if their position shifts (such an outcome has been noted on ceramics, see Forster et al. 2011, Figure 5). Despite this there is a need for further work with HHpXRF and non-ferrous metals to assess the combined effect of corrosion and statistical methodology in more detail.

A full archaeological interpretation of the results presented here will be undertaken in the next chapter.

CHAPTER 5: SILVER RESULTS

*Then came the bride, the lovely Medway came,
Clad in a vesture of unknown gear
And uncouth fashion, yet her well became,
That seem'd like silver sprinkled here and there
With glitt'ring spangs that did like stars appears*

(Spenser 1859, III:156)

5.1 INTRODUCTION

This chapter continues on from the statistical methodology (Chapter 4, page 181), which used the Eriswell silver dataset as a method to assess mathematical approaches. It includes an archaeological interpretation of the principal component and hierarchical clustering results, presented after a simpler consideration of objects that have analytically been determined to be silver in the context of their categorical variables.

5.2 IDENTIFICATION OF SILVER OBJECTS

Silver objects were initially identified visually as part of the post-excavation assessment. The visual identification was checked during analysis and confirmed (i.e. there were no objects wrongly identified as silver).

The decision to include or exclude an object from classification as 'silver' did not really solely on analytical confirmation of visual identification. All analyses were examined for silver content and a decision was made to count any of those where the silver net peak area was the near equal to or larger than that of other elements. Due to the corrosion processes noted in Chapter 3 (page 167) this leads to the inclusion of some potentially very low silver containing alloys. Consequently, where necessary, the data set was trimmed during statistical evaluation (see page 197).

5.3 OBJECT BREAKDOWN

Before considering the elemental makeup of the objects a simple breakdown is considered. This consists solely of considering those objects that have analytically been determined to be silver in the context of their categorical variables

This section involves a comparison of the objects analytically assessed to be silver against the categorical variables. It does not involve any consideration of the net peak areas themselves. Consequently shield mount 104-3675-2-A, excluded from the statistical evaluation because of inadvertent analysis of a gilt area, is included here.

5.3.1 SILVER OBJECTS BY CEMETERY AND GRAVE

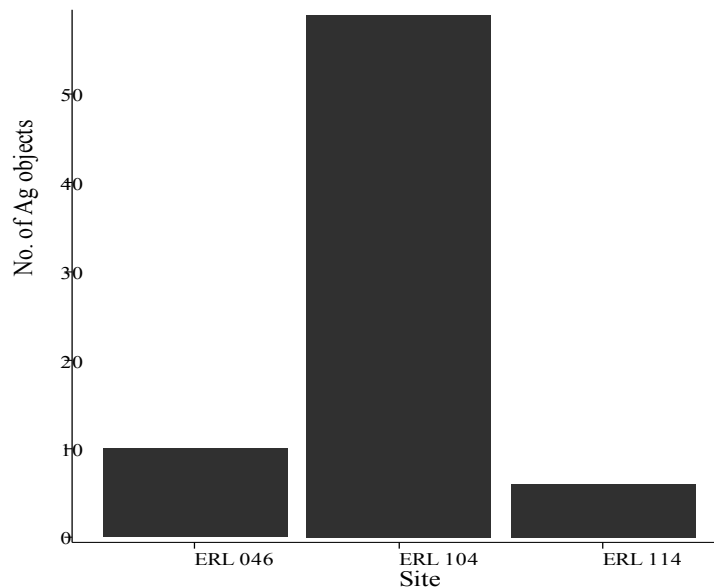


Figure 5-1: Bar chart of the number of silver objects by site.

Preliminary sorting of the data revealed there to be sixty-eight silver objects in the Eriswell assemblages (defined as discussed on page 45); 54 from ERL 104, six from ERL 114 and eight from ERL 046 (see Table 5-1 and Figure 5-1). These objects were defined as a subset by identifying those where silver formed the

largest individual component of the composition.⁷³ The eight objects from ERL 046 consist of four necklace pendants and four finger rings. The six objects from ERL 114 consist of four beads, one necklace pendant and one finger ring. The silver objects from ERL 104 have much greater typological variety and consists of a variety of wrist clasps (nine, all Form A), shield mounts, strap ends, beads, pendants, rings a variety of fittings associated with horse tack. The horse tack in ERL 104 is all from one grave (G323), which dominates the assemblage.

Site	Grave No.	No. of Ag objects
ERL 046	G002	2
	G005	2
	G042	4
ERL 046 Total		8
ERL 104	G116	2
	G139	1
	G168	4
	G213	1
	G245	2
	G264	1
	G266	4
	G273	1
	G305	4
	G315	5
	G323	17
	G339	1
	G357	1
	G364	4
	No Grave	6
ERL 104 Total		54
ERL 114	G417	1
	G445	1
	G450	4
ERL 114 Total		6
Grand Total		68

Table 5-1: Number of silver objects by site and grave number.

Out of four hundred and twenty-six inhumations at Eriswell only twenty (4.7%) contained gilded objects. In Table 5-2 a comparison across cemeteries shows that

⁷³ Surface analysis, as used here, means that this choice is not 100% watertight. See footnote 73 (page 8) and page 160 for more details.

silver objects are proportionally relatively equally distributed in terms of number of graves across the three cemeteries (although ERL 114 is ‘poorer’ than the other two).⁷⁴ This is a remarkably different distribution to gilt artefacts (as discussed in Chapter 6:).

	ERL 046	ERL 104	ERL 114
No. of inhumations that contain silver objects	3	14	3
No. of inhumations that contain no silver objects	56	247	95
% of inhumations that contain silver objects	5.08	5.36	3.06

Table 5-2: Number of inhumations that contain silver objects in cemeteries ERL 046, 104 and 114.

5.3.2 SILVER OBJECTS BY TYPOLOGY

Examining the object categories (Figure 5-2) reveals that the majority of silver objects are dress accessories (thirty-seven in total). In second place are equestrian associated objects (seventeen items in total). In third place are items associated with weaponry (six objects). Examining the second plot in Figure 5-3 shows that this consists exclusively of shield mounts. The breakdown of the dress accessories in the object class graph reveals that the silver dress accessories consist predominantly of wrist clasps (nine) and beads (ten). A summary of the data associated with these graphs is available in Table 5-3.

⁷⁴ It should be remembered that this thesis does not include cemetery ERL 008. This is ‘poorer’ still than ER: 114.

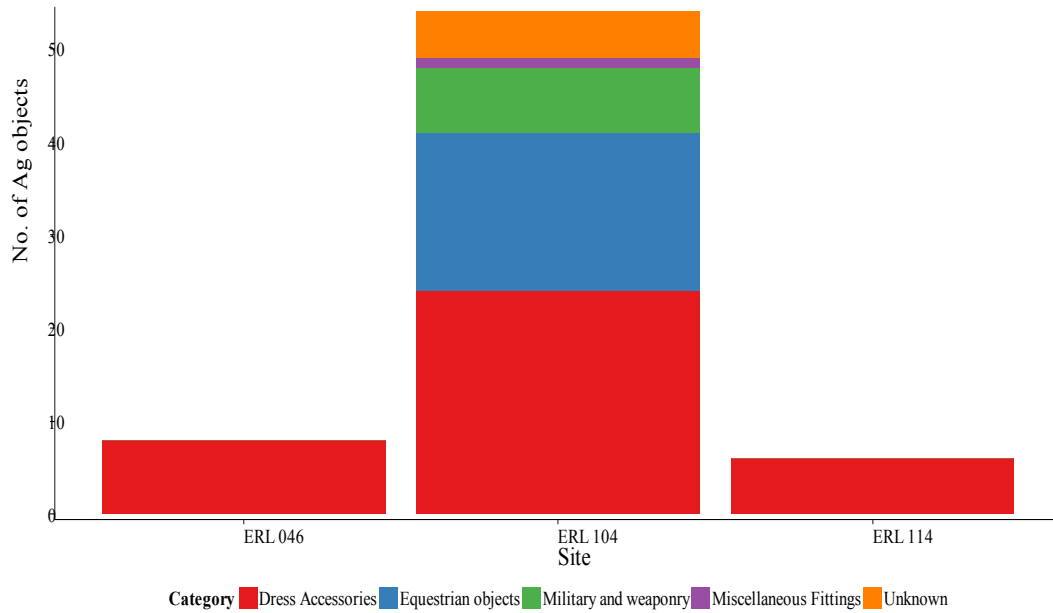


Figure 5-2: Bar chart showing the number of silver objects by cemetery and object category.

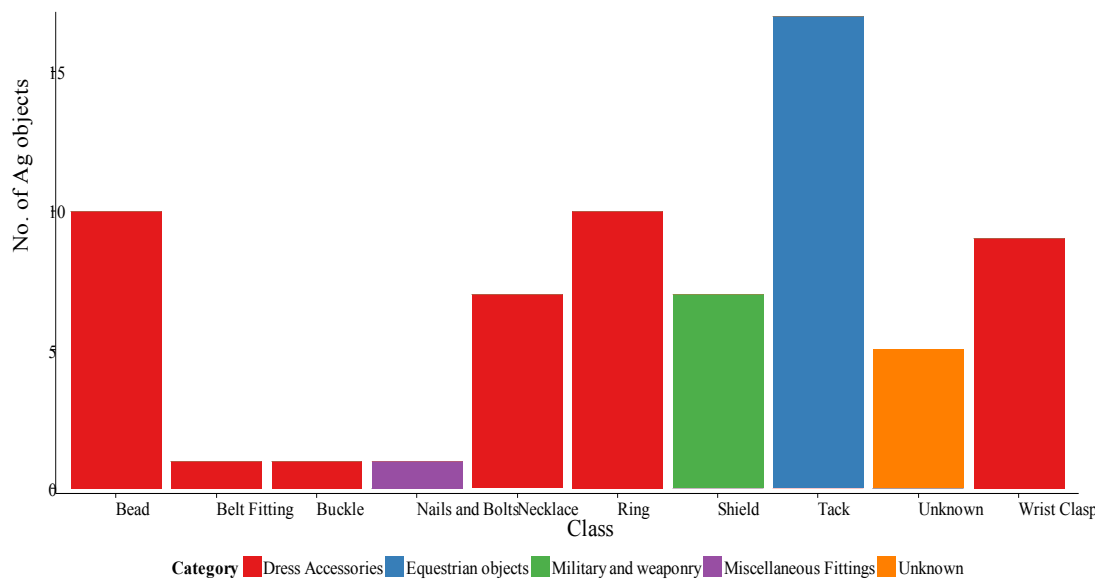


Figure 5-3: Silver objects by category (left) and class (right). The colour coding in the class graph is taken from the categories.

Site	Category	Class	Sub Class	No. of Ag objects
ERL 046	Dress Accessories	Necklace	Pendant	4
		Ring	Finger ring	4
ERL 104	Dress Accessories	Bead	Undefined Bead	6

Site	Category	Class	Sub Class	No. of Ag objects
		Belt Fitting	Strap-end	1
		Buckle	Undefined Buckle	1
		Necklace	Pendant	2
		Ring	Ear Ring	3
			Finger ring	2
		Wrist Clasp	Form A	9
	Equestrian objects	Tack	Bridle Fitting	16
			Bridle mount	1
	Military and weaponry	Shield	Shield Mount	6
	Miscellaneous Fittings	Nails and Bolts	Stud	1
	Unknown	Unknown	Unknown	5
ERL 114	Dress Accessories	Bead	Undefined Bead	4
		Necklace	Pendant	1
		Ring	Finger ring	1

Table 5-3: Table showing the number of silver objects by cemetery, object category, class and sub class.

5.3.3 SILVER OBJECTS BY SEX, GENDER AND PHASE

As noted earlier (page 43) the graves are categorized by both a biologically defined sex (determined by the osteoarchaeologist) and a gender assigned based on the suite of associated grave goods.

A quick consideration of the objects based on our ideas of contemporary gender norms may lead one to conclude that there is a breakdown by sex in the distribution of silver artefact (i.e. silver dress accessories tend to be associated with female burials and military with males, see Stoodley 1997 for an in-depth discussion on gender, sex and Anglo-Saxon burials).

Further examination suggests that this is not necessarily the case; although poor skeletal preservation means that large numbers of individuals remain unsexed (in this study it has been decided to make a distinction where possible between biological sex and assigned gender). The bar charts in Figure 5-4 suggest that where biological sex was determinable silver dress accessories were associated with both males and females (although more with females than males).

Upon examining the Dress Accessory object classes (Figure 5-6) some sex divisions do begin to suggest themselves. Silver beads appear to be associated with females, as do wrist clasps (although no sex is known for over 50% of burials with silver wrist clasps). Rings on the other hand (both finger and ear) are – where sex was determinable – wholly associated with males. It will be examined in the subsequent chapters if these trends in biological sex distribution are associated solely with silver or apply to other non-ferrous alloys.

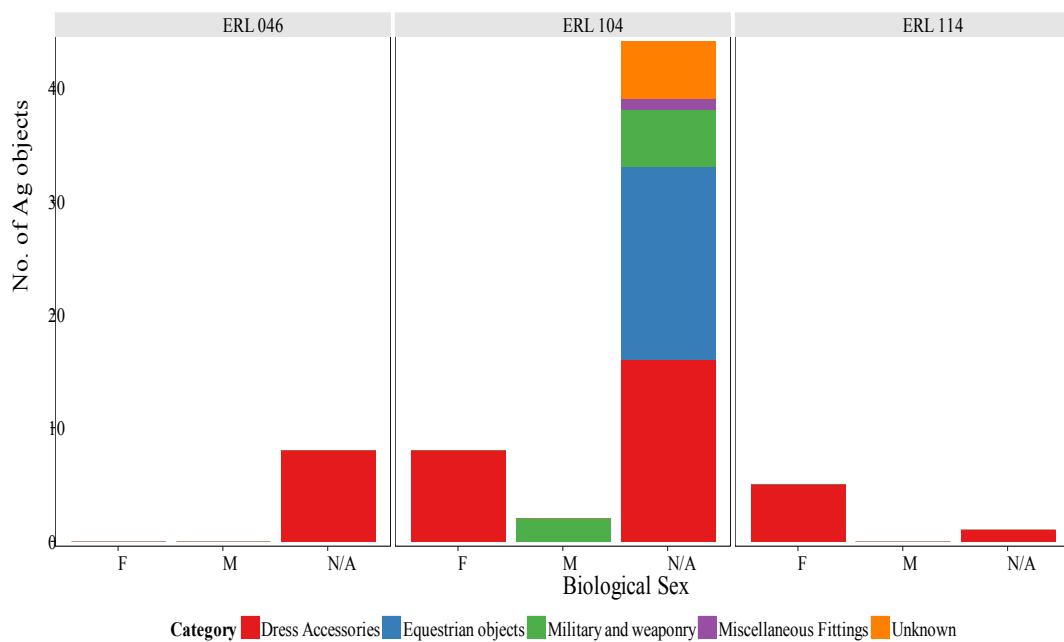


Figure 5-4: Bar chart showing the number of silver objects by cemetery with biological sex on the X axis and object category as the stratum variable.

The bar charts of assigned gender (Figure 5-5) show a distribution in line with what one may traditionally expect; weaponry and equestrian silver objects are associated with gendered males and dress accessories with gendered females. It should be noted that in ERL 114 there are no silver objects associated with male gendered burials. A series of bar charts of object class and assigned gender is provided in Figure 5-7 to act as a comparator to the biological sex equivalent (Figure 5-6).

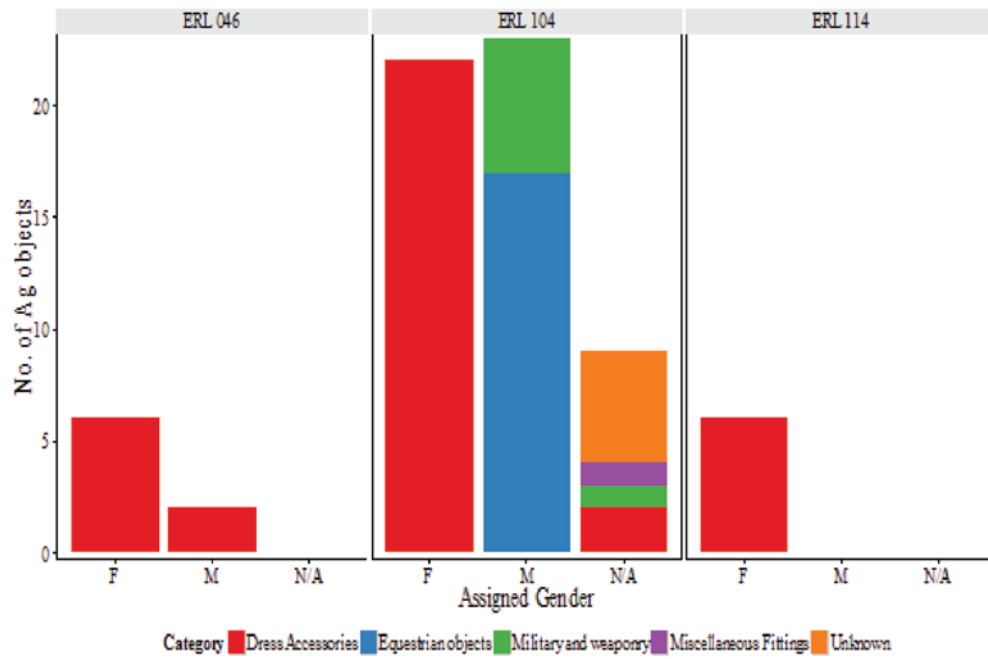


Figure 5-5: Bar charts of showing the number of silver objects by cemetery with assigned gender on the X axis and object category as the stratum variable.

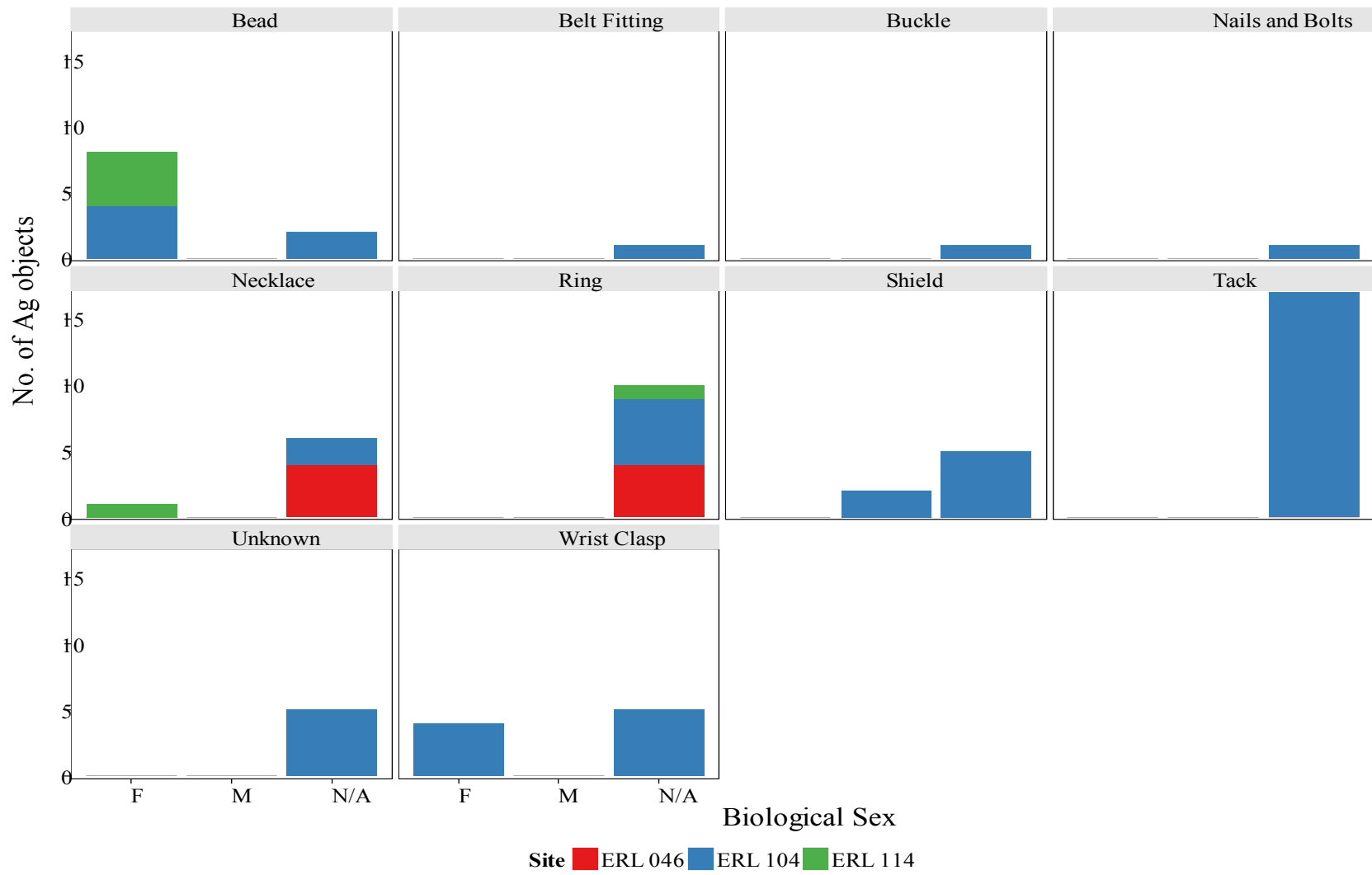


Figure 5-6: Bar charts of object classes with biological sex on the X axis and cemetery as the stratum variable

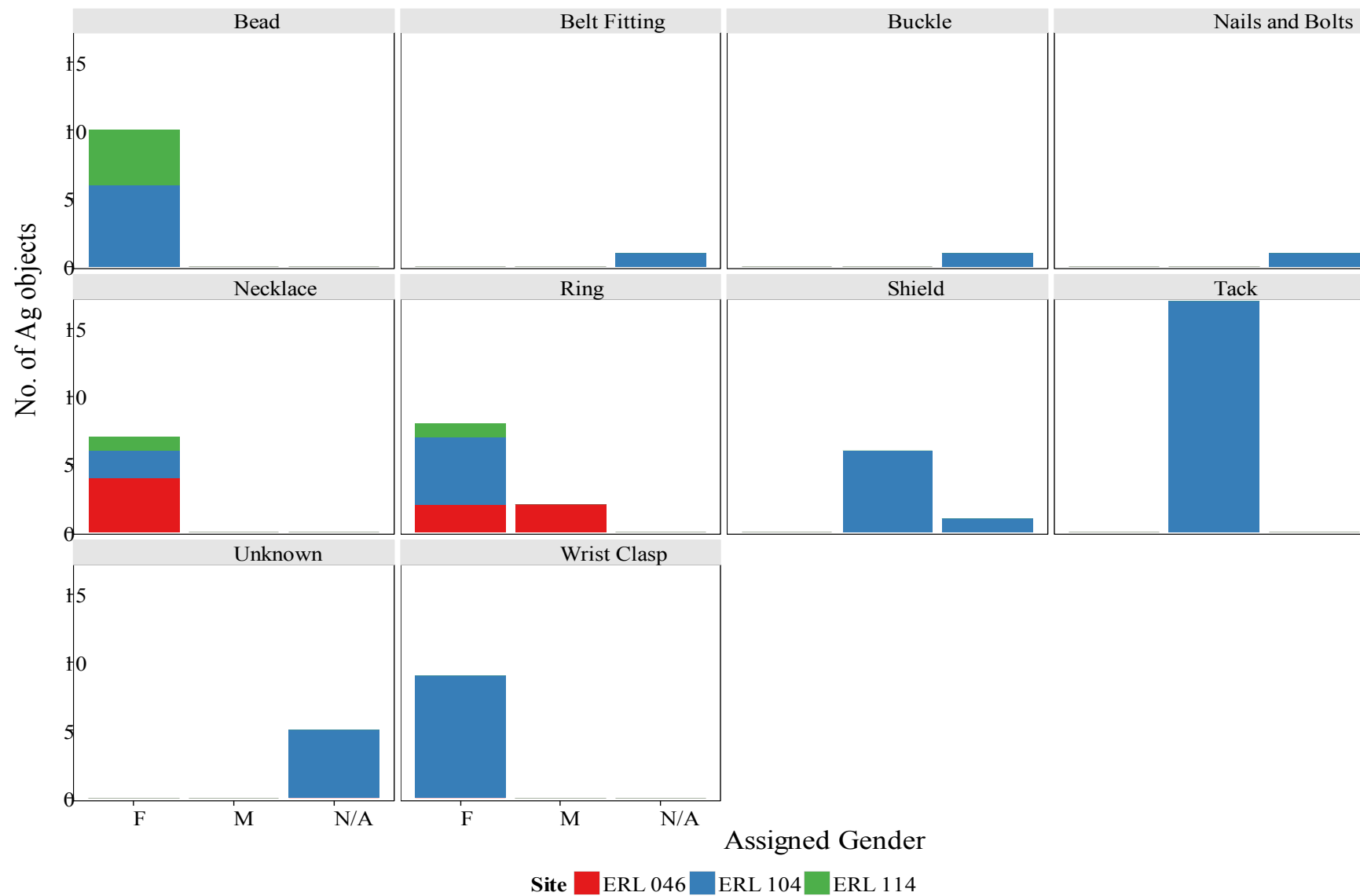


Figure 5-7: Bar charts of object classes with assigned gender on the X axis and cemetery as the stratum variable.

The burial phasing is gender specific (being based on groups of artefacts) and is presented in Figure 5-8. In ERL 046 the majority of the silver objects are associated with female phase A1. This is in contrast to ERL 104 and 114 where the majority of the gendered female objects are associated with phase A2. In the male gendered objects phase A(B) has the most objects. In ERL 046 male objects are only associated with phase B.

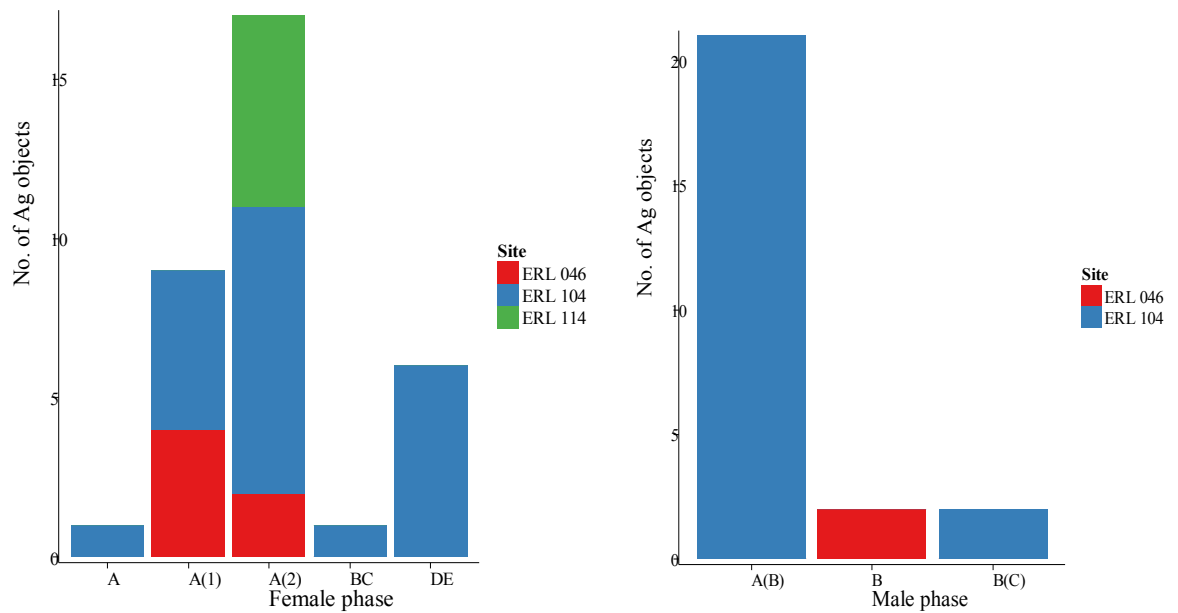


Figure 5-8: Bar charts showing the number of silver objects according female inhumation phasing (left) and male phasing (right). The cemetery is the stratum variable in both.

5.3.4 SILVER OBJECTS BY FABRICATION TECHNIQUE

The objects are predominantly made out of sheet metal (forty-nine objects) with the remainder being wire (sixteen) and cast (three). The cast objects are of unknown form, being predominantly ‘melted blobs’ possibly associated with cremations (i.e. they were objects that got melted in the cremation process). Wire and sheet objects are found in both ERL 046 and ERL 104 (Table 5-4). ERL 114 contains only sheet objects.

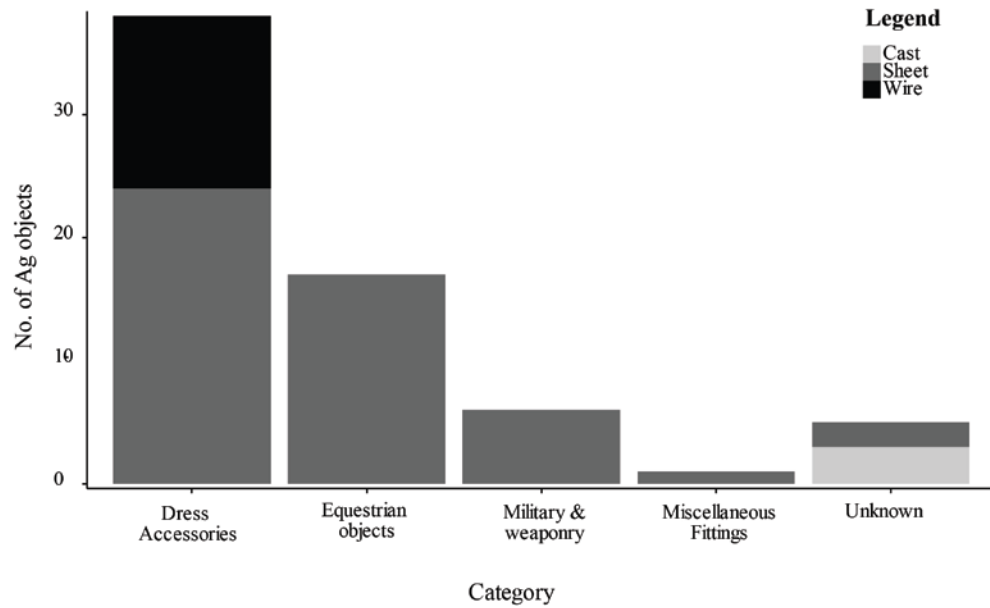


Figure 5-9: Bar chart of fabrication techniques and object class. It should be noted that the 'unknowns' in the cast category are predominantly formed of 'melted blobs' that are assumed to be associated with cremations, i.e. these could have represented sheet, wire or cast objects that were melted in the cremation process.

Site	Cast	Sheet	Wire
ERL 046		7	1
ERL 104	3	36	15
ERL 114		6	

Table 5-4: No of silver objects by fabrication technique and site.

Examining the object classes (Table 5-5) it can be seen that silver wire is only used for a narrow range of dress accessories; predominantly rings and wrist clasps.

Site	Category	Class	Cast	Sheet	Wire	
ERL 046	Dress Accessories	Necklace		4		
		Ring		3	1	
ERL 104	Dress Accessories	Bead		5	1	
		Belt Fitting		1		
		Buckle		1		
		Necklace		2		
		Ring		2	3	
		Wrist Clasp			9	
		Equestrian objects	Tack		17	
		Military and weaponry	Shield		6	
		Miscellaneous Fittings	Nails and Bolts		1	
		Unknown	Unknown	3		2
ERL 114	Dress Accessories	Bead		4		
		Necklace		1		
		Ring		1		

Table 5-5: No of silver objects by fabrication technique, site, object category and class.

5.4 ARCHAEOLOGICAL INTERPRETATION OF CLUSTERS

Previous analytical work on early medieval Anglo-Saxon silver alloys has, as stated, focussed on fineness. This, along with the small number of objects analysed, has resulted in discussion focusing on the concept of mixed alloys and debasement. The debasement is taken to indicate that there was not a good source of readily available ‘fresh’ silver available (Mortimer 1986, 241; Fleming 2012, 23), meaning that “*analysis of alloys, therefore, is of technological importance but because of the sources of metals used fails to assist in understanding dispersal*” (Arnold 2005, 135). This approach is reductive and reminiscent of “people as pots” (i.e. that silver content could be linked to the movement of peoples). By focussing on fineness agency has been removed from the communities / individuals that produced the objects and our understanding is hampered. It constrains our ability to understand the dimensionality of the data to a single variable: silver content.

The methodological approach used here means that this is not an option. As stated in the previous two chapters the analytical methodology means that silver content cannot be relied upon singularly to interpret the data. The focus has to be on dimensionality reduction and cluster results.

In the previous chapter two statistical methodologies were evaluated, with one — using centred log-ratio transformed data — proving superior. The principal component results on the clr transformed data (Table 4-16) indicated that the majority of the variance was related to gold, tin and zinc and this can be seen in the biplots and PCA results presented in the previous chapter (Table 4-16 on page 212 & Figure 4-13 on page 213). These results, when subjected to hierarchical clustering (see Figure 4-16 on page 217) suggested distinct compositional groups in the Eriswell silver alloys. The performance of these clusters was assessed (against the untransformed PCA clusters) in a series of ternary diagrams (see page 223). A brief recap is now presented (a full list of the clusters is available in Appendix II).

Figure 5-10 shows un-centred and centred gold-tin-zinc and silver-tin-zinc ternary and Figure 5-11 presents un-centred and centred 3D ternary diagrams of gold-silver-tin-zinc and copper-lead-tin-zinc.⁷⁵ In both individuals are identified by clr clusters.

⁷⁵ These are the same ternary diagrams presented in Figure 4-19, Figure 4-20, Figure 4-21 and Figure 4-22 with the untransformed cluster diagrams removed.

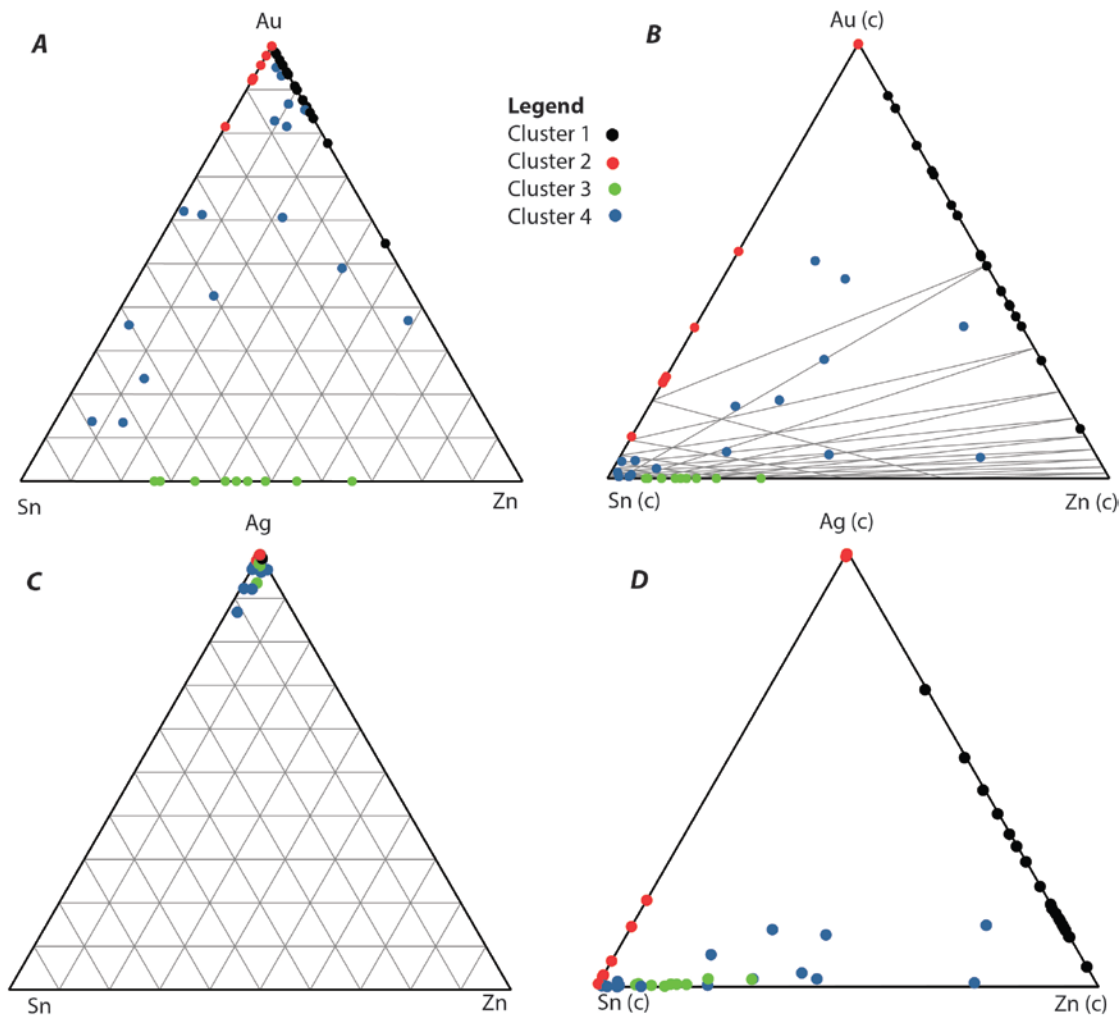


Figure 5-10: Ternary diagrams with individuals colour coded according to *clr* clusters. A & B show Au-Sn-Zn diagrams un-centred and centred respectively, C & D Ag-Sn-Zn diagrams centred and centred respectively.

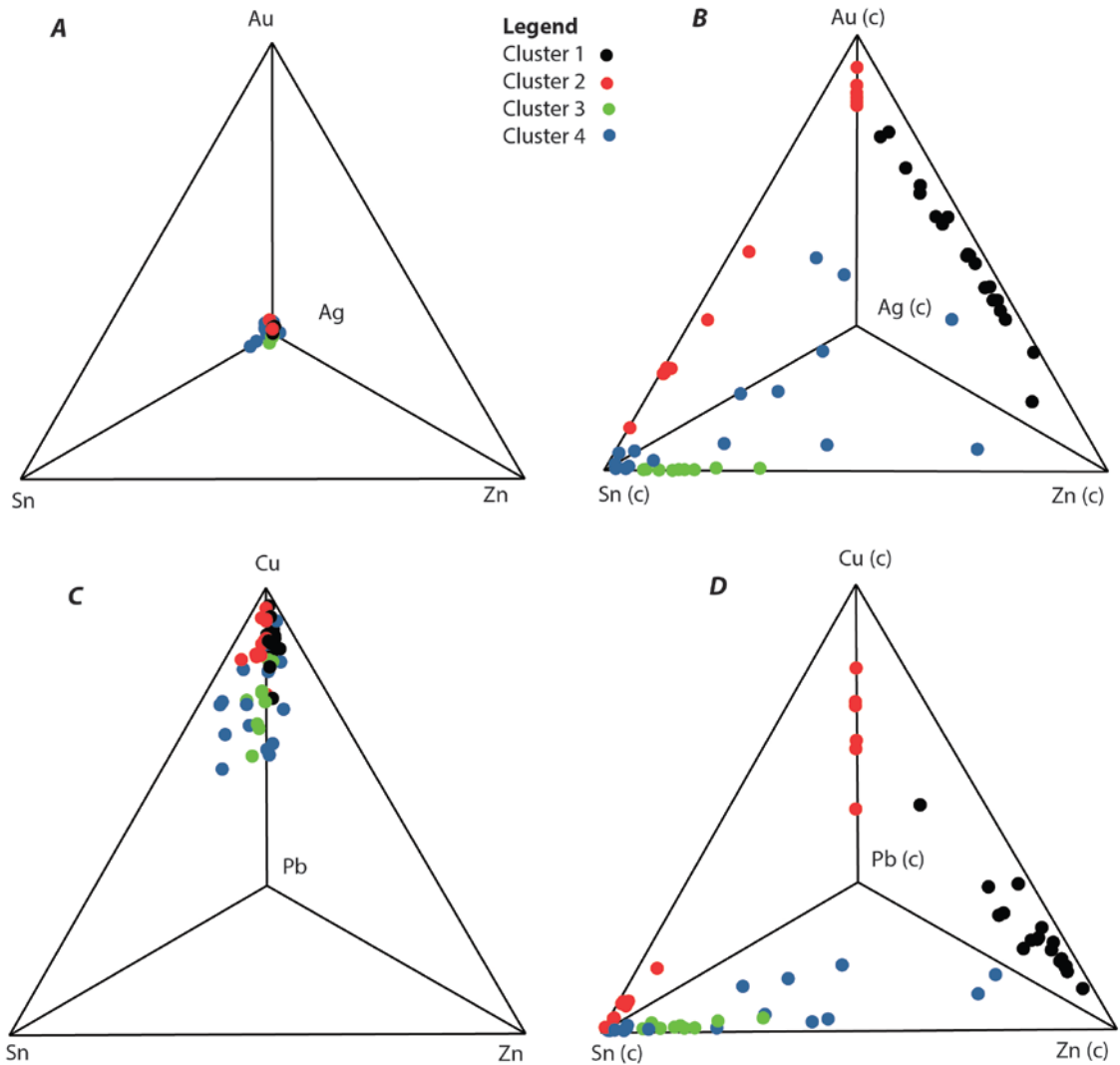


Figure 5-11: 3D ternary diagrams with individuals colour coded according to clr clusters. The top two (A & B) show Au-Ag-Sn-Zn un-centred (A) and centred (B). The bottom two (C & D) show Cu-Pb-Sn-Zn un-centred (C) and centred (D).

From these two diagrams and the principal component results the following conclusions can be drawn:

- Cluster 1 contains zinc and minimal tin.
- Cluster 2 contains tin and minimal zinc.
- Cluster 3 contains both tin and zinc and minimal gold.
- Cluster 4 is mixed and contains all three elements. Because of this it is not always well represented ternary diagrams, but it is clear in diagrams that

use the elements that explain the most variance according to the PCA (see diagram *A* in Figure 5-10).

- All of the silver alloys contain copper and lead.

The bullet points above provide a brief overview of the main elements which explain the variance within the dataset and define the clusters. Each of these elements adds specific qualities to the silver alloys:

- Zinc will ‘brighten’ the colour (particularly when other non-white metal alloying elements such as copper are present) and the addition of zinc makes for a more malleable alloy in a silver-copper alloy (Percy 1880, 169–170; Gowland 1921, 295).
- Silver tin alloys can be hard and brittle but the same colour as pure silver (Percy 1880, 183).
- The addition of copper makes silver much more malleable and hard wearing (Davis 2001a, 553) and, although 10% or more copper will begin to affect the colour of the silver, the alloy will remain white up to a 50% copper (Percy 1880, 150; Gowland 1921, 295).
- The addition of lead can produce a highly reflective alloy (i.e. the Speculum used for Roman mirrors), but small amounts can affect the malleability of the alloy (Percy 1880, 171; Gowland 1921, 296) .
- Finally silver-copper-tin-gold alloys are easily formed and form an alloy which is “firm, solid and durable” (Percy 1880, 184).

In addition to this the addition of both zinc and tin to silver help tarnish proof the alloy and reduce the melting point (Greiff 2012, 251).

The alloying components which explain the variance in the data proffer specific and useful properties to silver alloys and there are distinctive and reasonably well defined groups that reflect these. Some conclusions can be immediately drawn from this. None of the clusters are particularly ‘pure’, suggesting that older

material culture was probably the source material (i.e. recycling). Yet the very presence of clusters immediately challenges assumptions that this was a blind process. There were choices and decisions being made about what went into these objects; even with very mixed alloys (such as cluster 4).

Before this is considered further a re-examination of the clusters and categorical variables is undertaken. In this the ‘low silver’ individuals, which were removed during the statistical analysis, are reintegrated and added as a ‘low silver’ group.

5.4.1.1 CATEGORICAL VARIABLES AND CLUSTERS

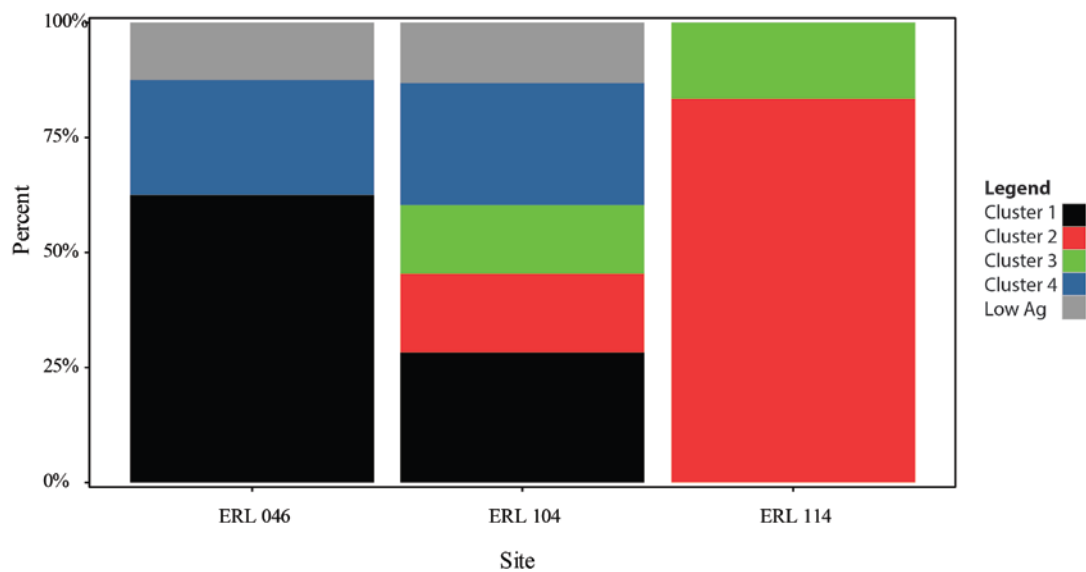


Figure 5-12: Bar chart showing the percentage of silver objects with cluster as the stratum variable and cemetery on the X axis.

In Figure 5-12 a bar chart showing the percentage of silver objects by cluster and cemetery is shown. All clusters are represented in ERL 104, but interestingly not in ERL 046 or ERL 114; Clusters 3 and 4 are not present in ERL 046 and clusters 1 and 4 are not present in ERL 114. Drilling down further and examining the clusters by grave number (Figure 5-13) shows further interesting distributions. Of the twenty graves considered here 60% (twelve) of them contain more than one silver object. In this group of multi silver object graves only four consist of one cluster. As a general rule it appears that the more silver

objects there are in a grave the more likely it is there will be more than one silver cluster represented, yet rarely will all objects be of a different cluster (bead 104-3483-A and pendant 104-3578-A from grave 116 is the only exception to his here).

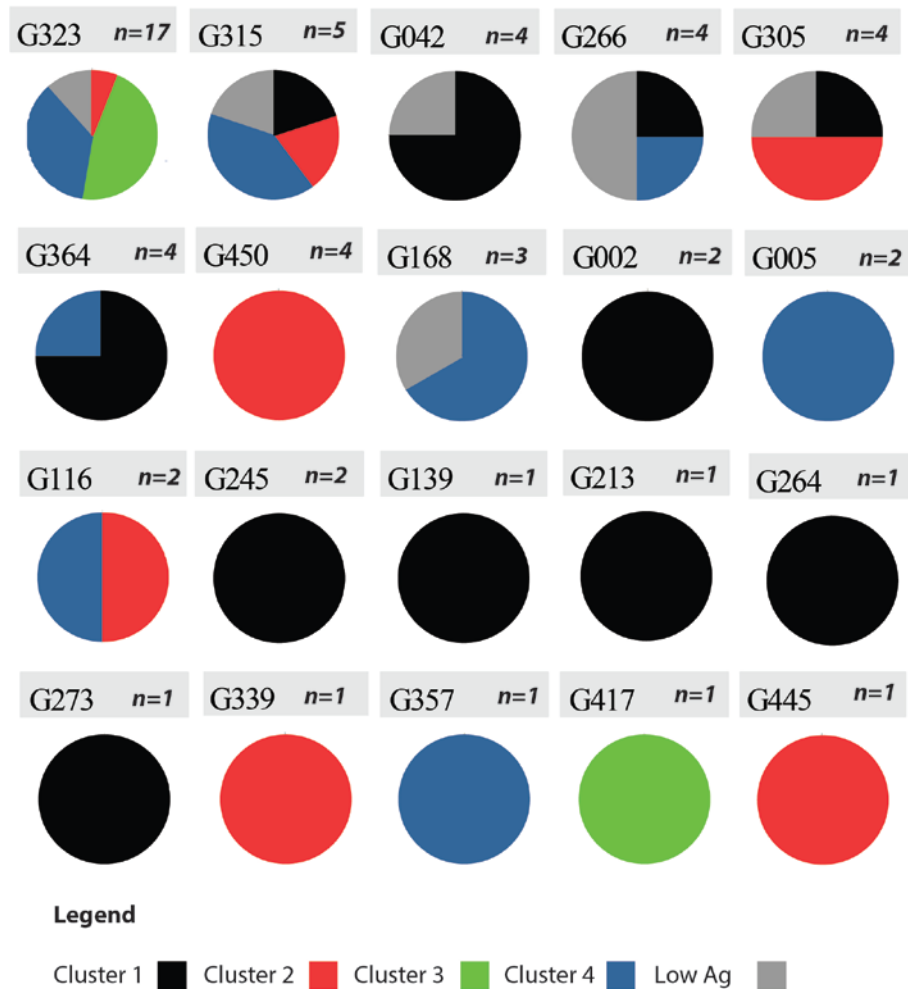


Figure 5-13: Pie charts showing the silver clusters present within each grave. The number of objects in each grave is presented adjacent to the right of the grave number.

5.4.1.1.1 SILVER ALLOYS BY GRAVE

As there are only a small number of graves that contain more than one silver object a brief summary is provided for each of the graves. It may be tempting here to see groups of similar objects from the same grave (such as wrist clasps and beads) that are grouping as the same cluster as made from the same source material (i.e. as a set). However, it should be remembered that the minor and

trace element data is not of particularly high quality (the focus being on broad compositional trends in the major elements) and that without these it is not possible to effectively match objects.

5.4.1.1.1.1 G002

A male inhumation (phase ERL-MB) from cemetery ERL 046. It contained two silver alloy objects 046-1708-A and 046-1714-A. The former is a wire spiral ring with a 25 mm diameter whilst the latter is a sheet spiral ring with a 24 mm diameter and punched dot decoration. Both, when analysed, fell into transformed cluster 1.

5.4.1.1.1.2 G005

A female inhumation (phase ERL-FA(2)) from cemetery ERL 046 that contained two sheet metal silver alloy pendants (046-1487-A and 046-1488-A). The pendants are both in transformed cluster type 4 and one (046-1487-A) had punched decoration. Both are part of a larger copper alloy necklace set (046-1375, 046-1375, 046-1377 and 046-1540) the results of which can be found in Chapter 8.

5.4.1.1.1.3 G042

A female inhumation (phase ERL-FA(1)) from cemetery ERL 046 that contained four silver alloy objects; two C-bracteate style silver pendants (046-1086-A and 046-1087-A) and two finger rings (046-1143-A and 046-1144-A). All were of transformed cluster 1 type with the exception of ring 046-1144-A, which appeared to have a relatively low silver content. It may be that this set should be evaluated further using more accurate analytical techniques as it may be interesting to see how closely related the three cluster 1 objects are and if the low silver object is indeed so. If the supposition here is confirmed it would be interesting to begin to hypothesise about what this tells us about the construction and acquisition of personal sets of precious metal dress accessories.

5.4.1.1.1.4 G116

A female inhumation (phase ERL-FDE) from cemetery ERL 104 that contained two silver alloy objects, a bead (104-3483-A) and pendant (104-3578-A). The pendant was decorated with three concentric circles of punched dots. Both were excavated from a soil block so their exact association is unknown.

5.4.1.1.1.5 G168

A male inhumation (phase ERL-MA(B)) from cemetery ERL 104 that contained three silver alloy objects: 104-3674-2-A, 104-3674-3-A and 104-3675-3-A. All three are copper alloy studs from a shield mount. Each stud had a small silver alloy sheet disc joined to the front (probably with the use of a filler alloy, all discs remained attached so it was not possible to ascertain this). Two of the silver alloy sheets were in transformed cluster 4 whilst the third (104-3675-3-A) appeared to be low silver with a significantly higher copper peak area than the other two. Before interpreting this as an addition from a different source material it should be remembered that these discs are relatively small and the the copper peak may have partially been contributed from the areas of the rivet irradiated by the beam (despite best attempts to position the object to avoid this). Therefore further analysis may be required on this object either with XRF (but using a unit with a collimator and the ability to focus the beam (no such unit is available at the department of Archaeology and Conservation in Cardiff) or with destructive sampling.

5.4.1.1.1.6 G245

A male inhumation (phase ERL-MB(C)) from cemetery ERL 104 that contained two silver alloy objects. Like G168 these were silver sheets adhered to the front of copper alloy studs from a shield mount. Both silver sheets belong to transformed cluster 1.

5.4.1.1.1.7 G266

A female inhumation (phase ERL-FDE) from cemetery ERL 104 that contained four silver alloy objects. These were all sheet metal beads, only two of which were from the same cluster: 104-1336-A (low silver), 104-1548-A (cluster 1), 104-1579-A (cluster 4) and 104-1583-A (low silver). It would be interesting to subject these to further analysis and assess if they are indeed substantially different.

5.4.1.1.1.8 G305

A female inhumation (phase ERL-FA(1)) from cemetery ERL 104 that contained four silver alloy objects. These were all Form A wire wrist clasps (104-1778-A, 104-1779-A, 104-1780-A and 104-1781-A). These are discussed in more detail below on page 255.

5.4.1.1.1.9 G315

A female inhumation (phase ERL-FA(2)) from cemetery ERL 104 that contained five silver alloy objects as follows:

- One sheet necklace pendant (104-2311-A), cluster type 2.
- One sheet finger ring (104-2309-A), cluster type 1.
- Three sheet ear ring pendants. Two are cluster type 4 (104-2317-E and 104-2317-H) and one had a proportionally low silver content (104-2317-D).

5.4.1.1.1.10 G323

Grave 323 is the horse and warrior burial in ERL 104 (phase ERL-MA(B)). It contained the largest amount of silver alloy objects (17 in total). These are discussed more on page 256 below.

5.4.1.1.1.11 G364

A female inhumation (phase ERL-FA(2)) from cemetery ERL 104 that contained four silver alloy objects. These were all Form A wire wrist clasps (104-2055-A, 104-2055-B, 104-2128-A and 104-2128-B). They are discussed in more detail on page 255 below.

5.4.1.1.1.12 G450

A female inhumation (phase ERL-FA(2)) from cemetery ERL 114 that contained four silver alloy sheet beads (114-1182-A, 114-1183-A, 114-1188-A and 114-1216-A). All belong to the same cluster (2) and it may be tempting to see them as part of set produced from the same source material. The data here is not of high enough quality to determine this and consequently these perhaps should be subjected to further, more detailed, analysis.

5.4.1.2 WRIST CLASPS

Some graves (excluding G116) appear to contain ‘pairs’ of objects. In Table 5-6 the silver wrist clasps are presented along with their clusters. Wrist clasps (hook and eye pieces) from graves 305 (104-1780-A and 104-1781-A) and 364 (104-2128-A and 104-2128-B) are highlighted, both pairs being from the same cluster. In Figure 5-14 these are plotted in ternary diagrams (along with the other wrist clasps featured in Table 5-6). It can be seen that these two pairs are apparently closer related than the other wrist clasps plotted. Whilst the analytical data here is not suitable for indicating if these are definitively compositional matches it may suggest that each pair was possibly from the same source material (although we need a full analysis including detailed information on trace elements to be certain).

Site	SF No.	Analysis Area	Grave No.	Wrist clasp form	Grave Phase	Fabrication	Cluster
ERL 104	1548	A	G264	Form A	A(1)	Wire	1
ERL 104	1778	A	G305	Form A	A(1)	Wire	1
ERL 104	1779	A	G305	Form A	A(1)	Wire	Low Ag
ERL 104	1780	A	G305	Form A	A(1)	Wire	2
ERL 104	1781	A	G305	Form A	A(1)	Wire	2
ERL 104	2055	A	G364	Form A	A(2)	Wire	1
ERL 104	2055	B	G364	Form A	A(2)	Wire	4
ERL 104	2128	A	G364	Form A	A(2)	Wire	1
ERL 104	2128	B	G364	Form A	A(2)	Wire	1

Table 5-6: Silver wrist clasps. Those from the same grave (i.e. a hook and eye piece) which fall in the same cluster are highlighted.

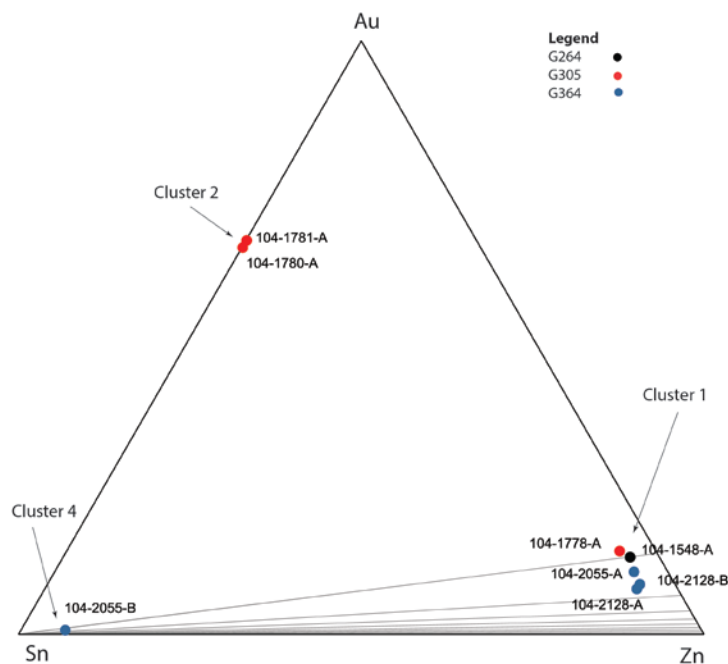


Figure 5-14: Centred ternary diagram showing silver wrist clasps colour coded according to clusters.

5.4.1.3 EQUESTRIAN GEAR

As can be seen in Figure 5-13 grave 323, the horse and warrior burial from ERL 104, is unusual for the number of silver objects it contains and the number of compositional clusters. The objects and clusters from this grave are presented below in Table 5-7. Again these are plotted in a ternary diagram (Figure 5-15). It is interesting to note that there is not the same close relationship between the objects that one might expect. For instance 104-BM6-7A-A and 104-BM6-7A-E (silver sheets attached to alternate sides of the bit) are of the same cluster (3) but well separated. It should be noted that apart from one object (114-1464-A from grave 417) objects from G323 form the entirety of cluster 3 and that no other cluster is dominated by an assemblage of objects from one grave in this way.

Site	SF no.	SF Sub div.	Analysis area	Sub class	Fabrication	Cluster
ERL 104	2623		B	Bridle mount	Sheet	4
ERL 104	2624		B	Bridle Fitting	Sheet	4
ERL 104	BM1		B	Bridle Fitting	Sheet	3
ERL 104	BM1		E	Bridle Fitting	Sheet	3
ERL 104	BM1		D	Bridle Fitting	Sheet	4
ERL 104	BM1		C	Bridle Fitting	Sheet	Low Silver
ERL 104	BM12		C	Bridle Fitting	Sheet	3
ERL 104	BM12		D	Bridle Fitting	Sheet	3
ERL 104	BM18		B	Bridle Fitting	Sheet	Low Silver
ERL 104	BM19		C	Bridle Fitting	Sheet	3
ERL 104	BM3		B	Bridle Fitting	Sheet	3
ERL 104	BM5		E	Bridle Fitting	Sheet	2
ERL 104	BM5		B	Bridle Fitting	Sheet	4
ERL 104	BM5		C	Bridle Fitting	Sheet	4
ERL 104	BM5		D	Bridle Fitting	Sheet	4
ERL 104	BM6	7A	A	Bridle Fitting	Sheet	3
ERL 104	BM6	7A	E	Bridle Fitting	Sheet	3

Table 5-7: Silver equestrian objects from grave 323.

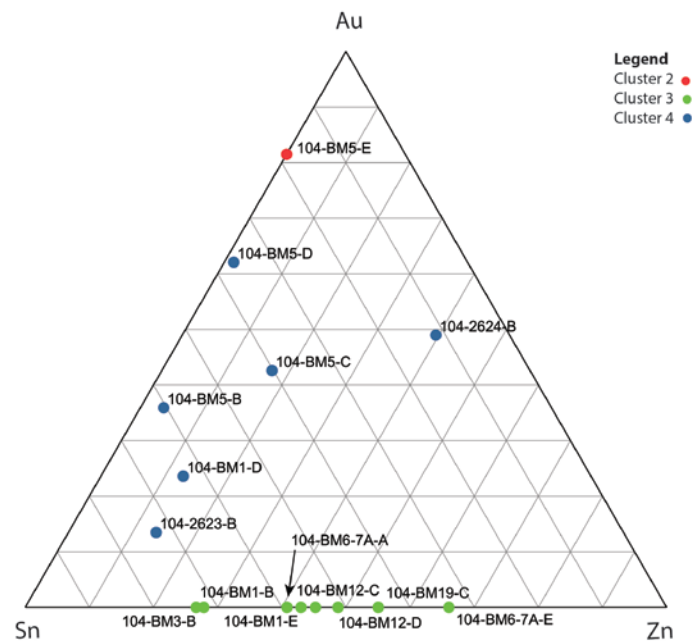


Figure 5-15: Un-centred ternary diagram showing the silver equestrian objects from grave 323.

5.4.1.4 CATEGORY AND CLUSTER DISTRIBUTIONS

Drawing back and examining the broad object categories shows that all four clusters are associated with dress accessories, with cluster 1 being predominant.

In equestrian objects cluster 1 is absent and in military and weaponry cluster 3 is absent.

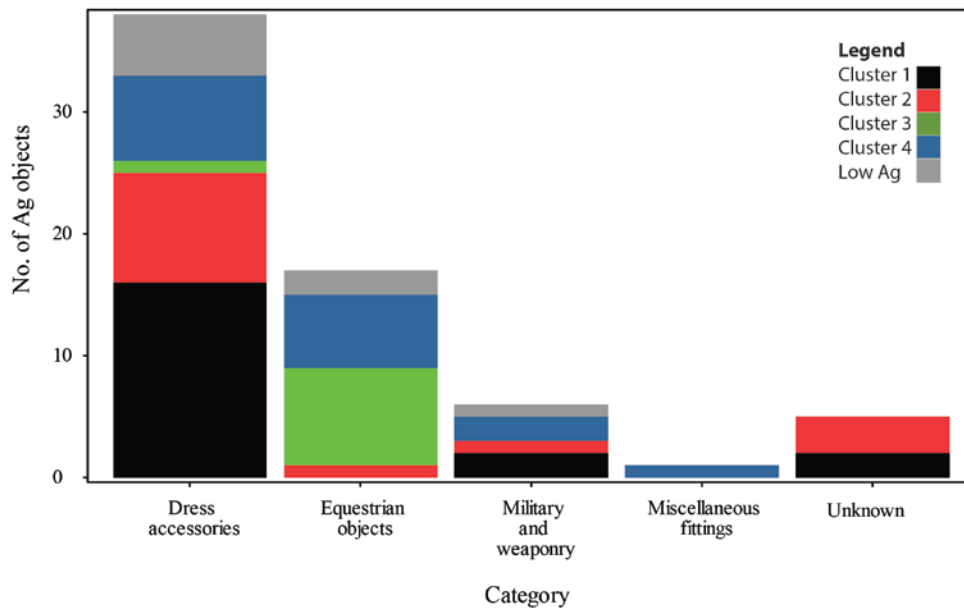


Figure 5-16: Bar chart showing the number of objects by object category with cluster as the stratum variable.

Drilling down into the object classes (Table 5-8 and Figure 5-17) shows further interesting results Cluster 1 is the dominant alloy type for finger rings, wrist clasps, and strap ends, cluster 2 dominant for beads and cluster 4 is dominant for ear rings. It should be noted that this is a relatively small set of objects and so care should be taken to avoid extrapolating beyond reason (for instance there is only one silver strap end).

Category	Class	Sub Class	Clusters				Low Ag
			1	2	3	4	
<i>Dress Accessories</i>	Bead	Undefined Bead	2	5		1	2
	Belt Fitting	Strap-end	1				
	Buckle	Undefined Buckle	1				
	Necklace	Pendant	2	1	1	3	
	Ring	Ear Ring				2	1
		Finger ring	5	1			1
		Wrist Clasp	Form A	5	2		1
<i>Equestrian objects</i>	Tack	Bridle Fitting		1	8	5	2
		Bridle mount				1	
<i>Military and weaponry</i>	Shield	Shield Mount	2	1		2	1
<i>Miscellaneous Fittings</i>	Nails and Bolts	Stud				1	
<i>Unknown</i>	Unknown	Unknown	2	3			
TOTAL			2	14	9	16	8

Table 5-8: Object categories, classes and sub classes with the number of objects by cluster.

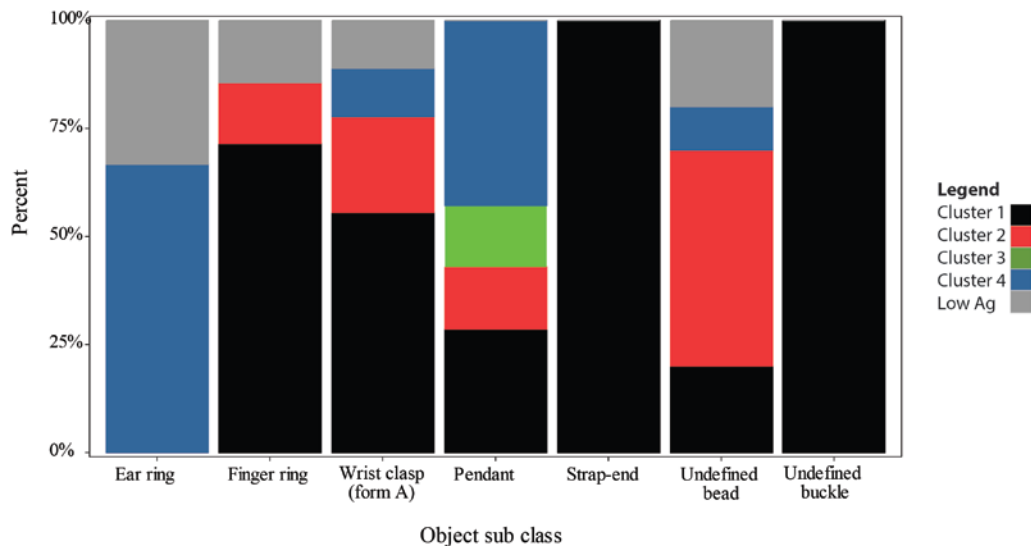


Figure 5-17: Bar chart showing the percentage of objects by object sub class with cluster type as the stratum variable. See Table 5-8 for the relevant data.

The differing distributions between these classes might lead one to wonder if this was linked to fabrication techniques. In Figure 5-18 it can be seen that there is a preference for using cluster 1 alloy type for wire objects (along with a complete lack of cluster 3). Sheet metal — the fabrication form used on most of the silver objects at Eriswell — is less clear. All clusters are represented and, although there

appears to be a slight preference for cluster 4, it is hard to draw any firm conclusions.

This is reinforced by incorporating object classes, fabrication and clusters into one bar chart (Figure 5-19). Some differences between clusters and object type can be seen. It appears that there is a preference to use cluster 1 for silver wrist clasps and an avoidance of cluster 3. Cluster 3 is also not present in beads, but here cluster 2 is most popular with only two beads made out of a cluster 1 alloy. At the same time there are no sheet metal silver wristclasps and only one wire bead. This suggests that, in specific cases, the composition, fabrication technique and form of an object may be interlinked (but that this is not necessarily an overriding consideration).

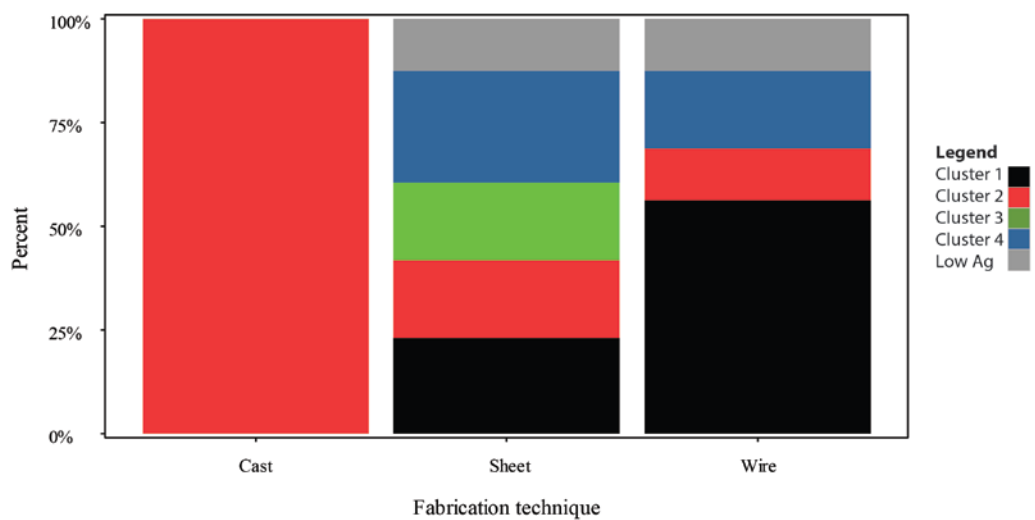


Figure 5-18: Bar chart showing the percentage of objects by object fabrication technique with cluster type as the stratum variable. The cast objects consisted solely of a few 'melted blobs' and so are not indicative of any particular object type. See Table 5-9 for the relevant data.

Cluster group	Fabrication technique		
	Cast	Sheet	Wire
1		11	9
2	3	9	2
3		9	
4		13	3
Low Silver		6	2

Table 5-9: Showing showing the number of objects by object fabrication technique and cluster type. The cast objects consisted solely of a few melted drops (predominantly associated with cremations and so are not indicative of any particular object type. See Figure 5-18 for a bar chart of the results.

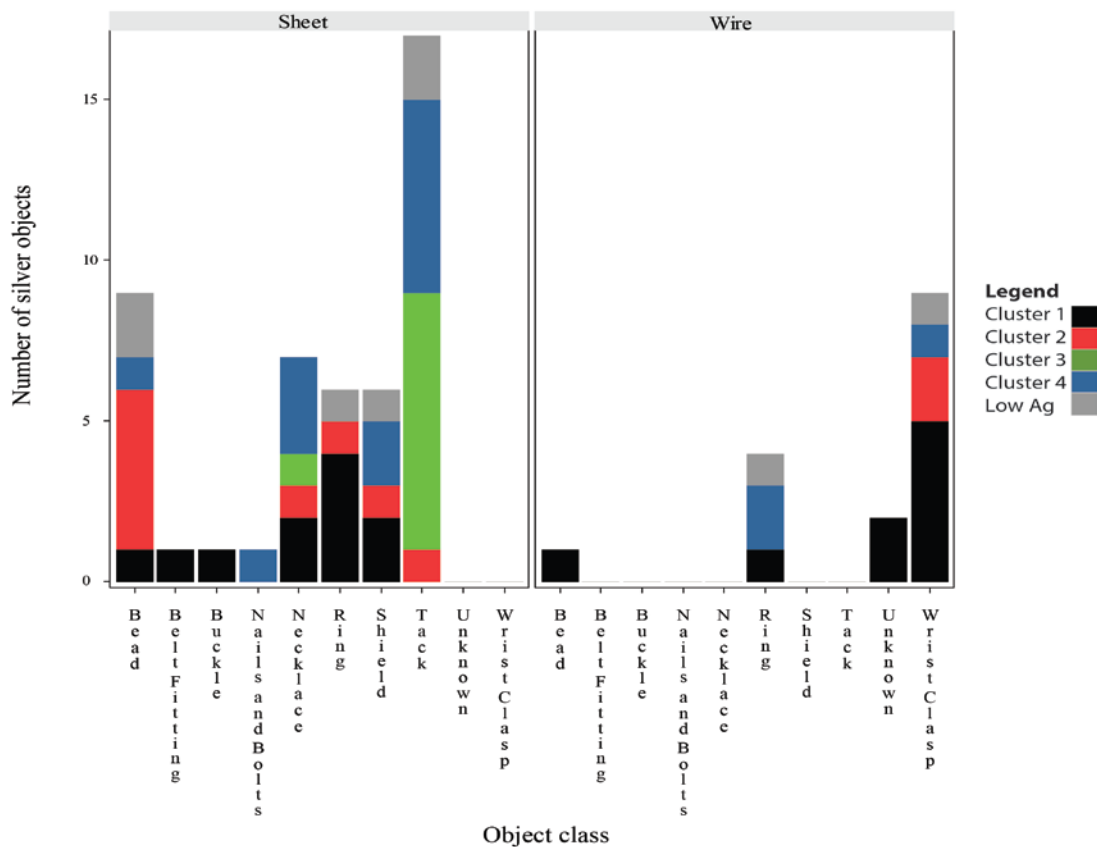


Figure 5-19: Bar chart showing object class with clusters in the stratum variable and fabrication as the facet available in the rows. The 'cast' objects have not been included here as they solely consisted of 'melted blobs'.

In the bar chart of site and cluster (Figure 5-12) it was clear that cluster 1 was absent from ERL 114. This is seen again in the bar chart of grave phasing, cemeteries and clusters (Figure 5-20). This chart also shows some potential interesting distributions between cemeteries and phases. In the female assigned gender inhumations ERL 104, with a larger number of objects than the other

cemeteries, provides the best cemetery to examine for cluster distribution within phases. In ERL 104 it can be seen that cluster 1 is present in every phase, yet most popular in phase A(2). Cluster 4 does not appear before phase A(2) in either ERL 046 or 104.

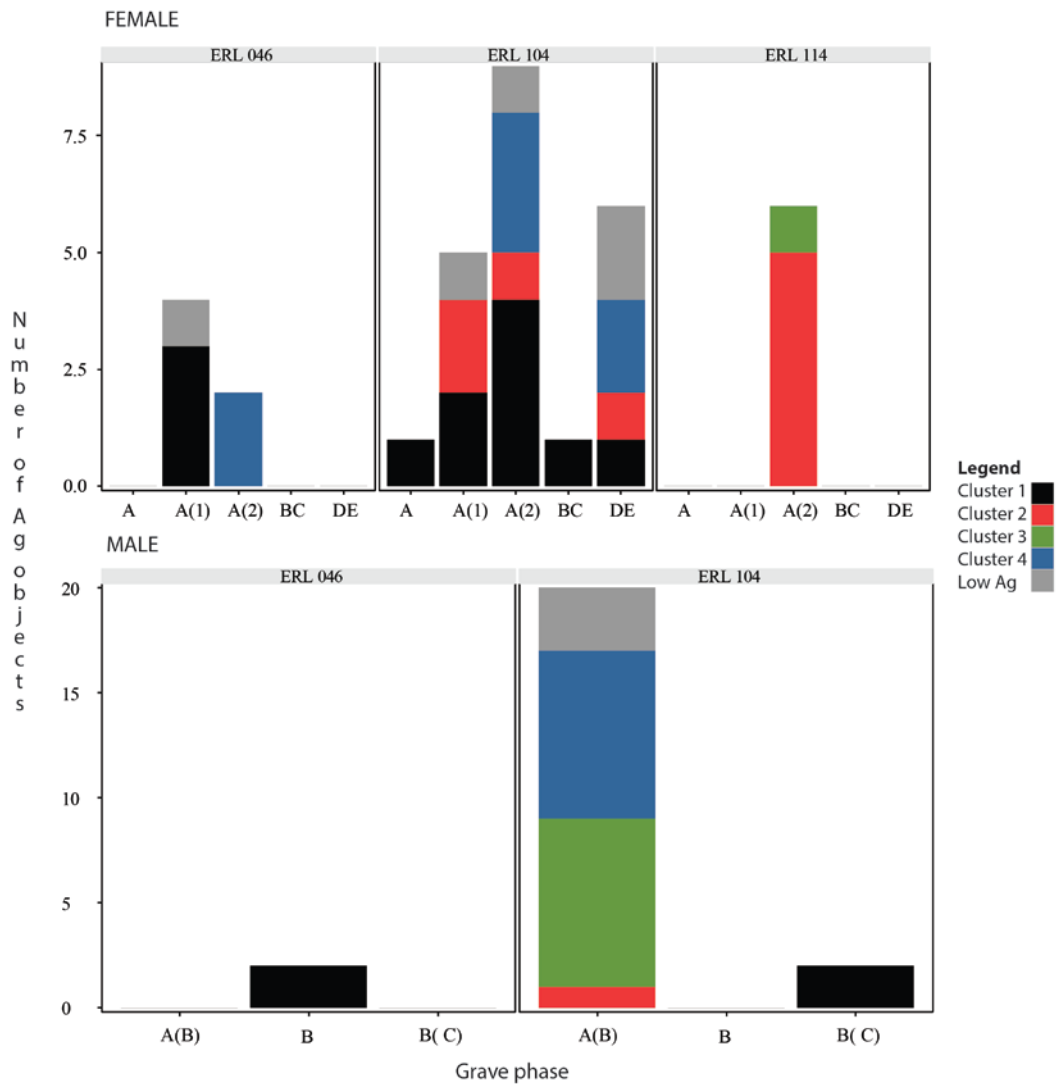


Figure 5-20: Bar chart showing grave phases (top row female, bottom row male) with clusters in the stratum variable and cemetery as the facet available in the rows.

Cluster 3 is not present in the female gendered inhumations of ERL 046 and 104 but is in ERL 114. In ERL 104 cluster 3 is entirely accounted for by the gendered male burial in grave 323. It is also interesting to note that, generally, silver objects are predominantly associated with female gendered burials. In a straight count of

the number of objects it may appear that there is a little more parity between males and females, but this is solely due to the horse and warrior burial of grave 323.

This has been a very basic attempt to interpret the clusters within the context of the archaeological categorical variables. Whilst there may be some hints of correlations between clusters and archaeological variables conclusive results are hard to deduce. It may be that more advanced techniques, such as using the clusters in a correspondence analysis, will prove more fruitful.

5.5 DISCUSSION

Previous work on early medieval Anglo-Saxon alloys (such as Brownsword and Hines 1993; Mortimer 1990; Leigh, Cowell, and Turgoose 1984) had limited amounts of objects to analyse. Where large number of early medieval silver objects were analysed they tended to be coins (Metcalf and Northover 1985; Metcalf and Northover 1988; Archibald 1985; Mackerrel and Stevenson 1972; Hawkes, Merrick, and Metcalf 1966). Consequently, with a shortage of non-numismatic analysis, the study of silver alloys has been dominated by an obsession with fineness. Unfortunately this subsequently became the dominant narrative and fineness / debasement became the sole prism through which this aspect of Anglo-Saxon metallurgy was viewed (see for example Arnold 2005, 135; Fleming 2012). Accordingly the debate has remained distorted despite the lack of a large body of evidence to truly support such a theory: we do not know if debasement was a concern for the early Anglo-Saxons (especially when concerned with dress accessories), perhaps it was simply enough for an object to look silver enough. The results here suggest that there are compositional groups (although one should be aware of the risk of false correlations due to the zero replacement method chosen here, see page 200) and, if correct, these results would challenge previous conclusions. It should be noted at this juncture that because of the lack of comparable data sets the interpretation has been deliberately limited to a primarily technological focus, unlike the copper alloys where large and much more accurate and precise data sets (see page xx) provide comparable material against which to test hypotheses that focus on social and cultural influences.

Four clusters have been identified using principal components on log-ratio transformed data and hierarchical clustering:

- Cluster 1 contains zinc and minimal tin.
- Cluster 2 contains tin and minimal zinc.

- Cluster 3 contains both tin and zinc and minimal gold.
- Cluster 4 is mixed and contains all three elements.
- All clusters contained copper and lead.

An examination of the clusters along with archaeological categorical variables has revealed some potentially interesting relationships between them and the clusters, but the small number of objects means that a degree of care must be used in their interpretation and extrapolation (if any) beyond Eriswell. The relationships can be summarised as:

- Cluster 1 is preferred for wire objects.
- Cluster 2 is used predominantly for sheet dress accessories.
- Cluster 3 is almost entirely associated with the bridle fittings from grave 323 in ERL 104.
- Cluster 4 appears to be a general use silver alloy with no particular pattern in its use.

Despite the clusters the alloys are mixed and all contain copper and lead. The relative levels of the additional elements in the silver here suggest that the silver was not purified by the metal smith using cupellation (a technique that archaeological evidence has indicated was practised in the early medieval period, Bayley 1991, 120). It is therefore likely that the non-silver elements (with the exception of gold) were deliberately added as alloying components (Wanhill 2002, 20–21; Wanhill 2005), most likely in the ‘original’ objects which formed the source. This mixed nature suggests that the source of material was recycled metals, previously identified as the production mechanism for early medieval silver alloys (Arnold 2005; Brownsword and Hines 1993). Consequently the silver is poor quality in economic ‘fineness’ terms. But, as can be seen above, the debased nature of the alloys does not mean that no useful information can be drawn from the compositions: production was not blind. There was choice and

selection being exercised; it just does not necessarily conform to our overriding focus on purity.

The addition of zinc to silver makes for a more malleable alloy (Percy 1880, 169–170; Gowland 1921, 295). The use of zinc as an additive to silver has been previously been identified as occurring from the late Romano-British period and through the post-Roman and early medieval period (Mortimer 1986, 240–241). Interestingly, in the late Romano-British period this is almost exclusively linked to dress accessories and other personal adornments and not coinage (see for instance the Snettisham Hoard, Pike et al. 1997). That it also helps prevent silver tarnish is another benefit (Percy 1880, 169–170; Gowland 1921, 295). Tin likewise makes silver tarnish resistant and makes the alloy more ductile, an ideal property for sheet objects (Greiff 2012, 251).

The addition of copper on its own is known in association with relatively high quality Roman silvers (Mortimer 1986, 240–241). It increases the hardness of silver and makes for a more durable alloy (Gowland 1921, 295). Its consistent presence here, along with lead, suggests that when tin or zinc were added to silver it was in the form of leaded alloys (a mechanism previously noted by Metcalf and Northover 1988, 104 and Kruse and Tatef 1992, 297).

The presence of gold is more difficult to explain. There is a chance it may have been added deliberately but it is more likely to be a by-product of the ores originally exploited; a majority of silver in antiquity was extracted from lead ores using cupellation, a process which gold survives (McKerrell and Stevenson 1972, 197–198). The presence / absence of gold in silver alloys has been used to suggest the exploitation of different ore bodies (Kruse and Tatef 1992, 297). Whilst a useful point to consider the presence absence of gold here is limited to the identification of different clusters.

Considering the above the cluster distributions make sense from a metallurgical perspective. Silver alloys containing zinc (cluster 1) are preferred for wire objects.

As noted above the presence of zinc makes for a more malleable silver alloy, a very desirable quality when working wire. The silver containing tin clusters (2, 3 and 4) are predominantly used for sheet objects, as tin increases the ductility of silver this again makes sense. The constant presence of copper will help make the alloys more hard wearing. It is true that these alloys are not 'pure' silver-zinc or silver-tin, but it should be remembered that these are small objects, not the Gundestrup cauldron.

All this does suggest that there was a shortage or lack of access to 'fresh' silver sources. However, this too is not necessarily a clear cut case. In the next chapter the use of mercury for gilding is discussed. Mercury is not found in the British Isles and was not recyclable, it had to be imported. Interestingly mercury ores are often found in common with silver ore bodies. This raises an interesting question; why were people willing and able to import mercury but not silver when both were likely available from similar sources?

5.5.1 RECYCLING MODELS

The alloys are mixed and 'debased', but clusters are identifiable. This suggests, as already stated, that recycled silver provided the source material for the Eriswell objects and that this process was not blind; there was choice involved. Can this be used to develop models for the production of early medieval silver in the East of England?

Yes and no.

We can rule out the idea that anything and everything was simply thrown into a melt. What is harder to deduce is how the compositional clusters were arrived at with two possibilities presenting themselves:

- The Eriswell object compositions represent those of the recycled objects, i.e. an object made an object (an existing silver

wire object would be selected to make a new silver wire object, a silver sheet would make a new silver sheet etc.).

- Relatively pure silver alloys were debased by the addition of copper alloys that were thought to contain desirable qualities, i.e. the addition of brass for a wire object, bronze for a sheet.
- A mixture of both methods was used.

Deducing which of these options was used is difficult with the relatively small number of objects here. There is also a requirement for a full and detailed understanding of silver alloy compositions of all preceding silver using cultures to properly understand how recycled material was being used (i.e. was there a focus on late Romano-British material that would be less tarnished than earlier objects? Do these compositions really differ that much from late Roman-British silver alloys?). It is clear that a much larger program of work is required.

5.6 CONCLUSION

Previous studies on early medieval silver alloys have been dominated by coinage. This numismatic focus has led to an overriding focus on the ‘fineness’ of silver alloys as the main object of study. It is the contention of this study that this focus has led to an erroneous focus on non-coinage objects and has distorted the discussion on the use of silver in the early medieval.

The investigation of the totality of silver objects from Eriswell here has revealed that there are groups within compositional data and that these are sometimes related to fabrication technique and object type. The analysis does suggest that recycled objects probably formed the source material, but there were choices being made and it was not a blind process. However, the data set is small and the mechanisms behind the choices made are difficult to elucidate. Further study that takes a broader chronological outlook is desperately needed to truly throw light on silver object production in the early medieval period.

CHAPTER 6: GILT OBJECTS

“The quick mercurius and the burning gold”

(Barlow 1793, 47)

6.1 INTRODUCTION

There were no ‘solid’ gold objects in the Eriswell assemblage seen by the author (there is one half of a Roman gold coin, but that was not available for analysis). Consequently this chapter deals with gilding; acts of making base metals appear gold.

As discussed in Chapter 2 (page 70) there are several methods of gilding a metal. The easiest to detect analytically using HHPXRF is mercury gilding, a technique using mercury to adhere the gold to the surface of the object.

Potential gilded objects were initially identified by eye during the post-excavation assessment. Methodologically it was decided that, in the first instance, HHPXRF analysis would be undertaken to see if mercury (Hg) and gold (Au) peaks were present (indicating mercury gilding). If not, then optical and electron microscopy would be undertaken to investigate the method further.

The results appear to suggest that all gilding on non-ferrous and ferrous objects was mercury gilding with clear gold and mercury peaks visible. No other gilding technique appears to have been used on non-ferrous metals in any of the Eriswell cemeteries.

A degree of care must be used when interpreting this result as gold-mercury mineralisation is known to have been exploited in antiquity (Patterson 1971, 302) and it cannot be ruled out that detectable mercury may occasionally result from the gold ore body (for a detailed examination on the formation and distribution of gold-mercury combined ore formations see Nekrasov 1996).

During the process of analysis the importance of analytically assessing gilding was driven home by a number of objects which, in the initial post-excavation assessment, had been visually identified gilt. However, analysis showed there to be no mercury and no gold; they were copper alloys that had less corrosion than the majority and simply retained their metallic sheen.

6.1.1 DIFFUSION

Mercury gilding produces a relatively thin gold layer on the surface of the object (approximately 3-9 μ m depth) with further diffusion layers into the non-ferrous substrate (approximately 10 μ m depth) (Salomon et al. 2008; Corregidor et al. 2011). The presence of diffusion layers on the Eriswell objects was illustrated by non-destructive surface X-Ray Diffraction (XRD) on one wrist clasp (046-1812). The XRD used an XPERT-PRO PAN analytical diffractometer. Wrist clasp 046-1812 was selected because it possessed the consistently greatest width and flat area of gilding on an Eriswell object (with a width of approx. 22mm). This enabled the object to be placed in situ on a fixed stage and analysed with a divergent beam with a footprint of 200 mm² for 11 sec/step (7-100°2 θ) acquisition time. Data was analysed with X'Pert HighScore V2.1.2 and PDF-02 database.

Analysis detected intermetallic compounds such as Kolymite (Cu₇Hg₆, PDF 00-033-0470), Luanheite (Ag₃Hg, PDF 00-041-1417), Eugenite (Au₅Hg, PDF 00-004-0781) and Goldamalgam (AuHg, PDF 00-039-0394) (see Figure 6-1 and Appendix VI).⁷⁶

⁷⁶ As with the copper in Kolymite the silver in Luanheite is from the substrate, see the next chapter for more details.

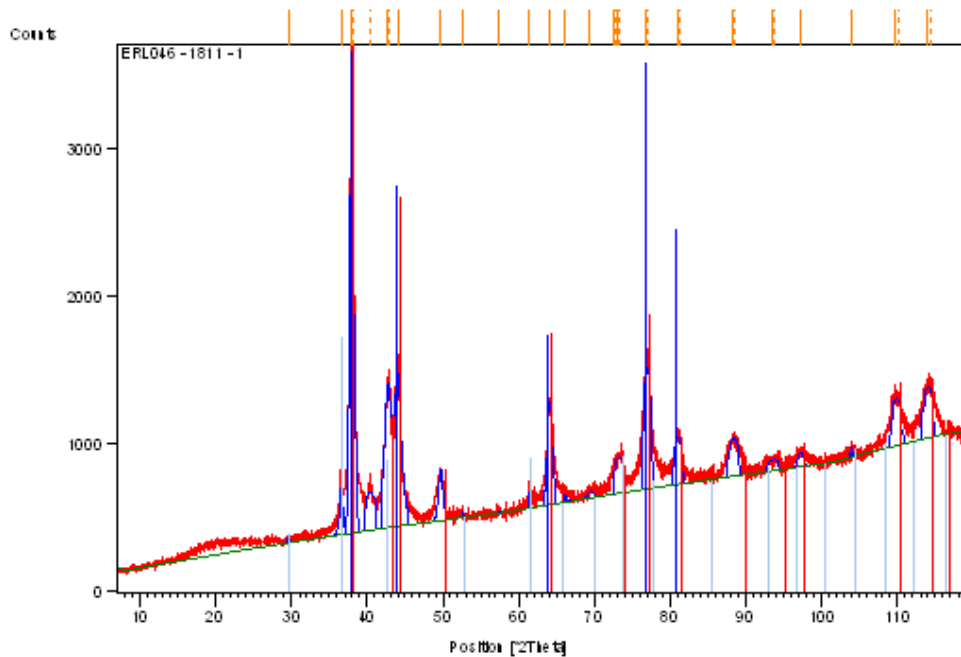


Figure 6-1: XRD spectra for gilding on wrist clasp 046 – 1811. Analysis was undertaken on a PANalytical X'pert PRO at the National Museum Wales. The full data for the analysis are available in .

6.1.2 HOT OR NOT?

As briefly mentioned earlier there are two methods of gilding using mercury: hot and cold. Cold gilding involves the application of mercury directly to the surface of the object to be gilded followed by gold leaf. Fire gilding involves the production of a mercury gold amalgam which is painted upon the surface of the object and heated (vaporising some, but not all, mercury). In the latter the mercury is used as little more than a “*sticking medium*” (Habashi 2008, 4). This does not mean the mercury is simply replacing another organic or inorganic adhesive (for an overview of the use of adhesives in gilding see Oddy 1981, 77) as cold mercury gilding will lead to surface diffusion between the mercury, substrate and the gold (Tylecote 1978, 80; Vittori 1979, 36).

Both techniques will leave traces of mercury (Lins and Oddy 1975, 370); so the XRF detection of mercury and gold peaks is not an indication of which form of mercury gilding was used. Both techniques will also lead to the formation of

intermetallic compounds; so the simple presence of said compounds (detected by XRD) is also not indicative of technique. Unfortunately it appears that little research has been undertaken into the intermetallic compounds one might expect to form dependent on the mercury gilding procedure. More common is an automatic assumption that fire gilding was used (for example Aufderhaar 2009; Šmit, Istenič, and Knific 2008).

Of the intermetallic compounds mentioned in the previous section only one is particularly diagnostic for our purposes: Kolymite. This compound, with a formula of Cu_7Hg_6 , has a weight percent composition of 26.8% copper and 73.02% mercury. Examining this in a phase diagram (Figure 6-2) shows that it forms at 128°C , i.e. above the temperatures that one would expect to be encountered in an everyday environment. This, it would seem, indicates that fire gilding was used (although one cannot discount the possibility of a cold mercury gilded wrist clasp accidentally being dropped in a domestic fireplace).

This is, of course, only one object and consequently we cannot securely extrapolate to definitively state that all Eriswell gilt objects were gilded this way. Nevertheless it does indicate that the technique was still practiced in the post-Roman period and it may be reasonable to assume that at least some Eriswell objects were fire gilded.

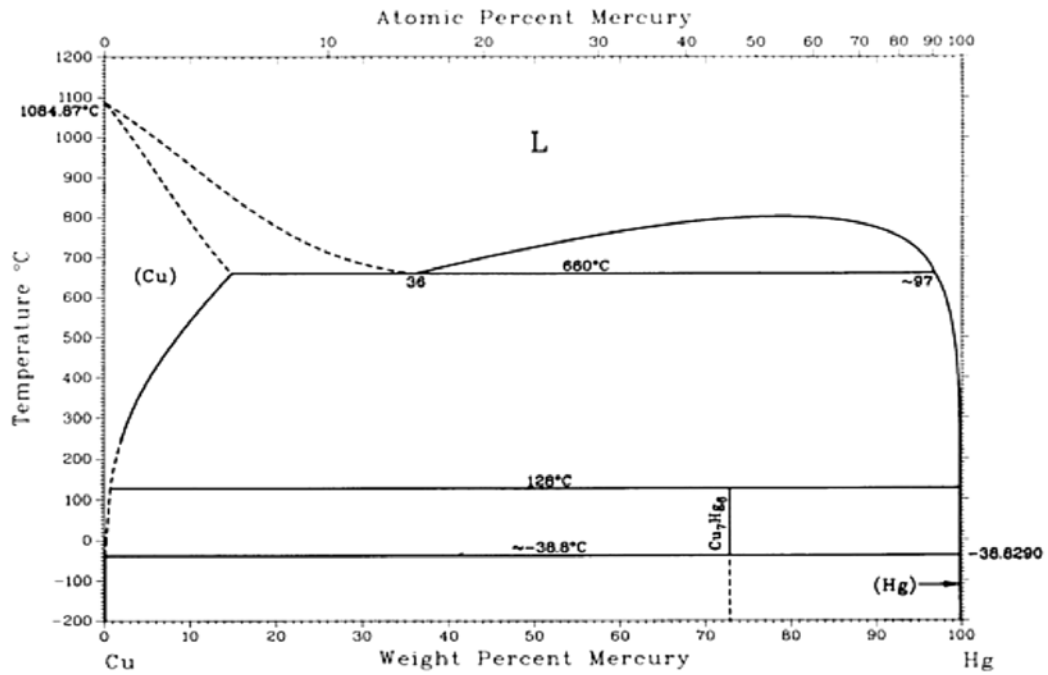


Figure 6-2: Phase diagram for the Cu-Hg system from Chakrabarti and Laughlin 1985, 522, Figure 1.

6.1.3 ANALYSIS DEPTH

Au has a density of $19.30 \text{ g}\cdot\text{cm}^{-3}$ and a mass absorption coefficient (μ/ρ) of $12.98 \text{ cm}^2/\text{g}$ at 40 keV. AuHg has a density of $15.893 \text{ g}\cdot\text{cm}^{-3}$ and a mass absorption coefficient (μ/ρ) of $13.20 \text{ cm}^2/\text{g}$ at 40 keV (absorption coefficient data from the NIST XCOM database v 1.5, see Berger et al. 2010). Therefore x-rays of 40 keV would have a $1/e$ penetration depth (i.e. the level at which the radiation has lost 63% of its original value) of $40 \text{ }\mu\text{m}$ in an infinitely thick gold layer and $48 \text{ }\mu\text{m}$ in an infinitely thick Gold amalgam layer.

These are, of course, significantly deeper than the escape volumes for the characteristic $K\alpha$ and $L\alpha$ energies for the elements of interest here. Calculating the critical penetration depth (t_{crit}) values for copper and tin $K\alpha$ energies in matrices of gold amalgam and gold allows us to see the maximum depth from which these characteristic energies could escape (Table 6-1).

Matrix	Peak	Attenuation coefficient (cm ² g ⁻¹)	μ_{tot}	t_{crit} (μm)
AuHg (density 15.89 g·cm ⁻³)	Cu K α	2.07E+02	309.84	15.89
	Sn Ka	4.34E+01	77.96	37.17
Au (density 19.30 g·cm ⁻³)	Cu K α	2.04E+02	304.75	7.87
	Sn Ka	4.28E+01	76.72	31.26

Table 6-1: Attenuation coefficients for fluorescent Cu–K α (8.05 KeV) and Sn–Ka (25.27 KeV) x-rays in gold amalgam and gold matrices. The t_{crit} shows the maximum from which Cu and Sn Ka x-rays would be able to escape from the respective matrices with an incident x-ray of 40 KeV). Calculated using the formula from Potts, Williams-Thorpe, and Webb 1997, 32, Equation 2. For a detailed discussion on calculating the critical penetration depth see page 162.

Realistically these depths are likely thicker than the gold layers encountered on the Eriswell objects (as mentioned in section 6.1.1 mercury gilt layers tend to have a maximum depth of 9 μm). Consequently we are not sampling solely the gilt layer (because it is too thin to fully attenuate the beam), but also the diffusion layer (up to 10 μm thick if present) and alloy substrate. Therefore the HHpXRF results here will not solely show gilding, but also elements from the diffusion layer and substrate. This limits the potential for interpretation of the analytical results thus there will be no statistical investigation of gilt compositions. Instead interpretation is in the form of characterizing the presence/absence of mercury and assessing possible correlations between categorical variables (such as object form) and gilding presence.

6.2 INTERPRETATION

6.2.1 SITE AND GRAVES

In this section only objects seen by the author and analytically demonstrated to have been gilded are included. This does mean that one or two objects are excluded as they were either not available for analysis, too delicate to analyse or suspected to be gilt but analysis prevented by the levels of corrosion (cruciform brooch 046-1369 is a good example of this). Consequently the figures here should be seen as the lower limit of gilt objects (although it is not expected that the full number would be much higher).

Out of 426 inhumations at Eriswell only nine contained gilded objects. There were no gilded objects associated with any of the seventeen cremations.

Table 6-2 shows a breakdown of the graves by cemetery. As can be seen ERL 046 and ERL 114 have one gilt containing grave respectively, whilst ERL 104 has seven. It should of course be remembered that this excludes a number of gilt objects that definitely belong to the early Anglo-Saxon period but were not in a grave context (i.e. the burials they were likely associated with had probably been heavily truncated).

	ERL 046	ERL 104	ERL 114
Non-gilt grave	51	252	97
Gilt grave	1	7	1
Gilt grave %	2	3	1

Table 6-2: Number of gilt and non-gilt graves for cemeteries ERL 046, 104 and 114.

In total these nine graves contained 33 gilded objects (the categorical data can be found in Appendix VII). The majority of these were from cemeteries ERL 104 (24 objects, 21 of which were from burial contexts) with ERL 046 and ERL 114 containing six (one from a grave) and three (all from a grave) respectively. As stated in the introduction all had gold and mercury peaks, showing evidence of

mercury gilding. Although no further interpretation of the peak data will be undertaken here a full table of the Net Peak data can be found in Appendix VIII.

Table 6-3 shows a list of the gilt containing graves with the object categories and number of gilt objects. Examining this shows that grave 323 (a horse burial from ERL 104) dominates the assemblage with its gilt tack. In total 33% of graves (three in total) contain more than one gilt object (24% of gilt objects are not assigned to a grave).

Site	Grave No.	Gilt object category	No. of objects
ERL 046	NG	Dress Accessories	5
	25	Dress Accessories	1
ERL 104	NG	Dress Accessories	2
	NG	Miscellaneous Fittings	1
	166	Dress Accessories	1
	206	Personal equipment	1
	245	Military and weaponry	2
	263	Dress Accessories	1
	322	Dress Accessories	1
	323	Equestrian objects	14
364	Dress Accessories	1	
ERL 114	405	Dress Accessories	3
Total			33

Table 6-3: Showing graves containing objects, the gilt object categories and the number of gilt objects.

6.2.2 OBJECT TYPOLOGIES

Considering the results by object category (Table 6-4) shows that dress accessories are the most frequent gilt objects (45% or 15 objects), with equestrian objects (all from grave 323) accounting for the majority of the remainder (42% or 14 objects). Delving deeper into the categories shows that brooches and wrist clasps are the most frequently gilded objects (13 objects), accounting for 86% of all dress accessories and 39% of all gilt objects (Table 6-4).

Site	Category	Class	Sub Class	Total		
046	Dress Accessories	Bead	Undefined Bead	2		
			Brooch	Cruciform	1	
					Fish	1
					Great square-headed	2
		Necklace	Necklace Ring	1		
			Pendant	1		
			Wrist Clasp	Form B 13 a	1	
					Form B 18	2
					Form B 7	2
					Form C 1	2
			Equestrian objects			1
	Unknown	Unknown	Unknown	1		
104	Dress Accessories	Belt Fitting	Strap-end	2		
			Brooch	Applied saucer	1	
					Bar	1
					Bird	1
					Great square-headed	1
		Ring	Ear Ring	2		
			Equestrian objects		15	
		Military and weaponry	Shield	Shield Mount	3	
		Miscellaneous Fittings	Miscellaneous	Sheet	1	
		Personal equipment	Purse	Purse Fitting	2	
		Unknown	Unknown	Unknown	1	
114	Dress Accessories	Wrist Clasp	Undefined Wrist Clasp	3		

Table 6-4: showing gilt objects by site, category, class and sub class.

Examining the object classes (Table 6-4) shows one particularly interesting result; of the seven gilt wrist clasps not one is associated with ERL 104 (four from ERL 046 and three from ERL 114). Gilt brooches appear only in ERL 046 and ERL 104 (two and four brooches respectively). It is uncertain if this actually indicates much; the small number of gilt objects means that care must be taken in extrapolating relationships between object types and distribution.

6.2.3 GENDER AND PHASING

The assigned genders show an apparent distinct split in distributions, with ERL 104 the only place where males have gilt objects (Table 6-5). Gilt objects in ERL 046 and ERL 114 in comparison completely associate with female gendered burials.

Site	Assigned Gender	Category	Total
046	N/A	Dress Accessories	5
	F	Dress Accessories	1
104	N/A	Dress Accessories	2
	N/A	Miscellaneous Fittings	1
	N/A	Personal equipment	1
	F	Dress Accessories	4
	M	Equestrian objects	14
	M	Military and weaponry	2
114	F	Dress Accessories	3

Table 6-5: Number of gilt objects by site and assigned gender.

Within the object categories and classes there is a ‘traditional’ breakdown. Gilt dress accessories are exclusively associated with gendered female burials. In contrast gendered male burials are almost exclusively associated with military and equestrian related artefacts (Table 6-5).

The majority of the female gendered objects fall within site phase ERL-FA2 and the majority of the male gendered objects with site phase ERL-MAB (see Table 6-6).

Site	Assigned Gender	Grave Phase	Total
046		N/A	5
	F	A2	1
104		N/A	4
	F	A2	4
	M	AB	14
		C	2
114	F	A2	3

Table 6-6: Number of objects by phase.

6.3 DISCUSSION

*Regard the capture here, O Janus-faced, / As double as the hands that twist this glass. / Such
eyes at search or rest you cannot see; / Reciting pain or glee, how can you bear!*

*Twin shadowed halves: the breaking, second holds t, / In each the skin alone, and so it is / I
crust a plate of vibrant mercury / Borne cleft to you, and brother in the half.*

(Crane 2001, stanza i-ii, 91)

With a relatively small number of gilt objects the conclusions that can be drawn are relatively small. Nevertheless there are some interesting results; the richness of horse burial 323 in ERL 104 is highlighted and there are some potentially curious distributions of gilt objects between the cemeteries (such as the lack of gilt wrist clasps in ERL 104). Perhaps the most provoking observation to draw from about the Eriswell gilt objects lies not in distributions and variable correlations but the totality of method employed.

Fire gilding became the most frequently used method of gilding from the 3rd Century CE onwards (Oddy 1980; Oddy 1991). The use of the process, as indicated by the XRD analysis on wrist clasp 046-1812, at Eriswell therefore suggests a degree of continuity of practice in at least one element of metallurgical technology from the late Romano-British period.

6.3.1 MERCURY SOURCES

The mercury gilding of post-Roman and early medieval objects raises an important question that has, so far, received little attention in early medieval scholarship; where was the mercury coming from?

Mercury is mined in the form of cinnabar and / or native mercury and the recycling of it is difficult and beyond the technology of the period (it is possible to recycle the gold from the gilding, but this process requires mercury, see Biringuccio 1966, 383). Whilst examples of cinnabar deposition have been identified in the UK (King 1982; Ambrose 2013) they are sparse, not readily

extractable and are of geological rather than economic interest. Consequently the mercury used in gilding will likely have been imported. Unfortunately we have little indication of where mining was taking place in the 5-7th centuries, the nature of the trade networks or even in what form it was transported.

Understanding where and how mercury was being sourced is important for our understanding of Anglo-Saxon metallurgy. As stated previously, current interpretations of the period's non-ferrous metallurgy have the period defined as a dark age; there was no access to fresh materials and recycling for non-ferrous alloys was an act of desperation. If this was the definitive case then one might expect there to be no fire gilding; instead foil or other techniques that did not require the importation of exotic materials would be used. The use of mercury challenges our traditional interpretations.

Deposits of cinnabar (HgS) and native mercury are known across Europe (see Figure 6-3 and Table 6-7) from Almadén (Spain), Avala (Serbia), Carnia (Austria, this location is uncertain, see Table 6-7 for further details), Ephesus (Turkey), Idrija (Slovenia), Moschellandsberg (Germany), Rosenau (Romania) and Tuscany (Italy) (Rapp 2009, 180; Maras, Botticelli, and Ballirano 2013, 686). The largest of these, the Almadén mine in Spain (containing one third of the world's total supply of mercury, Hernández et al. 1999, 539), was exploited from the Iron Age onwards with production only ceasing in 2000 (Edmondson 1989, 94). With some of the other sites, such as Moschellandsberg, activity is not recorded before the later medieval period. However, Roman mining sites outside of the Iberian peninsula and British Isles are poorly documented (Hirt 2010, 32) and with later mining activities often destroying remains of earlier workings one cannot not safely exclude them. It is unknown which mines were being exploited in the post-Roman period.

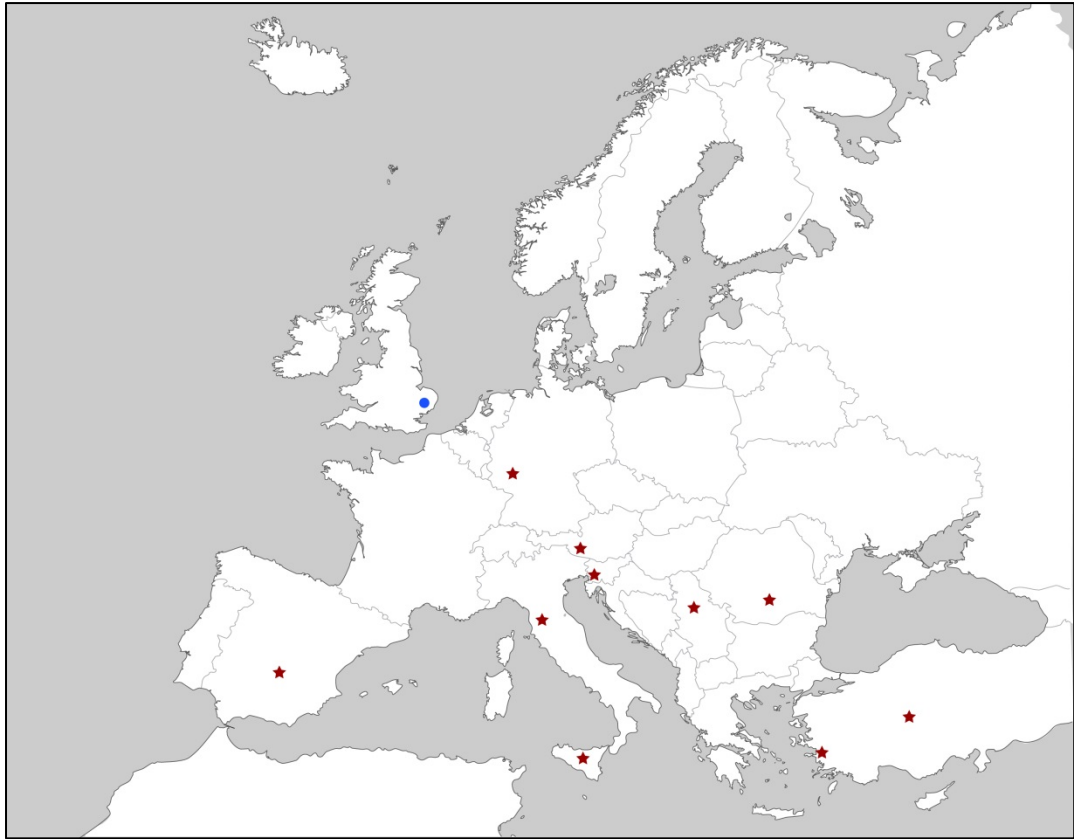


Figure 6-3: Modern political map of Europe showing cinnabar deposits known to have been exploited in the Roman and / or medieval (red stars) and Eriswell (blue circle). The locations are: Almadén (Spain), Avala (Serbia), Carnia (Austria), Ephesus (Turkey), Idrija (Slovenia), Moschellandsberg (Germany), Rosenau (Romania), Sicily (Italy), Sızma (Turkey) and Tuscany (Italy). See Table 6-7 for details and references of the antiquity of mining activities at each location. Data from Rapp (2009, 180) and Maras et al. (2013, 686), base vector map by Erind (2010).

Location	Country	Period of earliest currently confirmed mining
Almadén	Spain	Mining commonly cited as starting in the Roman period (for example see Edmondson 1989, 94) however, environmental evidence suggests the Iron Age to be more likely (Martínez-Cortizas 1999).
Avala	Serbia	?Iron Age (Davies 1934)
?Carnia	Austria	Uncertain. Rapp (2009, 180) mentions Austria as being a source of cinnabar but provides no further location. Maras et al. (2013, 686) use a mineral sample from Austria (Carnia) but provide no further reference for this being a location of cinnabar extraction in the Medieval periods or earlier. It may be that the reference to 'Austria' in Rapp (ibid.) refers to Idrija (see also below); a region of the Austrian Littoral until the dissolution of the Austro-Hungarian Empire in 1918. After a brief inter-war sojourn in Italy the area presently resides in Slovenia where it enjoys World Heritage Site status.
Ephesus	Turkey	Roman (Brunt 1990, 398)
Idrija	Slovenia	Late Medieval (UNESCO 2012, 228)
Moschellandsberg	Germany	Late Medieval (Krupp 1989)
Rosenau	Romania	Unknown. Significant Roman levels of mining activity (for a variety of minerals) are suspected, but there has been little study of the history of early extractive metallurgy in the region (Hirt 2010, 32).
Sicily	Italy	?Roman. Area known for its Roman sulphur production (Anonymous 2012, 8:136) but cinnabar does not appear to get mentioned. Mentioned as a source of cinnabar by early medieval Islamic traders and geographers such as Al-Dimashqi and al-Bakri (UNESCO 2001, 96).
Sizma	Turkey	?Roman (Anonymous 2012, 8:136)
Tuscany	Italy	Chalcolithic (Steiniger and Giardino 2013)

Table 6-7: Cinnabar mining areas shown in Figure 6-3 with dates for the earliest documented extraction activities. Those that are noted as medieval have sites as

As Anglo-Saxon fire gilding of non-ferrous objects appears to be a continuation of late-Roman practice it would seem that Roman evidence would be the best place to start to try and understand its trade. Unfortunately our understanding is slim and predominantly rests on the testimony of classical writers such as Strabo (for an erudite interpretation of Strabo and cinnabar see Leaf 1916) and Pliny the Elder. It was Pliny (writing in the first century AD) who provided perhaps the most detailed (and best known) account describing its processing and movement:

We are informed by Juba that minium [cinnabar or HgS] is also procured in Carmania; and by Timagines, that it is also found in Ethiopia. But it is not brought to us from either of these

*places nor indeed scarcely from any place except Spain. The most celebrated kind comes from the district of the Sisapo [Almadén], in Beetica; this mine of minium is a source of considerable revenue to the Romans, and is guarded with very great care. **The substance is not allowed to be purified or roasted on the spot, but is brought to Rome sealed up,** to the amount of 10,000 lbs weight annually; it is then washed at Rome. The price of it is fixed by an express statute...*" (Pliny the Elder and Bostock 1828, 57)

At the time Pliny was writing about fire gilding on non-ferrous objects it was relatively uncommon in Europe (W. A. Oddy 1991). Cinnabar was predominantly used as a pigment (either directly or after processing into vermilion) and mercury for medicinal purposes as treatments for Syphilis and oral hygiene (Prioreshi 1998, 206–7). Fire gilding rapidly increased in popularity from the 3rd century CE onwards across the Roman world. Unfortunately it is not known if the trade and processing of cinnabar remained as tightly controlled in the later Roman period as in Pliny's time. It is also unknown what degree of continuity there was in trade routes in the post-Roman period and this remains an area of significant debate: for every Nancy Edwards suggesting a degree of continuity (2013, 69) there is a Ward-Perkins (2005, 117–118) arguing for near complete collapse.

It is not known if mercury was imported processed or as cinnabar (with distilling occurring relatively locally) into the British Isles. If imported as liquid metal then it may be reasonable to suggest that the manner of its 'packaging' was not so different to that used in the post-medieval period (as described in *The Penny Cyclopædia*): "*the metal was poured into fresh sheep-skin, from which the wool was taken off, the ends were tied tight, and the sort of bag thus made was enclosed in a second skin, and that in a third...*" (Anonymous 1839, 102). In the 19th Century this method was replaced with the use of iron flasks.

Given the sheer dominance of the Almadén mine in the archaeological narratives and historical documentation it may be suspected that this remained a source in

the early Anglo-Saxon period. Environmental evidence indicates that, whilst production fell off in the immediate post-Roman period, it did not cease (Martínez-Cortizas 1999). Links between west Britain and the Iberian Peninsula in the early medieval period are well attested (Fulford 1989) and there may be some evidence to support Almadén as a source in Late Anglo-Saxon documentary evidence, with textual analysis of Bald's Leechbook (a mid-ninth century medical textbook) suggesting that mercury for medical purposes may have been imported from the region (Cameron 1993, 104). Arnold (2005, 118) also thought Iberia may have been the source, proposing that the large amount of Kentish metalwork found in the Bordeaux region may indicate trade in high value goods such as this.

Unfortunately, with our lack of knowledge about the operation of mining activities in other areas, this on its own is not enough to draw any firm conclusions. It may be that future work can help in this area. Recent Raman spectroscopic analysis of Anglo-Saxon illuminated manuscripts in the British Library has shown the use of vermilion as a pigment (K. L. Brown and Clark 2004) and the sourcing of cinnabar deposits used in pigments has shown promise (Damiani et al. 2003; Maras, Botticelli, and Ballirano 2013). If further and earlier examples of the use of cinnabar as a pigment in Anglo-Saxon cultural areas are discovered (in texts or on other materials) then it may be possible to use techniques such as XRD to illuminate the exploitation source(s) (assuming that cinnabar for pigmentation and mercury for gilding or medical purposes followed similar trade routes).

There may also be much archaeological evidence, currently rarely recognised, that could also throw light on the usage and trade of mercury. Recently Bayley and Russell (Bayley and Russel 2008) published the discovery of two mortars from Clausentum (located near Hamwic) and Hamwic (Figure 6-4). Both of these showed traces of microscopic gold particles and analysis showed clear mercury

peaks, indicating that these had been used in the production of amalgam (presumably for gilding).

Given the preponderance of mercury gilding as a technique throughout the post-Roman and Anglo-Saxon period it seems unlikely that these are the only two mortars of the period in existence. Instead it is perhaps more likely these are the only two for which a metallurgical usage was suspected and analysis undertaken to investigate further. Consequently it seems likely that there may be further archaeological evidence waiting to be discovered both in the archive and field which may throw light on this intriguing aspect of metallurgy.



Figure 6-4: Amalgam mortars from Hamwic (left) and Clausentum (right). From (Bayley and Russel 2008).

6.4 CONCLUSION

On all gilded objects the analytical results show the presence of mercury. This indicates that mercury gilding was the sole technique utilised.

Because of the analytical technique used and the depth of the gilding the interpretation of the results was relatively limited. Nevertheless there were some interesting results. Proportionally ERL 046 has significantly more gilt containing graves than either of the other two cemeteries. In contrast no grave in ERL 046 or 114 can match the richness of the warrior and horse burial (323) in ERL 104.

The usage of mercury also poses some interesting questions about metallurgy and trade in the period.

The continuing use of the technique suggests a certain degree of continuity of technological practice with late Roman techniques. The usage of mercury in itself is also interesting. There are no exploitable sources of cinnabar or native mercury in the British Isles. Consequently material had to be imported, an issue which has received little attention (apart from a brief mention in Arnold 2005, 118–9). Our lack of knowledge about extractive metallurgy in the period presents serious limitations in trying to understand from where the source(s) were located. Nevertheless it is interesting that in a period traditionally characterized as being one of ‘de-skilling’, suffering ‘a loss of basic technological know-how’ and alleged lack of raw materials (Fleming 2012, 35) the presence of mercury gilding suggests the opposite. It suggests a society that maintained continuity of technological knowledge and practice from the Romans and had the access to that strange and wondrous liquid metal: mercury.

CHAPTER 7: FILLER, LEAD AND TIN ALLOYS

*What says this leaden casket?
“Who chooseth me must give and hazard all he hath.”
Must give—for what? For lead? Hazard for lead?*

(Shakespeare, *The Merchant of Venice*, 2010, 50, Act II, Scene VII)

7.1 INTRODUCTION

This short chapter brings together the small group of (predominantly) lead rich alloys in use at Eriswell. The largest group of alloys that fall under this category are probable filler alloys used for joining non-ferrous components. There are also a handful of objects composed from lead and tin rich alloys (see section 7.3, page 299), four of which were nearly pure lead. Of this former group all but one were intrusive or spoil heap finds and do not date to the early-medieval period.

7.2 FILLER ALLOYS IN CONTEXT

Many of the Eriswell objects are composite and these composite parts need fixing together. There are several methods available for joining metals together, roughly classified as follows (Humpston and Jacobson 2004, 1):

- Mechanical fastening – no fusing of metals, objects physically fixed together. Used on a number of Eriswell objects.
- Adhesives – essentially ‘gluing’ metallic objects together with an organic adhesive. There was no obvious usage of this identified (either macro or microscopically) on the non-ferrous assemblage from Eriswell. It is not possible to chemically identify the presence of organic adhesives with the HHpXRF.
- Soldering & Brazing - the application of a molten filler metal or alloy (with lower melting point than the metals it’s joining) to join metallic

objects that are less readily fusible to each other. If the filler metal / alloy melts below 450°C then it is known as soldering, if over then brazing (Humpston and Jacobson 2004, 5).

- Welding – may involve a filler material. Involves fusing two separate pieces with the direct application of heat to the parts to be joined.
- Solid state - broad term that encompasses a variety of techniques including pressure welding and diffusion bonding (Humpston and Jacobson 2004, 6). It is achieved when prepared surfaces (usually fayed) are joined by heating (below the melting point of the alloys) and / or pressure, coalescing the two without the addition of any filler material (Davis 2001, 299). This group of joining technologies includes techniques such as diffusion gilding, the predominant method of gilding before the introduction of mercury gilding (Figueiredo et al. 2010, 285).

Variations of all these five joining techniques are known to have been used from the pre-Roman era onwards (for an overview of joining techniques in antiquity see Lang & Hughes 1980 and Lang & Hughes 1984). However, there is only definitive evidence for the use of two on the non-ferrous assemblage from Eriswell: mechanical fastening and soldering / brazing.

Mechanical fastening is readily identifiable even when an object has not broken down into its composite parts; rivets remain readily visible. In the non-ferrous assemblage at Eriswell they were most frequently used to attach alloys to organic materials such as wood (as on bucket 046-1036). The evidence for other joining techniques is less clear as it is only possible to analytically examine those where the join has failed after more than a millennia of burial. Consequently, being a self-selecting dataset, the results presented here cannot be extrapolated to represent a comprehensive assessment of non-ferrous joining technologies and materials.

7.2.1 ERISWELL FILLER ALLOYS

Possible areas that may have formed a joined surface were identified visually (and if necessary, microscopically). These areas were then subject to HHPXRF analysis. Any areas representing a potential join were assigned a separate area letter to prevent the analysis being amalgamated with analysis of areas of the base alloy. The results were then compared with the base alloy to examine the differences in the results. This process excludes the identification of any organic bonding agents (i.e. glues). This would have required an alternate technique such as FTIR. However, all potential joins appeared to show the presence of filler alloys and so this was a moot issue.

In total sixty-three possible areas of solder were visually identified and confirmed by HHPXRF analysis. The focus of this study is on the broad chemical and statistical categorisation of the non-ferrous alloys used in the Eriswell grave assemblages, particularly the copper alloys. It should be noted that the beam spot size on the HHPXRF is significantly larger than the areas of solder. Consequently there is a significant contribution from the base alloy in the net peak area results. This prevents any statistical analysis and evaluation of the qualitative results.

A table of all the filler alloys analysed and the associated categorical variables for the objects they are attached to can be found in Appendix IX. The associated net peak area data can be found in Appendix X. Included in the appendices is a column identifying the type of material the filler alloy was attached to (i.e. silver or copper alloy).

The majority of the filler alloys identified were associated with dress accessories (see Table 7-1). Most of the filler alloys were also associated with composite objects (i.e. soldering silver sheets to the front of a brooch or securing the parts of a bucket pendant). There were, however, a few that were clearly linked with repairs to broken objects. This includes 104-1704 (see Figure 7-1), a great square-headed brooch whose footplate was broken off in antiquity and repaired by

means of a strip of metal joined on the underside of the footplate (for the solder see 104-1704-B).

Site	Dress Accessories	Equestrian objects	Military & weaponry	Misc. Fittings	Unknown	Total
046	17					17
104	29	6	1	6	1	43
114	3					3
Total	49	6	1	6	1	63

Table 7-1: Areas of filler alloy associated with joining (i.e. soldering / brazing) by site and object category.

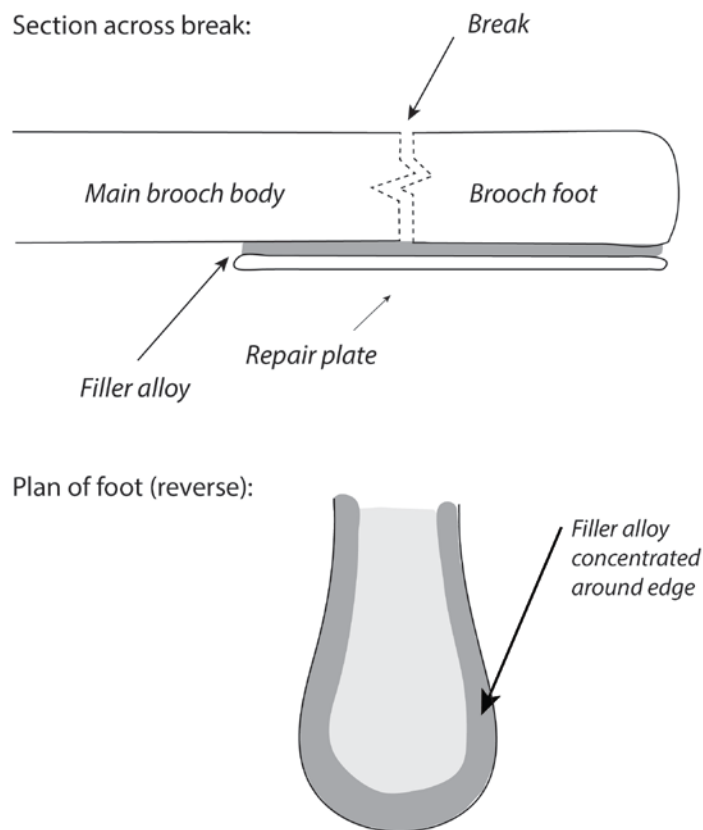


Figure 7-1: A schematic sketch cross section and plan illustrating how the break in great square head brooch 104-1704 was repaired with the use of a filler alloy and copper alloy plate. Not to scale.

7.2.2 FILLER ALLOYS: NET PEAK AREA RESULTS

The areas of analysis that identified the presence of filler alloys were removed from the main body of the relevant analyses (for the silver objects excluding filler alloys see chapters 4 and 5, for copper alloys see chapter 8 and 9).

The areas of filler alloy all contained elevated levels of lead and / or tin (as stated above the associated net peak area data can be found in Appendix X). These are briefly discussed in the context of the alloy type they are attached to (silver and copper alloy). It should be remembered here that the filler alloys are not uniformly distributed and so the analysis includes some of the substrate (i.e. the silver or copper alloy).

Site	SF No.	Analysis Area	Grave No.	Category	Sub Class
046	1487	B	005	Dress Accessories	Pendant
046	1488	B	005	Dress Accessories	Pendant
104	1061	D	No Grave	Dress Accessories	Strap-end
104	1176	E	245	Military and weaponry	Shield Mount
104	1191	E	245	Military and weaponry	Shield Mount
104	2317	D	315	Dress Accessories	Ear Ring
104	2317	I	315	Dress Accessories	Ear Ring

Table 7-2: Areas of filler alloy on silver objects. See Appendix X for full net peak area data (including coefficient of variation where applicable).

The areas of solder on the silver alloys all contained elevated levels of lead and tin. Plotting the results in a silver-tin-lead ternary diagram with base alloys from the same objects illustrates this. As can be seen (Figure 7-2, net peak area data in Table 7-2) the base alloys cluster close to the silver apex, whereas filler alloys are distributed along the lead axis whilst also showing a propensity to contain more tin than the base alloys.

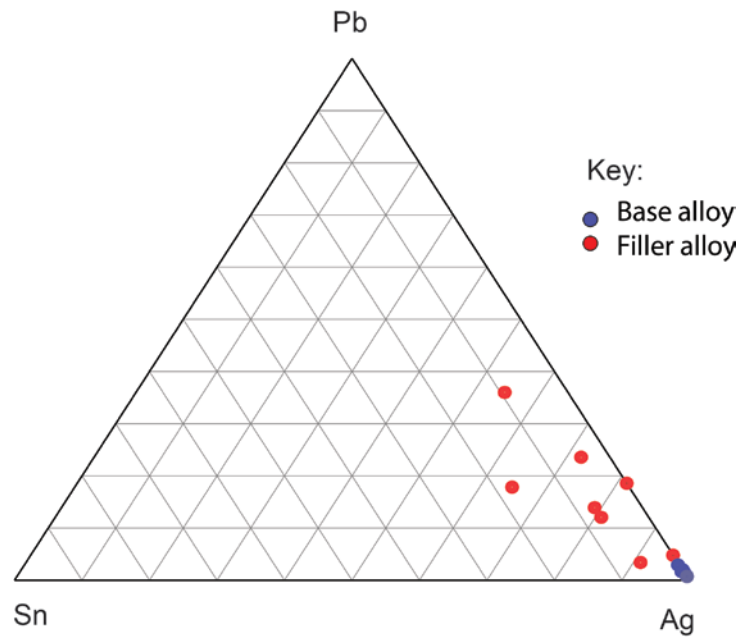


Figure 7-2: Ternary diagram showing solders and non-solder areas on silver objects. See Table 7-3 for net peak area data.

Site	SF No.	Analysis Area	Solder?	Cu	Pb	Sn	Ag	Au	Zn
046	1487	A	Non-solder	85228	101195	766	2009713	48886	2780
046	1487	B	Solder	108987	406340		1780585	30611	9679
046	1488	A	Non-solder	89680	30901	780	1864716	47996	1678
046	1488	B	Solder	108165	500751	90436	1532594	21997	13235
104	1061	C	Non-solder	109141	16764		812357	24333	6986
104	1061	D	Solder	239000	308136	80184	467537	3343	4856
104	1176	D	Non-solder	92704	15883		1792072	39047	4003
104	1176	E	Solder	214683	274921	267399	998273	7286	224550
104	1191	D	Non-solder	40039	10430		1191949	16506	1040
104	1191	E	Solder	140139	277202	141148	1574192	9389	12491
104	2317	D	Solder	933867	41057	66831	1099188	18851	22817
104	2317	E	Non-solder	933867	41057	3304	1357728	28324	44982
104	2317	H	Non-solder	202513	25530	5071	1471889	66449	9959
104	2317	I	Solder	439094	185326	108124	1242587	27016	9757

Table 7-3: Net peak areas for solders and non-solders. The full solder data (including the coefficients of variation) are in Appendix X, non-solder silver data are available in Appendix IV.

The analysis of the filler alloys on copper alloys shows a similar result with elevated levels of lead and tin (see Appendix X) compared to the non-soldered areas. A total of sixty-one areas of probable filler metal were analysed (see Appendix IX for a list of the objects and their categorical variables). The full set of net peak area data (including coefficient of variation where more than one reading was possible) are available in Appendix X.

Plotting the results in lead-tin-copper ternary diagram (Figure 7-3) against areas on the base alloys on the same objects (see Appendix XI for copper alloy filler alloys with base alloy results from the same objects) helps illustrate this. Whilst the results are not as tightly grouped as the silver version (due to the greater variance in the copper alloy compositions, see the next chapter for details) there is a separation with filler alloys extending along the lead axis.

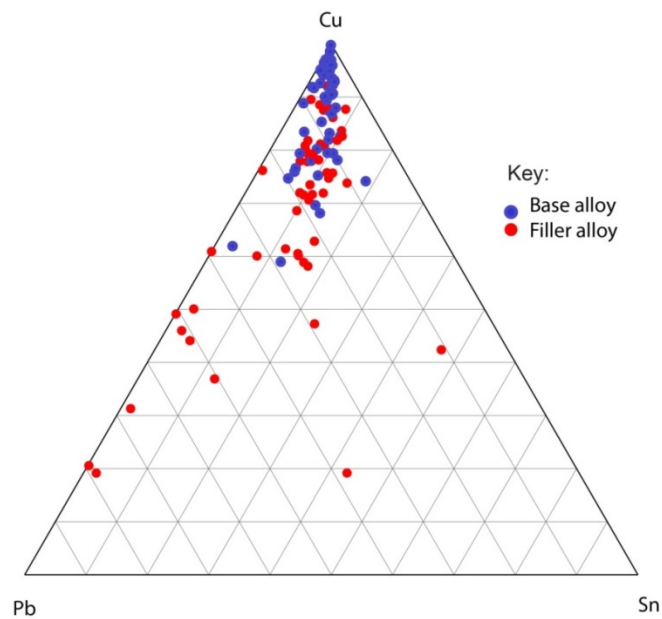


Figure 7-3: Ternary diagram showing solders and non-solder areas on copper alloy objects. The net peak area data can be found in Appendix XI.

The filler alloys appear to be richer in lead and tin than the surrounding base alloys, although sometimes they are only slightly richer than the quaternary leaded alloys they are joined to, despite being easily visible to the naked eye.

Similarities between the base alloy and the filler alloy are not uncommon (and have been noted on silver objects, see Lang and Hughes 1984, 86), but caution should be exercised here because of the beam size.

The results appear to suggest the use of lead – tin filler alloys. These are soft solders (i.e. for a joining process at below 450°C) as the phase diagram below (Figure 7-4) illustrates (the liquidus line at all points being significantly below the melting points for copper alloys).

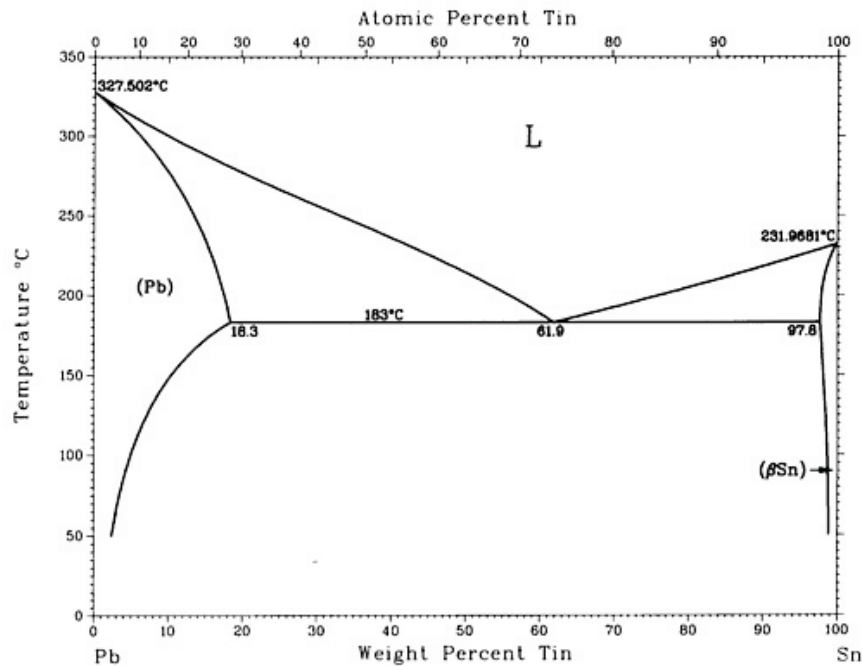


Figure 7-4: Lead-tin phase diagram from ASM International (1992, 1300) after Karakaya and Thompson (1988).

As stated earlier the large beam size used here means that it is not possible to assess the filler alloys in more detail. Consequently it is not possible to determine if any of the alloys were in the range of a eutectic composition (63 % tin, 37 % lead) which would have had the lowest melting point (183 °C) or a different composition which would have imparted different qualities (such as a slower solidifying time) that may have been sought by the smith.

There are some results that differ slightly from the norm and may suggest the use of different alloys for filler types. They must, however, be treated with caution.

The filler alloys associated with 104-2317 appear to be of particular interest. The object is a 20mm diameter copper alloy wire ear ring (104-2317-A) with two pierced copper alloy sheet discs (104-2317-B and 104-2317-G). These two discs had silver sheets (104-2317-D and 104-2317-H) fixed to them using a filler alloy (filler alloy analysis on the copper alloy sheets 104-2317-C and 104-2317-F; filler alloy analysis on the silver sheets 104-2317-E and 104-2317-I). The results (see Table 7-4 for net peak area data for all areas) show the presence of gold and silver in the filler alloys on the copper alloy sheet discs (104-2317-C and 104-2317-F). It may be tempting to interpret this as the use of different filler alloy, such as a gold-silver-copper based 'hard' filler alloy (see Roberts 1973 for an overview) used for brazing (see Figure 7-5 for a phase diagram for gold-silver-copper alloys).

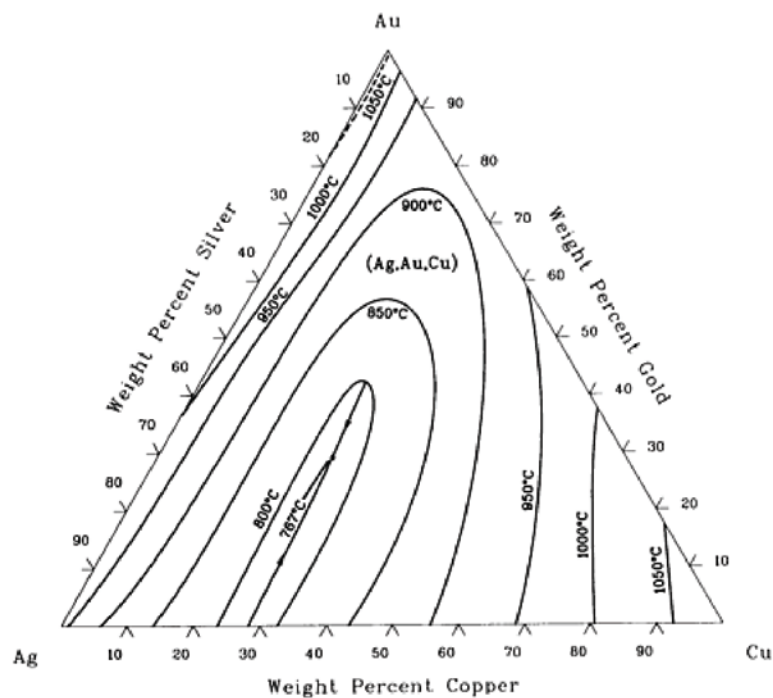


Figure 7-5: Silver-gold-copper phase diagram. From ASM International (1992, 1494) after Prince, Raynor, and Evans (1990, 65)

There is a problem with this though. These copper alloy discs were, as previously stated, attached to silver sheet discs. The silver alloys often contain — aside from the obvious silver — gold (see the discussion in Chapter 5, page 244 onwards). The silver sheet discs from 104-2317 contain gold. It is therefore not secure to interpret the filler alloys on the 104-2317 copper sheet discs based on their gold and silver contents as there can be no certainty that these are not contributed by particles of alloy from the silver discs.

<i>Site</i>	<i>SF Number</i>	<i>Anal. Area</i>	<i>XRF Location</i>	<i>Cu (K)</i>	<i>Pb (L)</i>	<i>Sn (K)</i>	<i>Ag (K)</i>	<i>As (K)</i>	<i>Sb (K)</i>	<i>Au (L)</i>	<i>Zn (K)</i>	<i>Hg (L)</i>
104	2317	A	Wire	918676	105879	96011	6763	3884	577	93	49424	
104	2317	B	Sheet disc A	4758745	44528	23405	7223		929			
104	2317	C	Sheet disc A (filler alloy side)	3012415	141848	114984	20304			1998		184
104	2317	D	Silver sheet assoc. with Cu disc A	580630	146103	66831	1099188	1		18851		22817
104	2317	E	Silver sheet assoc. with Cu disc A (filler alloy side)	933867	41057	3304	1357728	5495		28324		44982
104	2317	F	Sheet disc B (filler alloy side)	2923502	113834	133015	32298			2234		216
104	2317	G	Sheet disc B	5478340	9341	1624	6311					
104	2317	H	Silver sheet associated with Cu disc B	202513	25530	5071	1471889			66449		9959
104	2317	I	Silver sheet associated with Cu disc B (filler alloy side)	439094	185326	108124	1242587	1		27016		9757

Table 7-4: Net peak area data for necklace and pendants 104-2317. For data with the coefficient of variant (where applicable) see Appendix X and Appendix XI.

A similar degree of caution must be applied when looking at the silver alloys. Some of the filler alloys analysed here, such as 104-1176-E and 104-1191-E detected elevated tin and / or silver. Previous work of filler metals on Roman silver objects (Lang and Hughes 1984) identified the use of an assortment of alloys. These contained (in varying combinations and quantities) lead, silver, tin and copper. This bears some relation to Pliny the Elder's *stagnum* (see Forbes 1964, p.259; Humphrey et al. 2003, pp.213–214), some combinations of which were hard solders (i.e. for brazing, see Figure 7-6 and Figure 7-7 for phase diagrams of silver alloys used as filler alloys).

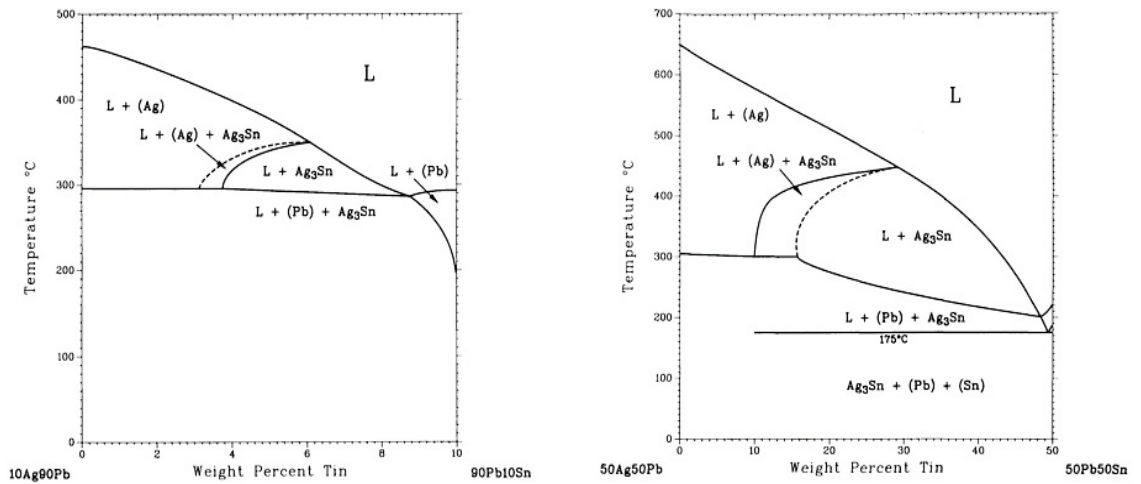


Figure 7-6; Ag-Pb-Sn phase diagram from ASM International (1992, 1503) after Petzow and Effenberg (1988).

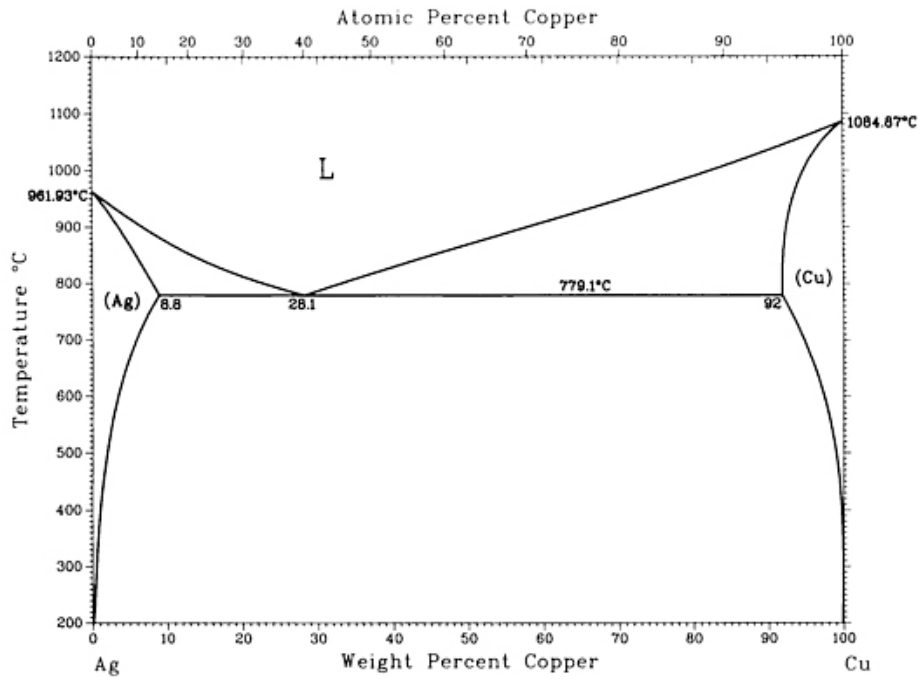


Figure 7-7: Silver – copper phase diagram. From Subramanian and Perepezko (1993, 63, Fig. 1)

It may be tempting to see the use of distinct filler alloys in the two silver examples mentioned in the previous paragraph. Again, however, it cannot be ascertained securely that these results are genuinely representative of the filler alloy composition (i.e. these peaks may have been contributed by the non-ferrous copper alloy object they were joined to).

7.3 LEAD RICH ALLOYS

Only seven objects had results that suggested such a high lead presence that they were better categorised as lead alloys rather than any other type (see Table 7-5 below for categorical variables.. These were all from cemeteries 104 and 114 with none from 046.

Site	SF No.	SF Sub Div.	Anal. Area	Grave No.	Manufacture method	Category	Class	Sub Class
104	1034		A		Cast	Coins, Tokens and Jettons	Token	Undefined Token
104	1166		A	110	Cast	Miscellaneous Fittings	Nails and Bolts	Stud
104	1705		B	322	Cast	Dress Accessories	Brooch	Annular
104	2905		A	348	Cast	Dress Accessories	Necklace	Pendant
114	1037		A	432	Cast	Military and weaponry	Shield	Misc. Shield Fragment
114	1039		A	432	Cast	Military and weaponry	Shield	Misc. Shield Fragment
114	1044		A	432	Cast	Military and weaponry	Shield	Misc. Shield Fragment
114	1323		A	445	Sheet	Dress Accessories	Bead	Undefined Bead
114	1331		A	445	Sheet	Dress Accessories	Bead	Undefined Bead
114	1336		A	445	Sheet	Dress Accessories	Bead	Undefined Bead
114	1499		A	415	Sheet	Unknown	Unknown	Unknown
114	1500		A	415	Sheet	Unknown	Unknown	Unknown

Table 7-5: 'Lead' objects. A full table of the categorical variables can be found in Appendix XII. See Table 7-6 for the net peak area data.

Site	SF Number	SF Sub Div.	Anal. Area	Cu (K)	Pb (L)	Sn (K)	Ag (K)	As (K)	Ni (K)	Sb (K)	Zn (K)	No. of anal.
104	1034		A	10090	1579360	2060					616	4
104	1166		A	518446	208729	136578	6436	15302	1253	1229	99004	2
104	1705		B	310702	260593	55780	2326		672		161113	2
104	2905		A	9449	1312570	7952					936	3
114	1037		A	175603	1468306	282505	4519				5030	2
114	1039		A	1402635	423357	174340	6953				35193	2
114	1044		A	836619	742153	241110	6109				28852	2
114	1323		A	10828	786246	37681					2666	2
114	1331		A	4793	786246	60845					1499	2
114	1336		A	4084	1038359	145933					3615	2
114	1499		A	3635	1665029	12705						4
114	1500		A	4126	1740073	18745						4

Table 7-6: Mean net peak area data for the 'lead' objects. A full version of the data, including coefficients of variation, is available in Appendix XIII. See Table 7-5 for related categorical variables.

The combination of a small data set and the methodological approach used in this study means that there is little that can be drawn from the results (see Table 7-6 for a summary of the mean net peak area data and Appendix XIII for the full data including the coefficient of variation). Consequently interpretation will be limited to a brief discussion of each object.

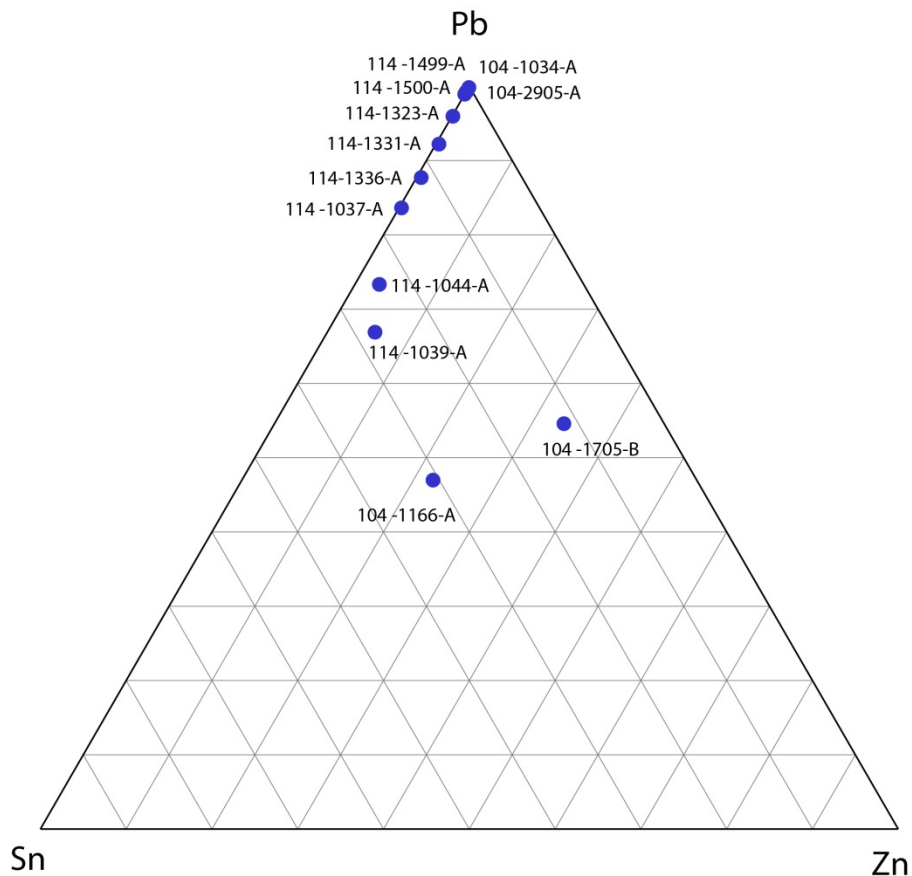


Figure 7-8: Ternary diagrams of 'lead' alloy NPA. See Table 7-6 for the NPA data.

7.3.1 LEAD AND TIN RICH ALLOYS: OBJECT OVERVIEW

Of the nine objects four are nearly pure lead. The remainder are tin and lead rich alloys that also contain copper and zinc. Of the four nearly pure objects only one is definitely of an early mediaeval date and associated with the cemeteries. The other three objects are intrusive.

7.3.1.1 OBJECT 104-1034-A

104-1034 is a possible token. Semi-circular in shape with a diameter of 23 mm it has a double cross on both sides and letters in the quadrants; on one face the letter 'N' on the other half the letter 'G'.

The token was not found in a grave context nor in a stratified context, but during metal detecting of the spoil heap. It is not early medieval and likely dates from the high medieval (i.e. post-Conquest) and analysis bears this out. With very little tin, zinc or copper present (see the ternary diagram in Figure 7-8) it is nearly pure lead. Previous analysis of tokens has indicated that near pure lead tokens are introduced from the beginning of the fourteenth century CE (Mitchiner and Skinner 1983, 41) and continue in use throughout the Plantagenet period (Mitchiner and Skinner 1984).

7.3.1.2 OBJECT 104-1166-A

With the lowest lead content of any of this group (see the ternary diagram in Figure 7-8) this 9 mm long cast rivet from grave 110 in ERL 104 is something of an enigma. There were no traces of filler alloy visible (either visually or microscopically) anywhere on the object.

A highly leaded alloy is not the most obvious choice for an object whose job is to assist in joining other materials. It is unknown if this was for aesthetic (i.e. the colour of the alloy) reasons, or simple expediency (i.e. that was the raw material available at the time to make the alloy in a recycling metallurgical economy).

7.3.1.3 OBJECT 104-1705-B

An annular brooch decorated with punched rings around the inner edge and a diameter of 49 mm with a pin attached. From grave 322 in ERL 104.

This analysis is from the pin (see 104-1705-A for the main brooch body analysis). Both are heavily leaded, high zinc alloys. The pin contains appears to contain significantly more lead though, perhaps suggesting it was produced at a different point in time from the brooch.

7.3.1.4 OBJECT 104-2905-A

A flat disc fragment (23 mm long and 22 mm wide) pierced in two places to form a pendant. The object was found in grave 348 in ERL 104. The burial had a number of other non-ferrous artefacts associated with it, but no other lead objects.

Although the analysis detected traces of copper, tin and zinc the object is otherwise almost pure lead (see Figure 7-8).

7.3.1.5 OBJECTS 114-1037-A, 114-1039-A AND 114-1044-A

Three disc-headed studs with short pins and sheet roves from grave 432 in ERL 114. The analyses are on the front of the heads. The pins (114-1037-B, 114-1039-B, and 114-1144-B) appeared to be made out of leaded quaternary copper alloys. In contrast the fronts had significantly higher levels of lead and tin present.

On the front of each copper alloy disc traces of a heavily abraded white metal remained (see Figure 7-9 for a sketch of 104-1039 illustrating this). These white metal deposits appeared to have fairly similar compositions (although differences in the amounts remaining make direct comparison difficult due to the beam size). The purpose of this is uncertain. There were no silver discs or any other fragments of metal that may have been joined onto the front in the assemblage (although these could have easily been missed in the excavation process). Consequently it is not clear whether this was a filler alloy or a form of decoration in itself.

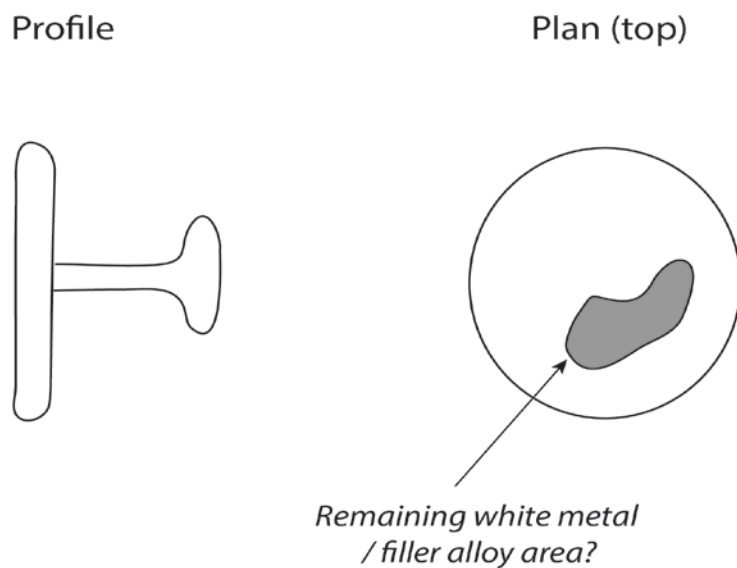


Figure 7-9: Sketch profile and plan of 114-1039. Studs 114-1037 and 114-1044 share the same form. Not to scale.

7.3.1.6 OBJECTS 114-1323-A, 114-1331-A AND 114-1336-A

Three lead alloy beads from grave 445 in ERL 114. One is a disc-headed stud with short pin and rove (114-1323-A) whilst the other two are wound sheets (114-1331-A and 114-1336-A). The beads were not found associated with a necklace or similar; the only other objects in the grave were a silver finger ring (114-1299-C) a copper alloy cruciform brooch (114-1298-A, 114-1298-C) with some filler alloy on (114-1298-B, see earlier in this chapter for details) and two copper alloy annular brooches (114-1296-A and 114-1297-A).

All three objects have relatively high lead content along with some tin. Although zinc was detected it appears to be minimal.

7.3.1.7 OBJECTS 114-1499-A AND 114-1500-A

Associated lead sheet strips from grave 415 in ERL 114. Analysis showed them both to be nearly pure lead. The grave was significantly truncated by modern services and construction related activity. The grave fill was disturbed and there is a strong chance that these two sheets are intrusive and from a later (unknown) period.

7.4 CONCLUSION

The majority of the evidence for the use of lead and lead-tin rich alloys at Eriswell in the early medieval comes from filler alloys. Lead objects themselves are extremely rare, with only one definitively lead object (104-2905-A) from the early-medieval period being found. The remainder of the objects are either highly leaded alloys or intrusive objects from later periods.

Post-Roman and early medieval filler alloys have received relatively little attention. Where they have been in receipt of detailed analysis and discussion it has been from later period sites, such as the Lindsey smith burial (Hinton 2000) or the workshops excavated in York (Bayley 1991; Bayley 1992). In the former rods of tin-lead filler alloys were found, ready to be applied in joining operations. Obviously both the previous references refer to production related contexts. At Eriswell we do not have the remains of any workshop space, nor the remains of a metalworker conveniently buried with their equipment. This means that many questions relating to the use of filler alloys must remain unanswered. We cannot know how the alloys were applied; with a rod to be rubbed on a heated surface as in the previous example or powdered as the Romans apparently often did (Lang and Hughes 1984, 92)? The interpretation is also hampered by the methodological approach used here, with the HHPXRF beam being too large to accurately focus on filler alloys and avoid any analysis of the base alloys.

It is therefore difficult to place the procurement of the raw materials in a conceptual framework of early-medieval alloy use. Were filler alloys sourced from recycled materials? What degree of control was exercised over filler alloy composition? These are important questions, ones that could help to significantly develop our understanding of the non-ferrous metal economy of the early medieval.

Unfortunately these are questions that we do not have the answers to, and the data here is not of high enough quality to significantly illuminate these points in detail. It is clear that early-medieval filler alloys require significantly more research and that this should be part of a wider study that examines how joining

technologies and associated material changed chronologically from the Roman to high medieval times, allowing the early medieval to be placed into greater context.

CHAPTER 8: COPPER ALLOYS

“If you were to say that poetry is more enduring, I would reply that the works of a coppersmith are even more enduring still...”

(da Vinci 2001, 24)

8.1 INTRODUCTION

This chapter presents the results of the HHPXRF analysis on the copper alloys. It includes an archaeological interpretation of the principal component and hierarchical clustering results, presented after a simpler consideration of objects that have analytically been determined to be copper alloy in the context of their categorical variables.

The data set presented here is large and comprises nearly the entirety of the copper alloy assemblage from the three Eriswell cemeteries (855 objects representing 610 small find numbers). Such a large data set proffers many possibilities for interpretation and analysis. Equally there is a risk in getting lost in the data and especially — given the method of analysis — of insecurely over-interpreting.

The focus here is on undertaking an assessment that seeks to understand the distribution of the alloys in relation to the major alloying components (tin, zinc and lead). Specifically there is a focus on understanding:

- Which elements explain the variance in the Eriswell copper alloys.
- Understanding how these elements affect distribution and interpretation thereof.
- To determine and delimitate the presence of groups representative of specific compositions.
- Assess how groups (if found) relate to any categorical variables, specifically: is there any indication that specific alloy types may have been used for specific purposes?

- Begin to understand what this tells us about the use of copper-alloys in the Early Anglo-Saxon period.

The nature of the data requires the use of a rigorous and adaptive methodology. Commonly used techniques — such as histograms of the frequency of element weight percentages — are not appropriate here. Following the process used in the data processing methodology (Chapter 4, page 181) Principal Component Analysis (PCA) will be used to understand the variance in the data (page 362) with Hierarchical Clustering (HC) undertaken on the PCA (page 371) to assess the presence of groups.

8.2 HOW ‘OBJECTS’ ARE DEFINED

For details on how the objects are categorised, numbered and counted please see page 45 in Chapter 1.

8.3 CORROSION

As previously mentioned the results presented here are from analyses on the surface of the objects in their as conserved state (i.e. no further cleaning was undertaken). Consequently there will be a significant margin of error from the ‘true’ compositions. This is discussed in depth (along with penetration depths) in the HHpXRF methodology (Chapter 3, page 162) and the data processing methodology (Chapter 4, page 181). These two chapters demonstrated that, despite the uncertainty introduced by the corrosion, the HHpXRF was capable of producing numerical data that could be analysed to discover broad trends in alloy usage.

As a further exploration of the impact of corrosion on a ‘real world’ scenario two objects with differing levels of corrosion were examined (suspension strip 104-2626 from grave 323 and belt suspension ring 104-2760 from grave 358).⁷⁷ Both these objects had relatively corrosion free areas and heavily corroded areas; normally the corroded areas would have been avoided for analysis, but instead

⁷⁷ Provided for those who may have skipped the methodology chapters!

both were analysed and kept separate (i.e. not amalgamated) to examine the impact of the corrosion on the results. The results (shown graphically in Figure 8-1) showed that corrosion does, as previously discussed, impact the results.

Where there was an area with shiny relatively patina free alloy available and an area with patina then the results agree (104-2626-D and 104-2626-E).

There can be a significant difference when comparing objects with pulvrescent corrosion (104-2626-B) or a deformed and destroyed surface (104-2760-A) and areas with little corrosion beyond a patina (104-2760-B, 104-2626-D and 104-2626-E). Consequently direct comparison between individual objects must be undertaken carefully. Broader comparisons can still be made however (again, as noted earlier). In the ternary diagram below it should be noticed that whilst there is significant variation between the two readings for 104-2760 in tin and lead both are still relatively lead free. Likewise the readings for 104-2626 show variation in tin and zinc, but the alloys are still mixed. The data processing and interpretation methodology applied here allows for such variations as it is focussed on a broad understanding of what is contributing the variation to the alloys as part of the whole assemblage. It is not focussed on matching individual objects (although this will be looked at as a broadly qualitative concern).

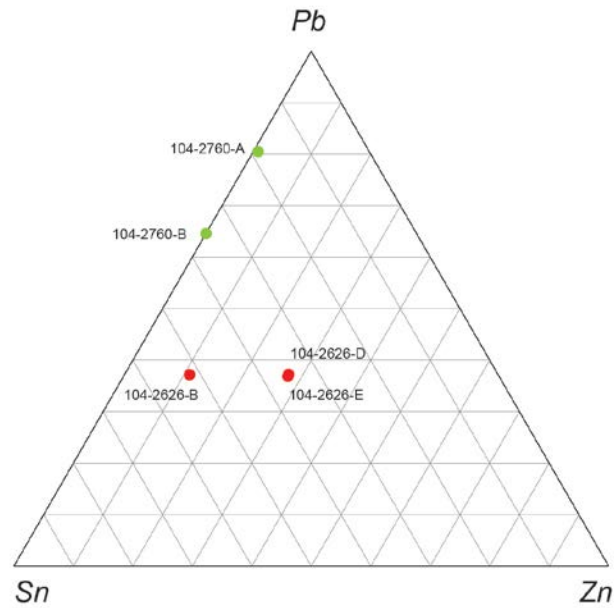


Figure 8-1: Example of the impact of corrosion on two objects that had areas of uncorroded and significantly corroded alloy available for analysis.

Of the readings mentioned in this subsection only those on the uncorroded areas will be taken forward for consideration.

8.4 EXCLUDED OBJECTS

Not all of the objects analysed are fully presented here. Table 8-1 provides a list of the eight objects which were not analysed and the reason why.

These objects are included in the introductory discussion of categorical variables, but will not be considered in any further detail beyond that point.

Further objects are excluded after outlier analysis. See page 336 for more details.

<i>Site</i>	<i>SF no.</i>	<i>SF sub div.</i>	<i>Grave no.</i>	<i>Category</i>	<i>Class</i>	<i>Sub Class</i>	<i>Reason not included</i>
046	1094		042	Dress Accessories	Brooch	Annular	Submitted for neutron diffraction analysis. To be published separately.
046	1367			Dress Accessories	Belt Fitting	Belt Ring	Submitted for neutron diffraction analysis. To be published separately.
046	1108		038	Dress Accessories	Belt Fitting	Girdle-hanger	Large amount of Fe corrosion prevents analysis.
104	2315		315	Dress Accessories	Bead	Undefined Bead	Spectra lost due to backup error.
104	2621		323	Equestrian objects	Tack	Bridle mount	Not analysed due to very delicate preserved fibres.
104	2901		348	Dress Accessories	Brooch	Annular	Spectra lost due to backup error.
104	3315		231	Dress Accessories	Buckle	Undefined Buckle	Spectra lost due to backup error.
104	3371		336	Dress Accessories	Brooch	Annular	Spectra lost due to backup error.
104	3574	2	168	Military and weaponry	Shield	Shield Mount	Large amount of Fe corrosion prevents analysis.
114	1321		459	Dress Accessories	Belt Fitting	Belt ring	Large amount of Fe corrosion prevents analysis.

Table 8-1: Copper alloy objects excluded from statistical interpretation in this chapter.

8.5 CATEGORICAL VARIABLES

8.5.1 DISTRIBUTION ACROSS CEMETERIES

Preliminary sorting of the data revealed there to be 808 copper alloy objects in the Eriswell assemblages; 148 from ERL 046, 503 from ERL 104 and 157 from ERL 114 (see Table 8-2). The majority of these objects were recovered from 142 inhumations in the three cemeteries. There are some objects included here whose context is insecure and consequently they are excluded from statistical analysis later on (see page 336). This includes a small number of Romano-British objects that may well have come from truncated burials (such as the coins in ERL 114). The volume of copper alloy objects identified is significantly higher than the number of silver, gold or lead objects; however this should not be confused with them being common. Copper alloys were only present in 34% of the inhumations across all the cemeteries.

Site	Total
ERL 046	148
ERL 104	503
ERL 114	157
Total	808

Table 8-2: Number of copper alloy objects by site.

Strikingly the percentage of inhumations that contained copper alloy grave goods is remarkable similar in cemeteries ERL 046 and 104 (See Table 8-3). In contrast ERL 114 has approximately 16% fewer graves containing copper alloy objects. This is in line with the results presented previously for the silver and gilt objects and confirms the feeling that ERL 114 is ‘poorer’ in non-ferrous grave goods than the other two cemeteries.

	ERL 046	ERL 104	ERL 114
No. of inhumations that contain Cu alloy objects	22	99	21
No. of inhumations that do not contain Cu alloy objects	37	162	77
% of inhumations that contain Cu alloy objects	37	38	21

Table 8-3: Number of inhumations that contain copper alloy objects in cemeteries ERL 046, 104 and 114.

8.5.2 OBJECTS BY TYPOLOGY

Examining the object categories reveals that the majority of copper alloy objects are dress accessories (589 objects in total representing 73% of the assemblage). The largest single grouping within this is brooches (213 objects), representing 26% of all copper alloy objects at Eriswell (see Table 8-4).

The majority of these brooches are annular (114 objects) and cruciform (46 objects). These brooch classes are also the only two that are represented in all three cemeteries (Table 8-6). Other large groups within the dress accessories category are wrist clasps (13.1% of all copper alloy objects) and beads (mainly bucket pendants, 12% of all copper alloy objects). Outside of dress accessories one of the largest categories are objects related to equestrian gear (5.2% of copper alloy objects). Nearly all of these come from the horse and warrior burial in ERL 104 (grave number 323).

Category	Class	Site			Total
		ERL 046	ERL 104	ERL 114	
Coins, Tokens and Jettons	Coin			2	2
	Coins, Tokens and Jettons Total			2	2
Dress Accessories	Bead	32	29	35	96
	<i>Belt Fitting</i>	12	41	17	70
	Brooch	43	129	41	213
	<i>Buckle</i>	1	43	2	46
	Miscellaneous		1		1
	<i>Necklace</i>	6	8	15	29
	Pin	1	5		6
	<i>Ring</i>	5	15	2	22
	Wrist Clasp	32	42	32	106
	Dress Accessories Total	132	313	144	589
Equestrian objects	Tack	3	39		42
	Equestrian objects Total	3	39		42
Household objects	Bucket	7			7
	Household objects Total	7			7
Military and weaponry	Shield		8	5	13
	<i>Spear</i>		1		1
	Military and weaponry Total		9	5	14
Miscellaneous Fittings	<i>Belt Fitting</i>		3		3
	Buckle		2		2
	<i>Fragment</i>	2	7		9
	Miscellaneous		55	3	58
	<i>Nails and Bolts</i>		12		12
	Miscellaneous Fittings Total	2	79	3	84
Personal equipment	<i>Implement</i>			1	1
	Purse		7		7
	Personal equipment Total		7	1	8
Toilet and surgical objects	Cosmetic Implements	1	11		12
	Toilet and surgical objects Total	1	11		12
Unknown	Unknown	3	44	2	49
	Unknown Total	3	44	2	49

Table 8-4: The number of copper alloy objects analysed by site, object category and object class.

It should be noted that there is a large amount of utilitarian ('miscellaneous') metalwork analysed here (84 objects, 10.39% of the assemblage), including a number of nails and bolts. At this juncture it should be remembered that the number of objects used here refers to the different fabricated parts that make up a composite object (as discussed on page 309). Consequently there are not seven

buckets listed in Table 8-5 but seven different parts to one bucket (small find 1306 from grave 031 in ERL 046).

Brooch sub class	Site			Total
	ERL 046	ERL 104	ERL 114	
Annular	26	67	21	114
Applied disc		4	7	11
Bar		1		1
Colchester	3			3
Cruciform	2	38	6	46
Fish	4			4
Great square-headed	1	3		4
Penannular	3	2		5
Radiate-head		1		1
Roman	3			3
Small-Long		2	7	9
Square /cross		2		2
Undefined Brooch	1	9		10
Total	43	129	41	213

Table 8-6: The number and type of brooches analysed by cemetery. It should be remembered that the number of objects refers to the different fabricated parts that make up a composite object (as discussed on page 309). Consequently the number presented here may differ from how Anglo-Saxon brooch scholar would normally consider or count.

8.5.3 MANUFACTURE METHOD

One of the key questions identified in Chapter 2 (page 80) was to determine if there was any difference between cast and sheet object compositions. Before considering the chemistry in detail this brief overview places the documentation of manufacture methods into context within the categorical variables.

In Table 8-7 below an overview of the broad manufacturing methods is presented, showing the number of objects by site and method. The table illustrates that cast and sheet metalwork account for the majority of the assemblage (48.14% and 43.44% respectively).

Site	Cast	Melted	Unknown	Sheet	Struck	Wire
ERL 046	73			67		8
ERL 104	232	30	7	223		10
ERL 114	84	1		61	2	9
Total	389	31	7	351	2	27

Table 8-7: Number of copper alloy objects by manufacture method.

If these figures are graphed as a percentage across each site (Figure 8-2) we can see that there is some differentiation in how different forms were used. Sheet and cast metal are the most frequent manufacturing methods in all cemeteries; however, in ERL 114 there is a slightly higher use of cast metal. ERL 046 and 114 also have a slightly higher percentage of wire objects present and ERL 104 has more melted drops (representing the presence of cremations in the cemetery).

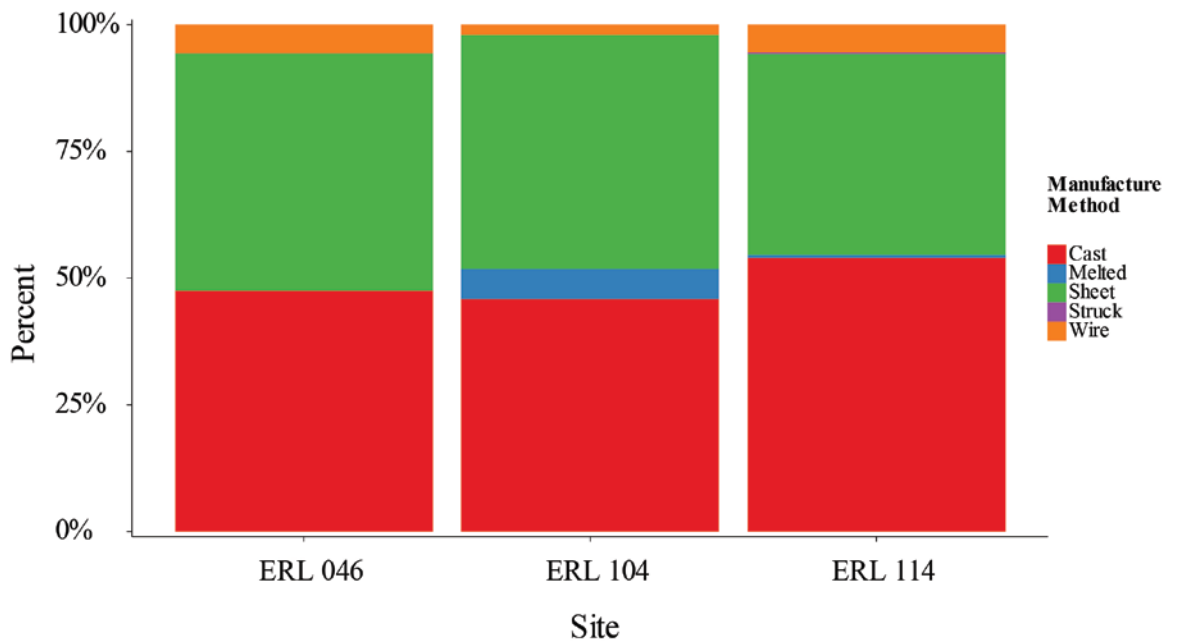


Figure 8-2: Bar chart of manufacture by site.

Table 8-8 below shows the number objects by site and by object category. Here it can be seen that the large number of sheet objects in ERL 104 is the result of an increased usage of sheet metal for miscellaneous fittings than when compared to ERL 046 and 114. A summary of these objects are provided in Table 8-9 below.

Site	Category	Cast	Melted	N/A	Sheet	Struck	Wire
ERL 046	Dress Accessories	73			51		8
	Equestrian objects				3		
	Household objects				7		
	Miscellaneous Fittings				2		
	Toilet and surgical objects				1		
	Unknown				3		
ERL 046 Total		73			67		8
ERL 104	Dress Accessories	172	15	5	115		6
	Equestrian objects	31		1	7		
	Military and weaponry	6		1	2		
	Miscellaneous Fittings	11			65		3
	Personal equipment	5			2		
	Toilet and surgical objects	3			7		1
	Unknown	4	15		25		
ERL 104 Total		232	30	7	223		10
ERL 114	Coins, Tokens and Jettons					2	
	Dress Accessories	78			57		9
	Military and weaponry	5					
	Miscellaneous Fittings				3		
	Personal equipment	1					
	Unknown		1		1		
ERL 114 Total		84	1		61	2	9
Total		389	31	7	351	2	27

Table 8-8: Showing the number of copper alloy objects by working type and object category.

Class	Sub Class	No. of sheet objects
Belt Fitting	Strap-end	3
	<i>Belt Fitting Total</i>	<i>3</i>
Buckle	Buckle Plate	2
	<i>Buckle Total</i>	<i>2</i>
Fragment	Bracket	1
	Sheet	5
	Strip	1
	<i>Fragment Total</i>	<i>7</i>
Miscellaneous	Binding Ring	1
	Box Fitting	1
	Clip	8
	Rove	1
	Sheet	42
	<i>Miscellaneous Total</i>	<i>53</i>
Nails and Bolts	Rivet	3
	Stud	2
	<i>Nails and Bolts Total</i>	<i>5</i>
Total		70

Table 8-9: Number of sheet objects within the miscellaneous fittings category from ERL 104.

Cast objects account for almost half of the copper alloy assemblage. Examining these for further degrees of working (Table 8-10) we can see that the majority are ‘as cast’ (i.e. they have no further degree of working). Interestingly it is ERL 046 that shows the greatest variation in the application of different further degrees of working (see Figure 8-3).

Site	As cast (%)	Incised (%)	Punched (%)	Wrought (%)	No. of individuals
ERL 046	32	15	27	25	71
ERL 104	230	10	48	44	235
ERL 114	76	8	10	25	85

Table 8-10: A breakdown of cast objects showing further degrees of working.

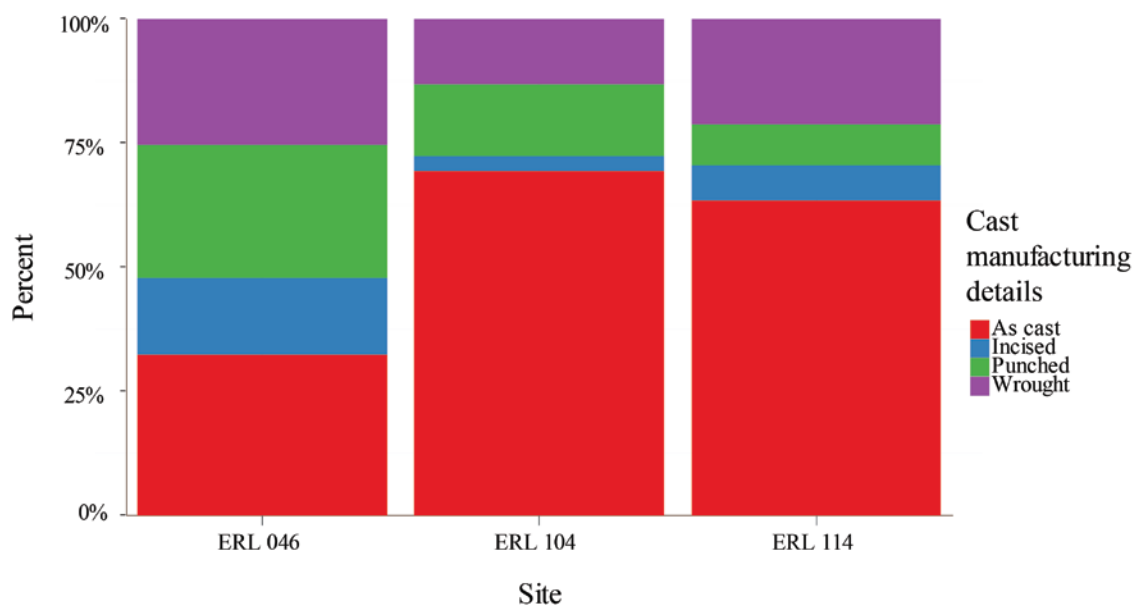


Figure 8-3: Bar chart showing a breakdown of cast objects and further degrees of working.

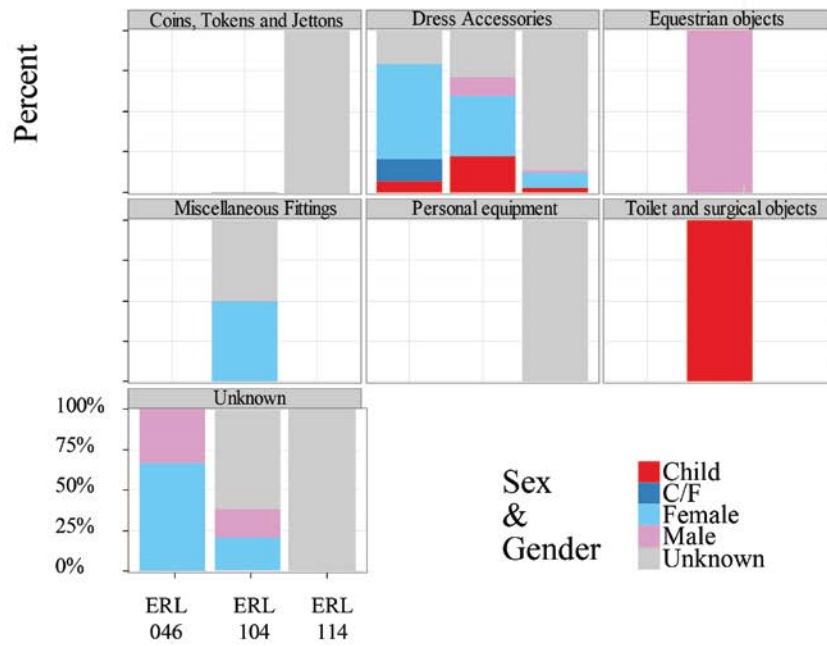
8.5.4 SEX, GENDER AND PHASE

Examining the objects by biological sex shows that the majority of the objects are associated (where it was possible for a sex to be assigned to skeletal remains) with female burials. There are two exceptions to this: equestrian and toilet and surgical objects from ERL 104 (see Figure 8-4 and Table 8-11).

In gender (where a gender has been assigned based on the suite of grave goods) a similar pattern emerges (Figure 8-4 and Table 8-11). In the process of assigning a gender the child category was assigned to male or female based on the suite of grave goods. A gender was also assigned to adult burials based on the grave good assemblage. It should be noted that no biologically sexed female graves became gendered male or vice versa during this process.

As with the silver objects earlier (see page 233) the distributions fall within what one may traditionally expect: weaponry and equestrian objects are associated with gendered males and dress accessories predominantly (but not exclusively with gendered females).

Biological Sex



Assigned Gender

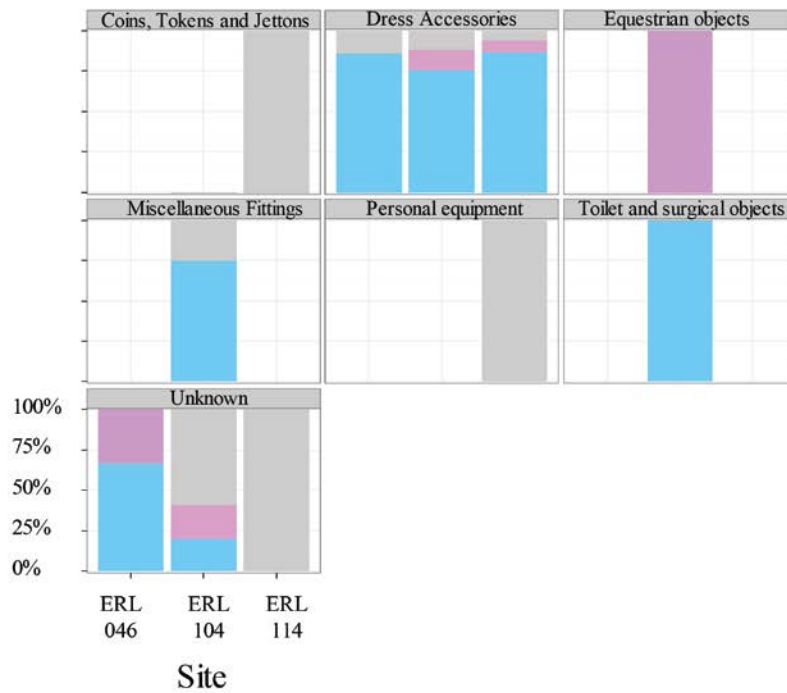


Figure 8-4: Bar charts showing object categories as the row variable, cemetery on the x-axis and sex and gender as the stratum variables. The data for the graphs can be found in Table 8-11.

Site	Category	Ost. Sex					Assigned Gender			
		C	C/F	F	M	N/A	F	M	N/A	Total
ERL 046	Dress Accessories	19	12	79		22	119		13	132
	Equestrian objects		3				3			3
	Household objects				7			7		7
	Miscellaneous Fittings			1		1	1		1	2
	Toilet and surgical objects					1	1			1
	Unknown			2	1		2	1		3
ERL 046 Total		19	15	82	8	24	126	8	14	148
ERL 104	Dress Accessories	42		133	15	123	246	24	43	313
	Equestrian objects				39			39		39
	Military and weaponry					9		9		9
	Miscellaneous Fittings	11		16	14	38	31	27	21	79
	Personal equipment	2				5	2		5	7
	Toilet and surgical objects	3		4		4	11			11
	Unknown			8	4	32	9	9	26	44
ERL 104 Total		58		161	72	212	299	108	96	502
ERL 114	Coins, Tokens and Jettons					2			2	2
	Dress Accessories	18		10	1	115	134	6	4	144
	Military and weaponry					5		5		5
	Miscellaneous Fittings					3	2		1	3
	Personal equipment					1			1	1
	Unknown					2			2	2
ERL 114 Total		18		10	1	128	136	11	10	157
Total		95	15	253	81	364	561	127	120	808

Table 8-11: Number of copper alloy objects by site, object category, biological sex and assigned gender.

As noted in the introduction the majority of the copper alloy objects are dress accessories. In female gendered burials these primarily consist of beads (mainly bucket beads), brooches and wrist clasps (Table 8-13). In male gendered burials the largest object class represented within dress accessories are buckles (Table 8-12).

Class	Sub Class	Site			Total
		ERL 046	ERL 104	ERL 114	
Brooch	Cruciform		1	1	2
	Undefined Brooch		1		1
Buckle	Undefined Buckle		21	1	22
	Buckle				
Pin	Undefined Pin		1		1
Wrist Clasp	Undefined Wrist Clasp			4	4
	Wrist Clasp				

Table 8-12: Copper alloy dress accessories associated with male gendered burials.

Class	Sub Class	Site			
		ERL 046	ERL 104	ERL 114	Total
Bead	Undefined Bead	32	29	32	93
	Undefined Buckle			3	3
Belt Fitting	Belt ring	1	2	3	6
	Girdle-hanger	5	6	7	18
	Latch-lifter		3		3
	Small-Long		11		11
	Strap-end	4	15	1	20
	Strap-mount			6	6
	Brooch	Annular	26	65	18
Applied disc			4	7	11
Bar			1		1
Cruciform		2	30	5	37
Fish		4			4
Great square-headed		1	3		4
Penannular		1	2		3
Radiate-head			1		1
Roman		3			3
Small-Long			1	7	8
Square/cross			2		2
Undefined Brooch		1	1		2
Buckle		Undefined Buckle	1	10	1
Miscellaneous	Chain		1		1
Necklace	Necklace Ring	3		1	4
	Pendant	3	7	14	24
Pin	Undefined Pin		2		2
Ring	Bracelet		2		2
	Ear Ring		5		5
	Finger ring	1	5	2	8
Wrist Clasp	Form A	4			4
	Form B 12		4		4
	Form B 13 a	9	4		13
	Form B 13 c	6	6		12
	Form B 17 a	5			5
	Form B 20	1	8		9
	Form B 7	3	13		16
	Form C 1	3			3
	Undefined Wrist Clasp		3	27	30

Table 8-13: Copper alloy dress accessories associated with female gendered burials.

In Table 8-14 the number of objects by grave phase is provided. In female gendered burials most copper alloy objects are associated with phase ERL-FA2, in male gendered burials it is phase ERL-MAB. These two phases — female ERL-FA2 and male ERL-MAB — cover a similar chronological period as can be

seen in the schematic phasing diagram in Chapter 1 (Figure 1-12, page 44). This suggests that there was a distinct chronological phase of activity when the burial of copper alloy in graves was at its peak.

Gender	Phase	Site				Manufacture method				
		ERL 046	ERL 104	ERL 114	Total	Cast	Melted	Sheet	Wire	Total
Female	A		1		1	1				1
	A1		28	3	31	23	1	7		31
	A2	50	241	131	422	195		208	15	418
	A2b	26	12	2	40	15		24		39
	AB	8			8	4			4	8
	B	11	2		13	12		1		13
	C	7			7	2		5		7
	DE	24	10		34	26		7	1	34
	FC		5		5	4		1		5
	Total		126	299	136	561	282	1	253	20
Male	A		7		7	3		3		6
	AB	7	60	5	72	38	1	32		71
	B	1	8	1	10	2		8		10
	BC		4	5	9	6		3		9
	C		6		6	4		2		6
	C/EF		17		17	7		10		17
	CDEF		5		5	1	1	3		5
	EF		1		1			1		1
	Total		8	108	11	127	61	2	62	

Table 8-14: Number of copper alloy objects by female (top) and male (bottom), grave phase, site and manufacturing method.

Considering the phasing in the context of other categorical variables, such as fabrication technique, does not reveal any immediately obvious trends (see Table 8-14). In ERL 046 and 114 there is a lack of any wire objects after phase ERL-FAB in the female graves and no wire objects at all in the male phases.

8.6 EXPLORATORY DATA ANALYSIS

8.6.1 NORMALITY

An examination of the data distribution in the form of density plots (Figure 8-5) indicates that the data are not normally distributed. Many elements are skewed with only copper and tin displaying a distribution that approaches a normal curve. It appears that there are outliers in the data. This is a matter of concern as principal components analysis can be distorted by outliers (discussed further on page 325).

Examining the data in quartile plots (where the distribution is plotted against a theoretical normal distribution) emphasises this (see Figure 8-6) with all distributions deviating from the theoretical normal distribution.

For many years, following the work of Ahrens (1953; 1954), a standard approach with geochemical data when dealing with non-normal distributions was to work with a logarithmic transformation under the assumption that it will have a log-normal distribution. As discussed in detail by Reimann and Filzmoser (2000) this is rarely the case in the real world, and Eriswell is no exception, as can be seen in quartile plots of log-normal distributions (Figure 8-7).

The distributions of the data are, with the potential exception of nickel, still skewed and still not normal, with numerous outliers. This remains the case with transformations more complex than simply taking the logarithm of the original value, as can be seen in the density plots of clr transformed data below (Figure 8-8).

The clr transformation has given some elements (such as lead and silver) the appearance of a 'normal' distribution but has changed the distribution of those that previously were closest to 'normal' (copper and tin). It should also be noted that assessments of normality are — no matter how the data are or are not transformed — dependent on sample size (Zhang et al. 2005, 1872) and the larger a sample size is the easier it becomes to reject a hypothesis. This is illustrated here in Table 8-15 below, where the p-value increases as the test is

undertaken on a random sample of a decreasing number of objects. When the number of individuals in the sample is reduced to a quarter of the total then the test returns a p-value returns a result above 0.05 (i.e. accepting the hypothesis that the data is normally distributed as true).

Sample size	p-value
796 (all objects)	0.0001623
398	0.005753
199	0.3957
100	0.7942
50	0.9221

Table 8-15: results of a Shapiro-Wilks test for normality on untransformed copper results with a decreasing sample size. The individuals in the reduced samples were randomly selected using the base R function 'sample'. It should be noted that although these samples were randomly selected there is a chance that if replicated multiple times the results would not follow the same pattern of an increasing p-value.

This has implications for how the data are to be explored, for principal components analysis — whether data transformed or not — is easily distorted by outliers and extreme values. It is therefore not a suitable technique for non-normal data unless robust methods that are less subject to distortion by outliers (Reimann and Filzmoser 2000, 1012–1013) are used. This reduces the impact of the outlying variables on the data and allows the underlying dominant trends to shine through.

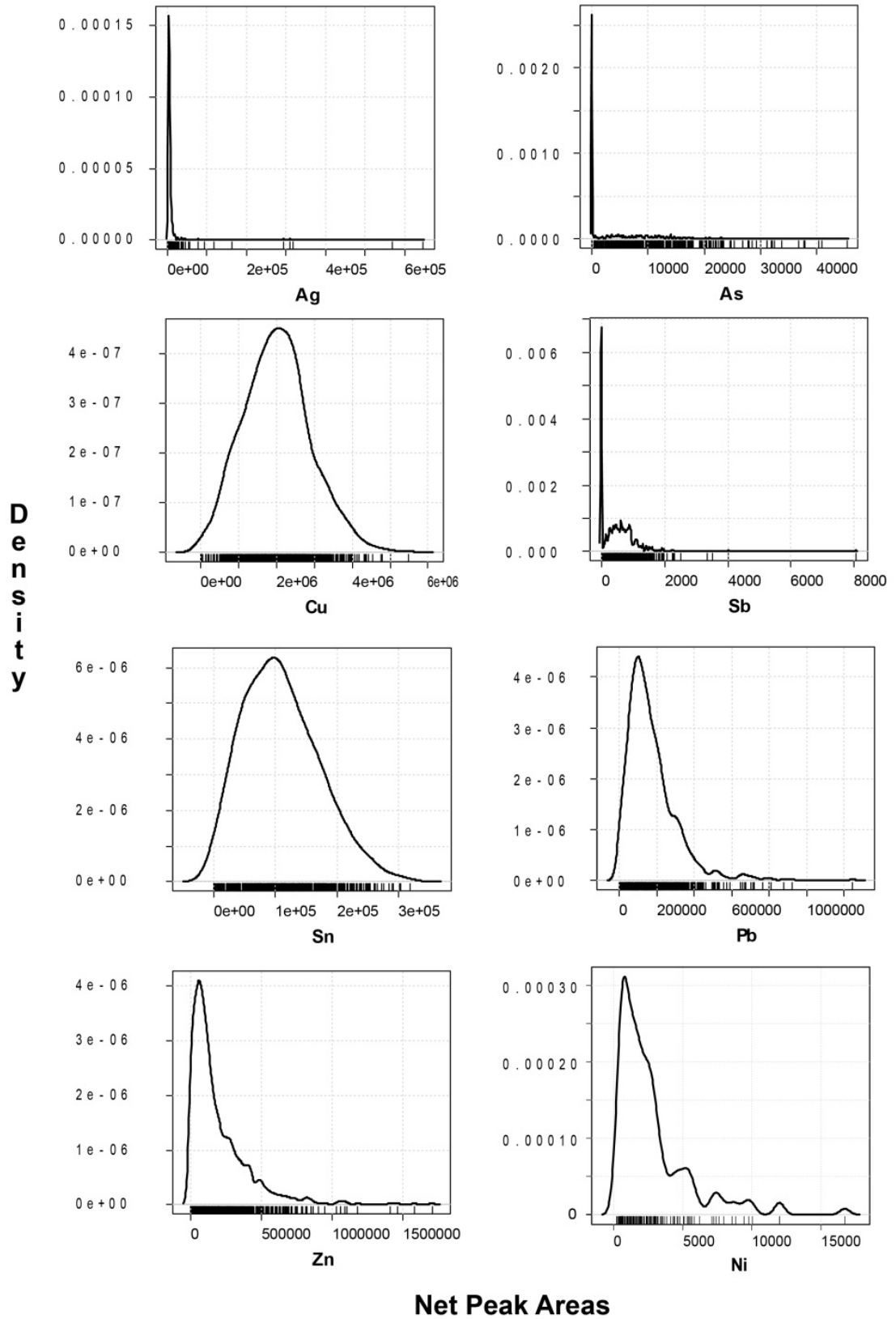


Figure 8-5: Density plots showing the distribution of the data for major elements.

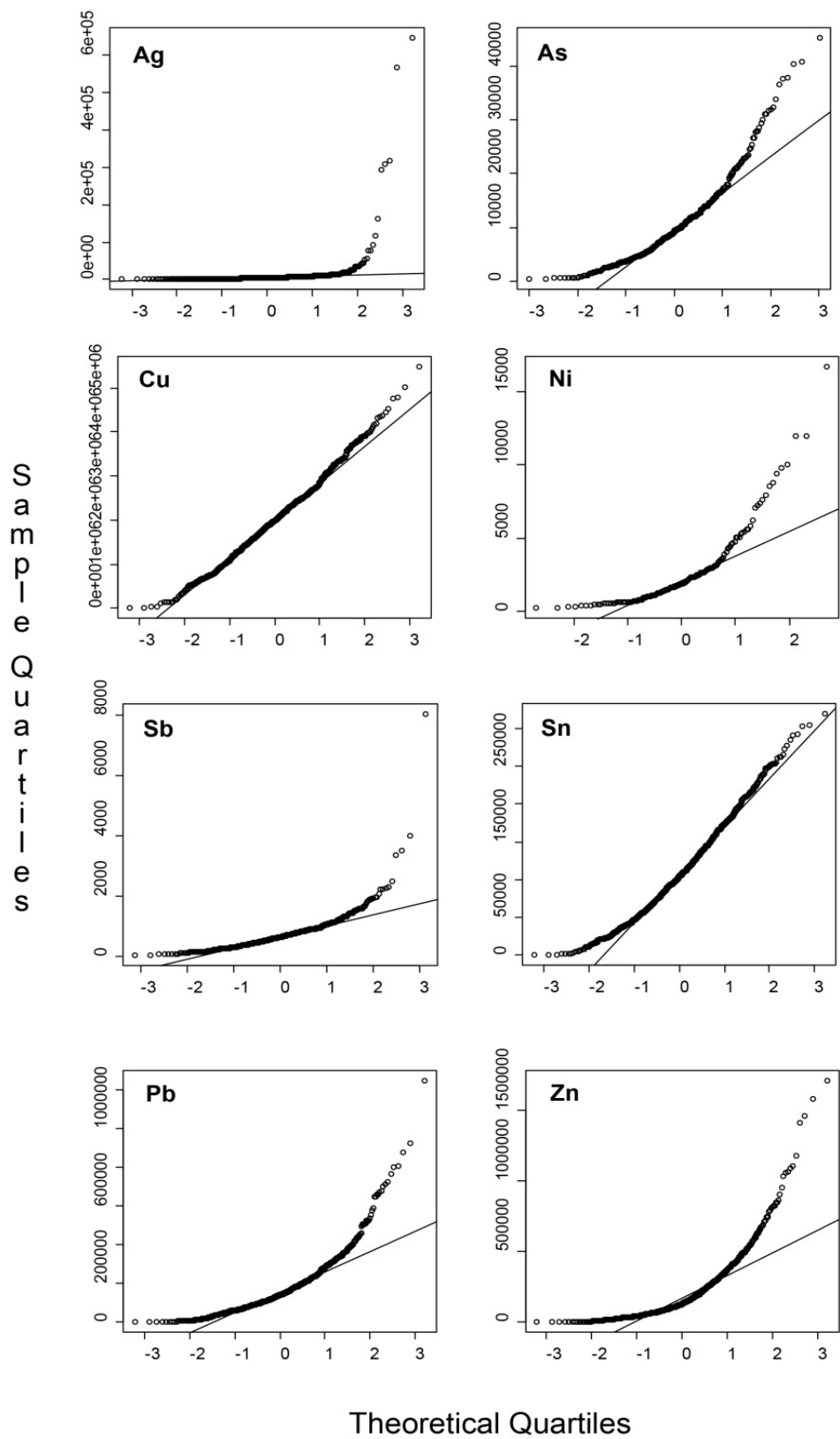


Figure 8-6: Q-Q plots for normal distribution. The black dots show the individuals and the straight line the theoretical normal distribution.

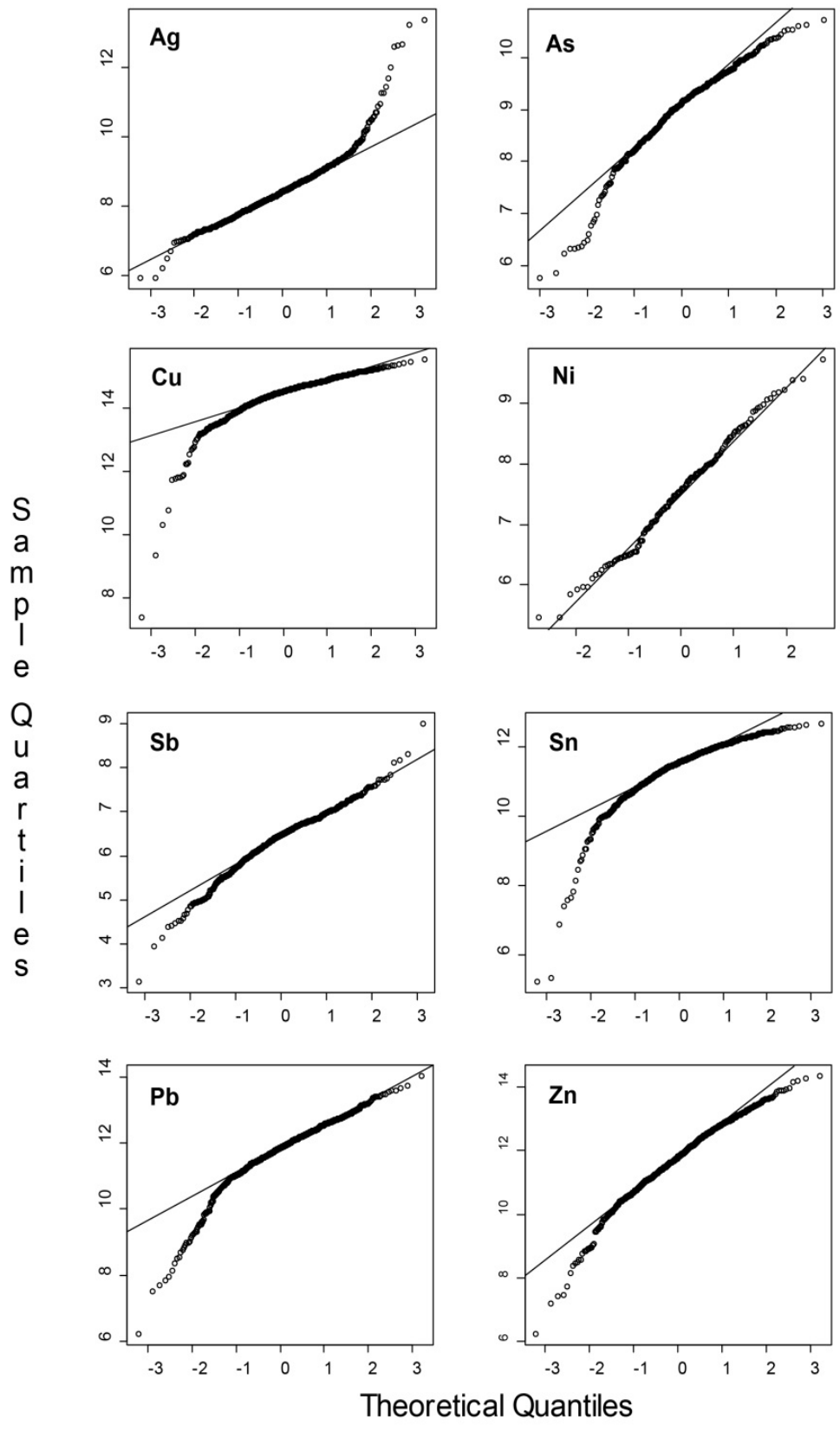


Figure 8-7: *Q-Q* plots for lognormal distribution. The black dots show the individuals and the straight line the theoretical lognormal distribution.

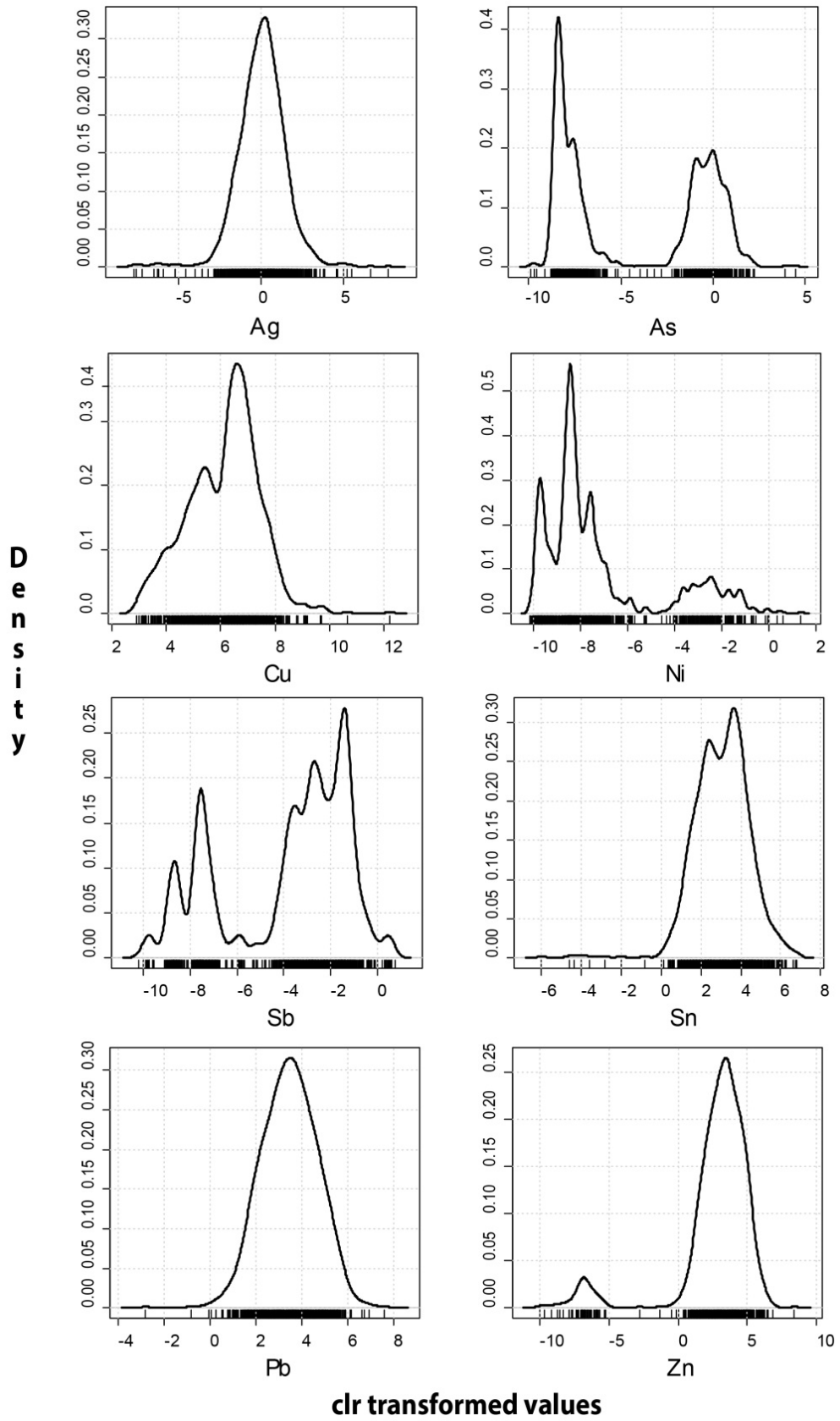


Figure 8-8: Density plots of clr transformed copper alloy data.

8.6.2 OUTLIERS

Defining outliers is a troublesome occupation with which to while away one's time when undertaking exploratory data analysis. The term carries with it an assumption that there is a pattern in the data that one is aware of and that you feel happy declaring an individual or population to be an interloper (from another pattern and representing a different process) or an extreme value (i.e. belonging to the pattern but being at an extreme end).

The data set here is non-normal. Standard tests for outliers tend to be based on the mean and standard deviation (such as defining all those values that deviate ± 2 SD from the mean as outlier) or the use of lower and upper quartiles. These processes are not suitable for non-normal data and therefore a robust statistical approach must be used (Reimann, Filzmoser, and Garrett 2005).⁷⁸ Here this will be implemented using the R package 'mvoutlier' (Filzmoser and Gschwandtner 2015). This package allows for multivariate outlier detection and can be undertaken on untransformed and transformed (using log-ratios) data using a Mahalanobis distance based test with distance calculations based upon a minimum covariance determinant providing the robustness (Filzmoser, Garrett, and Reimann 2005).

With both untransformed and transformed data, arsenic, cobalt, bismuth and gold are left out from the outlier detection. This is because of the large number of zeros in the minor and trace elements. Leaving them as missing values means that the 'x' and 'y' lengths differ and the Mahalanobis distance cannot be calculated. Using a replacement strategy (i.e. replacing the zeros with a minimal value) also does not work as it leaves a data set that forms a singular matrix. Although this means the results must be considered with care, it will still inform on the structure of the assemblage based on the major elements. Outliers and extreme values identified here (under both geometries) will not be automatically excluded from further analysis and interpretation, although they may be removed if investigation suggests that outlier status is the result of contamination or

⁷⁸ As an example: a very quick test using ANOVA reveals every single reading to be an outlier.

misclassification (i.e. the accidental inclusion of an object that should have been considered under a different material classification).

8.6.2.1 UNTRANSFORMED OUTLIERS

The biplots show the first and second robust principal components, which explain 87% of the variance in the data. In Figure 8-9 (top) a series of univariate scatterplots are provided, allowing the outliers to be visualised in the context of individual elements. It can be seen in this that there are several significant outliers containing silver (Ag). On one of these (rivet 104-2865-A) it becomes clear from re-examining notes made during analysis that the silver results from contamination of the spectra (the shape of the object making it difficult to analyse the copper alloy reverse whilst excluding the silver plating on the front). The remaining objects do not appear 'silver' or white in appearance; they simply appear to be copper alloys with a higher silver content than the majority of the copper alloy objects.

In these univariate plots these silver outliers have the impact of reducing the scale upon which the distribution in other elements can be seen. Redrawing the graph and excluding silver allows these to be investigated in a little more detail (bottom plot, Figure 8-9). Two of the elements stand out as being of particular interest here: zinc (Zn) and antimony (Sb). In antimony it can be seen that there appears to be a clear distinction between two groups; a main body and a group of outliers (those that contained no antimony). In zinc there also appears to be two groups consisting of the main body and a scatter of outlying higher zinc alloys. Lead also contains a spread of outliers. This may be due to the accidental clipping of areas of filler alloy. This is discussed on page 342 and continues to be evaluated throughout this chapter.

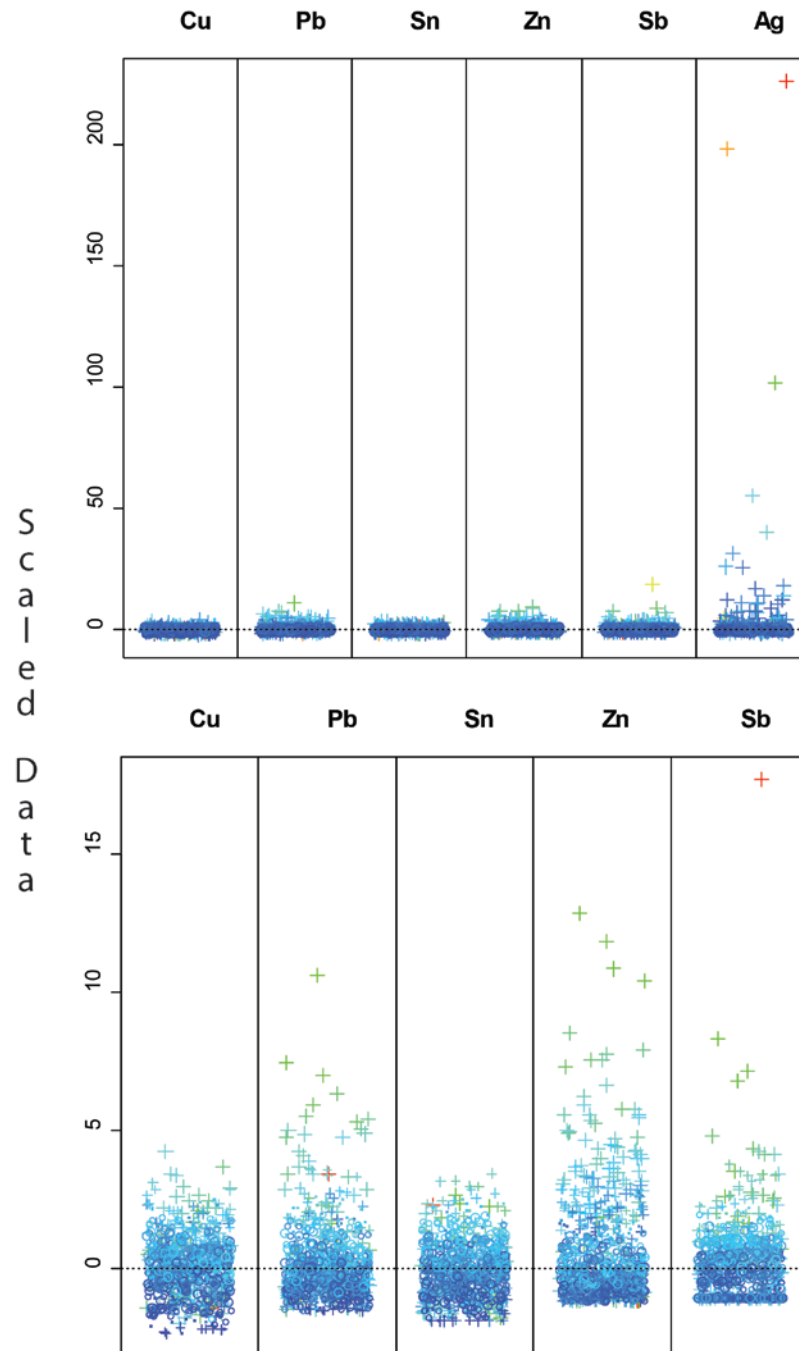


Figure 8-9: Univariate scatterplots for the (untransformed) elements. The top plot includes silver, the bottom excludes it. Circles indicate individuals that are within the main distribution, crosses outlying individuals. The colour scheme is based on a heat map (i.e. a cooler colour indicates the degree of how much an outlier outlies). Created using the R package 'mvoutlier' (Filzmoser and Gschwandtner 2015).

A close examination of the univariate scatter plots (Figure 8-9) shows that there are outliers (the crosses) that, at points, appear within the main distribution for an individual element. This is because the outlier technique is multivariate, i.e. it looks at the data set as a whole and not at each element individually and in isolation. Consequently an outlier may appear in the main distribution for an

element (such as copper), but is marked as an outlier because a value (or values) for another element (such as antimony) identify it as so.

8.6.2.2 TRANSFORMED OUTLIERS

The use of a multiplicative replacement strategy on zero values (see Chapter 4, page 200 for a discussion on zero replacement strategies) means that arsenic (As) can be included in the calculations here. Bismuth (Bi), cobalt (Co) and gold (Au) are still excluded as the large number of minimal values makes for a singular matrix. As a consequence two versions of the ilr outliers are presented; one set calculated with arsenic and one without, enabling easier comparison with the untransformed outliers. The log ratio transformed outlier results are presented in a biplot of the first two robust ilr transformed principle components (Figure 8-10). The projections explain 93.5% (including arsenic) and 92.2% (excluding arsenic) of the variance in the data set.

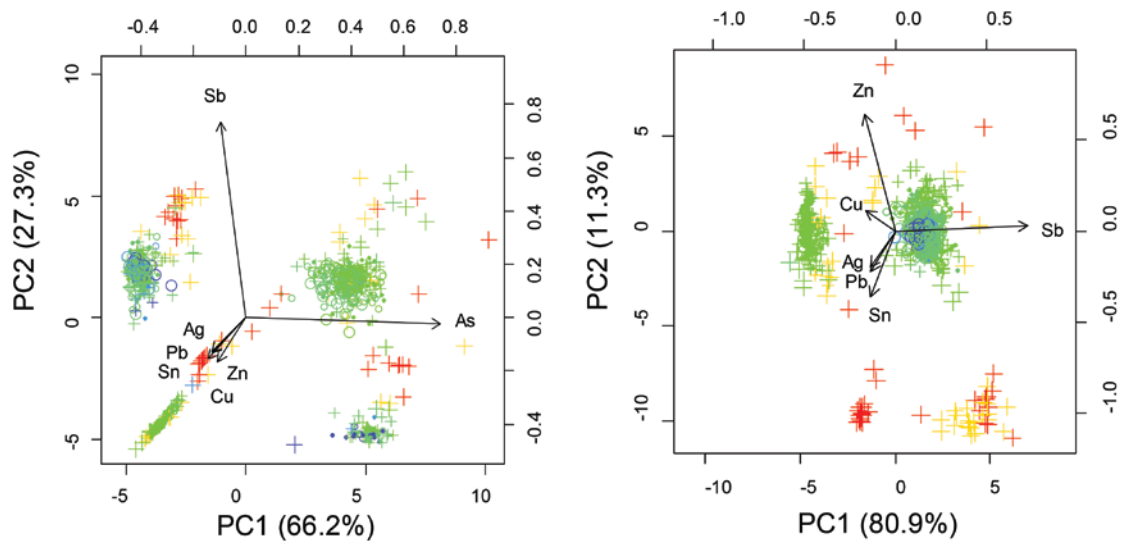


Figure 8-10: Biplot of ilr transformed data both including and excluding arsenic (left and right respectively) showing individuals within the main distribution outliers (circles) and outliers (crosses). The colour scheme is heat map based (i.e. the warmer the colour the more outlying it is). Created using the R package ‘mvoutlier’ (Filzmoser and Gschwandtner 2015).

There appear to be four primary groups within the data, with arsenic and antimony expressing the most variance (groups will be examined in more detail after hierarchical clustering). A number of other outliers are present, but these

(such as those near the copper rays) may be nothing more than extreme values from nearby groups.

The univariate scatter plots of the individual elements (Figure 8-11), not surprisingly, show the same discrete groups of outliers. There is also a degree of similarity with the untransformed plots: there is a distinct outlier group in antimony, there is the suggestion of distinct groups in zinc. This can also be visualised in a parallel coordinate plot (Figure 8-12). Parallel coordinate plots display individual variables for each unique object analysis joined by a line across the horizontal plane (i.e. imagine the points in Figure 8-11 being joined together across all the elements), allowing graphical interpretation of multivariate data across different variables and the identification of relatively homogeneous groups within the data.⁷⁹ Here it can be seen that the three main outlier groups share in common lower zinc content than the majority, a similar silver content to the majority and that the difference between the groups is most stark in antimony and arsenic content.

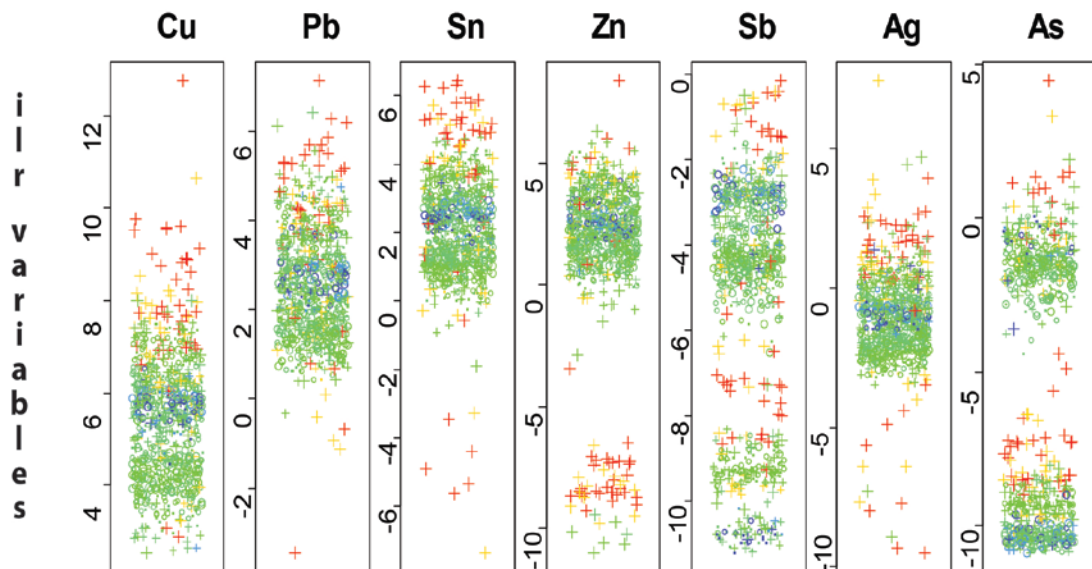


Figure 8-11: Univariate scatter plots of *ilr* transformed outliers. Circles indicate individuals that are within the main distribution, crosses outlying individuals. Created using the R package ‘*mvoutlier*’ (Filzmoser and Gschwandtner 2015).

⁷⁹ For further details on parallel coordinate plots and their application to archaeology see Herzog and Siegmund 2013)

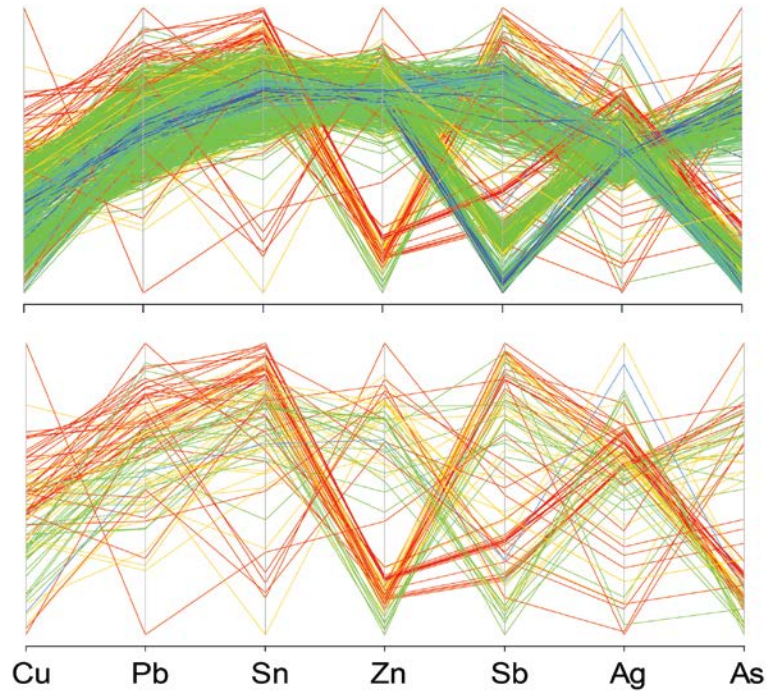


Figure 8-12: Two parallel coordinate plots, the top shows all data, the bottom outliers only. The colour scheme is based on a heat map (i.e. a warmer colour indicates the degree of how much an outlier outliers). The minimum of the variables is zero and the maximum is one. Created using the R package ‘mvoutlier’ (Filzmoser and Gschwandtner 2015).

A similar pattern can be seen, if not as clearly, in a parallel coordinate plot of the untransformed data (Figure 8-13). The majority of the outliers again share in common lower zinc content than the majority, a similar silver content to the majority and differing antimony and arsenic contents.

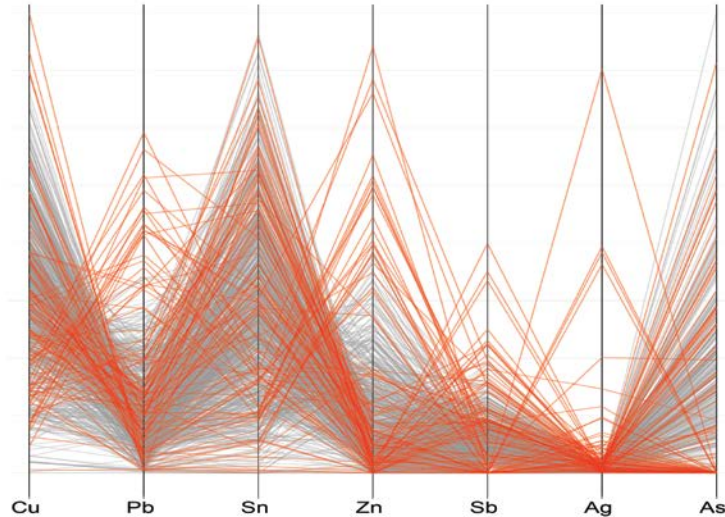


Figure 8-13: Parallel coordinate plot of untransformed data. Outliers are in red, non-outliers in grey. The minimum of the variables is zero and the maximum is one. Created using the R package 'ggally' (Schloerke et al. 2014).

8.6.2.3 OUTLIERS SUMMARY

All outliers identified – both transformed and untransformed - are listed in Appendix XVI with contextual information. The majority of the outliers identified appear to be representing different patterns in the metallurgy (as noted in the parallel coordinate plots). There are also a number of individual outliers and extreme values that stand out.

It should be noted at this point that there is no intention to automatically exclude any outliers from further interpretation.

8.6.2.3.1 OUTLYING CULTURES

One set of set of objects with a distinct categorical variable consistently stood out: those produced by different cultures. These are listed in Table 8-16 (categorical variables) and Table 8-17 (net peak areas) below.

The earliest object in the assemblage is the possible Bronze Age awl 114-1159-A. This object immediately stands out by being a relatively pure tin bronze (in common with Bronze Age metalwork analysed from elsewhere, see for instance Northover 1991). In contrast most of the copper alloy objects are quaternary copper alloys.

In Figure 8-14 all Roman objects from Eriswell (excluding the coins) — whether detected as outlier or not — are plotted in a tin-lead-zinc ternary diagram along with analyses of Roman copper alloy objects (predominantly dress accessories) from Richborough, Lincoln, Baldock, Nornour and St Albans (data from Bayley and Butcher 2004 and Blades 1995). As can be seen the Roman finds from Eriswell are largely consistent with the range of alloy compositions found elsewhere.

It can also be seen that the different components of composite objects are showing some dispersal in their distribution. This presents a useful reminder that one should be careful when interpreting the results here. It may be reasonably considered that the component parts of 046-1737 and 046-1160 (two brooches) were produced from the same alloy, yet the plot of the three components in the ternary diagram does not give this impression. As the analysis is on the corroded surface this could be expected. This does not mean that the data is not useful however. As can be seen the parts of each of these two objects are within the same areas, i.e. all parts of 046-1737 are a leaded bronze with low zinc and all parts of 046-1160 are a zinc brass with low lead and tin. As we are seeking to understand broad patterns in alloy composition and choice this is acceptable.

Other non-Anglo-Saxon objects include a possible high medieval or later spoon fragment, a melted 'drop' of unknown date and a farthing of Charles I.

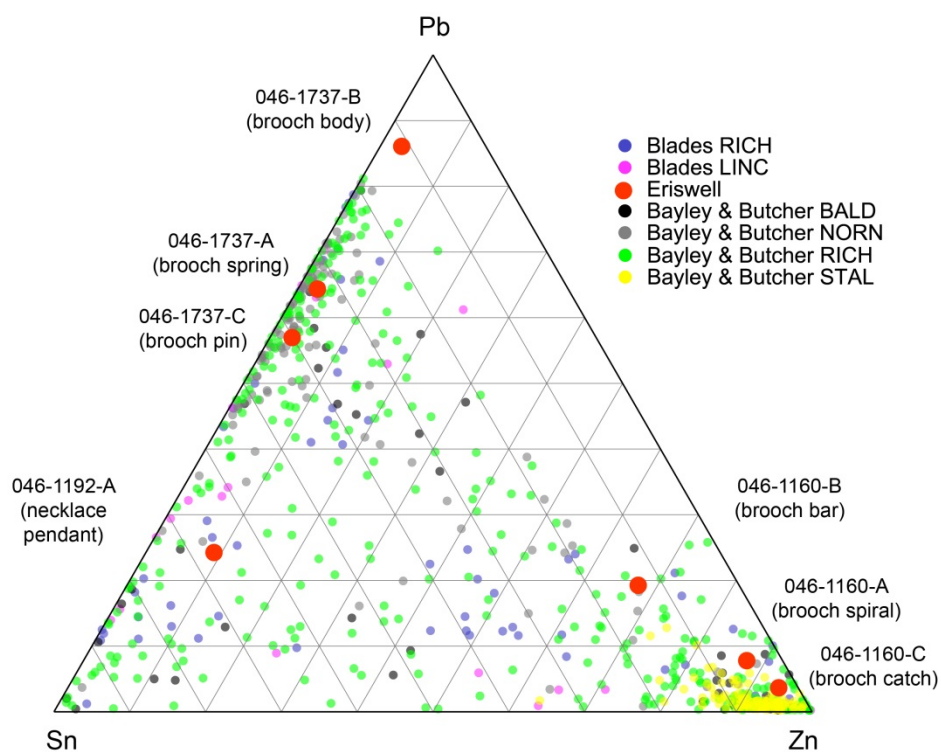


Figure 8-14: Ternary diagram showing Roman copper alloy objects from Eriswell (excluding coins) over analyses of Roman dress accessories from other sites in the UK. The comparable data are drawn from analyses by Bayley and Butcher (2004) and Blades (1995). The site codes are as follows: RICH – Richborough; LINC – Lincoln; BALD – Baldock, Hertfordshire; NORN - Nornour, Isles of Scilly; STAL - St Albans, Hertfordshire. Blades analysis was undertaken using ICP-MS, Bayley and Butcher's AAS. Each data set was closed as a sub composition before being combined with the others for the purposes of plotting the diagram.

ID	Untrans.	ilr trans. (ex. As)	ilr trans. (inc. As)	XRF Location	Grave No.	Mfr. method	Category	Class	Sub Class	Cultural Period
046-1160-A		Y	Y	Spiral		Cast	Dress Accessories	Brooch	Colchester	Roman
046-1160-B		Y	Y	Main bar		Cast	Dress Accessories	Brooch	Colchester	Roman
046-1160-C		Y	Y	Fragment with catch attached		Cast	Dress Accessories	Brooch	Colchester	Roman
046-1192-A	Y				024	Cast	Dress Accessories	Necklace	Pendant	Roman
046-1737-B	Y	Y	Y	Bow (front)	043	Cast	Dress Accessories	Brooch	Roman	Roman
046-1751-A		Y	Y			Cast	Dress Accessories	Pin	Undefined Pin	Unknown
104-2502-A	Y	Y	Y	Cast spoon fragment		Cast	Unknown	Unknown	Unknown	Unknown
104-3064-A		Y	Y	Melted blob		Melted	Unknown	Unknown	Unknown	Unknown
104-3327-A	Y	Y	Y			Struck	Coins, Tokens and Jettons	Coin	Undefined Coin	Post- medieval
104-4211-A	Y			Bow (front)		Cast	Unknown	Unknown	Unknown	Unknown
114-1000-A	Y	Y	Y	Head side		Struck	Coins, Tokens and Jettons	Coin	Undefined Coin	Roman
114-1159-A		Y	Y		434	Cast	Personal equipment	Implement	Awl	Bronze Age?
114-1501-A	Y	Y	Y	Reverse		Struck	Coins, Tokens and Jettons	Coin	Undefined Coin	Roman

Table 8-16: Non early medieval outliers and categorical variable. See Table 8-17 for associated net peak area data.

ID	XRF location	Manuf. method	Cu (K)	Pb (L)	Sn (K)	Ag (K)	As (K)	Ni (K)	Sb (K)	Au (L)	Bi (L)	Zn (K)	Co (K)	No. of analyses
046-1160-A	Spiral	Cast	1848527	10341	6279	3705						116205		1
046-1160-B	Main bar	Cast	2706554	20444	14126	6456						71588		2
			<i>0.03</i>	<i>0.12</i>	<i>0.11</i>	<i>0.08</i>						<i>0.11</i>		
046-1160-C	Fragment with catch attached	Cast	3903010	15118	10625	5489						387725		1
046-1192-A		Cast	2365527	90353	248854	6170	8058	5413	3364			33478		3
			<i>0.2</i>	<i>0.57</i>	<i>0.28</i>	<i>0.24</i>	<i>0.73</i>	<i>0.14</i>	<i>0.3</i>			<i>0.37</i>		
046-1737-A	Spring	Cast	812769	186352	95767	1527						7433		1
046-1737-A	Spring	Cast	812769	186352	95767	1527						7433		1
046-1737-B	Bow (front)	Cast	539192	721482	93020				1549			23752		4
			<i>0.16</i>	<i>0.06</i>	<i>0.18</i>				<i>0.17</i>			<i>0.35</i>		
046-1737-C	Pin	Cast	280128	101667	71570	369			189			5228		2
			<i>0.29</i>	<i>0.33</i>	<i>0.24</i>	<i>1.41</i>			<i>1.41</i>			<i>0.01</i>		
046-1751-A		Cast	2127987				987							2
			<i>0.01</i>				<i>0.02</i>							
104-2502-A		Cast	3188742	28305	20601	366	1522	3576	189			849271		4
			<i>0.12</i>	<i>0.15</i>	<i>0.1</i>	<i>1.16</i>	<i>1.18</i>	<i>1.2</i>	<i>1.19</i>			<i>0.24</i>		
104-3064-A	A	Melted	1014391	64149	236592	6695			391					2
			<i>0.16</i>	<i>0.17</i>	<i>0.17</i>	<i>0.16</i>			<i>0.28</i>					
104-3327-A		Struck	2556252	68677	54772	2077			477			161543		4
			<i>0.2</i>	<i>0.73</i>	<i>0.6</i>	<i>0.62</i>			<i>0.38</i>			<i>0.42</i>		
104-4211-A	Bow (front)	Cast	2111995	113458	110038	20827			1108			118599		5

ID	XRF location	Manuf. method	Cu (K)	Pb (L)	Sn (K)	Ag (K)	As (K)	Ni (K)	Sb (K)	Au (L)	Bi (L)	Zn (K)	Co (K)	No. of analyses
			0.21	0.24	0.17	0.1			0.15			0.36		
114-1000-A	Head side	Struck	1115027	1246433	5973	9512			1160					4
			0.1	0.05	0.6	0.11			0.16					
114-1159-A		Cast	1503593	2218	162183	5247	7482							5
			0.22	0.08	0.24	0.41	0.42							
114-1501-A	Reverse	Struck	2124690	307344	115025	118338	5184		1813	561		12889		4
			0.05	0.1	0.04	0.09	1.91		0.05	0.72		0.67		

Table 8-17: Non early medieval outliers. The unshaded row shows the net peak areas (mean if more than one analysis taken) for each element, the second (shaded) row shows the coefficient of variation. The final column shows the number of analyses. See Table 8-16 for associated categorical variables.

Should these non-Anglo-Saxon objects be included in further analysis? Our current model for early medieval Anglo-Saxon non-ferrous metallurgy postulates the recycling of other, earlier, cultures' metal as the predominant method of resource acquisition. A number of the earlier objects — such as the Bronze Age awl (114-1159-A), Roman pendant (046-1192-A), Roman brooch (046-1737-A, B & C) and undated tweezers (046-1026-A) — were found in grave contexts and appeared to have been deliberately selected for inclusion in the burials. The facets of these objects that led them to being perceived as being objects of value in themselves (and not as raw material) are unknown. Nevertheless, this re-use is a form of recycling; that they did not undergo the death and resurrection of being cast into new cultural forms does not mean that they should be considered as having played an active role in the metallurgical life of the communities at Eriswell. Indeed, what is to separate them from the sheet metal spangle clipped from a Romano-British sheet object? No metallurgical change has taken place, but the metal is now in a recognisable 'Anglo-Saxon' form. How can we include those objects and then exclude others simply because they do not fit our pre-conceived notion of what Anglo-Saxon copper alloy objects are? Consequently they should not be excluded from further statistical consideration; to do so would be to discard the complex life histories of non-ferrous artefacts in the post-Roman world (Eckardt and Williams 2003; Swift 2012b).

The same cannot be said for those earlier objects with no early medieval context. Although there is a chance that they were part of a (subsequently disturbed or truncated) grave assemblage it cannot be certain. They could easily be residual remnants / background 'noise. Consequently those objects from an earlier culture and that are not from a secure early medieval context will be excluded from further statistical interpretation.

8.6.2.3.2 CONTAMINATED MEASUREMENTS

All the outliers identified by both approaches were carefully examined for any evidence of contamination. This revealed several objects where contamination had occurred. In each case this had been a concern at the time of analysis. These

objects are listed with their associate categorical variables in Table 8-18 with the associated net peak area data in Table 8-19.

This group of objects will be excluded from any further statistical consideration.

ID	Reason for exclusion	XRF Location	Notes	Grave No.	Mfr. method	Category	Class	Sub Class
104-2865-A	Silver contamination	Rivet 1 (head)	Contaminated by nearby silver sheet?	323	Cast	Equestrian objects	Tack	Undefined Equestrian
104-1191-B	<i>Solder contamination</i>	<i>Non gilded area on front</i>	<i>Pb & Sn could be contribution from solder (no other areas of the 'base' alloy are accessible).</i>	245	<i>Cast</i>	<i>Military and weaponry</i>	<i>Shield</i>	<i>Shield Mount</i>
104-2624-E	Solder contamination	Front	Above head, possible area of solder.	323	Cast	Equestrian objects	Tack	Bridle Fitting
104-1176-B	<i>Solder contamination</i>	<i>Non gilded area on front</i>	<i>Pb & Sn could be contribution from solder (no other areas of the 'base' alloy were accessible).</i>	245	<i>Cast</i>	<i>Military and weaponry</i>	<i>Shield</i>	<i>Shield Mount</i>
104-3675-1-B	Poor quality spectra	Reverse of Stud	Large amount of ferrous corrosion.	168	Cast	Military and weaponry	Shield	Shield Mount
104-3674-2-B	<i>Poor quality spectra</i>	<i>Reverse of Stud</i>	<i>Small Cu peak but large amount of ferrous corrosion and mineralised wood.</i>	168	<i>Cast</i>	<i>Military and weaponry</i>	<i>Shield</i>	<i>Shield Mount</i>

Table 8-18: Contaminated measurements identified during outlier analysis with categorical variables.

ID	XRF location	Mfr. method	Cu (K)	Pb (L)	Sn (K)	Ag (K)	As (K)	Ni (K)	Sb (K)	Au (L)	Bi (L)	Zn (K)	Co (K)	No. of analyses
104-2865-A	Rivet 1 (head)	Cast	1226218	238128	188664	647101						182901		1
104-1191-B	Non gilded area on front	Cast	2186573	213638	167425	56833	564			6053		141233		3
			0.2	0.26	0.17	0.31	0.93			0.87		0.14		
104-2624-E	Front	Cast	1525696	223824	301844	45049						29003		1
104-1176-B	Non gilded area on front	Cast	2149388	160969	189670	16778		5825				575584		3
			0.21	0.17	0.27	0.38		0.19				0.14		
104-3675-1-B	Reverse of Stud	Cast	47888	2821								4755		2
			0.05	0.19								0.11		
104-3674-2-B	Reverse of Stud	Cast	1597	497		1076	316					499		2
			1.41	1.41		1.41	1.41					1.41		

Table 8-19: net peak area data for contaminated analyses. The unshaded row shows the net peak areas (mean if more than one analysis taken) for each element, the second (shaded) row shows the coefficient of variation. The final column shows the number of analyses. See Table 8-18 for associated categorical variable.

8.6.2.3.3 OUTLIERS CONCLUSION

Outlier analysis detected a number of groups that differ from the majority. These will be examined in more detail in the following principal component and hierarchical clustering analysis and will not be excluded.

A subset of outlying objects were identified where it was decided to exclude these from further assessment due to the lack of a secure context and association with the cemeteries (for non-Anglo Saxon objects) and contaminated analyses. These are listed in Table 8-20 over the page.

ID	Grave No.	Mfr.	Category	Class	Sub Class	Cultural Period	Reason for exclusion
046-1160-A	NG	Cast	Dress Accessories	Brooch	Colchester	Roman	UP
046-1160-B	NG	Cast	Dress Accessories	Brooch	Colchester	Roman	UP
046-1160-C	NG	Cast	Dress Accessories	Brooch	Colchester	Roman	UP
046-1751-A	NG	Cast	Dress Accessories	Pin	Undefined Pin	Unknown	UP
104-2502-A	NG	Cast	Unknown	Unknown	Unknown	Unknown	UP
104-3064-A	NG	Melted	Unknown	Unknown	Unknown	Unknown	UP
104-4211-A	NG	Cast	Unknown	Unknown	Unknown	Unknown	UP
114-1000-A	NG	Struck	Coins, Tokens and Jettons	Coin	Undefined Coin	Roman	UP
114-1501-A	NG	Struck	Coins, Tokens and Jettons	Coin	Undefined Coin	Roman	UP
104-2865-A	323	Cast	Equestrian objects	Tack	Undefined Equestrian	E. Sax.	C
104-1191-B	245	Cast	Military and weaponry	Shield	Shield Mount	E. Sax.	C
104-2624-E	323	Cast	Equestrian objects	Tack	Bridle Fitting	E. Sax.	C
104-1176-B	245	Cast	Military and weaponry	Shield	Shield Mount	E. Sax.	C
104-3675-1-B	168	Cast	Military and weaponry	Shield	Shield Mount	E. Sax.	C
104-3674-2-B	168	Cast	Military and weaponry	Shield	Shield Mount	E. Sax.	C

Table 8-20: Full list of the objects excluded from further analysis after outlier analysis. The final column details the reason: UP – unphased non-Anglo-Saxon object; C – contaminated analysis.

8.6.3 CLASSICAL STATISTICAL SUMMARY AND DISTRIBUTIONS

After the removal of a small number of objects as explained in the previous section, 781 individuals remain for further statistical consideration. The exploratory data analysis here will be undertaken using the methods outlined in Chapter 4, i.e. untransformed and centred log-ratio transformed data sets will be used. The use principal components analysis requires missing values to be imputed. This section will, however, initially focus on the original data with no transformations or zero replacements. In Table 8-21 the frequency of missing values by element is shown.

Element	Eriswell: Frequency of missing values (out of 781)	Blades: Frequency of missing values (out of 378)
Cu	0	0
Fe	0	0
Pb	0	0
Sn	3	1
Ag	12	119
Zn	48	2
Sb	225	0
As	410	15
Ni	639	0
Au	760	31
Bi	774	81
Co	774	261

Table 8-21: Showing elements and the number of missing values for the Eriswell data and Blades Early Saxon data (1995, 86–97) (two non-copper alloy objects have been excluded from Blades results here, these are Blades analysis numbers 762 & 766).

Those elements which were not identified in a significant number of individuals (gold, bismuth, nickel and cobalt) will be automatically excluded from further numerical statistical evaluation as estimating and imputing such a significant number of missing values may distort the results. These results will not be completely disregarded. Instead they will be considered as binary categorical variables (i.e. a ‘yes’ / ‘no’ based on their presence or absence).

This is not a definitive statement on the presence or absence of these elements in the Eriswell copper alloys. The table compares the number of missing values in

the Eriswell data with 378 analyses on Early Saxon objects from Nigel Blades' study (1995, 86–97). These copper alloy objects are from a similar chronological, cultural and geographical context and acquired using a more sensitive analytical technique (ICP-AES) on samples of uncorroded metal. An examination of the number of missing values in his data set reveals that elements missing here (with the exception of cobalt) *tend* to be present in his analyses.

There may be some concern about the validity of replacing zeroes for these elements with minimal values. As discussed earlier it may be considered unlikely — given the mixed and (probably) recycled nature of the alloys used — that these elements are true zeros. It is more that they are below the limit of detection for the analytical technique and practical methodology undertaken here (i.e. they are essentially rounded zeros).

In chapter 3, page 160 the limits of the analytical method (LDM) were examined. The results (Table 3-13, page 161) show are significantly higher than Blades detection limits (1995, 70, Table 8.6). As an example the weight percent LDM (see Table 8-22) for arsenic in a fully quantified analysis on an uncorroded surface is 0.75%, Blades arsenic detection limit was 0.02%. A comparison with Blades' data (1995, 86–97) shows that 380 out of 381 copper alloy objects had arsenic below this level; therefore we might reasonably expect the arsenic levels in the alloys here to be of a similarly low percentage.

As	
Weight %	0.75
NPA	56569

Table 8-22: Maximum LDM (±) values for arsenic across all MBH and IMMACO reference alloys as analysed at 40 kV - 7.9 μA. For the full table with all elements see Table 3-13, page 161. The NPA result should be considered valid only for flat uncorroded alloys that completely cover the HHpXRF window

Although the LDM is not the absolute minimum limit at which an instrument and methodology can detect an element (being a measure of the confidence with which the method will be able to return the same result), it does provide an indication of the minimum amount that can be identified (i.e. with an LDM of 0.75% an arsenic result of 0.6% has an error margin between existence or not). As the results are not quantified here this cannot be viewed as a hard and fast

guide, but it does provide an indication of the level at which arsenic is being regarded as present. Similar conclusions can be drawn for other elements such as gold and bismuth (most of Blades' results are to two or three decimal places). Consequently — because these elements are present in a majority of Blades' analyses at a level below the LDM of the method used here — the lack of identification of a peak cannot not be taken to mean that the element is not present, but that it may be present but at a level below the detection limit for the methodology used here.

Iron was detected in all analyses. The presence of iron as a trace element in ancient copper alloys is well attested (Cooke and Aschenbrenner 1975; Craddock, La Niece, and Hook 1990; Blades 1995, 135). Here, however, we need concern ourselves little with sulphurous ores and reducing atmospheres; the nature of the analysis (on the surface) means it is not possible to determine if the iron peak is a contribution from alloy or soil particulates and corrosion. Consequently iron will be excluded from any consideration here.

Antimony, arsenic and silver peaks were not identified in 25%, 52% and 2% of individuals respectively. Should these be retained for statistical consideration? Silver is present in nearly all alloys, antimony was present in all of Blades' analyses and arsenic in nearly all. As they are present in a majority (or near majority in the case of arsenic) they will, for the moment, be retained. There are, however, concerns about the quality of the arsenic results, discussed in more detail on page 352.

The major elements (copper, tin, lead and zinc) will, of course, be retained. Where there are zero values they will be replaced using a zero replacement strategy. This is believed to be a secure approach because of the highly mixed nature of the metals and a distinct lack of binary alloys (both as observed here during data acquisition and examination of previous data sets). It can therefore be reasonably securely suggested that zeros here are not true zeros. Nevertheless a degree of caution should be exercised and one should be aware that there is the

possibility that some of those objects that did not contain zinc or tin are genuine brasses or bronzes.

A brief summary of the data is provided below in Table 8-23. It can be seen that, in some cases, the standard deviation is larger than the mean (for instance silver and arsenic). This is no surprise. It has already been noted in the previous section that the data are non-normal in their distribution, and so the revelation that the data are well spread is not a revelation of particular importance.

	Mean	Std. Dev	Percentile				
			Min	25	50	75	Max
Cu	2020101	878437	11318	1423096	1980568	2545887	5478340
Pb	171487	129420	1837	86311	140964	225610	922863
Sn	110251	60269	185	63593	103797	147886	318868
Ag	7373	24465	369	2854	4475	6872	567910
As	10782	7693	352	5051	9481	14032	45290
Ni	2736	2683	234	974.5	1891	3153	16713
Sb	721	552	23	401	637	891	8050
Zn	206277	216522	1296	65261	133093	280813	1711181

Table 8-23: Classical statistical summary for the copper alloy data set.

In Table 8-24 below a correlation matrix is provided.

	Cu	Pb	Sn	Ag	As	Sb	Zn
Cu		-0.2574	-0.1899	-0.0892	-0.188	-0.0073	0.3249
Pb	-0.2574		0.2401	-0.0060	0.5892	0.2295	-0.0923
Sn	-0.1899	0.2401		0.1443	0.111	0.2724	-0.3618
Ag	-0.0892	-0.006	0.1443		0.0612	0.0673	-0.0643
As	-0.188	0.5892	0.111	0.0612		0.2604	0.0812
Sb	-0.0073	0.2295	0.2724	0.0673	0.2604		0.0513
Zn	0.3249	-0.0923	-0.3618	-0.0643	0.0812	0.0513	

Table 8-24: Correlation matrix for the copper alloy data set including arsenic.

The matrix shows the most significant relationships, predominantly being between pairs of major and minor elements (lead and arsenic, copper and nickel etc.). The most significant relationships between pairs of major elements feature zinc. This can be seen clearly in the table of top ten most highly correlated pairs below (Table 8-25). This table shows pairs of elements with Pearson's r correlation in the final column. This shows a score between 1 and -1 based on

the linear relationship between the two elements. A positive score suggests that when one element increases so does the other, a negative that when one increases the other decreases. The closer the value is to zero then the weaker the correlation (zero itself in no correlation). The repeated presence of zinc within the top five is of interest and is discussed further on page 358.

First variable	Second Variable	Correlation
Pb	As	0.5892
Sn	Zn	-0.3618
Cu	Zn	0.3249
Sn	Sb	0.2724
As	Sb	0.2604
Cu	Pb	-0.2574
Pb	Sn	0.2401
Pb	Sb	0.2295
Cu	Sn	-0.1899
Cu	As	-0.188

Table 8-25: Top ten most highly correlated pairs for the copper alloy data set including arsenic

8.6.3.1 ARSENIC AND LEAD CORRELATIONS

Particularly interesting in the previous table (Table 8-25) is the relationship between arsenic and lead. As noted in Chapter 3 (page 105) the arsenic $K\alpha$ and lead $L\alpha$ peaks overlap (both are at 10.5 K ν). The majority of these objects are leaded and therefore the presence of arsenic was identified via its $K\beta$ peak. When constructing a calibration, the overlap of lead and arsenic are accounted for using slope corrections. Here, where using a qualitative approach with net peak areas, no such correction was possible. Whilst a comparison of the arsenic and lead net peak areas on page 157 (an extract is presented in Figure 8-15 below) did suggest that net peak areas performed tolerably well at differentiation when compared against known values it should be borne in mind that only a small number of reference alloys was available and that these may not accurately represent the full range of compositions seen in early medieval copper alloys.

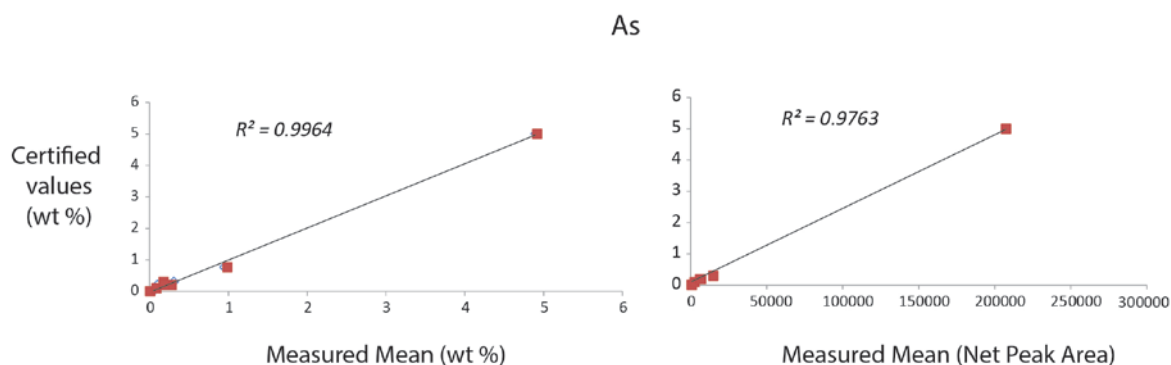


Figure 8-15: Extract from Figure 3-10 and Figure 3-13 showing scatter plots of measured mean ($n=10$) arsenic quantitative (left) and qualitative (right) results on reference alloys at 40 kV - 7.9 μA against certified values.

Consequently a large degree of caution should be used when interpreting relationships between lead and / or arsenic. Indeed, a comparison with the correlation matrix for Blades' Early Saxon data (Table 8-26) and scatterplot matrices of elements (for Eriswell data see Figure 8-16, for Blades' data see Figure 8-17) shows that Blades' data have no equivalent relationship between arsenic and lead.

	Cu	Zn	Pb	Sn	Ni	As	Sb	Ag
Cu		-0.3793	-0.5855	0.0008	-0.0211	-0.1254	-0.2033	0.1844
Zn	-0.3793		-0.1663	-0.6580	0.0055	0.3330	-0.0853	-0.0426
Pb	-0.5855	-0.1663		0.0683	0.0136	-0.0176	0.1495	-0.0905
Sn	0.0008	-0.6580	0.0683		-0.0139	-0.2422	0.1183	-0.0389
Ni	-0.0211	0.0055	0.0136	-0.0139		0.0183	-0.0046	-0.0197
As	-0.1254	0.3330	-0.0176	-0.2422	0.0183		-0.0503	-0.0139
Sb	-0.2033	-0.0853	0.1495	0.1183	-0.0046	-0.0503		-0.0390
Ag	0.1844	-0.0426	-0.0905	-0.0389	-0.0197	-0.0139	-0.0390	

Table 8-26: Correlation matrix for Blades (1995, 86–97) early Saxon copper alloy data set (excluding two non-copper alloy results, Blades analysis numbers 762 & 766).

There is a possibility that the correlation between lead and arsenic in the Eriswell matrices is representative of a real metallurgical relationship, but a greater likelihood that the correlation represents peak overlaps and a lack of correction. Because of this there is a need to consider how arsenic should be evaluated: included in the statistical interpretations as a numerical value or as a categorical variable (i.e. a binary 'yes' or 'no' for its presence and absence). As there is a lack of comparable 'mixed' reference alloys available with which to check the nature

of the relationship it is considered appropriate that the safer course of action is taken here and that arsenic be considered as categorical. Indeed it may be noted that the distribution of arsenic is already best viewed as a binary variable (i.e. in the distribution seen in outlier analysis in Figure 8-11).

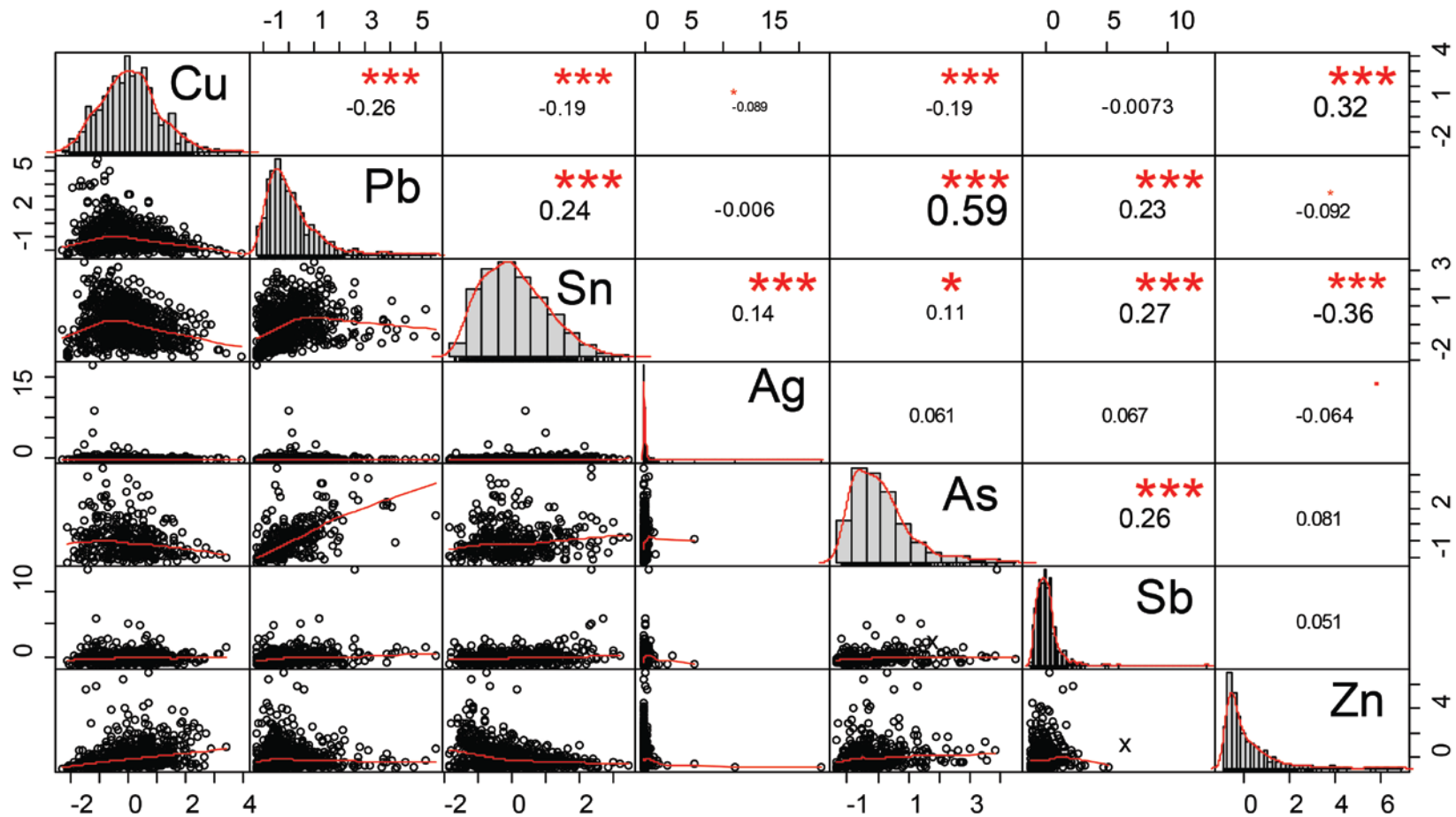


Figure 8-16: Scatterplot matrix of Eriswell untransformed data using the R package 'PerformanceAnalytics' (Peterson and Carl 2014). Pairwise complete observations only. Data has been scaled.

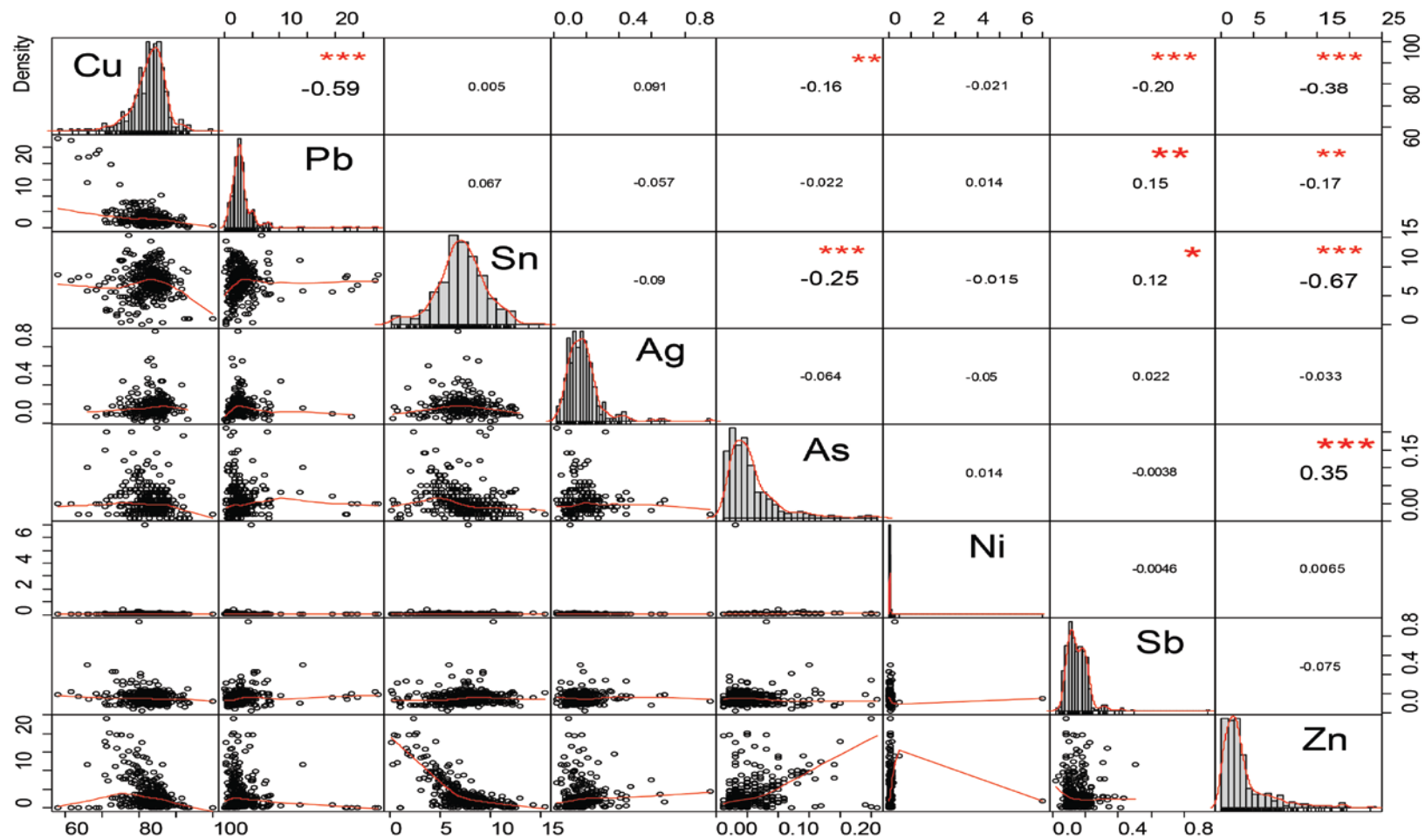


Figure 8-17: Scatterplot matrix for Blades (1995, 86–97) early Saxon copper alloy data set (excluding two non-copper alloy results, analysis numbers 762 & 766). No zero replacement used, pairwise observations only.

In Table 8-27 an overview of the presence / absence detection of arsenic is provided. Arsenic was definitely identified in 47% of Eriswell copper alloy objects.

Arsenic identified?	ERL 046	ERL 104	ERL 114	Total
No	85	238	87	410
Yes	56	248	67	371

Table 8-27: Summary showing number of objects and the identification of arsenic by site.

It should be restated that, although reduced to a binary variable, this is not a definitive statement on the presence or absence of arsenic in the Eriswell copper alloys. The weight percent LDM (see Table 8-22) for arsenic in a fully quantified analysis on an uncorroded surface is 0.75%. A comparison with Blades' data (1995, 86–97) shows that 380 out of 381 copper alloy objects had arsenic below this level; therefore we might reasonably expect the arsenic levels in the alloys here to be of a similarly low percentage and not identifiable with the approach used here.

The exclusion of arsenic does have some implications for the interpretation of the correlation matrix. As powerfully noted by Aitchison et al. (2002), coherence is not retained in a correlation matrix when data is subset. This can be seen in the reproduction tables of the correlation matrix and the top ten most highly correlated pairs with arsenic excluded in Table 8-28 and Table 8-29, and the scatter plot matrix in Figure 8-18.

	Ag	Cu	Pb	Sb	Sn	Zn
Ag		-0.0892	-0.006	0.0673	0.1443	-0.0643
Cu	-0.0892		-0.2574	-0.0073	-0.1899	0.3249
Pb	-0.006	-0.2574		0.2295	0.2401	-0.0923
Sb	0.0673	-0.0073	0.2295		0.2724	0.0513
Sn	0.1443	-0.1899	0.2401	0.2724		-0.3618
Zn	-0.0643	0.3249	-0.0923	0.0513	-0.3618	

Table 8-28: Correlation matrix for the Eriswell copper alloy data set excluding arsenic

First variable	Second Variable	Correlation
Sn	Zn	-0.3618
Cu	Zn	0.3249
Sb	Sn	0.2724
Cu	Pb	-0.2574
Pb	Sn	0.2401
Pb	Sb	0.2295
Cu	Sn	-0.1899
Ag	Sn	0.1443
Pb	Zn	-0.0923
Ag	Cu	-0.0892

Table 8-29: Top ten most highly correlated pairs for the copper alloy data set excluding arsenic.

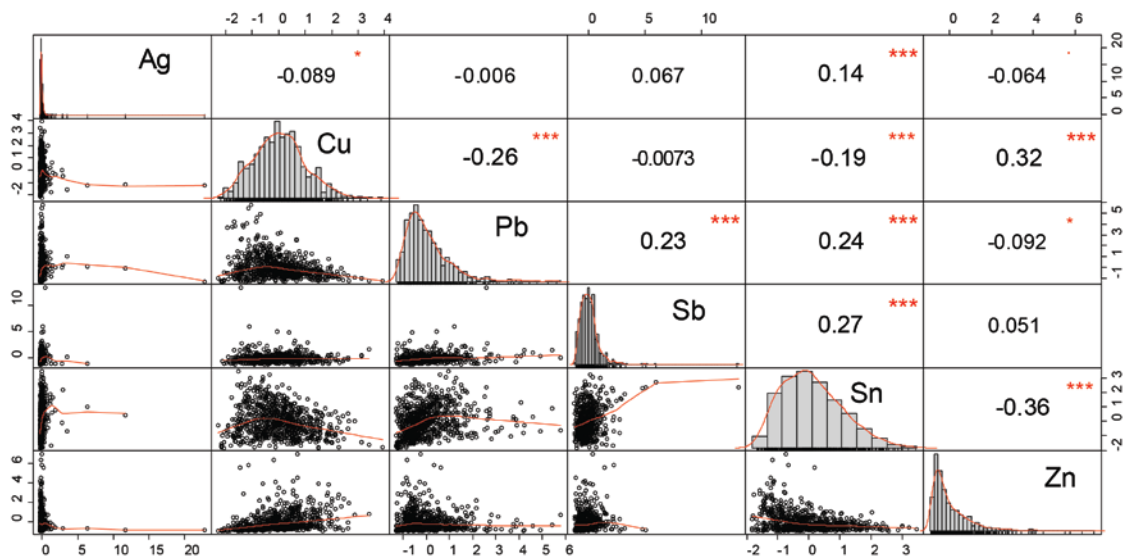


Figure 8-18: Scatterplot matrix of Eriswell untransformed data excluding arsenic using the R package 'PerformanceAnalytics' (Peterson and Carl 2014). Pairwise complete observations only. Data have been scaled.

8.6.3.2 OTHER CORRELATIONS

There are other relationships highlighted by the correlations that are of interest. Tin and zinc show an inverse relationship. Such a relationship has long been noted for Roman copper alloys (as noted by Dungworth 1997 in his overview of Craddock 1975 and Smythe 1934). As it is thought that Roman scrap metal (i.e. brass or bronze) was the raw material for the production of early Anglo-Saxon copper alloys (Blades 1995; Baker 2013) it is logical that we should expect some of this earlier correlation to survive — if diluted — in the alloys here. It may also be linked to the volatility of zinc (with its much lower boiling point), i.e. differing cycles of recycling have resulted in the loss of zinc. A similar relationship can be

seen in the correlation matrix and scatterplots of Blades' early medieval data (Table 8-26 and Figure 8-17). In Figure 8-19 a clr transformed ternary diagram scatterplot matrix is presented. Here the individuals form an almost linear pattern between tin and zinc (with a sub-composition of zinc free individuals also represented), again perhaps suggesting a relationship. A similar relationship can be seen between copper and lead. Again, this makes sense, higher lead content being matched by a decreased copper content. Interestingly there also appears to be a hint of a sub group in the zinc – silver plots.

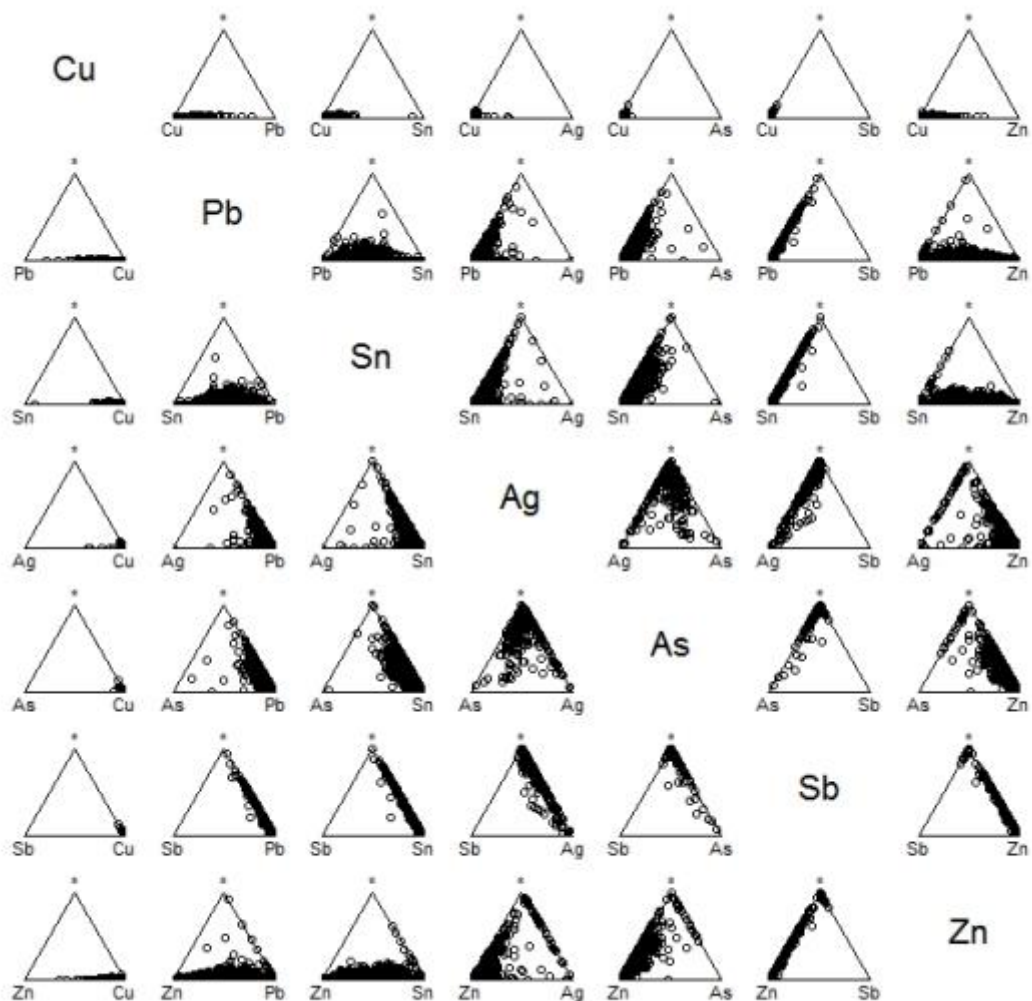


Figure 8-19: Scatterplot matrix of clr transformed data. The * at the apex of each diagram is the third component and represents the geometric mean of the remaining components.

The variation arrays in Table 8-30 and Table 8-31 shows the log-ratio mean and variances with and without arsenic. Two tables are presented as there may be some doubts in the reader’s mind about the applicability of the compositional approach here; however, it should be noted that (in contrast to the correlation matrices) the variations between the pairs of elements (see for example copper – zinc) remain stable in both ‘full’ and sub-composition versions as should be expected (see Aitchison, Barcelo-Vidal, and Pawlowsky-Glahn 2002, 299–301).

Xi\Xj	Cu	Pb	Sn	Ag	As	Sb	Zn	clr variances
Cu		1.0754	1.3376	1.6908	22.9722	9.9823	9.5011	1.4291
Pb	-2.6414		1.0989	1.619	22.6417	9.5519	9.311	1.2489
Sn	-3.0338	-0.3923		1.7812	22.7232	9.8514	11.2016	1.6341
Ag	-6.0905	-3.4491	-3.0568		23.4159	10.0312	11.1921	1.8821
As	-10.3378	-7.6963	-7.304	-4.2472		27.8535	28.627	15.954
Sb	-9.9807	-7.3393	-6.947	-3.8902	0.357		18.429	7.0205
Zn	-3.3985	-0.757	-0.3647	2.6921	6.9393	6.5823		7.3866
						Total Variance		36.5554

Table 8-30: Variation array for Eriswell copper alloys including arsenic. Upper triangle: log-ratio variances; lower triangle: log-ratio means. Bold values are those that have the largest variance.

Xi\Xj	Cu	Pb	Sn	Ag	Sb	Zn	clr variances
Cu		1.0754	1.3376	1.6908	9.9823	9.5011	0.9408
Pb	-2.6414		1.0989	1.619	9.5519	9.311	0.7856
Sn	-3.0338	-0.3923		1.7812	9.8514	11.2016	1.2214
Ag	-6.0905	-3.4491	-3.0568		10.0312	11.1921	1.3953
Sb	-9.9807	-7.3393	-6.947	-3.8902		18.429	6.6506
Zn	-3.3985	-0.757	-0.3647	2.6921	6.5823		6.9487
					Total Variance		17.9424

Table 8-31: Variation array for Eriswell copper alloys excluding arsenic. Upper triangle: log-ratio variances; lower triangle: log-ratio means. Bold values are those that have the largest variance.

As can be seen arsenic accounts for the largest amount of variation when included. When excluded tin – zinc, silver – zinc and tin – zinc are the largest. Considering the major elements alone for a moment it is interesting to note that the variances for copper, lead and tin against each other are low. When each is compared against zinc, however, the variance increases significantly. In the late Romano-British period Dungworth (1997a) noted that brass rarely appeared to have been recycled on its own, instead being mixed with bronzes. This could explain the variance here, although there are more variables to consider and it is not clear if this is the result of a conscious choice to mix (earlier) brasses with

bronzes and later mixed Romano-British alloys or a function of the mixing that had already occurred during the late Romano-British period.

To consider this in more detail we can examine a ternary diagram scatterplot matrix (Figure 8-20) where zinc is taken as a constant to plot against (as opposed to the geometric mean). Zinc is used because it appears to account for a lot of variation and it is relatively consistently present across all the analyses and, along with lead and tin, determines how we classify copper alloys.

Again the potential zinc – silver sub group division can be seen very clearly. It should also be noted that the zinc - lead – tin diagram nicely illustrates the highly mixed nature of the alloys. This supports the indication that can be gained from simply looking at the raw data: the alloys are highly mixed as can be expected from previous analyses on material from this period (Mortimer 1990; Mortimer 1991; Blades 1995; Baker 2013).

Of course there are limitations as to how far interpretation can be developed here. To develop further there is a need to understand which elements explain the variance in a multivariate manner, and for that we need principal components analysis.

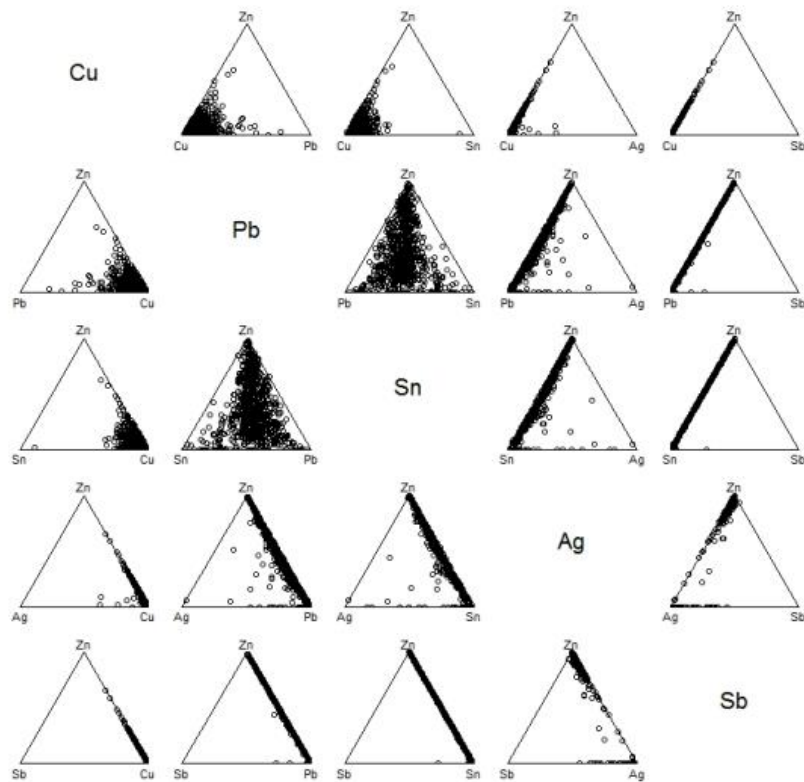


Figure 8-20: Scatterplot matrix of clr transformed data with zinc as a constant at the apex of the pyramid.

8.6.4 PRINCIPAL COMPONENTS

Please note that for ease of viewing all figures and tables for this subsection are presented at the end (for tables see pages 366-368, for figures 369-370).

In Chapter 4 two approaches to principal components were used: transformed using a centred log-ratio (clr) approach and untransformed. Both appeared to be producing results from which conclusions could be drawn and there were legitimate concerns about the applicability of both. Consequently both are used again here. As with the mentioned with the silver alloys earlier one should be aware of the risk of false correlations due to the zero replacement method chosen here (see page 200 for further details).

As mentioned earlier (page 325) PCA is sensitive to outliers. The impact of this sensitivity can be minimised by using robust statistical methods, although one should be cognizant that these outliers may represent groups that are of significant interest and that suppressing their influence may not be a desirable

outcome. Consequently both robust and non-robust methods will be used on the transformed and untransformed data (i.e. there are four sets of principal components produced here).

Both robust and non-robust transformed PCA is, unlike in Chapter 4, undertaken in R using the package ‘compositions’ (this was previously used only for hierarchical clustering with the standalone program CoDaPack used for PCA). This package uses the base R package ‘robustbase’ to apply a Minimum Covariance Determinant (MCD) estimator to the data (Boogaart and Tolosana-Delgado 2013, 241). This approach, developed by Rousseeuw (1984), examines the data for non-outlying individuals and estimates their covariance matrix. The full data set is then reassessed and individuals with large Mahalanobis distances are down weighted as required. The untransformed PCA is undertaken, as previously, with the R package ‘FactoMineR’ whilst the robust untransformed PCA is undertaken using the R package ‘pcaPP’ (Filzmoser, Fritz, and Kalcher 2014). This last uses projection pursuit, a method whereby principal components are deduced by “searching for directions that maximize a robust measure of variance of the data projected on it” (Croux, Filzmoser, and Fritz 2013, 202).

The results of the four sets of PCA are shown in Figure 8-23 (transformed PCA) and Figure 8-22 (untransformed PCA). Each diagram shows biplots of the first two components and scree plots of the variance explained by each component. The associated data can be found in Table 8-36 (clr transformed non-robust) Table 8-37 (clr transformed robust) Table 8-34 (untransformed) and Table 8-35 (untransformed robust).

The scree plots for the untransformed PCA are not particularly clear and suggest stopping around the third or fourth component. The transformed scree plots suggest the second (robust) and third (non-robust) respectively. Examining the variance using the Guttman-Kaiser Criterion indicates that the scree plots are not accurate indicators of component retention and that, with the exception of the robust transformed PCA (one component), only two components should be retained (Table 8-32). Bearing in mind the problems with scree plots and the

Guttman-Kaiser Criterion (see Chapter 4, page 208), Horn's Parallel Analysis can also be used to assess component retention. This is only undertaken on the untransformed non-robust data here. The results (see Table 8-33 and Figure 8-21) suggest retaining only two components and that the Guttman-Kaiser Criterion is performing better than the scree plots here in deciding how many components to retain.

For comparison's sake the first two components will be discussed for each PCA variation, although it should be remembered that the inclusion of the second component from the robust transformed PCA is not necessarily supported.

The first two components of each PCA can be summarised as follows:

- Untransformed non-robust (Table 8-34).
PC 1: copper, lead, tin and zinc (30.88% of total variance).
PC 2: copper, silver, antimony and zinc (20.97%).
- Untransformed robust (Table 8-35)
PC 1: copper, tin and zinc (37.64%).
PC 2: copper and tin (28.52%).
- Transformed non-robust (Table 8-36).
PC 1: antimony and zinc (51.67%).
PC 2: tin, silver, antimony and zinc (36.76%).
- Transformed robust (Table 8-37).
PC 1: tin and zinc (51.29%).
PC 2: copper and lead (18.11%).

The largest difference in the PCA results is between the robust and non-robust approaches. In the non-robust results (both transformed and untransformed) silver and antimony are shown as playing a significant role in explaining the variance. In contrast the robust results focus on the major elements. This is no great surprise as the robust approaches dampen the effect of outliers on the PCA (i.e. the presence / absence of antimony and silver). The projection of the first two components in the untransformed biplots (Figure 8-22) shows that copper,

tin and zinc account for the greatest spread. In the non-robust biplot copper and zinc are co-linear whilst in the robust version they are not. This is not a contradiction, but reflects the underlying data structure when the influence of antimony and silver is restricted. It is interesting to note that in both biplots tin and lead are relatively closely correlated and that tin and zinc are approximately negatively correlated.

The non-robust and robust transformed biplots (Figure 8-23) explain a greater proportion of the variance than their untransformed brethren (88.43 and 69.41% respectively). Most immediately noticeable in the biplots is the existence of an outlying group of high tin individuals. In the non-robust plot there is also a significant distinction between two groups based on antimony content. It is no surprise that, once again, antimony shows such an effect; of the remaining minor elements it is the one with the largest amount of absences. The robust PCA, as with its untransformed counterpart, dampens the effect of the antimony allowing the underlying structure in the major elements to be seen more clearly. It can be seen the copper and lead appear to lie on a common line suggesting a negative correlation between the two. There is possibly a similar relationship between zinc and tin. The length and distribution of the tin – lead – zinc rays suggests the log-ratios between these are highly variable, something backed up by the ternary diagrams displayed earlier in Figure 8-20. In the robust transformed PCA the distribution of the individuals — tin outliers excepted — is somewhat similar to the robust untransformed PCA biplot: a cloud of individuals not immediately showing any particular distribution pattern.

The variations between the different approaches are not necessarily of any concern; they are simply saying different things about the data structure depending on transformations and statistical approaches used. All are valid depending on how they are interpreted and one is aware that the variation they are ascribing may be linked more to the statistical approaches than the actual chemistry of the objects. To determine how ‘well’ they are performing hierarchical clustering will be used to distinguish groups and ascertain if there are useful conclusions about the metallurgy to be drawn.

	PC 1	PC 2	PC 3	PC 4	PC 5
Robust untransformed	<i>1.4709</i>	<i>1.1146</i>	0.6886	0.3584	0.2533
Untransformed	<i>1.8526</i>	<i>1.2583</i>	0.9012	0.8777	0.6048
Robust transformed	<i>1.5824</i>	0.5588	0.3858	0.3494	0.2085
Transformed	<i>9.2823</i>	<i>6.6049</i>	0.9723	0.6257	0.4803

Table 8-32: Variance of each component. Those components that should be retained according the Guttman-Kaiser Criterion are italicised. Only those components with a value above 1 (i.e. greater than the weight of an individual) should be retained according to the criterion.

Component	Adjusted Eigenvalue	Unadjusted Eigenvalue	Estimated Bias
1	1.685371	1.852551	0.167179
2	1.162212	1.25829	0.096077

Table 8-33: Results of Horn's Parallel Analysis for component retention with 23430 ($30 \times n$) iterations, using the 95th percentile estimate. Only those elements that should be retained are presented. See Figure 8-21 for the scree plot.

		PC 1	PC 2	PC 3	PC 4	PC 5	PC 6
Cu	Loadings (L)	-0.6125	0.3601	0.2139	0.4739	0.4187	-0.2223
	Contributions (%)	20.2515	10.3062	5.0754	25.5916	28.9942	9.7811
Pb	L	0.5936	0.3087	0.2311	-0.5498	0.4253	-0.1261
	%	19.0176	7.5737	5.9268	34.4345	29.9032	3.1442
Sn	L	0.7273	0.0841	0.0812	0.4778	0.1909	0.4389
	%	28.5516	0.5617	0.7321	26.0096	6.0289	38.1162
Ag	L	0.1075	-0.6063	0.7731	0.0769	-0.0860	-0.0991
	%	0.6235	29.2146	66.3204	0.6742	1.2234	1.9439
Sb	L	0.4156	0.7091	0.2304	0.1720	-0.4431	-0.2131
	%	9.3237	39.9592	5.8916	3.3719	32.4710	8.9825
Zn	L	-0.6418	0.3948	0.3804	-0.2950	-0.0913	0.4384
	%	22.2322	12.3846	16.0537	9.9183	1.3793	38.0319
Percentage of Variance		30.88	20.97	15.02	14.63	10.08	8.42
Cumulative Proportion		30.88	51.85	66.87	81.50	91.58	100

Table 8-34: untransformed principal components. Figures in bold are judged to be significant values (those making at least a 10% contribution).

		PC 1	PC 2	PC 3	PC 4	PC 5	PC 6
Cu	Loadings (L)	0.8161	0.4945	-0.0718	-0.1145	-0.2660	0.0219
	Contributions (%)	66.5971	24.4549	0.5153	1.3103	7.0742	0.0481
Pb	L	-0.2515	0.1556	0.7140	-0.3498	-0.5279	-0.0417
	%	6.3229	2.4210	50.9857	12.2330	27.8635	0.1739
Sn	L	-0.3966	0.7518	-0.0649	0.5219	-0.0246	0.0193
	%	15.7299	56.5148	0.4217	27.2356	0.0607	0.0373
Ag	L	0.0021	0.0538	0.1405	-0.0855	0.1852	0.9673
	%	0.0004	0.2897	1.9745	0.7313	3.4295	93.5746
Sb	L	0.1015	0.2769	0.4323	-0.2217	0.7845	-0.2482
	%	1.0302	7.6661	18.6853	4.9148	61.5432	6.1604
Zn	L	0.3212	-0.2942	0.5236	0.7319	-0.0170	0.0076
	%	10.3194	8.6533	27.4175	53.5751	0.0290	0.0057
Percentage of Variance		37.64	28.52	17.62	9.17	6.48	0.57
Cumulative Proportion		37.64	66.16	83.78	92.95	99.43	100

Table 8-35: untransformed robust principal components. Figures in bold are judged to be significant values (those making at least a 10% contribution).

		PC 1	PC 2	PC 3	PC 4	PC 5
Cu	Loadings (L)	0.0170	-0.2629	-0.2093	0.8054	-0.2673
	Contribution (%)	0.0289	6.9124	4.3814	64.8674	7.1432
Pb	L	0.0079	-0.2407	-0.2484	-0.0709	0.8418
	%	0.0062	5.7920	6.1722	0.5026	70.8603
Sn	L	-0.0618	-0.3268	-0.4206	-0.5754	-0.4634
	%	0.3816	10.6774	17.6901	33.1080	21.4762
Ag	L	-0.0549	-0.3172	0.8464	-0.1050	-0.0472
	%	0.3014	10.0620	71.6445	1.1027	0.2228
Sb	L	-0.6572	0.6335	-0.0015	0.0099	-0.0103
	%	43.1861	40.1265	0.0002	0.0098	0.0107
Zn	L	0.7490	0.5141	0.0334	-0.0640	-0.0535
	%	56.0958	26.4296	0.1116	0.4096	0.2867
Percentage of Variance		51.67	36.76	5.41	3.49	2.67
Cumulative Proportion		51.67	88.43	93.84	97.33	100

Table 8-36: clr transformed non-robust principal components. Figures in bold are judged to be significant values (those making at least a 10% contribution). For scree plot and biplot see Figure 8-23.

		PC 1	PC 2	PC 3	PC 4	PC 5
Cu	Loadings (L)	0.1684	-0.4762	-0.4766	0.3583	0.4719
	Contribution (%)	2.8343	22.6811	22.7115	12.8400	22.2665
Pb	L	-0.2537	0.8047	-0.1832	0.2229	0.1952
	%	6.4374	64.7605	3.3580	4.9670	3.8105
Sn	L	-0.4245	-0.2600	0.0310	0.3351	-0.6872
	%	18.0191	6.7584	0.0963	11.2286	47.2309
Ag	L	-0.1868	-0.1613	0.7733	-0.0980	0.4060
	%	3.4888	2.6009	59.7970	0.9598	16.4869
Sb	L	-0.1258	-0.0713	-0.3271	-0.8365	-0.0755
	%	1.5822	0.5083	10.7018	69.9716	0.5694
Zn	L	0.8224	0.1640	0.1826	0.0182	-0.3104
	%	67.6382	2.6910	3.3354	0.0330	9.6358
Percentage of Variance		51.29	18.11	12.51	11.33	6.76
Cumulative Proportion		51.29	69.41	81.96	93.29	100

Table 8-37: *clr* transformed robust principal components. Figures in bold are judged to be significant values (those making at least a 10% contribution). For scree plot and biplot see Figure 8-23.

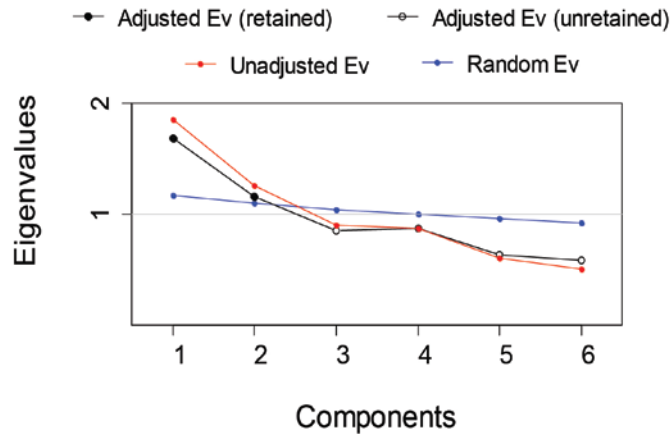


Figure 8-21: Scree plot of the results of Horn's Parallel Analysis for component retention with 23430 ($30 \times n$) iterations, using the 95th percentile estimate. See Table 8-33 for further details.

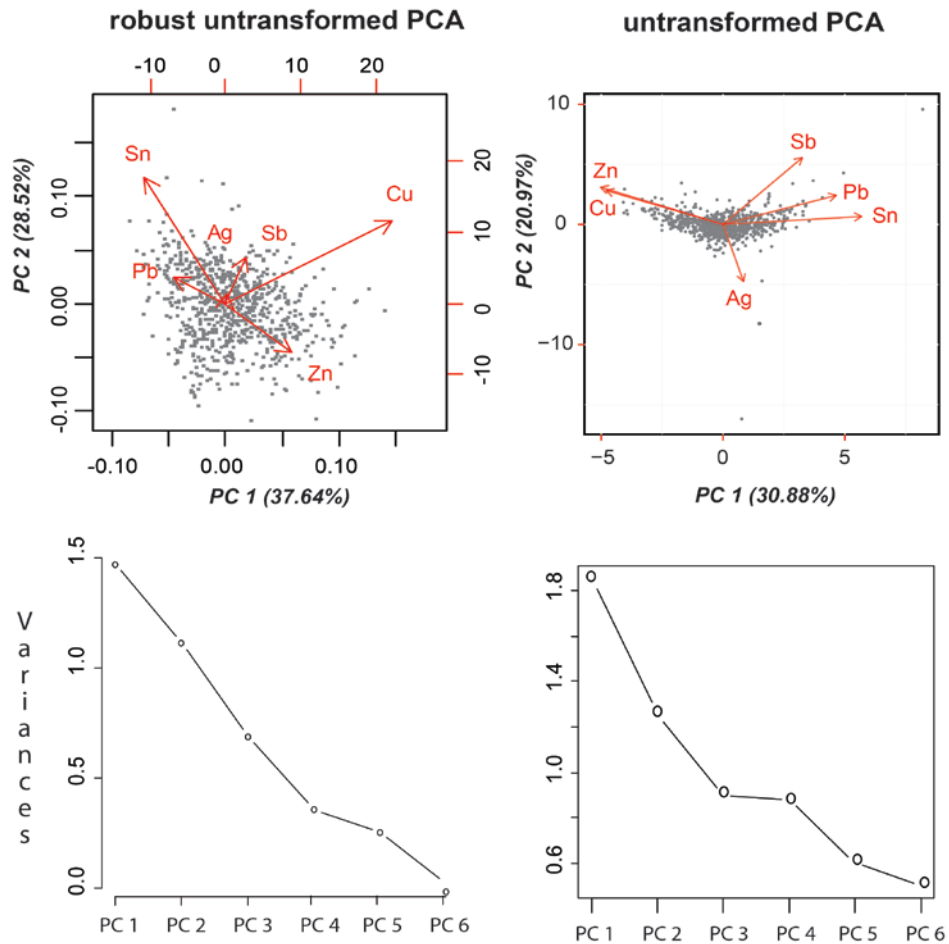


Figure 8-22: untransformed Principal Components Analysis. On the left are a biplot (top) and scree plot (bottom) showing the results of robust PCA (see also Table 8-35). On the right are a biplot (top) and scree plot (bottom) showing the results of non-robust PCA (see also Table 8-34). The robust PCA was undertaken using the R package 'pcaPP' (Filzmoser, Fritz, and Kalcher 2014), the non-robust using the R package 'FactoMineR'.

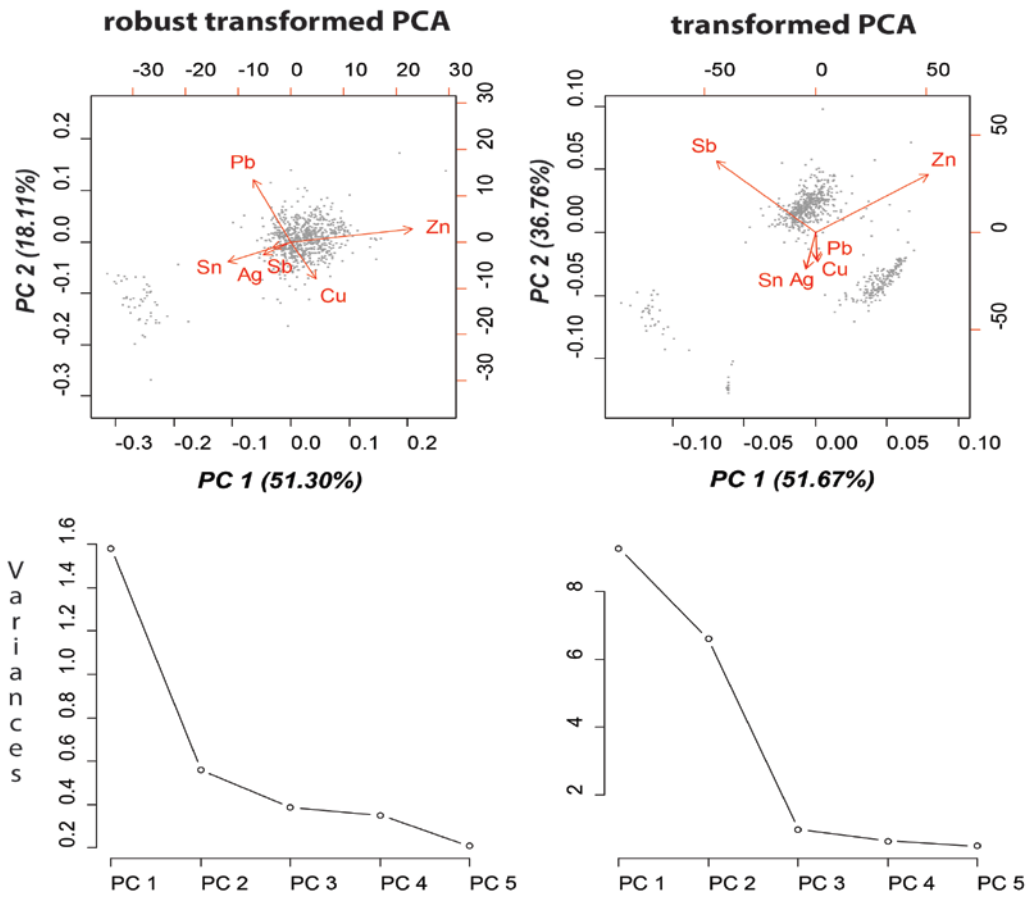


Figure 8-23: *clr* transformed Principal Components Analysis. On the left are a biplot (top) and screeplot (bottom) showing the results of robust PCA (see also Table 8-37). On the right are a biplot (top) and screeplot (bottom) showing the results of non-robust PCA (see also Table 8-36). All plots produced using the R package ‘compositions’.

8.6.5 HIERARCHICAL CLUSTERING

The hierarchical clustering was undertaken on the principal components and, as in the data processing methodology, Ward's distance was used to calculate the clusters. The clustering was undertaken on all four PCA variations. With so many individuals it is not useful to display the balance dendrograms here and it will have to suffice to say the decision was based on long height intervals with minimal agglomeration. In each case this led to the tree being cut into three clusters. The result of this clustering is illustrated in the series of colour coded biplots in Figure 8-24. A brief overview of the clustering results is provided in Table 8-38 below and a full table showing each individuals cluster membership for each PCA variation can be found in Appendix XVII on page 663.

Cluster groups	ERL 046	ERL 104	ERL 114	Total
<i>Untransformed</i>				
U 1	76	171	39	286
U 2	65	313	115	493
U 3		2		2
<i>Untransformed Robust</i>				
UR 1	80	218	52	350
UR 2	18	121	35	174
UR 3	43	147	67	257
<i>Transformed</i>				
T 1	7	35	6	48
T 2	41	411	85	537
T 3	93	40	63	196
<i>Transformed Robust</i>				
TR 1	7	35	6	48
TR 2	49	284	65	398
TR 3	85	167	83	335

Table 8-38: Cluster groups showing the number of objects by cluster and site. Please note that the group numbers do not mean that the clusters are directly comparable, i.e. U1 and UR1 are not exactly the same. For details on each individuals group membership see Appendix XVII on page 663.

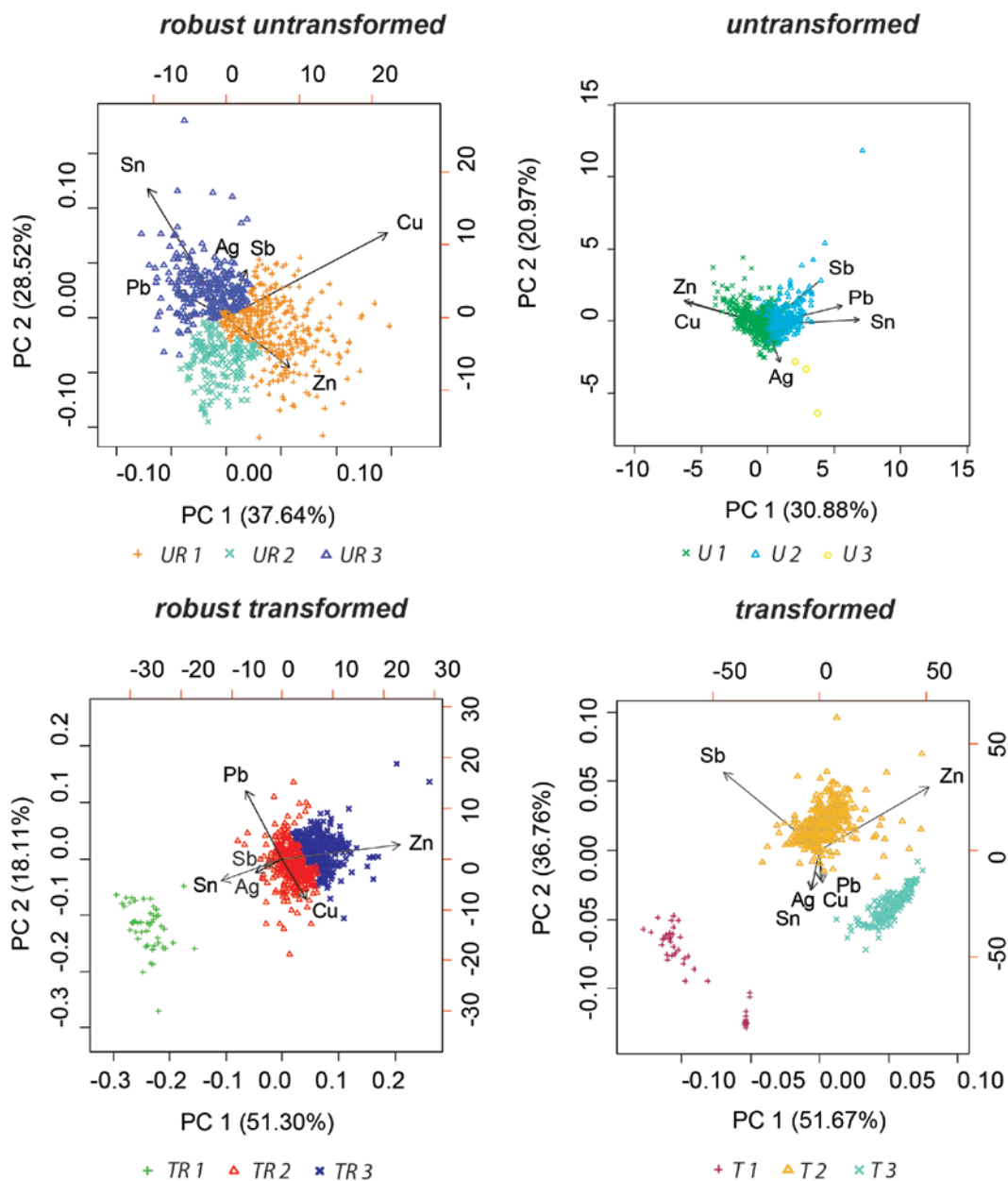


Figure 8-24: Biplots showing individuals coloured according to cluster membership. Please note that the group numbers do not mean that the clusters are directly comparable, i.e. U1 and UR1 are not exactly the same. For a summary of the clusters see Table 8-38. For details on each individual's group membership see Appendix XVII on page 663.

The clustering brings into focus some of the conclusions drawn from the PCA. The non-robust approaches (both untransformed and transformed) tend to be placing a lot of weight on outlying values. With the untransformed this leads to a dense spread with a few outliers based on silver and antimony contents being given significant weight. The transformed PCA is, as noted with the silver objects, producing more discrete groups. Again, however, these are based

predominantly on outliers (particularly antimony). Consequently the results of primary interest here are the two robust PCA implementations and the clusters based upon them. These are, as discussed, placing more weight on the major elements which are — given the limitations of the analytical technique used here and the questions we are seeking answers too (the decline of brass etc.) — of primary interest.

To understand what the groups from the robust PCA are illustrating they are plotted in parallel coordinate charts (Figure 8-25). In these charts the original data have been used with missing values as NAs (to see how the cluster groups apply when the data is not transformed etc.). The missing values are plotted here at 10% below the minimum of the variable for the missing value and the variables are ordered by skewness (i.e. the most skewed variables are first in the plots). The variables have been scaled univariately with a maximum of 1 and centred.

What is immediately clear from the two plots is that there is a high degree of similarity between untransformed robust group 1 (UR 1) and transformed robust group 3 (TR 3): both representing a high(ish) zinc and low(ish) tin composition. The distinction between clusters UR 2 and UR 3 in the untransformed robust plot is not immediately clear. Careful examination, however, reveals that distinction lies in tin with UR 2 apparently having a lower tin content than UR 3. Other than that they are remarkable similar. This is not a surprise as in the PCA results tin accounted for a significant amount of the variation in the first two components (Table 8-35, page 367). In contrast TR clusters TR 1 and TR 2 are primarily distinguished by the zinc content with TR 1 representing those objects where no zinc was detected (see Table 8-21 on page 348). Again this is no surprise: zinc accounting for the majority of the variation in the first principle component in the PCA results (Table 8-37 on page 368).

These are all valid observations the question is; which is most useful for understanding the Eriswell copper alloy objects?

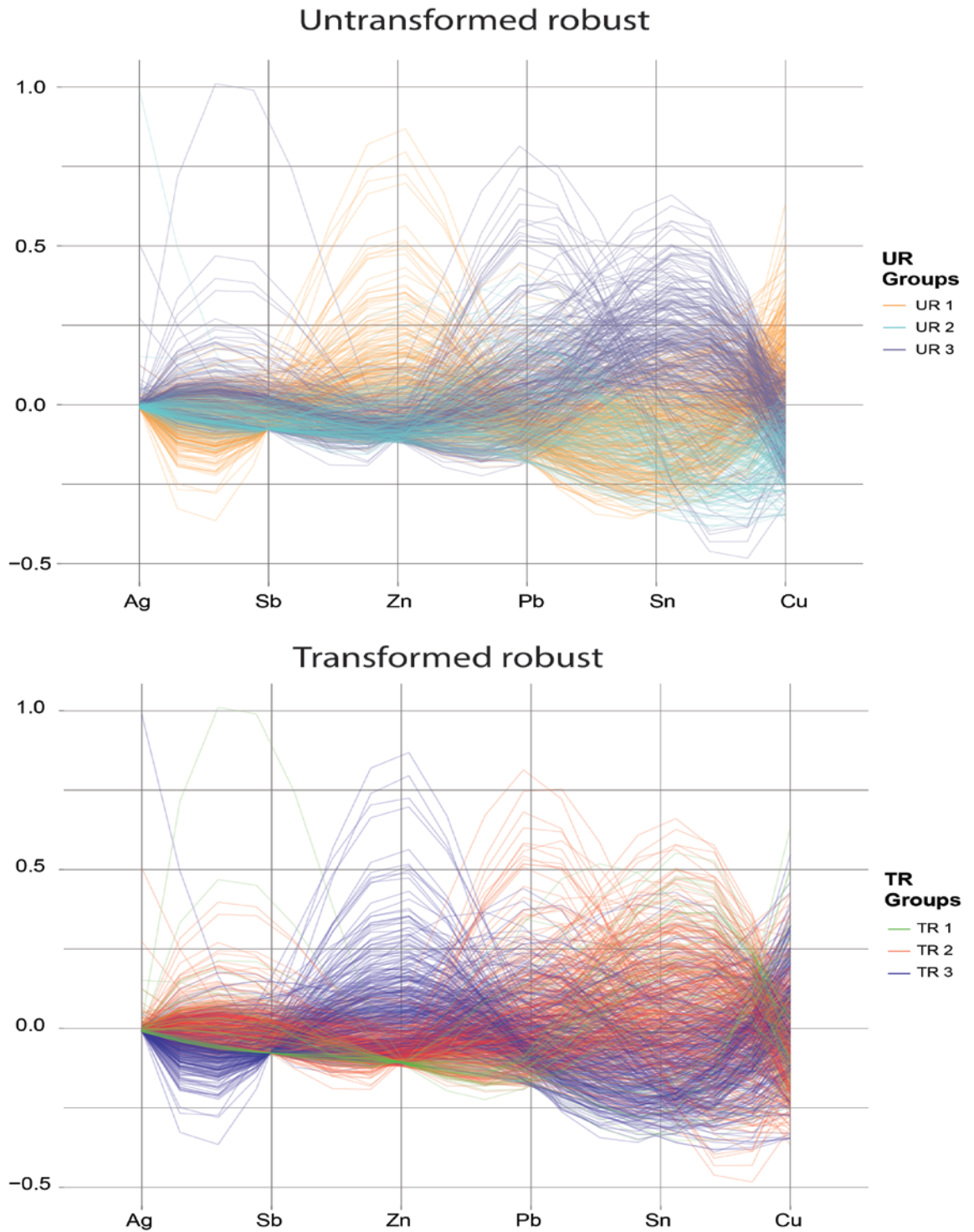


Figure 8-25: Parallel co-ordinate plots showing the variables scaled and centred with individuals colour coordinated according to cluster membership. The colours used are the same as in Figure 8-24. The top plot shows the clusters defined from the untransformed robust PCA, the bottom plot shows the transformed robust PCA clusters. Missing values are plotted at 10% below the minimum of the variable for the missing value and the variables are ordered by skewness (i.e. the most skewed variables are first in the plots). The variables have been scaled univariately with a maximum of 1 and centred. Created using the 'ggparcoord' function from the R package 'GGally' (Schloerke et al. 2014).

The graph below (Figure 8-26) show scatterplots of tin – copper, zinc – tin and lead – tin with individuals colour coded according to their group memberships. The plots have used the scaled original data (i.e. there are no transformations) with missing values as NAs (this approach means that group TR 1 is entirely missing from the robust transformed zinc – lead plot).

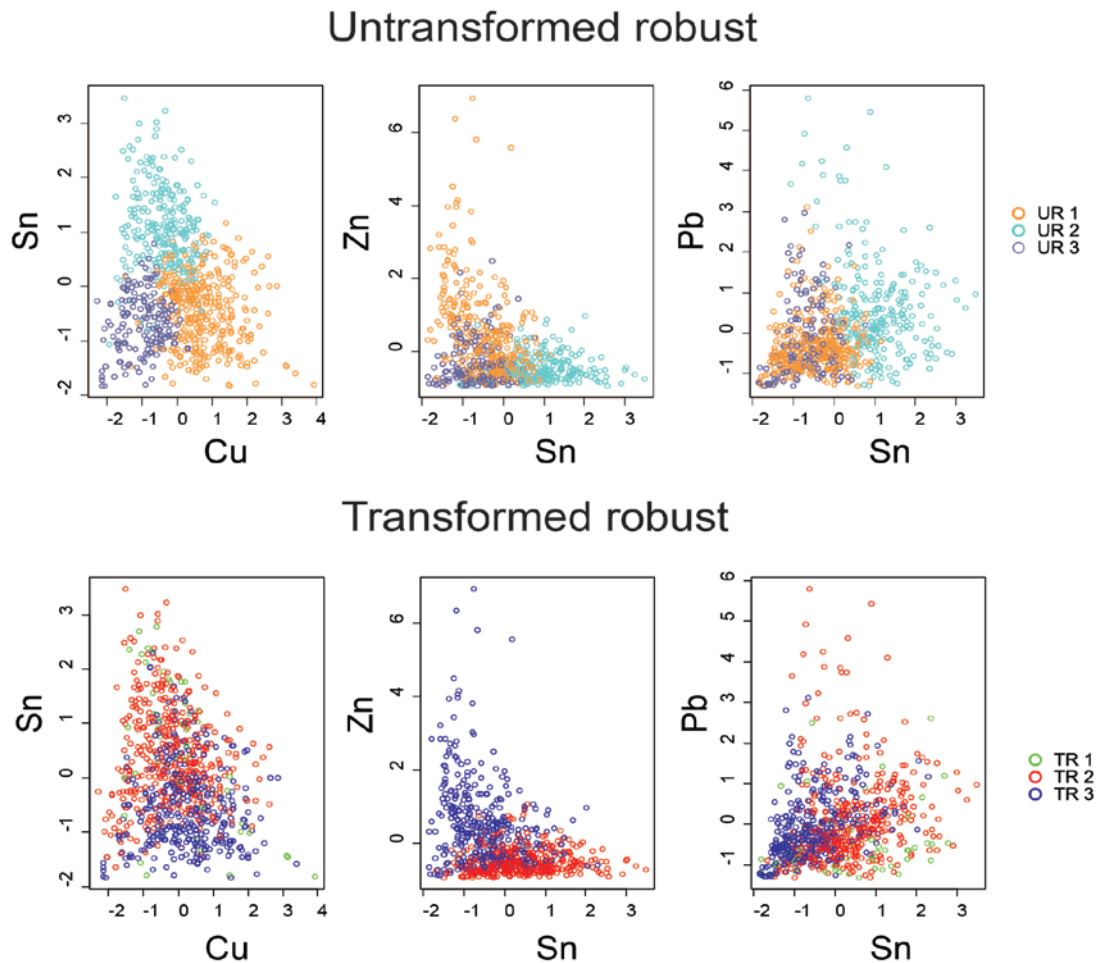


Figure 8-26: Scaled scatterplots with pairwise complete observations only (hence cluster group TR 1 being missing from the Zn – Sn transformed plot). Individuals are coloured according to cluster membership.

It can be seen the untransformed robust clusters appear particularly distinct in the tin – copper plot. In the zinc – tin plot the untransformed clusters UR 1 and UR 3 overlap but are relatively distinct from high tin – low zinc cluster UR 2. In the lead – tin plot a similar result is seen, UR1 and 3 overlap significantly and UR 2 is relatively well distinguished. In the transformed robust counterparts the clusters are relatively mixed in the tin – copper plot (although TR 3 tends to be displayed as having a lower tin content than TR 2) but clearly distinguished in the

zinc – tin plot (but note that group TR 1 is missing due to the use of pairwise complete observations only). In the lead – tin plot there is a degree of overlap, although TR appears as a lower tin group than TR 1 and 2.

It may appear that neither set of groups is outperforming the other at describing the metallurgy of the groups. A different story appears when the cluster groups are considered as three part compositions. In the ternary diagrams below tin – lead – zinc and copper – tin – zinc are plotted. The data in these have been subject to a zero replacement (i.e. zeros have been replaced with a value of 0.65 as previously discussed) but no further transformations or perturbations have been undertaken.

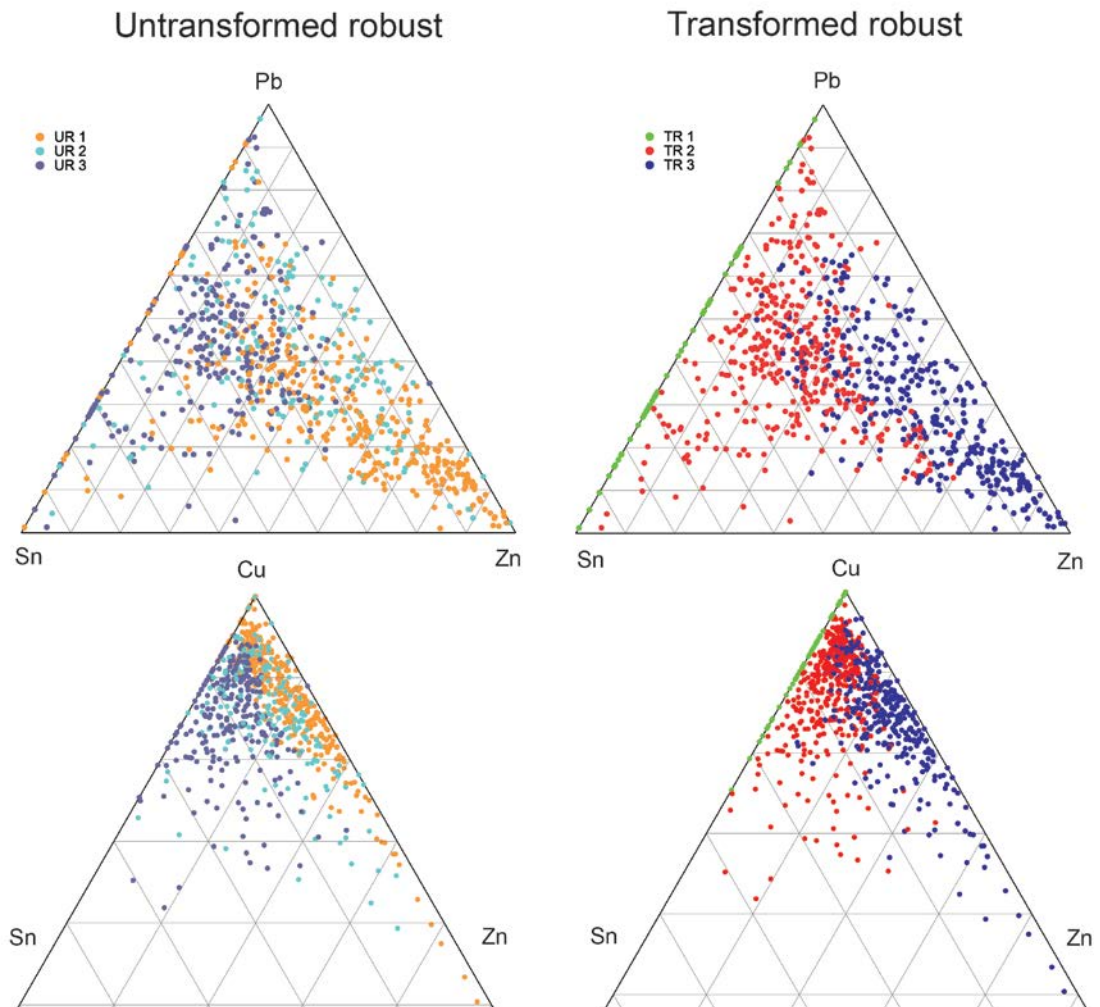


Figure 8-27: Ternary diagrams showing tin – lead – zinc (top) and the apex of a copper – tin – zinc diagram (bottom). Individuals are coloured according to cluster membership.

The untransformed clusters appear in the lead – tin – zinc ternary diagram as highly mixed with no clear pattern beyond cluster UR 3 tending to contain little zinc compared to the other two clusters. In the copper - tin - zinc diagram there is a little more clarity with UR 1 tending to be more ‘brass’ like than the other two. In contrast the transformed robust clusters appear to be offering a clearer insight. TR 1 is essentially a near bronze like composition (containing either very little or no zinc) whilst TR 2 is a mixed quaternary alloy and TR 3 – whilst mixed - leans towards being more of a brass like composition. There is, however, still a degree of crossover in the middle between TR 2 and TR 3 (perhaps to be expected given the noisy state of the data).

It appears that the untransformed robust PCA and clustering has delivered valid results, but they are relatively ‘one note’. It effectively describes the relationship between tin and copper, but fails to effectively distinguish differences when further elements from the alloy composition are considered. The transformed robust PCA and clustering is, in contrast, producing a more coherent series of groups that can help summarise and explain the alloy compositions more effectively. Consequently from here on the transformed robust cluster groups will be used for interpretation of the alloy data set.

8.7 CLUSTERS IN CONTEXT

The following section will provide a brief overview of the Eriswell clusters with a comparison to earlier studies and methodologies.

8.7.1 CLUSTERS IN A MAJOR CONTEXT

There have been three significant attempts to create typologies for early Anglo-Saxon copper alloys. These will be briefly discussed and compared to the Eriswell data in this section.

In 1991 Mortimer used data acquired from her analytical study of cruciform brooches (Mortimer 1990) to begin to develop a classification framework for Anglo-Saxon copper alloys. In this work there was a deliberate attempt to avoid the use of universal copper alloy typologies and to allow the alloys to delimitate themselves. The classification was descriptive and based on a scatterplot of the tin and zinc contents (these being approximately negatively correlated) with groups delimited by eye (1991, 105, Figure 1). Subsequent to the creation of the groups Mortimer introduced lead as a variable in the tin – zinc binary scatterplot by varying the individual point size according to lead content. When describing alloys as leaded Mortimer abandoned division by eye and set a content limit of 5 weight percent lead as the dividing line. The results of the inclusion of lead in the scatter plot showed no clear pattern. The description of her classification groups are reproduced in Table 8-39 below.

Alloy	Definition
Bronze	Copper alloyed with tin, with only small amounts of zinc present. A small number of bronzes were noted for their high tin and low zinc contents; those with tin contents of over 11% were given the type high-tin bronze.
Zinc bronze	Copper alloyed with tin, with significant amounts of zinc present.
Gunmetal	An alloy containing copper, tin and zinc.
Tin brass	Copper alloyed with zinc, with more than 1% tin present.
Brass	An alloy containing copper and zinc, with only small amounts of tin present (less than 1%).
Copper	An alloy with very little tin or zinc present (less than 4% of either element).

Table 8-39: Mortimer's (1991, 106) description of her copper alloy definitions.

In contrast to Mortimer, Blades (1995, 106) used a universal typology. Blades was producing a broad chronological piece of work that stretched from the Romano-

British period to the post-medieval, and consequently the use of a universal typology appears to have been dictated by the need to have comparable typology across all time periods. Blades' system eschewed grouping by eye and used a series of mathematical descriptions. These were a mixture of ratios (for tin and zinc) and absolute values (for lead content and 'impure copper') to be used as delimitating features. His descriptions are reproduced below in Table 8-40.

Alloy	Definition
Brass	Copper with zinc. Tin if present is less than one quarter the zinc content.
Bronze	Copper with tin. Zinc if present is less than one third the tin content.
Gunmetal	Copper with zinc and tin both present in significant amounts (i. e. exceeding the limits given above for brass and bronze).
'Leaded'	This term is applied to any of the above alloys containing more than 4% lead.
Impure copper	Copper with less than 5% total additions (i. e. zinc + lead + tin).

Table 8-40: Blades (1995, 126) description of his copper alloy definitions.

A universal typology was also the objective of Pollard et al. (2015) who used Blades' data set (along with many others) to examine broad chronological patterns during the first millennium CE in alloy types. Their approach differs from that of Blades and Mortimer in that they use much lower thresholds to define alloy categories in an attempt to avoid classifying by modern alloy definitions that are fixated on thresholds that impact on physical properties (2015, 699). A summary of Pollard et al.'s typology is reproduced in Table 8-41 below.

Alloy	Definition
Copper	Lead, tin and zinc each below 1%
Leaded copper	Tin and zinc below 1%, lead above 1%
Bronze	Zinc and lead below 1%, tin above 1%
Leaded bronze	Zinc below 1%, tin and lead above 1%
Brass	Tin and lead below 1%, zinc above 1%
Leaded brass	Tin below 1%, zinc and lead above 1%
Gunmetal	Lead below 1%, zinc and tin each above 1%
Leaded gunmetal	Lead, tin and zinc each above 1%

Table 8-41: Pollard et al.'s description of their copper alloy definitions (2015, 700, Table 2).

In Figure 8-28 binary scatterplots of tin and zinc are provided for Mortimer, Blades and Eriswell data sets. In each the classification of the individuals is shown according to the methodology defined for each. Plots of Blades' data set

are also reproduced with individuals identified according to Pollard et al.'s (2015) system and the HC on PCA used in this study (for information the PCA results are reported in Table 8-42 below). Binary plots are used here to allow visual comparison with Mortimer's method. A table with Blades, Pollard and TR groups and clusters for each Early Saxon copper alloy analysed by Blades can be found in Appendix XVIII on page 696.

		PC 1	PC 2	PC 3	PC 4	PC 5
Cu	Loadings (L)	0.1400	0.1930	-0.1693	-0.0478	0.8635
	Contribution (%)	1.9603	3.7235	2.8655	0.2283	74.5557
Zn	L	-0.8942	0.0355	-0.0962	-0.1286	-0.0819
	%	79.9553	0.1261	0.9261	1.6542	0.6716
Pb	L	0.1389	-0.8925	0.1303	-0.0193	0.0084
	%	1.9300	79.6622	1.6970	0.0371	0.0070
Sn	L	0.3549	0.2125	-0.2745	-0.6603	-0.3884
	%	12.5985	4.5163	7.5340	43.5974	15.0872
Sb	L	0.1591	0.1315	-0.4220	0.7267	-0.2907
	%	2.5326	1.7293	17.8061	52.8133	8.4521
Ag	L	0.1012	0.3200	0.8317	0.1292	-0.1107
	%	1.0233	10.2426	69.1713	1.6696	1.2265
Percentage of Variance		69.36	13.32	10.08	5.42	1.82
Cumulative Proportion		69.36	82.68	92.76	98.18	100

Table 8-42: Results of robust transformed PCA on Blades Early Saxon data set (1995, 86–97). Significant figures (those explaining over 10% of variance are in bold). Antimony and silver have been included to enable comparability with the Eriswell results.

Mortimer's method is entirely an expression of the variance in tin and zinc content (it should be remembered that the transformed robust PCA results on Eriswell and Blades showed tin and zinc to be most significant in explaining the variance in the respective alloy data sets). If creating groups that start from the position of modern alloy typologies then there are problems with this and, examining the Blades and Eriswell plots, it can be seen that there is crossover between groups as lead (and other elements) have played a lesser role in the classification (i.e. leaded variations overlay their non-leaded brethren). As a side note it is interesting to see that the Eriswell individuals have a relatively similar degree of distribution to Mortimer's and Blades' results: the majority of the individuals cluster around the tin baseline with a scatter of decreasing intensity as zinc content increases.

Below, in Figure 8-29, tin – zinc – lead ternary diagrams of Blades’ data are provided with his original groupings, Pollard et al.’s groupings and with individuals identified by clusters produced after robust transformed PCA and HC. The PCA and HC were undertaken using the procedures outlined earlier (zeros replaced etc.). To enable comparability with the Eriswell clusters the data was subset and consisted of copper, tin, zinc, lead, silver and antimony (remembering that the co-variances will remain stable when the data is subset).

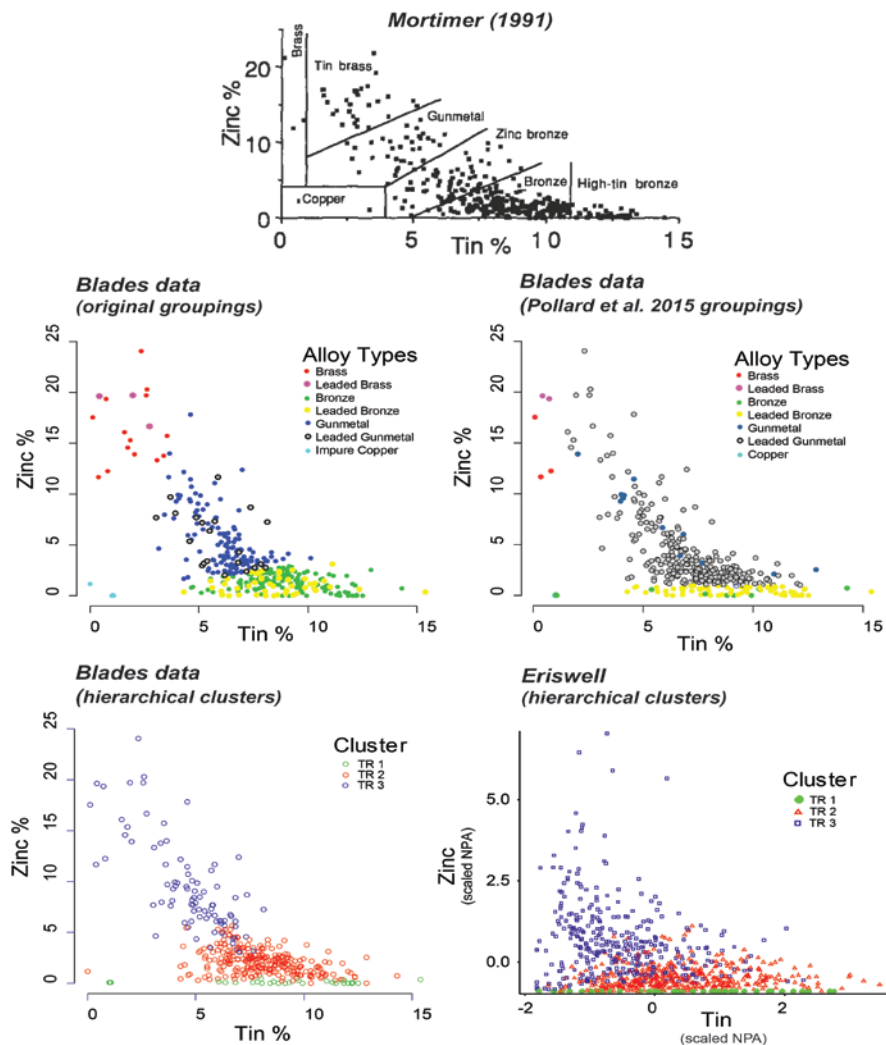


Figure 8-28: Comparison of alloy classification systems in tin – zinc scatterplots. The top plot (Mortimer 1991, 105, Figure 1) shows Mortimer’s classification system (reproduced in Table 8-39) based on her analysis of cruciform brooches (Mortimer 1990). The middle left, right and bottom left all show Blades’ Early Saxon data (1995, 86–97) classified according to his alloy types (reproduced in Table 8-40), Pollard et al.’s alloy types (reproduced in Table 8-41) and the hierarchical clustering used in this study respectively. On the bottom left is Eriswell (scaled and using the zero replaced data) with classification derived from the hierarchical clustering.

The ternary diagram of Blades groupings shows that, for the most part, the groups are coalescing into what appear to be coherent blocks. A closer examination does raise some questions however; and the tight boundaries between bronze / leaded bronze and bronze / gunmetal do make one wonder if strict definitions of compositions are drawing false boundaries. A similar issue can be seen in the Pollard et al. groups (for instance in gunmetal / leaded gunmetal and gun metal / leaded brass). Both Mortimer (1991, 105) and Pollard et al. (2015, 699) were concerned about the impact of applying modern metallurgical definitions and understandings to past alloys and both sought to minimise the impact of imposing classifications on past alloys. Yet both — along with Blades — are still using the terminology of the modern metallurgist. It may be argued that, despite best efforts, there is still an undeniable and false impact of this terminology (for, despite even the best efforts, it is indescribably difficult to avoid inserting one's own perspective when using contemporary terminology that — to some extent — controls the way one thinks).

When you examine the distribution of the alloys in both Blades and Eriswell data sets one of the first things that comes to mind is that there is little in the way of distinct and *discrete* groupings: the alloys are distributed as a continuum. Consequently it may be argued that any division that uses modern terminology as a starting point of reference — no matter how aware you are of the dangers of using modern terminology and how you try to mitigate the impact — is likely to create false divisions. Using HC on the PCA does — to a certain extent — alleviate this. Whilst the analyst is (of course) making decisions and choices based on their knowledge and experience (and the constraints of the statistical techniques chosen) there is also a degree of allowing alloys to define themselves: variance is as variance does.

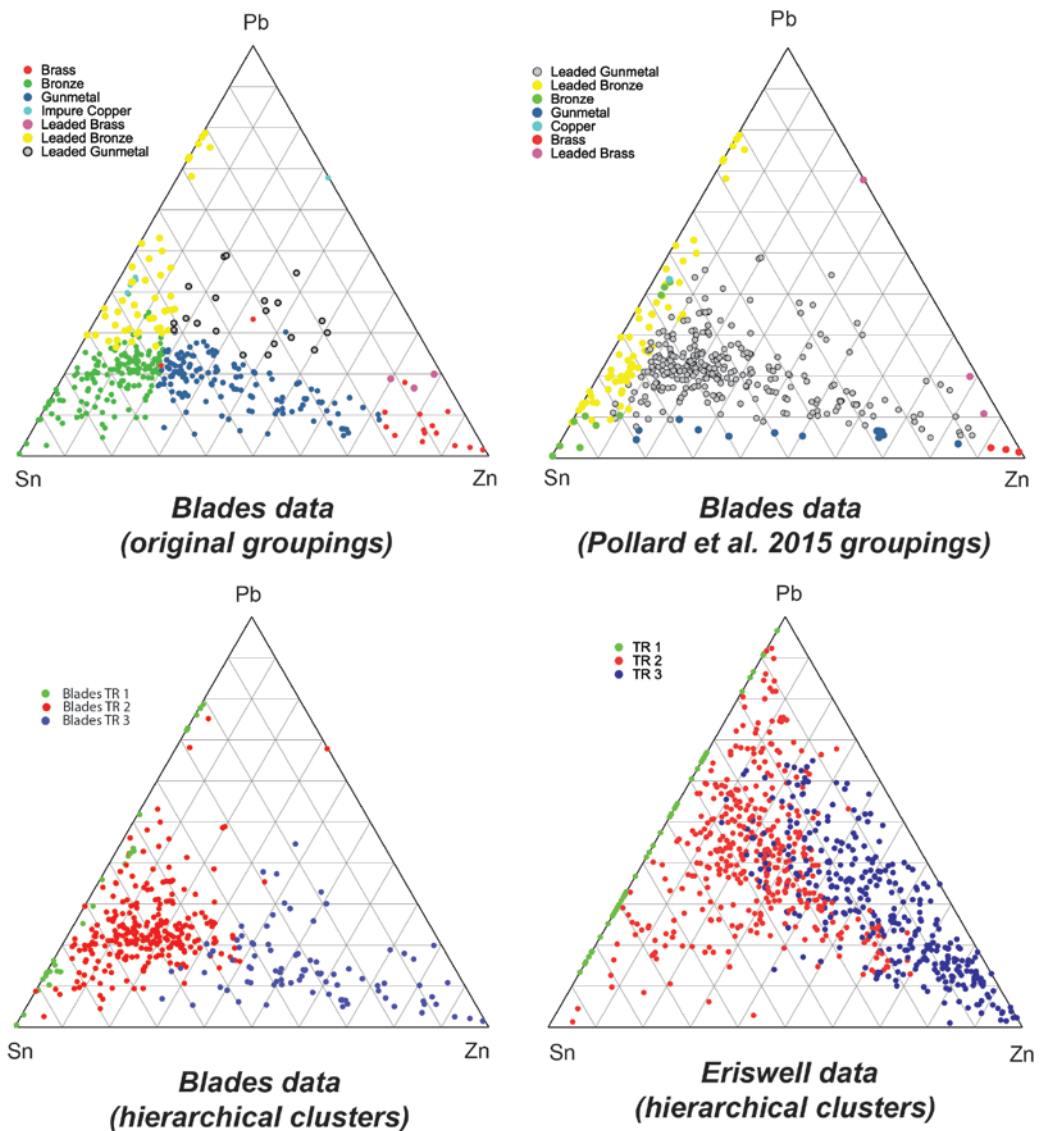


Figure 8-29: Tin – zinc – lead ternary diagrams. On the top left is Blades’ Early Saxon data (1995, 86–97) classified according to his alloy types (reproduced here in Table 8-40) and on the top right is the same data but with individuals identified classified according to Pollard et al.’s (2015, 700, Table 2) definitions (reproduced here in Table 8-41). The bottom left diagram shows individuals identified by clusters produced after robust transformed PCA and HC was performed on Blades data (using the processes outlined earlier). On the bottom right the Eriswell data is provided for comparison, again with individuals identified by clusters derived from the HC.

An example of this can be seen in the parallel coordinate plots of Blades data in Figure 8-30 in which each individual is identified by group / cluster membership (Blades, Pollard et al.’s and hierarchical clusters). In the first two plots a high copper individual can be seen (Blades analysis number 256). This was characterised as an impure copper by Blades and copper by Pollard et al. (the only copper they identified in Blades data set). Yet in the hierarchical clustering it is not separated out by its copper content, but by its near absence of zinc. The

decision to group as such by Blades and Pollard et al. was a choice based on preconceived perceptions of alloy types. In contrast in the clusters its assignment is based on an element which has been deduced to be significant in explaining significant variance in the data *not* on a preconceived choice of what an alloy should be.

This should be countenanced with an understanding that — with longitudinal studies — the Blades and Pollard et al. approach is more appropriate than using clusters. To understand variation over large cultural *and* chronological periods then a common linguistic metallurgical terminology is required (it should be also remembered that these names can represent very real differences in the physical alloys) and it is only through such approaches that we can determine changes such as the decline of brass (as discussed earlier in chapter 2 and also in Pollard et al. 2015, 703)

The clusters produced from the robust transformed PCA on the Blades data show an approximate distribution similar to the Eriswell set: TR 1 is a relatively pure bronze, TR 2 a more mixed bronze and TR 3 towards the brass end of the spectrum. In both there are occasional visual outliers, whose cluster or group membership may seem odd with the location in which they sit. This is to be expected as the diagrams are only expressing three parts of the compositions, leaving other elements (such as copper) which have contributed to the grouping or clustering choices unexpressed.

It is interesting to note at this juncture how, when we compare the Blades and Eriswell distributions in the ternary diagrams (Figure 8-29) and the parallel coordinate plots (Blades in Figure 8-30 and Eriswell in Figure 8-25), the individuals are relatively similarly distributed and the clusters are in agreement in how they interpret the assemblages. There are of course differences: the Eriswell assemblage appears to contain more lead than those sites analysed by Blades. It is suspected that this is unlikely to be a real feature of the Eriswell assemblage, but a function of the analytical approach (i.e. due to corrosion processes and analysing the corroded surface). Despite this difference, the HC transformed

clusters appear to be (approximately) describing early Anglo-Saxon alloys in a comparable manner even though the data were acquired and processed in very different ways. This last is particularly significant and suggests that, despite the concerns expressed at the start of Chapter 4 (page 182), approaching the NPA data with a compositional framework (i.e. using a clr transformation) is an appropriate approach.

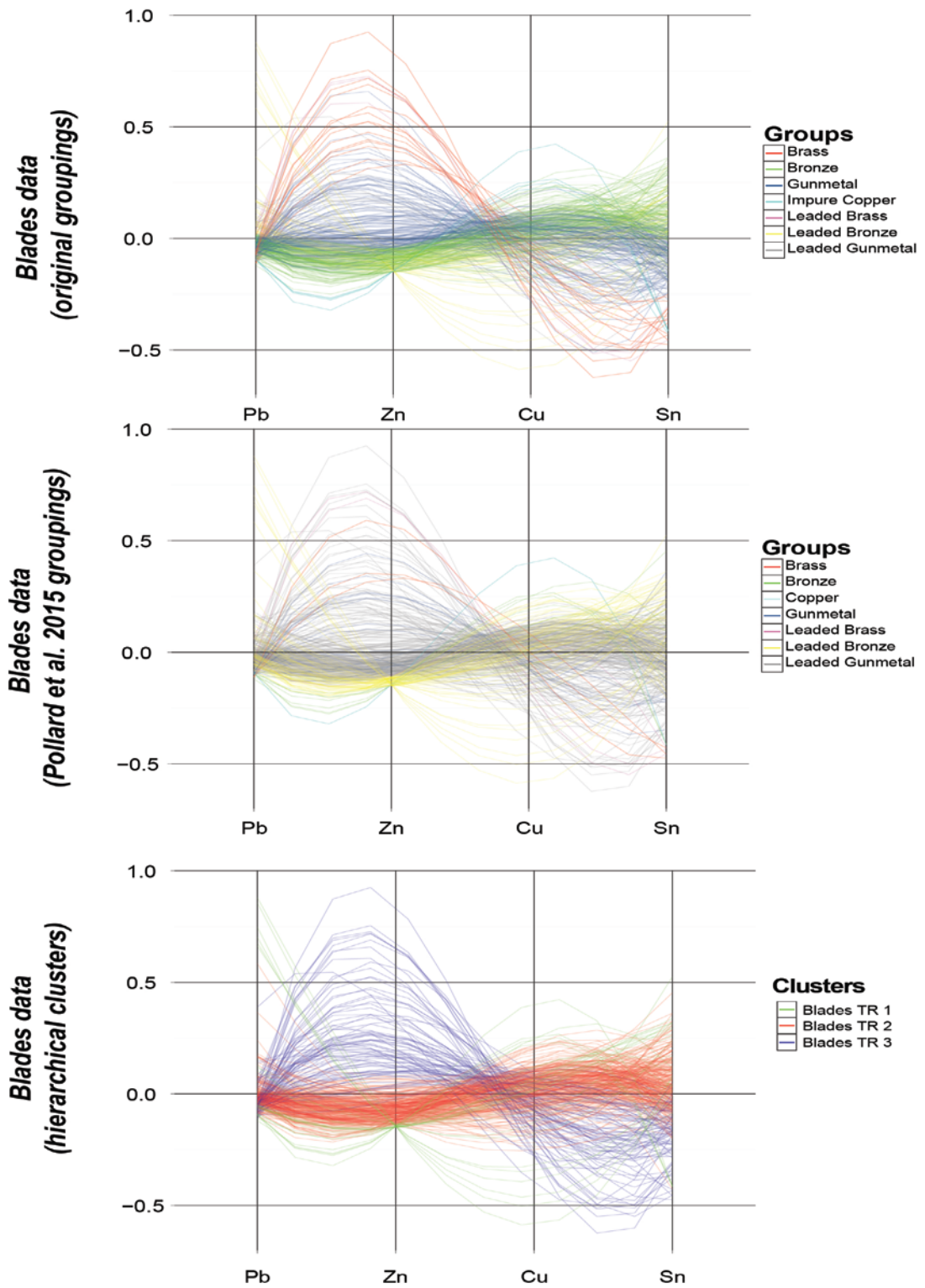


Figure 8-30: Parallel co-ordinate plots of Blades' Early Saxon data (1995, 86–97) showing the variables scaled and centred with individuals colour coordinated according to group membership as follows: top - Blades groups, middle - Pollard et al.'s (2015) groups, bottom – hierarchical clusters . Missing values are plotted at 10% below the minimum of the variable for the missing value and the variables are ordered from left to right by skewness. The variables have been scaled univariately with a maximum of 1 and centred.

With compositional data approaches in mind it is worth considering briefly the absolute prescriptive elements of Mortimer, Blades and Pollard et al.'s classification systems. All three use the percentage of specific elements (or combinations of elements) at various points to delimitate groups and depending on how the data is processed this can be problematic. As an example in Table 8-43 the results of an analysis on a wrist clasp from Morning Thorpe (Blades analysis number 351) are shown as reported by Blades (1995, 91) and normalised. Normalisation — a relatively common process in metallurgical studies — is often used to help comparability between different results which do not sum to 100%. However, when absolute values are used to define groups, normalisation can cause classification shift. This can be seen in the example below where normalisation shifts the weight percent of lead across the 4% boundary that Blades set for describing an alloy as leaded: the object is no longer gunmetal, it is leaded gunmetal. Similar issues can be expected with Blades' 'impure copper' classification (tin, zinc and lead add up to less than 5%), Mortimer's leaded classification (over 5% or more lead present) and Pollard et al.'s 1% boundary used for all classifications.

	Reported results	Normalised
Cu	84.1	84.56
Zn	3.51	3.53
Pb	3.99	4.01
Sn	6.99	7.03
Fe	0.21	0.21
Ni	0.03	0.03
As	0.03	0.03
Bi	0.02	0.02
Sb	0.23	0.23
S	0.1	0.1
Ag	0.25	0.25
Total	99.46	100.00
Type	Gunmetal	Leaded Gunmetal

Table 8-43: Showing the reported and normalised results (weight percent) from Blades' analysis (Blades analysis number 351) on a wrist clasp from Morning Thorpe (1995, 91). Note that normalised the lead crosses the 4% threshold set by Blades for distinguishing between leaded and unleaded alloys.

The reader will remember that in the introduction to Chapter 4 it was discussed that the key component of a compositional approach is the understanding that

absolute values do not matter; it is the ratios that are significant. By focussing on absolute values the previously discussed classification systems run into a possible issue as they are not technically compositionally coherent. This can be easily rectified however by using ratios instead of absolutes. Blades already does this for tin and zinc contents (see Table 8-40) and it is a relatively simple matter to adjust the remainder of the rules to ratios (in all three cases the ratios would be set against the total of the data rather than a specific element, i.e. 5:20 for Mortimer's lead, 1:25 for Blades' lead and 1:100 for Pollard et al.'s boundaries). With such an adjustment the boundaries become more responsive to the realities of the data type (i.e. changing all values to ppm would require no adjustment of any formula used to calculate groupings) and mathematical realities (rounding errors etc.).

8.7.2 CLUSTERS IN A MINOR CONTEXT

Earlier (on pages 348 and 352) the dropping of a number of minor and trace elements from the statistical evaluation was discussed. These elements were not completely discarded but reduced to binary variables based on their presence or absence and played no part in the PCA. At this juncture they will be reintroduced and assessed against the groups determined by hierarchical clustering using Multiple Correspondence Analysis (MCA). The MCA was undertaken using the R package 'FactoMineR' (previously used for some implementations of PCA).

Figure 8-31 shows a biplot of the first two components of an MCA analysis of arsenic, nickel, gold, cobalt and bismuth and the transformed robust clusters. Examining the diagram it becomes apparent that there is little structure to the distributions and that the majority of individuals are associated with the failure to detect trace and minor elements (a jitter has been added to make the individuals more visible, otherwise the majority overlap and appear singular) with little obvious relationship to the clusters. The main groups (TR 2 and 3) sit in the centre whilst the presence and absence of the arsenic and nickel sit astride them without revealing any particular structure to the distribution. The TR 1 cluster may appear to be of some interest; being definitively on the 'no' side of arsenic and cobalt and possibly associated with a gold presence, but it must be

remembered that it is a small group and that care must be taken not to over-interpret.

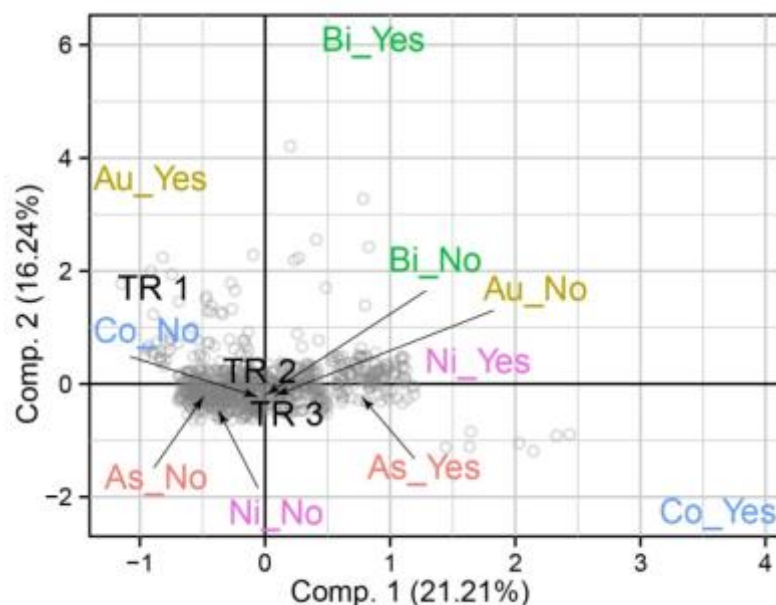


Figure 8-31: MCA biplot of clusters and minor element presence ('yes') or absence ('no'). A jitter has been added to make the individuals more visible, otherwise the majority overlap and appear singular

An alternate approach is that may prove more fruitful is to group using ubiquity analysis. Recently ubiquity analysis has been used to assess trace elements associated with copper (arsenic, antimony, silver and lead) as binary variables based. A technique usually associated with palaeobotany and zooarchaeology (VanDerwarker 2010, 65–66), ubiquity analysis is a presence / absence procedure of grouping variables to assess the frequency of occurrence. Its novel application to early medieval archaeometallurgical studies by Pollard et al. (2015, 706–711) demonstrated how the technique could simply and effectively be used to throw light on trace elements and the metallurgy of the period.

In Table 8-44 below is a reproduction of Pollard et al.'s trace element groups and the percentage of Early Saxon objects from Blades' data set that they identified as belonging to each. As a comparison the number and percentage of Eriswell objects is also presented. There are some similarities between the groups (such as the popularity of CC7) but generally there is poor agreement. Unfortunately it is not possible to ascertain if this is a real difference. The focus of this project has been on gaining a broad understanding of neither the metallurgical choices made

by the early medieval peoples of Eriswell, not the mining site of the metals nor smelting choices of earlier cultures. As such a ‘broad brush’ analytical methodology has been used that does not have any way near comparable sensitivity or accuracy for trace and minor elements when compared to Blades. Consequently it is unsafe and unwise to draw any direct comparisons between the Eriswell NPA data and the trace groups identified by Pollard et al. from Blades’ data.

Pollard et al. trace groups	Element Presence / Absence				Blades	Eriswell	No. of objects
	<i>As</i>	<i>Sb</i>	<i>Ag</i>	<i>Ni</i>	%	%	
CC1	N	N	N	N	3.7	0.8	6
CC2	Y	N	N	N	0.3	0.5	4
CC3	N	Y	N	N	28.9	0.1	1
CC4	N	N	Y	N	5	16.1	126
CC5	N	N	N	N	0.3		0
CC6	Y	Y	N	N	0.3	0.1	1
CC7	N	Y	Y	N	48.3	33.8	264
CC8	N	N	Y	Y	0	1.3	10
CC9	Y	N	Y	N	0.5	8.2	64
CC10	N	Y	N	Y	1.1		0
CC11	Y	N	N	Y	1.3		0
CC12	Y	Y	Y	N	4	22.2	173
CC13	N	Y	Y	Y	0.5	0.4	3
CC14	Y	Y	N	Y	1.6		0
CC15	Y	N	Y	Y	0.3	1.9	15
CC16	Y	Y	Y	Y	2.1	14.6	114

Table 8-44: Pollard et al.’s (2015, 708–9, Tables 5 & 6) trace element groups and the percentage of Early Saxon objects they found in Blades (1995) data. The final two columns show the number and percentage of objects from Eriswell that fall into the same categories. The Eriswell details are provided for interest only and should not be considered valid.

8.7.3 CLUSTERS AND TYPOLOGIES

The previous two sections have focussed on placing the cluster results in a wider context using data from comparable cultural groups and chronological periods. This next section will turn inwards and assess the clusters against the categorical variables for the Eriswell assemblage.

In Figure 8-32 below the results of a correspondence analysis between manufacture method and cluster type is shown. Intriguingly it suggests some relatively clear relationships between the two. Cluster TR 2 (tends to have a high

tin content, low to medium zinc content with lead varying) is associated with cast objects. Meanwhile cluster TR 3 (which tends to contain more zinc than the other two clusters) is associated more with wire and sheet metalwork. Cluster TR 1 (which is contains little to no zinc and is close to a bronze or leaded bronze composition) tends to be associated more with melted objects.

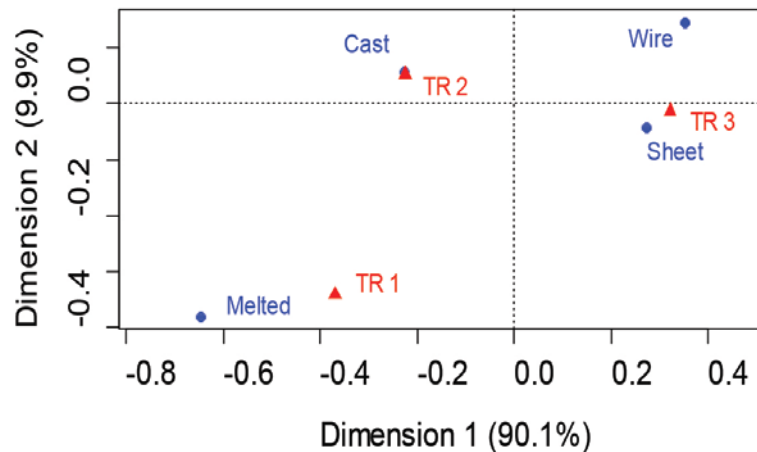


Figure 8-32: Results of a correspondence analysis between manufacture method and hierarchical clusters on the Eriswell data set.

The relationships between the clusters and manufacture methods are intriguing and something of a surprise as it would appear to contradict previous conclusions about the nature of the early Anglo-Saxon metallurgy: that we are dealing with a ‘metallurgy of survival’ and there is no choice or control being exercised. However, one should be wary of over interpreting this: manufacturing types are still mixed and not solely composed of one cluster. In reaching such a conclusion there is also the issue that we may have jumped the gun in deciding that the alloy cluster type is linked to a choice made before production. Alternatively it could be informing us about decisions made during production. It is possible that the lower zinc in cast objects is due to zinc volatilisation when melting alloys to cast them anew. Dungworth (1995, 133–134) undertook experimental melting of brass alloys (with no lids on the crucibles) and noted that the zinc loss could be substantial (up to 40% dependent on temperature and time). Baker (2013, 92), who modelled early medieval copper alloy recycling following Caple’s similar work (1986) and incorporating Dungworth’s

experimental discoveries, settled on a relative loss of 10% of zinc for each melting incidence (and the loss of 1% tin). Using this, and starting with a series of eight hypothetical source alloys (including recycled Roman scrap and fresh brasses), allowed Baker to produce a series of hypothetical compositions that matched the general distribution of early Anglo-Saxon copper alloys with regards to tin and zinc content (Baker 2013). We must therefore be aware that cast objects may tend to have lower zinc contents and higher tin contents because of zinc volatilisation during melting. If this was the case it might also indicate that sheet metal did not tend to undergo melting, but may have been scrap sheet metal that was simply re-forged and did not undergo a re-melting.

Truly understanding this process is, unfortunately, difficult. We have little archaeological evidence for working practices and consequently we have little idea how any re-melting occurred; type of crucibles, lidded or not etc. are questions that we cannot currently answer. We cannot adequately explain with any certainty why sheet metal objects may be richer in zinc and cast richer in tin.

The basic interpretation of the CA can be confirmed by looking at a simple bar chart of manufacturing against clusters (Figure 8-33, data in Table 8-45).

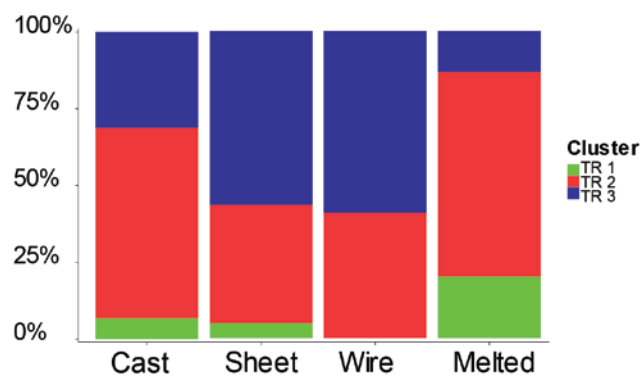


Figure 8-33: Bar chart of clusters and manufacturing method. For the raw figures see Table 8-45.

	TR 1	TR 2	TR 3	Total
Cast	25	231	117	373
Melted	6	20	4	30
Sheet	17	135	198	350
Wire		11	16	27
Total	48	398	335	780

Table 8-45: Manufacture method and cluster membership. For a bar chart of the data see Figure 8-33.

the bottom left of Figure 8-34 and made of wire) and Form B 12 (associated with cluster TR 2 in the bottom right of Figure 8-34).

Wrist clasp type	Cluster			<i>Total</i>
	TR 1	TR 2	TR 3	
Form A			4	4
Form B	1			1
Form B 12		4		4
Form B 13 a		6	7	13
Form B 13 c		3	9	12
Form B 17 a		3	2	5
Form B 18	1			1
Form B 20		6	4	10
Form B 7		9	8	17
Form C 1	3			3
Undefined Wrist Clasp	3	18	15	36
<i>Total</i>	8	49	49	106

Table 8-46: Number of wrist clasps by hierarchical cluster type.

Blades (1995) does not use Hines' (1993) wrist clasp typology (as is used here), so a direct comparison is difficult, although we can broadly compare across sites.⁸¹ In Table 8-47 the number of wrist clasps from each site that Blades analysed is displayed by cluster type with Eriswell as a comparison. As can be seen there is variation between the sites with only Bergh Apton and West Heslerton sharing in common with Eriswell the production of wrist clasps using cluster type TR 1.

Site	Cluster			Total
	TR 1	TR 2	TR 3	
Bergh Apton	4	3	2	9
Empingham		3	4	7
Morning Thorpe		13	2	15
Spong Hill		10	1	11
West Garth Gardens		4		4
West Heslerton	3	2	5	10
<i>Eriswell</i>	8	49	49	106

Table 8-47: The number of alloy cluster types used for the production of wrist clasps analysed by Blades (1995). Eriswell is provided for comparison at the bottom of the table.

⁸¹ There are also no accession numbers (quite probably because the objects had not been accessioned or catalogued) and infrequent find numbers / codes (most likely because of the excavation methodologies), making it difficult to match up the analyses with the site catalogues.

In Figure 8-35 below the CA is repeated, but with the three TR 1 associated wrist clasp types (Form C 1, Form B and Form B 18) excluded to enable easier visualisation of the remaining mass of object sub classes.

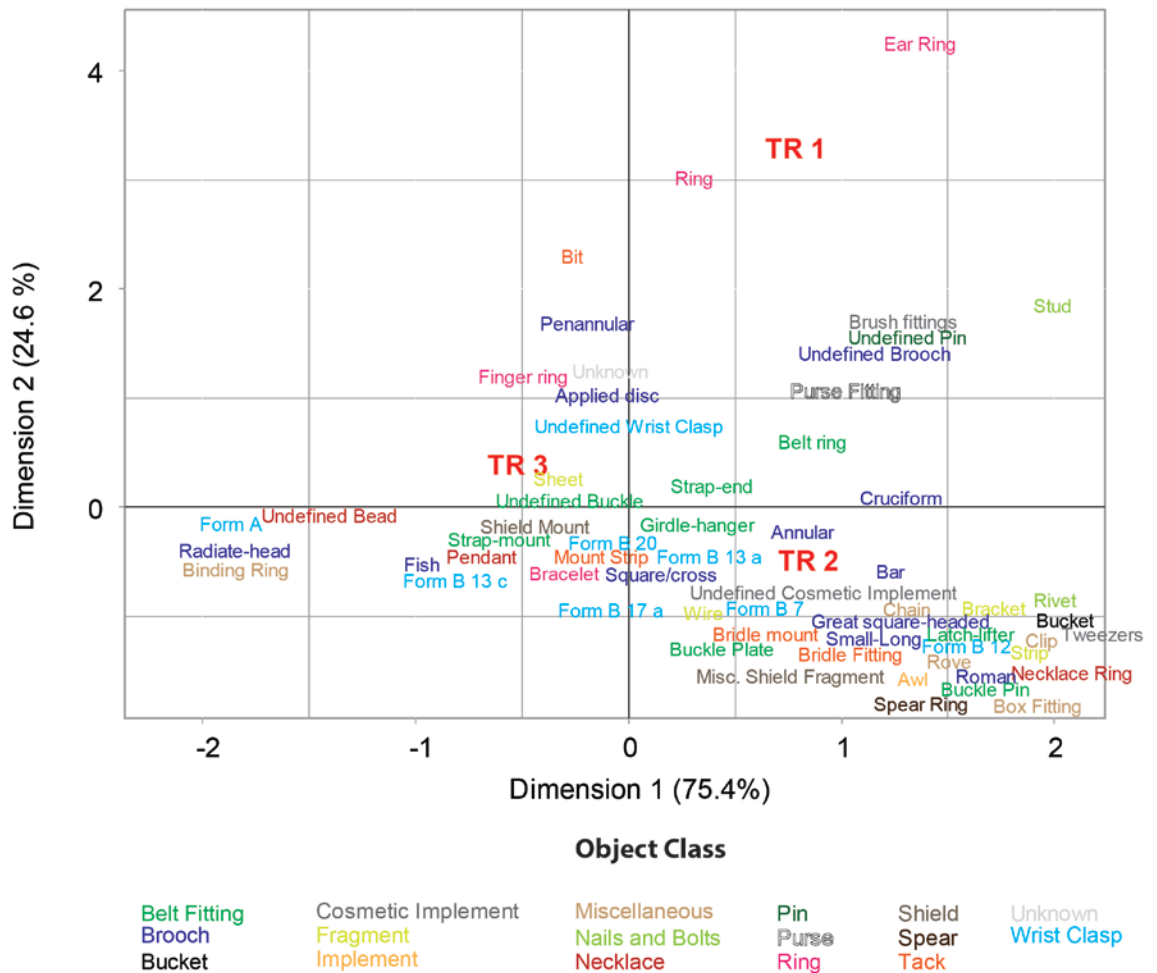


Figure 8-35: Results of a correspondence analysis between hierarchical clusters and object sub class on the Eriswell data set excluding wrist clasp forms Form C 1, Form B and Form B 18. The object categories are colour coded according to object class membership.

8.7.3.2 BROOCHES

Although the plot may appear confusing at first there are several useful conclusions to be drawn. Many of the brooches appear associated with cluster type TR 2. A table of brooch sub classes and clusters supports this (Table 8-48), with 61% of all brooches being assigned to TR 2. This, however, is not the whole story. The largest sub class of brooch present in the Eriswell assemblage are annular. Annular brooches are one of the few object types produced in both cast and sheet forms. In Table 8-49 below a breakdown by manufacturing method is

provided and it can be seen that cluster TR 3 is (slightly) preferred for the manufacture of sheet metal annular brooches whilst TR 2 is preferred for the cast equivalents. Nigel Blades analysed a large number of annular brooches (125). Unfortunately he did not provide any details on the manufacturing methods used.⁸² Nevertheless a comparison of the alloy types used at each of the sites he analysed is provided in Table 8-50. It can be seen that there is significant variation between the sites and it would be interesting to know if this is linked to different manufacturing techniques at different sites (i.e. are annular brooches from Empingham predominantly made out of sheet metal?).

Brooch Sub Class	Cluster			Total
	TR 1	TR 2	TR 3	
Annular	5	65	41	111
Applied disc	1	3	7	11
Bar		1		1
Cruciform	5	35	6	46
Fish		1	3	4
Great square-headed		3	1	4
Penannular	1	2	2	5
Radiate-head			1	1
Roman		3		3
Small-Long		8	1	9
Square/cross		1	1	2
Undefined Brooch	2	6	2	10
Total	14	128	65	207

Table 8-48: Number of brooches by hierarchical cluster type.

Annular brooch manufacture method	Cluster			No. of objects
	TR 1 (%)	TR 2 (%)	TR 3 (%)	
Cast	6	62	32	87
Sheet		40	60	22

Table 8-49: Showing the percentage of annular brooches by manufacture method in each cluster. The final column shows the actual number of objects.

It would be particularly interesting to compare the annular brooch results with the penannular brooches. However; there are only five penannular brooches analysed (Table 8-48) and, whilst there appears to be a similar degree of distribution, one must maintain a degree of caution.

⁸² It should be possible to reunite the analyses with the individual brooches to enable one to calculate this. Unfortunately there was not the time to undertake this in this project.

Site	Cluster			No. of objects
	TR 1 (%)	TR 2 (%)	TR 3 (%)	
Bergh Apton	10	90		10
Empingham		33	67	6
Morning Thorpe		86	14	56
Spong Hill		89	11	18
West Garth Gardens		100		4
West Heselton	16	55	29	31
Eriswell	5	59	37	111

Table 8-50: The percentage of the alloy types used for the production of annular brooches analysed by Blades (1995). Eriswell is provided as a comparison at the bottom of the table. Blades did not provide any details of the manufacturing processes used on the objects he analysed so it is not possible to provide a breakdown by cast and sheet.

It is interesting to note the cruciform brooches are almost wholly associated with cluster TR 2. Cruciform brooches were the sole type of artefact upon which Mortimer began to develop her classification and interpretation of early medieval copper alloys. Mortimer was explicit about the limits of using a data set composed of results from a single cast object type to draw conclusions about alloy design and choices (1991, 105). Nevertheless a narrative of collapse and lack of choice (Fleming 2012) has taken hold and dominates discussion. Yet, as we can see here, Mortimer's concerns were well founded as cruciform brooches are predominantly represented by one cluster type and are not representative of the full range of copper alloys in use.

Bead manufacture method	TR 2	TR 3	Total
Cast	2	1	3
Sheet	9	79	88
Total	11	80	91

Table 8-51: Showing number beads by manufacture and cluster type.

8.7.3.3 BUCKET PENDANTS

In the previous two CA plots beads were one of four object sub classes to be linked almost exclusively with cluster TR 3. The other three objects it shares this distinction with are extremely small and distinctive groups (one radiate headed brooch, one binding ring and four Form A wrist clasps). In contrast there are 91 beads (summarised by manufacture and cluster type Table 8-51) meaning that this association is of significant interest.

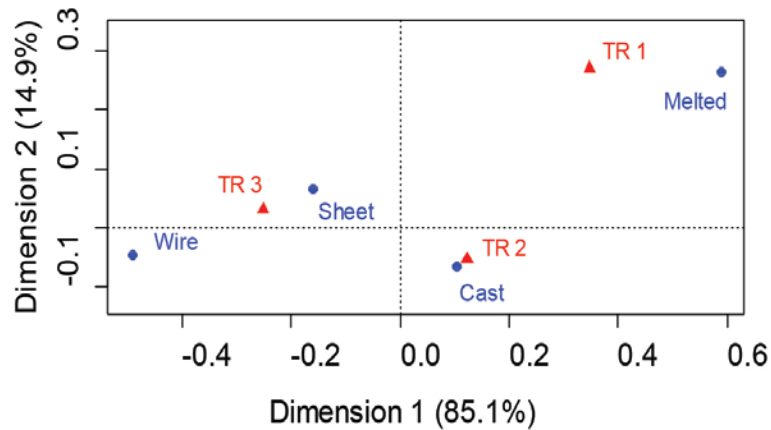


Figure 8-36: Results of a correspondence analysis between manufacture method and hierarchical clusters on the Eriswell data set with all beads excluded. See Figure 8-32 for the same plot with beads included.

As can be seen nearly 90% of sheet beads (predominantly bucket beads or bucket pendants, see Table 8-53) are made out of a cluster TR 3 type of alloy (these 79 beads represent 23% of all sheet metal objects from Eriswell). Indeed, so significant are the beads that their exclusion from the dataset before undertaking CA significantly weakens (but does not break) the relationship between cluster TR 3 and sheet metal (see Figure 8-36).

Object Class	TR 1	TR 2	TR 3	No. of objects
	%	%	%	
Bead		12	88	91
Belt Fitting	4	61	34	70
Brooch	7	62	31	207
Buckle	2	49	49	47
Cosmetic Implements	8	83	8	12
Miscellaneous	10	53	37	59
Nails and Bolts	17	83		12
Necklace	3	41	55	29
Ring	14	41	45	22
Tack	3	62	35	37
Unknown	13	41	46	46
Wrist Clasp	8	46	46	106

Table 8-52: Showing the percentage of objects by category and their cluster membership. The final column shows the actual number of objects. Only those object classes with 10 or more objects are displayed here.

Beads are different; not in their metallurgy but in the near singular use of a single alloy type. No other class of object (with 10 or more objects analysed) leans so heavily in favour of one cluster (see Table 8-52). This includes other object classes where the majority of the objects are sheet metal, suggesting their

difference is less to do with being made of sheet metal but because of the object typology itself. Is there something different about bucket beads (which all the sheet beads are)?

	TR 2 %	TR 3 %	No. of Objects
Bucket pendants	6	94	70
Other beads	33	67	21
Total	12	88	91

Table 8-53: The percentage of bucket pendants and other bead types by cluster.

Bucket beads are complex little objects composed of three separate pieces of sheet metal sheet: the hoop (from which it was suspended), the bucket side (a cylinder) and a base. All three components are soldered together. There is some suggestion that, at least in continental Europe, the beads may have contained sweet smelling animal fats (Eckardt 2014a, 44).

Bucket beads — whilst not common — are a relatively frequent occurrence in early medieval cemeteries, having been discovered in burials at Bergh Apton (Green 1978), Harford Farm, Holywell Row (Geake 1995, 94, 100), Nassington (Leeds and Atkinson 1944), Norton Cleveland (Sherlock and Welch 1992) and West Heslerton (Haughton and Powlesland 1999).⁸³ As an artefact category they are often — in the Roman period — associated with north and eastern

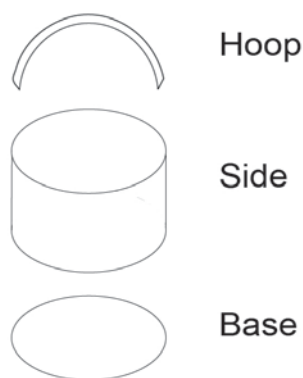


Figure 8-37: Schematic diagram of a bucket bead.

continental Europe cemeteries (specifically present day Denmark, Germany, Hungary, Poland, Romania and the Ukraine) (Eckardt 2014b). In Britain — in post-Roman and early medieval burial contexts — they are generally considered as representative of a different culture and possibly demonstrative of either strong cultural influence or physical movement of individuals (Hines 1984, 13; Montgomery et al. 2005) as they are exceptionally rare in Roman burials (Eckardt 2014a, 43–45).

⁸³ In the literature the cemetery at Eastry Updown (Welch 2008) is often noted as containing bucket pendants. Recent work has suggested that this is a misclassification (pers. comm. Professor John Hines).

However; it should be noted that their distribution during the Roman period is so varied and covers so many different archaeological cultures beyond the borders of Rome that some (Greene 1987; Eckardt 2014a, 42) have raised significant questions as to their usefulness as an indicator of ethnic or cultural identity. Nevertheless it is inescapable that they are rare in the British Isles during the Romano-British period and more frequent after, raising the tantalising potential that cultural identity may, in certain circumstances, be intrinsically linked to metallurgical choices.

The Eriswell results tilt alluringly in this direction. Unfortunately there is a lack of corroborating analyses from comparable assemblages (none were analysed by Blades although they were present in two of the assemblages — Bergh Apton and West Heslerton — that he analysed). Indeed, bucket beads have been the subject of such little study that they are, perhaps, the only Anglo-Saxon non-ferrous dress accessory that returns less than a dozen results on Google Scholar (in English). Consequently — and sadly — it cannot be certain that the result here is not an isolated example or something more mundane.

8.7.3.4 BUCKETS

There was one ‘proper’ copper-alloy bound bucket in the assemblage (there are other iron bound buckets in the assemblage): 1306 from ERL 046. This was received for analysis relatively late in the analysis stage of this study (conservation necessarily and rightly taking a priority). As a result there was not enough available time to ascertain if each horizontal band (overlain by vertical bands and with well-preserved wood attached) was a single piece or several individual sections riveted together (rivets were visible at each horizontal / vertical intersection). Consequently each was treated as (potentially) being a separate piece.

All pieces of the bucket analysed belonged to the same cluster and all had relatively similar results. Indeed when amalgamated the coefficient of variation between each area (Table 8-54) is less than it is from some objects where the results were definitely amalgamated from a single object (such as 046-1068-A).

ID	Cu	Pb	Sn	Zn	Cluster
046-1306-A	2445736	238236	127035	65261	TR 2
046-1306-B	2412608	200728	117818	74997	TR 2
046-1306-C	2624373	61533	106474	187736	TR 2
046-1306-D	2445736	238236	127035	65261	TR 2
046-1306-E	2445736	238236	127035	65261	TR 2
046-1306-F	2587925	190545	123828	111643	TR 2
046-1306-G	2445736	238236	127035	65261	TR 2
Coefficient of Variation	0.03	0.32	0.06	0.51	

Table 8-54: Analysis of bucket SF 1306 from ERL 046. The coefficient of variation provided is across the amalgamated analyses presented above. Major elements only. For full results see Appendix XV on page 584.

This leads one to suspect that it is either one piece or several sheets produced at a similar/the same time. Most interesting about the result is the cluster: all belong to TR 2. Blades (1995) also analysed three buckets (Morning Thorpe - analysis no. 207; West Heslerton - analysis no. 290; Spong Hill - analysis no. 411) which were also all from cluster TR 2.

Full sized buckets are different from their miniature brethren, suggesting that — whilst there may have been a preference for the use of different alloys based on fabrication techniques — this was not necessarily an overriding concern. Moreover it is a stark reminder that, whilst it is tempting to focus on modern metallurgical typologies and their perceived technological limits, the early medieval craftsperson was perfectly capable of producing objects (items good enough to survive a millennia or so) with alloys that would be considered unsuitable today for the form and function today.

8.7.3.5 TACK

Of course it was not a bucket that captured the imagination when the Eriswell cemeteries were excavated. It was the horse and warrior burial from ERL 104 (grave no. 323). In contrast to the buckets (big or small) there is a much more mixed approach to the alloys used. All three alloy clusters make an appearance (see Table 8-55), perhaps suggesting that this was not a set produced in a single event.

Of more interest is the fact that, where more than a couple of objects are involved (i.e. both cast and sheet bridle fittings), TR 2 is the most populous

cluster. This is not surprising as this cluster type appears to be most frequent with object types that are, in modern terms, typologically considered as being of most interest (i.e. the majority of brooch types, excluding annular brooches) and potentially elite.

The equestrian gear from grave 323 is considered in further detail on page 418.

Equestrian Sub Class	Manufacturing method	Cluster			No. of objects
		TR 1 (%)	TR 2 (%)	TR 3 (%)	
Bit	Cast	50	50		2
	Sheet			100	2
Bridle fitting	Cast		71	29	21
	Sheet		75	25	4
Bridle mount	Cast		67	33	3
	Sheet		100		1
Strap-mount	Cast			100	1

Table 8-55: Showing the percentage of equestrian object from grave 323 (ERL 104) by object sub class, manufacturing method and cluster membership. The final column shows the actual number of objects.

8.7.3.6 GIRDLE-HANGERS

In Table 8-56 below a breakdown by cluster type of suspension related belt fitting objects is presented. This object class is dominated by girdle-hangers. The cast girdle-hangers in the Eriswell assemblage have an interesting cluster distribution, with membership nearly evenly distributed between TR 2 and TR 3.

Belt fitting Sub class	Mfr. method	Cluster			No. of objects
		TR 1 (%)	TR 2 (%)	TR 3 (%)	
Belt ring	Cast	14.3	71	14	7
Girdle-hanger	Cast		56	44	16
	Sheet			100	1
Latch-lifter	Cast		100		3

Table 8-56: Showing the percentage of suspension related belt fitting objects by object sub class, manufacturing method and cluster membership. The final column shows the actual number of objects. The latch-lifters are 104-3313-A, 104-2787-A-A and 104-2787-C-A.

The one entry for sheet in the above table is 114-1061-C-B; a piece of metal used to join composite girdle-hanger parts 114-1061-C-A and 114-1061-C-C (from grave 447 in ERL 114). Intriguingly the trident end (114-1061-C-A) appears to be made from a different cluster type to the sheet and main shaft (Table 8-58). This would appear to suggest that it is a genuinely composite object (created from two

separate girdle-hangers). Having said this one should be aware that the lead and tin levels on 114-1061-C-A are much higher and there is also a possibility that some filler alloy was accidentally caught during the analysis (probably the more likely scenario).

ID	Mfr. method	Cu	Pb	Sn	Zn	Cluster
114-1061-C-A	Cast	1595359	524463	132090	51049	TR 2
114-1061-C-B	Sheet	2364904	100013	97898	328241	TR 3
114-1061-C-C	Cast	3040499	121710	68036	146830	TR 3

Table 8-57: NPA data for composite girdle-hanger 1061 from ER 114.

Girdle-hangers are complex objects (Mortimer and Stoney 1996; Felder 2014, 43–47) and are often decorated with a litany of punch marks, i.e. they can be subject to significant amounts of post-casting working.⁸⁴ As this study did not focus on individual object categories the precise level of post-casting work was not recorded in detail (a more detailed overview of the girdle-hangers in question is displayed in Table 8-59 below). A comparison with the girdle-hangers analysed by Blades (1995) shows that cluster TR 2 represents the totality of the alloys at the majority of the sites except Bergh Apton and Morning Thorpe (Table 8-58). It may be interesting to speculate that cluster TR 3 (generally preferred for sheet work) was preferentially selected for girdle-hangers that were highly worked post-casting, but equally this may simply be the result of individual communities exploiting the metal resources in their hinterland. Further work is required.

Site	Cluster		No. of objects
	TR 2 (%)	TR 3 (%)	
Bergh Apton	33	67	3
Empingham	100		5
Morning Thorpe	60	40	5
Spong Hill	100		6
West Garth Gardens	100		1
Eriswell	53	47	17

Table 8-58: The percentage of the alloy types used for the production of girdle-hangers analysed by Blades (1995). Eriswell is provided as a comparison at the bottom of the table. Blades did not provide any details of the manufacturing processes used on the objects he analysed so it is not possible to provide a breakdown.

⁸⁴ They have traditionally been considered by archaeologists as high status objects, although recent research has suggested a much more nuanced and complex situation (Felder 2015, 14).

Site	ID	Hines Description	Analysis Areas	Grave No.	Mfr. Method	Gender	Grave Phase	Cluster
046	46-1636-A	Single girdle-hanger. Trident head. Appears to have been broken and re-bored for suspension.	Central shaft.	025	Cast	F	A2	TR 3
046	46-1108-A	Plain trident head. Single row of dot punch marks along shaft and some transverse moulding. 1108: part of strip suspension ring for these, with Fe bar.	Central shaft.	038	Cast	F	DE	TR 3
046	46-1107-A	Plain trident head. Single row of dot punch marks along shaft and some transverse moulding. 1108: part of strip suspension ring for these, with Fe bar.	Distal terminal and main shaft.	038	Cast	F	DE	TR 3
046	46-1106-A	Plain trident head. Single row of dot punch marks along shaft and some transverse moulding. 1108: part of strip suspension ring for these, with Fe bar.	Distal terminal and main shaft.	038	Cast	F	DE	TR 2
104	104-3596-A	Stem of girdle hanger	Central shaft.	350	Cast	F	A2	TR 2
104	104-3090-B	Pair, with 3089. Head only, closed trident. Punch decoration.	Front only (traces of solder on reverse).	172	Cast	F	A2	TR 2
104	104-3089-A	Ae girdle hanger with large Fe concretion, probably the remains of latch lifter shafts. All attached to a short Fe bar for suspension. Girdle hanger has punched decoration on borders.	Distal terminal and main shaft.	172	Cast	F	A2	TR 3
104	104-2787-b-A	Remains of set of three associated with Ae girdle-hangers.	Distal terminal and main shaft.	189	Cast	F	A2	TR 2
104	104-2140-A	With 2139. Matching pair; trident heads with profile zoomorphic terminals.	Distal terminal and main shaft.	242	Cast	F	A2	TR 3
104	104-2139-A	With 2140. Matching pair; trident heads with profile zoomorphic terminals.	Distal terminal and main shaft.	242	Cast	F	A2	TR 2
114	114-1405-A	Pair with 1402.	Reverse of Distal terminal and main shaft.	422	Cast	F	A2	TR 2
114	114-1402-A	Pair with 1405. Broken shaft. Trident over notched crescent terminal. Moulding.	Distal terminal, proximal terminal and main shaft	422	Cast	F	A2	TR 2

Site	ID	Hines Description	Analysis Areas	Grave No.	Mfr. Method	Gender	Grave Phase	Cluster
114	114-1061-C-C	3 GH: 1 pair, 1 additional. Pair with trident terminal; incised shaft. Other is broken and composite, with what is similar to head plate of SLB attached to terminal: with bulls-eye decoration and 2-4 Ae rivets.	Central and lower main shaft. This is the broken composite girdle-hanger.	447	Cast	F	A2	TR 3
114	114-1061-C-B	3 GH: 1 pair, 1 additional. Pair with trident terminal; incised shaft. Other is broken and composite, with what is similar to head plate of SLB attached to terminal: with bulls-eye decoration and 2-4 Ae rivets.	Sheets joining the two halves This is the broken composite girdle-hanger.	447	Sheet	F	A2	TR 3
114	114-1061-C-A	3 GH: 1 pair, 1 additional. Pair with trident terminal; incised shaft. Other is broken and composite, with what is similar to head plate of SLB attached to terminal: with bulls-eye decoration and 2-4 Ae rivets.	Distal terminal. This is the broken composite girdle-hanger.	447	Cast	F	A2	TR 2
114	114-1061-B-A	3 GH: 1 pair, 1 additional. Pair with trident terminal; incised shaft. Other is broken and composite, with what is similar to head plate of SLB attached to terminal: with bulls-eye decoration and 2-4 Ae rivets.	Central shaft.	447	Cast	F	A2	TR 2
114	114-1061-A-A	3 GH: 1 pair, 1 additional. Pair with trident terminal; incised shaft. Other is broken and composite, with what is similar to head plate of SLB attached to terminal: with bulls-eye decoration and 2-4 Ae rivets.	Central and upper shaft.	447	Cast	F	A2	TR 3

Table 8-59: Girdle-hangers from Eriswell with cluster memberships. The column 'Hines Description' is an amalgamation of information provided to the author in two batches in 2010 and 2013 by Professor John Hines.

8.7.4 CLUSTERS AND GRAVES

Was there any selection of alloy types for suites of objects associated with individuals (i.e. were items made as a set)?

There are 105 graves at Eriswell that contain more than one copper alloy object. Examining all would require a prohibitive amount of time and space. Consequently it was decided to focus only on those that contain 10 or more objects. It should be borne in mind that these graves are unusual because of the number of objects within them and consequently they — and conclusions drawn from them — may not be representative of trends in the wider community.

The 17 graves selected contained 307 objects, representing 39.4% of the total analysed copper alloy objects from Eriswell. In Table 8-60 below details of the graves and the number of objects are presented.

Grave No.	Site	Burial overview				Clusters as percentage of grave alloy type			No. of Cu alloy objects
		Ost. Sex	Gender	Phase	Burial Age	TR 1	TR 2	TR 3	
005	046	F	F	A2b	MA?	12	8	80	25
015	046	F	F	A2	Y-MA	8	42	50	12
024	046	C/F	F	A2	10 to 14		20	80	15
025	046	C	F	A2	15-16		11	89	19
038	046	F	F	DE	25-30		53	47	15
172	104	F	F	A2	Young		9	91	11
231	104	C	F	A2	Sub-adult?		92	8	13
242	104	F	F	A2	Old	9	73	18	11
255	104	M	M	AB	MA		90	10	10
315	104	F	F	A2	Y-MA	11	41	48	27
323	104	M	M	AB	Young	6	63	31	33
350	104	N/A	F	A2	18	7	21	71	14
362	104	F	F	A2	Old		92	8	12
405	114	N/A	F	A2	N/A		50	50	12
422	114	N/A	F	A2	N/A		19	81	48
447	114	N/A	F	A2	N/A		25	75	12
458	114	C	F	A2	9 to 10		22	78	18

Table 8-60: Graves at Eriswell that contain more than 10 copper alloy objects.

To examine the grave assemblages a series of lead-tin-zinc ternary diagrams were produced. Each diagram is presented individually in the context of the grave being discussed.

Before beginning it must be noted that close proximity between two points in a ternary diagram cannot be read as indicating items have the same composition. These diagrams are expressing only three parts of the composition. Close points suggest similarity in the alloying components plotted, but the other elemental data is missing (particularly trace elements) which would be more suited to see if objects were produced from the same melt. It should also be remembered that the methodological approach here has focussed on the acquisition of qualitative data to assess the assemblage for broad trends in metallurgical changes and choices. Consequently the data itself is not well suited to matching objects (due to corrosion etc.). Nevertheless one may deduce that where there is good reason to suspect that objects may have been produced together in the same mould (i.e. the wrist clasp example in footnote 4, page 45) then proximity of points may suggest that there is a reasonable probability (but not definitively demonstrate) that they were produced at the same time as a 'set'.

8.7.4.1 G005

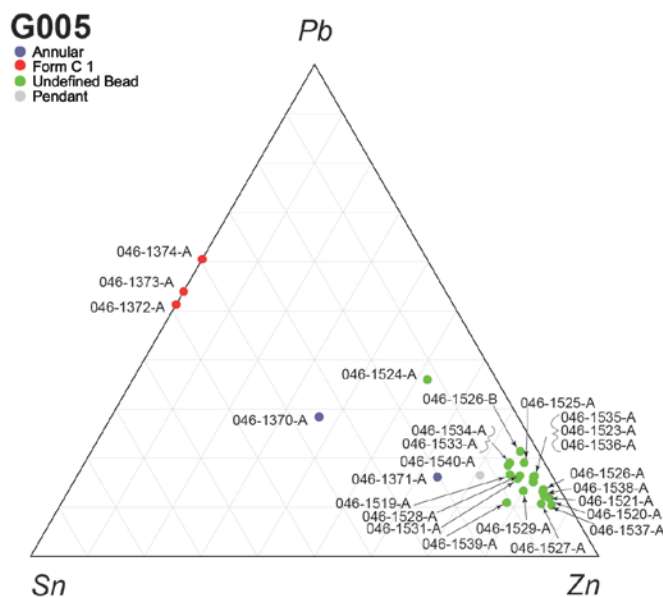


Figure 8-38: Ternary diagram of grave 005 from ERL 046.

Immediately a cluster of beads in the zinc corner jumps out (Figure 8-38). These are bucket pendants and the relatively tight grouping immediately makes one wonder if these were produced together as a set (either through re-melting or simply reforging existing sheet metal objects). One bucket pendant (046-1524-A) does fall outside the grouping. This object is a high zinc alloy (like the others) but appears to contain more lead. As these are composite objects soldered together this is likely the result of filler alloy accidentally being analysed, however, there is a chance that the pendant is indeed from a relatively different alloy and may represent an addition made separately from the bulk. This bead should be subject to further analysis to assess this. It is interesting to note that the pendant (046-1540-A) from the same necklace also falls within the grouping.

The three Form C 1 wrist clasps (046-1374-A, 046-1373-A, 046-1372-A) are also relatively closely grouped on the tin – lead axis (none contain zinc). This suggests that either they were produced from the same metal (the variation being accounted for here by analytical approach) or a selection of very similar source materials.

The two annular brooches are not particularly close. Whilst this may be due to the methodological approach their difference is such that it is tempting to see it as two objects made from different source materials. It may be that this is simply due to expediency or production at different times, but we should be aware of the possibility of the use of ‘ancestor’ alloys. For a discussion on this last possibility see Caple (2010) (in relation to saucer brooches), this is also discussed further in Chapter 9.

8.7.4.2 G015

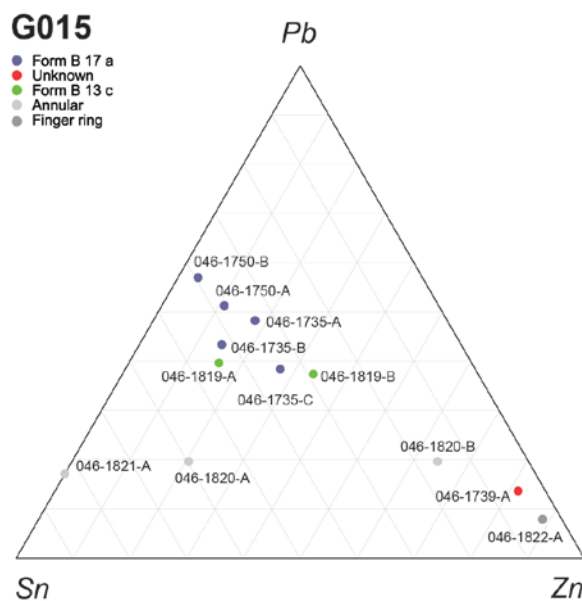


Figure 8-39: Ternary diagram of grave 015 from ERL 046.

The Form B 17 A wrist clasps (046-1750-B, 046-1750-A, 046-1735-A, 046-1735-B and 046-1735-C) are relatively tightly grouped (Figure 8-39) as low zinc alloys suggesting either selection of similar source alloys for production or production at the same time (with variation accounted for by corrosion etc.). The two Form B13 C wrist clasps are not as closely grouped; of these one is the main eye piece (046-1819-A) and the other a repousse sheet (046-1819-B). It is interesting that the eye piece is closely associated with the other main wrist clasp fragments whilst the repousse sheet appears to contain more zinc (as could be expected for sheet metal work). That it also appears to have a relatively high lead content is of

interest, although again one cannot be certain that this does not result from the accidental clipping of an area of filler alloy on a highly fragmentary sheet.

The wire finger ring (046-1822-A) is made out of a high zinc alloy. It will be remembered that wire objects tend to be made out of zinc rich alloys (cluster type TR 3, page 392).

As with grave 005 there is a suggestion that the annular brooches seem to be made out of a variety of alloys.

8.7.4.3 G024

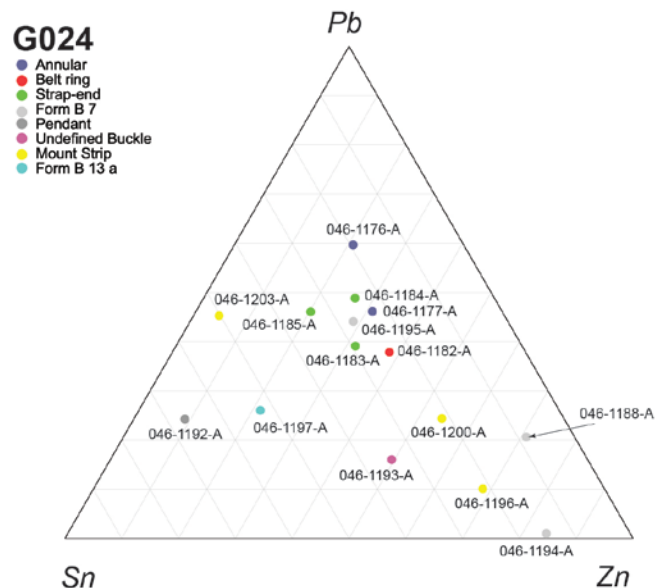


Figure 8-40: Ternary diagram of grave 024 from ERL 046.

The strap ends in grave 024 appear relatively closely grouped whilst in contrast the mount strips are much more diverse (Figure 8-40).

In contrast to graves 005 and 015 two of the wrist clasps (046-118-A and 046-1194-A) are made out of zinc rich (as opposed to tin rich alloys). These wrist clasps (Form B 7) are both made out of sheet metal (those in the previous graves were cast), supporting previous assertions that zinc rich alloys are preferred for sheet metal.

8.7.4.4 G025

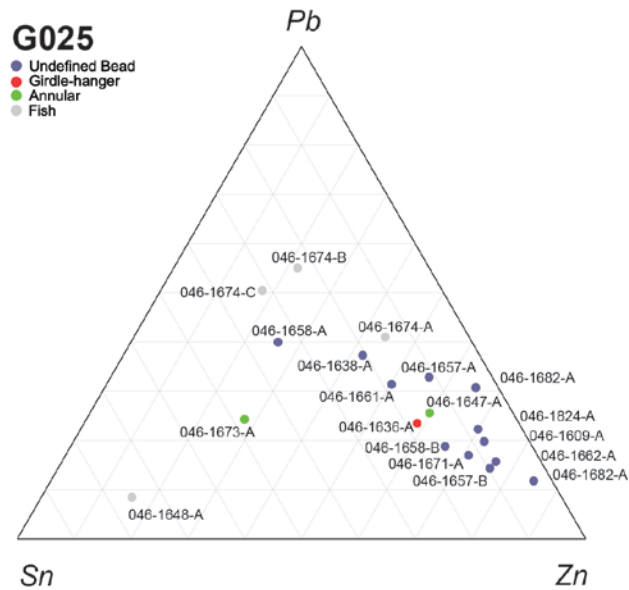


Figure 8-41: Ternary diagram of grave 025 from ERL 046.

The bucket pendants in grave 025 — as with grave 005 — fall towards the zinc rich end of the spectrum (Figure 8-41). Those outliers (such as 046-1658-A and 046-1638-A) that appear to contain more lead and tin may (as with 046-1524-A in 005) result from the accidental analysis of filler alloy.

Of primary interest in this grave is the fish brooch (the only example of this style from Eriswell). The main body of the brooch (046-1648-A) appears to be a high tin, low lead and zinc alloy (on the interface between clusters TR2 and TR 3). Believed to be associated with the brooch was a pin (046-1674-B) and two fragments of sheet metal (046-1674-A and 046-1674-C). These last three appear substantially different from, the main body. Were these later additions / repairs?

8.7.4.5 G038

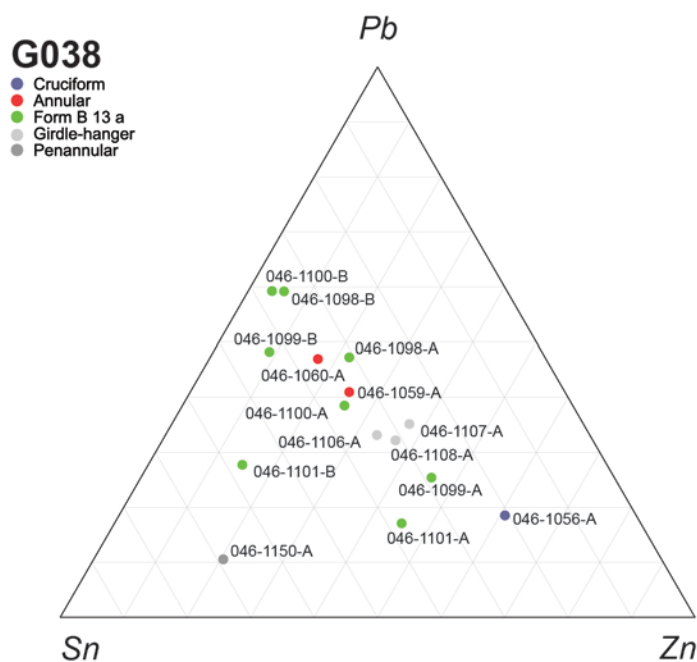


Figure 8-42: Ternary diagram of grave 038 from ERL 046.

In grave 038 (see Figure 8-42) the girdle hangers appear to be of most interest: all three components (two girdle hangers and a suspension ring; 046-1106-A, 046-1107-A and 046-1108-A respectively) are relatively closely grouped. It is not possible to say if these are made from the same casting operation here, but it does raise the tantalising possibility that this entire group of belt fittings was produced as a set. This is not always the case with pairs of girdle-hangers (see the example from West Heslerton grave 113 in Baker 2013, 410) raising the interesting question of what we could deduce about an individual's status from the metallurgy: what does it say about the status of an individual who can 'afford' (or needs) to have two girdle hangers produced from the same melt? Are those whose girdle hangers are produced from different alloy types adding to their collection at later dates, is one a replacement for a lost or broken one? Is it related to the quantities of material available at the time (i.e. both produced at approximately the same point but requiring two different melting operations) or are we looking at the use and incorporation of 'ancestor' alloys?

8.7.4.6 G172

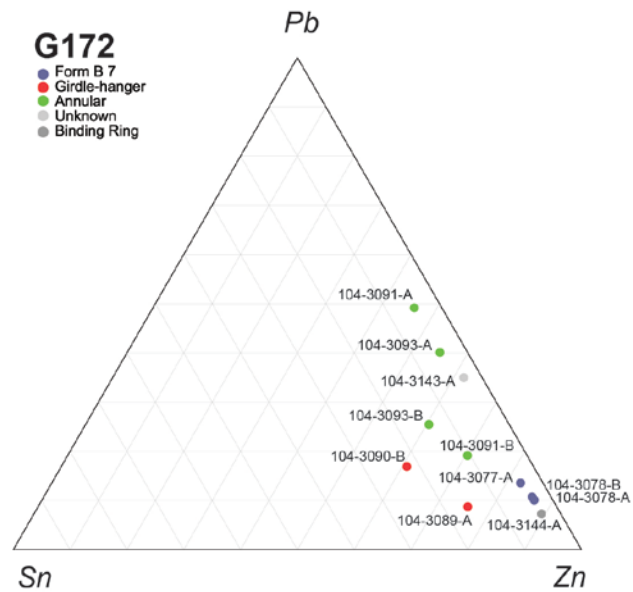


Figure 8-43: Ternary diagram of grave 172 from ERL 104.

All objects are on the zinc rich side of the spectrum (Figure 8-43). Apart from two pins (104-3091-B and 104-3093-B, associated with annular brooches 104-3091-A and 104-3093-A) and two girdle-hangers (104-3089-A and 104-3090-B) all objects are sheet metal. The three Form B 7 wrist clasps (104-3077-A, 104-3078-A and 104-3078-B) are very tightly grouped.

8.7.4.7 G231

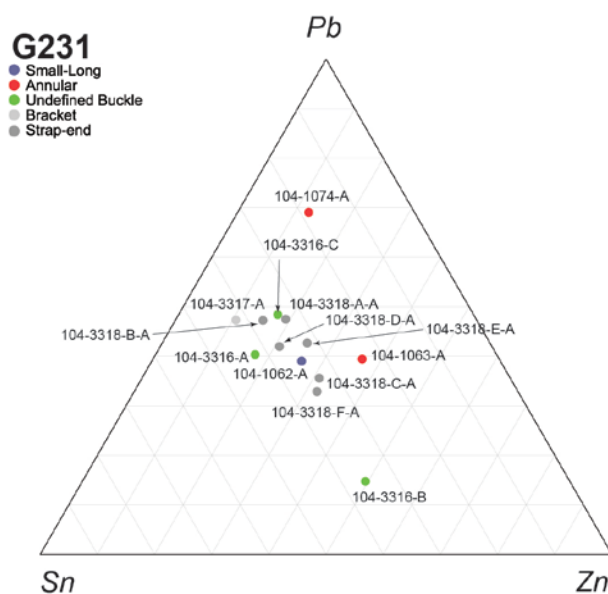


Figure 8-44 Ternary diagram of grave 231 from ERL 104.

Four strap ends (104-3318-A-A, 104-3318-B-A, 104-3318-C-A and 104-3318-F-A) are the closest grouped individual sub class of object in grave 231 (Figure 8-44). The reverse of the strap ends were covered in filler alloys (see Chapter 7). That they do not closely group could be due to the accidental clipping of filler alloys (104-3318-A-A and 104-3318-B-A show more lead and tin than the other two) and it may be worth undertaking further destructive or semi-destructive analysis to determine if the four were indeed made as a single set or are slightly different (but similar) alloys.

The buckle is made out of three composite parts: the buckle plate (104-3316-A), frame 104-3316-B and a rolled sheet (104-3316-C). Most interesting about this is that the buckle frame and tongue appears to be made out of a much lower leaded alloy. As always a large degree of care must be taken in interpreting this, but it is interesting to speculate that the object may have been made out different alloys (repairs / adaption of an earlier buckle?).

As in many other graves the annular brooches do not appear particularly closely related in alloy types.

8.7.4.8 G242

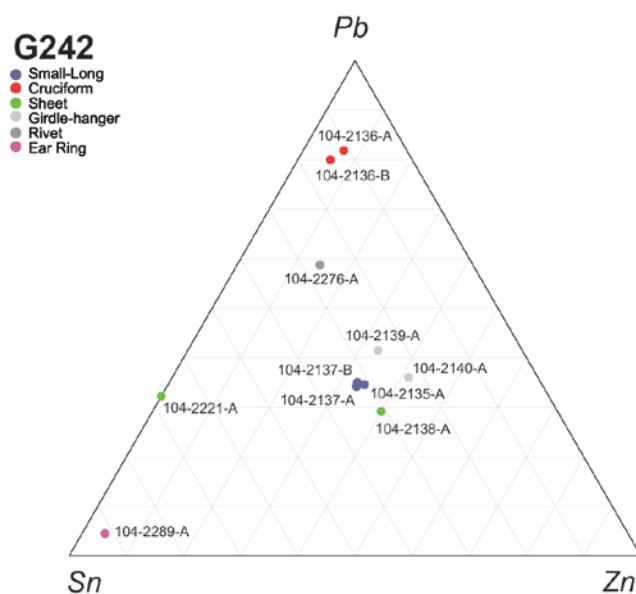


Figure 8-45: Ternary diagram of grave 242 from ERL 104.

Of particular interest in grave 242 are a cruciform brooch and two small-long brooches (Figure 8-45). The cruciform brooch is a two part composite object with the cast main body (104-2137-A) and a cast catch (104-2137-B) soldered on. Both are tightly grouped suggesting that both were probably manufactured at the same time and possibly from the same alloy. A series of fragments from a rolled sheet (104-2276-A) were thought to also possibly be associated with this brooch. In contrast to the body and catch the fragments appear to be of a different composition, containing much less lead.

The pair of small long brooches (104-2135-A and 104-2137-A) are tightly grouped. One brooch had a catch soldered on which it was possible to analyse separately (104-2137-B). Like the catch associated with the cruciform brooch, this was tightly grouped with the parent main brooch body. The tight grouping suggests (but does not prove) that both brooches and the catch were manufactured at the same time.

8.7.4.9 G255

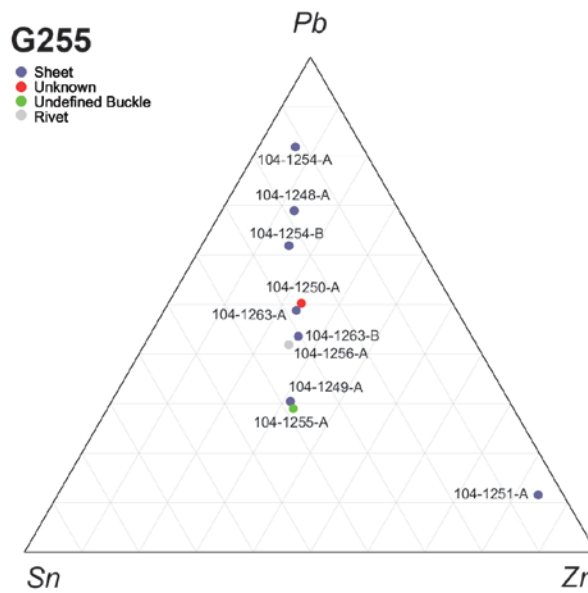


Figure 8-46: Ternary diagram of grave 255 from ERL 104.

Grave 255 (Figure 8-46) contained less in the way of immediately identifiable dress accessories than the other graves featured here and the assemblage mainly consists of sheet metal fragments. These are notable (with the exception of 104-1251-A) for their high lead content (when compared with sheet objects from other graves).

8.7.4.10 G315

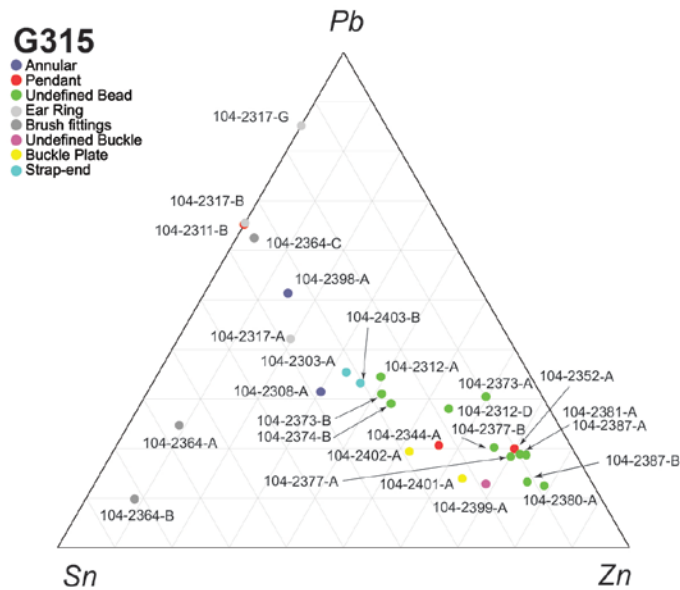


Figure 8-47: Ternary diagram of grave 315 from ERL 104.

Grave 315 (Figure 8-47) contained a number of bucket pendants. The majority of these are — like those elsewhere — clustered towards the zinc rich apex. Those that are not (104-2312-A, 104-2373-B and 104-2374-B) may be the result of accidental contamination by filler alloys. Further analysis may be necessary to confirm if this is the case or whether this small group were indeed made of a significantly different alloy to the others in the grave.

The two strap ends (104-2303-A and 104-2403-B) are closely related in the ternary diagram.

The copper alloy ear ring accoutrements appear particularly interesting in this grave, there being relatively few at Eriswell (one each in G232 and G242; 104-1095-A and 104-2289-A respectively). In grave 315 there are three copper alloy ear ring parts: wire (104-2317-A, possibly looped through the piercing?) and two copper alloy discs (104-2317-B and 104-2317-G). Both of these disks had had silver sheets soldered onto them.⁸⁵ In common with the ear ring in grave 242

⁸⁵ For copper alloy disc 104-2317-B: filler alloy on copper alloy is 104-2317-C, silver disc is 104-2317-D (filler alloy side) and 104-2317-E (silver side).

(104-2289-A) all three components are low zinc alloys, indeed the two discs are possibly zinc free (cluster TR 1).

As with the other graves examined here the annular brooches do not appear particularly closely related.

8.7.4.11 G323

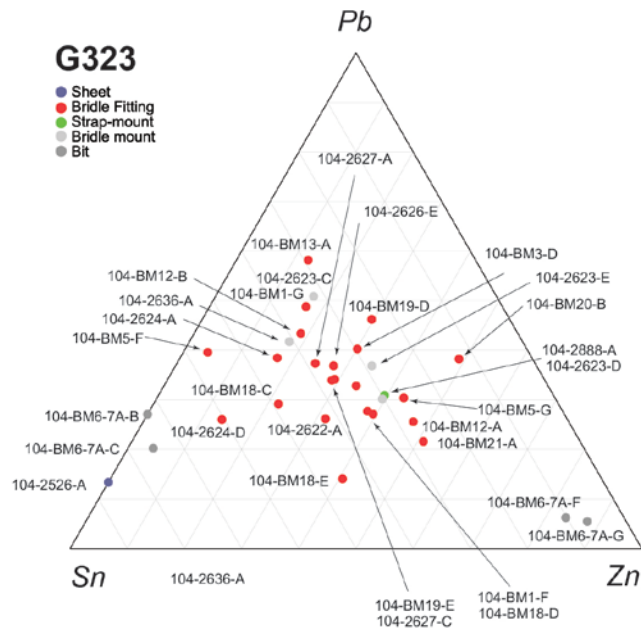


Figure 8-48: Ternary diagram of grave 323 from ERL 104.

Grave 323 (Figure 8-48) contained the horse and warrior burial. The tack has already been briefly discussed (page 401) and will be further so here. It should be noted that these objects (having been prepared for display) had been cleaned and conserved to a much higher standard than the others (which had undergone preliminary conservation only). Consequently the surface readings here are likely to be much more secure than on other objects.

As mentioned earlier all three alloy clusters make an appearance in the tack, perhaps suggesting that this was not a set produced in a single event. Having said that there are three very closely related pairs:

For copper alloy disc 104-2317-G: filler alloy on copper alloy is 104-2317-F, silver disc is 104-2317-I (filler alloy side) and 104-2317-H (silver side).

- 104-BM19-E and 104-2627-C: two square headed pendant strips.
- 104-BM1-F and 104-BM18-D: two cruciform shaped bridle mounts. The front of both were gilded and had silver sheets soldered on. Both these analyses were on the reverse of the objects where microscopic investigation suggested no filler alloys were present and there were no other adornments or decoration. It is particularly interesting that these two so closely match as the other two cross shaped mounts (104-BM5-F and 104-2623-D) are not closely related to either each other or to these two (all four were relatively 'clean' and not too heavily corroded).
- 104-2623-D and 104-2888-A: a cross shaped bridle mount and a small rivet. It is unknown if the rivet was used in direct association with the mount.

As has now been said repeatedly (and probably to the point of the reader's tedium) the margin of error is such that it cannot be guaranteed that these objects do indeed have highly similar compositions. Nevertheless it is interesting that there is the suggestion of some objects being very closely related. If this is so (and this will require further work to determine more securely) then it raises some interesting questions. We have no real models, theoretical or practical, of how assemblages (such as this tack) are produced and / or acquired in the post-Roman / Early Saxon period. The results, whilst qualitative, do tentatively suggest that some objects might have been made together. Yet others that one may have strongly suspected to match, such as the two gilt bridle fittings with style 1 faces (104-BM12-A and 104-2624-A), do not appear to do so. There are three broad possibilities for this:

- The entire set (as found in the grave) was accumulated / produced over time. Some pieces were made from the same source alloy.
- The entire set (as found in the grave) was produced in a single event but from a variety of different scrap resources. Occasionally there was enough scrap from a single recycled object to produce one or more new objects.
- A mixture of the two.

The second point may perhaps be favoured by many, but has some unanswered and significant issues to be considered. Given the mixed nature of the alloys used to produce the tack (what we would now term leaded gunmetals) why are some ‘companion’ pieces (i.e. the style 1 fittings) so different? Would not it have been ‘easier’ to combine the scrap into a single melt and produce both at the same time, or was there some taboo or prescription on how pieces should be produced (i.e. certain types of objects not being mixed in a melt)? This is a stark reminder that in terms of understanding the post-Roman metalsmiths working practices and cultural considerations we are still in the starting blocks.

8.7.4.12 G350

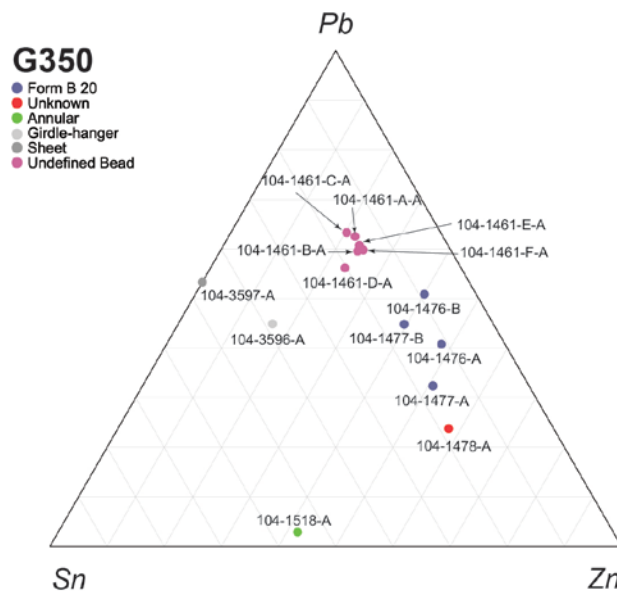


Figure 8-49: Ternary diagram of grave 350 from ERL 104.

The form B 20 sheet metal wrist clasp eye and hook pieces (104-1476-A, 104-1476-B, 104-1477-A and 104-1477-B) are all zinc rich alloys (as one would expect from sheet metal objects here). They do not appear particularly closely grouped (Figure 8-49), but this could be due to corrosion and it may be of interest to analyse them further and determine if they are indeed separate (if similar) alloys.

In contrast to the other graves featured here the beads (104-1461-C-A, 104-1461-A-A, 104-1461-E-A, 104-1461-F-A, 104-1461-B-A and 104-1461-D-A) are

significantly different, tightly clustering as lead rich alloys. These are cylinder beads not bucket pendants (i.e. they are composed of a single short strip of sheet metal worked into a cylinder through which they are suspended). It may be that the high lead comes from the accidental clipping of filler alloys, but given the tight grouping across all six this seems somewhat unlikely. It is of interest that the composition appears so different to the bucket pendants, and this may be an area of interest for future study.

8.7.4.13 G362

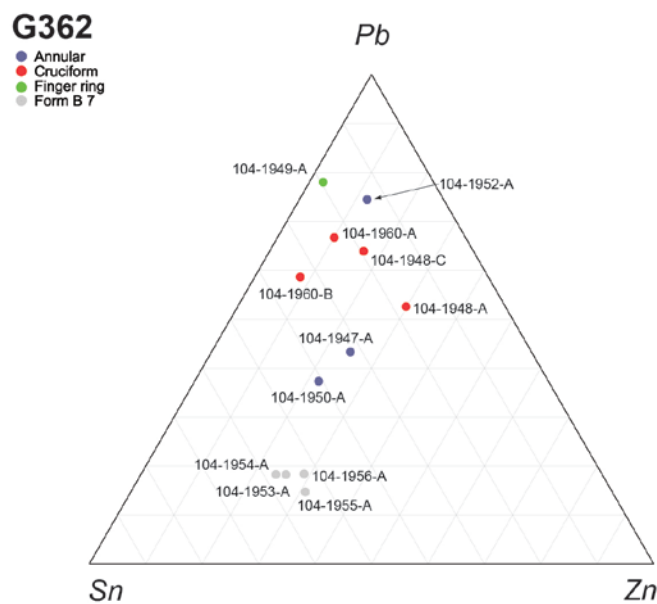


Figure 8-50: Ternary diagram of grave 362 from ERL 104.

There are two composite cruciform brooches in grave 362 (Figure 8-50):

- Main brooch body (104-1948-A), a separate side knob (104-1948-C) that was soldered on (see 104-1948-B for the filler alloy)
- Main brooch body (104-1960-A) and catch (104-1960-B)

All parts share a similar alloy composition, containing both zinc and tin and a relatively high amount of lead. Caveats about accuracy aside, it is interesting to note that the largest variation is between the brooch that has a side knob soldered on. This leads one to suspect that it is a later repair.

The Form B 7 wrist clasps (104-1953-A, 104-1954-A, 104-1955-A and 104-1956-A) are a very tightly grouped tin rich alloy. They are all sheet metal and this composition, along with their tight grouping, makes them stand out from many other sheet objects. It is tempting to see them as a set produced from the same source material.

Of the three annular brooches two are relatively closely grouped (104-1947-A and 104-1950-A) whilst the third (104-1952-A) is somewhat removed and contains significantly more lead.

8.7.4.14 G405

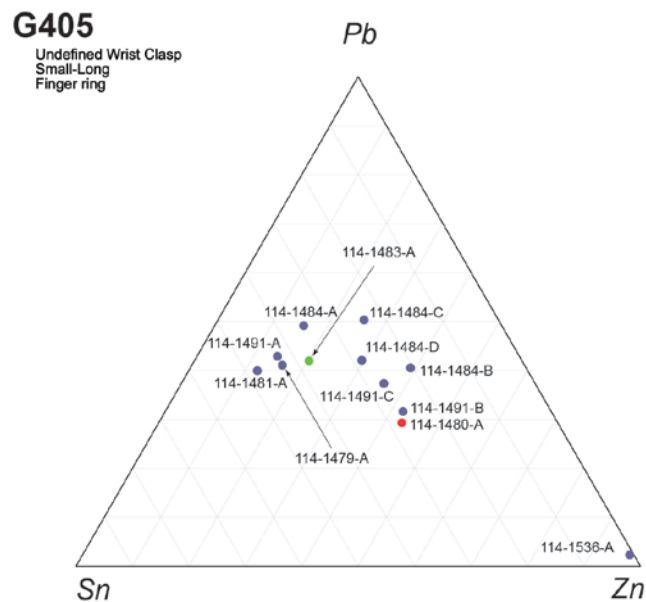


Figure 8-51: Ternary diagram of grave 405 from ERL 114.

The wrist clasps in grave 405 were composite with cast and sheet elements (Figure 8-51). Some were also highly fragmentary (114-1491 and 114-1484). Nevertheless they group together approximately in the centre of the ternary diagram. Alongside the wrist clasp was a small-long brooch (114-1480-A) and a finger ring (114-1483-A). These two fall in the same area of the diagram as the wrist clasps.

8.7.4.15 G422

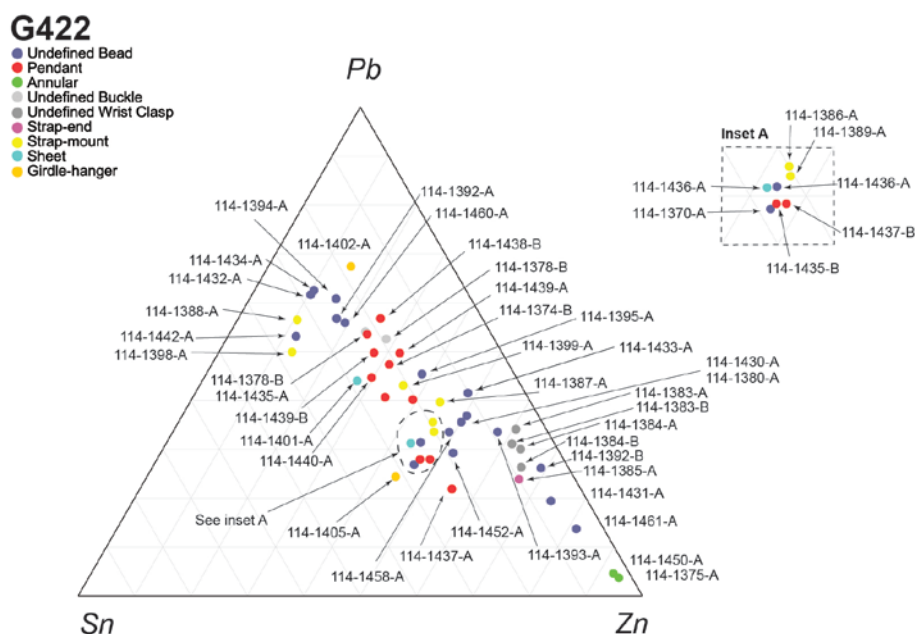


Figure 8-52: Ternary diagram of grave 422 from ERL 114.

Grave 422 is the most populous grave in all three cemeteries for non-ferrous artefacts (Figure 8-52). In total it contained 48 objects, the vast majority of which were pendants and beads (Table 8-61).

Object Sub Class	No. of objects
Annular	2
Girdle-hanger	2
Pendant	11
Sheet	2
Strap-end	1
Strap-mount	6
Undefined Bead	18
Undefined Buckle	2
Undefined Wrist Clasp	4

Table 8-61: Objects from grave 422

The pendants are composed of two parts; a wire ring and a perforated sheet tag. In each of the analyses presented here the tag is always ‘A’ (i.e. 114-1374-A) and the wire ring always B (i.e. 114-1374-B). The pendants have a roughly linear distribution along zinc – lead in the ternary diagram. Although some appear relatively high in lead there is a tendency for them to be slightly more zinc rich than tin rich. It would be interesting to subject these to further destructive

analysis and see if any tighter grouping may form or if they are indeed from different source alloys.

The beads, all bucket pendants, show a much more varied composition with a relatively distinct high tin – lead group. Many of these beads were fragmentary and some of the high lead may result from inadvertent clipping of filler alloys. If this is not the case then it is interesting to speculate why six of the beads were made with what appears to be a very different alloy from the remainder.

Interestingly, and in contrast to the beads and pendants, the cast wrist clasps in this grave (114-1383-A, 114-1383-B, 114-1384-A and 114-1384-B) group very closely as zinc rich alloys.

A further object class of particular note in this grave is the two annular brooches (114-1375-A and 114-1450-A), which appear (with normal caveats) to be very closely related. In the graves so far examined there has not always been a high degree of similarity between pairs of annular brooches (as one might expect), which makes these (if the results are confirmed) as something of an outlier.

8.7.4.16 G447

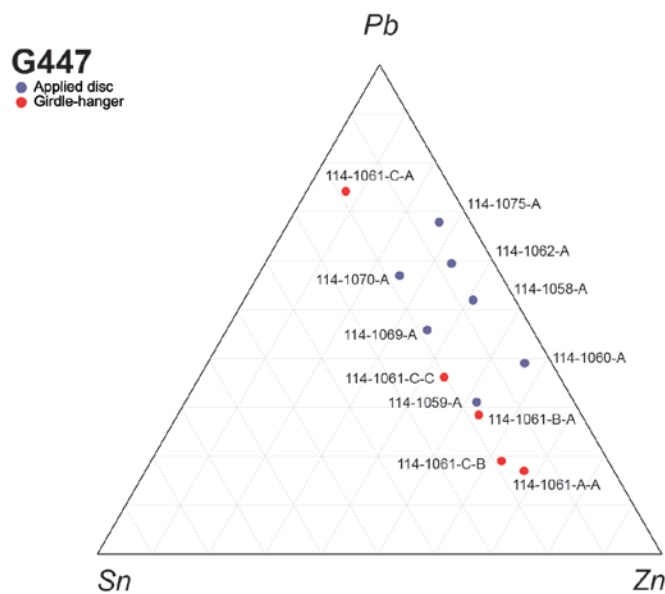


Figure 8-53: Ternary diagram of grave 447 from ERL 114.

Grave 447 (Figure 8-53) contains only two types of objects: girdle-hangers and applied disc brooches.

There were three girdle-hangers, two of which were complete (114-1061-A-A and 114-1061-B-A) and one which was composite / repaired consisting of the main body (114-1061-C-C) and a proximal terminal (114-1061-C-A) joined the main body by a sheet (114-1061-C-B). All the girdle-hangers (both complete and composite) appear relatively closely together in the ternary diagram except the proximal terminal, which has a much higher lead content. This perhaps suggests that the terminal is not a simple repair (i.e. a broken girdle-hanger repaired with the use of an extra sheet) but the combination of two objects.

The applied disc brooch individuals shown in the ternary diagram are thought to be from the same highly fragmentary object as follows:

- 114-1058-A - fragmentary back plate and rim
- 114-1059-A - fragmentary back plate
- 114-1060-A - fragmentary back plate and rim
- 114-1062-A - rim fragment
- 114-1069-A - catch
- 11A-1070-A - applied decoration?
- 114-1075-A - rim fragment

There is considerable variation in the ternary diagram (especially in lead content), but one thing remains constant: they all contain more zinc than tin. It is of course likely that all these fragments are from the same object (although intrusion as the result of bioturbation is always a risk) and it is likely that the high degree of corrosion present (on what is predominantly very thin sheet) has resulted in the spread.

8.7.4.17 G458

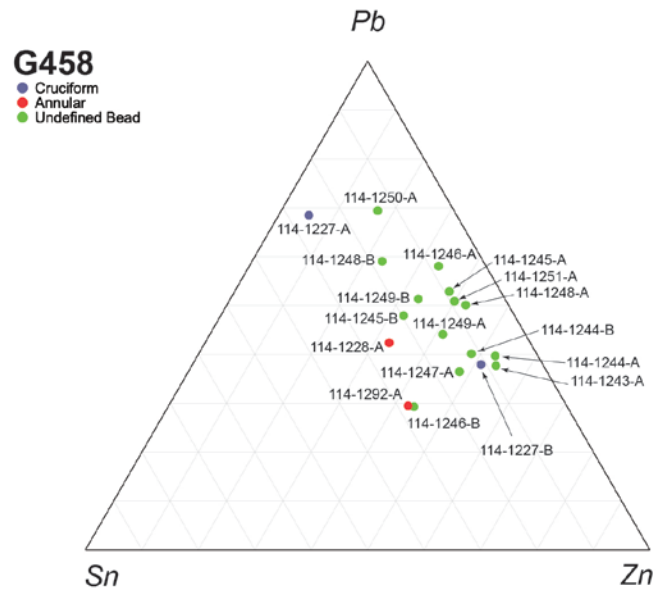


Figure 8-54: Ternary diagram of grave 458 from ERL 114.

The final grave in this section primarily contained bucket pendants (Figure 8-54). These — with the exception of 114-1250-A — all fell within cluster type TR 3 (the cluster where zinc tends to dominate more than tin). The remaining objects are a single cruciform brooch and two annular brooches. The two annular brooches are in the same area of the ternary diagram.

8.7.5 CLUSTERS AND PHASES

Is there any chronological variation in the use of the clusters? In Figure 8-55 below a bar chart of the female and male phases with cluster types is presented. The male phasing shows little in the way of a coherent narrative. In contrast the female phasing appears to document the rise and fall in popularity of cluster TR 3 between phases A1 and B, yet a quick examination of the raw numbers (Table 8-62) would counsel caution: excluding phases A2 (male) and AB (female) relatively few objects are present. It is unlikely that the graph is truly representative.

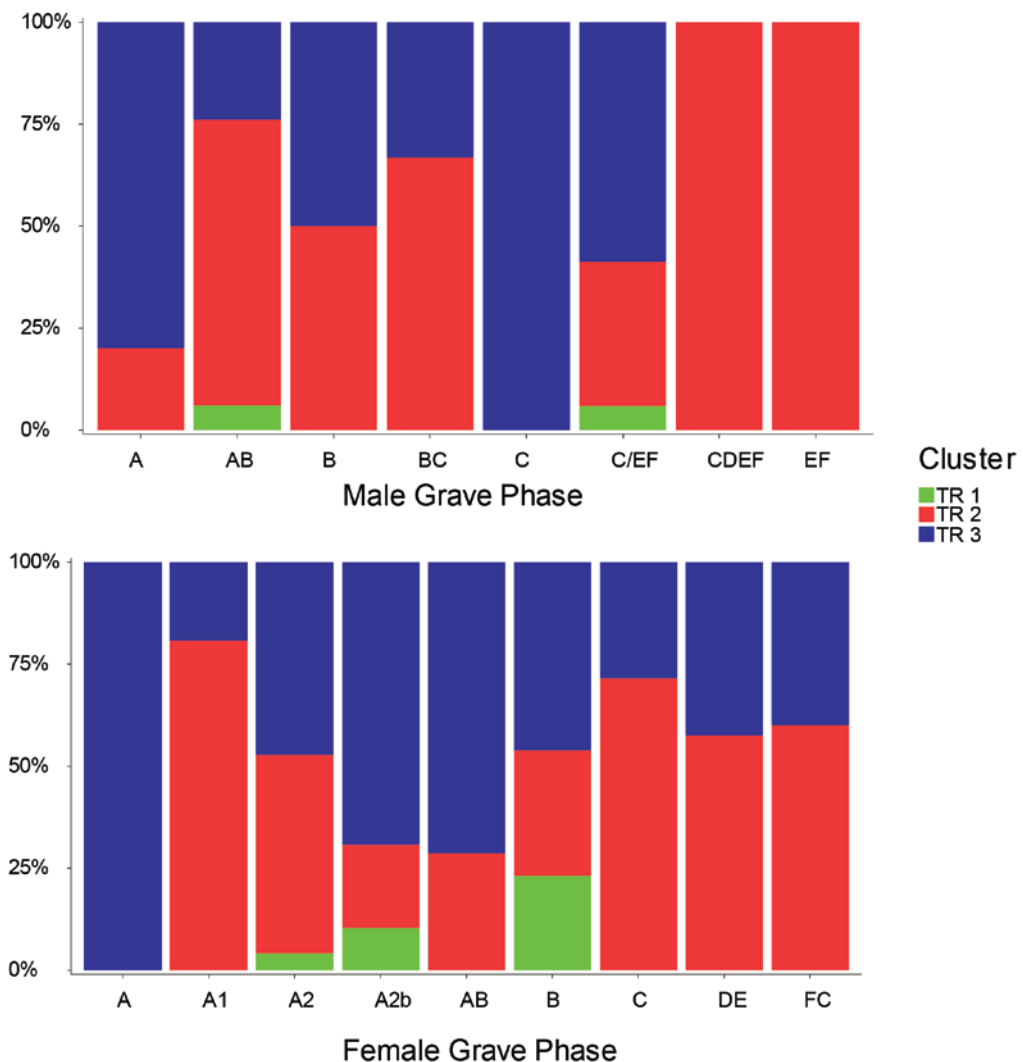


Figure 8-55: Bar chart showing the percentage of cluster type by male and female grave phase (top and bottom respectively). See Table 8-62 for the actual number of objects.

Gender	Grave Phase	Cluster			Total
		TR 1	TR 2	TR 3	
<i>Female</i>	A			1	1
	A1		25	6	31
	A2	17	203	197	417
	A2b	4	8	27	39
	AB		2	5	7
	B	3	4	6	13
	C		5	2	7
	DE		19	14	33
	FC		3	2	5
<i>Male</i>	A		1	4	5
	AB	4	47	16	67
	B		5	5	10
	BC		6	3	9
	C			4	4
	C/EF	1	6	10	17
	CDEF		5		5
	EF		1		1

Table 8-62: Number of objects per cluster in each phase. The final column shows the actual number of objects in each phase.

The data set does not have enough depth (we need more objects from the other phases to be sure) to see if there are variations in the choices being made on major alloying elements, but can we compare these to broader chronological assessments? As noted earlier (in comparison to other methods of grouping, see page 378) broad comparisons can be drawn between the clusters and groupings previously derived. Direct comparisons are, however, more difficult (i.e. cluster TR 2 covers a mixture of what many have previously called both leaded bronze and gunmetals). It can be said with some confidence and with a visual examination of the NPA results that the Eriswell alloys are highly mixed: pure alloys are a rarity and it would seem that — broadly speaking — they would not significantly alter the general distributions that have previously been produced (for instance Caple 1986, 543; Blades 1995, 189–190; Bayley, Crossley, and Ponting 2008, 50; Pollard et al. 2015).

The trace element data acquired here (see page 388) are not of high enough quality to see if there are any introductions of fresh alloys as suggested by Pollard et al (2015).

8.8 CONCLUSION

The application of robust transformed (using a clr transformation) PCA indicated that zinc accounts for the majority of the variation in the Eriswell data set (although one should be aware of the risk of false correlations due to the zero replacement method chosen here, see page 200). A comparison with Blades early Saxon data (acquired using ICP-AES and offering superior accuracy and precision than achieved in this study) — processed using the statistical methodology applied to the Eriswell data — showed a similar result. That the statistical methodology produced similar results on Blades data as on Eriswell supports the choice to treat the NPA data here as compositional (i.e. using a clr transformation), as Blades data is definitely compositional in the statistical sense (see Figure 8-56).

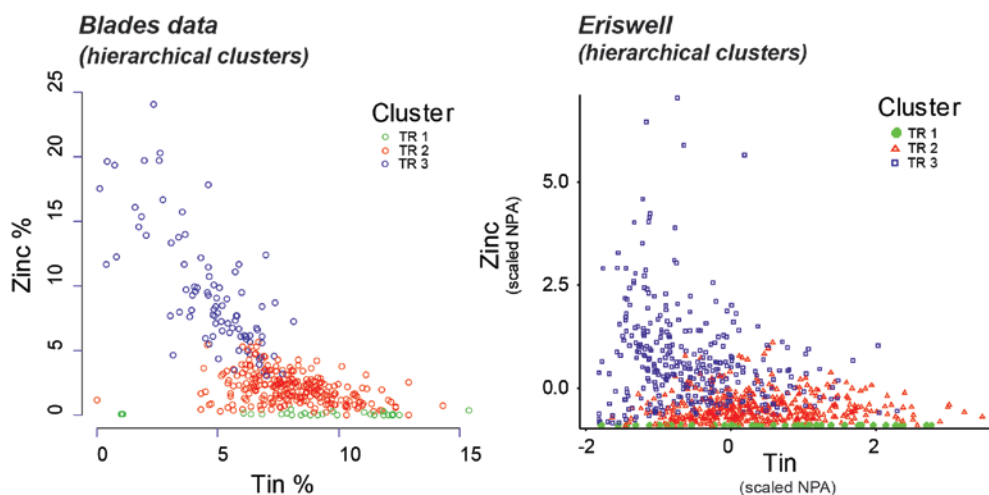


Figure 8-56: Extract from Figure 8-28. The left plot shows Blades' Early Saxon data (1995, 86–97) classified according to the HC used in this study, on the right is Eriswell (scaled and using the zero replaced data) with classification derived from the HC. It can be seen that there is similarity in the distribution of the clusters, supporting the decision to treat the Eriswell NPA data compositionally.

The application of HC to the principal components resulted in the delineation of three clusters:

- TR 1: No or very low zinc content, tin content varies but tends to be high. Could be approximately described as a bronze.

- TR 2: Low to medium zinc content, tin content varies but tends to be high. Could be approximately described as bronze or leaded bronze. Its interface with TR 3 is diffuse, and in this area it can be seen in this area as gunmetal or leaded gunmetal (with tin more dominant than zinc).
- TR 3: High zinc content and low tin. Could be approximately described as brass or leaded brass. Its interface with TR 2 is diffuse, and in this area it can be seen in this area as gunmetal or leaded gunmetal (with zinc more dominant than tin).

These descriptions can be seen visually in the parallel coordinate plots of major elements in Figure 8-57.

These clusters were compared against grouping and classification methods applied previously by Mortimer (1991, 106) , Blades (1995, 126) and Pollard et al. (2015, 700). All three used modern metallurgical definitions to label groups (leaded gunmetal, brass, leaded brass etc.). Although the authors were all explicit about the impact of modern metallurgical definitions and understandings on archaeological alloys they are still using the terminology of the modern metallurgist. Examination of the distribution of the alloys in the Blades and Eriswell data makes one aware that there is little in the ways of distinct and *discrete* groupings and that the alloys are distributed as a continuum. Therefore it may be argued that any system of grouping alloys that uses modern terminology as a starting point is likely to create false divisions: the language is controlling the interpretation. Using HC on the PCA does — to a certain extent — alleviate this. Whilst the analyst is (of course) making decisions and choices based on their knowledge and experience (and the constraints of the statistical techniques chosen) there is also a degree of allowing alloys to define themselves: variance is as variance does. Consequently it is argued that the HC applied here is producing a more useful and effective method of interpreting and grouping Anglo-Saxon copper alloys.

The comparison of the clusters against the categorical variables suggests that there was a preference for the usage of cluster TR 3 (the high zinc cluster) when

producing sheet metal objects. Although only a tentative result this is a surprising and intriguing result. The lack of binary alloy types has previously led to suppositions that “[*metal smiths*] had not sorted very carefully by alloy type before reforging” (Fleming 2012, 23), indicating a “*metallurgy of survival - adequate but not technically fastidious*” (Mortimer 1990, 397). This would suggest a lack of choice, and yet it appears that there were choices and decisions being made during production that affected the metal composition or based on the types of the metals before production (although, to be clear the alloys are still very mixed).

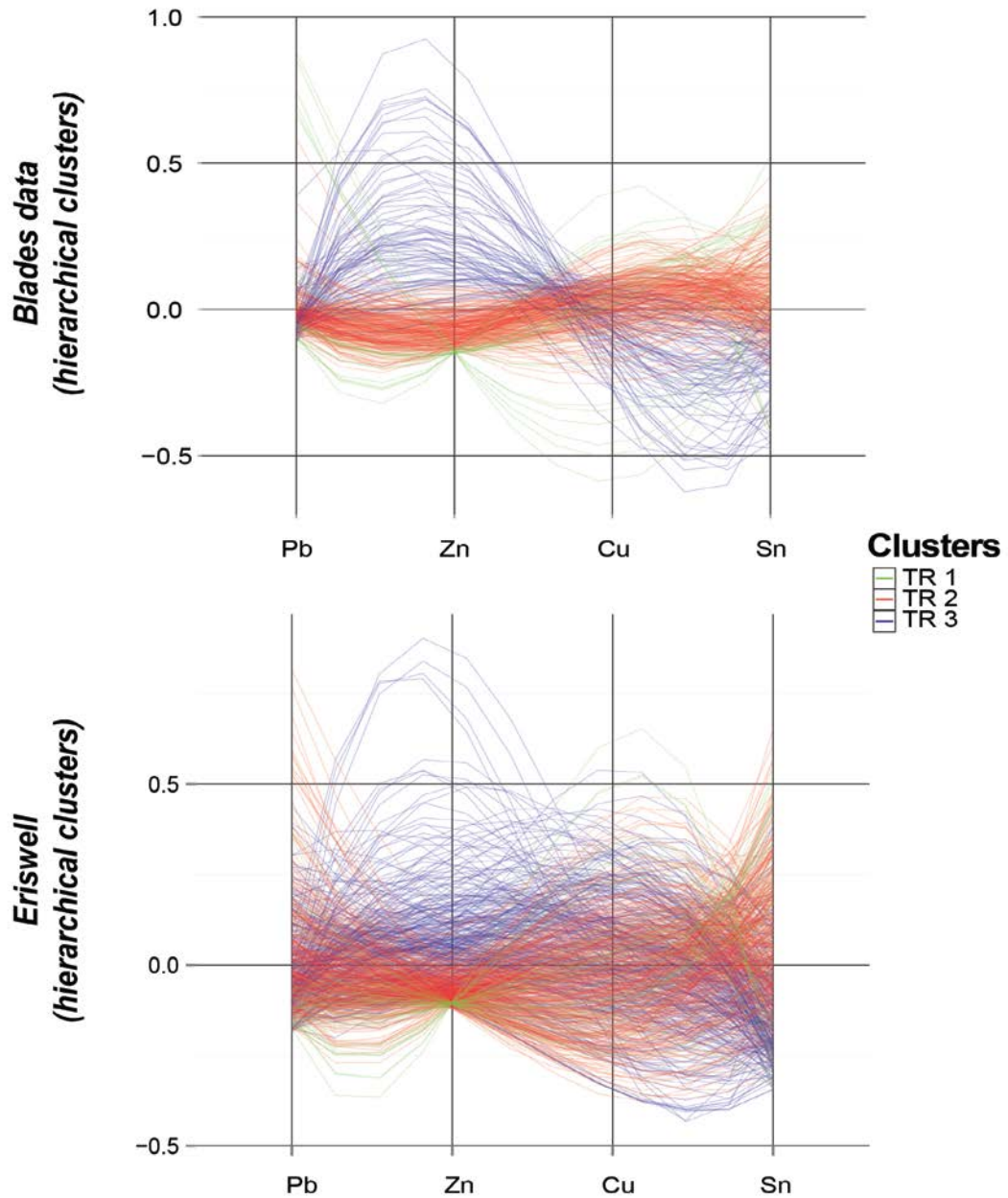


Figure 8-57: Parallel co-ordinate plot of Blades' Early Saxon data (1995, 86–97) (top) and Eriswell (bottom) showing the variables scaled and centred with individuals colour coordinated according to cluster membership. Missing values are plotted at 10% below the minimum of the variable for the missing value. The variables have been scaled univariately with a maximum of 1 and centred.

A further intriguing result emerged from examination of the bucket pendants / beads. The near complete lack of this object type in Roman Britain and its presence in the post-Roman and early medieval periods has led to suggestions that they are possibly demonstrative of either strong external cultural influence or physical movement of individuals.

The analysis here showed that 90% of the bucket beads at Eriswell were made using a cluster TR 3 type of alloy. This near singular use of a single cluster type is unique at Eriswell and does enticingly suggest something different about this object type.

Cast objects tended to be out of cluster type TR 2. Previous studies of non-ferrous metallurgical objects from this period have focussed nearly exclusively on cast dress accessories (see for example Mortimer 1990; Blades 1995). Consequently it is not surprising that rather narrow interpretations of alloy usage in the period have developed. Having said this there are problems attempting to extrapolate from a single site to create a framework for Anglo-Saxon non-ferrous metallurgy. We have no idea of how valid the conclusions are beyond the limits of that site and, as was seen earlier (when comparing the alloy clusters for annular brooches, wrist clasps and girdle-hangers Blades' sites) there *is* significant variation between sites. Unfortunately at present we cannot be certain if this is due to a sampling strategies (i.e. what percentage of site assemblages did Blades analyse and are these figures a real representation?) or genuinely representative of variance between cemeteries.

CHAPTER 9: ENDINGS

“...what you end up remembering isn't always the same as what you have witnessed.”

(Barnes 2011, 3)

There is always a tendency in a project such as this to recast hindsight as foresight; to pretend (to a degree) that one had planned it this way from the start. Of course that is not the case (even though one may want to remember it so). It is only when the nature and extent of an assemblage can be experienced by the person(s) studying it that — much like a person edging cautiously across a marsh under a New Moon — a path through it can be revealed.

The nature of this project meant there was a lot of path finding. This study was not constructed around a hypothesis and tested against objects selected for the purpose: questions were dictated by the cemeteries and their assemblages. This presented two main challenges when analysing the non-ferrous metalwork: there was a need to produce work relevant to the site narrative as — to a certain extent — dictated by the assemblage itself and there was a desire to place analysis within the wider research context for metallurgy and archaeology in the Early Anglo-Saxon period. It may seem that the two are natural bedfellows, but the sheer size of the assemblage meant that certain choices had to be made about what it was feasible to achieve.

Before beginning to discuss the results of this study the original research objectives as identified in the post-excavation assessment (Freestone and Mortimer 2005, 119) and previously discussed in Chapter 2 (page 80) will be re-discussed here. It should be remembered that these points were written in the context of a prior belief that Early Anglo-Saxon communities were reliant on recycling as a purely economic reflex to the collapse of Empire. The main points identified were:

- How potential recycling was organized remains unexplored. Could sufficient material simply be collected locally, or was it imported from continental Europe or even further afield?
- To what extent artefacts were produced locally, in regional centres, or imported?
- In the case of indigenous production, were the craftsmen peripatetic or attached to specific communities?
- Were there specialist producers of different types of artefact in the same material?

In Chapter 2 these questions were examined within the context of our current state of knowledge and assumptions (see page 80). Previous analysis on Early Anglo-Saxon objects by Mortimer (1990; 1991) and Blades (1995) showed that copper alloys were highly mixed and did not easily fit into our pre-conceived notions of alloy nomenclature. The narrative developed from this has focussed exclusively on resource management within the context of an assumed collapse of economies, trade links and cultural identities in the post-Roman era (see for example Mortimer 1990, 397; Fleming 2012, 23). It was suggested by the author that this narrative slant, being based on analysis of a relatively narrow and predominantly cast object forms (see page 72), was a little crude. It was also felt that there was too much focus on using modern pre-conceived notions of what a 'good' alloy was and (by extension) what 'good' metallurgical economy and practice are. This, it is believed, is a risky interpretative route: for whilst we can use our scientific knowledge to understand the physical limitations of a particular alloy we must be wary of judging it by our own standards. Taking this route has isolated the copper alloys; reducing complex composite objects to a singular facet of their identity despite the fact that the objects can be composed of many different metals (i.e. gilt surfaces, silver sheets, filler alloys, niellos). A cohesive and more holistic approach may tell a very different story about resource acquisition and management.

Because of these issues a slightly different methodological approach to previous studies was needed. Rather than focus in detail on a narrow subset of objects it was decided to take a broader approach and attempt to analyse as a large a proportion of the assemblage as possible (see page 95). In practice this meant a qualitative approach based on non-invasive surface analysis using hand held portable X-ray fluorescence (HHpXRF, see Chapter 3 for the full practical methodology). Whilst this necessitated the loss of analytical resolution on individual objects (when compared with other techniques such as scanning electron microscopy or mass spectrometry) it is believed that the greater breadth it allows the interpretation to be sited in adds a degree of archaeological accuracy that cannot be found from detailed trace element data on a subset of objects. This also necessitated a reassessment of the original research agenda which had been very much sited in the methodological and narrative approach set by previous studies (the revised questions can be found on page 91 and the same questions are used to structure the discussion in this chapter).

The methodological approach used here does, however, introduce some difficulties, particularly in interpreting the data. This will especially be the case for the archaeologist or Anglo-Saxon brooch specialist who is used to receiving the results of analysis as weight percent. There is no such comforting familiarity or security with the figures produced here and the net peak area data (NPA) can appear relatively incomprehensible. The data are presented in this manner due to the qualitative nature of the analysis and whilst it is perfectly possible to process the spectra in a quantitative manner (i.e. using an empirical calibration) to do so could be a grave error, presenting a false degree of accuracy (as discussed on page 158). For, whilst there is nothing inherently quantitative about presenting data in weight percent (when provided with appropriate limits of determination and qualifications etc.) the fact remains that much of the wider archaeological community often view it as such.

As stated the analysis is on the corroded surfaces. This means that, due to a host of corrosion processes (tin enrichment, de-zincification etc.), the results will not match an analysis of the un-corroded alloy (discussed on pages 110, 145, 162 and

309). This corrosion also increases the inhomogeneity of an object. Despite this experimental work (see page 158 and Nicholas and Manti 2014) has shown that processing data as NPA can result in data that are less numerically accurate than those produced using an empirical calibration. At the same time the experimental results have shown that NPA results, whilst deviating from given values on experimentally corroded alloys, still produce results that are within the broad alloy categorisations we use (i.e. a leaded bronze remains a leaded bronze). With a small number of objects there may be issues about the reliability of any conclusions drawn from the data set, but with a large data set (like here) the more reliable the data becomes. The key issue is to remember the limitations of the data and not over interpret.

In practical terms what does this mean? It means that it is not possible to use the results here to look at two objects and determine if their compositions match (i.e. to hypothesise that they were produced at the same time). It does mean that we can examine broad trends in alloy compositions (one of the main research focuses study, see page 91) and see if there is any relationship between various categorical variables (brooch type, manufacture method etc.) and alloy usage.

9.1 MORPHING INTO THE FUTURE

Before discussing the results there will be a brief consideration of what lessons this project can provide in the event that a similarly furnished large early medieval cemetery is excavated in the future. It is hoped that the work here has demonstrated that qualitative non-invasive surface analysis can produce numerical data which, when appropriately interpreted, can tell us much about the assemblage.

In this project the non-ferrous metalwork was submitted to assessment of its potential as part of the broader post-excavation assessment undertaken on the three cemeteries (Caruth and Anderson 2005). This included a brief breakdown of object manufacturing methods based on a visual examination of the objects (Freestone and Mortimer 2005).

The assessment of potential is a standard process for MAP 2 and MoRPHE (Lee 2006) compliant projects on all periods. For non-ferrous artefacts of all periods this rarely strays beyond the quantification of the number of objects and the composition is ignored and not investigated until the analysis phase (if at all, see McSloy 2013 for an example where there appears to have been little consideration of the potential for analytical work, indeed there is little meaningful attempt at interpretation of the non-ferrous objects full stop).⁸⁶ In comparison a post-excavation assessment for ceramics will involve not only a quantification of the number of sherds but also initial fabric descriptions (pers. comm. Dr Alice Forward), something akin to beginning to investigate the composition of a metal beyond that which is visually identifiable.

It may be that we are better served by undertaking a degree of qualitative analysis as part of the post-excavation assessment. The increasing affordability and rapidity of non-destructive analytical techniques certainly make this a more financially viable option than it was previously and doing so would allow us to assess the potential of the assemblage in a deeper and more meaningful way. It would enable limited resources to be more effectively deployed and the academic objectives of the project (a key consideration in the planning of archaeological excavation projects, see Historic England 2008, 15) to be developed with a tighter and more cost effective focus. Specifically — for early medieval cemeteries — it would allow the development of a detailed invasive sampling strategy for quantitative analysis that is based on the potential of the assemblage and not on pre-conceived notions of what the metallurgy *might* tell us. It would also enable more effective organisation: where there is already a proposal for objects to go on museum display it would enable a sampling strategy to be developed after discussion with relevant conservation staff in the planning stage.

Such a shift may seem somewhat unlikely, but it should be remembered that many scientific dating methods (particularly radiocarbon) were once undertaken only as a post-excavation measure, whereas now they are very much incorporated

⁸⁶ This should not be read as a criticism of the cited author, but of a failing in the project design and post-excavation assessment that led to metallurgy not being considered worthy of consideration.

into the excavation process itself (especially on long term projects or sites). Equally — as already noted — other material specialists already incorporate a similar degree of material analysis into the assessment phase. Adapting a similar position for non-ferrous metals may require a shift in the attitudes of project managers, but it should be noted that there has been recent discussion about post-excavation assessment standards (see the presentation from the 2009 IFA conference on this issue by Bryant, Glazebrook, and Hutcheson). Consequently there may be an opportunity, based on the experience of this and other similar studies, to develop an assessment process that can enable a simpler and more effective outcome (especially with a product-based planning project management process, see Lee 2006, 26). It goes without saying that, following the Historic England Archaeometallurgy Guidelines (Dungworth 2015), analytical work on the non-ferrous metals should always be undertaken by an appropriately trained specialist.

9.2 DISCUSSION

Although the methodological approach used in this study has differed from (some) previous work in its choice of breadth over analytical detail it is believed that there are still some very interesting results. Whilst it is not possible to discuss pairings of objects or sourcing and resource management based on trace and minor element data (à la Blades 1995 and Pollard et al. 2015), there are some broad trends that can be derived from the results of the three major data sets: the copper alloys, silver alloys and gilding.

9.2.1 PATTERNS OF ALLOY USAGE

As has been note regularly through this study the dominant narrative is that the Early Anglo-Saxon peoples had little control over their non-ferrous metallurgy. It is believed by the author, based on the results of this study, that this characterization is a little crude. The results suggest that the compositions are not random and that there is a degree of choice and skill being exercised. It is not Dark Age metallurgy.

This is not to suggest that the results are showing there to be clear and distinct alloy groups: the alloys are still very mixed (and one should be aware of the risk of false correlations due to the zero replacement method chosen here, see page 200 for further details). But there is perhaps an indication that there was a slight preference for different alloy types dependent on manufacturing process.

9.2.1.1 SILVER ALLOYS

It was noted in the silver results (Chapter 5) that previous analytical work on early medieval Anglo-Saxon silver alloys has focussed on fineness and debasement as the sole prism for interpretation (see page 263). The impact of this focus has been compounded by the very small number of silver objects so far analysed, the results of which (see Brownsword and Hines 1993; Mortimer and Draper 1997, compositions in see Table 3-18 on page 169) show these objects to have a relatively low silver content. This debasement is taken to indicate that there was no good source of readily available ‘fresh’ silver available (Mortimer 1986, 241; Fleming 2012, 23), and that tends to be where the interpretation ceases. Yet by focussing on fineness have not we removed agency from the communities and individuals that produced the objects? We have forgotten that the value of metals in a society can shift readily (despite some such shifts happening within living memory: during the Second World War in the USA base metals became of more importance to the state than sterling silver, which replaced them in costume jewellery, see Schroy 2004, 283) and are forcing our own value system on the past. We are constraining our ability to understand the dimensionality of the data to a single variable: silver content.

The nature of the surface analysis meant that studying fineness was not really an option here (due to corrosion processes, see page 167). Instead the focus was on the major alloying elements and assessing these against the archaeological categorical variables. Sixty-seven silver objects were analysed here and the results were processed using cluster analysis on the principal components (see Chapter 4). The results (see from page 244 onwards) suggested the following groups:

- Silver cluster 1 contains zinc and minimal tin. Preferred for wire objects.

- Silver cluster 2 contains tin and minimal zinc. Used predominantly for sheet dress accessories.
- Silver cluster 3 contains both tin and zinc and minimal gold. Almost entirely associated with the bridle fittings from grave 323 in ERL 104.
- Silver cluster 4 is mixed and contains all three elements. A general use silver alloy with no particular pattern in its use.

Of course one should not overstate this: the alloys are mixed and all contain copper and lead. The relative levels of the additional elements in the silver here suggest that the silver was not purified by the metal smith using cupellation, a technique that archaeological evidence has indicated was practised from the Bronze Age in Europe (Rehren and Eckstein 2002) and was widespread in both the Romano-British and middle Anglo-Saxon periods (Bayley and Eckstein 2006). Our evidence for early Anglo-Saxon cupellation is currently lacking — see Bayley 1991, 120 — although it is unknown if this is absence of evidence or evidence of absence. It is therefore likely that the non-silver elements (with the exception of gold) were deliberately added as alloying components (Wanhill 2002, 20–21; Wanhill 2005), although we do not know if they were added by the Anglo-Saxon smiths or by those who made the objects they were recycling (i.e. were they highly mixed Romano-British silver alloys). The mixed nature suggests that the source of material was recycled metals, previously identified as the production mechanism for early medieval silver alloys (Arnold 2005; Brownsword and Hines 1993). Consequently the silver is poor quality in modern economic ‘fineness’ terms. But, as can be seen above, the debased nature of the alloys does not mean that no useful information can be drawn from the compositions: production was not blind. There was choice and selection being exercised; it just does not necessarily conform to our overriding focus on purity.

9.2.1.2 COPPER ALLOYS

As has been stated throughout this study previous studies have tended to focus on cast dress accessories and ignore sheet and wire objects. As part of this study 808 copper alloy objects were investigated, of which 781 were considered in

detail (for details of the excluded objects see page 336). The data exploration followed the same process as used on the silver alloys. To check the validity of the process and provide comparable data the Nigel Blade's (1995) Early Anglo-Saxon analyses were also investigated in the same statistical manner (see Table 8-42 on page 380 for the results). The results of the principal components on both Eriswell and Blades' data showed that zinc and tin explained the variance. Hierarchical clustering on the results (see page 371) indicated the following groups:

- TR 1: No or very low zinc content, tin content varies but tends to be high. Lead content varies. Could be approximately described as a bronze.
- TR 2: Low to medium zinc content, tin content varies but tends to be high. Lead content varies from low to high. Could be approximately described as bronze or leaded bronze. Its interface with TR 3 is diffuse, and in this area it can be seen in this area as gunmetal or leaded gunmetal (with tin more dominant than zinc).
- TR 3: High zinc content and low tin. Lead content varies from low to high. Could be approximately described as brass or leaded brass. Its interface with TR 2 is diffuse, and in this area it can be seen in this area as gunmetal or leaded gunmetal (with zinc more dominant than tin).

It will be noticed that lead has played very little role in defining the clusters. This is not unexpected; the principal components analysis showed that most of the variation is explained by zinc and tin (see page 362). Mortimer (1991) noted similar results and incorporating leaded variations into her typology showed no discernible pattern (see page 381 for more on this). Blades also noted varying lead levels (1995, 145–146). He was not able to distinguish any particular distribution between lead and the other major alloying components and limited himself to classifying alloy types as leaded (see Table 8-40, page 379 for a detailed breakdown of Blades' alloy classification). The one exception was with cast rings from Morning Thorpe, which had a slightly higher lead content than other objects from the same cemetery (Blades was not able to see any such relationship

in the other cemeteries he analysed). There was no obvious similar relationship to be detected here, although further work may be required to investigate this in detail. Both Mortimer and Blades concluded that the presence of lead indicated that recycled scrap was forming the raw material resource (late Romano-British copper alloys also often being leaded, see page 78 for a discussion on this), and this is also the conclusion here.

This is a relatively small number of alloy groups compared with other copper alloy classification systems. Consequently the clusters were compared (see page 378) with the terminology used by Mortimer (1991), Blades (1995) and Pollard et al. (2015). All three used modern metallurgical definitions to label groups. Although the authors were all explicit about the impact of using modern definitions and understandings on archaeological alloys they are still using the terminology of the modern metallurgist (leaded gunmetal, brass, leaded brass etc.). It was felt that the results of both Blades and Eriswell data suggested that there was little in the way of distinct and *discrete* groupings: the alloys were distributed as a continuum. Consequently it may be argued that any division that uses modern terminology as a starting point of reference — no matter how aware you are of the dangers of using modern terminology and how you try to mitigate the impact — is likely to create false divisions. Using hierarchical clustering on the principal components does — to a certain extent — alleviate this. Whilst the analyst is (of course) making decisions and choices based on their knowledge and experience (and the constraints of the statistical techniques chosen) there is also a degree of allowing alloys to define themselves: variance is as variance does.

The data were not of high enough quality to investigate trace and minor elements in detail (see page 388).

A comparison of the categorical variables and the alloy clusters showed some intriguing results (see page 390). There appears to be a preference for the usage of cluster TR 3 (where zinc is more abundant than tin) for sheet metal objects and TR 2 for cast objects (where tin is more abundant than zinc). The situation

with cluster TR 1 (a zinc free nor near zinc free alloy) is more complex. It tends to be associated with melted drops, i.e. objects which have been through the cremation process. Consequently it may be that the zinc has simply volatilised off. Those cast and sheet objects made from TR 1 are more intriguing further work is required to understand if there is anything particularly significant about the presence of a near zinc free alloy.

Although only a tentative result this is a surprising and intriguing. The lack of binary alloy types has previously led to suppositions that this was a “*metallurgy of survival*” (Mortimer 1990, 397), suggesting a lack of choice. Yet, as discussed in the previous paragraph, it appears that there were choices and decisions being made during production that affected the metal composition. And, whilst the alloys are still very mixed and it is still uncertain exactly what decisions these clusters may represent (re-use and re-working of existing sheet metal work or choice and control of the alloys melted?) the very presence of alloy types (however broad) would suggest against a blind metallurgy of survival. It should be noted at this point the Mortimer was explicit about the limits of extrapolating from a data set drawn from the analysis of a single cast object type (1991, 105), but this message seems to have been ignored by many non-metallurgists.

The relationship between clusters and objects typologies was more limited. There appeared to be little relationship between cultural style and alloy usage *unless* the form of object appeared intrinsically linked to being produced in either cast or sheet metal. The most interesting result in this area was the bucket pendants (see page 397). Bucket pendants differ; not in their metallurgy but in the near singular use of a single alloy type. No other class of object (with 10 or more objects analysed) leans so heavily in favour of one cluster (see Table 8-52 on page 398). This includes other object classes where the majority of the objects are sheet metal, suggesting their difference is less to do with being made of sheet metal but because of the object typology itself. Is there something different about bucket pendants?

Bucket pendants are often — in the Roman period — associated with north and eastern continental European cemeteries (Eckardt 2014b). They are exceptionally rare in Romano-British burials (Eckardt 2014a, 43–45). In Britain — in post-Roman and early medieval burial contexts when they begin to appear — they are generally considered as representative of a different culture and possibly demonstrative of either strong cultural influence or physical movement of individuals (Hines 1984, 13; Montgomery et al. 2005). However; it should be noted that their distribution during the Roman period is so varied and covers so many different archaeological cultures beyond the borders of Rome that some (Greene 1987; Eckardt 2014a, 42) have raised significant questions as to their usefulness as an indicator of ethnic or cultural identity. Nevertheless it is inescapable that they are rare during the Romano-British period and more frequent after, raising the tantalising potential that cultural identity may, in certain circumstances, be intrinsically linked to metallurgical choices.

The Eriswell results tilt alluringly in this direction. Unfortunately there is a lack of corroborating analyses from comparable assemblages (none were analysed by Blades although they were present in two of the assemblages — Bergh Apton and West Heslerton — that he analysed). Consequently — and sadly — it cannot be certain that the result here is not an isolated example or something more mundane. It is recommended that bucket pendants should be subject to significantly more analytical work to try and throw further light on this interesting object category.

9.2.1.3 LEAD ALLOYS

The majority of the evidence for the use of lead and lead-tin rich alloys at Eriswell in the early Anglo-Saxon period comes from filler alloys (see Chapter 7, starting on page 286). Lead objects themselves are extremely rare, with only one definitively lead object (104-2905-A, see page 304) from the early-medieval period being found.

The bulk of our evidence for lead rich alloys are from filler alloys (solders etc.). Many of the Eriswell objects are composite. Where components had broken

away the opportunity was taken to investigate the joining technique. Mechanical fastening and soldering / brazing appeared to be the most popular joining techniques (it should be remembered that this is a skewed dataset, predominantly investigating joins that had failed). Where visual examination suggested the use of a filler alloy the area was subjected to analysis. This allowed the filler alloys to be broadly compared, but more detailed analysis was not possible as the HHpXRF beam is too large to accurately focus on a filler alloy and avoid any analysis of the base alloy.

The results appear to suggest the use of lead – tin filler alloys but the constraints presented by the methodology mean that many questions relating to the use of filler alloys must remain unanswered. We cannot know how the alloys were applied; with a rod to be rubbed on a heated surface or powdered as the Romans apparently often did (Lang and Hughes 1984, 92).

Post-Roman and early medieval filler alloys have received relatively little attention. Where they have been in receipt of detailed analysis and discussion it has been from later period sites, such as the Lindsey smith burial (Hinton 2000) or the workshops excavated in York (Bayley 1991; Bayley 1992). At Eriswell — as already noted — we do not have the remains of any workshop space, nor the remains of a metalworker conveniently buried with their equipment. It is therefore difficult to place the procurement of the raw materials in a conceptual framework of early-medieval alloy use. Were filler alloys sourced from recycled materials? What degree of control was exercised over filler alloy composition? These are important questions, ones that could help to significantly develop our understanding of the non-ferrous metal economy of the early medieval period. Consequently it is recommended that in future work filler alloys should be the subject of detailed quantitative analysis that would help us begin to answer some of these questions.

9.2.1.4 GILDING

There are not a large number of gilt objects (see Chapter 6). The analysis of the gilt objects showed the presence of mercury in every gilt layer analysed. X-Ray

Diffraction (XRD) of one object suggested that hot (or fire) mercury gilding was used (see page 270). The use of mercury gilding on post-Roman and early medieval objects raises an important question that has, so far, received little attention in early medieval scholarship (apart from a brief mention in Arnold 2005, 118–9); where was the mercury coming from?

Mercury is mined in the form of cinnabar and / or native mercury and there are no viable deposits known in the British Isles. Consequently the mercury used in gilding will likely have been imported (this is discussed in detail on page 278). Unfortunately we have little indication of where mining was taking place in the 5-7th centuries, the nature of the trade networks or even in what form it was transported. Understanding where and how mercury was being sourced is important for our understanding of Anglo-Saxon metallurgy.

The use of the technique suggests a certain degree of continuity of technological practice with late Roman techniques. Our lack of knowledge about extractive metallurgy in the period presents serious limitations in trying to understand from where the source(s) were located. Nevertheless it is interesting that in a period traditionally characterized as being one of ‘de-skilling’, suffering ‘a loss of basic technological know-how’ and alleged lack of raw materials (Fleming 2012, 35) the presence of mercury gilding suggests the opposite. It suggests a society that, at least for elite objects, maintained a continuity of technological knowledge and practice from the Romans and had the access to some of the same raw materials. The use of mercury challenges our traditional interpretations.

9.2.2 DISTRIBUTION AND SITE VARIATION

Just as there were problems in extrapolating an Anglo-Saxon non-ferrous metallurgy from an unrepresentative set of object types so there are issues with trying to use a single site: we have no idea of how valid the conclusions are beyond the limits of that site. Consequently there will be a brief examination of the Eriswell results in the context of analytical work from other cemeteries.

As noted there is a paucity of analytical work on silver alloys. Thus it is not possible to compare the results here with those from other cemeteries.

Archaeological evidence and analytical results appear to show that mercury gilding was the standard method of gilding throughout the Anglo-Saxon period (Lins and Oddy 1975; Bayley 1991, 119; Bayley and Russel 2008). In this respect Eriswell does not appear to differ from other sites and cemeteries.

Examining the usage of the Eriswell copper alloys with comparable sites featured in Blades (1995) suggests that there may be significant site based variation in alloy usage. This particularly appeared to be the case for annular brooches (see Table 8-50 on page 397), wrist clasps (see Table 8-47, page 394) and girdle-hangers (see Table 8-58, page 403). Unfortunately we cannot be certain at present if this is due to sampling strategies or genuinely representative of variance between cemeteries. Blades does not provide detail on the percentage of each site assemblage he analysed, therefore we have no real idea of how representative these analyses are of the wider assemblages.

The results here do not contradict that general consensus that the majority of the metal resource is acquired through the mechanism of recycling. Yet we do not understand how that process functioned within different communities. We are assuming that fen-edge and ‘inland’ communities exploited the metal resource in the same way because there are shared artistic and cultural styles, but we do not yet have the evidence to confirm or deny this hypothesis.

Currently we tend to focus our interpretation on very simplistic economic factors (i.e. the loss of imperial networks) and miss the opportunity to understand that resource acquisition can be strongly influenced by society and culture. Gerrard has argued that this is a period when personal power, local relationships and local structures come to the fore as there was no need to sublimate them to an imperial state (2013, 274–276). Whether you agree or not it should at least make one aware that there may be hyperlocal issues at play in the exploitation of the metal resource. Some of the issues we need to consider include:

- Did (presumably itinerant) metal craftspeople carry their own supply of scrap with them?
- Did individuals or communities collect scrap from their own hinterlands?

- If individuals or communities were collecting from their hinterlands would there be any variation in the types of site available to exploit and would these sites have had any particular practices associated that would impact on the nature of the metal resource available for recycling? We tend to assume that there was relatively equal access to the same ‘scrap’ resource in the Early Anglo-Saxon period without considering that there may have been hyperlocal variation in the usage and depositional practice of alloys by the previous culture whose metallurgy is being exploited (for a relevant example — if not directly geographically related — see Dungworth’s study of Romano-British copper alloys in Northern Britain: 1997b, 908)
- Were there any taboos or other cultural considerations / restrictions on the type of objects that could be recycled (an issue raised by Caple 1986, 531) *or* the locations that material could be collected from?

It is not possible to answer these questions here as there is not the comparable data available. It is clear that significant further work is required. This must focus on much broader approaches to analysis: there needs to be less focus on specific object typologies, instead our approaches need to ensure a reasonable representative sample of the whole assemblage is analysed.

9.2.3 PRIMARY METAL PRODUCTION AND THE NATURE OF TRADE IN METALS

The highly mixed nature of the silver and copper alloys suggests that current model of recycled objects as the predominant raw material resource is correct.

It should be noted, however, that the minor and trace element data was not of particularly high quality. Previous studies have suggested that there were periodic introductions of fresh metal into the supply chain in the early medieval period (Caple 1986, 530; Blades 1995, 194–197) and the recent study by Pollard et al. (2015, 712–713) appears to confirm this. It would be interesting to undertake further more detailed analysis on the Eriswell objects (i.e. invasive) to assess the trace elements in more detail and investigate if any similar trends are visible. It

would be particularly interesting to focus on the TR 3 cluster objects (i.e. the zinc rich alloys) and see if there is any indication at this stage that the mid-Saxon new metal group Pollard et al. identified (named by them CC12) can already be detected. The evidence for the extraction of other metals (lead, tin etc.) is more circumspect at Eriswell (although there is evidence for elsewhere in the country during the Anglo-Saxon period, see Chapter 2, page 66). To investigate this area further and see if any trace and minor element data can throw light on this it would be worthwhile focussing on collecting quantitative data from objects in cluster TR 1 (the zinc free cluster) and TR 2 (the cluster where tin is more abundant than zinc) to see if there is any indication of ‘new’ or different copper tin alloys entering the system.

It was not possible in this study to analyse the lead and tin rich filler alloys (i.e. the alloys used for soldering) in detail and, for the moment, our interpretation is limited to conjecture. It is unknown if the filler alloys (which at Eriswell are lead and tin rich) were sourced through recycling or fresh supplies. It would be interesting to undertake further work on this. If the results of further quantitative analysis suggest clean and ‘fresh’ alloys then ascertaining the source must be a priority. There is evidence for tin (Thorndycraft, Pirrie, and Brown 1999; Thorndycraft, Pirrie, and Brown 2004) and lead extraction (Fleming 1994) during the early medieval period (and further afield, see for instance the evidence for possible post-Roman lead mining in Northern Spain documented by Camarero et al. 2015). Understanding trade links (or their absence) such as these will help us throw considerable light on the networks within which the Early Anglo-Saxons operated.

In this data set the evidence for the acquisition of ‘fresh’ metals comes from the gilt objects. As mentioned all the gilt objects analysed here were mercury gilded. There are no cinnabar deposits in the British Isles, therefore the producers of the Eriswell gilt objects had access to trade networks that enabled them to access this (presumably) elite material. The most likely source for this is Almadén in Spain (although there may be other possibilities, see the map in Figure 6-3 on page 280).

On many different fronts the evidence suggests that, whilst the primary source of material for non-ferrous alloys was recycling, there was access to fresh sources of material.

9.2.4 CONTINUITY?

“The collapse of the metal economy in Britain also lays bare the extraordinary transformations people lived through as complex systems of production disappeared, and as they were left without access to very basic commodities like freshly smelted metal and nails, things that their great-grandparents would have bought with money. It also underscores the ways in which the collapse of the Roman economy was accompanied by the rapid and dramatic deskilling of Britain’s population.”

(Fleming 2012, 34)

The quotation from Fleming above illustrates the generally accepted narrative of non-ferrous metals in the Early Anglo-Saxon period. It is viewed as a period of near catastrophic technological decline, an uncivilised interlude before advancement continued onto the medieval society that (eventually) led us to capitalism and the now. The big assumption in this hypothesis is that the end of Roman Britain marked a complete technological break from the past: the loss of financial complexity meant a collapse in international trade and a reversal of technological skills to sub-standard prehistoric technological levels. Setting aside that this is somewhat misrepresenting the technological skills and abilities of Iron Age craftspeople, it is a disturbing backwards and reductive projection of what drives technological change. This approach was challenged long ago in prehistoric studies (Budd and Taylor 1995), yet still holds sway in early Anglo-Saxon studies. Is this because the evidence supports this position?

Not really.

The importation of mercury suggests a degree of continuity. We do not know the exact trade route mechanisms by which it was acquired, but it is suspected that it was mined at Almadén. It indicates a degree of continuity in trade and technological practice from the Roman period. Of course one must not overstate the case in this example as we are dealing with relatively elite materials. This raises a question: is continuity something we see only in relation to high status individuals who have the social influence or wealth to maintain connections and

continuity with the past in a way that others cannot? To examine this we turn to copper alloys, and again the situation is more complex.

It was demonstrated earlier that the position is potentially more multifaceted and nuanced (with regards to the major alloying elements in copper alloys) than previously suggested, but can we detect any continuity of practice between late Romano-British and Early Anglo-Saxon non-ferrous metallurgy? Re-examining the chart of manufacturing technique and cluster (Figure 8-33, page 392) and looking beyond the manufacturing divisions we can see that cluster TR 2 (low to medium zinc content, tin content varies but tends to be high) is the most plentiful alloy type overall. Mapping these clusters on to the standard alloy terminology is not easy, but generally this cluster type can be considered a bronze (or gunmetal towards its interface with TR 3 in a scatterplot of tin and zinc, see page 381). This — to some extent — fits in with the general trend of alloy usage in this period discussed in Chapter 2 (see Figure 2-7, page 79), with alloys where tin is more abundant than zinc being dominant. Putting this in a still broader context (again see Figure 2-7 on page 79) this alloy usage is not occurring in a vacuum and it is generally accepted that brass alloys reach their zenith in the early Romano-British period before declining and with ternary and quaternary alloys seeing much higher usage (Dungworth 1996; Bayley 1998; Bayley, Crossley, and Ponting 2008, 48–49). Indeed, as Pollard et al. point out, there is actually a very high degree of similarity visible in late Romano-British and Early Anglo-Saxon copper alloy compositions (2015, 700). This, naturally, suggests that there is a degree of continuity of practice in resource exploitation and alloy usage.⁸⁷ It is hoped that both further analysis and reinterpretation of existing analyses in the light of refined chronologies (such as Hines et al. 2013) can throw further light upon this.⁸⁸

⁸⁷ It should be noted that, whilst Roman objects are being recycled into Anglo-Saxon objects, Roman coins (particularly precious metal coinage) appear — to some degree — to still be in circulation as the original in the early medieval period, see for instance Eagles and Mortimer (1993) and Bradley (1987).

⁸⁸ As stated at the start of this section one must not overstate or over extrapolate continuity, there being many examples of significant changes in society in post-Roman Britain (see for instance Lane 2015).

9.3 THE END OF THE AFFAIR

“Unlike flint, pottery and wood whose reuse and recycling is strictly limited and involves more or less rapid depletion — finished metal products are just as good as the raw material ore. Far better in fact, as all the energy involved in the conversion to metal is now gratis”

(Taylor 1999)

Early Anglo-Saxon non-ferrous metallurgy is a complex area that has (outside of archaeometallurgical circles) been reduced to an overly simplistic narrative of technological decline. Much is often made of Mortimer’s ‘metallurgy of survival’ (1990, 397) in the archaeological and historical literature, but Mortimer herself was explicit about the limitations of the analysis so far undertaken and the preliminary nature of the conclusions (1991, 107). Sadly this nuance seems to have been lost, despite a host of metallurgical work suggesting a much more complex situation including the periodic injection of fresh metal supplies and the social complexities involved in the production of alloys (Caple 1986; Blades 1995; Baker 2013; Pollard et al. 2015).

The results here have suggested that there are different alloys used for different manufacturing purposes. There is also a hint that, in some cases, the metallurgy of some specific object classes (bucket pendants) may be a form of cultural expression. This should not be over-interpreted: the alloys are still very mixed. They do not form neat groupings and are best understood as a continuum rather than in modern, neat, technological distinctions (brass, bronze, gunmetal etc.). As with other studies it is believed that recycled scrap formed the majority of the raw material for the production of the metalwork from Eriswell. This brings us to the question of recycling, the widespread usage of which has led to a consensus that *“in the face of widespread recycling the knowledge used to produce new metal disappeared.”* (Fleming 2012, 35). This attitude is problematic, assuming that mining and smelting is superior to recycling without really considering if there is any evidence base to support this (not an uncommon position, as noted by

Korom recycling tends to be maligned across the contemporary world on both social and religious grounds, 1998, 197–198). A strong reminder of this comes from the quote at the opening of this section. Although from a paper focussing on the Eneolithic (or Chalcolithic) its point remains valid: recycling of non-ferrous metals is an effective technique and should not be considered inferior to mining and smelting (both approaches of resource acquisition have benefits and drawbacks), it is simply different. Indeed, recycling has formed part of the metal economy since humans started using metal.

It is believed that a significant reason for why this attitude to recycling has become so entrenched in Anglo-Saxon studies is the prism through which it is viewed: an economic interpretation framed by imperial decline. It is almost as if moral judgement is being passed (for an interesting discussion on how we often pass moral judgements on objects and production techniques see Saito 2010, 210–211). Empire provided an order that appears recognisable to us in our modern nation states; in contrast the Early Anglo-Saxon alloys are ‘dirty’ and representative of something out of place. They are offending our own cultural concepts of cleanliness and good order (Douglas 2002, 44). Yet it is clear there was a very real degree of continuity between different cultural periods. The challenge now is to become more aware of the litany of complex choices that lay behind the technological decision made in the Early Anglo-Saxon period and try and understand how this impacted upon the metallurgical compositions. We have to re-frame our views and remember that recycling is not only an economic act, but can be the product of active social and cultural choices. This is something we are already aware of when it comes to the recycling and reuse of monuments (Williams 1998) and masonry (Moreland 1999), but it is an awareness that is generally skipped when it comes to non-ferrous metals. Where this has been investigated (Meaney 1981; White 1990; Eckardt and Williams 2003) it has tended to focus on recognisable objects (predominantly Roman) that were re-used rather than those that were fully recycled (i.e. melted) into new forms of cultural identity. When full recycling is considered it tends to, again, be

reduced a to a function of scarcity (Swift 2012a, 110), even while more complex motivations are considered for other forms of re-use.

There has been one significant attempt to move beyond this by Caple (2010) who used saucer brooches as a case study. Saucer brooches, he noted, are often found in pairs and share enough visible production traits that it is thought they were likely made by the same hand and at the same time. Yet Caple notes that in his examples the composition of the pairs differ (2010, 312), indicative of two different melts where one would do and two adds extra requirements (preparing a crucible twice etc.). It is suggested that the reason for this may be the use of ancestor alloys, i.e. objects with meaning are being selected for recycling precisely because they have meaning(s) that will be incorporated into the new object. This should not be a surprising conclusion. There is no rule that states the incorporation or recycling of material from an object means the memory of that object is lost in the process; it can be a way of an individual or community incorporating one past as part of the construction of a new past and present. This is further compounded because, as anthropology can teach us, there is no need for physical material from an old object to be incorporated into a new one for a sense of age and continuity to be retained even when made completely afresh (P. Lane 2005, 19).

The breadth of analysis on the Eriswell assemblage means that it may be possible to spot similar patterns in sets of objects where one might have expected them to have shared the same composition (although issues with corrosion affecting results mean that further quantitative analysis will be needed). Of particular interest in this regard is the tack from grave 323 (page 418) and pairs of annular brooches that do not match (such as those from grave 005: see page 408). There may also be intermediary degrees between reuse and recycling that need to be examined. Sheet metal (which could potentially have been clipped and re-forged rather than melted afresh, see page 392) may be a particularly fruitful area for this, as current research has tended to focus solely on those objects with recognisable Roman traits (see Swift 2012b).

If these kinds of activities are occurring at Eriswell then it should not surprise us. They bury their dead around a Bronze Age barrow (ERL 114, see page 42) and incorporate Romano-British and Prehistoric artefacts in graves (see page 336). Why should such activity stop at the level of readily (to us) visibly identifiable material culture? This does not mean that we should throw away or ignore economic considerations; just that we need to be much more aware of the potential complexity and not reach for our (current) default position. Of course it is easy to say this, but the reality of incorporating such approaches into our understanding of the non-ferrous metallurgy will not be easy. As Caple notes “*functional and cultural meaning are often combined*” (2010, 315), making it conceptually difficult to understand resource selection and management choices made in the past. We must also remember to consider our interpretations within a communal context and not overly focus on individual actors; even choices such as the incorporation of an heirloom are, after all, made within a framework of shared cultural and social values.

It is not a de-skilled period. It is not the metallurgy of survival. It is not the twilight of technology, waiting for a new dawn. It is its own metallurgy, with its own complexities and nuances. We can use our scientific knowledge to understand the physical limitations of a particular alloy, but we must be wary of judging it by our own assumptions of what ‘good’ technology is.

BIBLIOGRAPHY

- Abdi, Hervé, and Lynne J. Williams. 2010. "Principal Component Analysis." *Wiley Interdisciplinary Reviews: Computational Statistics* 2 (4) (July 30): 433–459. doi:10.1002/wics.101. <http://doi.wiley.com/10.1002/wics.101>.
- Agterberg, Frits. 2014. *Geomathematics: Theoretical Foundations, Applications and Future Developments*. Quantitative Geology and Geostatistics. Cham: Springer International Publishing. doi:10.1007/978-3-319-06874-9. <http://link.springer.com/10.1007/978-3-319-06874-9>.
- Ahrens, L. H. 1953. "A Fundamental Law of Geochemistry." *Nature* 172 (4390) (December 19): 1148. doi:10.1038/1721148a0. <http://dx.doi.org/10.1038/1721148a0>.
- . 1954. "The Lognormal Distribution of the Elements (A Fundamental Law of Geochemistry and Its Subsidiary)." *Geochimica et Cosmochimica Acta* 5 (2) (February): 49–73. doi:10.1016/0016-7037(54)90040-X. <http://www.sciencedirect.com/science/article/pii/001670375490040X>.
- Aitchison, John. 1982. "The Statistical Analysis of Compositional Data." *Journal of the Royal Statistical Society. Series B (Methodological)* 44 (2): 139–177. <http://www.jstor.org/stable/2345821>.
- . 2003. "A Concise Guide to Compositional Data Analysis." In *2nd Compositional Data Analysis Workshop; Girona, Italy*. http://ima.udg.edu/activitats/codawork05/A_concise_guide_to_compositional_data_analysis.pdf.
- Aitchison, John, Carles Barceló-Vidal, and Vera Pawlowsky-Glahn. 2002. "Some Comments on Compositional Data Analysis in Archaeometry, in Particular the Fallacies in Tangri and Wright's Dismissal of Logratio Analysis." *Archaeometry* 44 (2) (May): 295–304. doi:10.1111/1475-4754.t01-1-00061. <http://doi.wiley.com/10.1111/1475-4754.t01-1-00061>.
- Aitchison, John, and J. J. Egozcue. 2005. "Compositional Data Analysis: Where Are We and Where Should We Be Heading?" *Mathematical Geology* 37 (7) (October): 829–850. doi:10.1007/s11004-005-7383-7. <http://www.springerlink.com/index/10.1007/s11004-005-7383-7>.
- Aitchison, John, and J.W. Kay. 2003. "Possible Solutions of Some Essential Zero Problems in Compositional Data Analysis." In *CoDaWork '03: Proceedings of Compositional Data Analysis Workshop, 2003*. Girona. http://ima.udg.edu/Activitats/CoDaWork03/paper_Aitchison_and_Kay.pdf.
- Akerman, John Yonge. 1853a. "An Account of Excavations in an Anglo-Saxon Burial Ground at Harnham Hill, near Salisbury." *Archaeologia* 35: 259–278.
- . 1853b. "Note on Some Further Discoveries in the Anglo-Saxon Burial-Ground at Harnham Hill, near Salisbury." *Archaeologia* 35: 475–479.
- . 1855. *Remains of Pagan Saxondom*. London: J. R. Smith. <http://books.google.com/books?id=HTHYAAAAMAAJ&pgis=1>.
- . 1857. "An Account of the Discovery of Anglo-Saxon Remains at Kemble, in North Wilts; with Observations on a Grant of Land at Ewelme at the Abbey of Malmesbury by King Ethelstan, in the Year 931." *Archaeologia* 37: 113–121.
- . 1863. "Report on Further Researches in an Anglo-Saxon Burial Ground at

- Long Wittenham, Berkshire, in the Summer of 1860.” *Archaeologia* 39: 135–142.
- Alcock, Leslie. 1989. *Arthur's Britain*. London: Penguin Books.
- Alvarez, R.A.V. 2007. “When Zero Doesn’t Mean It and Other Geomathematical Mischief.” In *Geomathematics and GIS Analysis of Resources, Environment and Hazards: Proceedings of LAMG 2007*, edited by P Zhao, F Agterberg, and Q Cheng. Kingston, ON, Canada: International Association for Mathematical Geology. [http://dugi-doc.udg.edu/bitstream/handle/10256/711/VALLS_new_When zero doesn't mean it.pdf](http://dugi-doc.udg.edu/bitstream/handle/10256/711/VALLS_new_When_zero_doesn't_mean_it.pdf)
- Ambrose, Keith. 2013. “Breedon Hill.” *Mercian Geologist* 18 (2): 139–143. <http://nora.nerc.ac.uk/503473/>.
- Anonymous. 1839. *The Penny Cyclopaedia of the Society for the Diffusion of Useful Knowledge (Volume 15)*. London: Charles Knight and Co.
- . 1946. “Early Mining and Metallurgy Group.” *Man* 46: 99.
- . 2012. *The Cambridge Companion to the Roman Economy*. Edited by Walter Scheidel. Vol. 8. Cambridge: Cambridge University Press. http://books.google.com/books?id=InbNvsEB_pkC&pgis=1.
- . 2013. “Norfolk & Suffolk Brecks: Landscape Character Assessment.” Ipswich: Suffolk County Council. [http://www.suffolklandscape.org.uk/userfiles/pdfs/Brecks LCA/Part 1 Brecks LCA - Final Report %5B%20res_23_Oct_2013%5D.pdf](http://www.suffolklandscape.org.uk/userfiles/pdfs/Brecks_LCA/Part_1_Brecks_LCA_-_Final_Report_%5B%20res_23_Oct_2013%5D.pdf).
- Archibald, Marion. 1985. “The Coinage of Beonna in Light of the Middle Harling Hoard.” *British Numismatic Journal* 55: 10–54. <http://www.bcin.ca/Interface/openbcin.cgi?submit=submit&Chinkey=86637>.
- Arnold, C.J. 2005. *An Archaeology of the Early Anglo-Saxon Kingdoms*. London/New York: Routledge.
- Arrhenius, B. 1982. “Technical Properties as a Discriminant in Migration Period.” In *Aspects of Production and Style in Dark Age Metal (Occasional Paper 34)*, edited by L. Webster, 1–19. British Museum.
- Artioli, G. 2007. “Crystallographic Texture Analysis of Archaeological Metals: Interpretation of Manufacturing Techniques.” *Applied Physics A* 89 (4) (August 9): 899–908. doi:10.1007/s00339-007-4215-2. <http://www.springerlink.com/index/10.1007/s00339-007-4215-2>.
- ASM International. 1992. *ASM Handbook: Volume 3: Alloy Phase Diagrams*. Materials Park, Russell Township, OH: ASM International.
- Aucouturier, Marc, and Evelyne Darque-Ceretti. 2007. “The Surface of Cultural Heritage Artefacts: Physicochemical Investigations for Their Knowledge and Their Conservation.” *Chemical Society Reviews* 36 (10) (October 24): 1605–21. doi:10.1039/b605304c. <http://www.ncbi.nlm.nih.gov/pubmed/17721585>.
- Aufderhaar, Iris. 2009. “From the Goldsmith’s Point of View.” *ArcheoSciences* (33) (December 31): 243–253. <http://archeosciences.revues.org/2269>.
- Bacon-Shone, John. 2011. “A Short History of Compositional Data Analysis.” In *Compositional Data Analysis: Theory and Applications*, edited by Vera Pawlowsky-Glahn and Antonella Buccianti, 3–11. Chichester, UK: John Wiley & Sons, Ltd. doi:10.1002/9781119976462. <http://doi.wiley.com/10.1002/9781119976462>.
- Baker, Jocelyn Margaret. 2013. “The Colour and Composition of Early Anglo-Saxon

- Copper Alloy Jewellery.” University of Durham. <http://etheses.dur.ac.uk/10550/>.
- Bakka, E. 1958. *On the Beginning of Salin's Style I in England*. Universitet I Bergen Arbok Historik-Antikvarisk Rekke 3. Bergen: Universitet i Bergen.
- Barlow, J. 1793. *Vision of Columbus: A Poem in Nine Books*. 5th ed. Paris: The English Press.
- Barnes, Julian. 2011. *The Sense of an Ending*. London: Random House.
- Baxter, Michael J. 1993. “Comment On D. Tangri And R. V. S. Wright, ‘Multivariate Analysis Of Compositional Data?’, *Archaeometry*, 35 (1) (1993).” *Archaeometry* 35 (1) (February): 112–115. doi:10.1111/j.1475-4754.1993.tb01027.x. <http://doi.wiley.com/10.1111/j.1475-4754.1993.tb01027.x>.
- Baxter, Michael J., and Ian C. Freestone. 2006. “Log-Ratio Compositional Data Analysis in *Archaeometry*.” *Archaeometry* 48 (3) (August): 511–531. doi:10.1111/j.1475-4754.2006.00270.x. <http://doi.wiley.com/10.1111/j.1475-4754.2006.00270.x>.
- Bayley, Justine. 1991. “Anglo-Saxon Non-Ferrous Metalworking: A Survey.” *World Archaeology* 23 (1) (December): 115–130. <http://www.jstor.org/stable/124732>.
- . 1992. *Anglo-Scandinavian Non-Ferrous Metalworking from 16-22 Coppergate*. The Archaeology of York 17/7. York: Council for British Archaeology for the York Archaeological Trust.
- . 1998. “The Production of Brass in Antiquity with Particular Reference to Roman Britain.” In *2000 Years of Zinc and Brass. London: British Museum (Occasional Paper 50, Revised Edition)*, edited by Paul Terence Craddock, 7–26. London: British Museum.
- Bayley, Justine, and Sarnia Butcher. 2004. *Roman Brooches in Britain: A Technological and Typological Study Based on the Richborough Collection*. London: Society of Antiquaries of London. <http://archaeologydataservice.ac.uk/archives/view/68fiche/>.
- Bayley, Justine, David Crossley, and Matthew Ponting. 2008. *Metals and Metalworking: A Research Framework for Archaeometallurgy*. HMS Occasional Publications. London: Historical Metallurgy Society. <http://hist-met.org/images/Frameworks-Met&Mat-2008.pdf>.
- Bayley, Justine, and K Eckstein. 2006. “Roman and Medieval Litharge Cakes: Structure and Composition.” In *34th International Symposium on Archaeometry, 3-7 May 2004, Zaragoza, Spain*, edited by J Pérez-Arantegui, 145–153. Zaragoza: Institución “Fernando el Católico.
- Bayley, Justine, and Andy Russel. 2008. “Making Gold-Mercury Amalgam: The Evidence for Gilding From Southampton.” *The Antiquaries Journal* 88 (2008): 37. doi:10.1017/S0003581500001335.
- Bayley, Justine, and Jacqui Watson. 2009. “Emerging from the Appendices: The Contribution of Scientific Examination and Analysis to Medieval Archaeology.” In *50 Years of Medieval Archaeology, 1957-2007*, edited by Roberta Gilchrist and Andrew Reynolds. Society for Medieval Archaeology Monographs. Leeds: Maney Publishing.
- Beck, L., S. Bosonnet, S. Réveillon, D. Eliot, and F. Pilon. 2004. “Silver Surface Enrichment of Silver–copper Alloys: A Limitation for the Analysis of Ancient Silver Coins by Surface Techniques.” *Nuclear Instruments and Methods in Physics Research Section B: Beam Interactions with Materials and Atoms* 226 (1-2) (November): 153–162. doi:10.1016/j.nimb.2004.06.044.

<http://www.sciencedirect.com/science/article/pii/S0168583X04008316>.

- Beldjoudi, T, F Bardet, N Lacoudre, S Andrieu, A Adriaens, Ina Constantinides, and Philippe Brunella. 2001. "Surface Modification Processes on European Union Bronze Reference Materials for Analytical Studies of Cultural Artefacts." *Surface Engineering* 17 (3): 231–235. doi:1854/12834. <http://hdl.handle.net/1854/LU-434112>.
- Berger, M.J., J.H. Hubbell, S.M. Seltzer, J. Chang, J.S. Coursey, R. Sukumar, D.S. Zucker, and K. Olsen. 2010. "XCOM: Photon Cross Sections Database (NIST Standard Reference Database 8 (XGAM))." Gaithersburg, MD: National Institute of Standards and Technology (NIST). <http://www.nist.gov/pml/data/xcom/>.
- Best, Stephen, and Sharon Marcus. 2009. "Surface Reading: An Introduction." *Representations* 108 (1) (November): 1–21. doi:10.1525/rep.2009.108.1.1. <http://academiccommons.columbia.edu/catalog/ac:157279>.
- Beutel, J., H.L. Kundel, and R.L. Van Metter. 2000. *Handbook of Medical Imaging: Physics and Psychophysics*. Bellingham (Washington): SPIE Press.
- Bezur, Aniko, and Francesca Casadio. 2012. "The Analysis of Porcelain Using Handheld and Portable X-Ray Fluorescence Spectrometers." In *Handheld XRF for Art and Archaeology*, edited by Aaron N. Shugar and Jennifer L. Mass, 249–312. Leuven: Leuven University Press. <http://upers.kuleuven.be/en/book/9789058679079>.
- Biek, L. 1994. "Tin Ingots Found at Praa Sands, Beagrie, 1974." *Cornish Archaeology* 33: 57–95.
- Bintliff, John. 1991. "Post-Modernism, Rhetoric and Scholasticism at TAG: The Current State of British Archaeological Theory." *Antiquity* 65 (247) (June 1): 274–278. <https://openaccess.leidenuniv.nl/handle/1887/11982>.
- . 2011. "The Death of Archaeological Theory?" In *The Death of Archaeological Theory?*, edited by John Bintliff and M Pearce, 7–22. Oxford: Oxford Books.
- Biringuccio, Vannoccio. 1666. *Pirotechnia*. Edited and translated by Cyril Stanley Smith and Martha T Gnudi. Cambridge, Massachusetts: MIT Press.
- Blades, Nigel William. 1995. "Copper Alloys From English Archaeological Sites 400–1600 AD: An Analytical Study Using ICP-AES." *October*. Royal Holloway University of London. <http://ethos.bl.uk/OrderDetails.do?did=1&uin=uk.bl.ethos.261778>.
- Blair, C, and John Blair. 1991. "Copper Alloys." In *English Medieval Industries: Craftsmen, Techniques, Products*, edited by John Blair and N Ramsey, 81–106. London: The Hambleton Press.
- Bogen, J. 2010. "Theory and Observation in Science." *The Stanford Encyclopedia of Philosophy*. <http://plato.stanford.edu/archives/spr2010/entries/science-theory-observation/>>.
- Boivin, N. 2004. "Mind over Matter? Collapsing the Mind-Matter Dichotomy in Material Culture Studies." In *Rethinking Materiality: The Engagement of Mind with the Material World*, edited by E. DeMarrais, C. Gosden, and C. Renfrew, 63–71. Cambridge: McDonald Institute Monograph.
- Bonizzoni, Letizia, Anna Galli, Marco Gondola, and Marco Martini. 2013. "Comparison between XRF, TXRF, and PXRF Analyses for Provenance Classification of Archaeological Bricks." *X-Ray Spectrometry* 42 (4) (July 24): 262–267.

- doi:10.1002/xrs.2465. <http://doi.wiley.com/10.1002/xrs.2465>.
- Booth, A. 2015. "SF-66EDD6: A EARLY MEDIEVAL CLASP." <https://finds.org.uk/database/artefacts/record/id/717229>.
- Bos, M., and J.A.M. Vrieling. 1998. "Constraints, Iteration Schemes and Convergence Criteria for Concentration Calculations in X-Ray Fluorescence Spectrometry with the Use of Fundamental Parameter Methods." *Analytica Chimica Acta* 373 (2-3) (November): 291–302. doi:10.1016/S0003-2670(98)00412-7. [http://dx.doi.org/10.1016/S0003-2670\(98\)00412-7](http://dx.doi.org/10.1016/S0003-2670(98)00412-7).
- Bradley, Richard. 1987. "Time Regained: The Creation of Continuity." *Journal of the British Archaeological Association* 40 (1) (July 18): 1–17. <http://www.maneyonline.com/doi/abs/10.1179/jba.1987.140.1.1>.
- Bragg, W.L. 1913. "The Diffraction of Short Electromagnetic Waves by a Crystal." *Proceedings of the Cambridge Philosophical Society* 17: 43–57.
- Bray, Peter, and A. Mark Pollard. 2005. "Comments Ii: The Underpinnings And Consequences Of The Materiality Approach." *Archaeometry* 47 (1) (February): 179–182. doi:10.1111/j.1475-4754.2005.195-2.x. <http://doi.wiley.com/10.1111/j.1475-4754.2005.195-2.x>.
- Briscoe, Grace. 1953. "A Romano-British Settlement at Lakenheath, Suffolk." *Proceedings of the Suffolk Institute of Archaeology* 26: 69 – 84. [http://suffolk.institute.pdfsrv.co.uk/customers/SuffolkInstitute/2014/01/10/Volume XXVI Part 2 \(1953\)_A Romano-British settlement at Lakenheath Suffolk G Briscoe_68 to 84.pdf](http://suffolk.institute.pdfsrv.co.uk/customers/SuffolkInstitute/2014/01/10/VolumeXXVI%20Part%20(1953)_A%20Romano-British%20settlement%20at%20Lakenheath%20Suffolk%20G%20Briscoe_68%20to%2084.pdf).
- Briscoe, Grace, and W. E. Le Bard. 1960. "Archaeological Notes: An Anglo-Saxon Cemetery on Lakenheath Airfield." *Proceedings of the Cambridge Antiquarian Society* 53: 56–57. http://archaeologydataservice.ac.uk/catalogue/adsdata/arch-1895-1/dissemination/pdf/PCAS/1960_LIII/PCAS_LIII_1960_055-057_Wilkersonetal.pdf.
- British Museum. 2012. "Energy Dispersive X-Ray Fluorescence (ED-XRF)." Accessed May 23. http://www.britishmuseum.org/about_us/departments/conservation_and_science/research/scientific_techniques/x-ray_fluorescence.aspx.
- Brooks, D.A. 1994. "The Theory and Methodology of Classifications of the Fifth and Sixth Centuries A.D. in Anglo-Saxon England with Reference to Great Square-Headed Brooches." University College, University of London.
- Brown, Katherine L., and Robin J. H. Clark. 2004. "Analysis of Key Anglo-Saxon manuscripts(8–11th Centuries) in the British Library: Pigment Identification by Raman Microscopy." *Journal of Raman Spectroscopy* 35 (3) (March): 181–189. doi:10.1002/jrs.1127. <http://doi.wiley.com/10.1002/jrs.1127>.
- Brown, N., P Murphy, B Ayers, S Bryant, and T Malim. 2000. "Research Themes." In *Research and Archaeology: A Framework for the Eastern Counties 2: Research Agenda and Strategy*, edited by N Brown and J Glazebrook. Norwich: The Scole Archaeological Committee for East Anglia.
- Brownsword, R., and John Hines. 1993. "The Alloys of a Sample of Anglo-Saxon Great Square-Headed Brooches." *The Antiquaries Journal* 73 (1): 1–10. doi:<http://dx.doi.org/10.1017/S000358150007164X>.
- Brugmann, Birte. 1999. "The Role of Continental Artefact-Types in Sixth-Century

- Kentish Chronology.” In *The Pace of Change: Studies in Early Medieval Chronology*, edited by John Hines, Karen Høiland Nielsen, and Frank Siegmund, 37–64. Cardiff Studies in Archaeology. Oxford: Oxbow Books.
- Bruker Elemental. 2010. “User Guide: Tracer Series (Version 0.30.0002.02.0).” Madison, WI.
- Brunt, P. 1990. *Roman Imperial Themes*. Oxford: Clarendon Press.
- Bryant, Stewart, Jenny Glazebrook, and Andy Hutcheson. 2009. “Standards For Post-Excavation Assessment: A View From The East Of England.” In *IfA Conference (Torquay) Post Excavation in Archaeology*. <https://postexcavation.wordpress.com/presentations/standards-for-post-excavation-assessment-a-view-from-the-east-of-england/>.
- Bucciante, Antonella, and Vera Pawlowsky-Glahn. 2005. “New Perspectives on Water Chemistry and Compositional Data Analysis.” *Mathematical Geology* 37 (7) (October): 703–727. doi:10.1007/s11004-005-7376-6. <http://link.springer.com/10.1007/s11004-005-7376-6>.
- Budd, Paul, and Timothy Taylor. 1995. “The Faerie Smith Meets the Bronze Industry: Magic versus Science in the Interpretation of Prehistoric Metal Making.” *World Archaeology* 27 (1) (June 15): 133–143. doi:10.1080/00438243.1995.9980297. <http://www.tandfonline.com/doi/abs/10.1080/00438243.1995.9980297>.
- Bullis, W.M. 1990. “Silicon Material Properties.” In *Handbook of Semiconductor Silicon Technology*, edited by W.C O’Mara, R.B Herring, and L.P Hunt, 422–434. New Jersey: Noyes Publications.
- Burley, David V., Peter J. Sheppard, and Maia Simonin. 2011. “Tongan and Samoan Volcanic Glass: pXRF Analysis and Implications for Constructs of Ancestral Polynesian Society.” *Journal of Archaeological Science* 38 (10) (October): 2625–2632. doi:10.1016/j.jas.2011.05.016. <http://www.sciencedirect.com/science/article/pii/S0305440311001762>.
- Camarero, L., P. Masqué, W. Devos, I. Ani-Ragolta, J. Catalan, H.C. Moor, S. Pla, and J.A. Sanchez-Cabeza. 2015. “Historical Variations in Lead Fluxes in the Pyrenees (Northeast Spain) from a Dated Lake Sediment Core.” *Water, Air, and Soil Pollution* 105 (1-2): 439–449. doi:10.1023/A:1005005625972. <http://link.springer.com/article/10.1023/A%3A1005005625972>.
- Cameron, M.L. 1993. *Anglo-Saxon Medicine*. Cambridge: Cambridge University Press.
- Campbell, Ewan. 2007. “Continental and Mediterranean Imports to Atlantic Britain and Ireland, AD 400-800.” York: Council for British Archaeology. <http://eprints.gla.ac.uk/49272/>.
- Campbell, Ewan, and Alan Lane. 1994. “Excavations at Longbury Bank, Dyfed, and Early Medieval Settlement in South Wales.” *Medieval Archaeology* 38: 15–77.
- Caple, Chris. 1986. “An Analytical Appraisal of Copper Alloy Pin Production: 400-1600 AD.” University of Bradford. <http://hdl.handle.net/10454/3423>.
- . 2010. “Ancestor Artefacts – Ancestor Materials.” *Oxford Journal of Archaeology* 29 (3): 305–318. <http://onlinelibrary.wiley.com/doi/10.1111/j.1468-0092.2010.00350.x/full>.
- Caruth, Jo, and Sue Anderson. 2005. “An Assessment of the Potential for Analysis and Publication for Archaeological Work Carried out at RAF Lakenheath between 1987 and June 2005: Volume I: The Anglo-Saxon Cemeteries ERL 104, ERL 046

- and ERL 114.” 2005/94. SCCAS Report. Ipswich: Suffolk County Council.
- Casaletto, M. P., G. M. Ingo, C. Riccucci, and F. Faraldi. 2010. “Production of Reference Alloys for the Conservation of Archaeological Silver-Based Artifacts.” *Applied Physics A* 100 (3) (April 22): 937–944. doi:10.1007/s00339-010-5677-1. <http://link.springer.com/10.1007/s00339-010-5677-1>.
- Cesareo, Roberto, and GE Gigante. 2008. “Portable Systems for Energy Dispersive X-Ray Fluorescence Analysis of Works of Art.” In *Portable X-Ray Fluorescence Spectrometry: Capabilities for In Situ Analysis*, edited by P.J. Potts and M. West, 206–246. London: The Royal Society of Chemistry. doi:10.1039/9781847558640-00206. <http://pubs.rsc.org/en/content/chapter/bk9780854045525-00206/978-1-84755-864-0>.
- Chakrabarti, D. J., and D. E. Laughlin. 1985. “The Cu-Hg (Copper-Mercury) System.” *Bulletin of Alloy Phase Diagrams* 6 (6) (December): 522–527. doi:10.1007/BF02887149. <http://link.springer.com/10.1007/BF02887149>.
- Chamón, J., P. Carolina Gutiérrez, J. Barrio, Aurelio Climent-Font, and M. Arroyo. 2010. “Study of Medieval Enamelling on Gilded Objects Combining SEM-EDAX and PIXE.” *Applied Physics A* 99 (2) (March 26): 377–381. doi:10.1007/s00339-010-5634-z. <http://www.springerlink.com/content/e838638477852682/>.
- Charlton, Michael F., Eleanor Blakelock, Marcos Martín-Torres, and Tim Young. 2012. “Investigating the Production Provenance of Iron Artifacts with Multivariate Methods.” *Journal of Archaeological Science* 39 (7) (July): 2280–2293. doi:10.1016/j.jas.2012.02.037. <http://www.sciencedirect.com/science/article/pii/S0305440312001021>.
- Clarke, David L. 1968. *Analytical Archaeology*. Michigan: Methuen. <http://books.google.com/books?id=vzRmAAAAMAAJ&pgis=1>.
- Collins, A.E.P, and H.H Beeny. 1950. “Ancient Mining and Metallurgy Committee: Report on Pattern-Welding on a Viking Period Spearhead.” *Man* 50: 124–125.
- Colman, Tim. 2010. “Gold in Britain : Past, Present and Future.” *Mercian Geologist* 17 (3): 173–180. <http://nora.nerc.ac.uk/11831/>.
- Comas-Cufí, M, and Santiago Thió-Henestrosa. 2011. “CoDaPack 2.0: A Stand-Alone, Multi-Platform Compositional Software.” In *Proceedings of CoDaWork'11: 4th International Workshop on Compositional Data Analysis*. Sant Feliu de Guíxols. <http://www.ma3.upc.edu/users/ortego/codawork11-Proceedings/Admin/Files/FilePaper/p28.pdf>.
- Condamin, J., and M. Picon. 1964. “The Influence of Corrosion and Diffusion on the Percentage of Silver in Roman Denarii.” *Archaeometry* 7 (1) (June): 98–105. doi:10.1111/j.1475-4754.1964.tb00603.x. <http://doi.wiley.com/10.1111/j.1475-4754.1964.tb00603.x>.
- Cook, Ian. 2004. “Follow the Thing: Papaya.” *Antipode* 36 (4) (September): 642–664. doi:10.1111/j.1467-8330.2004.00441.x. <http://doi.wiley.com/10.1111/j.1467-8330.2004.00441.x>.
- Cooke, Strathmore R.B., and Stanley Aschenbrenner. 1975. “The Occurrence of Metallic Iron in Ancient Copper.” *Journal of Field Archaeology* 2 (1): 251–266. doi:10.1179/009346975791491015. <http://www.maneyonline.com/doi/abs/10.1179/009346975791491015>.
- Corregidor, V., L.C. Alves, N.P. Barradas, M.A. Reis, M.T. Marques, and J.A. Ribeiro.

2011. "Characterization of Mercury Gilding Art Objects by External Proton Beam." *Nuclear Instruments and Methods in Physics Research Section B: Beam Interactions with Materials and Atoms* 269 (24) (December): 3049–3053. doi:10.1016/j.nimb.2011.04.070. <http://www.sciencedirect.com/science/article/pii/S0168583X11004216>.
- Craddock, Paul Terence. 1975. "The Composition of Copper Alloys in the Classical World." University College London (University of London). <http://ethos.bl.uk/OrderDetails.do?uin=uk.bl.ethos.452458>.
- Craddock, Paul Terence, Susan La Niece, and Duncan Hook. 1990. "Brass in the Medieval Islamic World." In *2000 Years of Zinc and Brass*, edited by Paul Terence Craddock, Revised ed, 73–80. British Museum.
- Craddock, Paul Terence, Jonathan M. Wallis, and John F. Merkel. 2001. "The Rapid Qualitative Analysis of Groups of Metalwork: Making a Dream Come True." In *Pattern and Purpose in Insular Art*, edited by Mark Redknap, Nancy Edwards, Alan Lane, Susan Youngs, and Jeremy Knight, 117–124. Oxford: Oxbow Books.
- Craig, Nathan, Robert J. Speakman, Rachel S. Popelka-Filcoff, Michael D. Glascock, J. David Robertson, M. Steven Shackley, and Mark S. Aldenderfer. 2007. "Comparison of XRF and PXRF for Analysis of Archaeological Obsidian from Southern Perú." *Journal of Archaeological Science* 34 (12) (December): 2012–2024. doi:10.1016/j.jas.2007.01.015. <http://dx.doi.org/10.1016/j.jas.2007.01.015>.
- Crane, Hart. 2001. "Recitative." In *The Complete Poems of Hart Crane*, edited by Harold Bloom, 91. New York: Liveright Publishing Corporation.
- Croux, Christophe, Peter Filzmoser, and Heinrich Fritz. 2013. "Robust Sparse Principal Component Analysis." *Technometrics* 55 (2) (May 22): 202–214. doi:10.1080/00401706.2012.727746. <http://www.tandfonline.com/doi/abs/10.1080/00401706.2012.727746>.
- da Vinci, Leonardo di ser Piero. 2001. *Leonardo on Painting: An Anthology of Writings by Leonardo Da Vinci, with a Selection of Documents Relating to His Career as an Artist*. Edited by Martin Kemp. Translated by Martin Kemp and Margaret Walker. New Haven, Connecticut: Yale University Press.
- Damiani, D., E. Gliozzo, I. Memmi Turbanti, and J. E. Spangenberg. 2003. "Pigments and Plasters Discovered in the House of Diana (Cosa, Grosseto, Italy): An Integrated Study Between Art History, Archaeology and Scientific Analyses*." *Archaeometry* 45 (2) (May): 341–354. doi:10.1111/1475-4754.00112. <http://doi.wiley.com/10.1111/1475-4754.00112>.
- Darby, H. C. 1934. "The Fenland Frontier in Anglo-Saxon England." *Antiquity* 8 (30) (June 1): 185–199. doi:10.1017/S0003598X00009157. http://journals.cambridge.org/abstract_S0003598X00009157.
- Daston, L, and P Galison. 2010. *Objectivity*. New York: Zone Books.
- Davies, O. 1934. "Roman and Medieval Mining Techniques." *Transactions of Institute of Mining and Metallurgy* XLIII: 3–54.
- Davis, Joseph R. 2001a. "Nobel Metal Alloys." In *Alloying: Understanding the Basics*, edited by Joseph R. Davis, 550–570. Materials Park, Russell Township, OH: ASM International.
- . 2001b. *Copper and Copper Alloys*. Materials Park, Russell Township, OH: ASM International.

- Davis, Mary. 2014. "Technology at the Transition: Relationships between Culture, Style and Function in the Late Iron Age Determined through the Analysis of Artefacts." Cardiff. <http://orca.cf.ac.uk/73215/2/davism.pdf>.
- Day, J. 1998. "Brass and Zinc in Europe from the Middle Ages until the Nineteenth Century." In *2000 Years of Zinc and Brass (Occasional Paper 50, Revised Edition)*, 133–158. London: British Museum.
- De Vries, J.L., and B.A.R. Vrebos. 2002. "Quantification of Infinitely Thick Specimens by XRF Analysis." In *Handbook of X-Ray Spectrometry - Second Edition, Revised and Expanded*, edited by R.E. Van Grieken and A.A Markowicz, 2nd ed., 341–406. New York - Basel: Marcel Dekker, Inc.
- de Waal, Edmund. 2011. *The Hare With Amber Eyes*. London: Vintage Books.
- Deetz, J. 1968. "The Inference of Residence and Descent Rules from Archeological Data." In *New Perspectives in Archeology*, edited by S. R. Binford and L. R. Binford, 41–48. New York: Aldine.
- Delton, A. W., M. M. Krasnow, L. Cosmides, and J. Tooby. 2011. "Evolution of Direct Reciprocity under Uncertainty Can Explain Human Generosity in One-Shot Encounters." *Proceedings of the National Academy of Sciences* (July 25): 1102131108–. doi:10.1073/pnas.1102131108. <http://www.pnas.org/cgi/content/abstract/1102131108v1>.
- Demoli, N, K Sariri, Z Stanic, V Mastruko, and O Milat. 2004. "Toolmarks Identification Using SEM Images in an Optoelectronic Correlator Device." *Optik - International Journal for Light and Electron Optics* 115 (11-12): 487–492. doi:10.1078/0030-4026-00404. <http://linkinghub.elsevier.com/retrieve/pii/S0030402605703995>.
- Demoli, Nazif, Jörn Kamps, Sven Krüger, Hartmut Gruber, and Günther Wernicke. 2002. "Recognition of Cuneiform Inscription Signs by Use of a Hybrid-Optoelectronic Correlator Device." *Applied Optics* 41 (23) (August 10): 4762. doi:10.1364/AO.41.004762. <http://ao.osa.org/abstract.cfm?URI=ao-41-23-4762>.
- Dennis, M. 1999. "X-Ray Fluorescence Analysis of Non-Ferrous Metalworking Debris from the Royal Opera House Site, Lundenwic, 1995." London. <http://research.english-heritage.org.uk/report/?5453>.
- Derevenski, Joanna Sofaer. 2000. "Rings of Life: The Role of Early Metalwork in Mediating the Gendered Life Course." *World Archaeology* 31 (3): 389–406.
- Dickinson, Tania M. 2002. "Translating Animal Art: Salin's Style I and Anglo-Saxon Cast Saucer Brooches." *Hikuin* 29: 163–186.
- Dinno, Alexis. 2012. "Paran: Horn's Test of Principal Components/Factors." <http://cran.r-project.org/package=paran>.
- . 2014. "Gently Clarifying the Application of Horn's Parallel Analysis to Principal Component Analysis Versus Factor Analysis." *Community Health Faculty Publications and Presentations*. http://doyenne.com/Software/files/PA_for_PCA_vs_FA.pdf.
- Dobres, M-A, and J.E Robb. 2000. *Agency in Archaeology*. London: Routledge.
- Dockrill, S.J., J.M. Bond, V.E. Turner, L.D. Brown, D.J. Bashford, J.E. Cussans, and R.A. Nicholson. 2010. *Excavations at Old Scatness, Shetland Volume 1: The Pictish Village and Viking Settlement*. Lerwick: Shetland Heritage Publications.
- Douglas, Mary. 2002. *Purity and Danger: An Analysis of Concepts of Pollution and Taboo*.

- London: Routledge.
- Drobny, J.G. 2010. *Radiation Technology for Polymers*. Boca Raton, FL: CRC Press.
- Dube, R.K. 2006. "Interrelation between Gold and Tin: A Historical Perspective." *Gold Bulletin*. doi:10.1007/BF03215537.
- Dungworth, David Barry. 1995. "Iron Age and Roman Copper Alloys from Northern Britain." University of Durham. <http://etheses.dur.ac.uk/1024/>.
- . 1996. "Caley's 'Zinc Decline' Reconsidered." *The Numismatic Chronicle* 156: 228–234. <http://www.jstor.org/stable/42667954>.
- . 1997a. "Iron Age and Roman Copper Alloys from Northern Britain." *Internet Archaeology* 2. doi:10.11141/ia.2.2. http://intarch.ac.uk/journal/issue2/dungworth_index.html.
- . 1997b. "Roman Copper Alloys: Analysis of Artefacts from Northern Britain." *Journal of Archaeological Science* 24 (10): 901–910. doi:10.1006/jasc.1996.0169. http://www.researchgate.net/publication/240442220_Roman_Copper_Alloys_Analysis_of_Artefacts_from_Northern_Britain.
- . 2000. "Analysis of Non-Ferrous Tudor and Stuart Artefacts from Southwark, London." 39/2000. Ancient Monuments Laboratory Report. London: English Heritage. <http://research.historicengland.org.uk/redirect.aspx?id=4944>.
- . 2001. "Metal Working Evidence from Housesteads Roman Fort, Northumberland." 109/2001. Centre for Archaeology Reports. London: English Heritage. <http://research.historicengland.org.uk/redirect.aspx?id=5079>.
- . 2015. *Archaeometallurgy: Guidelines for Best Practice*. London: Historic England. <http://historicengland.org.uk/images-books/publications/archaeometallurgy-guidelines-best-practice/>.
- Dungworth, David Barry, and Matthew Nicholas. 2004. "Caldarium? An Antimony Bronze Used for Medieval and Post-Medieval Cast Domestic Vessels." *Historical Metallurgy* 38 (1): 24–34. http://www.researchgate.net/publication/237100389_Caldarium_An_antimony_bronze_used_for_medieval_and_post-medieval_cast_domestic_vessels.
- Eagles, Bruce, and Catherine Mortimer. 1993. "Early Anglo-Saxon Artefacts from Hod Hill Dorset." *The Antiquaries Journal* 73 (1) (April 21): 132–140. doi:10.1017/S0003581500071717. http://journals.cambridge.org/abstract_S0003581500071717.
- Eckardt, Hella. 2014a. *Objects and Identities: Roman Britain and the North-Western Provinces*. Oxford: Oxford University Press.
- . 2014b. "Objects and Identities in Roman Britain and the North-Western Provinces [Data-Set]: Appendix 1: Bucket Pendants." York: Archaeology Data Service [distributor]. doi:10.5284/1018083. <http://dx.doi.org/10.5284/1018083>.
- Eckardt, Hella, and Howard M. R. Williams. 2003. "Objects without a Past? The Use of Roman Objects in Early Anglo-Saxon Graves." In *Archaeologies of Remembrance: Death and Memory in Past Societies*, edited by Howard M. R. Williams, 141–170. New York and London: Kluwer/Plenum.
- Eco, Umberto. 1984. *The Name of the Rose*. Translated by Martin Seeker. London: Picador.
- Economou-Eliopoulos, M. 2000. "Palladium, Platinum and Gold Concentration in

- Porphyry Copper Systems of Greece and Their Genetic Significance.” *Ore Geology Reviews* 16 (1-2) (March): 59–70. doi:10.1016/S0169-1368(99)00024-4. [http://dx.doi.org/10.1016/S0169-1368\(99\)00024-4](http://dx.doi.org/10.1016/S0169-1368(99)00024-4).
- Edmondson, J. C. 1989. “Mining in the Later Roman Empire and beyond: Continuity or Disruption?” *The Journal of Roman Studies* 79: 84–102. <http://www.jstor.org/stable/301182>.
- Edwards, Nancy. 2013. *The Archaeology of Early Medieval Ireland*. New York: Routledge.
- Egozcue, Juan José, Vera Pawlowsky-Glahn, Glòria Mateu-Figueras, and Carles Barceló-Vidal. 2003. “Isometric Logratio Transformations for Compositional Data Analysis.” *Mathematical Geology* 35 (3): 279–300. doi:10.1023/A:1023818214614. <http://link.springer.com/article/10.1023/A%3A1023818214614>.
- Ellis, Andrew T. 2002. “Energy-Dispersive X-Ray Fluorescence Analysis Using X-Ray Tube Excitation.” In *Handbook of X-Ray Spectrometry - Second Edition, Revised and Expanded*, edited by Rene Van Grieken and Andrzej A Markowicz, 2nd ed., 199–238. New York - Basel: Marcel Dekker, Inc.
- Emery, Virginia L., and Maury Morgenstein. 2007. “Portable EDXRF Analysis of a Mud Brick Necropolis Enclosure: Evidence of Work Organization, El Hibe, Middle Egypt.” *Journal of Archaeological Science* 34 (1) (January): 111–122. doi:10.1016/j.jas.2006.04.001. <http://dx.doi.org/10.1016/j.jas.2006.04.001>.
- English Heritage. 2006. “MoRPHE for Users of MAP2.” London: English Heritage. <https://www.english-heritage.org.uk/publications/morphe-for-users-of-map2/>.
- Erind. 2010. “Vector Maps of Europe.” *Vecteezy*. <http://www.vecteezy.com/map-vector/5918-vector-maps-of-europe>.
- Etzioni, A. 2009. “A Crisis of Consumerism.” In *Aftershocks: Economic Crisis and Institutional Choice*, edited by A.B Hemerijck, E Knapen, and E Doorne, 155–162. Amsterdam: Amsterdam University Press.
- . 2011a. “Shifting Sands.” *Journal of International Security Affairs* 20: 87–89.
- . 2011b. “On Communitarian and Global Sources of Legitimacy.” *The Review of Politics* 73 (1): 105–122.
- Evison, Vera I. 1968. “Quoit Brooch Style Buckles.” *Antiquaries Journal* XLVIII: 231–249.
- . 1977. “Supporting Arm Brooches and Equal-Arm Brooches in England.” In *Studien Zur Sachsenforschung*, 127–147. Hildesheim: Lax.
- . 1978. “Early Anglo-Saxon Applied Disc Brooches, Part II.” *Antiquaries Journal* LVIII: 260–278.
- Evison, Vera I., H Hodges, and J.G Hurst. 1974. “A Bibliography of the Works of G.C. Dunning.” In *Medieval Pottery from Excavations: Studies Presented to Gerald Clough Dunning with a Bibliography of His Works*, edited by V.I Evison, H Hodges, and J.G Hurst, 17–32. London: J. Baker.
- Felder, Kathrin. 2014. “Girdle-Hangers in 5th- and 6th-Century England. A Key to Early Anglo-Saxon Identities: Volume 1.” University of Cambridge.
- . 2015. “Networks of Meaning and the Social Dynamics of Identity. An Example from Early Anglo-Saxon England.” *Papers from the Institute of Archaeology* 25 (1): 1–20. doi:10.5334/pia.478. <http://www.pia-journal.co.uk/articles/10.5334/pia.478/>.

- Fernandes, Ricardo, Bertil JH van Os, and Hans DJ Huisman. 2013. "The Use of Hand-Held XRF for Investigating the Composition and Corrosion of Roman Copper-Alloyed Artefacts." *Heritage Science* 1 (1) (September 16): 30. doi:10.1186/2050-7445-1-30. <http://www.heritagesciencejournal.com/content/1/1/30>.
- Ferretti, Marco. 2004. "Fluorescence from the Collimator in Si-PIN and Si-Drift Detectors: Problems and Solutions for the XRF Analysis of Archaeological and Historical Materials." *Nuclear Instruments and Methods in Physics Research Section B: Beam Interactions with Materials and Atoms* 226 (3) (November): 453–460. doi:10.1016/j.nimb.2004.07.001. <http://dx.doi.org/10.1016/j.nimb.2004.07.001>.
- Ferretti, Marco, G. Cristoforetti, S. Legnaioli, V. Palleschi, A. Salvetti, E. Tognoni, E. Console, and P. Palaia. 2007. "In Situ Study of the Porticello Bronzes by Portable X-Ray Fluorescence and Laser-Induced Breakdown Spectroscopy." *Spectrochimica Acta Part B: Atomic Spectroscopy* 62 (12) (December): 1512–1518. doi:10.1016/j.sab.2007.09.004. <http://dx.doi.org/10.1016/j.sab.2007.09.004>.
- Figueiredo, Elin, Rui J. C. Silva, M. Fátima Araújo, and João C. Senna-Martinez. 2010. "Identification of Ancient Gilding Technology and Late Bronze Age Metallurgy by EDXRF, Micro-EDXRF, SEM-EDS and Metallographic Techniques." *Microchimica Acta* 168 (3-4) (January 30): 283–291. doi:10.1007/s00604-009-0284-6. <http://www.springerlink.com/index/10.1007/s00604-009-0284-6>.
- Fillery-Travis, Ruth. 2010. "Experimental Archaeology? Exploratory Statistical Examination of Romano-British Copper Alloys."
- Filzmoser, Peter, Heinrich Fritz, and Klaudius Kalcher. 2014. "pcaPP: Robust PCA by Projection Pursuit." <http://cran.r-project.org/package=pcaPP>.
- Filzmoser, Peter, Robert G. Garrett, and Clemens Reimann. 2005. "Multivariate Outlier Detection in Exploration Geochemistry." *Computers & Geosciences* 31 (5) (June): 579–587. doi:10.1016/j.cageo.2004.11.013. <http://www.sciencedirect.com/science/article/pii/S0098300404002304>.
- Filzmoser, Peter, and Moritz Gschwandtner. 2015. "Mvoutlier: Multivariate Outlier Detection Based on Robust Methods." <http://cran.r-project.org/package=mvoutlier>.
- Filzmoser, Peter, Karel Hron, and Clemens Reimann. 2009. "Principal Component Analysis for Compositional Data with Outliers." *Environmetrics* 20 (6) (September): 621–632. doi:10.1002/env.966. <http://doi.wiley.com/10.1002/env.966>.
- Flannery, K.V. 1982. "The Golden Marshalltown: A Parable for the Archeology of the 1980s." *American Anthropologist (New Series)* 84 (2): 265–278.
- Fleming, Andrew. 1994. "Swadal, Swar (and Erechwydd?): Early Medieval Polities in Upper Swaledale." *Landscape History* 16 (1) (January 3): 17–30. doi:10.1080/01433768.1994.10594463. <http://www.tandfonline.com/doi/abs/10.1080/01433768.1994.10594463?journalCode=rlsh20>.
- Fleming, Robin. 2012. "Recycling in Britain after the Fall of Rome's Metal Economy." *Past & Present* 217 (1) (October 29): 3–45. doi:10.1093/pastj/gts027. <http://past.oxfordjournals.org/cgi/doi/10.1093/pastj/gts027>.
- Forbes, Robert James. 1964. *Metallurgy in Antiquity: A Notebook for Archaeologists and Technologists*. Leiden and Boston: Brill Archive.
- Forouzan, Firoozeh, Jeffrey B. Glover, Frank Williams, and Daniel Deocampo. 2012.

- “Portable XRF Analysis of Zoomorphic Figurines, ‘tokens,’ and Sling Bullets from Chogha Gavaneh, Iran.” *Journal of Archaeological Science* 39 (12) (December): 3534–3541. doi:10.1016/j.jas.2012.04.010. <http://www.sciencedirect.com/science/article/pii/S0305440312001306>.
- Forster, Nicola, and Peter Grave. 2012. “Non-Destructive PXRF Analysis of Museum-Curated Obsidian from the Near East.” *Journal of Archaeological Science* 39 (3) (March): 728–736. doi:10.1016/j.jas.2011.11.004. <http://dx.doi.org/10.1016/j.jas.2011.11.004>.
- Forster, Nicola, Peter Grave, Nancy Vickery, and Lisa Kealhofer. 2011. “Non-Destructive Analysis Using PXRF: Methodology and Application to Archaeological Ceramics.” *X-Ray Spectrometry* 40 (5) (September 26): 389–398. <http://doi.wiley.com/10.1002/xrs.1360>.
- Fox, Aileen. 1995. “Tin Ingots from Bigbury Bay.” *Proceedings of the Devon Archaeological Society* 53: 11–24.
- Fox, Cyril. 1923. *The Archaeology of the Cambridge Region: A Topographical Study of the Bronze, Early Iron, Roman and Anglo-Saxon Ages, with an Introductory Note on the Neolithic Age*. Cambridge: Cambridge University Press.
- Frahm, Ellery, Roger C.P. Doonan, and V. Kilikoglou. 2014. “Handheld Portable X-Ray Fluorescence of Aegean Obsidians.” *Archaeometry* 56 (2) (April 10): 228–260. doi:10.1111/arcm.12012. <http://doi.wiley.com/10.1111/arcm.12012>.
- Frahm, Ellery, Beverly A. Schmidt, Boris Gasparyan, Benik Yeritsyan, Sergei Karapetian, Khachatur Meliksetian, and Daniel S Adler. 2014. “Ten Seconds in the Field: Rapid Armenian Obsidian Sourcing with Portable XRF to Inform Excavations and Surveys.” *Journal of Archaeological Science* 41 (September): 333–348. doi:10.1016/j.jas.2013.08.012. <http://dx.doi.org/10.1016/j.jas.2013.08.012>.
- Frame, Lesley Diana. 2009. “Technological Change in Southwestern Asia: Metallurgical Production Styles and Social Values during the Chalcolithic and Early Bronze Age.” University of Arizona. <http://arizona.openrepository.com/arizona/handle/10150/195816>.
- Freestone, Ian C., and Catherine Mortimer. 2005. “Technological Study of Non-Ferrous Artefacts.” In *An Assessment of the Potential for Analysis and Publication for Archaeological Work Carried out at RAF Lakenheath between 1987 and June 2005: Volume I: The Anglo-Saxon Cemeteries ERL 104, ERL 046 and ERL 114*, edited by Jo Caruth and Sue Anderson, 119–120. SCCAS Report 2005/94. Ipswich: Suffolk County Council.
- Fulford, M.J. 1989. “Byzantium and Britain: A Mediterranean Perspective on Post-Roman Mediterranean Imports in Western Britain and Ireland.” *Medieval Archaeology* 33: 1–6.
- Fyodorov, Nikolai Fedorovich. 1990. *What Was Man Created for? The Philosophy of the Common Task: Selected Works*. Edited and translated by Elisaeth Koutaissoff and Marilyn Minto. London: Honeyglan Publishing Ltd.
- Gao, Yuxi. 2010. “X-Ray Fluorescence.” In *Nuclear Analytical Techniques for Metallomics and Metalloproteomics*, edited by Chunying Chen, Zhifang Chai, and Yuxi Gao, 62–94. Cambridge: Royal Society of Chemistry. doi:10.1039/9781847559913.
- Gauss, Roland K., J. Batora, Erich Nowaczinski, Knut Rassmann, and Gerd Schukraft. 2013. “The Early Bronze Age Settlement of Fidvár, Vráble (Slovakia): Reconstructing Prehistoric Settlement Patterns Using Portable XRF.” *Journal of Archaeological Science* 40 (7) (July): 2942–2960. doi:10.1016/j.jas.2013.01.029.

- <http://www.sciencedirect.com/science/article/pii/S0305440313000435>.
- Geake, Helen. 1995. "The Use of Grave-Goods in Conversion-Period England C. 600 - C. 850 A.D." University of York. <http://etheses.whiterose.ac.uk/id/eprint/2461>.
- Gerrard, Christopher. 2003. *Medieval Archaeology: Understanding Traditions and Contemporary Approaches*. London: Routledge.
- Gerrard, James. 2013. *The Ruin of Roman Britain: An Archaeological Perspective*. Cambridge University Press.
- Giauque, Robert D., Frank Asaro, Fred H. Stross, and Thomas R. Hester. 1993. "High-Precision Non-Destructive X-Ray Fluorescence Method Applicable to Establishing the Provenance of Obsidian Artifacts." *X-Ray Spectrometry* 22 (1) (January): 44–53. doi:10.1002/xrs.1300220111. <http://doi.wiley.com/10.1002/xrs.1300220111>.
- Gilchrist, Roberta. 2009. "Medieval Archaeology and Theory: A Disciplinary Leap of Faith." In *Reflections: 50 Years of Medieval Archaeology 1957-2007*, edited by Roberta Gilchrist and Andrew Reynolds, 385–408. Society for Medieval Archaeology Monographs. Leeds: Maney Publishing. <http://centaur.reading.ac.uk/1698/>.
- Goodale, Nathan, David G. Bailey, George T. Jones, Catherine Prescott, Elizabeth Scholz, Nick Stagliano, and Chelsea Lewis. 2012. "pXRF: A Study of Inter-Instrument Performance." *Journal of Archaeological Science* 39 (4) (April): 875–883. doi:10.1016/j.jas.2011.10.014. <http://dx.doi.org/10.1016/j.jas.2011.10.014>.
- Goren, Yuval, Hans Mommsen, and Jörg Klinger. 2011. "Non-Destructive Provenance Study of Cuneiform Tablets Using Portable X-Ray Fluorescence (pXRF)." *Journal of Archaeological Science* 38 (3) (March): 684–696. doi:10.1016/j.jas.2010.10.020. <http://dx.doi.org/10.1016/j.jas.2010.10.020>.
- Gosden, Chris. 2005a. "Comments Iii: Is Science A Foreign Country?" *Archaeometry* 47 (1) (February): 182–185. doi:10.1111/j.1475-4754.2005.195-3.x. <http://doi.wiley.com/10.1111/j.1475-4754.2005.195-3.x>.
- . 2005b. "What Do Objects Want?" *Journal of Archaeological Method and Theory* 12 (3) (September): 193–211. doi:10.1007/s10816-005-6928-x. <http://www.springerlink.com/index/R673K55117676561.pdf>.
- Gowland, William. 1912. "The Metals in Antiquity." *Journal of the Royal Anthropological Institute of Great Britain and Ireland* 42: 235–287. <http://www.jstor.org/stable/2843191>.
- . 1921. *The Metallurgy of the Non-Ferrous Metals*. London: Charles Griffin and Company Limited. <https://archive.org/details/metallurgynonfe00gowlgoog>.
- Grave, Peter, Val Attenbrow, Lin Sutherland, Ross Pogson, and Nicola Forster. 2012. "Non-Destructive pXRF of Mafic Stone Tools." *Journal of Archaeological Science* 39 (6) (June): 1674–1686. doi:10.1016/j.jas.2011.11.011. <http://dx.doi.org/10.1016/j.jas.2011.11.011>.
- Green, Barbara. 1978. *The Anglo-Saxon Cemetery at Bergh Apton, Norfolk: Catalogue*. East Anglian Archaeology: Report No. 7. Norwich: Norfolk Archaeological Unit.
- Greene, Kevin. 1987. "Gothic Material Culture." In *Archaeology as Long-Term History*, edited by Ian Hodder, 117–131. Cambridge: Cambridge University Press.
- Greiff, Susanne. 2012. "Silver Grave Goods from Early Hungarian Contexts: Technological Implications of Debased Alloy Compositions With Zinc, Tin and Lead." In *Die Archäologie Der Frühen Ungarn: Chronologie, Technologie Und Methodik*

- (*Römisch-Germanischen Zentralmuseums Mainz* 2012), edited by Evelyn Garvey, Reinhard Köster, Bendeguz Tobias, and Hans Jung, 241–260. Mörlenbach: Römisch-Germanischen Zentralmuseum & Strauss GmbH.
- Gullayanon, Rutchanee. 2011. “A Calibration Methodology for Energy Dispersive X-Ray Fluorescence Measurements Based upon Synthetically Generated Reference Spectra.” Georgia Institute of Technology. <http://smartech.gatech.edu/handle/1853/42771>.
- Guttman, L. 1954. “Some Necessary Conditions for Common-Factor Analysis.” *Psychometrika* 19: 149–161.
- Habashi, Fathi. 2008. *Alloys: Preparation, Properties, Applications*. Weinheim: Wiley-VCH. <http://eu.wiley.com/WileyCDA/WileyTitle/productCd-3527611924.html>.
- Halsall, Guy. 1995. *Settlement and Social Organization: The Merovingian Region of Metz*. Cambridge University Press.
- Harvey, D. 2007. *A Brief History of Neoliberalism*. Oxford: Oxford University Press.
- Haseloff, Gunther. 1974. “Salin’s Style I.” *Medieval Archaeology* 18: 1–15.
- Haughton, Christine A, and Dominic Powlesland. 1999. *West Heslerton: The Anglian Cemetery: Catalogue of the Anglian Graves and Associated Assemblages with Specialist Contributions*. Vol. 2. Landscape Research Centre Archaeological Monographs. Yeddingham: Landscape Research Centre.
- Hawkes, S.C., J.M. Merrick, and D.M. Metcalf. 1966. “X-Ray Fluorescent Analysis of Some Dark Age Coins and Jewellery.” *Archaeometry* 9 (1) (June): 98–138. doi:10.1111/j.1475-4754.1966.tb00911.x. <http://www.blackwell-synergy.com/doi/abs/10.1111/j.1475-4754.1966.tb00911.x>.
- He, Bob B. 2009. *Two-Dimensional X-Ray Diffraction*. Hoboken, N.J: Wiley.
- Heaney, Seamus. 1984. *Station Island*. London: Faber and Faber.
- Heginbotham, Arlen, Aniko Bezur, Michel Bouchard, Jeffrey M Davis, Katherine Eremin, James H Frantz, Lisha Glinsman, et al. 2011. “Interlaboratory Reproducibility of Quantitative XRF Analysis of Historic Copper Alloys.” In *Metal 2010, Proceedings of the Interim Meeting of the ICOM-CC Metal Working Group, Charleston, South Carolina, USA, 11-15 October 2010*, edited by P Mardikian, C Chemello, C Watters, and P Hull, 178–188. Clemson, South Carolina: Clemson University.
- Helleiner, Eric. 1996. *States and the Reemergence of Global Finance: From Bretton Woods to the 1990s*. Ithaca (NY): Cornell University Press. <http://books.google.com/books?id=jcg6YICLiIYC&pgis=1>.
- Helsen, J.A., and A. Kuczumow. 2009. “Wavelength-Dispersive X-Ray Fluorescence.” In *Handbook of X-Ray Spectrometry - Second Edition, Revised and Expanded*, 2nd ed., 95–198. New York - Basel: Marcel Dekker, Inc.
- Hernández, A., M. Jébrak, P. Higuera, R. Oyarzun, D. Morata, and J. Munhá. 1999. “The Almadén Mercury Mining District, Spain.” *Mineralium Deposita* 34 (5-6) (July 7): 539–548. doi:10.1007/s001260050219. <http://www.springerlink.com/content/q0vg85u59tub90tw/>.
- Herzog, Irmela, and Frank Siegmund. 2013. “Parallel Coordinate Plots in Archaeology.” In *Algorithms from and for Nature and Life*, edited by Berthold Lausen, Dirk Van den Poel, and Alfred Ultsch, 299–308. Studies in Classification, Data Analysis, and Knowledge Organization. Cham: Springer International Publishing.

doi:10.1007/978-3-319-00035-0. <http://link.springer.com/10.1007/978-3-319-00035-0>.

- Hines, John. 1984. *The Scandinavian Character of Anglian England in the Pre-Viking Period*. British Series 124. Oxford: British Archaeological Reports.
- . 1993. *Clasps, Hektespenner, Agraffen. Anglo-Scandinavian Clasps of Classes A-C of the 3rd to 6th Centuries A.D. Typology, Diffusion and Function*. By J. Hines *Clasps, Hektespenner, Agraffen. Anglo-Scandinavian Clasps of Classes A-C of the 3rd to 6th Centuries A*. Stockholm: Kungl. Vitterhets Historie och Antikvitets Akademien.
- . 1997. *A New Corpus of Anglo-Saxon Great Square-Headed Brooches*. London: Society of Antiquaries of London.
- . 2003. "Foreword." In *The Anglo-Saxons from the Migration Period to the Eighth Century: An Ethnographic Perspective*, edited by John Hines, 2nd ed., 1–6. Studies in Historical Archaeoethnology. Woodbridge: Boydell Press.
- . 2013a. "The Origins of East Anglia in a North Sea Zone." In *East Anglia and Its North Sea World in the Middle Ages*, edited by David Bates and Robert Liddiard, 16–43. Woodbridge, Suffolk: Boydell & Brewer. <http://www.boydellandbrewer.com/store/viewItem.asp?idProduct=14243>.
- . 2013b. "The Archaeological Study of Early Anglo-Saxon Cemeteries." In *Anglo-Saxon Graves and Grave Goods of the 6th and 7th Centuries AD: A Chronological Framework*, edited by John Hines and Alexandra Louise Bayliss, 13–30. Society for Medieval Archaeology Monograph 33. London: Society for Medieval Archaeology.
- Hines, John, Alexandra Louise Bayliss, Karen Høilund Nielsen, and Christopher Scull. 2013. *Anglo-Saxon Graves and Grave Goods of the Sixth and Seventh Centuries AD: A Chronological Framework*. Edited by John Hines and Alexandra Louise Bayliss. Society for Medieval Archaeology Monograph 33. Leeds: Society for Medieval Archaeology. <http://orca.cf.ac.uk/31504/>.
- Hinton, David A. 1987. "Archaeology and the Middle Ages. Recommendations by the Society for Medieval Archaeology to the Historic Buildings and Monuments Commission for England." *Medieval Archaeology* 31: 1–12. doi:10.5284/1000320. http://archaeologydataservice.ac.uk/catalogue/adsdata/arch-769-1/dissemination/pdf/vol31/31_001_012.pdf.
- . 2000. *A Smith in Lindsey: The Anglo-Saxon Grave at Tattershall Thorpe, Lincolnshire*. The Society for Medieval Archaeology Monograph Series No. 16. Leeds: The Society for Medieval Archaeology.
- Hirt, Alfred Michael. 2010. *Imperial Mines and Quarries in the Roman World: Organizational Aspects, 27 BC - AD 235*. Oxford University Press. http://books.google.com/books?id=RxD6gb_HAFsC&pgis=1.
- Historic England. 2008. *MoRPHE Project Planning Note 3: Archaeological Excavation*. London: Historic England. <http://historicengland.org.uk/images-books/publications/morphe-project-planning-note-3/>.
- Hodginson, J.S. 1999. "Romano-British Iron Production in the Sussex and Kent Weald: A Review of Current Data." *Historical Metallurgy* 33 (2): 68–72.
- Horn J.L. 1965. "A Rationale and a Test for the Number of Factors in Factor Analysis." *Psychometrika* 30: 179–185.
- Hughes, M.J., and J.A. Hall. 1979. "X-Ray Fluorescence Analysis of Late Roman and Sassanian Silver Plate." *Journal of Archaeological Science* 6 (4) (December): 321–344.

- doi:10.1016/0305-4403(79)90017-7.
<http://www.sciencedirect.com/science/article/pii/0305440379900177>.
- Humphrey, John W., John P. Oleson, and Andrew N. Sherwood. 2003. *Greek and Roman Technology: A Sourcebook: Annotated Translations of Greek and Latin Texts and Documents*. Routledge.
- Humpston, Giles, and David M. Jacobson. 2004. *Principles of Soldering*. Materials Park, Russell Township, OH: ASM International.
- Husson, F., J. Josse, and J. Pages. 2010. "Principal Component Methods-Hierarchical Clustering-Partitional Clustering: Why Would We Need to Choose for Visualizing Data?" *Applied Mathematics Department*. Rennes: Institut supérieur des sciences agronomiques, agroalimentaires, horticoles et du paysage.
http://factominer.free.fr/docs/HPCP_husson_josse.pdf.
- Husson, Francois, and Julie Josse. 2014. "missMDA: Handling Missing Values With/in Multivariate Data Analysis (Principal Component Methods)." <http://cran.r-project.org/package=missMDA>.
- Husson, Francois, Julie Josse, Sebastien Le, and Jeremy Mazet. 2014. "FactoMineR: Multivariate Exploratory Data Analysis and Data Mining with R." <http://cran.r-project.org/package=FactoMineR>.
- Hutchinson, Patricia. 1966. "The Anglo-Saxon Cemetery at Little Eriswell, Suffolk." *Proceedings of the Cambridge Antiquarian Society*. 59: 1–32.
http://archaeologydataservice.ac.uk/catalogue/adsdata/arch-1895-1/dissemination/pdf/PCAS/1966_LIX/PCAS_LIX_1966_001-032_Hutchinson.pdf.
- Ice, G. E., and B. C. Larson. 2000. "3D X-Ray Crystal Microscope." *Advanced Engineering Materials* 2 (10) (October): 643–646. doi:10.1002/1527-2648(200010)2:10<643::AID-ADEM643>3.0.CO;2-U.
[http://doi.wiley.com/10.1002/1527-2648\(200010\)2:10<643::AID-ADEM643>3.0.CO;2-U](http://doi.wiley.com/10.1002/1527-2648(200010)2:10<643::AID-ADEM643>3.0.CO;2-U).
- Ingelbrecht, C, A Adriaens, and E.A. Maier. 2001. *The Certification of Arsenic, Lead, Tin and Zinc (Mass Fractions) in Five Copper Alloys, BCR-691*. European Commission, Directorate-General for Research and Innovation.
- Inker, Peter. 2000. "Technology as Active Material Culture: The Quoit-Brooch Style." *Medieval Archaeology* 44: 25–52.
<http://www.ingentaconnect.com/content/maney/med/2000/00000044/00000001/art00002>.
- Ishiguro, Kazuo. 2015. *The Buried Giant*. London: Faber & Faber.
- James, E. 2001. *Britain in the First Millennium*. London: Arnold.
- Janssens, Koen. 2003. "X-Ray Fluorescence Analysis." In *Handbook of Spectroscopy*, edited by Guenter Gauglitz and Tuan Vo-Dinh, 363–420. Chichester: John Wiley & Sons, Ltd. doi:10.1002/3527602305.ch11.
<http://onlinelibrary.wiley.com/book/10.1002/3527602305>.
- . 2013. "X-Ray Based Methods of Analysis." In *Archaeological and Historical Glass*, edited by Koen Janssens, 79–128. Chichester: John Wiley & Sons, Ltd. doi:10.1002/9781118314234.ch5.
- Johnson, Jack. 2014. "Accurate Measurements of Low Z Elements in Sediments and Archaeological Ceramics Using Portable X-Ray Fluorescence (PXRF)." *Journal of*

- Archaeological Method and Theory* 21 (3) (October 17): 563–588. doi:10.1007/s10816-012-9162-3. <http://link.springer.com/10.1007/s10816-012-9162-3>.
- Johnson, M. 2007. *Archaeological Theory: An Introduction*. Oxford: Blackwell Publishers.
- Jones, A.M. 2002. *Archaeological Theory and Scientific Practice*. Cambridge: Cambridge University Press.
- . 2004. “Archaeometry and Materiality: Materials Based Analysis in Theory and Practice.” *Archaeometry* 46 (3) (August): 327–338. doi:10.1111/j.1475-4754.2004.00161.x. <http://onlinelibrary.wiley.com/doi/10.1111/j.1475-4754.2004.00161.x/full>.
- Jope, E.M. 1947. “Medieval Pottery in Berkshire.” *Berkshire Archaeological Journal* 50: 49–76.
- Kaiser, B., and A. Wright. 2009. “Bruker XRF Spectroscopy User Guide: Spectral Interpretation And Sources Of Interference.” Madison, WI.
- Kaiser, H. F. 1960. “The Application of Electronic Computers to Factor Analysis.” *Educational and Psychological Measurement* 20: 141–151.
- Karakaya, I., and W. T. Thompson. 1988. “The Pb–Sn (Lead-Tin) System.” *Journal of Phase Equilibria* 9 (2) (April): 144–152. doi:10.1007/BF02890552. <http://link.springer.com/10.1007/BF02890552>.
- Karkov, Catherine E. 1999. *The Archaeology of Anglo-Saxon England: Basic Readings*. Basic Readings in Anglo-Saxon England. New York: Garland Publishing.
- Karydas, A. G. 2007. “Application of a Portable XRF Spectrometer for the Non-Invasive Analysis of Museum Metal Artefacts.” *Annali Di Chimica* 97 (7) (June): 419–432. doi:10.1002/adic.200790028. <http://doi.wiley.com/10.1002/adic.200790028>.
- Karydas, A.G., D. Kotzamani, R. Bernard, Jean-Noël Barrandon, and Ch. Zarkadas. 2004. “A Compositional Study of a Museum Jewellery Collection (7th–1st BC) by Means of a Portable XRF Spectrometer.” *Nuclear Instruments and Methods in Physics Research Section B: Beam Interactions with Materials and Atoms* 226 (1-2) (November): 15–28. doi:10.1016/j.nimb.2004.02.034. <http://dx.doi.org/10.1016/j.nimb.2004.02.034>.
- Kato, N., I. Nakai, and Y. Shindo. 2009. “Change in Chemical Composition of Early Islamic Glass Excavated in Raya, Sinai Peninsula, Egypt: On-Site Analyses Using a Portable X-Ray Fluorescence Spectrometer.” *Journal of Archaeological Science* 36 (8) (August): 1698–1707. doi:10.1016/j.jas.2009.03.020. <http://dx.doi.org/10.1016/j.jas.2009.03.020>.
- Kemble, John Mitchell. 1863. *Horæ Ferales: Or, Studies in the Archaeology of the Northern Nations*. Edited by Robert Gordon Latham and Augustus Wollaston Franks. London: Lovell, Reeve and Company. <https://books.google.com/books?id=MkwxAQAAAJ&pgis=1>.
- Killick, D. 2005. “Comments Iv: Is There Really A Chasm Between Archaeological Theory And Archaeological Science?” *Archaeometry* 47 (1) (February): 185–189. doi:10.1111/j.1475-4754.2005.195-4.x. <http://doi.wiley.com/10.1111/j.1475-4754.2005.195-4.x>.
- King, R.J. 1982. “The Occurrence of Cinnabar in Leicestershire.” *Transactions of the Leicester Literary and Philosophical Society* 76: 51–53. <http://www2.le.ac.uk/hosted/litandphil/documents->

1/transactions/transactions_1982.

- Kingsley, Charles. 1866. *Hereward the Wake*. Leipzig: Bernhard Tauchnitz.
- Kitov, B. I. 2000. "Calculation Features of the Fundamental Parameter Method in XRF." *X-Ray Spectrometry* 29 (4) (July): 285–290. doi:10.1002/1097-4539(200007/08)29:4<285::AID-XRS428>3.0.CO;2-C.
[http://doi.wiley.com/10.1002/1097-4539\(200007/08\)29:4<285::AID-XRS428>3.0.CO;2-C](http://doi.wiley.com/10.1002/1097-4539(200007/08)29:4<285::AID-XRS428>3.0.CO;2-C).
- Klockenkämper, R., H. Bubert, and K. Hasler. 1999. "Detection of near-Surface Silver Enrichment on Roman Imperial Silver Coins by X-Ray Spectral Analysis." *Archaeometry* 41 (2) (August): 311–320. doi:10.1111/j.1475-4754.1999.tb00985.x.
<http://doi.wiley.com/10.1111/j.1475-4754.1999.tb00985.x>.
- Konrád, György. 1992. *A Feast in the Garden*. Translated by Imre Goldstein. London: Faber and Faber.
- Korom, Frank J. 1998. "On the Ethics and Aesthetics of Recycling in India." In *Purifying the Earthly Body of God: Religion and Ecology in Hindu India*, edited by Lance E. Nelson, 197–224. Albany, New York: State University of New York Press.
- Kristiansen, K. 2004. "Genes versus Agents: A Discussion of Widening Theoretical Gaps in Archaeology." *Archaeological Dialogues* 11 (2): 185–189.
- Krupp, R.E. 1989. "Paragenesis and Conditions of Formation of the Moschellandsberg Mercury Deposit, SW Germany." *Mineralium Deposita* 24 (2) (April). doi:10.1007/BF00206305. <http://link.springer.com/10.1007/BF00206305>.
- Kruse, Susan E, and James Tatef. 1992. "XRF Analysis of Viking Age Silver Ingots." *Proceedings of the Society of Antiquaries of Scotland* 122: 295–328. doi:10.5284/1000184.
http://archaeologydataservice.ac.uk/catalogue/adsdata/arch-352-1/dissemination/pdf/vol_122/122_295_328.pdf.
- Kuhn, T.S. 1962. *The Structure of Scientific Revolutions*. Chicago: University of Chicago Press.
- La Niece, Susan. 1983. "Niello: An Historical and Technical Survey." *The Antiquaries Journal* 63 (2): 279–297. doi:10.1017/S000358150006652X.
<http://dx.doi.org/10.1017/S000358150006652X>.
- Lane, Alan. 2015. "Wroxeter and the End of Roman Britain." *Antiquity* 88 (340) (January 2): 501–515. doi:10.1017/S0003598X00101140.
http://journals.cambridge.org/abstract_S0003598X00101140.
- Lane, Paul. 2005. "The Material Culture of Memory." In *The Qualities of Time: Anthropological Approaches*, edited by Wendy James and David Mills, 19–34. ASA Monographs 41. Oxford and New York: BERG.
- Lang, J., and Michael J. Hughes. 1980. "Joining Techniques." In *Aspects of Early Metallurgy: Papers Presented at a Symposium Organized by the Historical Metallurgy Society and the British Museum Research Laboratory and Held at the British Museum on 22nd and 23rd April 1977*, edited by W.A. Oddy, 169–177. London: British Museum.
- . 1984. "Soldering Roman Silver Plate." *Oxford Journal of Archaeology* 3 (3) (November): 77–107. doi:10.1111/j.1468-0092.1984.tb00124.x.
<http://doi.wiley.com/10.1111/j.1468-0092.1984.tb00124.x>.
- Larkin, Philip. 2003. *Collected Poems*. Edited by Anthony Thwaite. New York: Farrar, Straus and Giroux.

- Larsen, Benner. 1987. "SEM-Identification and Documentation of Tool Marks and Surface Textures on the Gundestrup Cauldron." In *Recent Advances in the Conservation and Analysis of Artifacts*, edited by James Black, 393–408. London: University Of London Summer Schools Press.
- Latour, Bruno. 2004. "Why Has Critique Run out of Steam? From Matters of Fact to Matters of Concern." *Critical Inquiry* 30 (2): 225–248.
- Latour, Bruno, and S Woolgar. 1979. *Laboratory Life: The Construction of Scientific Facts*. 2nd ed. New Jersey: Princeton University Press.
- Law, Peter A. 2014. *The History, Heritage and Haraldry of the 48th Fighter Wing*. Lakenheath: 48th Fighter Wing History Office. <http://www.lakenheath.af.mil/shared/media/document/AFD-140410-022.pdf>.
- Leaf, Walter. 1916. "The Commerce of Sinope." *The Journal of Hellenic Studies* 36 (November 1): 1. doi:10.2307/625746. http://journals.cambridge.org/abstract_S007542690009087X.
- Lee, Edmund. 2006. "Management of Research Projects in the Historic Environment The MoRPHE Project Managers' Guide." London: English Heritage.
- Leeds, Edward Thurlow. 1913. *The Archaeology of the Anglo-Saxon Settlements*. Oxford: Clarendon Press.
- . 1945. "The Distribution of the Angles and Saxons Archaeologically Considered." *Archaeologia* 91: 1–106.
- . 1949. *A Corpus of Early Anglo-Saxon Great Square-Headed Brooches*. Oxford: Clarendon Press.
- Leeds, Edward Thurlow, and R. J. C. Atkinson. 1944. "An Anglo-Saxon Cemetery at Nassington, Northants." *The Antiquaries Journal* 24 (3-4) (January 8): 100–128. doi:10.1017/S0003581500016577. http://journals.cambridge.org/abstract_S0003581500016577.
- Leigh, D., M. Cowell, and S. Turgoose. 1984. "The Composition of Some Sixth Century Kentish Silver Brooches." *Historical Metallurgy* 18 (1): 35–41.
- Leigh, David. 1980. "The Square-Headed Brooches of Sixth Century Kent." University College, Cardiff, <http://ethos.bl.uk/OrderDetails.do?did=1&uin=uk.bl.ethos.276763>.
- . 1990. "Aspects of Early Brooch Design and Production." In *Anglo-Saxon Cemeteries: A Reappraisal: Proceedings of a Conference Held at Liverpool Museum, 1986*, edited by Edmund Southworth, 107–124. Stroud, Gloucestershire: Sutton.
- Lem, Stanislaw. 1976. *The Investigation*. Translated by Adele Milch. New York: Avon Books.
- Levine, Philippa. 2003. *The Amateur and the Professional: Antiquarians, Historians and Archaeologists in Victorian England 1838-1886*. Cambridge: Cambridge University Press. <http://books.google.com/books?id=N6Yv2zB-HVIC&pgis=1>.
- Linke, R., M. Schreiner, G. Demortier, and M. Alram. 2003. "Determination of the Provenance of Medieval Silver Coins: Potential and Limitations of X-Ray Analysis Using Photons, Electrons or Protons." *X-Ray Spectrometry* 32 (5) (September): 373–380. doi:10.1002/xrs.654. <http://doi.wiley.com/10.1002/xrs.654>.
- Lins, P.A, and W.A. Oddy. 1975. "The Origins of Mercury Gilding." *Journal of Archaeological Science* 2 (4) (December): 365–373. doi:10.1016/0305-4403(75)90007-

2. <http://www.sciencedirect.com/science/article/pii/S0305440375900072>.
- Liu, S., Q. H. Li, Q. Fu, F. X. Gan, and Z. M. Xiong. 2013. "Application of a Portable XRF Spectrometer for Classification of Potash Glass Beads Unearthed from Tombs of Han Dynasty in Guangxi, China." *X-Ray Spectrometry* 42 (6) (November 16): 470–479. doi:10.1002/xrs.2505. <http://doi.wiley.com/10.1002/xrs.2505>.
- Liu, S., Q.H. Li, F. Gan, P. Zhang, and J.W. Lankton. 2012. "Silk Road Glass in Xinjiang, China: Chemical Compositional Analysis and Interpretation Using a High-Resolution Portable XRF Spectrometer." *Journal of Archaeological Science* 39 (7) (July): 2128–2142. doi:10.1016/j.jas.2012.02.035. <http://www.sciencedirect.com/science/article/pii/S0305440312001008>.
- Lowery, P.R., R.D.A. Savage, and R.L. Williams. 1971. "Scriber, Graver, Scorper, Tracer: Notes on Experiments in Bronzeworking Technique." *Proceedings of the Prehistoric Society* 37 (1): 167–182.
- MacIntyre, Alasdair. 1988. *Whose Justice? Which Rationality?* London: Duckworth. <http://books.google.com/books?id=32XbAAAAMAAJ&pgis=1>.
- Mackerrel, H., and R.B.K. Stevenson. 1972. "Some Analysis of Anglo-Saxon Associated Oriental Silver Coinage." In *Methods of Chemical and Metallurgical Investigation of Ancient Coinage; a Symposium Held by the Royal Numismatic Society at Burlington House, London on 9-11 December 1970*, edited by E.T. Hall and D.M. Metcalf, 195–209. London: Royal Numismatic Society. <http://www.bcin.ca/Interface/openbcin.cgi?submit=submit&Chinkey=20053>.
- Mahuteau, L. 2008. "Study of Algorithms for Analysis of XRF Spectra to Automate Inspection of Carpets." Georgia Institute of Technology. <https://smartech.gatech.edu/handle/1853/26625>.
- Maia, J.M., J.M.F. Dos Santos, and C.A.N. Conde. 1997. "Source-to-Sample Distance Independent Efficiency Technique for XRF Analysis." *Applied Radiation and Isotopes* 48 (10-12) (October): 1649–1656. doi:10.1016/S0969-8043(97)00165-6. [http://dx.doi.org/10.1016/S0969-8043\(97\)00165-6](http://dx.doi.org/10.1016/S0969-8043(97)00165-6).
- Malim, T, and John Hines. 1998. *The Anglo-Saxon Cemetery at Edix Hill (Barrington A), Cambridgeshire*. CBA Research Report Series 112. York: Council for British Archaeology.
- Maras, A, M Botticelli, and P Ballirano. 2013. "Archaeometric Investigations on Cinnabar Provenance and Origin by X-Ray Powder." *International Journal of Conservation Science* 4: 685–692. <http://www.ijcs.uaic.ro/public/IJCS-SI-Maras.pdf>.
- Marett, R. R. 1914. "Presidential Address: Folklore and Psychology." *Folklore* 25 (1): 12–33. doi:10.1080/0015587X.1914.9718802. <http://www.jstor.org/stable/1255347>.
- Markowicz, Andrzej A. 2002. "X-Ray Physics." In *Handbook of X-Ray Spectrometry - Second Edition, Revised and Expanded*, edited by R.E. Van Grieken and A.A. Markowicz, 1–94. New York - Basel: Marcel Dekker, Inc.
- . 2008. "Quantification and Correction Procedures." In *Portable X-Ray Fluorescence Spectrometry: Capabilities for In Situ Analysis*, edited by P.J. Potts and M West, 13–37. London: Royal Society of Chemistry.
- Marriner, Nick. 2009. "Currents and Trends in the Archaeological Sciences." *Journal of Archaeological Science* 36 (12) (December): 2811–2815. doi:10.1016/j.jas.2009.09.009. <http://dx.doi.org/10.1016/j.jas.2009.09.009>.
- Martin, E. A., J. Plouviez, and H. Ross. 1982. "Archaeology in Suffolk, 1981." *Proceedings*

- of the Suffolk Institute for Archaeology & History* 35 (2): 155–167.
[http://suffolkinststitute.pdfsrv.co.uk/customers/SuffolkInstitute/2014/01/10/VolumeXXXV Part 2 %281982%29_Archaeology in Suffolk 1981 E A Martin J Plouviez H Ross_155 to 170.pdf](http://suffolkinststitute.pdfsrv.co.uk/customers/SuffolkInstitute/2014/01/10/VolumeXXXVPart2%281982%29_ArchaeologyinSuffolk1981EA MartinJPlouviezHRoss_155to170.pdf).
- Martin, Toby F. 2015. *The Cruciform Brooch and Anglo-Saxon England*. Woodbridge, Suffolk: Boydell & Brewer Ltd.
<http://www.jstor.org/stable/10.7722/j.ctt9qdmn6>.
- Martínez-Cortizas, A. 1999. “Mercury in a Spanish Peat Bog: Archive of Climate Change and Atmospheric Metal Deposition.” *Science* 284 (5416) (May 7): 939–942.
 doi:10.1126/science.284.5416.939.
<http://www.sciencemag.org/content/284/5416/939.abstract>.
- Martín-Fernández, J. A., Carles Barceló-Vidal, and Vera Pawlowsky-Glahn. 2000. “Zero Replacement in Compositional Data Sets.” In *Studies in Classification, Data Analysis, and Knowledge Organization, Proceedings of the 7th Conference of the International Federation of Classification Societies (IFCS'2000)*, edited by H. Kiers, J. Rasson, P. Groenen, and M. Shader, 155–160. Berlin: Springer-Verlag.
- . 2003. “Dealing with Zeros and Missing Values in Compositional Data Sets Using Nonparametric Imputation.” *Mathematical Geology* 35 (3) (April 1): 253–278.
 doi:10.1023/A:1023866030544.
<http://link.springer.com/article/10.1023/A:1023866030544>.
- Martín-Fernández, J. A., J. Palarea-Albaladejo, and R.A. Olea. 2011. “Dealing with Zeros.” In *Compositional Data Analysis: Theory and Applications*, edited by V. Pawlowsky-Glahn and A. Buccianti, 43–58. Chichester: John Wiley & Sons, Ltd.
- McCormac, F G, Alexandra Louise Bayliss, M G L Baillie, and D M Brown. 2004. “Radiocarbon Calibration in the Anglo-Saxon Period; AD 495-725.” *Radiocarbon* 46 (3) (November 20): 1123–1125. doi:10.2458/azu_js_rc.46.4173.
<http://journals.uair.arizona.edu/index.php/radiocarbon/article/view/4173>.
- McCormac, F G, Alexandra Louise Bayliss, D M Brown, P J Reimer, and M M Thompson. 2008. “Extended Radiocarbon Calibration in the Anglo-Saxon Period, AD 395-485 and AD 735-805.” *Radiocarbon*. doi:10.2458/azu_js_rc.50.3031.
<http://journals.uair.arizona.edu/index.php/radiocarbon/article/view/3031>.
- McKerrell, H, and R.B.K Stevenson. 1972. “Some Analyses of Anglo-Saxon and Associated Oriental Silver Coinage.” In *Methods of Chemical and Metallurgical Investigation of Ancient Coinage*, edited by E.T Hall and D. M. Metcalf, 195–209. London: Royal Numismatic Society.
- McNeil, J.A., and F.E. Cecil. 2009. “X-Ray Fluorescence Measurements of Manganese in Petroglyphs and Graffiti in the Bluff, Utah Area.”
http://inside.mines.edu/~jamcneil/XRF_Report_Bluff_Ut.pdf.
- McSloy, E.RR. 2013. “Metal and Other Small Finds.” In *Friars, Quakers, Industry and Urbanisation: The Archaeology of the Broadmead Expansion Project, Cabot Circus, Bristol, 2005-2008*, edited by Victoria Ridgeway and Martin Watts, 237–243. Cirencester and London: CAPCA. <http://www.cotswoldarchaeology.co.uk/friars-quakers-industry-and-urbanisation/>.
- Meaney, Audrey Lilian. 1981. *Anglo-Saxon Amulets and Curing Stones*. British Archaeology Series (BAR) 96. Oxford: Archaeopress.
- Metcalf, D.M., and J.P. Northover. 1985. “Debasement of the Coinage in Southern England in the Age of King Alfred.” *Numistics Chronicle* 145: 150–176.

- <http://www.jstor.org/stable/42667536>.
- . 1988. “Carolingian and Viking Coins from the Cuerdale Hoard: An Interpretation and Comparison of Their Metal Contents.” *The Numismatic Chronicle* 148: 97–116. <http://www.jstor.org/stable/42668130>.
- Milazzo, M., and C. Cicardi. 1997. “Simple Methods for Quantitative X-Ray Fluorescence Analysis of Ancient Metal Objects of Archaeological Interest.” *X-Ray Spectrometry* 26 (4) (July): 211–216. doi:10.1002/(SICI)1097-4539(199707)26:4<211::AID-XRS214>3.0.CO;2-G. [http://doi.wiley.com/10.1002/\(SICI\)1097-4539\(199707\)26:4<211::AID-XRS214>3.0.CO;2-G](http://doi.wiley.com/10.1002/(SICI)1097-4539(199707)26:4<211::AID-XRS214>3.0.CO;2-G).
- Millhauser, John K, Enrique Rodríguez-Alegría, and Michael D. Glascock. 2011. “Testing the Accuracy of Portable X-Ray Fluorescence to Study Aztec and Colonial Obsidian Supply at Xaltocan, Mexico.” *Journal of Archaeological ...* 38 (11) (November): 3141–3152. doi:10.1016/j.jas.2011.07.018. <http://www.sciencedirect.com/science/article/pii/S0305440311002585>.
- Milligan, Glenn W. 1980. “An Examination of the Effect of Six Types of Error Perturbation on Fifteen Clustering Algorithms.” *Psychometrika* 45 (3) (September): 325–342. doi:10.1007/BF02293907. <http://link.springer.com/10.1007/BF02293907>.
- Mitchell, Darren, Peter Grave, Michael Maccheroni, and Evgenia Gelman. 2012. “Geochemical Characterisation of North Asian Glazed Stonewares: A Comparative Analysis of NAA, ICP-OES and Non-Destructive pXRF.” *Journal of Archaeological Science* 39 (9) (September): 2921–2933. doi:10.1016/j.jas.2012.04.044. <http://www.sciencedirect.com/science/article/pii/S030544031200177X>.
- Mitchiner, M, and A Skinner. 1983. “English Tokens, C. 1200 to 1425.” *British Numismatic Journal* 53: 29–77. http://www.britnumsoc.org/publications/DigitalBNJ/pdfs/1983_BNJ_53_7.pdf.
- . 1984. “English Tokens, C. 1425 to 1672.” *British Numismatic Journal* 54: 86–163. http://www.britnumsoc.org/publications/DigitalBNJ/pdfs/1984_BNJ_54_11.pdf.
- Mithen, S. 2005. “Comments V: The Need For An Evolutionary Perspective On The Human Mind.” *Archaeometry* 47 (1) (February): 189–192. doi:10.1111/j.1475-4754.2005.195-5.x. <http://doi.wiley.com/10.1111/j.1475-4754.2005.195-5.x>.
- Montgomery, Janet, Jane A Evans, Dominic Powlesland, and Charlotte A Roberts. 2005. “Continuity or Colonization in Anglo-Saxon England? Isotope Evidence for Mobility, Subsistence Practice, and Status at West Heslerton.” *American Journal of Physical Anthropology* 126 (2) (February): 123–38. doi:10.1002/ajpa.20111. <http://www.ncbi.nlm.nih.gov/pubmed/15386290>.
- Moreland, John. 1999. “The World(s) of the Cross.” *World Archaeology* 31 (2) (July 15): 194–213. doi:10.1080/00438243.1999.9980441. <http://www.tandfonline.com/doi/abs/10.1080/00438243.1999.9980441>.
- Morgenstein, Maury, and Carol A. Redmount. 2005. “Using Portable Energy Dispersive X-Ray Fluorescence (EDXRF) Analysis for on-Site Study of Ceramic Sherds at El Hibeh, Egypt.” *Journal of Archaeological Science* 32 (11) (November): 1613–1623. doi:10.1016/j.jas.2005.05.004. <http://dx.doi.org/10.1016/j.jas.2005.05.004>.
- Mortimer, Catherine. 1986. “Early Use of Brass in Silver Alloys.” *Oxford Journal of Archaeology* 5 (2) (July): 233–242. doi:10.1111/j.1468-0092.1986.tb00355.x.

- <http://doi.wiley.com/10.1111/j.1468-0092.1986.tb00355.x>.
- . 1990. “Some Aspects of Early Medieval Copper-Alloy Technology, as Illustrated by a Study of the Anglian Cruciform Brooch.” University of Oxford.
- . 1991. “A Descriptive Classification of Early Anglo-Saxon Copper-Alloy Compositions: Towards a General Typology of Early Medieval Copper Alloys.” *Medieval Archaeology* 35 (December 1): 104–107. doi:10.1179/174581308X381074. <http://ads.ahds.ac.uk/catalogue/ARCHway/toc.cfm?rcn=1089&vol=35>.
- Mortimer, Catherine, and A. Draper. 1997. “Technological Study of the Non-Ferrous Artefacts from Boss Hall and Buttermarket (St. Stephen’s Lane) Anglo-Saxon Cemeteries, Ipswich, Suffolk.” 112/97. Ancient Monuments Laboratory Report. London: English Heritage. <http://services.english-heritage.org.uk/ResearchReportsPdfs/112-1997.pdf>.
- Mortimer, Catherine, and M Stoney. 1996. “Decorative Punchmarks on Non-Ferrous Artefacts from Barrington Edix Hill Anglo-Saxon Cemetery 1989—91, Cambridgeshire, Cambridgeshire, in Their Regional Context (Ancient Monuments Laboratory Reports 21).” London.
- Moss, A. A. 1953. “Niello.” *Studies in Conservation* 1 (2) (November 11): 49–62 . <http://www.jstor.org/pss/1505039>.
- Myres, John Nowell Linton. 1969. *Anglo-Saxon Pottery and the Settlement of England*. Oxford: Clarendon Press.
- . 1977. *A Corpus of Anglo-Saxon Pottery of the Pagan Period*. Cambridge: Cambridge University Press.
- Nagel, Christopher J, and Dudley R Herschbach. 2009. “Unique Properties of Thermally Tailored Copper: Magnetically Active Regions and Anomalous X-Ray Fluorescence Emissions.” *The Journal of Physical Chemistry. C, Nanomaterials and Interfaces* 113 (51) (December): 21428–21440. doi:10.1021/jp908299q. <http://dx.doi.org/10.1021/jp908299q>.
- Nazaroff, A, and M. Steven Shackley. 2009. “Testing the Size Dimension Limitation of Portable XRF Instrumentation for Obsidian Provenance.” *2009 Portland GSA Annual Meeting*. Portland, OR.: Geological Society of America Annual Meeting, Portland, Oregon (18-21 October, 2009). https://gsa.confex.com/gsa/2009AM/finalprogram/abstract_158668.htm.
- Nekrasov, I.Y. 1996. *Geochemistry, Mineralogy and Genesis of Gold Deposits*. Translated by P.M. Rao. Rotterdam: Balkema. <http://books.google.com/books?id=HUWRZecignoC&pgis=1>.
- Neuwirth, Erich. 2011. “RColorBrewer: ColorBrewer Palettes.” <http://cran.r-project.org/package=RColorBrewer>.
- Newell, A, and HA Simon. 1976. “Computer Science as Empirical Inquiry: Symbols and Search.” *Communications of the ACM* 19 (3): 113–126. doi:10.1145/360018.360022. <http://dl.acm.org/citation.cfm?id=360022>.
- Newman, R., J. R. Dennis, and E. Farrell. 2007. “A Technical Note on Niello.” *Journal of the American Institute for Conservation* 21 (2) (November 9): 80–85. <http://www.jstor.org/pss/3179381>.
- Nicholas, Matthew. 2003. “Copper Alloy Objects from Seven Sites within Mid Saxon London (Lundenwic).” 36/2003. Centre for Archaeology Report Series. London: English Heritage. <http://research.english-heritage.org.uk/report/?8819>.

- . 2008. “Metal-Working Debris from Park Street.” In *The Bull Ring Uncovered: Excavations at Edgbaston Street, Moor Street, Park Street and The Row, Birmingham City Centre, 1997-2001*, edited by Stephanie Ratkai, 227 – 235, 348 – 361. Oxford: Oxbow Books. <http://www.oxbowbooks.com/oxbow/the-bull-ring-uncovered.html>.
- . 2012. “X-Ray Fluorescence Analysis of the Copper-Alloy Objects.” In *Lundenwic: Excavations in Middle Saxon London, 1987–2000*, edited by Robert Cowie and Lynne Blackmore, 286–288. London: Museum of London Archaeology Service.
- Nicholas, Matthew, and Dan Hicks. 2013. “Oxfordshire.” In *World Archaeology at the Pitt Rivers Museum: A Characterization*, edited by Dan Hicks and Alice Stevenson, 279–301. Oxford: Archaeopress. <http://www.scribd.com/doc/125482256/Chapter-13-Oxfordshire-World-Archaeology-at-the-Pitt-Rivers-Museum>.
- Nicholas, Matthew, and Panagiota Manti. 2014. “Testing the Applicability of Handheld Portable XRF to the Characterisation of Archaeological Copper Alloys.” In *ICOM-CC 17th Triennial Conference Preprints, Melbourne, 15–19 September 2014*, edited by J Bridgland. Paris: International Council of Museums.
- Nielson, Kirk K. 1977. “Matrix Corrections for Energy Dispersive X-Ray Fluorescence Analysis of Environmental Samples with Coherent/incoherent Scattered X-Rays.” *Analytical Chemistry* 49 (4) (April): 641–648. doi:10.1021/ac50012a034. <http://dx.doi.org/10.1021/ac50012a034>.
- Nilfanion. 2010a. “Suffolk UK Location Map.” *Wikimedia Commons*. https://commons.wikimedia.org/wiki/File:Suffolk_UK_location_map.svg.
- . 2010b. “Suffolk UK Locator Map 2010.” *Wikimedia Commons*. https://commons.wikimedia.org/wiki/File:Suffolk_UK_locator_map_2010.svg.
- Northover, J.P. 1991. “Non-Ferrous Metalwork and Metallurgy.” In *Maiden Castle: Excavation and Field Survey, 1985-86*, edited by N Sharples, 156–162. London: English Heritage. doi:10.5284/1028203. http://archaeologydataservice.ac.uk/archives/view/eh_monographs_2014/content.sfm?mono=1089042.
- Northover, Peter. 1977. “Bronze in the British Bronze Age.” In *Aspects of Early Metallurgy: Papers Presented at a Symposium Organized by the Historical Metallurgy Society and the British Museum Research Laboratory and Held at the British Museum on 22nd and 23rd April 1977*, edited by W.A. Oddy, 63–70. British Museum Occasional Papers, No. 17. London: British Museum Press.
- . 1995. “Analyses of Early Medieval Metalwork from Cadbury Castle.” In *Cadbury Castle, Somerset: The Early Medieval Archaeology*, edited by L Alcock, S.J Stevenson, and C.R Musson, 73–74. Cardiff: University of Wales Press.
- O’Connor, T. 1991. “Science, Evidential Archaeology, and the New Scholasticism.” *Scottish Archaeological Review* 8: 1–7.
- O’Connor, T. P. 2005. “Animal Bones.” In *An Assessment of the Potential for Analysis and Publication for Archaeological Work Carried out at RAF Lakenbeath between 1987 and June 2005: Volume I: The Anglo-Saxon Cemeteries ERL 104, ERL 046 and ERL 114*, edited by Jo Caruth and Sue Anderson, 76–88. SCCAS Report. Ipswich: Suffolk County Council.
- Oddy, Andrew. 1981. “Gilding through the Ages.” *Gold Bulletin* 14 (2) (June): 75–79. doi:10.1007/BF03214601. <http://link.springer.com/10.1007/BF03214601>.

- Oddy, W.A. 1980. "Gilding and Tinning in Anglo-Saxon England." In *Aspects of Early Metallurgy*, edited by W.A. Oddy, 129–134. British Museum Occasional Paper. London: British Museum.
- . 1983. "Bronze Alloys in Dark-Age Europe." In *The Sutton Hoo Ship Burial: Volume 3: Part II*, 945–961. London: British Museum.
- . 1991. "Gilding: An Outline of the Technological History of the Plating of Gold on to Silver or Copper in the Old World." *Endeavour* 15 (1) (January): 29–33. doi:10.1016/0160-9327(91)90085-P. [http://dx.doi.org/10.1016/0160-9327\(91\)90085-P](http://dx.doi.org/10.1016/0160-9327(91)90085-P).
- Oddy, W.A., M. Bimson, and Susan La Niece. 1983. "The Composition of Niello Decoration on Gold, Silver and Bronze in the Antique and Mediaeval Periods." *Studies in Conservation* 28 (1) (November 11): 29–35. <http://www.jstor.org/pss/1506104>.
- Ohlsson, Stellan. 1990. "Models of Thought, Vol. 2, H. A. Simon (Ed.) (Book Review)." *Applied Cognitive Psychology* 4 (6) (November): 501–504. doi:10.1002/acp.2350040609. <http://doi.wiley.com/10.1002/acp.2350040609>.
- Olsen, Bjørnar. 2003. "Material Culture after Text: Re-Membering Things." *Norwegian Archaeological Review* 36 (2) (October 1): 87–104. doi:10.1080/00293650310000650. <http://www.ingentaconnect.com/content/routledg/sarc/2003/00000036/00000002/art00001;jsessionid=1cu2z6js7uss.alice>.
- Orfanou, V., and Thilo Rehren. 2014. "A (Not so) Dangerous Method: pXRF vs. EPMA-WDS Analyses of Copper-Based Artefacts." *Archaeological and Anthropological Sciences* (June 13). doi:10.1007/s12520-014-0198-z. <http://link.springer.com/10.1007/s12520-014-0198-z>.
- Orwell, George. 1975. "A Hanging." In *The Collected Essays Journalism and Letters of George Orwell Volume 1: An Age Like This, 1920-1940*, edited by Sonia Orwell and Ian Angus, 66–71. London: Penguin Books.
- Otero, N, R Tolosana-Delgado, A Soler, Vera Pawlowsky-Glahn, and A Canals. 2005. "Relative vs. Absolute Statistical Analysis of Compositions: A Comparative Study of Surface Waters of a Mediterranean River." *Water Research* 39 (7) (April 1): 1404–14. doi:10.1016/j.watres.2005.01.012. <http://europepmc.org/abstract/MED/15862341>.
- Pader, Ellen-Jane. 1982. *Symbolism, Social Relations and the Interpretation of Mortuary Remains*. B.A.R. International Series No. 130. Oxford: Archaeopress.
- Palarea-Albaladejo, Javier, Josep A. Martín-Fernández, and Juan Gómez-García. 2007. "A Parametric Approach for Dealing with Compositional Rounded Zeros." *Mathematical Geology* 39 (7) (September 14): 625–645. doi:10.1007/s11004-007-9100-1. <http://link.springer.com/10.1007/s11004-007-9100-1>.
- Pantazis, T., A.G. Karydas, C. Doumas, A. Vlachopoulos, P. Nomikos, and M. Dinsmore. 2002. "X-Ray Fluorescence Analysis of a Gold Ibex and Other Artifacts from Akrotiri." <http://www.therafoundation.org/Projects/analysis/Metron Paper - Rev B2.pdf>.
- Papadopoulou, D. N., G. A. Zachariadis, A. N. Anthemidis, N. C. Tsirliganis, and J. A. Stratis. 2006. "Development and Optimisation of a Portable Micro-XRF Method for in Situ Multi-Element Analysis of Ancient Ceramics." *Talanta* 68 (5) (February 28): 1692–9. doi:10.1016/j.talanta.2005.08.051. <http://www.ncbi.nlm.nih.gov/pubmed/18970516>.

- Pappalardo, G, E Costa, C Marchetta, L Pappalardo, F.P Romano, A Zucchiatti, P Prati, et al. 2004. "Non-Destructive Characterization of Della Robbia Sculptures at the Bargello Museum in Florence by the Combined Use of PIXE and XRF Portable Systems." *Journal of Cultural Heritage* 5 (2) (April): 183–188. doi:10.1016/j.culher.2003.08.002. <http://dx.doi.org/10.1016/j.culher.2003.08.002>.
- Parker-Pearson, Mike. 1984. "Social Change, Ideology and the Archaeological Record." In *Marxist Perspectives in Archaeology*, edited by M Spriggs, 59–71. Cambridge: Cambridge University Press.
- Patterson, C.C. 1971. "Native Copper, Silver, and Gold Accessible to Early Metallurgists." *American Antiquity* 36 (3): 286–321.
- Pawlak, Z. 1991. *Rough Sets: Theoretical Aspects of Reasoning about Data*. Dordrecht: Kluwer Academic Publishers. <http://books.google.com/books?id=MJPLCqIniGsC>.
- Pawłowsky-Glahn, Vera, and Juan José Egozcue. 2006. "Compositional Data and Their Analysis: An Introduction." *Geological Society, London, Special Publications* 264 (1) (January 1): 1–10. doi:10.1144/GSL.SP.2006.264.01.01. <http://sp.lyellcollection.org/cgi/doi/10.1144/GSL.SP.2006.264.01.01>.
- Pawłowsky-Glahn, Vera, Juan José Egozcue, and R Tolosana Delgado. 2007. "Lecture Notes on Compositional Data Analysis." <http://dugi-doc.udg.edu/handle/10256/297>.
- Peake, James Robert Nicholas. 2013. "Early Anglo-Saxon Glass Beads: Composition and Origins Based on the Finds from RAF Lakenheath, Suffolk." Cardiff University. <http://orca.cf.ac.uk/47677/13/peakejrn.pdf>.
- Pearson, Karl, and Alice Lee. 1896. "Mathematical Contributions to the Theory of Evolution. On Telegony in Man, &c." *Proceedings of the Royal Society of London (1854-1905)* 60 (1) (January 1): 273–283. doi:10.1098/rspl.1896.0048. <http://rspl.royalsocietypublishing.org>.
- Penn, Kenneth, and Birte Brugmann. 2007. *Aspects of Anglo-Saxon Inhumation Burial: Morning Thorpe, Spong Hill, Bergh Apton and Westgarth Gardens*. East Anglian Archaeology Monograph 119. Dereham: East Anglian Archaeology & Norfolk Museums and Archaeology Series.
- Percy, John. 1861. *Metallurgy: The Art of Extracting Metals from Their Ores, and Adapting Them to Various Purposes of Manufacture: Fuel, Fire-Clays, Copper, Zinc, Brass, Etc.* London: J. Murray.
- . 1880. *Metallurgy: The Art of Extracting Metals from Their Ores: On Silver and Gold (Volume IV)*. London: John Murray. <https://archive.org/details/metallurgyartex00percgoog>.
- Peterson, Brian G., and Peter Carl. 2014. "PerformanceAnalytics: Econometric Tools for Performance and Risk Analysis." <http://cran.r-project.org/package=PerformanceAnalytics>.
- Petzow, G., and G. Effenberg. 1988. *Ternary Alloys: A Comprehensive Compendium of Evaluated Constitutional Data and Phase Diagrams, Volume 1*. Weinheim: VCH Verlagsgesellschaft.
- Phillips, Patricia. 1985. "Introduction." In *The Archaeologist and the Laboratory*, edited by Patricia Phillips, 1. CBA Research Report No 58. London: Council for British Archaeology. doi:10.5284/1000332. http://archaeologydataservice.ac.uk/archives/view/cba_rr/rr58.cfm.

- Phillips, S. Colby, and Robert J. Speakman. 2009. "Initial Source Evaluation of Archaeological Obsidian from the Kuril Islands of the Russian Far East Using Portable XRF." *Journal of Archaeological Science* 36 (6) (June): 1256–1263. doi:10.1016/j.jas.2009.01.014. <http://linkinghub.elsevier.com/retrieve/pii/S0305440309000302>.
- Piestrzyński, Adam, Jadwiga Pieczonka, and Adam Gluszek. 2002. "Redbed-Type Gold Mineralisation, Kupferschiefer, South-West Poland." *Mineralium Deposita* 37 (5) (June 1): 512–528. doi:10.1007/s00126-002-0256-9. <http://www.springerlink.com/content/m3clxxqywxalpeb6/>.
- Pike, A., C. Cartwright, M. Cowell, and J. Lang. 1997. "The Scientific Examination of the Hoard." In *The Snettisham Roman Jeweller's Hoard*, edited by C Jones, 50–68. London: The British Museum Press.
- Pitt-Rivers, A.H.L.F. 1883. "Excavations at Caesar's Camp, near Folkestone, Conducted in 1878." *Archaeologia* 47: 429–465.
- Pliny the Elder, and John Bostock. 1828. *The First and Thirty-Third Books of Pliny's Natural History; A Specimen of a Proposed Translation of the Whole Work with Notes, Etc.* London: Baldwin and Cradock.
- Pollard, A. Mark, Peter Bray, Chris Gosden, Andrew Wilson, and Helena Hamerow. 2015. "Characterising Copper-Based Metals in Britain in the First Millennium AD: A Preliminary Quantification of Metal Flow and Recycling." *Antiquity* 89 (345) (June 1): 697–713. doi:10.15184/aqy.2015.20. http://journals.cambridge.org/abstract_S0003598X15000204.
- Ponting, Matthew. 2002. "Keeping up with the Romans? Romanisation and Copper Alloys in First Revolt Palestine." *Institute for Archaeo-Metallurgical Studies* 22: 3–6.
- Potts, Philip J., Peter C. Webb, and Olwen Williams-Thorpe. 1997. "Investigation of a Correction Procedure for Surface Irregularity Effects Based on Scatter Peak Intensities in the Field Analysis of Geological and Archaeological Rock Samples by Portable X-Ray Fluorescence Spectrometry." *Journal of Analytical Atomic Spectrometry* 12 (7): 769–776. doi:10.1039/a606639i. <http://pubs.rsc.org/en/content/articlehtml/1997/ja/a606639i>.
- Potts, Philip J., Olwen Williams-Thorpe, and Peter C. Webb. 1997. "The Bulk Analysis of Silicate Rocks by Portable X-Ray Fluorescence: Effect of Sample Mineralogy in Relation to the Size of the Excited Volume." *Geostandards and Geoanalytical Research* 21 (1) (June 22): 29–41. doi:10.1111/j.1751-908X.1997.tb00529.x. <http://doi.wiley.com/10.1111/j.1751-908X.1997.tb00529.x>.
- Presbyter, Theophilus. 2000. *Theophilus: On Diverse Arts: The Foremost Medieval Treatise on Painting, Glassmaking and Metalwork*. Translated by G.J. Hawthorne and Cyril Stanley Smith. New York: Dover Publications Ltd.
- Prince, Alan, Geoffrey V. Raynor, and Dain Stedman Evans. 1990. *Phase Diagrams of Ternary Gold Alloys*. London: Institute of Metals.
- Prioreschi, Plinio. 1998. *A History of Medicine: Roman Medicine (Volume III)*. Omaha: Horatius Press.
- Pylyshyn, Zenon W., and Liam Bannon. 1989. *Perspectives on the Computer Revolution*. 2nd ed. Norwood, New Jersey: Ablex Publishing.
- R Core Team. 2014. "R: A Language and Environment for Statistical Computing." Vienna, Austria: R Foundation for Statistical Computing. <http://www.r->

project.org/.

- Rapp, George. 2009. *Archaeomineralogy*. 2nd ed. Natural Science in Archaeology. Berlin, Heidelberg: Springer Berlin Heidelberg. doi:10.1007/978-3-540-78594-1. <http://link.springer.com/10.1007/978-3-540-78594-1>.
- Rehren, Thilo, and K Eckstein. 2002. "The Development of Analytical Cupellation in the Middle Ages." In *Archaeometry 98: Proceedings of the 31st Symposium Budapest, April 26-May 3 1998*, edited by Erzsébe Jerem and Katalin T. Biro, 445–448. Oxford: Archaeopress.
- Reimann, Clemens, and Peter Filzmoser. 2000. "Normal and Lognormal Data Distribution in Geochemistry: Death of a Myth. Consequences for the Statistical Treatment of Geochemical and Environmental Data." *Environmental Geology* 39 (9) (July 14): 1001–1014. doi:10.1007/s002549900081. <http://link.springer.com/10.1007/s002549900081>.
- Reimann, Clemens, Peter Filzmoser, and Robert G Garrett. 2005. "Background and Threshold: Critical Comparison of Methods of Determination." *The Science of the Total Environment* 346 (1-3) (June): 1–16. doi:10.1016/j.scitotenv.2004.11.023. <http://www.sciencedirect.com/science/article/pii/S0048969704007983>.
- Richards, Julian. 1999. "Meet the Ancestors: Warrior." UK: BBC. <http://www.bbc.co.uk/programmes/b0074lbw>.
- . 2013. "Stories from the Dark Earth: Meet the Ancestors Revisited: The First Anglo-Saxons." UK: BBC. <http://www.bbc.co.uk/programmes/b01skwfd>.
- Richards, Julian D. 1987. *The Significance of Form and Decoration of Anglo-Saxon Cremation Urns*. Vol. 166. BAR British Series. Oxford: Archaeopress.
- Rickard, T.A. 1932. "The Nomenclature of Copper and Its Alloys." *The Journal of the Royal Anthropological Institute of Great Britain and Ireland* 62: 281–290.
- Roach Smith, Charles. 1848. *Collectanea Antiqua: Etchings and Notices of Ancient Remains, Illustrative of the Habits, Customs, and History of Past Ages*. London: J. R. Smith. <https://books.google.com/books?id=q826mwEACAAJ&pgis=1>.
- . 1871. *A Catalogue of Anglo-Saxon and Other Antiquities, Discovered at Faversham, in Kent, and Bequeathed by E. Gibbs to the South Kensington Museum*. London: Chapman and Hall.
- Robbiola, L, J-M Blengino, and C. Fiaud. 1998. "Morphology and Mechanisms of Formation of Natural Patinas on Archaeological Cu–Sn Alloys." *Corrosion Science* 40 (12) (December): 2083–2111. doi:10.1016/S0010-938X(98)00096-1. [http://dx.doi.org/10.1016/S0010-938X\(98\)00096-1](http://dx.doi.org/10.1016/S0010-938X(98)00096-1).
- Roberts, P. M. 1973. "Gold Brazing in Antiquity." *Gold Bulletin* 6 (4) (December): 112–119. doi:10.1007/BF03215024. <http://link.springer.com/10.1007/BF03215024>.
- Rousseau, RM. 2001. "Detection Limit and Estimate of Uncertainty of Analytical XRF Results." *The Rigaku Journal* 18 (2): 33 – 47. <http://www.citeulike.org/group/10232/article/5197419>.
- Rousseuw, Peter J. 1984. "Least Median of Squares Regression." *Journal of the American Statistical Association* 79 (388): 871–880. doi:10.2307/2288718. <http://www.jstor.org/stable/2288718>.
- RStudio. 2014. "RStudio." Boston, MA: RStudio. <http://www.rstudio.org/>.
- Saito, Yuriko. 2010. *Everyday Aesthetics*. Oxford: Oxford University Press.

- Salomon, J., J.-C. C. Dran, T. Guillou, B. Moignard, L. Pichon, P. Walter, and F. Mathis. 2008. "Ion-Beam Analysis for Cultural Heritage on the AGLAE Facility: Impact of PIXE/RBS Combination." *Applied Physics A: Materials Science and Processing* 92 (1) (May 23): 43–50. doi:10.1007/s00339-008-4512-4. <http://link.springer.com/10.1007/s00339-008-4512-4>.
- Sanford, Richard F., Charles T. Pierson, and Robert A. Crovelli. 1993. "An Objective Replacement Method for Censored Geochemical Data." *Mathematical Geology* 25 (1) (January): 59–80. doi:10.1007/BF00890676. <http://link.springer.com/10.1007/BF00890676>.
- Schaller, R.R. 1997. "Moore's Law: Past, Present and Future." *IEEE Spectrum* 34 (6) (June): 52–59. doi:10.1109/6.591665. <http://ieeexplore.ieee.org/lpdocs/epic03/wrapper.htm?arnumber=591665>.
- Schloerke, Barret, Jason Crowley, Di Cook, Heike Hofmann, Hadley Wickham, Francois Briatte, Moritz Marbach, and Edwin Thoen. 2014. "GGally: Extension to ggplot2." <http://cran.r-project.org/package=GGally>.
- Schoonjans, Tom, Laszlo Vincze, Vicente Armando Solé, Manuel Sanchez del Rio, Philip Brondeel, Geert Silversmit, Karen Appel, and Claudio Ferrero. 2012. "A General Monte Carlo Simulation of Energy Dispersive X-Ray Fluorescence Spectrometers — Part 5." *Spectrochimica Acta Part B: Atomic Spectroscopy* (April). doi:10.1016/j.sab.2012.03.011. <http://www.citeulike.org/article/10547636>.
- Schroy, Ellen T., ed. 2004. *Warman's Americana & Collectibles*. Iola, Wisconsin: Krause Publications.
- Scott, David A. 1991. *Metallography and Microstructure of Ancient and Historic Metals*. Marina del Rey; Santa Monica: Getty Conservation Institute and J. Paul Getty Museum in association with Archtype Books. <http://www.bcin.ca/Interface/openbcin.cgi?submit=submit&Chinkey=128658>.
- Searle, John R. 1995. *The Construction of Social Reality*. Simon and Schuster.
- Sebald, W G. 2002. *The Rings Of Saturn*. Translated by Michael Hulse. London: Cintage.
- Shackley, M. Steven. 2010. "Is There Reliability and Validity in Portable X-Ray Fluorescence Spectrometry (PXRF)?" *The SAA Archaeological Record* 10 (5): 17–18 & 20.
- . 2011. "An Introduction to X-Ray Fluorescence (XRF) Analysis in Archaeology." In *X-Ray Fluorescence Spectrometry (XRF) in Geoarchaeology*, edited by M. Steven Shackley, 7–44. New York, NY: Springer New York. doi:10.1007/978-1-4419-6886-9. <http://www.springerlink.com/index/10.1007/978-1-4419-6886-9>.
- Shakespeare, William. 2010. *The Merchant of Venice*. Edited by Jonathan Bate and Eric Rasmussen. The RSC Sh. London: Palgrave Macmillan.
- Shalev, S, S Sh Shilstein, and Yu Yekutieli. 2006. "XRF Study of Archaeological and Metallurgical Material from an Ancient Copper-Smelting Site near Ein-Yahav, Israel." *Talanta* 70 (5) (December): 909–13. doi:10.1016/j.talanta.2006.05.052.
- Shepherd, Tom J., Jon E. Bouch, Andrew G. Gunn, John A. McKervey, Jonathan Naden, Richard C. Scrivener, Michael T. Styles, and Duncan E. Large. 2005. "Permo–Triassic Unconformity-Related Au-Pd Mineralisation, South Devon, UK: New Insights and the European Perspective." *Mineralium Deposita* 40 (1) (May 14): 24–44. doi:10.1007/s00126-004-0459-3. <http://www.springerlink.com/content/m618355108t22163/>.

- Sheppard, Peter J., Geoff J. Irwin, Sam C. Lin, and Cameron P. McCaffrey. 2011. "Characterization of New Zealand Obsidian Using PXRF." *Journal of Archaeological Science* 38 (1) (January): 45–56. doi:10.1016/j.jas.2010.08.007. <http://www.sciencedirect.com/science/article/pii/S0305440310002815>.
- Sherlock, S.J., and Martin G. Welch. 1992. *An Anglo-Saxon Cemetery at Norton, Cleveland*. CBA Research Report No 82. York: Council for British Archaeology. doi:10.5284/1000332. <http://dx.doi.org/10.5284/1000332>.
- Shilstein, S. S., and S. Shalev. 2011. "Making Sense out of Cents: Compositional Variations in European Coins as a Control Model for Archaeometallurgy." *Journal of Archaeological Science* 38 (7) (July): 1690–1698. doi:10.1016/j.jas.2011.02.036.
- Sim, Susan Elliott, Steve Easterbrook, and Richard C. Holt. 2003. "Using Benchmarking to Advance Research: A Challenge to Software Engineering." In *ICSE '03: Proceedings of the 25th International Conference on Software Engineering*, 74–83. <http://dl.acm.org/citation.cfm?id=776816.776826>.
- Simsek, Gulsu, Francesca Casadio, Philippe Colomban, Ludovic Bellot-Gurlet, Katherine T. Faber, Ghenete Zelleke, V. Milande, and Eric Moinet. 2014. "On-Site Identification of Early BÖTTIGER Red Stoneware Made at Meissen Using Portable XRF: 1, Body Analysis." Edited by H. Chan. *Journal of the American Ceramic Society* 97 (9) (September 11): 2745–2754. doi:10.1111/jace.13032. <http://doi.wiley.com/10.1111/jace.13032>.
- Sitko, Rafał. 2009. "Quantitative X-Ray Fluorescence Analysis of Samples of Less than 'infinite Thickness': Difficulties and Possibilities." *Spectrochimica Acta Part B: Atomic Spectroscopy* 64 (11-12) (November): 1161–1172. doi:10.1016/j.sab.2009.09.005. <http://dx.doi.org/10.1016/j.sab.2009.09.005>.
- Šmit, Ž., J. Istenič, and T. Knific. 2008. "Plating of Archaeological Metallic Objects – Studies by Differential PIXE." *Nuclear Instruments and Methods in Physics Research Section B: Beam Interactions with Materials and Atoms* 266 (10) (May): 2329–2333. doi:10.1016/j.nimb.2008.03.057. <http://linkinghub.elsevier.com/retrieve/pii/S0168583X08002619>.
- Smythe, J.A. 1934. "Roman Objects of Copper and Iron from the North of England." *Proceedings of the University of Durham Philosophical Society* 9: 382–405.
- Snyder, R.L. 2009. "X-Ray Diffraction." In *X-Ray Characterization of Materials*, edited by E/ Lifshin, 1–105. Weinheim: Wiley-VCH.
- Sokal, A. 1996. "A Physicist Experiments with Cultural Studies." *Lingua Franca* 6 (May/June): 62–64.
- Sotnikov, V. 2001. "Palladium, Platinum and Gold Distribution in Porphyry Cu±Mo Deposits of Russia and Mongolia." *Ore Geology Reviews* 18 (1-2) (April): 95–111. doi:10.1016/S0169-1368(01)00018-X. [http://dx.doi.org/10.1016/S0169-1368\(01\)00018-X](http://dx.doi.org/10.1016/S0169-1368(01)00018-X).
- Southport Group. 2011. "Realising the Benefits of Planning-Led Investigation in the Historic Environment: A Framework for Delivery." Reading.
- Souvatzi, S.G. 2008. *A Social Archaeology of Households in Neolithic Greece: An Anthropological Approach*. Cambridge: Cambridge University Press.
- Speakman, Robert J., Nicole C. Little, Darrell Creel, Myles R. Miller, and Javier G. Iñáñez. 2011. "Sourcing Ceramics with Portable XRF Spectrometers? A Comparison with INAA Using Mimbres Pottery from the American Southwest."

- Journal of Archaeological Science* 38 (12) (December): 3483–3496.
doi:10.1016/j.jas.2011.08.011.
<http://www.sciencedirect.com/science/article/pii/S0305440311002822>.
- Spenser, Edmund. 1859. *The Poetical Works of Edmund Spenser: With Memoir and Critical Dissertations, Volume 3*. Edited by George Gilfillan. Vol. III. Edinburgh: James Nichol. <https://books.google.com/books?id=HTkrAQAIAAJ>.
- Standley, E, Dan Hicks, and Alice Forward. 2013. “Post-Roman Europe.” In *World Archaeology at the Pitt Rivers Museum: A Characterization*, edited by D Hicks and Alice Stevenson, 262–278. Oxford: Archaeopress.
- Steiniger, D, and C Giardino. 2013. “Prehistoric Mining in Central Italy: New Evidence from the Monti Della Tolfa (Latium).” In *Mining in European History and Its Impact on Environment and Human Societies: Proceedings for the 1st Mining in European History-Conference of the SFB-HIMAT, 12.-15. November 2009, Innsbruck*, edited by Peter Anreiter, Gert Goldenberg, Klaus Hanke, Rüdiger Krause, Walter Leitner, Franz Mathis, Kurt Nicolussi, et al., 81–87. Innsbruck University Press.
- Stoodley, Nicholas. 1997. “The Spindle and the Spear: A Critical Enquiry into the Construction of Meaning of Gender in the Early Anglo-Saxon Inhumation Burial Rite.” University of Reading.
<http://ethos.bl.uk/OrderDetails.do?uin=uk.bl.ethos.363709>.
- Subramanian, P. R., and J. H. Perepezko. 1993. “The Ag-Cu (Silver-Copper) System.” *Journal of Phase Equilibria* 14 (1) (February): 62–75. doi:10.1007/BF02652162.
<http://link.springer.com/10.1007/BF02652162>.
- Suffolk County Council Archaeological Service. 2009. “ERL 058 - Lakenheath Airfield; Swimming Pool.” Ipswich: Suffolk County Council.
<https://heritage.suffolk.gov.uk/hbsmr-web/record.aspx?UID=MSF10699-Lakenheath-Airfield-Swimming-Pool&pageid=16&mid=9>.
- Sussams, Kate. 1996. “The Breckland Archaeological Survey 1994-1996: A Characterisation of the Archaeology and Historic Landscape of the Breckland Environmental Sensitive Area.” Ipswich: Suffolk County Council.
- Suzuki, S. 2000. *The Quoit Brooch Style and Anglo-Saxon Settlement: A Casting and Recasting of Cultural Identity Symbols*. London: Boydell & Brewer.
- . 2007. *Anglo-Saxon Button Brooches: Typology, Genealogy, Chronology*. London: Boydell & Brewer.
- Swift, Ellen. 2012a. “The Analysis of Reused Material Culture for Late Antique Studies.” *Late Antique Archaeology* 9 (1) (January 1): 91–119. doi:10.1163/22134522-12340006.
<http://booksandjournals.brillonline.com/content/journals/10.1163/22134522-12340006>.
- . 2012b. “Object Biography, Re-Use and Recycling in the Late to Post-Roman Transition Period and Beyond: Rings Made from Romano-British Bracelets.” *Britannia* 43 (August 30): 167–215. doi:10.1017/S0068113X12000281.
http://journals.cambridge.org/abstract_S0068113X12000281.
- Tanenbaum, A.S. 1988. *Computer Networks*. 2nd ed. New Jersey: Prentice Hall Inc.
- Tangri, D., and R. V. S. Wright. 1993. “Multivariate Analysis of Compositional Data: Applied Comparisons Favour Standard Principal Components Analysis Over Aitchison’s Loglinear Contrast Method.” *Archaeometry* 35 (1) (February): 103–112.

doi:10.1111/j.1475-4754.1993.tb01026.x. <http://doi.wiley.com/10.1111/j.1475-4754.1993.tb01026.x>.

- Taylor, Christopher. 1984. *Village and Farmstead: A History of Rural Settlement in England*. London: G. Philip.
<http://books.google.com/books?id=FOnWAAAAMAAJ&pgis=1>.
- Taylor, H.F.W. 1962. "The Dehydration of Hemimorphite." *The American Mineralogist* 47: 932–944.
- Taylor, Timothy. 1999. "Envaluing Metal: Theorizing the Eneolithic 'Hiatus.'" In *Metals in Antiquity*, edited by Susan M. M. Young, A. Mark Pollard, and Paul Budd, 22–32. BAR International Series: 792. Oxford: Archaeopress.
- . 2005. "Comments Vii: A Cunning Duplicate In Mind-Materiality And The Interpretive Dilemma." *Archaeometry* 47 (1) (February): 196–198. doi:10.1111/j.1475-4754.2005.195-7.x. <http://doi.wiley.com/10.1111/j.1475-4754.2005.195-7.x>.
- Thomas, J. 2005. "Comments Viii: Between 'Material Qualities' And 'Materiality.'" *Archaeometry* 47 (1) (February): 198–201. doi:10.1111/j.1475-4754.2005.195-8.x. <http://doi.wiley.com/10.1111/j.1475-4754.2005.195-8.x>.
- Thorndycraft, Varyl R., D. Pirrie, and A. G. Brown. 1999. "Tracing the Record of Early Alluvial Tin Mining on Dartmoor, UK." *Geological Society, London, Special Publications* 165 (1) (January 1): 91–102. doi:10.1144/GSL.SP.1999.165.01.07. <http://sp.lyellcollection.org/cgi/content/abstract/165/1/91>.
- Thorndycraft, Varyl R., Duncan Pirrie, and Antony G. Brown. 2004. "Alluvial Records of Medieval and Prehistoric Tin Mining on Dartmoor, Southwest England." *Geoarchaeology* 19 (3) (March): 219–236. doi:10.1002/gea.10114. <http://doi.wiley.com/10.1002/gea.10114>.
- Tilley, Christopher. 1990. *Reading Material Culture*. Oxford: Blackwell Publishing, Ltd.
- Tolosana-Delgado, Raimon. 2012. "Uses and Misuses of Compositional Data in Sedimentology." *Sedimentary Geology* 280 (December): 60–79. doi:10.1016/j.sedgeo.2012.05.005. <http://www.sciencedirect.com/science/article/pii/S003707381200142X>.
- Tolosana-Delgado, Raimon, N. Otero, and Vera Pawlowsky-Glahn. 2005. "Some Basic Concepts of Compositional Geometry." *Mathematical Geology* 37 (7) (October): 673–680. doi:10.1007/s11004-005-7374-8. <http://www.springerlink.com/content/fm432427p4573545/>.
- Tomtlund, J-E. 1978. "Tools." In *Excavations at Helgö V:1: Workshop, Part II*, edited by K Lamm, A Lundström, and H Clarke, 15–29. Stockholm: KVHAA.
- Toulmin, Stephen Edelston. 1992. *Cosmopolis: The Hidden Agenda of Modernity*. Chicago: Chicago University Press.
- Trigger, Bruce. 2006. *A History of Archaeological Thought*. 2nd ed. Cambridge: Cambridge University Press.
- Tykot, R.H. 2010. "Sourcing of Sardinian Obsidian Collections in the Museo Preistorico-Etnografico 'Luigi Pigorini' Using Non-Destructive Portable XRF." In *L'ossidiana Del Monte Arci Nel Mediterraneo. Nuovi Apporti Sulla Diffusione, Sui Sistemi Di Produzione E Sulla Loro Cronologia. Atti Del 5 Convegno Internazionale*, edited by C. Lugliè, 85–97. Alès: NUR.
- Tylecote, R. F. 1978. "The Solid Phase Bonding of Gold to Metals." *Gold Bulletin* 11 (3)

- (September): 74–80. doi:10.1007/BF03215091.
<http://link.springer.com/10.1007/BF03215091>.
- Tylecote, R.F. 1976. *A History of Metallurgy*. London: The Metals Society.
- U.S. Environmental Protection Agency. 2007. “Field Portable X-Ray Fluorescence Spectrometry for the Determination of Elemental Concentrations in Soil and Sediment.” Washington D.C.
<http://www.epa.gov/osw/hazard/testmethods/sw846/pdfs/6200.pdf>.
- UNESCO. 2001. *Science and Technology in Islam: Technology and Applied Sciences*. Paris: UNESCO.
- . 2012. “Heritage of Mercury: Almadén and Idrija (36 COM 8B.39).” Paris.
- Untracht, Oppi. 2005. *Metal Techniques for Craftsmen: A Basic Manual for Craftsmen on the Methods of Forming and Decorating Metals*. London: Robert Hale.
- van den Boogaart, K. Gerald, R. Tolosana, and M. Bren. 2014. “Compositions: Compositional Data Analysis.” <http://cran.r-project.org/package=compositions>.
- van den Boogaart, K. Gerald, and Raimon Tolosana-Delgado. 2006. “Compositional Data Analysis with ‘R’ and the Package ‘Compositions.’” *Geological Society, London, Special Publications* 264 (1) (January 1): 119–127. doi:10.1144/GSL.SP.2006.264.01.09.
<http://sp.lyellcollection.org/content/264/1/119.abstract>.
- van den Boogaart, K.G, and Raimon Tolosana-Delgado. 2013. *Analyzing Compositional Data with R. Use R!* Berlin, Heidelberg: Springer. doi:10.1007/978-3-642-36809-7.
<http://dx.doi.org/10.1007/978-3-642-36809-7>.
- VanDerwarker, Amber M. 2010. “Simple Measures for Integrating Plant and Animal Remains.” In *Integrating Zooarchaeology and Paleoethnobotany: A Consideration of Issues, Methods, and Cases*, edited by Amber M VanDerwarker and Tanya M Peres, 65–74. New York: Springer-Verlag.
- Vittori, Ottavio. 1979. “Pliny the Elder on Gilding: A New Interpretation of His Comments.” *Gold Bulletin* 12 (1): 35–39. doi:10.1007/BF03215105.
<http://link.springer.com/article/10.1007/BF03215105>.
- von Eynatten, Hilmar, Vera Pawlowsky-Glahn, and Juan José Egozcue. 2002. “Understanding Perturbation on the Simplex: A Simple Method to Better Visualize and Interpret Compositional Data in Ternary Diagrams.” *Mathematical Geology* 34 (3): 249–257–257. doi:10.1023/A:1014826205533.
<http://www.springerlink.com/content/r1yexkq8wenwywva/>.
- Wade, K. 2000. “Anglo-Saxon and Medieval (Rural).” In *Research and Archaeology: A Framework for the Eastern Counties 2: Research Agenda and Strategy*, edited by N Brown and J Glazebrook. Norwich: The Scole Archaeological Committee for East Anglia.
- Wadsak, Michael, Ina Constantinides, Guido Vittiglio, Annemie Adriaens, Koen Janssens, Manfred Schreiner, Freddy C Adams, Philippe Brunella, and Michel Wuttmann. 2000. “Multianalytical Study of Patina Formed on Archaeological Metal Objects from Bliesbruck-Reinheim.” *Mikrochimica Acta* 133: 159–164. doi:10.1007/s006040070086. <http://dx.doi.org/10.1007/s006040070086>.
- Wang, C.Y. 1919. *Antimony: It's History, Chemistry, Mineralogy, Geology, Metallurgy, Uses, Preparations, Analyses, Production, and Valuation*. London: Charles Griffin & Company Ltd.
- Wanhill, R. J. H. 2005. “Embrittlement of Ancient Silver.” *Journal of Failure Analysis and*

- Prevention* 5 (1) (February): 41–54. doi:10.1361/15477020522294. <http://link.springer.com/10.1361/15477020522294>.
- Wanhill, R.J.H. 2002. “Archaeological Silver Embrittlement: A Metallurgical Inquiry (NLR-TP-2002-224).” Amsterdam. <http://reports.nlr.nl:8080/xmlui/bitstream/handle/10921/680/TP-2002-224.pdf?sequence=1>.
- Ward Perkins, J.B. 1937. “English Medieval Embossed Tiles.” *Archaeological Journal* 94: 128–141.
- Ward, J.H. 1963. “Hierarchical Grouping to Optimize an Objective Function.” *Journal of the American Statistical Association* 58: 236–244. doi:10.1080/01621459.1963.10500845. http://www.tandfonline.com/doi/abs/10.1080/01621459.1963.10500845#.U_MOH_ISZH4.
- Ward-Perkins, Bryan. 2005. *The Fall of Rome: And the End of Civilization*. Oxford: Oxford University Press.
- Watanabe, Satosi. 1985. *Pattern Recognition: Human and Mechanical*. New York: Wiley.
- Welch, Martin. 2008. “Report on Excavations of the Anglo-Saxon Cemetery at Updown, Eastry, Kent.” *Anglo-Saxon Studies in Archaeology and History* 15: 1–146.
- West, Stanley E. 1998. *A Corpus of Anglo-Saxon Material from Suffolk*. East Anglian Archaeology No. 84. East Anglian Archaeology.
- White, Leslie A. 1947. “The Locus of Mathematical Reality: An Anthropological Footnote.” *Philosophy of Science* 14 (4): 289–303. <http://www.jstor.org/stable/184988>.
- White, R. 1990. “Scrap or Substitute: Roman Material in Anglo-Saxon Graves.” In *Anglo-Saxon Cemeteries: A Reappraisal*, edited by E. Southworth, 125–152. Stroud, Gloucestershire: Sutton.
- Whittle, A. 2003. *The Archaeology of People: Dimensions of Neolithic Life*. London: Routledge.
- Whorf, B.L. 1956. “The Relation of Habitual Thought and Behavior to Language?.” In *Language, Thought and Reality: Selected Writings of Benjamin Lee Whorf*, edited by John B. Carroll, 134–159. Cambridge, MA: MIT Press.
- Wickham, Hadley. 2009. “ggplot2: Elegant Graphics for Data Analysis.” New York: Springer. <http://had.co.nz/ggplot2/book>.
- Williams, Howard M. R. 1998. “Monuments and the Past in Early Anglo-Saxon England.” *World Archaeology* 30 (1): 90–108. doi:10.1080/00438243.1998.9980399.
- . 2004. “Death Warmed up: The Agency of Bodies and Bones in Early Anglo-Saxon Cremation Rites.” *Journal of Material Culture* 9 (3) (November 1): 263–291. doi:10.1177/1359183504046894. <http://mcu.sagepub.com/content/9/3/263>.
- Williams-Thorpe, O., P.C. Webb, and M.C. Jones. 2003. “Non-Destructive Geochemical and Magnetic Characterisation of Group XVIII Dolerite Stone Axes and Shaft-Hole Implements from England.” *Journal of Archaeological Science* 30 (10) (October): 1237–1267. doi:10.1016/S0305-4403(02)00274-1. <http://www.sciencedirect.com/science/article/pii/S0305440302002741>.
- Williams-Thorpe, Olwen, Philip J. Potts, and Peter C. Webb. 1999. “Field-Portable Non-Destructive Analysis of Lithic Archaeological Samples by X-Ray Fluorescence Instrumentation Using a Mercury Iodide Detector: Comparison with

- Wavelength-Dispersive XRF and a Case Study in British Stone Axe Provenancing.” *Journal of Archaeological Science* 26 (2) (February): 215–237. doi:10.1006/jasc.1998.0323. <http://dx.doi.org/10.1006/jasc.1998.0323>.
- Wilson, D. M., and J. G. Hurst. 1958. “Medieval Britain in 1957.” *Medieval Archaeology* 2: 183–213. doi:10.5284/1000320. http://archaeologydataservice.ac.uk/catalogue/adsdata/arch-769-1/dissemination/pdf/vol02/2_183_213_med_britain.pdf.
- Wilson, Paul, and Colin Cooper. 2008. “Finding the Magic Number.” *The Psychologist* 21 (10): 866–867.
- Wilthew, P. 1984. “Analysis of Pins and Other Middle Saxon Copper Alloy Objects from Southampton, Hampshire.” In *The Anglo-Saxon Cemetery at Finglesham, Kent*, edited by S.C Hawkes and G Grainger, 371–380. Oxford: Oxford University School of Archaeology.
- Wire. 2011. “Bad Worn Thing.” In *Red Barked Tree (Album)*. Pink Flag / Mutesong.
- Worthington, A.M. 1895. *The Splash of a Drop*. London: Society for Promoting Christian Knowledge.
- Wylie, Alison. 1989. “The Interpretive Dilemma.” In *Critical Traditions in Contemporary Archaeology*, edited by A Pinsky and Alison Wylie, 18–27. Cambridge: Cambridge University Press.
- . 1992. “The Interplay of Evidential Constraints and Political Interests: Recent Archaeological Research on Gender.” *American Antiquity* 57 (1): 15–35. <http://www.jstor.org/stable/2694833>.
- Yeomans, Keith A., and Paul A. Golder. 1982. “The Guttman-Kaiser Criterion as a Predictor of the Number of Common Factors.” *The Statistician* 31 (3) (September): 221–229. doi:10.2307/2987988. <http://www.jstor.org/stable/2987988>.
- Zhang, Chaosheng, Frank T. Manheim, John Hinde, and Jeffrey N. Grossman. 2005. “Statistical Characterization of a Large Geochemical Database and Effect of Sample Size.” *Applied Geochemistry* 20 (10) (October): 1857–1874. doi:10.1016/j.apgeochem.2005.06.006. <http://www.sciencedirect.com/science/article/pii/S0883292705001344>.
- Zimmermann, H.J. 2001. *Fuzzy Set Theory and Its Applications*. Dordrecht (Netherlands): Kluwer Academic Publishers.
- Zwick, William R., and Wayne F. Velicer. 1986. “Comparison of Five Rules for Determining the Number of Components to Retain.” *Psychological Bulletin* 99 (3): 432–442.
- Zwicky, Christoph N., and Peter Lienemann. 2004. “Quantitative or Semi-Quantitative?—laboratory-Based WD-XRF versus Portable ED-XRF Spectrometer: Results Obtained from Measurements on Nickel-Base Alloys.” *X-Ray Spectrometry* 33 (4) (July 7): 294–300. doi:10.1002/xrs.730. <http://doi.wiley.com/10.1002/xrs.730>.

DIGITAL APPENDECIES

All the appendices provided here can be downloaded from figshare. The file set DOI is:

<https://dx.doi.org/10.6084/m9.figshare.3179314>

All the original unprocessed spectra files (along with reference alloy analyses) are also provided on figshare as a digital only appendix. The file set DOI is:

<https://dx.doi.org/10.6084/m9.figshare.3179296>

Appendix I. MBH STANDARDS

The first (shaded) row for each alloy shows the value in weight percent (V), the second shows the uncertainty (U). Values in brackets are not certified and are presented for information only.

Name	Batch	Type	B	Mg	Al	Si	P	S	Cr	Mn	Fe	Co	Ni	Cu	Zn	As	Se	Ag	Cd	In	Sn	Sb	Au	Hg	Pb	Bi
32X SN6	A	Bronze (chill cast)	✓		.0313			.018	.0074	.0024	.099	.655	.203	86.39	1.17	.765		1.159	.0903		7.31	.323	.0073		1.559	.158
			U		.0013			.003	.0009	.0001	.004	.003	.002	.08	.02	.006		.012	.0012		.03	.004	.0005		.015	.002
32X LB10	E	Leaded bronze (chill cast)	✓		(.0005)			.0116		.0004	.013	.0456	.687	77.98	.566	(.001)		(.001)			8.16	.591	.042		11.74	.0608
			U				.0011		.0001	.001	.0014	.01	.1	.009							.09	.008	.002		.07	.001
31X B5	K	Major Elements in brass (chill cast)	✓	.0002	(.001)	(.001)			.0002	.0006	.056	.0062	.0085	76.22	23.6	.0054			.0005		0.045	.0057			.021	.0063
			U	.0001					.0001	.0001	.002	.0004	.0005	.08	.7	.0003			.00005		.002	.0006			.001	.004
33X GM29	A	Gun metal (continuous cast)	✓		(.0004)	.0027	.138	.0024	(.0004)	(.0005)	.0102		.0289	89.36	4.23	.0017		.0026			6.12	.0015			.05	.0019
			U			.0004	.003	.0004			.0007		.0014	.08	.03	.0002		.0004				.04	.0003			.002
32X PB10	N	Phosphoric bronze (chill cast)	✓		(<.001)	(.0036)	.003	.0162		.0005	.014		.054	87.85	.0494	.0138	.0058				11.87	.0201			.067	.0128
			U		.001		.001	.0016		.0001	.002		.002	.12	.0014	.0008	.0005				.08	.0011			.003	.0009
74X CA7	A	Tin-base lead-free solder (cast)	✓				.003				.0047		.0007	.333		.0095		4.21	.0045	.0026		.0103		.053	.0965	.0081
			U				.001				.0004		.0001	.008		.0005		.05	.0002	.0002		.0007		.005	.0016	.0003
91X S62AG2	A	Lead-tin-silver solder (cast)	✓		(.0011)						.0065		(.0016)	.069	.0011	.022		2.03	.0016		61.68	.347	.002			.168
			U								.0005			.003	.0002	.0002		.04	.0002		.1	.005	.0002			.003

Appendix II. SILVER ALLOY CLUSTERS

Table showing the two sets of clusters identified using both hierarchical clustering on Euclidean data and on CLR transformed data. The cluster numbers correspond to the cluster identifiers in the respective diagrams (Figure 4-15, page 216 and Figure 4-16, page 217).

<i>Site</i>	SF No.	SF Sub Division	Analysis Area	Grave No.	Cat.	Class	Sub Class	Assigned Gender	Grave Phase	Euclidean Clusters	clr Clusters
ERL 046	1086		A	G042	Dress Accessories	Necklace	Pendant	F	A(1)	3	1
ERL 046	1087		A	G042	Dress Accessories	Necklace	Pendant	F	A(1)	3	1
ERL 046	1143		A	G042	Dress Accessories	Ring	Finger ring	F	A(1)	3	1
ERL 114	1182		A	G450	Dress Accessories	Bead	Undefined Bead	F	A(2)	2	2
ERL 114	1183		A	G450	Dress Accessories	Bead	Undefined Bead	F	A(2)	2	2
ERL 114	1188		A	G450	Dress Accessories	Bead	Undefined Bead	F	A(2)	3	2
ERL 114	1216		A	G450	Dress Accessories	Bead	Undefined Bead	F	A(2)	2	2
ERL 114	1299		A	G445	Dress Accessories	Ring	Finger ring	F	A(2)	2	2
ERL 114	1464		A	G417	Dress Accessories	Necklace	Pendant	F	A(2)	3	3
ERL 046	1487		A	G005	Dress Accessories	Necklace	Pendant	F	A(2)	3	4
ERL 046	1488		A	G005	Dress Accessories	Necklace	Pendant	F	A(2)	3	4
ERL 104	1548		A	G264	Dress Accessories	Wrist Clasp	Form A	F	A(1)	3	1
ERL 104	1579		A	G266	Dress Accessories	Bead	Undefined Bead	F	DE	3	4
ERL 104	1584		A	G266	Dress Accessories	Bead	Undefined Bead	F	DE	2	1
ERL 104	1778		A	G305	Dress Accessories	Wrist Clasp	Form A	F	A(1)	3	1
ERL 104	1780		A	G305	Dress Accessories	Wrist Clasp	Form A	F	A(1)	3	2
ERL 104	1781		A	G305	Dress Accessories	Wrist Clasp	Form A	F	A(1)	3	2
ERL 104	2055		A	G364	Dress Accessories	Wrist Clasp	Form A	F	A(2)	3	1
ERL 104	2055		B	G364	Dress Accessories	Wrist Clasp	Form A	F	A(2)	3	4

<i>Site</i>	SF No.	SF Sub Division	Analysis Area	Grave No.	Cat.	Class	Sub Class	Assigned Gender	Grave Phase	Euclidean Clusters	clr Clusters
ERL 104	2128		A	G364	Dress Accessories	Wrist Clasp	Form A	F	A(2)	2	1
ERL 104	2128		B	G364	Dress Accessories	Wrist Clasp	Form A	F	A(2)	2	1
ERL 104	2309		A	G315	Dress Accessories	Ring	Finger ring	F	A(2)	3	1
ERL 104	2311		A	G315	Dress Accessories	Necklace	Pendant	F	A(2)	3	2
ERL 104	2317		E	G315	Dress Accessories	Ring	Ear Ring	F	A(2)	1	4
ERL 104	2317		H	G315	Dress Accessories	Ring	Ear Ring	F	A(2)	3	4
ERL 104	2466		A	G213	Dress Accessories	Ring	Finger ring	F	A	2	1
ERL 104	3330	B	A	G273	Dress Accessories	Bead	Undefined Bead	F	BC	2	1
ERL 104	3483		A	G116	Dress Accessories	Bead	Undefined Bead	F	DE	2	2
ERL 104	3578		A	G116	Dress Accessories	Necklace	Pendant	F	DE	2	4
ERL 104	1176		D	G245	Military and weaponry	Shield	Shield Mount	M	B(C)	3	1
ERL 104	1191		D	G245	Military and weaponry	Shield	Shield Mount	M	B(C)	2	1
ERL 046	1708		A	G002	Dress Accessories	Ring	Finger ring	M	B	2	1
ERL 046	1714		A	G002	Dress Accessories	Ring	Finger ring	M	B	2	1
ERL 104	2623		B	G323	Equestrian objects	Tack	Bridle mount	M	A(B)	1	4
ERL 104	2624		B	G323	Equestrian objects	Tack	Box Fitting	M	A(B)	3	4
ERL 104	3674	2	A	G168	Military and weaponry	Shield	Shield Mount	M	A(B)	2	4
ERL 104	3674	3	A	G168	Military and weaponry	Shield	Shield Mount	M	A(B)	2	4
ERL 104	BM1		B	G323	Equestrian objects	Tack	Bridle Fitting	M	A(B)	3	3
ERL 104	BM1		D	G323	Equestrian objects	Tack	Bridle Fitting	M	A(B)	3	4
ERL 104	BM1		E	G323	Equestrian objects	Tack	Bridle Fitting	M	A(B)	1	3
ERL 104	BM12		C	G323	Equestrian objects	Tack	Bridle Fitting	M	A(B)	3	3
ERL 104	BM12		D	G323	Equestrian objects	Tack	Bridle Fitting	M	A(B)	3	3
ERL 104	BM19		C	G323	Equestrian objects	Tack	Bridle Fitting	M	A(B)	3	3

<i>Site</i>	SF No.	SF Sub Division	Analysis Area	Grave No.	Cat.	Class	Sub Class	Assigned Gender	Grave Phase	Euclidean Clusters	clr Clusters
ERL 104	BM3		B	G323	Equestrian objects	Tack	Bridle Fitting	M	A(B)	3	3
ERL 104	BM5		B	G323	Equestrian objects	Tack	Bridle Fitting	M	A(B)	3	4
ERL 104	BM5		C	G323	Equestrian objects	Tack	Bridle Fitting	M	A(B)	3	4
ERL 104	BM5		D	G323	Equestrian objects	Tack	Bridle Fitting	M	A(B)	3	4
ERL 104	BM5		E	G323	Equestrian objects	Tack	Bridle Fitting	M	A(B)	3	2
ERL 104	BM6	7A	A	G323	Equestrian objects	Tack	Bridle Fitting	M	A(B)	3	3
ERL 104	BM6	7A	E	G323	Equestrian objects	Tack	Bridle Fitting	M	A(B)	3	3
ERL 104	1007		A		Unknown	Unknown	Unknown	N/A	N/A	2	2
ERL 104	1061		C		Dress Accessories	Belt Fitting	Strap-end	N/A	N/A	2	1
ERL 104	1465		A	G339	Military and weaponry	Shield	Shield Mount	N/A	N/A	3	2
ERL 104	1669		A		Unknown	Unknown	Unknown	N/A	N/A	2	2
ERL 104	2498		A		Unknown	Unknown	Unknown	N/A	N/A	2	1
ERL 104	2950		A	G357	Miscellaneous Fittings	Nails and Bolts	Stud	N/A	N/A	1	4
ERL 104	3232		A	G139	Dress Accessories	Buckle	Undefined Buckle	N/A	N/A	2	1
ERL 104	3375		A		Unknown	Unknown	Unknown	N/A	N/A	2	1
ERL 104	3618		E		Unknown	Unknown	Unknown	N/A	N/A	2	2

Appendix III. SILVER ALLOY CATEGORICAL VARIABLES

Site	SF No.	SF Sub Div.	Analysis Area	XRF Location	Grave No.	Ctx	Category	Class	Sub Class	Grave Bio. Sex	Grave Assigned Gender	Grave Phase
046	1086		A	Main body	042	146	Dress Accessories	Necklace	Pendant	N/A	F	A(1)
046	1087		A	Main body	042	146	Dress Accessories	Necklace	Pendant	N/A	F	A(1)
046	1143		A	Main body	042	146	Dress Accessories	Ring	Finger ring	N/A	F	A(1)
046	1144		A	Main body	042	146	Dress Accessories	Ring	Finger ring	N/A	F	A(1)
046	1487		A	Front	005	178	Dress Accessories	Necklace	Pendant	N/A	F	A(2)
046	1487		B	Reverse	005	178	Dress Accessories	Necklace	Pendant	N/A	F	A(2)
046	1488		A	Front	005	178	Dress Accessories	Necklace	Pendant	N/A	F	A(2)
046	1488		B	Reverse	005	178	Dress Accessories	Necklace	Pendant	N/A	F	A(2)
046	1708		A	Main body	002	178	Dress Accessories	Ring	Finger ring	N/A	M	B
046	1714		A	Main body	002	178	Dress Accessories	Ring	Finger ring	N/A	M	B
104	1007		A	Main body		1	Unknown	Unknown	Unknown	N/A	N/A	N/A
104	1061		C	Small disc		1	Dress Accessories	Belt Fitting	Strap-end	N/A	N/A	N/A
104	1061		D	Small disc		1	Dress Accessories	Belt Fitting	Strap-end	N/A	N/A	N/A
104	1176		D	Loose sheet	245	232	Military and weaponry	Shield	Shield Mount	M	M	B(C)
104	1176		E	Loose sheet	245	232	Military and weaponry	Shield	Shield Mount	M	M	B(C)
104	1191		D	Loose sheet	245	232	Military and weaponry	Shield	Shield Mount	M	M	B(C)
104	1191		E	Loose sheet	245	232	Military and weaponry	Shield	Shield Mount	M	M	B(C)
104	1336		A	Outer	266	412	Dress Accessories	Bead	Undefined Bead	F	F	DE
104	1465		A	Main body	339	377	Military and weaponry	Shield	Shield Mount	N/A	N/A	N/A
104	1548		A	Main body	264	564	Dress Accessories	Wrist Clasp	Form A	N/A	F	A(1)
104	1579		A	Main body	266	412	Dress Accessories	Bead	Undefined Bead	F	F	DE
104	1583		A	Outside edge	266	412	Dress Accessories	Bead	Undefined Bead	F	F	DE

Site	SF No.	SF Sub Div.	Analysis Area	XRF Location	Grave No.	Ctx	Category	Class	Sub Class	Grave Bio. Sex	Grave Assigned Gender	Grave Phase
104	1584		A	Outside edge	266	412	Dress Accessories	Bead	Undefined Bead	F	F	DE
104	1669		A	Main body		1	Unknown	Unknown	Unknown	N/A	N/A	N/A
104	1778		A	Hook piece	305	725	Dress Accessories	Wrist Clasp	Form A	F	F	A(1)
104	1779		A	Hook piece	305	725	Dress Accessories	Wrist Clasp	Form A	F	F	A(1)
104	1780		A	Eye piece	305	725	Dress Accessories	Wrist Clasp	Form A	F	F	A(1)
104	1781		A	Hook piece	305	725	Dress Accessories	Wrist Clasp	Form A	F	F	A(1)
104	2055		A	Eye piece	364	777	Dress Accessories	Wrist Clasp	Form A	N/A	F	A(2)
104	2055		B	Hook piece	364	777	Dress Accessories	Wrist Clasp	Form A	N/A	F	A(2)
104	2128		A	Eyepiece (front)	364	777	Dress Accessories	Wrist Clasp	Form A	N/A	F	A(2)
104	2128		B	Hookpiece (front)	364	777	Dress Accessories	Wrist Clasp	Form A	N/A	F	A(2)
104	2309		A	Main body	315	988	Dress Accessories	Ring	Finger ring	N/A	F	A(2)
104	2311		A	Silver sheet	315	988	Dress Accessories	Necklace	Pendant	N/A	F	A(2)
104	2317		D	Silver sheet	315	988	Dress Accessories	Ring	Ear Ring	N/A	F	A(2)
104	2317		E	Silver sheet	315	988	Dress Accessories	Ring	Ear Ring	N/A	F	A(2)
104	2317		H	Silver sheet	315	988	Dress Accessories	Ring	Ear Ring	N/A	F	A(2)
104	2317		I	Silver sheet	315	988	Dress Accessories	Ring	Ear Ring	N/A	F	A(2)
104	2466		A	Main body	213	4037	Dress Accessories	Ring	Finger ring	N/A	F	A
104	2498		A	Main body		4033	Unknown	Unknown	Unknown	N/A	N/A	N/A
104	2623		B	Silver plate	323	4116	Equestrian objects	Tack	Bridle mount	N/A	M	A(B)
104	2624		B	Front (applique)	323	4116	Equestrian objects	Tack	Box Fitting	N/A	M	A(B)
104	2950		A	Front of stud	357	4200	Miscellaneous Fittings	Nails and Bolts	Stud	N/A	N/A	N/A
104	3232		A	Sheet metal	139	4519	Dress Accessories	Buckle	Undefined Buckle	N/A	N/A	N/A
104	3330	B	A	Main body	273	4542	Dress Accessories	Bead	Undefined Bead	N/A	F	BC
104	3375		A	Wriste lasp fragment	001	N/A	Unknown	Unknown	N/A	N/A	N/A	
104	3483		A	Main body	116	96	Dress Accessories	Bead	Undefined Bead	N/A	F	DE

Site	SF No.	SF Sub Div.	Analysis Area	XRF Location	Grave No.	Ctx	Category	Class	Sub Class	Grave Bio. Sex	Grave Assigned Gender	Grave Phase
104	3578		A	Main body	116	96	Dress Accessories	Necklace	Pendant	N/A	F	DE
104	3618		B	Drop B		1	Unknown	Unknown	Unknown	N/A	N/A	N/A
104	3618		E	Drop E		1	Unknown	Unknown	Unknown	N/A	N/A	N/A
104	3674	2	A	Thin plate on front of stud	168	4741	Military and weaponry	Shield	Shield Mount	N/A	M	A(B)
104	3674	3	A	Front	168	4741	Military and weaponry	Shield	Shield Mount	N/A	M	A(B)
104	3675	2	A	Thin plate on front of stud	168	4741	Military and weaponry	Shield	Shield Mount	N/A	M	A(B)
104	3675	3	A	Thin plate on front.	168	4741	Military and weaponry	Shield	Shield Mount	N/A	M	A(B)
104	BM1		B	Silver plate	323	4116	Equestrian objects	Tack	Bridle Fitting	N/A	M	A(B)
104	BM1		C	Silver plate	323	4116	Equestrian objects	Tack	Bridle Fitting	N/A	M	A(B)
104	BM1		D	Silver plate	323	4116	Equestrian objects	Tack	Bridle Fitting	N/A	M	A(B)
104	BM1		E	Silver plate	323	4116	Equestrian objects	Tack	Bridle Fitting	N/A	M	A(B)
104	BM1 2		C	Silver plate (foot)	323	4116	Equestrian objects	Tack	Bridle Fitting	N/A	M	A(B)
104	BM12		D	Silver plate (head)	323	4116	Equestrian objects	Tack	Bridle Fitting	N/A	M	A(B)
104	BM1 8		B	Silver plate	323	4116	Equestrian objects	Tack	Bridle Fitting	N/A	M	A(B)
104	BM19		C	Silver sheet	323	4116	Equestrian objects	Tack	Bridle Fitting	N/A	M	A(B)
104	BM3		B	Silver sheet	323	4116	Equestrian objects	Tack	Bridle Fitting	N/A	M	A(B)
104	BM5		B	Silver plate	323	4116	Equestrian objects	Tack	Bridle Fitting	N/A	M	A(B)
104	BM5		C	Silver plate	323	4116	Equestrian objects	Tack	Bridle Fitting	N/A	M	A(B)
104	BM5		D	Silver plate	323	4116	Equestrian objects	Tack	Bridle Fitting	N/A	M	A(B)
104	BM5		E	Silver plate	323	4116	Equestrian objects	Tack	Bridle Fitting	N/A	M	A(B)
104	BM6	7A	A	Silver plate	323	4116	Equestrian objects	Tack	Bridle Fitting	N/A	M	A(B)
104	BM6	7A	E	Silver plate	323	4116	Equestrian objects	Tack	Bridle Fitting	N/A	M	A(B)
114	1182		A	Main body	450	344	Dress Accessories	Bead	Undefined Bead	F	F	A(2)
114	1183		A	Main body	450	344	Dress Accessories	Bead	Undefined Bead	F	F	A(2)
114	1188		A	Main body	450	344	Dress Accessories	Bead	Undefined Bead	F	F	A(2)

Site	SF No.	SF Sub Div.	Analysis Area	XRF Location	Grave No.	Ctx	Category	Class	Sub Class	Grave Bio. Sex	Grave Assigned Gender	Grave Phase
114	1216		A	Main body	450	344	Dress Accessories	Bead	Undefined Bead	F	F	A(2)
114	1299		A	Main body	445	467	Dress Accessories	Ring	Finger ring	N/A	F	A(2)
114	1464		A	Front	417	848	Dress Accessories	Necklace	Pendant	F	F	A(2)

Appendix IV. SILVER ALLOY NPA DATA

Full HHPXRF analytical data from Eriswell silver objects (sorted by small find number). The shaded row shows the net peak areas (mean if more than one analysis taken) for each element, the second (shaded) row shows the coefficient of variation. The final column shows the number of analyses.

<i>Site</i>	SF No.	SF Sub Div.	Analysis Area	Ca	Cu	Fe	Pb	Sn	Ag	As	Ti	Mn	Ni	Sb	Au	Bi	Zn	Hg	Zr	No. of analyses
<i>046</i>	1086		A		111134	6685	15968		1743259						30588		3107			4
					<i>0.07</i>	<i>0.63</i>	<i>0.23</i>		<i>0.02</i>						<i>0.34</i>		<i>0.36</i>			
<i>046</i>	1087		A		118790	7033	18195		1749257						25390		4082			2
					<i>0.01</i>	<i>0.63</i>	<i>0.1</i>		<i>0.14</i>						<i>0.22</i>		<i>0.21</i>			
<i>046</i>	1143		A		137522	4419	17995		1578443						31423	3236	5101			4
					<i>0.26</i>	<i>0.06</i>	<i>0.04</i>		<i>0.03</i>						<i>0.16</i>	<i>0.12</i>	<i>0.21</i>			
<i>046</i>	1144		A		986615	7849	11269		966551						13068		23990			4
					<i>0.39</i>	<i>0.45</i>	<i>0.13</i>		<i>0.13</i>						<i>0.45</i>		<i>0.16</i>			
<i>046</i>	1487		A		85228	10113	101195	766	2009713						48886		2780			2
					<i>0.04</i>	<i>0.02</i>	<i>0.37</i>	<i>1.41</i>	<i>0.02</i>						<i>0.12</i>		<i>0.24</i>			
<i>046</i>	1487		B		108987	10992	406340		1780585						30611		9679			2
					<i>0.55</i>	<i>0.5</i>	<i>0.32</i>		<i>0.14</i>						<i>0.46</i>		<i>0.72</i>			
<i>046</i>	1488		A		89680	9819	30901	780	1864716						47996		1678			2
					<i>0.09</i>	<i>0.05</i>	<i>0.03</i>	<i>1.41</i>	<i>0.04</i>						<i>0.12</i>		<i>0.01</i>			
<i>046</i>	1488		B		108165	15103	500751	90436	1532594						21997		13235			2
					<i>0.1</i>	<i>0.12</i>	<i>0.07</i>	<i>0.68</i>	<i>0.17</i>						<i>0.2</i>		<i>0.02</i>			
<i>046</i>	1708		A		25825	4105	13574		1212425						21111		933			3
					<i>0.03</i>	<i>0.05</i>	<i>0.05</i>		<i>0.1</i>						<i>0.13</i>		<i>0.31</i>			

<i>Site</i>	SF No.	SF Sub Div.	Analysis Area	Ca	Cu	Fe	Pb	Sn	Ag	As	Ti	Mn	Ni	Sb	Au	Bi	Zn	Hg	Zr	No. of analyses
046	1714		A	19348	48148	52692	13239		1302685						17814		821			4
				<i>0.23</i>	<i>0.42</i>	<i>1.56</i>	<i>0.21</i>		<i>0.11</i>						<i>0.37</i>		<i>0.13</i>			
104	BM1		B	481	191967	1912	110649	19161	1666053		454						7390			1
104	BM1		C	399	1157560	4820	36814	54235	1046820		379						13717			1
104	BM1		D	2175	272453	3931	25254	38107	1550942						14144		7691			1
104	BM1		E	849	346109	5834	137450	52303	1275694		477						36057			1
104	BM3		B	536	157393	1924	29615	26775	1580775		363						9731			2
				<i>0.42</i>	<i>0.02</i>	<i>0.14</i>	<i>0.01</i>	<i>0.02</i>	<i>0.17</i>		<i>0.21</i>						<i>0.05</i>			
104	BM5		B		159842	1419	19950	43061	1671145		294				25576	1317	2591			1
104	BM5		C	2349	330718	3304	49734	62691	1049445						66391		26757			1
104	BM5		D		210277	27285	30941	52601	1586259		400				89601		2124			1
104	BM5		E		161074	3079	19168	19258	1495836		1272				84851					1
104	BM6	7A	A	303	143666	10794	34323	14164	1170007		379						10679			2
				<i>0.03</i>	<i>0.21</i>	<i>1.03</i>	<i>0.18</i>	<i>0.26</i>	<i>0.16</i>		<i>0.13</i>						<i>0.18</i>			
104	BM6	7A	E	426	131077	5178	21558	4393	1192193		404						8548			2
				<i>0.4</i>	<i>0.02</i>	<i>0.02</i>	<i>0.09</i>	<i>0.12</i>	<i>0.01</i>		<i>0.02</i>						<i>0</i>			
104	BM12		C	148	124122	1115	13667	16171	1287751		402						13363			1

<i>Site</i>	SF No.	SF Sub Div.	Analysis Area	Ca	Cu	Fe	Pb	Sn	Ag	As	Ti	Mn	Ni	Sb	Au	Bi	Zn	Hg	Zr	No. of analyses
<i>104</i>	BM12		D	4	155549	1625	24399	20388	1559527		272						19411			1
<i>104</i>	BM18		B	5172	699096	12745	130113	148379	775388		361						58588			1
<i>104</i>	BM19		C	212	133428	1814	19565	6214	1602101		481						7606			2
				<i>0.42</i>	<i>0.13</i>	<i>0.12</i>	<i>0.11</i>	<i>0.31</i>	<i>0.01</i>		<i>0.04</i>						<i>0.23</i>			
<i>104</i>	1007		A	535	22510	6901	5638	588	1002421		987				12930				1231	2
				<i>0.03</i>	<i>0.18</i>	<i>0.1</i>	<i>0.86</i>	<i>0.5</i>	<i>0.07</i>		<i>0.05</i>				<i>0.06</i>				<i>0.44</i>	
<i>104</i>	1061		C		109141	4189	16764		812357		871				24333		6986			1
<i>104</i>	1061		D		239000	5305	308136	80184	467537	1	834				3343		4856			1
<i>104</i>	1176		D		92704	4586	15883		1792072		322				39047		4003			3
					<i>0.02</i>	<i>0.1</i>	<i>0.02</i>		<i>0.04</i>		<i>0.29</i>				<i>0.03</i>		<i>0.28</i>			
<i>104</i>	1176		E		214683	3737	274921	267399	998273				790	133	7286		224550		1181	1
<i>104</i>	1191		D	1195	40039	2342	10430		1191949		218				16506		1040			3
				<i>1.39</i>	<i>0.87</i>	<i>0.89</i>	<i>0.87</i>		<i>0.87</i>		<i>0.87</i>				<i>0.87</i>		<i>0.87</i>			
<i>104</i>	1191		E		140139	1998	277202	141148	1574192						9389		12491		492	1
<i>104</i>	1336		A	497	1302209	11793	25287	7354	1385292	5956	495				43491		34532			3
				<i>1.73</i>	<i>0.28</i>	<i>0.14</i>	<i>0.17</i>	<i>0.13</i>	<i>0.12</i>	<i>0.13</i>	<i>0.35</i>				<i>0.21</i>		<i>0.09</i>			
<i>104</i>	1465		A		71204	5141	14582		1466303		968				21128				347	4
					<i>0.05</i>	<i>0.09</i>	<i>0.04</i>		<i>0.08</i>		<i>0.06</i>				<i>0.05</i>				<i>0.26</i>	

<i>Site</i>	SF No.	SF Sub Div.	Analysis Area	Ca	Cu	Fe	Pb	Sn	Ag	As	Ti	Mn	Ni	Sb	Au	Bi	Zn	Hg	Zr	No. of analyses
104	1548		A		157232	7622	12605		1475717		705				33054		3691			4
					<i>0.36</i>	<i>0.66</i>	<i>0.75</i>		<i>0.21</i>		<i>0.59</i>				<i>0.31</i>		<i>0.53</i>			
104	1579		A		163602	4060	55282	26984	1474606						93407	1263	33641			6
					<i>0.46</i>	<i>0.17</i>	<i>0.23</i>	<i>1.31</i>	<i>0.16</i>						<i>0.34</i>	<i>0.36</i>	<i>0.39</i>			
104	1583		A	11974	834726	9071	38660	6803	1449061		437				38270	263	22195			3
				<i>1.2</i>	<i>0.44</i>	<i>0.19</i>	<i>0.11</i>	<i>0.08</i>	<i>0.05</i>		<i>0.28</i>				<i>0.23</i>	<i>1.73</i>	<i>0.16</i>			
104	1584		A		58053	1311	6485		577688		97				12998		1838			3
					<i>1.73</i>	<i>1.73</i>	<i>1.73</i>		<i>1.73</i>		<i>1.73</i>				<i>1.73</i>		<i>1.73</i>			
104	1669		A		46557	6877	5501		773444		965				14720				332	2
					<i>0</i>	<i>0.01</i>	<i>0.05</i>		<i>0.02</i>		<i>0.01</i>				<i>0</i>					
104	1778		A		264686	7013	12594		1409841		398				28778		2902			4
					<i>0.47</i>	<i>0.1</i>	<i>0.04</i>		<i>0.07</i>		<i>0.19</i>				<i>0.13</i>		<i>0.26</i>			
104	1779		A	3273	1149000	23856	2655		1111796	9731	766				13591		1084		3278	4
				<i>0.45</i>	<i>0.34</i>	<i>0.43</i>	<i>2</i>		<i>0.08</i>	<i>0.68</i>	<i>0.23</i>				<i>0.36</i>		<i>2</i>		<i>0.7</i>	
104	1780		A		15276	3932	8507		1658019		357				20375				432	4
					<i>0.38</i>	<i>0.33</i>	<i>0.3</i>		<i>0.1</i>		<i>0.14</i>				<i>0.49</i>				<i>0.43</i>	
104	1781		A		38879	3711	8812		1627471		424				21485				382	4
					<i>0.5</i>	<i>0.13</i>	<i>0.36</i>		<i>0.07</i>		<i>0.12</i>				<i>0.25</i>				<i>0.51</i>	
104	2055		A		94127	5412	13346		1574156		398				23114		3254			4
					<i>0.04</i>	<i>0.35</i>	<i>0.04</i>		<i>0.08</i>		<i>0.08</i>				<i>0.07</i>		<i>0.02</i>			
104	2055		B		87850	21726	13111	158	1549537		398	147			19719		3221			4
					<i>0.23</i>	<i>1.06</i>	<i>0.21</i>	<i>2</i>	<i>0.13</i>		<i>0.69</i>	<i>2</i>			<i>0.3</i>		<i>0.18</i>			
104	2128		A		72057	4237	10405		988106		958				13876		2754			4
					<i>0.17</i>	<i>0.2</i>	<i>0.18</i>		<i>0.21</i>		<i>0.09</i>				<i>0.17</i>		<i>0.15</i>			
104	2128		B		86135	3907	12168		1203525		979				17789		3200			4

<i>Site</i>	SF No.	SF Sub Div.	Analysis Area	Ca	Cu	Fe	Pb	Sn	Ag	As	Ti	Mn	Ni	Sb	Au	Bi	Zn	Hg	Zr	No. of analyses
					0.05	0.03	0.06		0.06		0.09				0.08		0.03			
104	2309		A		84038	3995	14042		1901876		303				28124		1966			4
					0.13	0.08	0.09		0.03		0.2				0.08		0.13			
104	2311		A		185209	3583	13509		1926810		288				60352				696	1
104	2317		D		580630	5405	146103	66831	1099188	1	235				18851		22817			1
104	2317		E		933867	30282	41057	3304	1357728	5495	322				28324		44982			1
104	2317		H	1714	202513	2539	25530	5071	1471889		260				66449		9959		611	1
104	2317		I		439094	2468	185326	108124	1242587	1	313				27016		9757			1
104	2466		A	319	65506	6678	11959		1171029		993				15492	148	224		437	4
				2	0.23	0.25	0.22		0.24		0.05				0.29	2	2		0.68	
104	2498		A		34807	4699	6924		789979		482	80			12197		397		277	2
					0.15	0.19	0.14		0.06		1.41	1.41			0.17		1.41		1.41	
104	2623		B	1925	394597	270131	88998	124413	973285						23018		23363		528	1
104	2624		B		162319	1405	19464	4642	1653956		394				19782		15967			1
104	2950		A		210387	13830	126038	80499	1050415	1	1083				14033		7531			2
					0.21	0.03	0.16	0.11	0.07		0.08				0.13		0.37			
104	3232		A	1119	73822	129314	14076		1294475		929				2171		1800			1

<i>Site</i>	SF No.	SF Sub Div.	Analysis Area	Ca	Cu	Fe	Pb	Sn	Ag	As	Ti	Mn	Ni	Sb	Au	Bi	Zn	Hg	Zr	No. of analyses
104	3330	B	A	552	44781	4635	3503		446149		1048				12142		846			2
				<i>0.13</i>	<i>0.01</i>	<i>0.01</i>	<i>0.05</i>		<i>0.01</i>		<i>0.12</i>				<i>0.08</i>		<i>0.06</i>			
104	3375		A		21168	9353	7008		1023443		355	228			20508		381		222	3
					<i>0.08</i>	<i>0.18</i>	<i>0.05</i>		<i>0.05</i>		<i>1.73</i>	<i>0.88</i>			<i>0.05</i>		<i>0.87</i>		<i>1.73</i>	
104	3483		A	774	68820	14264	13721	1415	950735		1074				17416				1530	2
				<i>0.69</i>	<i>0.21</i>	<i>0.43</i>	<i>0.04</i>	<i>0.3</i>	<i>0.06</i>		<i>0.19</i>				<i>0.1</i>				<i>1.24</i>	
104	3578		A		20835	1415	6603	1044	617904	6375	115				27349		3150			3
					<i>1.73</i>	<i>1.73</i>	<i>1.73</i>	<i>1.73</i>	<i>1.73</i>	<i>1.73</i>	<i>1.73</i>				<i>1.73</i>		<i>1.73</i>			
104	3618		B	727	59161	14915	14455		1286548		1292				32684					2
				<i>0.11</i>	<i>0.05</i>	<i>0.04</i>	<i>0.09</i>		<i>0.03</i>		<i>0.01</i>				<i>0.11</i>					
104	3618		E	717	46210	8516	5785		784182		904				12518					2
				<i>0.08</i>	<i>0.08</i>	<i>0.19</i>	<i>0.29</i>		<i>0.11</i>		<i>0.05</i>				<i>0.13</i>					
104	3674	2	A		41952	453151	45830	879	941298			978			9116		1008			3
					<i>0.4</i>	<i>0.92</i>	<i>0.75</i>	<i>1.73</i>	<i>0.25</i>			<i>0.85</i>			<i>0.45</i>		<i>0.04</i>			
104	3674	3	A		61104	162873	33824	8281	1151623			520			15276		1370			1
104	3675	2	A		301979	5198	126198	739	1678788			296			6109	1330	8114	75		3
					<i>0.55</i>	<i>0.38</i>	<i>0.84</i>	<i>1.01</i>	<i>0.06</i>			<i>0.15</i>			<i>0.19</i>	<i>1.73</i>	<i>0.77</i>	<i>1.61</i>		
104	3675	3	A		594249	8262	40846	30024	1001812			83			4680		64624			2
					<i>0.78</i>	<i>0.39</i>	<i>0.58</i>	<i>1.01</i>	<i>0.03</i>			<i>1.41</i>			<i>0.36</i>		<i>0.27</i>			
114	1182		A	500	109458	2702	8995	2143	528160		282				24989					2
				<i>0.07</i>	<i>0.13</i>	<i>0.17</i>	<i>0.1</i>	<i>0.21</i>	<i>0.08</i>		<i>0.17</i>				<i>0.2</i>					
114	1183		A	409	46656	2636	9536	2311	624022		314				27383					2
				<i>0.01</i>	<i>0.1</i>	<i>0.17</i>	<i>0.09</i>	<i>0.12</i>	<i>0.08</i>		<i>0.04</i>				<i>0.05</i>					
114	1188		A	642	220211	3343	18297	3989	1031508		395				50403					2

<i>Site</i>	SF No.	SF Sub Div.	Analysis Area	Ca	Cu	Fe	Pb	Sn	Ag	As	Ti	Mn	Ni	Sb	Au	Bi	Zn	Hg	Zr	No. of analyses
				0.52	0.62	0.38	0.03	0.06	0.06		0.08				0.05					
114	1216		A	374	52168	2188	11583	2502	754121		369				29456					2
				0.03	0	0.05	0.04	0.08	0.02		0.11				0.05					
114	1299		A	586	49564	5827	10026	441	1161945		402				19931					4
				0.31	0.3	0.19	0.27	0.11	0.13		0.05				0.21					
114	1464		A		139338	2271	77032	31481	1411435								16773			2
					0.45	0.09	0.15	0.11	0.04								0.04			

APPENDIX VI: GILT XRD PEAK LIST

Peak list for XRD on gilding on wrist clasp 046 - 1811

Pos.[°2Th.]	Height[cts]	FWHM[°2Th.]	d-spacing[Å]	Rel.Int.[%]	Tipwidth[°2Th.]	Matched by
29.6387	47.99	0.4015	3.01416	1.42	0.4818	01-077-0199;00..
36.4895	443.79	0.4531	2.46041	13.13	0.5438	01-077-0199;00..
36.5834	221.89	0.4531	2.46041	6.56	0.5438	
37.9113	3380.79	0.4901	2.37135	100	0.5881	01-071-4614;00..
38.0021	3262.8	1.3807	2.36589	96.51	1.6568	01-071-4614;00..
38.0091	1690.39	0.4901	2.37135	50	0.5881	
38.1002	1631.4	1.3807	2.36589	48.26	1.6568	
40.3762	270.29	2.3296	2.23208	7.99	2.7955	00-039-0394;00..
40.4809	135.14	2.3296	2.23208	4	2.7955	
42.6557	977.24	1.1521	2.11793	28.91	1.3825	01-077-0199;00..
42.7669	488.62	1.1521	2.11793	14.45	1.3825	
44.0057	1043.47	1.1065	2.05603	30.86	1.3278	01-071-4614;00..
44.1208	521.74	1.1065	2.05603	15.43	1.3278	
49.649	320.03	0.6691	1.83474	9.47	0.8029	00-033-0470;00..
52.5478	59.16	0.1338	1.74015	1.75	0.1606	01-077-0199;00..
57.3592	8.68	0.2342	1.60509	0.26	0.281	00-033-0470
61.3928	151.35	0.1004	1.50894	4.48	0.1204	01-077-0199;00..
64.0054	664.96	0.736	1.45351	19.67	0.8832	01-071-4614;00..
66.097	78.29	0.2007	1.41249	2.32	0.2409	01-077-0199;00..
69.3583	50.57	0.8029	1.35382	1.5	0.9635	01-077-0199;00..
72.6022	196.98	0.268	1.30112	5.83	0.3216	00-041-1417;00..

Pos.[°2Th.]	Height[cts]	FWHM[°2Th.]	d-spacing[Å]	Rel.Int.[%]	Tipwidth[°2Th.]	Matched by
72.8115	98.49	0.268	1.30112	2.91	0.3216	
73.1927	264.52	2.2485	1.29207	7.82	2.6981	01-077-0199;00..
73.4043	132.26	2.2485	1.29207	3.91	2.6981	
76.8711	850.07	1.4468	1.23915	25.14	1.7362	01-071-4614;00..
77.0972	425.03	1.4468	1.23915	12.57	1.7362	
80.9076	334.88	1.4289	1.1872	9.91	1.7146	01-071-4614;00..
81.1506	167.44	1.4289	1.1872	4.95	1.7146	
88.2778	271.75	1.8408	1.10612	8.04	2.209	00-041-1417;00..
88.5544	135.87	1.8408	1.10612	4.02	2.209	
93.444	79.23	2.807	1.05805	2.34	3.3684	01-077-0199;00..
93.7468	39.62	2.807	1.05805	1.17	3.3684	
97.0958	108.4	0.6691	1.02774	3.21	0.8029	01-071-4614;01..
103.86	77.83	0.1224	0.97846	2.3	0.1469	01-077-0199;00..
109.723	330.11	2.11	0.94196	9.76	2.532	01-071-4614
110.128	165.05	2.11	0.94196	4.88	2.532	
113.844	353.23	2.195	0.91929	10.45	2.634	01-071-4614
114.283	176.61	2.195	0.91929	5.22	2.634	

Pattern list for XRD on wrist clasp 046 - 1811

Ref.Code	Score	Compound Name	Scale Fac.	Chem. Formula
01-071-4614	64	Gold	0.784	Au
00-004-0781	63	Eugenite, syn	0.465	Au ₅ Hg
01-077-0199	80	copper(I) oxide	0.217	Cu ₂ O
00-039-0394	63	Goldamalgam-ã (NR)	0.408	(Au , Ag) Hg
00-041-1417	55	Luanheite	0.07	Ag ₃ Hg
00-033-0470	50	ã-brass	0.138	Cu ₇ Hg ₆
00-004-0836	36	á-brass	0.123	Cu

APPENDIX VII: GILT OBJECT CATEGORICAL VARIABLES

Summary table of Eriswell gilded Eriswell objects and categorical variables.

Site	SF Number	SF Sub Division	Anal. Area	Grave No.	Ctx	Category	Class	Sub Class	Ost. Sex	Assigned Gender	Grave Phase
104	1000		B	0	36	Miscellaneous Fittings	Miscellaneous	Sheet			
104	1046		A	0	1	Dress Accessories	Belt Fitting	Strap-end			
104	1061		B	0	1	Dress Accessories	Belt Fitting	Strap-end			
104	1176		A	245	232	Military and weaponry	Shield	Shield Mount	M	M	C
104	1191		A	245	232	Military and weaponry	Shield	Shield Mount	M	M	C
104	1361		A	263	459	Dress Accessories	Brooch	Bird	F	F	A2
104	1704		E	322	644	Dress Accessories	Brooch	Great square-headed	F	F	A2
104	2027		A	364	777	Dress Accessories	Brooch	Applied saucer	F	F	A2
104	3453		A	166	4698	Dress Accessories	Brooch	Bar	F	F	A2
104	3532		B	206	322	Personal equipment	Purse	Purse Fitting			
104	2865		B	323	4116	Equestrian objects	Tack	Undefined Equestrian	M	M	AB
104	BM18		A	323	4116	Equestrian objects	Tack	Bridle Fitting	M	M	AB
104	2623		A	323	4116	Equestrian objects	Tack	Bridle mount	M	M	AB
104	BM19		A	323	4116	Equestrian objects	Tack	Bridle Fitting	M	M	AB
104	2624		C	323	4116	Equestrian objects	Tack	Bridle Fitting	M	M	AB
104	2636		B	323	4116	Equestrian objects	Tack	Bridle mount	M	M	AB
104	BM3		A	323	4116	Equestrian objects	Tack	Bridle Fitting	M	M	AB
104	BM3		C	323	4116	Equestrian objects	Tack	Bridle Fitting	M	M	AB
104	BM12		E	323	4116	Equestrian objects	Tack	Bridle Fitting	M	M	AB
104	BM13		B	323	4116	Equestrian objects	Tack	Bridle Fitting	M	M	AB
104	BM1		A	323	4116	Equestrian objects	Tack	Bridle Fitting	M	M	AB

Site	SF Number	SF Sub Division	Anal. Area	Grave No.	Ctx	Category	Class	Sub Class	Ost. Sex	Assigned Gender	Grave Phase
104	BM5		A	323	4116	Equestrian objects	Tack	Bridle Fitting	M	M	AB
104	BM33		A	323	4116	Equestrian objects	Tack	Bridle Fitting	M	M	AB
104	BM6	7A	D	323	4116	Equestrian objects	Tack	Bit	M	M	AB
114	1481		C	405	904	Dress Accessories	Wrist Clasp	Undefined Wrist Clasp	N/A	F	A2
114	1484		D	405	904	Dress Accessories	Wrist Clasp	Undefined Wrist Clasp	N/A	F	A2
114	1491		E	405	904	Dress Accessories	Wrist Clasp	Undefined Wrist Clasp	N/A	F	A2
46	1372		B	NG	242	Dress Accessories	Wrist Clasp	Form C 1			
46	1373		B	NG	242	Dress Accessories	Wrist Clasp	Form C 1			
46	1374		C	NG	242	Dress Accessories	Wrist Clasp	Form C 1			
46	1648		B	25	284	Dress Accessories	Brooch	Fish	C	F	A2
46	1727		B	0	294	Dress Accessories	Wrist Clasp	Form B 18			
46	1811		B	NG	415	Dress Accessories	Brooch	Great square-headed			

APPENDIX VIII: GILT OBJECT NPA DATA

HHpXRF NPA analytical data from Eriswell gilt objects (sorted by small find number). The shaded row shows the net peak areas (mean if more than one analysis taken) for each element, the second (shaded) row shows the coefficient of variation. The final column shows the number of analyses. It should be remembered that the purpose of analysing the gilt surfaces was to simply to check for the presence of gold and mercury. The figures should not be used for anything more than presence absence. The other elements (i.e. those that are not gold and mercury) are present because the gilding layers are thin enough that the alloy substrate is being analysed as well. Again, these figures should not be used to infer anything about the alloys. For the analytical detail on the alloy substrates please see copper alloy NPA data appendix.

<i>Site</i>	SF No.	SF Sub Div.	Anal. Area	Cu (K)	Pb (L)	Sn (K)	Ag (K)	As (K)	Sb (K)	Au (L)	Zn (K)	Hg (L)	No. of analyses
104	1000		B	569506	23521	56215	103326			978442		66763	2
				<i>0.67</i>	<i>1.06</i>	<i>0.87</i>	<i>0.33</i>			<i>0.33</i>		<i>0.57</i>	
104	1046		A	435207	37299	72190	54571		325	1225819		8467	2
				<i>0.24</i>	<i>0.10</i>	<i>0.15</i>	<i>0.50</i>		<i>1.41</i>	<i>0.05</i>		<i>1.41</i>	
104	1061		B	291165	18834	47757	38055			1212044		120391	2
				<i>0.66</i>	<i>0.44</i>	<i>0.19</i>	<i>0.11</i>			<i>0.12</i>		<i>0.08</i>	
104	1176		A	521053		21408	49907			1521425	99409	170523	2
				<i>0.01</i>		<i>0.01</i>	<i>0.00001</i>			<i>0.00</i>	<i>0.003</i>	<i>0.00</i>	
104	1191		A	376460	12225	11378	58321			1544021		208132	2
				<i>0.56</i>	<i>0.61</i>	<i>0.13</i>	<i>0.01</i>			<i>0.02</i>		<i>0.03</i>	

<i>Site</i>	SF No.	SF Sub Div.	Anal. Area	Cu (K)	Pb (L)	Sn (K)	Ag (K)	As (K)	Sb (K)	Au (L)	Zn (K)	Hg (L)	No. of analyses
<i>104</i>	1361		A	1504033	8997	1821	457625	1118	112	14445	18962	2499	3
				<i>0.17</i>	<i>0.29</i>	<i>1.05</i>	<i>0.29</i>	<i>1.73</i>	<i>1.73</i>	<i>0.90</i>	<i>0.09</i>	<i>0.87</i>	
<i>104</i>	1704		E	1785067	141919	165894	4889			200953	31385	32326	3
				<i>0.16</i>	<i>0.67</i>	<i>0.87</i>	<i>0.54</i>			<i>0.88</i>	<i>0.17</i>	<i>0.89</i>	
<i>104</i>	2027		A	1306809	52831	30407	3461		329	1363	8211	2028	5
				<i>0.20</i>	<i>0.68</i>	<i>1.50</i>	<i>0.35</i>		<i>2.24</i>	<i>1.18</i>	<i>1.82</i>	<i>0.50</i>	
<i>104</i>	3453		A	3392503	34080	76256	16855		484	14001		4007	1
<i>104</i>	3532		B	310581	8090	39196	141206			927465		280590	2
				<i>0.09</i>	<i>0.06</i>	<i>0.02</i>	<i>0.13</i>			<i>0.11</i>		<i>0.13</i>	
<i>104</i>	2865		B	532080	1328509		12199			2673		19801	1
<i>104</i>	BM18		A	1009111	53967	74482	39165			872546	84399	135924	1
<i>104</i>	2623		A	894499	50743	59513	39623			1015048	50069	131090	1
<i>104</i>	BM19		A	918783	54208	86650	21295			941211	99354	129571	2
				<i>0.80</i>	<i>0.76</i>	<i>0.51</i>	<i>0.07</i>			<i>0.33</i>	<i>0.93</i>	<i>0.32</i>	
<i>104</i>	2624		C	1147836	81428	102665	65949			868772	22877	135168	1
<i>104</i>	2636		B	338713	68155	81275	89874			1222794	38213	280333	1
<i>104</i>	BM3		A	418762	119968	74688	19815			954983	44075	128877	1

<i>Site</i>	SF No.	SF Sub Div.	Anal. Area	Cu (K)	Pb (L)	Sn (K)	Ag (K)	As (K)	Sb (K)	Au (L)	Zn (K)	Hg (L)	No. of analyses
104	BM3		C	1003282	249555	166623	22917			575294	176665	76009	1
104	BM12		E	642868	146151	68623	44203			779566	59608	154548	1
104	BM13		B	218452	25068	38270	97341			1479952		344589	1
104	BM1		A	1005069	137366	125224	28988			682008	121903	101217	1
104	BM5		A	689076	50322	78214	36972			873986	58158	117067	1
104	BM33		A	1177413	77194	79611	15826			605076	91301	86990	1
104	BM6	7A	D	12662	10021	7671	14829			322144		35700	1
114	1481		C	2012621	160333	63532	30264		578	292211	41060	33533	1
114	1484		D	1654630	204540	67722	42759		620	506630	51615	47005	2
				0.19	0.21	0.07	0.19		0.11	0.31	0.08	0.27	
114	1491		E	2137206	163374	103140	42078		887	261803	97446	49500	2
				0.06	0.34	0.10	0.08		0.33	0.05	0.18	0.04	
46	1372		B	2229148	83572	30526	362536		206	317518		35068	1
46	1373		B	2130263	31993	37044	38225		398	789599		49776	2
				0.12	0.19	0.12	0.11		0.04	0.15		0.17	

<i>Site</i>	SF No.	SF Sub Div.	Anal. Area	Cu (K)	Pb (L)	Sn (K)	Ag (K)	As (K)	Sb (K)	Au (L)	Zn (K)	Hg (L)	No. of analyses
46	1374		C	2212896	68851	45427	33210		483	673435		70595	2
				<i>0.03</i>	<i>0.12</i>	<i>0.05</i>	<i>0.09</i>		<i>0.28</i>	<i>0.08</i>		<i>0.08</i>	
46	1648		B	2305372	5555	131448	2893			448162	22984	64824	2
				<i>0.34</i>	<i>0.16</i>	<i>0.12</i>	<i>0.48</i>			<i>0.68</i>	<i>0.37</i>	<i>0.64</i>	
46	1727		B	1665923	37146	59628	47119			676276		123521	1
46	1811		B	1145480	118900	43487	11943		588	345714	78356	28216	2
				<i>0.85</i>	<i>0.16</i>	<i>0.38</i>	<i>0.04</i>		<i>0.28</i>	<i>0.24</i>	<i>1.41</i>	<i>0.21</i>	

APPENDIX IX: FILLER ALLOYS ON NON-FERROUS OBJECTS: CATEGORICAL VARIABLES

Site	SF No.	SF Sub Div.	Anal. Area	XRF Location	Alloy type filler material attached to.	Grave No.	Category	Class	Sub Class	Ost. Sex	Assigned Gender	Grave Phase	Burial Age
046	1183		B		Copper alloy	024	Dress Accessories	Belt Fitting	Strap-end	C/F	F	A(2)	10 to 14
046	1487		B	Reverse	Silver	005	Dress Accessories	Necklace	Pendant	F	F	A(2)	MA?
046	1488		B	Reverse	Silver	005	Dress Accessories	Necklace	Pendant	F	F	A(2)	MA?
046	1519		B		Copper alloy	005	Dress Accessories	Bead	Undefined Bead	F	F	A(2)	MA?
046	1520		B		Copper alloy	005	Dress Accessories	Bead	Undefined Bead	F	F	A(2)	MA?
046	1521		B		Copper alloy	005	Dress Accessories	Bead	Undefined Bead	F	F	A(2)	MA?
046	1523		B		Copper alloy	005	Dress Accessories	Bead	Undefined Bead	F	F	A(2)	MA?
046	1527		B		Copper alloy	005	Dress Accessories	Bead	Undefined Bead	F	F	A(2)	MA?
046	1528		B		Copper alloy	005	Dress Accessories	Bead	Undefined Bead	F	F	A(2)	MA?
046	1529		B		Copper alloy	005	Dress Accessories	Bead	Undefined Bead	F	F	A(2)	MA?
046	1531		B		Copper alloy	005	Dress Accessories	Bead	Undefined Bead	F	F	A(2)	MA?
046	1533		B		Copper alloy	005	Dress Accessories	Bead	Undefined Bead	F	F	A(2)	MA?
046	1537		B		Copper alloy	005	Dress	Bead	Undefined	F	F	A(2)	MA?

Site	SF No.	SF Sub Div.	Anal. Area	XRF Location	Alloy type filler material attached to.	Grave No.	Category	Class	Sub Class	Ost. Sex	Assigned Gender	Grave Phase	Burial Age
							Accessories		Bead				
046	1538		B		Copper alloy	005	Dress Accessories	Bead	Undefined Bead	F	F	A(2)	MA?
046	1539		B		Copper alloy	005	Dress Accessories	Bead	Undefined Bead	F	F	A(2)	MA?
046	1682		C	Disc	Copper alloy	025	Dress Accessories	Bead	Undefined Bead	C	F	A(2)	15-16
046	1824		B		Copper alloy	025	Dress Accessories	Bead	Undefined Bead	C	F	A(2)	15-16
104	1060		A		Copper alloy		Miscellaneous Fittings	Nails and Bolts	Stud				
104	1061		A		Copper alloy		Dress Accessories	Belt Fitting	Strap-end				
104	1362		A	Eye Piece (front)	Copper alloy	263	Dress Accessories	Wrist Clasp	Form B 13 c	F	F	A(2)	Young
104	1458		A	Face	Copper alloy	341	Dress Accessories	Brooch	Applied disc	F	F	A(2)	MA
104	1458		D	Bag of fragments	Copper alloy	341	Dress Accessories	Brooch	Applied disc	F	F	A(2)	MA
104	1691		B	Hook piece (front)	Copper alloy		Dress Accessories	Wrist Clasp	Form B 7				
104	1704		B	Foot near edge where solder is concentrated (reverse)	Copper alloy	322	Dress Accessories	Brooch	Great square-headed	F	F	A(2)	MA
104	1782		B	White conglomerate, prob. Solder	Copper alloy	305	Miscellaneous Fittings	Miscellaneous	Ring	F	F	A(1)	Y-MA
104	1948		B	Separate side knob (front). On plate used to attach it to main brooch	Copper alloy	362	Dress Accessories	Brooch	Cruciform	F	F	A(2)	Old

Site	SF No.	SF Sub Div.	Anal. Area	XRF Location	Alloy type filler material attached to.	Grave No.	Category	Class	Sub Class	Ost. Sex	Assigned Gender	Grave Phase	Burial Age
				<i>body.</i>									
104	2124		B	Sheet metal fragment	Copper alloy	364	Miscellaneous Fittings	Miscellaneous	Ring	F	F	A(2)	Adult
104	2124		C	<i>Second sheet metal fragment</i>	<i>Copper alloy</i>	<i>364</i>	<i>Miscellaneous Fittings</i>	<i>Miscellaneous</i>	<i>Ring</i>	<i>F</i>	<i>F</i>	<i>A(2)</i>	<i>Adult</i>
104	2317		C	Sheet disc A (alternate side to 3). Also appears to be traces of Au & Hg - soldered to a gilded object or an Hg containing solder?	Copper alloy	315	Dress Accessories	Ring	Ear Ring	F	F	A(2)	Y-MA
104	2317		E	<i>Silver sheet assoc. with Cu disc A (alt. side to 5)</i>	<i>Silver</i>	<i>315</i>	<i>Dress Accessories</i>	<i>Ring</i>	<i>Ear Ring</i>	<i>F</i>	<i>F</i>	<i>A(2)</i>	<i>Y-MA</i>
104	2317		F	Sheet disc B. Also appears to be traces of Au & Hg - soldered to a gilded object or an Hg containing solder?	Copper alloy	315	Dress Accessories	Ring	Ear Ring	F	F	A(2)	Y-MA
104	2317		I	<i>Silver sheet associated with Cu disc B (alt. side to 9)</i>	<i>Silver</i>	<i>315</i>	<i>Dress Accessories</i>	<i>Ring</i>	<i>Ear Ring</i>	<i>F</i>	<i>F</i>	<i>A(2)</i>	<i>Y-MA</i>

Site	SF No.	SF Sub Div.	Anal. Area	XRF Location	Alloy type filler material attached to.	Grave No.	Category	Class	Sub Class	Ost. Sex	Assigned Gender	Grave Phase	Burial Age
104	2380		B	Disc	Copper alloy	315	Dress Accessories	Bead	Undefined Bead	F	F	A(2)	Y-MA
104	2381		B	Hoop (?solder area)	Copper alloy	315	Dress Accessories	Bead	Undefined Bead	F	F	A(2)	Y-MA
104	2381		C	Disc	Copper alloy	315	Dress Accessories	Bead	Undefined Bead	F	F	A(2)	Y-MA
104	2381		D	Disc	Copper alloy	315	Dress Accessories	Bead	Undefined Bead	F	F	A(2)	Y-MA
104	2495		A		Copper alloy	144	Dress Accessories	Brooch	Annular	F	F	A(1)	MA+
104	2626		A	Reverse	Copper alloy	323	Equestrian objects	Tack	Bridle Fitting	M	M	AB	Young
104	2626		C	Front (end)	Copper alloy	323	Equestrian objects	Tack	Bridle Fitting	M	M	AB	Young
104	2627		B	Reverse	Copper alloy	323	Equestrian objects	Tack	Bridle Fitting	M	M	AB	Young
104	2909		A	White concretion – poss. solder - on majority of surface	Copper alloy	184	Dress Accessories	Necklace	Pendant				
104	2909		B	White concretion - poss solder - on majority of surface	Copper alloy	184	Dress Accessories	Necklace	Pendant				
104	3090		A	Reverse	Copper alloy	172	Dress Accessories	Belt Fitting	Girdle-hanger	F	F	A(2)	Young
104	3223		B		Copper alloy	311	Miscellaneous Fittings	Miscellaneous	Sheet	M	M	B	Y-MA
104	3299		A	Side with white material	Copper alloy	359	Miscellaneous Fittings	Fragment	Sheet	C	F	A(2)	12 to 15

Site	SF No.	SF Sub Div.	Anal. Area	XRF Location	Alloy type filler material attached to.	Grave No.	Category	Class	Sub Class	Ost. Sex	Assigned Gender	Grave Phase	Burial Age
				adhering									
104	3318	a	B		Copper alloy	231	Dress Accessories	Belt Fitting	Strap-end	C	F	A	Sub-adult?
104	3318	b	B		Copper alloy	231	Dress Accessories	Belt Fitting	Strap-end	C	F	A	Sub-adult?
104	3318	d	B		Copper alloy	231	Dress Accessories	Belt Fitting	Strap-end	C	F	A	Sub-adult?
104	3318	e	B		Copper alloy	231	Dress Accessories	Belt Fitting	Strap-end	C	F	A	Sub-adult?
104	3318	f	B		Copper alloy	231	Dress Accessories	Belt Fitting	Strap-end	C	F	A	Sub-adult?
104	3348	b	B		Copper alloy	292	Unknown	Unknown	Unknown	F	F	A	MA
104	3349		D		Copper alloy	292	Dress Accessories	Wrist Clasp	Form B 13 a	F	F	A	MA
104	3350		A	Hook piece (front; white area, probably solder.	Copper alloy	292	Dress Accessories	Wrist Clasp	Form B 13 c	F	F	A	MA
104	3350		C	Hook piece, repousse sheet (front)	Copper alloy	292	Dress Accessories	Wrist Clasp	Form B 13 c	F	F	A	MA
104	3350		E	Eye piece, front area	Copper alloy	292	Dress Accessories	Wrist Clasp	Form B 13 c	F	F	A	MA
104	3350		G	Eye piece, reverse of repousse sheet	Copper alloy	292	Dress Accessories	Wrist Clasp	Form B 13 c	F	F	A	MA
104	3674	3	B	Reverse	Copper alloy	168	Military and weaponry	Shield	Shield Mount	N/A	M	B	MA
104	BM20		A	Reverse (convex face)	Copper alloy	323	Equestrian objects	Tack	Bridle Fitting	M	M	AB	Young

Site	SF No.	SF Sub Div.	Anal. Area	XRF Location	Alloy type filler material attached to.	Grave No.	Category	Class	Sub Class	Ost. Sex	Assigned Gender	Grave Phase	Burial Age
104	BM21		B	Reverse	Copper alloy	323	Equestrian objects	Tack	Bridle Fitting	M	M	AB	Young
104	BM33		B	Front	Copper alloy	323	Equestrian objects	Tack	Bridle Fitting	M	M	AB	Young
114	1298		B	Top panel	Copper alloy	445	Dress Accessories	Brooch	Cruciform	N/A	F	A(2)	N/A
114	1452		B	Reverse	Copper alloy	422	Dress Accessories	Bead	Undefined Bead	N/A	F	A(2)	N/A
114	1481		B	Concretion. High Sn - ?Solder remains	Copper alloy	405	Dress Accessories	Wrist Clasp	Undefined Wrist Clasp	N/A	F	A(1)	N/A

APPENDIX X: FILLER ALLOYS ON NON-FERROUS OBJECTS: NPA DATA

The unshaded row shows the net peak areas (mean if more than one analysis taken) for each element, the second (shaded) row shows the coefficient of variation. The final column shows the number of analyses.

Site	SF No.	SF Sub Div.	Anal. Area	XRF Location	Cu (K)	Pb (L)	Sn (K)	Ag (K)	As (K)	Ni (K)	Sb (K)	Au (L)	Bi (L)	Zn (K)	No. of anal.
046	1183		B		2474856	390942	159714	10747						11574 5	1
046	1487		B	Reverse	108987	406340		1780585				30611		9679	2
					<i>0.55</i>	<i>0.32</i>		<i>0.14</i>				<i>0.46</i>		<i>0.72</i>	
046	1488		B	Reverse	108165	500751	90436	1532594				21997		13235	2
					<i>0.10</i>	<i>0.07</i>	<i>0.68</i>	<i>0.17</i>				<i>0.20</i>		<i>0.02</i>	
046	1519		B	Area of solder	1659888	302365	123226	1652						34156 2	1
046	1520		B	Area of solder	1792320	334466	167158	3969			583			38813 3	1
046	1521		B	Area of solder	1390554	238433	91583	2928			440			32219 8	1

Site	SF No.	SF Sub Div.	Anal. Area	XRF Location	Cu (K)	Pb (L)	Sn (K)	Ag (K)	As (K)	Ni (K)	Sb (K)	Au (L)	Bi (L)	Zn (K)	No. of anal.
046	1523		B	Area of solder	1805125	248997	170253	3349			305			31384 3	1
046	1527		B	Area of solder	1641733	315999	151615	1550				788		49039 3	1
046	1528		B	Area of solder	2105849	200809	44919	1753	11528					50637 3	1
046	1529		B		1488810	196605	153918	1522	10731					36739 7	1
046	1531		B		1791398	318389	131509	1907	21725					45522 9	1
046	1533		B		1755861	362770	134251	2024	34386					34767 1	1
046	1537		B		1212273	203684	112531	2976				458		21407 4	2
					<i>0.66</i>	<i>0.32</i>	<i>0.33</i>	<i>0.48</i>				<i>0.21</i>		<i>0.87</i>	
046	1538		B		2134731	182587	121015	3882	10907					37403 0	1
046	1539		B		1720144	230883	180507	3071	14842					28016 7	1
046	1682		C	Disc	1619118	125762	190475							43751 6	1

Site	SF No.	SF Sub Div.	Anal. Area	XRF Location	Cu (K)	Pb (L)	Sn (K)	Ag (K)	As (K)	Ni (K)	Sb (K)	Au (L)	Bi (L)	Zn (K)	No. of anal.
046	1824		B		735505	313043	200878	1452		1121				13320 2	1
104	1060		A		283640	904727	20163	1315	49585					42307	2
					<i>0.12</i>	<i>0.63</i>	<i>0.42</i>	<i>0.25</i>	<i>0.63</i>					<i>0.46</i>	
104	1061		A	Reverse	941928	396444	228417	10382	8600		343	429		43228	5
					<i>0.33</i>	<i>0.29</i>	<i>0.33</i>	<i>0.97</i>	<i>1.55</i>		<i>1.40</i>	<i>0.94</i>		<i>0.47</i>	
104	1362		A	Eye Piece (front)	1210959	211814	197889	2132			337			23454 7	3
					<i>0.26</i>	<i>0.28</i>	<i>0.13</i>	<i>0.10</i>			<i>0.46</i>			<i>0.32</i>	
104	1458		A	Face	435929	268246	217975	2946	14480		141			16990	4
					<i>0.26</i>	<i>0.37</i>	<i>0.13</i>	<i>0.22</i>	<i>0.41</i>		<i>2.00</i>			<i>0.35</i>	
104	1458		D	Bag of fragments	202831	400259	454429	864			10			6846	3
					<i>0.09</i>	<i>0.03</i>	<i>0.02</i>	<i>0.02</i>			<i>1.43</i>			<i>0.08</i>	
104	1691		B	Hook piece (front)	1381403	217968	225961	8209	9158		835			10839 3	3
					<i>0.06</i>	<i>0.05</i>	<i>0.08</i>	<i>0.11</i>	<i>0.87</i>		<i>0.34</i>			<i>0.30</i>	
104	1704		B	Foot near edge where solder is concentrated (reverse)	1411289	754021	184347	2156			304			26072	1
104	1782		B	White conglomerate, prob. Solder?	587990	1259749	30492	7676	24655		468			7139	5
					<i>0.39</i>	<i>0.21</i>	<i>0.85</i>	<i>0.63</i>	<i>1.40</i>		<i>1.17</i>			<i>1.27</i>	

Site	SF No.	SF Sub Div.	Anal. Area	XRF Location	Cu (K)	Pb (L)	Sn (K)	Ag (K)	As (K)	Ni (K)	Sb (K)	Au (L)	Bi (L)	Zn (K)	No. of anal.
104	1948		B	Separate side knop (front). On plate used to attach it to main brooch body.	893719	380446	263007	41695			491			57031	2
					<i>0.36</i>	<i>0.05</i>	<i>0.37</i>	<i>0.59</i>			<i>0.30</i>			<i>0.13</i>	
104	2124		B	Sheet metal fragment	839976	285326	211590	2793	4012		97			29317	2
					<i>0.34</i>	<i>0.74</i>	<i>0.32</i>	<i>0.71</i>	<i>1.41</i>		<i>1.41</i>			<i>0.72</i>	
104	2124		C	Second sheet metal fragment	686577	285849	162223	2036	2413		133			15965	2
					<i>0.21</i>	<i>0.87</i>	<i>0.75</i>	<i>0.39</i>	<i>1.41</i>		<i>1.41</i>			<i>0.21</i>	
104	2317		C	Sheet disc A (alternate side to area B). Also appears to be traces of Au & Hg - soldered to a gilded object or an Hg containing solder?	3012415	141848	114984	20304				1998			1
104	2317		E	Silver sheet assoc. with Cu disc A (alt. side to 5)	933867	41057	3304	1357728	5495			28324		44982	1
104	2317		F	Sheet disc B. Also appears to be traces of Au & Hg - soldered to a gilded object or an Hg containing solder?	2923502	113834	133015	32298				2234			1
104	2317		I	Silver sheet associated with Cu disc B (alt. side to 9)	439094	185326	108124	1242587	1			27016		9757	1

Site	SF No.	SF Sub Div.	Anal. Area	XRF Location	Cu (K)	Pb (L)	Sn (K)	Ag (K)	As (K)	Ni (K)	Sb (K)	Au (L)	Bi (L)	Zn (K)	No. of anal.
104	2380		B	Disc	2456738	106479	237805	2146			167			235459	2
					<i>0.80</i>	<i>0.13</i>	<i>0.73</i>	<i>0.49</i>			<i>0.18</i>			<i>0.88</i>	
104	2381		B	Hoop (white area)	3179294	144937	49588	2959			183			309465	1
104	2381		C	Disc	2932775	215765	189156	4389			459			62785	1
104	2381		D	Disc	1655242	236107	351366	2391			159			45946	1
104	2495		A	White concretion (poss solder) on both faces makes it hard to get a sense of the Cu alloy. Possibly best to exclude this object.	597844	875255	111068	7160	36193		484			20204	6
					<i>0.38</i>	<i>0.20</i>	<i>0.09</i>	<i>0.12</i>	<i>0.51</i>		<i>0.52</i>			<i>0.27</i>	
104	2626		A	Reverse	2030019	336922	230468	3970			527			52706	2
					<i>0.17</i>	<i>0.44</i>	<i>0.01</i>	<i>0.02</i>			<i>0.03</i>			<i>0.07</i>	
104	2626		C	Front (end)	1999119	198234	245391	2862			331			56710	1
104	2627		B	Reverse	1483754	251556	223474	2629			355			39722	4
					<i>0.49</i>	<i>0.44</i>	<i>0.41</i>	<i>0.21</i>			<i>0.64</i>			<i>0.44</i>	
104	2909		A	White concretion - poss solder - on majority of surface	497814	1919184	4450	2800		631	115				2

Site	SF No.	SF Sub Div.	Anal. Area	XRF Location	Cu (K)	Pb (L)	Sn (K)	Ag (K)	As (K)	Ni (K)	Sb (K)	Au (L)	Bi (L)	Zn (K)	No. of anal.
					0.08	0.02	0.05	0.67		1.41	1.41				
104	2909		B	White concretion - poss solder - on majority of surface	1363045	1407771	3202	3444		5164	391				1
104	3090		A	Reverse (poss. solder)	1484638	317018	263041	27433	15793		1585			31609 4	3
					0.15	0.26	0.15	0.08	0.35		0.18			0.10	
104	3223		B	White concretion, prob. Solder	1398157	120168	60684	4836	14645		1241			31865 4	1
104	3299		A	Side with white material adhering	1021128	966385	51746	1338			806			15990	2
					0.14	0.08	0.07	0.03			0.01			0.01	
104	3318	a	B	White concretion, prob. Solder	1276180	396638	187553	3528			651			71170	1
104	3318	b	B	White concretion, prob. Solder	1043228	454699	201275	2844	20408		360		4058	58408	1
104	3318	d	B	White concretion, prob. Solder	1433754	376124	192934	2489						76528	1
104	3318	e	B	White concretion, prob. Solder	1285109	341488	158718	2677			283			58991	1
104	3318	f	B	White concretion, prob. Solder	1367428	311329	182189	3375			613			47767	1

Site	SF No.	SF Sub Div.	Anal. Area	XRF Location	Cu (K)	Pb (L)	Sn (K)	Ag (K)	As (K)	Ni (K)	Sb (K)	Au (L)	Bi (L)	Zn (K)	No. of anal.
104	3348	b	B	Poss. Solder	1131049	272706	175064	8206	3598	502	1010			20535 4	4
					<i>0.40</i>	<i>0.19</i>	<i>0.03</i>	<i>0.12</i>	<i>2.00</i>	<i>2.00</i>	<i>0.07</i>			<i>0.16</i>	
104	3349		D	White concretion	217184	892442	23650	904			216			73892	1
104	3350		A	Hook piece (front; white area, probably solder.	645097	720843	36450	1369			755			16666 4	1
104	3350		C	Hook piece, repousse sheet (front)	3622302	64129	16565	1871			2030			69492 2	3
					<i>0.02</i>	<i>0.06</i>	<i>0.09</i>	<i>0.05</i>			<i>0.06</i>			<i>0.08</i>	
104	3350		E	Eye piece, front area	422845	579447	143437	1469			408			46693	1
104	3350		G	Eye piece, reverse of repousse sheet.	1930796	585845	17651	1631			1509			65063 9	1
104	3674	3	B	Reverse	2577	1653			788					1261	1
104	BM20		A	Reverse (convex face)	1487273	253954	135365	11279			1147			19973 3	2
					<i>0.00</i>	<i>0.08</i>	<i>1.41</i>	<i>0.03</i>			<i>0.57</i>			<i>0.73</i>	
104	BM21		B	Reverse	2490170	192453	207801	13027			858			23224 6	2
					<i>0.09</i>	<i>0.10</i>	<i>0.08</i>	<i>0.08</i>			<i>0.44</i>			<i>0.47</i>	
104	BM33		B	Front (solder?)	1372359	114893	173747	50268			212			85818	2
					<i>0.39</i>	<i>0.00</i>	<i>0.08</i>	<i>0.04</i>			<i>1.41</i>			<i>0.36</i>	

Site	SF No.	SF Sub Div.	Anal. Area	XRF Location	Cu (K)	Pb (L)	Sn (K)	Ag (K)	As (K)	Ni (K)	Sb (K)	Au (L)	Bi (L)	Zn (K)	No. of anal.
114	1298		B	Top panel	1221246	317763	190773	4728			208			185638	1
114	1452		B	Reverse	965622	1116220	107085	2960			590			61085	1
114	1481		B	Concretion. High Sn - ?Solder remains	542783	139307	598735	1883						37174	1

APPENDIX XI: BASE AND FILLER ALLOYS ON COPPER ALLOY OBJECTS: NPA DATA

Showing areas of filler alloy with areas of the 'base' alloy from the same object. The unshaded row shows the net peak areas (mean if more than one analysis taken) for each element, the second (shaded) row shows the coefficient of variation. The final column shows the number of analyses.

Site	SF No,	SF Sub Div.	Anal. Area	Alloy Type	Cu (K)	Pb (L)	Sn (K)	Ag (K)	As (K)	Ni (K)	Sb (K)	Au (L)	Bi (L)	Zn (K)	No. of analyses
046	1183		A	Cast	3769260	187070	140440	9374						151066	3
					<i>0.17</i>	<i>0.49</i>	<i>0.17</i>	<i>0.07</i>						<i>0.2</i>	
046	1183		B	Filler alloy	2474856	390942	159714	10747						115745	1
046	1519		A	Sheet	2232090	90655	39644	1306					667	414002	3
					<i>0.09</i>	<i>0.12</i>	<i>0.16</i>	<i>0.91</i>					<i>1.73</i>	<i>0.2</i>	
046	1519		B	Filler alloy	1659888	302365	123226	1652						341562	1
046	1520		A	Sheet	3790566	92546	21620	3600			653			664769	1
046	1520		B	Filler alloy	1792320	334466	167158	3969			583			388133	1
046	1521		A	Sheet	2648620	80508	22102	3498	8789					549712	3

Site	SF No,	SF Sub Div.	Anal. Area	Alloy Type	Cu (K)	Pb (L)	Sn (K)	Ag (K)	As (K)	Ni (K)	Sb (K)	Au (L)	Bi (L)	Zn (K)	No. of analyses
					<i>0.03</i>	<i>0.31</i>	<i>0.07</i>	<i>0.01</i>	<i>0.21</i>					<i>0.1</i>	
046	1521		B	Filler alloy	1390554	238433	91583	2928			440			322198	1
046	1523		A	Sheet	3775496	114772	22292	4231			1052			564306	1
046	1523		B	Filler alloy	1805125	248997	170253	3349			305			313843	1
046	1527		A	Sheet	3005864	90468	39984	2196	4651					711342	1
046	1527		B	Filler alloy	1641733	315999	151615	1550				788		490393	1
046	1528		A	Sheet	2437223	107182	36876	1748	6487					507617	3
					<i>0.15</i>	<i>0.14</i>	<i>0.13</i>	<i>0.05</i>	<i>0.17</i>					<i>0.2</i>	
046	1528		B	Filler alloy	2105849	200809	44919	1753	11528					506373	1
046	1529		A	Sheet	3407823	81985	40323	1878	3718					490065	1
046	1529		B	Filler alloy	1488810	196605	153918	1522	10731					367397	1
046	1531		A	Sheet	3257829	86148	34402	1225	5963					421356	1
046	1531		B	Filler alloy	1791398	318389	131509	1907	21725					455229	1
046	1533		A	Sheet	3593978	107413	34489	1500	7989					421382	1

Site	SF No,	SF Sub Div.	Anal. Area	Alloy Type	Cu (K)	Pb (L)	Sn (K)	Ag (K)	As (K)	Ni (K)	Sb (K)	Au (L)	Bi (L)	Zn (K)	No. of analyses
046	1533		B	Filler alloy	1755861	362770	134251	2024	34386					347671	1
046	1537		A	Sheet	3789140	86764	25453	4436	6819					717992	1
046	1537		B	Filler alloy	1212273	203684	112531	2976				458		214074	2
					<i>0.66</i>	<i>0.32</i>	<i>0.33</i>	<i>0.48</i>				<i>0.21</i>		<i>0.9</i>	
046	1538		A	Sheet	3629193	92686	22807	3714				294		584069	1
046	1538		B	Filler alloy	2134731	182587	121015	3882	10907					374030	1
046	1539		A	Sheet	3717373	58158	56516	2532	5003					413990	1
046	1539		B	Filler alloy	1720144	230883	180507	3071	14842					280167	1
046	1682		A	Sheet	2517809	196394	25417	1605						417522	2
					<i>0.07</i>	<i>0.51</i>	<i>0.19</i>	<i>0.04</i>						<i>0.1</i>	
046	1682		B	Sheet	3070721	104346	28911	2358						753356	1
046	1682		C	Filler alloy	1619118	125762	190475							437516	1
046	1824		A	Sheet	2482403	146623	51305	2658						460336	1
046	1824		B	Filler alloy	735505	313043	200878	1452		1121				133202	1

Site	SF No,	SF Sub Div.	Anal. Area	Alloy Type	Cu (K)	Pb (L)	Sn (K)	Ag (K)	As (K)	Ni (K)	Sb (K)	Au (L)	Bi (L)	Zn (K)	No. of analyses
104	1061		A	Filler alloy	941928	396444	228417	10382	8600		343	429		43228	5
					<i>0.33</i>	<i>0.29</i>	<i>0.33</i>	<i>0.97</i>	<i>1.55</i>		<i>1.40</i>	<i>0.94</i>		<i>0.5</i>	
104	1362		A	Filler alloy	1210959	211814	197889	2132			337			234547	3
					<i>0.26</i>	<i>0.28</i>	<i>0.13</i>	<i>0.10</i>			<i>0.46</i>			<i>0.3</i>	
104	1362		B	Sheet	2370338	70691	41371	1696			304			342370	5
					<i>0.06</i>	<i>0.30</i>	<i>0.07</i>	<i>0.06</i>			<i>0.26</i>			<i>0.2</i>	
104	1458		A	Filler alloy	435929	268246	217975	2946	14480		141			16990	4
					<i>0.26</i>	<i>0.37</i>	<i>0.13</i>	<i>0.22</i>	<i>0.41</i>		<i>2.00</i>			<i>0.4</i>	
104	1458		B	Cast	1760888	183605	171504	6627	14034	1295	554			132128	4
					<i>0.37</i>	<i>0.43</i>	<i>0.18</i>	<i>0.18</i>	<i>0.27</i>	<i>1.16</i>	<i>1.16</i>			<i>0.1</i>	
104	1458		C	Cast	732308	187109	132239	7564		1367				66017	1
104	1458		D	Filler alloy	202831	400259	454429	864			10			6846	3
					<i>0.09</i>	<i>0.03</i>	<i>0.02</i>	<i>0.02</i>			<i>1.43</i>			<i>0.1</i>	
104	1458		E	Sheet	1564771	286186	155067	5793			221				4
					<i>0.26</i>	<i>0.38</i>	<i>0.20</i>	<i>0.19</i>			<i>0.33</i>				
104	1458		F	Cast	2943018	142783	160194	11865	7668		1550			113905	2
					<i>0.10</i>	<i>0.13</i>	<i>0.11</i>	<i>0.06</i>	<i>0.18</i>		<i>0.21</i>			<i>0.1</i>	
104	1691		A	Cast	1637071	206471	218157	7554	10607		628			98267	4
					<i>0.12</i>	<i>0.21</i>	<i>0.14</i>	<i>0.35</i>	<i>0.26</i>		<i>0.76</i>			<i>0.4</i>	
104	1691		B	Filler alloy	1381403	217968	225961	8209	9158		835			108393	3
					<i>0.06</i>	<i>0.05</i>	<i>0.08</i>	<i>0.11</i>	<i>0.87</i>		<i>0.34</i>			<i>0.3</i>	
104	1704		A	Cast	2095670	319456	196767	2920			467			45060	4

Site	SF No,	SF Sub Div.	Anal. Area	Alloy Type	Cu (K)	Pb (L)	Sn (K)	Ag (K)	As (K)	Ni (K)	Sb (K)	Au (L)	Bi (L)	Zn (K)	No. of analyses
					<i>0.37</i>	<i>0.49</i>	<i>0.49</i>	<i>0.10</i>			<i>0.27</i>			<i>0.1</i>	
104	1704		B	Filler alloy	1411289	754021	184347	2156			304			26072	1
104	1704		C	Cast	2940848	106208	111854	2981			605			62417	4
					<i>0.14</i>	<i>0.53</i>	<i>0.23</i>	<i>0.32</i>			<i>0.16</i>			<i>0.4</i>	
104	1704		D	Cast	2969023	225610	203413	2939			2321			50922	3
					<i>0.14</i>	<i>0.31</i>	<i>0.14</i>	<i>0.19</i>			<i>0.11</i>			<i>0.1</i>	
104	1782		A	Cast	2597714	295546	30430	7586			827				3
					<i>0.08</i>	<i>0.33</i>	<i>0.20</i>	<i>0.21</i>			<i>0.29</i>				
104	1782		B	Filler alloy	587990	1259749	30492	7676	24655		468			7139	5
					<i>0.39</i>	<i>0.21</i>	<i>0.85</i>	<i>0.63</i>	<i>1.40</i>		<i>1.17</i>			<i>1.3</i>	
104	1948		A	Cast	1626937	386337	129404	3903			1962			219305	5
					<i>0.17</i>	<i>0.41</i>	<i>0.21</i>	<i>0.19</i>			<i>0.22</i>			<i>0.3</i>	
104	1948		B	Filler alloy	893719	380446	263007	41695			491			57031	2
					<i>0.36</i>	<i>0.05</i>	<i>0.37</i>	<i>0.59</i>			<i>0.30</i>			<i>0.1</i>	
104	1948		C	Cast	2065317	314067	95501	3552			898			81903	4
					<i>0.24</i>	<i>0.60</i>	<i>0.16</i>	<i>0.24</i>			<i>0.27</i>			<i>0.2</i>	
104	2124		A	Cast	1533227	404346	115551	7451	15315		558			44408	6
					<i>0.31</i>	<i>0.22</i>	<i>0.45</i>	<i>0.60</i>	<i>0.86</i>		<i>0.79</i>			<i>0.3</i>	
104	2124		B	Filler alloy	839976	285326	211590	2793	4012		97			29317	2
					<i>0.34</i>	<i>0.74</i>	<i>0.32</i>	<i>0.71</i>	<i>1.41</i>		<i>1.41</i>			<i>0.7</i>	
104	2124		C	Filler alloy	686577	285849	162223	2036	2413		133			15965	2
					<i>0.21</i>	<i>0.87</i>	<i>0.75</i>	<i>0.39</i>	<i>1.41</i>		<i>1.41</i>			<i>0.2</i>	
104	2317		A	Wire	918676	105879	96011	6763	3884		577	93		49424	2

Site	SF No,	SF Sub Div.	Anal. Area	Alloy Type	Cu (K)	Pb (L)	Sn (K)	Ag (K)	As (K)	Ni (K)	Sb (K)	Au (L)	Bi (L)	Zn (K)	No. of analyses
104	2317		B	Sheet	4758745	44528	23405	7223	1.22		929	1.41		0.1	1
104	2317		C	Filler alloy	3012415	141848	114984	20304				1998			1
104	2317		F	Filler alloy	2923502	113834	133015	32298				2234			1
104	2317		G	Sheet	5478340	9341	1624	6311							1
104	2380		A	Sheet	3104862	61932	43134	2666			330			391881	2
104	2380		B	Filler alloy	2456738	106479	237805	2146			0.72			0.3	2
104	2381		A	Sheet	3326459	77025	40008	2690			0.18			0.9	2
104	2381		B	Filler alloy	3179294	144937	49588	2959			0.25			0.1	1
104	2381		C	Filler alloy	2932775	215765	189156	4389			459			62785	1
104	2381		D	Filler alloy	1655242	236107	351366	2391			159			45946	1
104	2626		A	Filler alloy	2030019	336922	230468	3970			527			52706	2
104	2626		B	Cast	2132890	187440	261572	4282			0.03			0.1	1

Site	SF No,	SF Sub Div.	Anal. Area	Alloy Type	Cu (K)	Pb (L)	Sn (K)	Ag (K)	As (K)	Ni (K)	Sb (K)	Au (L)	Bi (L)	Zn (K)	No. of analyses
104	2626		C	Filler alloy	1999119	198234	245391	2862			331			56710	1
104	2626		D	Cast	3314968	157115	151272	4944			904			117729	2
					<i>0.03</i>	<i>0.04</i>	<i>0.01</i>	<i>0.06</i>			<i>0.02</i>			<i>0.0</i>	
104	2626		E	Cast	3251930	161302	152415	4735			914			119352	1
104	2627		B	Filler alloy	1483754	251556	223474	2629			355			39722	4
					<i>0.49</i>	<i>0.44</i>	<i>0.41</i>	<i>0.21</i>			<i>0.64</i>			<i>0.4</i>	
104	2627		C	Cast	3415354	132744	145601	4846	10530					112553	1
104	2627		A	Cast	2757614	144177	148358	4819	11259					93440	3
					<i>0.23</i>	<i>0.22</i>	<i>0.08</i>	<i>0.06</i>	<i>0.35</i>					<i>0.2</i>	
104	2627		Ignore	Cast	3390178	134527	144938	4273	10425					112132	1
104	2909		A	Filler alloy	497814	1919184	4450	2800		631	115				2
					<i>0.08</i>	<i>0.02</i>	<i>0.05</i>	<i>0.67</i>		<i>1.41</i>	<i>1.41</i>				
104	2909		B	Filler alloy	1363045	1407771	3202	3444		5164	391				1
104	3090		A	Filler alloy	1484638	317018	263041	27433	15793			1585		316094	3
					<i>0.15</i>	<i>0.26</i>	<i>0.15</i>	<i>0.08</i>	<i>0.35</i>			<i>0.18</i>		<i>0.1</i>	
104	3090		B	Cast	3293116	104158	137471	14061	4542			547		375057	5
					<i>0.21</i>	<i>0.47</i>	<i>0.27</i>	<i>0.30</i>	<i>0.61</i>			<i>0.93</i>		<i>0.1</i>	
104	3223		A	Sheet	3136850	138472	55937	3546	20881			1314		603270	3

Site	SF No,	SF Sub Div.	Anal. Area	Alloy Type	Cu (K)	Pb (L)	Sn (K)	Ag (K)	As (K)	Ni (K)	Sb (K)	Au (L)	Bi (L)	Zn (K)	No. of analyses
					<i>0.21</i>	<i>0.41</i>	<i>0.30</i>	<i>0.88</i>	<i>0.54</i>		<i>0.04</i>			<i>0.3</i>	
104	3223		B	Filler alloy	1398157	120168	60684	4836	14645		1241			318654	1
104	3299		A	Filler alloy	1021128	966385	51746	1338			806			15990	2
					<i>0.14</i>	<i>0.08</i>	<i>0.07</i>	<i>0.03</i>			<i>0.01</i>			<i>0.0</i>	
104	3299		B	Sheet	1424093	808182	67659	1993			947			23932	2
					<i>0.02</i>	<i>0.11</i>	<i>0.27</i>	<i>0.32</i>			<i>0.25</i>			<i>0.1</i>	
104	3299		C	Sheet	705459	69594	176391	2051			543			8200	2
					<i>0.48</i>	<i>0.37</i>	<i>0.25</i>	<i>0.15</i>			<i>0.23</i>			<i>0.0</i>	
104	3318	a	B	Filler alloy	1276180	396638	187553	3528			651			71170	1
104	3318	a	A	Sheet	1296144	250798.7	176047.3	6482.333	10451.67		889			101266.3	3
					<i>0.673188</i>	<i>0.2364</i>	<i>0.265722</i>	<i>0.346648</i>	<i>0.896704</i>		<i>0.398377</i>			<i>0.219511</i>	
104	3318	b	A	Sheet	1004706	262339.8	207740.3	6320	9184.5	345.75	874.75		1872.75	85091.5	4
					<i>0.519757</i>	<i>0.391396</i>	<i>0.191051</i>	<i>0.432423</i>	<i>0.720573</i>	<i>2</i>	<i>0.417651</i>		<i>0.724341</i>	<i>0.453952</i>	
104	3318	b	B	Filler alloy	1043228	454699	201275	2844	20408		360		4058	58408	1
104	3318	d	A	Sheet	1479974	202606.3	179407	4261						100653	3
					<i>0.341553</i>	<i>0.20791</i>	<i>0.365011</i>	<i>0.354726</i>						<i>0.399215</i>	
104	3318	d	B	Filler alloy	1433754	376124	192934	2489						76528	1
104	3318	e	A	Sheet	2144785	146091.3	109416.3	3860			371.3333			86786	3
					<i>0.207309</i>	<i>0.331355</i>	<i>0.188188</i>	<i>0.103642</i>			<i>0.866231</i>			<i>0.119839</i>	
104	3318	e	B	Filler alloy	1285109	341488	158718	2677			283			58991	1

Site	SF No,	SF Sub Div.	Anal. Area	Alloy Type	Cu (K)	Pb (L)	Sn (K)	Ag (K)	As (K)	Ni (K)	Sb (K)	Au (L)	Bi (L)	Zn (K)	No. of analyses
104	3318	f	A	Sheet	2774029	91846.67	98186	3389.333			387			89330.33	3
					<i>0.080947</i>	<i>0.365875</i>	<i>0.176317</i>	<i>0.194307</i>			<i>0.280371</i>			<i>0.171364</i>	
104	3318	f	B	Filler alloy	1367428	311329	182189	3375			613			47767	1
104	3348	b	A	Sheet	2837543	92195	124972.3	6192			825.3333			195885.8	6
					<i>0.063259</i>	<i>0.145814</i>	<i>0.103885</i>	<i>0.141946</i>			<i>0.127074</i>			<i>0.177597</i>	
104	3348	b	B	Filler alloy	1131049	272705.8	175064.3	8206.25	3598	502	1010			205353.8	4
					<i>0.398531</i>	<i>0.192243</i>	<i>0.031802</i>	<i>0.123864</i>	<i>2</i>	<i>2</i>	<i>0.067118</i>			<i>0.157012</i>	
104	3349		A	Sheet	1944938	202937	131359	6182	15115	4430	946			260662	4
					<i>0.42</i>	<i>0.47</i>	<i>0.06</i>	<i>0.13</i>	<i>0.59</i>	<i>0.16</i>	<i>0.09</i>			<i>0.2</i>	
104	3349		B	Cast	2395068	69418	56453	1934			1436			488805	4
					<i>0.16</i>	<i>0.41</i>	<i>0.18</i>	<i>0.16</i>			<i>0.15</i>			<i>0.1</i>	
104	3349		C	Sheet	2607307	198287	37846	1741			1653			781448	3
					<i>0.18</i>	<i>0.62</i>	<i>0.39</i>	<i>0.33</i>			<i>0.26</i>			<i>0.2</i>	
104	3349		D	Filler alloy	217184	892442	23650	904			216			73892	1
104	3349		E	Cast	1691850	329145	110272	5041			789			113796	4
					<i>0.29</i>	<i>0.39</i>	<i>0.39</i>	<i>0.24</i>			<i>0.33</i>			<i>0.4</i>	
104	3350		A	Filler alloy	645097	720843	36450	1369			755			166664	1
104	3350		B	Sheet	2587466	49496	58975	1612			1517			412546	2
					<i>0.02</i>	<i>0.10</i>	<i>0.07</i>	<i>0.13</i>			<i>0.09</i>			<i>0.0</i>	
104	3350		C	Filler alloy	3622302	64129	16565	1871			2030			694922	3

Site	SF No,	SF Sub Div.	Anal. Area	Alloy Type	Cu (K)	Pb (L)	Sn (K)	Ag (K)	As (K)	Ni (K)	Sb (K)	Au (L)	Bi (L)	Zn (K)	No. of analyses
					<i>0.02</i>	<i>0.06</i>	<i>0.09</i>	<i>0.05</i>			<i>0.06</i>			<i>0.1</i>	
104	3350		D	Sheet	2872952	58846	59074	1894			1534			383654	3
					<i>0.12</i>	<i>0.33</i>	<i>0.12</i>	<i>0.23</i>			<i>0.05</i>			<i>0.2</i>	
104	3350		E	Filler alloy	422845	579447	143437	1469			408			46693	1
					<i>0.02</i>	<i>0.15</i>	<i>0.02</i>	<i>0.02</i>			<i>0.10</i>			<i>0.1</i>	
104	3350		F	Sheet	2408850	103480	17100	1629			1391			527968	2
					<i>0.02</i>	<i>0.15</i>	<i>0.02</i>	<i>0.02</i>			<i>0.10</i>			<i>0.1</i>	
104	3350		G	Filler alloy	1930796	585845	17651	1631			1509			650639	1
					<i>0.02</i>	<i>0.15</i>	<i>0.02</i>	<i>0.02</i>			<i>0.10</i>			<i>0.1</i>	
104	3674	3	B	Filler alloy	2577	1653			788					1261	1
					<i>0.08</i>	<i>0.38</i>	<i>1.41</i>	<i>0.15</i>	<i>1.41</i>		<i>1.41</i>			<i>0.1</i>	
104	BM20		B	Sheet	1200045	274333	92367	12715	5184		799			350986	2
					<i>0.08</i>	<i>0.38</i>	<i>1.41</i>	<i>0.15</i>	<i>1.41</i>		<i>1.41</i>			<i>0.1</i>	
104	BM20		A	Filler alloy	1487273	253954	135365	11279			1147			199733	2
					<i>0.00</i>	<i>0.08</i>	<i>1.41</i>	<i>0.03</i>			<i>0.57</i>			<i>0.7</i>	
104	BM21		B	Filler alloy	2490170	192453	207801	13027			858			232246	2
					<i>0.09</i>	<i>0.10</i>	<i>0.08</i>	<i>0.08</i>			<i>0.44</i>			<i>0.5</i>	
104	BM21		A	Sheet	1884574	113264	143900	8797	4600		318			267596	3
					<i>0.30</i>	<i>0.52</i>	<i>0.19</i>	<i>0.20</i>	<i>1.13</i>		<i>1.73</i>			<i>0.3</i>	
104	BM33		B	Filler alloy	1372359	114893	173747	50268			212			85818	2
					<i>0.39</i>	<i>0.00</i>	<i>0.08</i>	<i>0.04</i>			<i>1.41</i>			<i>0.4</i>	
104	BM33		C	Cast	1986704	148979	152358	12776			1147			152635	2
					<i>0.64</i>	<i>0.36</i>	<i>0.09</i>	<i>0.07</i>			<i>0.08</i>			<i>0.6</i>	
114	1298		A	Cast	3273607	146509	24376	6554			651			152920	5

Site	SF No,	SF Sub Div.	Anal. Area	Alloy Type	Cu (K)	Pb (L)	Sn (K)	Ag (K)	As (K)	Ni (K)	Sb (K)	Au (L)	Bi (L)	Zn (K)	No. of analyses
					<i>0.17</i>	<i>0.56</i>	<i>0.19</i>	<i>0.19</i>			<i>0.93</i>			<i>0.2</i>	
114	1298		B	Filler alloy	1221246	317763	190773	4728			208			185638	1
114	1298		C	Sheet	1022360	498761	212700	2224			198			39756	2
					<i>0.10</i>	<i>0.26</i>	<i>0.29</i>	<i>0.15</i>			<i>1.41</i>			<i>0.2</i>	
114	1452		A	Sheet	2658473	178253	115633	8462			1907			316188	1
114	1452		B	Filler alloy	965622	1116220	107085	2960			590			61085	1
114	1481		A	Cast	1572018	199905	239932	78401						60897	5
					<i>0.40</i>	<i>0.33</i>	<i>0.77</i>	<i>1.79</i>						<i>0.3</i>	
114	1481		B	Filler alloy	542783	139307	598735	1883						37174	1

APPENDIX XII: LEAD ALLOY OBJECT CATEGORICAL VARIABLES

Site	SF No.	SF Sub Div.	Anal. Area	Additional Notes	Grave No.	Manufacture method	Category	Class	Sub Class	Ost. Sex	Gender	Grave Phase	Burial Age
104	1034		A			Cast	Coins, Tokens and Jettons	Token	Undefined Token				
104	1166		A		110	Cast	Miscellaneous Fittings	Nails and Bolts	Stud				
104	1705		B		322	Cast	Dress Accessories	Brooch	Annular	F	F	A(2)	MA
104	2905		A	Analysed in bag as highly fragmentary	348	Cast	Dress Accessories	Necklace	Pendant	C	F	A(2)	9
114	1037		A		432	Cast	Military and weaponry	Shield	Misc. Shield Fragment	N/A	M	BC	N/A
114	1039		A		432	Cast	Military and weaponry	Shield	Misc. Shield Fragment	N/A	M	BC	N/A
114	1044		A		432	Cast	Military and weaponry	Shield	Misc. Shield Fragment	N/A	M	BC	N/A
114	1323		A		445	Sheet	Dress Accessories	Bead	Undefined Bead	N/A	F	A2	N/A
114	1331		A		445	Sheet	Dress Accessories	Bead	Undefined Bead	N/A	F	A2	N/A
114	1336		A		445	Sheet	Dress Accessories	Bead	Undefined Bead	N/A	F	A2	N/A
114	1499		A		415	Sheet	Unknown	Unknown	Unknown				

114	1500	A	415	Sheet	Unknown	Unknown	Unknown
-----	------	---	-----	-------	---------	---------	---------

APPENDIX XIII: LEAD ALLOY OBJECT NPA DATA

The unshaded row shows the net peak areas (mean if more than one analysis taken) for each element, the second (shaded) row shows the coefficient of variation. The final column shows the number of analyses.

Site	SF No.	SF Sub Division	Anal. Area	XRF Location	Additional Notes	Cu (K)	Pb (L)	Sn (K)	Ag (K)	As (K)	Ni (K)	Sb (K)	Zn (K)	Number of analyses
104	1034		A			10090	1579360	2060					616	4
						<i>0.04</i>	<i>0.06</i>	<i>0.12</i>					<i>0.17</i>	
104	1166		A			518446	208729	136578	6436	15302	1253	1229	99004	2
						<i>0.01</i>	<i>0.09</i>	<i>0.03</i>	<i>0.06</i>	<i>0.10</i>	<i>0.12</i>	<i>0.04</i>	<i>0.02</i>	
104	1705		B			310702	260593	55780	2326		672		161113	2
						<i>0.13</i>	<i>0.27</i>	<i>0.05</i>	<i>0.06</i>		<i>0.24</i>		<i>0.08</i>	
104	2905		A		Analysed in bag as highly fragmentary	9449	1312570	7952					936	3
						<i>0.07</i>	<i>0.03</i>	<i>0.19</i>					<i>0.19</i>	
114	1037		A			175603	1468306	282505	4519				5030	2
						<i>0.88</i>	<i>0.22</i>	<i>0.21</i>	<i>0.18</i>				<i>0.89</i>	
114	1039		A			1402635	423357	174340	6953			516	35193	2
						<i>0.35</i>	<i>0.32</i>	<i>0.29</i>	<i>0.02</i>			<i>0.14</i>	<i>0.33</i>	
114	1044		A			836619	742153	241110	6109				28852	2
						<i>0.33</i>	<i>0.3</i>	<i>0.01</i>	<i>0.08</i>				<i>0.29</i>	
114	1323		A			10828	786246	37681					2666	2
						<i>0.07</i>	<i>0.29</i>	<i>0.04</i>					<i>0.08</i>	

Site	SF No.	SF Sub Division	Anal. Area	XRF Location	Additional Notes	Cu (K)	Pb (L)	Sn (K)	Ag (K)	As (K)	Ni (K)	Sb (K)	Zn (K)	Number of analyses
114	1331		A			4793	786246	60845					1499	2
						0.39	0.25	1.30					0.69	
114	1336		A			4084	1038359	145933					3615	2
						0.03	0.07	0.41					0.22	
114	1499		A			3635	1665029	12705						4
						0.04	0.08	0.14						
114	1500		A			4126	1740073	18745						4
						0.13	0.12	0.17						

Appendix XIV. SUMMARY OF COPPER ALLOY OBJECTS

Below is a table of the objects as analysed with the associated categorical variables. See Appendix XV for the net peak area data.

Site	SF no.	SF sub div.	Ana l. area	XRF Location	Grave no.	Manuf. method	Category	Class	Sub class	Cultural period	Ost. Sex	Assigned Gender	Grave Phase
046	1002		A	Reverse	044	Cast	Dress Accessories	Brooch	Annular	E. Sax	N/A	F	A(2)
046	1006		A	Front	044	Cast	Dress Accessories	Brooch	Annular	E. Sax	N/A	F	A(2)
046	1012		A	Front	044	Sheet	Dress Accessories	Necklace	Pendant	E. Sax	N/A	F	A(2)
046	1026		A	Pincer end	053	Sheet	Toilet and surgical objects	Cosmetic Implements	Tweezers	Undated	N/A	N/A	N/A
046	1056		A	Central panel (front)	038	Cast	Dress Accessories	Brooch	Cruciform	E. Sax	F	F	A(2)
046	1059		A	Front	038	Cast	Dress Accessories	Brooch	Annular	E. Sax	F	F	A(2)
046	1060		A	Front	038	Cast	Dress Accessories	Brooch	Annular	E. Sax	F	F	A(2)
046	1068		A		042	Cast	Dress Accessories	Brooch	Annular	E. Sax	F	F	A
046	1095		A		042	Cast	Dress Accessories	Necklace	Necklace Ring	E. Sax	F	F	A
046	1097		A		042	Cast	Dress Accessories	Necklace	Necklace Ring	E. Sax	F	F	A
046	1098		A	Plate	038	Cast	Dress Accessories	Wrist Clasp	Form B 13 a	E. Sax	F	F	A(2)
046	1098		B	Bar	038	Cast	Dress Accessories	Wrist Clasp	Form B 13 a	E. Sax	F	F	A(2)
046	1099		A	Plate	038	Cast	Dress Accessories	Wrist Clasp	Form B 13 a	E. Sax	F	F	A(2)
046	1099		B	Bar	038	Cast	Dress Accessories	Wrist Clasp	Form B 13 a	E. Sax	F	F	A(2)
046	1100		A	Plate	038	Cast	Dress Accessories	Wrist Clasp	Form B 13 a	E. Sax	F	F	A(2)
046	1100		B	Bar	038	Cast	Dress Accessories	Wrist Clasp	Form B 13 a	E. Sax	F	F	A(2)
046	1101		A	Plate	038	Cast	Dress Accessories	Wrist Clasp	Form B 13 a	E. Sax	F	F	A(2)
046	1101		B	Bar	038	Cast	Dress Accessories	Wrist Clasp	Form B 13 a	E. Sax	F	F	A(2)
046	1106		A	Distal Terminal (front)	038	Cast	Dress Accessories	Belt Fitting	Girdle-hanger	E. Sax	F	F	A(2)

Site	SF no.	SF sub div.	Ana l. area	XRF Location	Grave no.	Manuf. method	Category	Class	Sub class	Cultural period	Ost. Sex	Assigned Gender	Grave Phase
046	1107		A	Distal Terminal (front)	038	Cast	Dress Accessories	Belt Fitting	Girdle-hanger	E. Sax	F	F	A(2)
046	1108		A	Central Shaft (front)	038	Cast	Dress Accessories	Belt Fitting	Girdle-hanger	E. Sax	F	F	A(2)
046	1140		A	Spiral (part of broken whole)	042	Wire	Dress Accessories	Wrist Clasp	Form A	E. Sax	F	F	A
046	1140		B	Spiral, not attached to A.	042	Wire	Dress Accessories	Wrist Clasp	Form A	E. Sax	F	F	A
046	1141		A	Spiral	042	Wire	Dress Accessories	Wrist Clasp	Form A	E. Sax	F	F	A
046	1141		B	Spiral	042	Wire	Dress Accessories	Wrist Clasp	Form A	E. Sax	F	F	A
046	1150		A		038	Cast	Dress Accessories	Brooch	Penannular	Roman	F	F	A(2)
046	1160		A	Spiral	Appendix IV	Cast	Dress Accessories	Brooch	Colchester	Roman			
046	1160		B	Main bar		Cast	Dress Accessories	Brooch	Colchester	Roman			
046	1160		C	Fragment with catch attached		Cast	Dress Accessories	Brooch	Colchester	Roman			
046	1162		A		040	Cast	Dress Accessories	Wrist Clasp	Form B 20	E. Sax	F	F	A(2)
046	1163		A	Front	040	Cast	Dress Accessories	Brooch	Annular	E. Sax	F	F	A(2)
046	1167		A	Front	040	Cast	Dress Accessories	Brooch	Annular	E. Sax	F	F	A(2)
046	1168		A	Foot (reverse)	037	Cast	Dress Accessories	Brooch	Cruciform	E. Sax	F	F	A
046	1176		A		024	Cast	Dress Accessories	Brooch	Annular	E. Sax	c/f	F	A(2)
046	1177		A		024	Cast	Dress Accessories	Brooch	Annular	E. Sax	c/f	F	A(2)
046	1182		A		024	Cast	Dress Accessories	Belt Fitting	Belt ring	E. Sax	c/f	F	A(2)
046	1183		A		024	Cast	Dress Accessories	Belt Fitting	Strap-end	E. Sax	c/f	F	A(2)
046	1184		A		024	Cast	Dress Accessories	Belt Fitting	Strap-end	E. Sax	c/f	F	A(2)
046	1185		A		024	Sheet	Dress Accessories	Belt Fitting	Strap-end	E. Sax	c/f	F	A(2)
046	1188		A		024	Sheet	Dress Accessories	Wrist Clasp	Form B 7	E. Sax	c/f	F	A(2)
046	1192		A		024	Cast	Dress Accessories	Necklace	Pendant	Roman	c/f	F	A(2)
046	1193		A		024	Sheet	Dress Accessories	Buckle	Undefined Buckle	E. Sax	c/f	F	A(2)
046	1194		A		024	Sheet	Dress Accessories	Wrist Clasp	Form B 7	E. Sax	c/f	F	A(2)

Site	SF no.	SF sub div.	Ana l. area	XRF Location	Grave no.	Manuf. method	Category	Class	Sub class	Cultural period	Ost. Sex	Assigned Gender	Grave Phase
046	1195		A		024	Sheet	Dress Accessories	Wrist Clasp	Form B 7	E. Sax	c/f	F	A(2)
046	1196		A		024	Sheet	Equestrian objects	Tack	Mount Strip	E. Sax	c/f	F	A(2)
046	1197		A		024	Cast	Dress Accessories	Wrist Clasp	Form B 13 a	E. Sax	c/f	F	A(2)
046	1200		A		024	Sheet	Equestrian objects	Tack	Mount Strip	E. Sax	c/f	F	A(2)
046	1202		A		219	Sheet	Miscellaneous Fittings	Fragment	Sheet	E. Sax	F	F	A(2)
046	1203		A		024	Sheet	Equestrian objects	Tack	Mount Strip	E. Sax	c/f	F	A(2)
046	1225		A	Reverse	003	Sheet	Dress Accessories	Belt Fitting	Strap-end	E. Sax	F	F	A(2)
046	1306		A	Side E - top band	031	Sheet	Household objects	Bucket	Bucket	E. Sax	M	M	AB
046	1306		B	Side N - bottom band	031	Sheet	Household objects	Bucket	Bucket	E. Sax	M	M	AB
046	1306		C	Side N - middle band	031	Sheet	Household objects	Bucket	Bucket	E. Sax	M	M	AB
046	1306		D	Side N - top band	031	Sheet	Household objects	Bucket	Bucket	E. Sax	M	M	AB
046	1306		E	Side S - top band	031	Sheet	Household objects	Bucket	Bucket	E. Sax	M	M	AB
046	1306		F	Side W - bottom band	031	Sheet	Household objects	Bucket	Bucket	E. Sax	M	M	AB
046	1306		G	Side W adjacent N - top band	031	Sheet	Household objects	Bucket	Bucket	E. Sax	M	M	AB
046	1348		A			Wire	Dress Accessories	Ring	Bracelet	E. Sax			
046	1352		A	Front	045	Cast	Dress Accessories	Brooch	Annular	E. Sax	F	F	A(2)
046	1353		A	Front	045	Cast	Dress Accessories	Brooch	Annular	E. Sax	F	F	A(2)
046	1355		A	Large fragment	007	Sheet	Dress Accessories	Wrist Clasp	Form B 13 c	E. Sax	F	F	A
046	1355		B	Smaller fragment	007	Sheet	Dress Accessories	Wrist Clasp	Form B 13 c	E. Sax	F	F	A
046	1356		A	Large fragment	007	Sheet	Dress Accessories	Wrist Clasp	Form B 13 c	E. Sax	F	F	A
046	1356		B	Smaller fragment	007	Sheet	Dress Accessories	Wrist Clasp	Form B 13 c	E. Sax	F	F	A
046	1360		A	Front	007	Cast	Dress Accessories	Brooch	Annular	E. Sax	F	F	A
046	1361		A	Front	007	Cast	Dress Accessories	Brooch	Annular	E. Sax	F	F	A
046	1364		A		023	Wire	Dress Accessories	Ring	Bracelet	E. Sax			

Site	SF no.	SF sub div.	Ana l. area	XRF Location	Grave no.	Manuf. method	Category	Class	Sub class	Cultural period	Ost. Sex	Assigned Gender	Grave Phase
046	1366		A			Cast	Dress Accessories	Belt Fitting	Belt ring	E. Sax			
046	1370		A		005	Cast	Dress Accessories	Brooch	Annular	E. Sax	F	F	A(2)
046	1371		A		005	Cast	Dress Accessories	Brooch	Annular	E. Sax	F	F	A(2)
046	1372		A		005	Cast	Dress Accessories	Wrist Clasp	Form C 1	E. Sax	F	F	A(2)
046	1373		A		005	Cast	Dress Accessories	Wrist Clasp	Form C 1	E. Sax	F	F	A(2)
046	1374		A		005	Cast	Dress Accessories	Wrist Clasp	Form C 1	E. Sax	F	F	A(2)
046	1519		A		005	Sheet	Dress Accessories	Bead	Undefined Bead	E. Sax	F	F	A(2)
046	1520		A		005	Sheet	Dress Accessories	Bead	Undefined Bead	E. Sax	F	F	A(2)
046	1521		A		005	Sheet	Dress Accessories	Bead	Undefined Bead	E. Sax	F	F	A(2)
046	1523		A		005	Sheet	Dress Accessories	Bead	Undefined Bead	E. Sax	F	F	A(2)
046	1524		A		005	Sheet	Dress Accessories	Bead	Undefined Bead	E. Sax	F	F	A(2)
046	1525		A		005	Sheet	Dress Accessories	Bead	Undefined Bead	E. Sax	F	F	A(2)
046	1526		A		005	Sheet	Dress Accessories	Bead	Undefined Bead	E. Sax	F	F	A(2)
046	1526		B		005	Sheet	Dress Accessories	Bead	Undefined Bead	E. Sax	F	F	A(2)
046	1527		A		005	Sheet	Dress Accessories	Bead	Undefined Bead	E. Sax	F	F	A(2)
046	1528		A		005	Sheet	Dress Accessories	Bead	Undefined Bead	E. Sax	F	F	A(2)
046	1529		A		005	Sheet	Dress Accessories	Bead	Undefined Bead	E. Sax	F	F	A(2)
046	1531		A		005	Sheet	Dress Accessories	Bead	Undefined Bead	E. Sax	F	F	A(2)
046	1533		A		005	Sheet	Dress Accessories	Bead	Undefined Bead	E. Sax	F	F	A(2)
046	1534		A		005	Sheet	Dress Accessories	Bead	Undefined Bead	E. Sax	F	F	A(2)
046	1535		A		005	Sheet	Dress Accessories	Bead	Undefined Bead	E. Sax	F	F	A(2)
046	1536		A		005	Sheet	Dress Accessories	Bead	Undefined Bead	E. Sax	F	F	A(2)
046	1537		A		005	Sheet	Dress Accessories	Bead	Undefined Bead	E. Sax	F	F	A(2)
046	1538		A		005	Sheet	Dress Accessories	Bead	Undefined Bead	E. Sax	F	F	A(2)

Site	SF no.	SF sub div.	Ana l. area	XRF Location	Grave no.	Manuf. method	Category	Class	Sub class	Cultural period	Ost. Sex	Assigned Gender	Grave Phase
046	1539		A		005	Sheet	Dress Accessories	Bead	Undefined Bead	E. Sax	F	F	A(2)
046	1540		A		005	Cast	Dress Accessories	Necklace	Pendant	E. Sax	F	F	A(2)
046	1605		A	Front	017	Cast	Dress Accessories	Brooch	Annular	E. Sax	F	F	A(2)
046	1606		A	Smaller fragment	017	Sheet	Dress Accessories	Brooch	Annular	E. Sax	F	F	A(2)
046	1606		B	Large fragment	017	Sheet	Dress Accessories	Brooch	Annular	E. Sax	F	F	A(2)
046	1609		A		025	Sheet	Dress Accessories	Bead	Undefined Bead	E. Sax	c	F	A(2)
046	1636		A	Upper shaft (front)	025	Cast	Dress Accessories	Belt Fitting	Girdle-hanger	E. Sax	c	F	A(2)
046	1638		A	Hoop (outer)	025	Sheet	Dress Accessories	Bead	Undefined Bead	E. Sax	c	F	A(2)
046	1639		A		002	Sheet	Unknown	Unknown	Unknown	E. Sax	M	M	B
046	1647		A	Front	025	Cast	Dress Accessories	Brooch	Annular	E. Sax	c	F	A(2)
046	1648		A	Head (reverse)	025	Cast	Dress Accessories	Brooch	Fish	E. Sax	c	F	A(2)
046	1657		A	Hoop	025	Sheet	Dress Accessories	Bead	Undefined Bead	E. Sax	c	F	A(2)
046	1657		B	Disc	025	Sheet	Dress Accessories	Bead	Undefined Bead	E. Sax	c	F	A(2)
046	1658		A	Hoop frag	025	Sheet	Dress Accessories	Bead	Undefined Bead	E. Sax	c	F	A(2)
046	1658		B	Disc	025	Sheet	Dress Accessories	Bead	Undefined Bead	E. Sax	c	F	A(2)
046	1661		A	Hoop	025	Sheet	Dress Accessories	Bead	Undefined Bead	E. Sax	c	F	A(2)
046	1662		A	Hoop (outer)	025	Sheet	Dress Accessories	Bead	Undefined Bead	E. Sax	c	F	A(2)
046	1671		A	Hoop (outer)	025	Sheet	Dress Accessories	Bead	Undefined Bead	E. Sax	c	F	A(2)
046	1673		A	Front	025	Cast	Dress Accessories	Brooch	Annular	Undated	c	F	A(2)
046	1674		A	Sheet metal	025	Sheet	Dress Accessories	Brooch	Fish	Undated	c	F	A(2)
046	1674		B	Pin	025	Cast	Dress Accessories	Brooch	Fish	Undated	c	F	A(2)
046	1674		C	Sheet fragment	025	Sheet	Dress Accessories	Brooch	Fish	Undated	c	F	A(2)
046	1682		A	Hoop	025	Sheet	Dress Accessories	Bead	Undefined Bead	E. Sax	c	F	A(2)
046	1682		B	Disc	025	Sheet	Dress Accessories	Bead	Undefined Bead	E. Sax	c	F	A(2)

Site	SF no.	SF sub div.	Ana l. area	XRF Location	Grave no.	Manuf. method	Category	Class	Sub class	Cultural period	Ost. Sex	Assigned Gender	Grave Phase
046	1713		A		010	Wire	Dress Accessories	Ring	Bracelet	E. Sax			
046	1715		A		010	Wire	Dress Accessories	Ring	Bracelet	E. Sax			
046	1727		A			Cast	Dress Accessories	Wrist Clasp	Form B 18	E. Sax			
046	1729		A			Sheet	Miscellaneous Fittings	Fragment	Sheet	E. Sax			
046	1735		A	Fragment 1 (eyes, one broken)	015	Cast	Dress Accessories	Wrist Clasp	Form B 17 a	E. Sax	F	F	A
046	1735		B	Fragment 2 (eyes, both complete)	015	Cast	Dress Accessories	Wrist Clasp	Form B 17 a	E. Sax	F	F	A
046	1735		C	Fragment 3 (no eyes)	015	Cast	Dress Accessories	Wrist Clasp	Form B 17 a	E. Sax	F	F	A
046	1737		A	Spring	043	Cast	Dress Accessories	Brooch	Roman	Roman	F	F	A(2)
046	1737		B	Bow (front)	043	Cast	Dress Accessories	Brooch	Roman	Roman	F	F	A(2)
046	1737		C	Pin	043	Cast	Dress Accessories	Brooch	Roman	Roman	F	F	A(2)
046	1739		A		015	Sheet	Unknown	Unknown	Unknown	E. Sax	F	F	A
046	1750		A	Eye piece	015	Cast	Dress Accessories	Wrist Clasp	Form B 17 a	E. Sax	F	F	A
046	1750		B	Bar	015	Cast	Dress Accessories	Wrist Clasp	Form B 17 a	E. Sax	F	F	A
046	1751		A			Cast	Dress Accessories	Pin	Undefined Pin	Undated			
046	1774		A		007	Sheet	Unknown	Unknown	Unknown	E. Sax	F	F	A
046	1782		A		033	Cast	Dress Accessories	Brooch	Penannular	E. Sax			
046	1782		B		033	Cast	Dress Accessories	Brooch	Penannular	E. Sax			
046	1792		A		018	Cast	Dress Accessories	Bead	Undefined Bead	E. Sax			
046	1811		A	Foot (front)	018	Cast	Dress Accessories	Brooch	Great square-headed	E. Sax			
046	1814		A		018	Cast	Dress Accessories	Necklace	Necklace Ring	E. Sax			
046	1815		A		018	Cast	Dress Accessories	Brooch	Undefined Brooch	E. Sax			
046	1817		A	Reverse	018	Cast	Dress Accessories	Brooch	Annular	E. Sax			
046	1818		A	Reverse	018	Cast	Dress Accessories	Brooch	Annular	E. Sax			

Site	SF no.	SF sub div.	Ana l. area	XRF Location	Grave no.	Manuf. method	Category	Class	Sub class	Cultural period	Ost. Sex	Assigned Gender	Grave Phase
046	1819		A	Eye piece (outer)	015	Sheet	Dress Accessories	Wrist Clasp	Form B 13 c	E. Sax	F	F	A
046	1819		B	Sheet with Repousse	015	Sheet	Dress Accessories	Wrist Clasp	Form B 13 c	E. Sax	F	F	A
046	1820		A	Front	015	Cast	Dress Accessories	Brooch	Annular	E. Sax	F	F	A
046	1820		B	Pin	015	Cast	Dress Accessories	Brooch	Annular	E. Sax	F	F	A
046	1821		A	Front	015	Cast	Dress Accessories	Brooch	Annular	E. Sax	F	F	A
046	1822		A		015	Sheet	Dress Accessories	Ring	Finger ring	E. Sax	F	F	A
046	1824		A	Disc	025	Sheet	Dress Accessories	Bead	Undefined Bead	Undated	c	F	A(2)
104	1000		A	Reverse		Cast	Miscellaneous Fittings	Miscellaneous	Sheet	E. Sax			
104	1001		A			Cast	Dress Accessories	Belt Fitting	Belt ring	E. Sax			
104	1003		A			Cast	Dress Accessories	Brooch	Cruciform	E. Sax			
104	1004		A	Reverse		Melted	Dress Accessories	Brooch	Cruciform	E. Sax			
104	1005		A			Melted	Dress Accessories	Buckle	Undefined Buckle	E. Sax			
104	1006		A			Melted	Dress Accessories	Buckle	Undefined Buckle	E. Sax			
104	1026		A	Frame & prong	115	Cast	Dress Accessories	Buckle	Undefined Buckle	E. Sax	F	f	DE
104	1026		B	Buckle sheet	115	Sheet	Dress Accessories	Buckle	Undefined Buckle	E. Sax	F	f	DE
104	1026		C	Buckle sheet	115	Sheet	Dress Accessories	Buckle	Undefined Buckle	E. Sax	F	f	DE
104	1027		A	Reverse	115	Cast	Dress Accessories	Brooch	Annular	E. Sax	F	f	DE
104	1033		A		118	Sheet	Dress Accessories	Buckle	Buckle Plate	E. Sax			
104	1035		A	Front		Cast	Dress Accessories	Brooch	Cruciform	E. Sax			
104	1038		A	Reverse		Melted	Dress Accessories	Brooch	Annular	E. Sax			
104	1046		B	Reverse		Cast	Dress Accessories	Belt Fitting	Strap-end	E. Sax			
104	1047		A			Melted	Unknown	Unknown	Unknown	E. Sax			
104	1048		A			Cast	Dress Accessories	Brooch	Cruciform	E. Sax			

Site	SF no.	SF sub div.	Ana l. area	XRF Location	Grave no.	Manuf. method	Category	Class	Sub class	Cultural period	Ost. Sex	Assigned Gender	Grave Phase
104	1049		A			Melted	Unknown	Unknown	Unknown	E. Sax			
104	1057		A		116	Cast	Dress Accessories	Buckle	Undefined Buckle	E. Sax	N/A	F	DE
104	1058		A	Tweezers	116	Sheet	Toilet and surgical objects	Cosmetic Implements	Tweezers	E. Sax	N/A	F	DE
104	1058		B	Hoop	116	Cast	Toilet and surgical objects	Cosmetic Implements	Tweezers	E. Sax	N/A	F	DE
104	1062		A	Bow (front)	231	Cast	Dress Accessories	Belt Fitting	Small-Long	E. Sax	c	F	A
104	1063		A		231	Cast	Dress Accessories	Brooch	Annular	E. Sax	c	F	A
104	1074		A		231	Cast	Dress Accessories	Brooch	Annular	E. Sax	c	F	A
104	1095		A		232	Wire	Dress Accessories	Ring	Ear Ring	E. Sax	c	F	A(2)
104	1098		A	Shiny area	237	Cast	Dress Accessories	Ring	Bracelet	E. Sax	N/A	F	BC
104	1148		A		237	Sheet	Miscellaneous Fittings	Miscellaneous	Sheet	E. Sax	N/A	F	BC
104	1161		A	Reverse	237	Cast	Dress Accessories	Brooch	Annular	E. Sax	N/A	F	BC
104	1162		A		237	Cast	Dress Accessories	Brooch	Annular	E. Sax	N/A	F	BC
104	1169		A	Front		Melted	Dress Accessories	Brooch	Cruciform	E. Sax			
104	1171		A	Front		Sheet	Dress Accessories	Brooch	Small-Long	E. Sax			
104	1173		A		219	Cast	Dress Accessories	Brooch	Annular	E. Sax	F	F	A(2)
104	1174		A	Reverse	219	Cast	Dress Accessories	Buckle	Undefined Buckle	E. Sax	F	F	A(2)
104	1176		B	Un gilded area on front	245	Cast	Military and weaponry	Shield	Shield Mount	E. Sax	M	M	C
104	1176		C	Rivet on reverse	245	Cast	Military and weaponry	Shield	Shield Mount	E. Sax	M	M	C
104	1178		A		245	Sheet	Unknown	Unknown	Unknown	E. Sax	M	M	C
104	1182		A		252	Cast	Miscellaneous Fittings	Nails and Bolts	Stud	E. Sax			
104	1191		B	Non gilded area on front	245	Cast	Military and weaponry	Shield	Shield Mount	E. Sax	M	M	C
104	1191		C	Rivet on reverse	245	Cast	Military and weaponry	Shield	Shield Mount	E. Sax	M	M	C
104	1195		A		245	Sheet	Unknown	Unknown	Unknown	E. Sax	M	M	C

Site	SF no.	SF sub div.	Ana l. area	XRF Location	Grave no.	Manuf. method	Category	Class	Sub class	Cultural period	Ost. Sex	Assigned Gender	Grave Phase
104	1213		A	Large fragment	219	Cast	Dress Accessories	Brooch	Annular	E. Sax	F	F	A(2)
104	1227		A		247	Sheet	Unknown	Unknown	Unknown	E. Sax			
104	1228		A		246	Sheet	Unknown	Unknown	Unknown	E. Sax	F	M	AB
104	1239		A		252	Sheet	Miscellaneous Fittings	Miscellaneous	Clip	E. Sax			
104	1248		A		255	Sheet	Miscellaneous Fittings	Miscellaneous	Sheet	E. Sax	M	M	AB
104	1249		A		255	Sheet	Miscellaneous Fittings	Miscellaneous	Sheet	E. Sax	M	M	AB
104	1250		A		255	Sheet	Unknown	Unknown	Unknown	E. Sax	M	M	AB
104	1251		A	Brass	255	Sheet	Miscellaneous Fittings	Miscellaneous	Sheet	E. Sax	M	M	AB
104	1254		A		255	Sheet	Miscellaneous Fittings	Miscellaneous	Sheet	E. Sax	M	M	AB
104	1254		B		255	Sheet	Miscellaneous Fittings	Miscellaneous	Sheet	E. Sax	M	M	AB
104	1255		A		255	Sheet	Dress Accessories	Buckle	Undefined Buckle	E. Sax	M	M	AB
104	1256		A		255	Sheet	Miscellaneous Fittings	Nails and Bolts	Rivet	E. Sax	M	M	AB
104	1263		A	Sheet	255	Sheet	Miscellaneous Fittings	Miscellaneous	Sheet	E. Sax	M	M	AB
104	1263		B	Tube	255	Sheet	Miscellaneous Fittings	Miscellaneous	Sheet	E. Sax	M	M	AB
104	1277		A		221	Cast	Dress Accessories	Buckle	Undefined Buckle	E. Sax	M	M	C/EF
104	1293		A		252	Melted	Dress Accessories	Pin	Undefined Pin	E. Sax			
104	1296		A		251	Sheet	Miscellaneous Fittings	Miscellaneous	Clip	E. Sax	N/A	M	BC
104	1317		A	Reverse		Cast	Dress Accessories	Brooch	Undefined Brooch	E. Sax			
104	1318		A			Cast	Dress Accessories	Brooch	Cruciform	E. Sax			
104	1323		A		297	Sheet	Unknown	Unknown	Unknown	E. Sax	M	M	AB
104	1324		A	Buckle sheet	208	Sheet	Dress Accessories	Buckle	Undefined Buckle	E. Sax			
104	1324		B	Buckle frame and tongue	208	Cast	Dress Accessories	Buckle	Undefined Buckle	E. Sax			
104	1325		A		268	Cast	Dress Accessories	Brooch	Annular	E. Sax	F	F	A(2)

Site	SF no.	SF sub div.	Ana l. area	XRF Location	Grave no.	Manuf. method	Category	Class	Sub class	Cultural period	Ost. Sex	Assigned Gender	Grave Phase
104	1357		A	Folded sheet	220	Sheet	Miscellaneous Fittings	Miscellaneous	Sheet	E. Sax			
104	1357		B	Rivet	220	Cast	Miscellaneous Fittings	Miscellaneous	Sheet	E. Sax			
104	1359		A	Bow (front)	263	Cast	Dress Accessories	Belt Fitting	Small-Long	E. Sax	F	F	A(2)
104	1360		A		263	Sheet	Miscellaneous Fittings	Miscellaneous	Sheet	E. Sax	F	F	A(2)
104	1362		B	Eye Piece (reverse)	263	Sheet	Dress Accessories	Wrist Clasp	Form B 13 c	E. Sax	F	F	A(2)
104	1363		A	Eye Piece (front)	263	Sheet	Dress Accessories	Wrist Clasp	Form B 13 c	E. Sax	F	F	A(2)
104	1363		B	Hook Piece (front)	263	Sheet	Dress Accessories	Wrist Clasp	Form B 13 c	E. Sax	F	F	A(2)
104	1364		A	Outer	261	Sheet	Miscellaneous Fittings	Fragment	Strip	E. Sax			
104	1366		A	Bow (front)	263	Cast	Dress Accessories	Belt Fitting	Small-Long	E. Sax	F	F	A(2)
104	1368		A		267	Cast	Dress Accessories	Brooch	Annular	E. Sax	M	f	BC (-D?)
104	1413		A	Analysed in bag	263	Sheet	Dress Accessories	Bead	Undefined Bead	E. Sax	F	F	A(2)
104	1443		A		334	Sheet	Dress Accessories	Ring	Bracelet	E. Sax			
104	1444		A		334	Sheet	Dress Accessories	Ring	Finger ring	E. Sax			
104	1445		A		334	Sheet	Dress Accessories	Wrist Clasp	Undefined Wrist Clasp	E. Sax			
104	1449		A		338	Sheet	Unknown	Unknown	Unknown	E. Sax			
104	1450	d	A	Front	268	Sheet	Dress Accessories	Wrist Clasp	Form B 7	E. Sax	F	F	A(2)
104	1450	c	A	Front	268	Sheet	Dress Accessories	Wrist Clasp	Form B 7	E. Sax	F	F	A(2)
104	1450	b	A	Front	268	Sheet	Dress Accessories	Wrist Clasp	Form B 7	E. Sax	F	F	A(2)
104	1450	a	A	Front	268	Sheet	Dress Accessories	Wrist Clasp	Form B 7	E. Sax	F	F	A(2)
104	1458		B	Reverse	341	Cast	Dress Accessories	Brooch	Applied disc	E. Sax	F	F	A(2)
104	1458		C	Catch	341	Cast	Dress Accessories	Brooch	Applied disc	E. Sax	F	F	A(2)
104	1458		E	Repousse sheet (front)	341	Sheet	Dress Accessories	Brooch	Applied disc	E. Sax	F	F	A(2)
104	1458		F	Rivet	341	Cast	Dress Accessories	Brooch	Applied disc	E. Sax	F	F	A(2)
104	1461	f	A	Side	350	Sheet	Dress Accessories	Bead	Undefined Bead	E. Sax	N/A	F	A(2)

Site	SF no.	SF sub div.	Ana l. area	XRF Location	Grave no.	Manuf. method	Category	Class	Sub class	Cultural period	Ost. Sex	Assigned Gender	Grave Phase
104	1461	e	A	Side	350	Sheet	Dress Accessories	Bead	Undefined Bead	E. Sax	N/A	F	A(2)
104	1461	d	A	Side	350	Sheet	Dress Accessories	Bead	Undefined Bead	E. Sax	N/A	F	A(2)
104	1461	c	A		350	Sheet	Dress Accessories	Bead	Undefined Bead	E. Sax	N/A	F	A(2)
104	1461	b	A	Side	350	Sheet	Dress Accessories	Bead	Undefined Bead	E. Sax	N/A	F	A(2)
104	1461	a	A	Side	350	Sheet	Dress Accessories	Bead	Undefined Bead	E. Sax	N/A	F	A(2)
104	1466		A		339	Sheet	Miscellaneous Fittings	Nails and Bolts	Stud	E. Sax	M	M	BC
104	1476		A	Hook Piece (front)	350	Cast	Dress Accessories	Wrist Clasp	Form B 20	E. Sax	N/A	F	A(2)
104	1476		B	Eye Piece (front)	350	Cast	Dress Accessories	Wrist Clasp	Form B 20	E. Sax	N/A	F	A(2)
104	1477		A	Eye Piece (front)	350	Cast	Dress Accessories	Wrist Clasp	Form B 20	E. Sax	N/A	F	A(2)
104	1477		B	Hook Piece (front)	350	Cast	Dress Accessories	Wrist Clasp	Form B 20	E. Sax	N/A	F	A(2)
104	1478		A		350	Sheet	Unknown	Unknown	Unknown	E. Sax	N/A	F	A(2)
104	1509		A	Bow (front)	341	Cast	Dress Accessories	Brooch	Cruciform	E. Sax	F	F	A(2)
104	1509		B	Sheet from soil block	341	Sheet	Dress Accessories	Brooch	Cruciform	E. Sax	F	F	A(2)
104	1518		A	Reverse	350	Cast	Dress Accessories	Brooch	Annular	E. Sax	N/A	F	A(2)
104	1543		A	Bow (front)	258	Cast	Dress Accessories	Brooch	Cruciform	E. Sax	F	F	A(1)
104	1545		A	Bow (front)	258	Cast	Dress Accessories	Brooch	Cruciform	E. Sax	F	F	A(1)
104	1546		A	Hook Piece (front)	258	Cast	Dress Accessories	Wrist Clasp	Form B 12	E. Sax	F	F	A(1)
104	1547		A	Hook Piece (front)	258	Cast	Dress Accessories	Wrist Clasp	Form B 12	E. Sax	F	F	A(1)
104	1547		B	Eye Piece (front)	258	Cast	Dress Accessories	Wrist Clasp	Form B 12	E. Sax	F	F	A(1)
104	1563		A	Outer curve	210	Sheet	Miscellaneous Fittings	Fragment	Sheet	E. Sax	F	f	DE
104	1568		A		266	Wire	Miscellaneous Fittings	Miscellaneous	Ring	E. Sax	F	F	DE
104	1570		A		258	Sheet	Toilet and surgical objects	Cosmetic Implements	Tweezers	E. Sax	F	F	A(1)
104	1570		B		258	Sheet	Toilet and surgical objects	Cosmetic Implements	Tweezers	E. Sax	F	F	A(1)
104	1589		A	Buckle plate	340	Sheet	Dress Accessories	Buckle	Undefined	E. Sax	N/A	M	C/EF

Site	SF no.	SF sub div.	Ana l. area	XRF Location	Grave no.	Manuf. method	Category	Class	Sub class	Cultural period	Ost. Sex	Assigned Gender	Grave Phase
									Buckle				
104	1589		B	Buckle frame and tongue	340	Cast	Dress Accessories	Buckle	Undefined Buckle	E. Sax	N/A	M	C/EF
104	1592	c	A	Strap end 1	277	Sheet	Dress Accessories	Belt Fitting	Strap-end	E. Sax	c	F	A(2)
104	1592	c	B	Strap end 2	277	Cast	Dress Accessories	Belt Fitting	Strap-end	E. Sax	c	F	A(2)
104	1593		A		277	Sheet	Miscellaneous Fittings	Miscellaneous	Sheet	E. Sax	c	F	A(2)
104	1593	b	A		277	Sheet	Toilet and surgical objects	Cosmetic Implements	Brush fittings	E. Sax	c	F	A(2)
104	1605		A	Reverse	277	Cast	Dress Accessories	Brooch	Square/cross	E. Sax	c	F	A(2)
104	1620		A		329	Melted	Dress Accessories	Buckle	Undefined Buckle	E. Sax	M	M	C/EF
104	1621		A		329	Cast	Dress Accessories	Brooch	Undefined Brooch	E. Sax	M	M	C/EF
104	1622		A			Melted	Unknown	Unknown	Unknown	E. Sax			
104	1643		A	Front	277	Cast	Dress Accessories	Brooch	Square/cross	E. Sax	c	F	A(2)
104	1656		A			Cast	Miscellaneous Fittings	Nails and Bolts	Stud	E. Sax			
104	1668		A			Sheet	Miscellaneous Fittings	Nails and Bolts	Rivet	E. Sax			
104	1681		A		279	Cast	Dress Accessories	Brooch	Annular	E. Sax	c	F	A(2)
104	1691		A	Hook piece (reverse)		Cast	Dress Accessories	Wrist Clasp	Form B 7	E. Sax			
104	1692		A			Melted	Unknown	Unknown	Unknown	E. Sax			
104	1693		A			Cast	Unknown	Unknown	Unknown	E. Sax			
104	1694		A			Melted	Unknown	Unknown	Unknown	E. Sax			
104	1695		A	Front		Cast	Dress Accessories	Belt Fitting	Small-Long	E. Sax			
104	1696		A			Sheet	Unknown	Unknown	Unknown	E. Sax			
104	1698		A			Cast	Dress Accessories	Brooch	Annular	E. Sax			
104	1704		A	Adjacent break between main body and foot (reverse)	322	Cast	Dress Accessories	Brooch	Great square-headed	E. Sax	F	F	A(2)
104	1704		C	Head panel (reverse)	322	Cast	Dress Accessories	Brooch	Great square-headed	E. Sax	F	F	A(2)

Site	SF no.	SF sub div.	Ana l. area	XRF Location	Grave no.	Manuf. method	Category	Class	Sub class	Cultural period	Ost. Sex	Assigned Gender	Grave Phase
104	1705		A		322	Sheet	Dress Accessories	Brooch	Annular	E. Sax	F	F	A(2)
104	1706		A		322	Sheet	Dress Accessories	Brooch	Annular	E. Sax	F	F	A(2)
104	1713		A	Foot (front)	290	Cast	Dress Accessories	Brooch	Radiate-head	E. Sax	c	F	A
104	1752		A	Hook piece (front)	322	Cast	Dress Accessories	Wrist Clasp	Form B 20	E. Sax	F	F	A(2)
104	1752		B	Eye piece (reverse)	322	Cast	Dress Accessories	Wrist Clasp	Form B 20	E. Sax	F	F	A(2)
104	1753		A	Hook piece (front)	322	Cast	Dress Accessories	Wrist Clasp	Form B 20	E. Sax	F	F	A(2)
104	1753		B	Eye piece (front)	322	Cast	Dress Accessories	Wrist Clasp	Form B 20	E. Sax	F	F	A(2)
104	1768		A	Buckle plate	287	Sheet	Dress Accessories	Buckle	Undefined Buckle	E. Sax	M	M	B
104	1776		A	Reverse	305	Sheet	Dress Accessories	Brooch	Annular	E. Sax	F	F	A(1)
104	1777		A		305	Sheet	Dress Accessories	Brooch	Annular	E. Sax	F	F	A(1)
104	1782		A		305	Cast	Miscellaneous Fittings	Miscellaneous	Ring	E. Sax	F	F	A(1)
104	1786		A		291	Sheet	Unknown	Unknown	Unknown	E. Sax	M	M	C/EF
104	1887		A	Bow (front)	363	Cast	Dress Accessories	Brooch	Cruciform	E. Sax	F	F	A(1)
104	1888		A	Bow (front)	363	Cast	Dress Accessories	Brooch	Cruciform	E. Sax	F	F	A(1)
104	1900		A	Reverse		Melted	Dress Accessories	Brooch	Undefined Brooch	E. Sax			
104	1903		A		364	Cast	Dress Accessories	Brooch	Cruciform	E. Sax	F	F	A(2)
104	1942		A		363	Melted	Unknown	Unknown	Unknown	E. Sax	F	F	A(1)
104	1947		A		362	Cast	Dress Accessories	Brooch	Annular	E. Sax	F	F	A(2)
104	1948		A	Bow (front)	362	Cast	Dress Accessories	Brooch	Cruciform	E. Sax	F	F	A(2)
104	1948		C	Separate side knop (reverse). On plate used to attach it to main brooch.	362	Cast	Dress Accessories	Brooch	Cruciform	E. Sax	F	F	A(2)
104	1949		A		362	Cast	Dress Accessories	Ring	Finger ring	E. Sax	F	F	A(2)
104	1950		A	Front	362	Cast	Dress Accessories	Brooch	Annular	E. Sax	F	F	A(2)
104	1952		A		362	Cast	Dress Accessories	Brooch	Annular	E. Sax	F	F	A(2)

Site	SF no.	SF sub div.	Ana l. area	XRF Location	Grave no.	Manuf. method	Category	Class	Sub class	Cultural period	Ost. Sex	Assigned Gender	Grave Phase
104	1952		B		362	Cast	Dress Accessories	Brooch	Annular	E. Sax	F	F	A(2)
104	1953		A	Eye piece (front)	362	Sheet	Dress Accessories	Wrist Clasp	Form B 7	E. Sax	F	F	A(2)
104	1954		A	Hook piece (front)	362	Sheet	Dress Accessories	Wrist Clasp	Form B 7	E. Sax	F	F	A(2)
104	1955		A	Hook piece (front)	362	Sheet	Dress Accessories	Wrist Clasp	Form B 7	E. Sax	F	F	A(2)
104	1956		A	Eye piece (rear)	362	Sheet	Dress Accessories	Wrist Clasp	Form B 7	E. Sax	F	F	A(2)
104	1960		A	Bow (front)	362	Cast	Dress Accessories	Brooch	Cruciform	E. Sax	F	F	A(2)
104	1960		B	Catch	362	Cast	Dress Accessories	Brooch	Cruciform	E. Sax	F	F	A(2)
104	2028		A	Bow (front)	318	Cast	Dress Accessories	Brooch	Cruciform	E. Sax	F	F	A(1)
104	2028		B	Separate side knob (front)	318	Cast	Dress Accessories	Brooch	Cruciform	E. Sax	F	F	A(1)
104	2028		C	Second separate side knob (front)	318	Cast	Dress Accessories	Brooch	Cruciform	E. Sax	F	F	A(1)
104	2029		A	Bow (front)	318	Cast	Dress Accessories	Brooch	Cruciform	E. Sax	F	F	A(1)
104	2030		A	Bow (front)	318	Cast	Dress Accessories	Brooch	Cruciform	E. Sax	F	F	A(1)
104	2030		B	Catch	318	Cast	Dress Accessories	Brooch	Cruciform	E. Sax	F	F	A(1)
104	2031		A		309	Sheet	Miscellaneous Fittings	Miscellaneous	Sheet	E. Sax	F	F	A(2)
104	2054		A	Bow (front)	364	Cast	Dress Accessories	Brooch	Cruciform	E. Sax	F	F	A(2)
104	2057		A	Bow (front)	309	Cast	Dress Accessories	Belt Fitting	Small-Long	E. Sax	F	F	A(2)
104	2059		A	Bow (front)	309	Cast	Dress Accessories	Belt Fitting	Small-Long	E. Sax	F	F	A(2)
104	2124		A	Knop	364	Cast	Miscellaneous Fittings	Miscellaneous	Ring	E. Sax	F	F	A(2)
104	2125		A		364	Wire	Dress Accessories	Ring	Finger ring	E. Sax	F	F	A(2)
104	2126		A		364	Sheet	Dress Accessories	Ring	Finger ring	E. Sax	F	F	A(2)
104	2135		A		242	Cast	Dress Accessories	Belt Fitting	Small-Long	E. Sax	F	F	A(2)
104	2136		A	Bow (front)	242	Cast	Dress Accessories	Brooch	Cruciform	E. Sax	F	F	A(2)
104	2136		B	Catch	242	Cast	Dress Accessories	Brooch	Cruciform	E. Sax	F	F	A(2)
104	2137		A	Bow (front)	242	Cast	Dress Accessories	Belt Fitting	Small-Long	E. Sax	F	F	A(2)

Site	SF no.	SF sub div.	Ana l. area	XRF Location	Grave no.	Manuf. method	Category	Class	Sub class	Cultural period	Ost. Sex	Assigned Gender	Grave Phase
104	2137		B	Catch	242	Cast	Dress Accessories	Belt Fitting	Small-Long	E. Sax	F	F	A(2)
104	2138		A		242	Sheet	Miscellaneous Fittings	Miscellaneous	Sheet	E. Sax	F	F	A(2)
104	2139		A		242	Cast	Dress Accessories	Belt Fitting	Girdle-hanger	E. Sax	F	F	A(2)
104	2140		A		242	Cast	Dress Accessories	Belt Fitting	Girdle-hanger	E. Sax	F	F	A(2)
104	2221		A		242	Sheet	Miscellaneous Fittings	Miscellaneous	Sheet	E. Sax	F	F	A(2)
104	2276		A		242	Sheet	Miscellaneous Fittings	Nails and Bolts	Rivet	E. Sax	F	F	A(2)
104	2289		A		242	Wire	Dress Accessories	Ring	Ear Ring	E. Sax	F	F	A(2)
104	2294		A			Melted	Unknown	Unknown	Unknown	E. Sax			
104	2298		A	Bow (front)	244	Cast	Dress Accessories	Brooch	Cruciform	E. Sax	F	F	A(1)
104	2299		A	Hook piece (front)	244	Cast	Dress Accessories	Wrist Clasp	Form B 12	E. Sax	F	F	A(1)
104	2300		A		244	Sheet	Toilet and surgical objects	Cosmetic Implements	Brush fittings	E. Sax	F	F	A(1)
104	2301		A		244	Sheet	Dress Accessories	Brooch	Undefined Brooch	E. Sax	F	F	A(1)
104	2308		A	Front	315	Cast	Dress Accessories	Brooch	Annular	E. Sax	F	F	A(2)
104	2311		B	Reverse	315	Sheet	Dress Accessories	Necklace	Pendant	E. Sax	F	F	A(2)
104	2312		A		315	Sheet	Dress Accessories	Bead	Undefined Bead	E. Sax	F	F	A(2)
104	2312		D	Clip	315	Sheet	Dress Accessories	Bead	Undefined Bead	E. Sax	F	F	A(2)
104	2317		A	Wire	315	Wire	Dress Accessories	Ring	Ear Ring	E. Sax	F	F	A(2)
104	2317		B	Sheet disc A	315	Sheet	Dress Accessories	Ring	Ear Ring	E. Sax	F	F	A(2)
104	2344		A		315	Sheet	Dress Accessories	Necklace	Pendant	E. Sax	F	F	A(2)
104	2352		A		315	Sheet	Dress Accessories	Necklace	Pendant	E. Sax	F	F	A(2)
104	2364		A	Wire	315	Wire	Toilet and surgical objects	Cosmetic Implements	Brush fittings	E. Sax	F	F	A(2)
104	2364		B	Sheet attachment	315	Sheet	Toilet and surgical objects	Cosmetic Implements	Brush fittings	E. Sax	F	F	A(2)
104	2364		C	Cast attachment	315	Cast	Toilet and surgical objects	Cosmetic Implements	Brush fittings	E. Sax	F	F	A(2)

Site	SF no.	SF sub div.	Ana l. area	XRF Location	Grave no.	Manuf. method	Category	Class	Sub class	Cultural period	Ost. Sex	Assigned Gender	Grave Phase
104	2373		A	Hoop	315	Sheet	Dress Accessories	Bead	Undefined Bead	E. Sax	F	F	A(2)
104	2373		B	Clip	315	Sheet	Dress Accessories	Bead	Undefined Bead	E. Sax	F	F	A(2)
104	2374		B	Clip	315	Sheet	Dress Accessories	Bead	Undefined Bead	E. Sax	F	F	A(2)
104	2377		A	Hoop A	315	Sheet	Dress Accessories	Bead	Undefined Bead	E. Sax	F	F	A(2)
104	2377		B	Hoop B	315	Sheet	Dress Accessories	Bead	Undefined Bead	E. Sax	F	F	A(2)
104	2380		A	Hoop	315	Sheet	Dress Accessories	Bead	Undefined Bead	E. Sax	F	F	A(2)
104	2381		A	Hoop	315	Sheet	Dress Accessories	Bead	Undefined Bead	E. Sax	F	F	A(2)
104	2387		A	Hoop	315	Sheet	Dress Accessories	Bead	Undefined Bead	E. Sax	F	F	A(2)
104	2387		B	Clip	315	Sheet	Dress Accessories	Bead	Undefined Bead	E. Sax	F	F	A(2)
104	2398		A	Reverse	315	Cast	Dress Accessories	Brooch	Annular	E. Sax	F	F	A(2)
104	2399		A		315	Sheet	Dress Accessories	Buckle	Undefined Buckle	E. Sax	F	F	A(2)
104	2401		A		315	Sheet	Miscellaneous Fittings	Buckle	Buckle Plate	E. Sax	F	F	A(2)
104	2402		A	Buckle sheet	315	Sheet	Miscellaneous Fittings	Buckle	Buckle Plate	E. Sax	F	F	A(2)
104	2403		A	Strap end A	315	Sheet	Miscellaneous Fittings	Belt Fitting	Strap-end	E. Sax	F	F	A(2)
104	2403		B	Strap end B	315	Sheet	Miscellaneous Fittings	Belt Fitting	Strap-end	E. Sax	F	F	A(2)
104	2411		A			Melted	Dress Accessories	Belt Fitting	Small-Long	E. Sax			
104	2413		A		212	Melted	Unknown	Unknown	Unknown	E. Sax			
104	2450		A		213	Cast	Dress Accessories	Bead	Undefined Bead	E. Sax			
104	2456		A			Sheet	Dress Accessories	Wrist Clasp	Form B	E. Sax			
104	2462		A		213	Cast	Dress Accessories	Brooch	Annular	E. Sax			
104	2463		A		213	Cast	Dress Accessories	Brooch	Annular	E. Sax			
104	2479		A		197	Sheet	Dress Accessories	Necklace	Pendant	E. Sax			
104	2494		A	Bow (front)	144	Cast	Dress Accessories	Brooch	Cruciform	E. Sax	F	F	A(1)
104	2494		B	Catch (loose sheet)	144	Sheet	Dress Accessories	Brooch	Cruciform	E. Sax	F	F	A(1)

Site	SF no.	SF sub div.	Ana l. area	XRF Location	Grave no.	Manuf. method	Category	Class	Sub class	Cultural period	Ost. Sex	Assigned Gender	Grave Phase
104	2499		A			Melted	Dress Accessories	Brooch	Undefined Brooch	E. Sax			
104	2500		A	Hook piece (front)		Cast	Dress Accessories	Wrist Clasp	Form B 20	E. Sax			
104	2501		A	Front		Cast	Dress Accessories	Brooch	Undefined Brooch	E. Sax			
104	2502		A			Cast	Unknown	Unknown	Unknown	E. Sax			
104	2503		A			Melted	Dress Accessories	Brooch	Undefined Brooch	E. Sax			
104	2507		A	Large fragment	141	Sheet	Miscellaneous Fittings	Miscellaneous	Sheet	E. Sax	M	M	C/EF
104	2507		B	Small fragment	141	Sheet	Miscellaneous Fittings	Miscellaneous	Sheet	E. Sax	M	M	C/EF
104	2510		A		212	Melted	Unknown	Unknown	Unknown	E. Sax			
104	2524		A		141	Sheet	Miscellaneous Fittings	Miscellaneous	Sheet	E. Sax	M	M	C/EF
104	2525		A		141	Sheet	Unknown	Unknown	Unknown	E. Sax	M	M	C/EF
104	2526		A		323	Sheet	Miscellaneous Fittings	Miscellaneous	Sheet	E. Sax	M	M	AB
104	2528		A			Melted	Dress Accessories	Brooch	Cruciform	E. Sax			
104	2529		A	Buckle plate	141	Cast	Dress Accessories	Buckle	Undefined Buckle	E. Sax	M	M	C/EF
104	2529		B	Buckle frame & prong	141	Cast	Dress Accessories	Buckle	Undefined Buckle	E. Sax	M	M	C/EF
104	2532		A			Sheet	Unknown	Unknown	Unknown	E. Sax			
104	2533		A			Melted	Unknown	Unknown	Unknown	E. Sax			
104	2540		A	Shaft (reverse, base)	144	Cast	Dress Accessories	Brooch	Cruciform	E. Sax	F	F	A(1)
104	2540	b	A	Side knob for 2494	144	Cast	Dress Accessories	Brooch	Cruciform	E. Sax	F	F	A(1)
104	2540	b	B	Side knob for 2494	144	Cast	Dress Accessories	Brooch	Cruciform	E. Sax	F	F	A(1)
104	2541		A	Bow (front)	144	Cast	Dress Accessories	Brooch	Cruciform	E. Sax	F	F	A(1)
104	2577		A	Front	191	Cast	Dress Accessories	Buckle	Undefined Buckle	E. Sax	M	M	AB
104	2587		A	Sheet front		Sheet	Miscellaneous Fittings	Nails and Bolts	Stud	E. Sax			
104	2587		B	Cast rivet		Cast	Miscellaneous Fittings	Nails and Bolts	Stud	E. Sax			
104	2588		A	Rivet head		Cast	Miscellaneous Fittings	Nails and Bolts	Stud	E. Sax			

Site	SF no.	SF sub div.	Ana l. area	XRF Location	Grave no.	Manuf. method	Category	Class	Sub class	Cultural period	Ost. Sex	Assigned Gender	Grave Phase
104	2589		A			Melted	Dress Accessories	Brooch	Undefined Brooch	E. Sax			
104	2590		A	Front	199	Cast	Dress Accessories	Buckle	Undefined Buckle	E. Sax			
104	2590		B	Reverse	199	Cast	Dress Accessories	Buckle	Undefined Buckle	E. Sax			
104	2591		A	Sheet metal	199	Sheet	Dress Accessories	Buckle	Undefined Buckle	E. Sax			
104	2591		B	Buckle' part	199	Cast	Dress Accessories	Buckle	Undefined Buckle	E. Sax			
104	2613		A	Buckle sheet	215	Sheet	Dress Accessories	Buckle	Undefined Buckle	E. Sax	M	M	BC
104	2613		B	Buckle frame and tongue	215	Cast	Dress Accessories	Buckle	Undefined Buckle	E. Sax	M	M	BC
104	2622		A	Front	323	Sheet	Equestrian objects	Tack	Bridle Fitting	E. Sax	M	M	AB
104	2623		C	Arm (no plate)	323	Cast	Equestrian objects	Tack	Bridle mount	E. Sax	M	M	AB
104	2623		D	Reverse (arm)	323	Cast	Equestrian objects	Tack	Bridle mount	E. Sax	M	M	AB
104	2623		E	Rivet	323	Cast	Equestrian objects	Tack	Bridle mount	E. Sax	M	M	AB
104	2624		A	Reverse (foot)	323	Cast	Equestrian objects	Tack	Bridle Fitting	E. Sax	M	M	AB
104	2624		D	Catch (reverse)	323	Cast	Equestrian objects	Tack	Bridle Fitting	E. Sax	M	M	AB
104	2624		E	Front	323	Cast	Equestrian objects	Tack	Bridle Fitting	E. Sax	M	M	AB
104	2626		B	Reverse	323	Cast	Equestrian objects	Tack	Bridle Fitting	E. Sax	M	M	AB
104	2626		D	Front	323	Cast	Equestrian objects	Tack	Bridle Fitting	E. Sax	M	M	AB
104	2626		E	Front	323	Cast	Equestrian objects	Tack	Bridle Fitting	E. Sax	M	M	AB
104	2627		A	Front	323	Cast	Equestrian objects	Tack	Bridle Fitting	E. Sax	M	M	AB
104	2627		C	Reverse	323	Cast	Equestrian objects	Tack	Bridle Fitting	E. Sax	M	M	AB
104	2627		Igno re	Front	323	Cast	Equestrian objects	Tack	Bridle Fitting	E. Sax	M	M	AB
104	2631		A		198	Sheet	Miscellaneous Fittings	Miscellaneous	Clip	E. Sax	M	M	C/EF
104	2633		A		198	Sheet	Miscellaneous Fittings	Miscellaneous	Clip	E. Sax	M	M	C/EF
104	2634		A	Buckle sheet	203	Sheet	Dress Accessories	Buckle	Undefined Buckle	E. Sax			

Site	SF no.	SF sub div.	Ana l. area	XRF Location	Grave no.	Manuf. method	Category	Class	Sub class	Cultural period	Ost. Sex	Assigned Gender	Grave Phase
104	2634		B	Buckle frame and tongue	203	Cast	Dress Accessories	Buckle	Undefined Buckle	E. Sax			
104	2636		A	Reverse	323	Sheet	Equestrian objects	Tack	Bridle mount	E. Sax	M	M	AB
104	2646		A	Buckle sheet	146	Sheet	Dress Accessories	Buckle	Undefined Buckle	E. Sax	M	M	C/EF
104	2646		B	Frame & Prong	146	Cast	Dress Accessories	Buckle	Undefined Buckle	E. Sax	M	M	C/EF
104	2646		C	Loose sheet	146	Sheet	Dress Accessories	Buckle	Undefined Buckle	E. Sax	M	M	C/EF
104	2647		A	Frame & Prong	146	Cast	Dress Accessories	Buckle	Undefined Buckle	E. Sax	M	M	C/EF
104	2647		B	Buckle sheet	146	Sheet	Dress Accessories	Buckle	Undefined Buckle	E. Sax	M	M	C/EF
104	2648		A		205	Cast	Dress Accessories	Brooch	Annular	E. Sax	F	F	A(2)
104	2649		A		205	Cast	Dress Accessories	Brooch	Annular	E. Sax	F	F	A(2)
104	2650		A	Rolled sheet	205	Sheet	Dress Accessories	Bead	Undefined Bead	E. Sax	F	F	A(2)
104	2651		A		205	Sheet	Dress Accessories	Bead	Undefined Bead	E. Sax	F	F	A(2)
104	2655		A			Sheet	Miscellaneous Fittings	Miscellaneous	Sheet	E. Sax			
104	2657		A		198	Sheet	Miscellaneous Fittings	Miscellaneous	Clip	E. Sax	M	M	C/EF
104	2671		A		214	Sheet	Dress Accessories	Brooch	Annular	E. Sax	c	F	A(2)
104	2672		A		214	Sheet	Dress Accessories	Brooch	Annular	E. Sax	c	F	A(2)
104	2672		B	Pin	214	Sheet	Dress Accessories	Brooch	Annular	E. Sax	c	F	A(2)
104	2679		A			Sheet	Miscellaneous Fittings	Miscellaneous	Sheet	E. Sax			
104	2681		A	Uncorroded area	190	Sheet	Unknown	Unknown	Unknown	E. Sax	F	F	A(2)
104	2682		A		190	Sheet	Unknown	Unknown	Unknown	E. Sax	F	F	A(2)
104	2706		A		205	Sheet	Dress Accessories	Bead	Undefined Bead	E. Sax	F	F	A(2)
104	2714		A		202	Cast	Dress Accessories	Brooch	Annular	E. Sax	F	F	A(2)
104	2715		A		202	Cast	Dress Accessories	Brooch	Annular	E. Sax	F	F	A(2)
104	2716		A		190	Sheet	Unknown	Unknown	Unknown	E. Sax	F	F	A(2)

Site	SF no.	SF sub div.	Ana l. area	XRF Location	Grave no.	Manuf. method	Category	Class	Sub class	Cultural period	Ost. Sex	Assigned Gender	Grave Phase
104	2717		A		185	Cast	Dress Accessories	Pin	Undefined Pin	E. Sax	N/A	F	A(2)
104	2719		A		152	Sheet	Military and weaponry	Spear	Spear Ring	E. Sax	N/A	M	EF
104	2748		A		148	Sheet	Miscellaneous Fittings	Miscellaneous	Sheet	E. Sax	c	F	A(1)
104	2749		A		148	Sheet	Miscellaneous Fittings	Miscellaneous	Sheet	E. Sax	c	F	A(1)
104	2750		A	Front	148	Cast	Dress Accessories	Brooch	Penannular	E. Sax	c	F	A(1)
104	2757		A	Bow (front)	358	Cast	Dress Accessories	Brooch	Cruciform	E. Sax	c	F	A(2)
104	2757		B	Catch	358	Cast	Dress Accessories	Brooch	Cruciform	E. Sax	c	F	A(2)
104	2758		A	Front	358	Cast	Dress Accessories	Brooch	Annular	E. Sax	c	F	A(2)
104	2759		A		358	Cast	Dress Accessories	Brooch	Annular	E. Sax	c	F	A(2)
104	2760		A	Reverse	358	Cast	Dress Accessories	Belt Fitting	Belt ring	E. Sax	c	F	A(2)
104	2760		B	Front	358	Cast	Dress Accessories	Belt Fitting	Belt ring	E. Sax	c	F	A(2)
104	2770		A	Large fragment	358	Sheet	Miscellaneous Fittings	Miscellaneous	Sheet	E. Sax	c	F	A(2)
104	2770		B	Rolled sheet	358	Sheet	Miscellaneous Fittings	Miscellaneous	Sheet	E. Sax	c	F	A(2)
104	2780		A		190	Sheet	Unknown	Unknown	Unknown	E. Sax	F	F	A(2)
104	2781		A	Cast hoop	358	Cast	Toilet and surgical objects	Cosmetic Implements	Undefined Cosmetic Implement	E. Sax	c	F	A(2)
104	2781		B	Sheet attached to ring	358	Sheet	Toilet and surgical objects	Cosmetic Implements	Undefined Cosmetic Implement	E. Sax	c	F	A(2)
104	2782		A		190	Cast	Dress Accessories	Brooch	Annular	E. Sax	F	F	A(2)
104	2783		A	Bow (front)	190	Cast	Dress Accessories	Brooch	Cruciform	E. Sax	F	F	A(2)
104	2784		A	Front	190	Sheet	Dress Accessories	Brooch	Annular	E. Sax	F	F	A(2)
104	2785		A	Reverse	189	Cast	Dress Accessories	Brooch	Annular	E. Sax	N/A	F	A(2)
104	2785		B	Pin	189	Cast	Dress Accessories	Brooch	Annular	E. Sax	N/A	F	A(2)
104	2786		A	Reverse	189	Cast	Dress Accessories	Brooch	Annular	E. Sax	N/A	F	A(2)
104	2786		B	Pin	189	Cast	Dress Accessories	Brooch	Annular	E. Sax	N/A	F	A(2)

Site	SF no.	SF sub div.	Ana l. area	XRF Location	Grave no.	Manuf. method	Category	Class	Sub class	Cultural period	Ost. Sex	Assigned Gender	Grave Phase
104	2787	c	A		189	Cast	Dress Accessories	Belt Fitting	Latch-lifter	E. Sax	N/A	F	A(2)
104	2787	b	A		189	Cast	Dress Accessories	Belt Fitting	Girdle-banger	E. Sax	N/A	F	A(2)
104	2787	a	A		189	Cast	Dress Accessories	Belt Fitting	Latch-lifter	E. Sax	N/A	F	A(2)
104	2788		A		189	Cast	Dress Accessories	Belt Fitting	Strap-end	Roman?	N/A	F	A(2)
104	2789		A		189	Wire	Miscellaneous Fittings	Fragment	Wire	E. Sax	N/A	F	A(2)
104	2798		A		352	Cast	Dress Accessories	Brooch	Annular	E. Sax	F	F	A(2)
104	2799		A	Front	352	Cast	Dress Accessories	Brooch	Annular	E. Sax	F	F	A(2)
104	2800		A		352	Sheet	Dress Accessories	Necklace	Pendant	E. Sax	F	F	A(2)
104	2821		A	Front	185	Sheet	Dress Accessories	Brooch	Annular	E. Sax	N/A	F	A(2)
104	2821		B	Reverse	185	Sheet	Dress Accessories	Brooch	Annular	E. Sax	N/A	F	A(2)
104	2823		A		185	Cast	Dress Accessories	Brooch	Annular	E. Sax	N/A	F	A(2)
104	2825		A		344	Cast	Dress Accessories	Belt Fitting	Small-Long	E. Sax	F	F	A(1)
104	2826		A		344	Sheet	Miscellaneous Fittings	Miscellaneous	Clip	E. Sax	F	F	A(1)
104	2827		A		344	Sheet	Miscellaneous Fittings	Miscellaneous	Clip	E. Sax	F	F	A(1)
104	2863		A		188	Cast	Dress Accessories	Buckle	Undefined Buckle	E. Sax	M	M	B
104	2865		A	Rivet 1 (head)	323	Cast	Equestrian objects	Tack	Undefined Equestrian	E. Sax	M	M	AB
104	2865		C	Rivet 2	323	Cast	Equestrian objects	Tack	Undefined Equestrian	E. Sax	M	M	AB
104	2865		E	Rivet 4	323	Cast	Equestrian objects	Tack	Undefined Equestrian	E. Sax	M	M	AB
104	2866		A	Bow (front)	180	Cast	Dress Accessories	Brooch	Small-Long	E. Sax	F	F	A(2)
104	2867		A		180	Cast	Dress Accessories	Brooch	Annular	E. Sax	F	F	A(2)
104	2868		A	Piece A	180	Sheet	Dress Accessories	Belt Fitting	Strap-end	E. Sax	F	F	A(2)
104	2868		B	Piece B	180	Sheet	Dress Accessories	Belt Fitting	Strap-end	E. Sax	F	F	A(2)
104	2869		A		180	Sheet	Unknown	Unknown	Unknown	E. Sax	F	F	A(2)

Site	SF no.	SF sub div.	Ana l. area	XRF Location	Grave no.	Manuf. method	Category	Class	Sub class	Cultural period	Ost. Sex	Assigned Gender	Grave Phase
104	2870		A	'Base' metal area	180	Sheet	Dress Accessories	Belt Fitting	Strap-end	E. Sax	F	F	A(2)
104	2870		B	Recorded as being a gilded in post ex. assessment. Analysis shows not gilded, simply uncorroded.	180	Sheet	Dress Accessories	Belt Fitting	Strap-end	E. Sax	F	F	A(2)
104	2879		A		180	Cast	Dress Accessories	Bead	Undefined Bead	E. Sax	F	F	A(2)
104	2888		A	Front	323	Cast	Equestrian objects	Tack	Strap-mount	E. Sax	M	M	AB
104	2895		A	Bow (front)	182	Cast	Dress Accessories	Belt Fitting	Small-Long	E. Sax	F	F	A(2)
104	2897		A		182	Cast	Dress Accessories	Brooch	Annular	E. Sax	F	F	A(2)
104	2899		A		182	Cast	Dress Accessories	Belt Fitting	Strap-end	E. Sax	F	F	A(2)
104	2902		A	Brooch	348	Cast	Dress Accessories	Brooch	Annular	E. Sax	c	F	A(2)
104	2902		B	Pin	348	Cast	Dress Accessories	Brooch	Annular	E. Sax	c	F	A(2)
104	2937		A		359	Sheet	Miscellaneous Fittings	Miscellaneous	Sheet	E. Sax	c	F	A(2)
104	2943		A		359	Sheet	Dress Accessories	Brooch	Annular	E. Sax	c	F	A(2)
104	2949		A		357	Sheet	Miscellaneous Fittings	Belt Fitting	Strap-end	E. Sax	M	M	AB
104	2950		B	Reverse	357	Cast	Miscellaneous Fittings	Nails and Bolts	Stud	E. Sax	M	M	AB
104	2993		A		349	Cast	Dress Accessories	Brooch	Annular	E. Sax	c	F	A(2)
104	2995		A	Large fragment	178	Sheet	Unknown	Unknown	Unknown	E. Sax	M	M	B
104	2995		B	Small fragment	178	Sheet	Unknown	Unknown	Unknown	E. Sax	M	M	B
104	3026		A	Curved sheet strip	176	Sheet	Personal equipment	Purse	Purse Fitting	E. Sax	c	F	A(2)
104	3026		B	Cast hoop	176	Cast	Personal equipment	Purse	Purse Fitting	E. Sax	c	F	A(2)
104	3045		A	Tube	176	Sheet	Dress Accessories	Bead	Undefined Bead	E. Sax	c	F	A(2)
104	3045		B	Sheet fragment	176	Sheet	Dress Accessories	Bead	Undefined Bead	E. Sax	c	F	A(2)
104	3045		C	Sheet fragment	176	Sheet	Dress Accessories	Bead	Undefined Bead	E. Sax	c	F	A(2)
104	3048		A	Pin head	176	Cast	Dress Accessories	Pin	Undefined Pin	E. Sax	c	F	A(2)

Site	SF no.	SF sub div.	Ana l. area	XRF Location	Grave no.	Manuf. method	Category	Class	Sub class	Cultural period	Ost. Sex	Assigned Gender	Grave Phase
104	3051		A	Front	176	Cast	Dress Accessories	Brooch	Annular	E. Sax	c	F	A(2)
104	3052		A	Front	176	Sheet	Dress Accessories	Brooch	Annular	E. Sax	c	F	A(2)
104	3059		A		366	Melted	Dress Accessories	Brooch	Cruciform	E. Sax	F	M	AB
104	3064		A			Melted	Unknown	Unknown	Unknown	E. Sax			
104	3077		A		172	Sheet	Dress Accessories	Wrist Clasp	Form B 7	E. Sax	F	F	A(2)
104	3078		A	Hook piece (front)	172	Sheet	Dress Accessories	Wrist Clasp	Form B 7	E. Sax	F	F	A(2)
104	3078		B	Eye piece (front)	172	Sheet	Dress Accessories	Wrist Clasp	Form B 7	E. Sax	F	F	A(2)
104	3088		A		175	Sheet	Unknown	Unknown	Unknown	E. Sax			
104	3089		A	Distal terminal (front right)	172	Cast	Dress Accessories	Belt Fitting	Girdle-hanger	E. Sax	F	F	A(2)
104	3090		B	Front	172	Cast	Dress Accessories	Belt Fitting	Girdle-hanger	E. Sax	F	F	A(2)
104	3091		A	Brooch	172	Sheet	Dress Accessories	Brooch	Annular	E. Sax	F	F	A(2)
104	3091		B	Pin	172	Cast	Dress Accessories	Brooch	Annular	E. Sax	F	F	A(2)
104	3093		A	Brooch	172	Sheet	Dress Accessories	Brooch	Annular	E. Sax	F	F	A(2)
104	3093		B	Pin	172	Sheet	Dress Accessories	Brooch	Annular	E. Sax	F	F	A(2)
104	3143		A		172	Sheet	Unknown	Unknown	Unknown	E. Sax	F	F	A(2)
104	3144		A		172	Sheet	Miscellaneous Fittings	Miscellaneous	Binding Ring	E. Sax	F	F	A(2)
104	3161		A		317	Sheet	Dress Accessories	Buckle	Undefined Buckle	E. Sax	M	M	AB
104	3165		A		310	Sheet	Miscellaneous Fittings	Miscellaneous	Sheet	E. Sax	M	M	B
104	3169		A		310	Sheet	Miscellaneous Fittings	Miscellaneous	Sheet	E. Sax	M	M	B
104	3170		A		310	Sheet	Miscellaneous Fittings	Miscellaneous	Clip	E. Sax	M	M	B
104	3203		A		302	Sheet	Dress Accessories	Ring	Bracelet	E. Sax	c	F	A(2)
104	3206		A		360	Sheet	Personal equipment	Purse	Purse Fitting	E. Sax			
104	3209		A			Wire	Miscellaneous Fittings	Fragment	Wire	E. Sax			
104	3210		A			Cast	Dress Accessories	Buckle	Buckle Pin	E. Sax			

Site	SF no.	SF sub div.	Ana l. area	XRF Location	Grave no.	Manuf. method	Category	Class	Sub class	Cultural period	Ost. Sex	Assigned Gender	Grave Phase
104	3223		A		311	Sheet	Miscellaneous Fittings	Miscellaneous	Sheet	E. Sax	M	M	B
104	3232		B	Cast buckle frame & prong	139	Cast	Dress Accessories	Buckle	Undefined Buckle	E. Sax	M	M	AB
104	3236		A			Melted	Unknown	Unknown	Unknown	E. Sax			
104	3249		A		221	Cast	Dress Accessories	Pin	Undefined Pin	E. Sax	M	M	C/EF
104	3283		A		309	Cast	Dress Accessories	Ring	Finger ring	E. Sax	F	F	A(2)
104	3299		B	Reverse	359	Sheet	Miscellaneous Fittings	Fragment	Sheet	E. Sax	c	F	A(2)
104	3299		C	Tube	359	Sheet	Miscellaneous Fittings	Fragment	Sheet	E. Sax	c	F	A(2)
104	3300		A		359	Sheet	Dress Accessories	Necklace	Pendant	E. Sax	c	F	A(2)
104	3313		A		263	Cast	Dress Accessories	Belt Fitting	Latch-lifter	E. Sax	F	F	A(2)
104	3314		A		263	Sheet	Dress Accessories	Belt Fitting	Strap-end	E. Sax	F	F	A(2)
104	3316		A	Buckle sheet	231	Sheet	Dress Accessories	Buckle	Undefined Buckle	E. Sax	c	F	A
104	3316		B	Frame and tongue	231	Cast	Dress Accessories	Buckle	Undefined Buckle	E. Sax	c	F	A
104	3316		C	Rolled sheet	231	Sheet	Dress Accessories	Buckle	Undefined Buckle	E. Sax	c	F	A
104	3317		A		231	Sheet	Miscellaneous Fittings	Fragment	Bracket	E. Sax	c	F	A
104	3318	f	A		231	Sheet	Dress Accessories	Belt Fitting	Strap-end	E. Sax	c	F	A
104	3318	e	A		231	Sheet	Dress Accessories	Belt Fitting	Strap-end	E. Sax	c	F	A
104	3318	d	A		231	Sheet	Dress Accessories	Belt Fitting	Strap-end	E. Sax	c	F	A
104	3318	c	A		231	Sheet	Dress Accessories	Belt Fitting	Strap-end	E. Sax	c	F	A
104	3318	b	A		231	Sheet	Dress Accessories	Belt Fitting	Strap-end	E. Sax	c	F	A
104	3318	a	A		231	Sheet	Dress Accessories	Belt Fitting	Strap-end	E. Sax	c	F	A
104	3327		A			Struck	Coins, Tokens and Jettons	Coin	Undefined Coin	E. Sax			
104	3328		A			Cast	Miscellaneous Fittings	Nails and Bolts	Stud	E. Sax			
104	3329		A			Cast	Miscellaneous Fittings	Nails and Bolts	Stud	E. Sax			

Site	SF no.	SF sub div.	Ana l. area	XRF Location	Grave no.	Manuf. method	Category	Class	Sub class	Cultural period	Ost. Sex	Assigned Gender	Grave Phase
104	3332		A		218	Wire	Dress Accessories	Miscellaneous	Chain	E. Sax	N/A	F	A(2)
104	3342		A	Front (wood on reverse). Fragment A.	153	Sheet	Miscellaneous Fittings	Miscellaneous	Sheet	E. Sax	c	M	AB
104	3342		B	Front (wood on reverse). Fragment B.	153	Sheet	Miscellaneous Fittings	Miscellaneous	Sheet	E. Sax	c	M	AB
104	3342		C	Front (wood on reverse). Fragment C.	153	Sheet	Miscellaneous Fittings	Miscellaneous	Sheet	E. Sax	c	M	AB
104	3348	b	A		292	Sheet	Unknown	Unknown	Unknown	E. Sax	F	F	A
104	3349		A	Eye piece (front)	292	Sheet	Dress Accessories	Wrist Clasp	Form B 13 a	E. Sax	F	F	A
104	3349		B	Hook piece (reverse)	292	Cast	Dress Accessories	Wrist Clasp	Form B 13 a	E. Sax	F	F	A
104	3349		C	Repousse sheet (front)	292	Sheet	Dress Accessories	Wrist Clasp	Form B 13 a	E. Sax	F	F	A
104	3349		E	Bar	292	Cast	Dress Accessories	Wrist Clasp	Form B 13 a	E. Sax	F	F	A
104	3350		B	Hook piece (reverse)	292	Sheet	Dress Accessories	Wrist Clasp	Form B 13 c	E. Sax	F	F	A
104	3350		D	Eye piece (reverse)	292	Sheet	Dress Accessories	Wrist Clasp	Form B 13 c	E. Sax	F	F	A
104	3350		F	Eye piece, repousse sheet (front)	292	Sheet	Dress Accessories	Wrist Clasp	Form B 13 c	E. Sax	F	F	A
104	3355		A	Bow (front)	292	Cast	Dress Accessories	Belt Fitting	Small-Long	E. Sax	F	F	A
104	3363		A	Large folded sheet with wood	157	Sheet	Miscellaneous Fittings	Miscellaneous	Sheet	E. Sax			
104	3363		B	Small fragment	157	Sheet	Miscellaneous Fittings	Miscellaneous	Sheet	E. Sax			
104	3363		C	Large sheet fragment (anaoiding bar)	157	Sheet	Miscellaneous Fittings	Miscellaneous	Sheet	E. Sax			
104	3363		D	Loose sheet strip	157	Sheet	Miscellaneous Fittings	Miscellaneous	Sheet	E. Sax			
104	3364		A		157	Sheet	Miscellaneous Fittings	Miscellaneous	Sheet	E. Sax			
104	3372		A		336	Cast	Dress Accessories	Brooch	Annular	E. Sax	c	F	A(2)
104	3373		A	Reverse	336	Sheet	Dress Accessories	Necklace	Pendant	E. Sax	c	F	A(2)
104	3373		B	Whitish residue	336	Sheet	Dress Accessories	Necklace	Pendant	E. Sax	c	F	A(2)
104	3387		A	Knot'	156	Wire	Dress Accessories	Ring	Bracelet	E. Sax			
104	3389		A		286	Cast	Dress Accessories	Brooch	Annular	E. Sax	N/A	F	A(2)

Site	SF no.	SF sub div.	Ana l. area	XRF Location	Grave no.	Manuf. method	Category	Class	Sub class	Cultural period	Ost. Sex	Assigned Gender	Grave Phase
104	3391		A	Front	286	Cast	Dress Accessories	Wrist Clasp	Undefined Wrist Clasp	E. Sax	N/A	F	A(2)
104	3393		A	Hook piece (front)	165	Cast	Dress Accessories	Wrist Clasp	Form B 7	E. Sax	F	F	A(2)
104	3393		B	Eye piece (reverse)	165	Cast	Dress Accessories	Wrist Clasp	Form B 7	E. Sax	F	F	A(2)
104	3394		A		165	Cast	Dress Accessories	Brooch	Annular	E. Sax	F	F	A(2)
104	3395		A	Front	165	Sheet	Dress Accessories	Brooch	Annular	E. Sax	F	F	A(2)
104	3396		A		171	Sheet	Unknown	Unknown	Unknown	E. Sax			
104	3443		A		166	Sheet	Miscellaneous Fittings	Miscellaneous	Rope	E. Sax	F	F	A(2)
104	3444		A		166	Cast	Dress Accessories	Brooch	Annular	E. Sax	F	F	A(2)
104	3453		B	Top	166	Cast	Dress Accessories	Brooch	Bar	E. Sax	F	F	A(2)
104	3460		A		166	Sheet	Dress Accessories	Brooch	Annular	E. Sax	F	F	A(2)
104	3475		A		171	Cast	Unknown	Unknown	Unknown	E. Sax			
104	3482		A	Only large enough for one analysis	116	Cast	Dress Accessories	Ring	Finger ring	E. Sax	N/A	F	DE
104	3494		A			Sheet	Unknown	Unknown	Unknown	E. Sax			
104	3495		A			Sheet	Unknown	Unknown	Unknown	E. Sax			
104	3524		A	Front	185	Cast	Dress Accessories	Wrist Clasp	Undefined Wrist Clasp	E. Sax	N/A	F	A(2)
104	3525		A		185	Sheet	Dress Accessories	Wrist Clasp	Undefined Wrist Clasp	E. Sax	N/A	F	A(2)
104	3530		A		206	Sheet	Dress Accessories	Pin	Undefined Pin	E. Sax			
104	3532		A	Reverse	206	Cast	Personal equipment	Purse	Purse Fitting	E. Sax			
104	3532	a	A		206	Cast	Personal equipment	Purse	Purse Fitting	E. Sax			
104	3532	1	A		206	Cast	Personal equipment	Purse	Purse Fitting	E. Sax			
104	3532		C	Reverse	206	Cast	Personal equipment	Purse	Purse Fitting	E. Sax			
104	3534		A	Front	182	Sheet	Miscellaneous Fittings	Miscellaneous	Box Fitting	E. Sax	F	F	A(2)
104	3573		A		166	Sheet	Miscellaneous Fittings	Miscellaneous	Sheet	E. Sax	F	F	A(2)

Site	SF no.	SF sub div.	Ana l. area	XRF Location	Grave no.	Manuf. method	Category	Class	Sub class	Cultural period	Ost. Sex	Assigned Gender	Grave Phase
104	3577		A		232	Sheet	Dress Accessories	Bead	Undefined Bead	E. Sax	c	F	A(2)
104	3579		A		268	Cast	Dress Accessories	Brooch	Penannular	E. Sax	F	F	A(2)
104	3580		A	Reverse	359	Cast	Dress Accessories	Brooch	Annular	E. Sax	c	F	A(2)
104	3581		A	Repousse sheet (small fragment, reverse)	221	Sheet	Miscellaneous Fittings	Miscellaneous	Sheet	E. Sax	M	M	C/EF
104	3582		A	Outer edge	309	Cast	Dress Accessories	Brooch	Annular	E. Sax	F	F	A(2)
104	3596		A		350	Cast	Dress Accessories	Belt Fitting	Girdle-hanger	E. Sax	N/A	F	A(2)
104	3597		A		350	Sheet	Miscellaneous Fittings	Miscellaneous	Sheet	E. Sax	N/A	F	A(2)
104	3616		A			Melted	Dress Accessories	Brooch	Undefined Brooch	E. Sax			
104	3618		A	Drop A		Melted	Unknown	Unknown	Unknown	E. Sax			
104	3618		C	Drop C		Melted	Unknown	Unknown	Unknown	E. Sax			
104	3618		D	Drop D		Melted	Unknown	Unknown	Unknown	E. Sax			
104	3674	2	B	Reverse of Stud	168	Cast	Military and weaponry	Shield	Shield Mount	E. Sax	N/A	M	B
104	3675	1	A	Thin plate on front of stud	168	Sheet	Military and weaponry	Shield	Shield Mount	E. Sax	N/A	M	B
104	3675	3	B	Reverse	168	Sheet	Military and weaponry	Shield	Shield Mount	E. Sax	N/A	M	B
104	3675	1	B	Reverse of Stud	168	Cast	Military and weaponry	Shield	Shield Mount	E. Sax	N/A	M	B
104	3677		A	Front	168	Sheet	Dress Accessories	Buckle	Undefined Buckle	E. Sax	N/A	M	B
104	3677		B	Front	168	Sheet	Dress Accessories	Buckle	Undefined Buckle	E. Sax	N/A	M	B
104	4211		A	Bow (front)	Unknown	Cast	Unknown	Unknown	Unknown	Unknown			
104	BM1		F	Reverse (arm)	323	Cast	Equestrian objects	Tack	Bridle Fitting	E. Sax	M	M	AB
104	BM1		G	Stud	323	Cast	Equestrian objects	Tack	Bridle Fitting	E. Sax	M	M	AB
104	BM1 2		A	Reverse (foot)	323	Cast	Equestrian objects	Tack	Bridle Fitting	E. Sax	M	M	AB
104	BM1 2		B	Reverse	323	Sheet	Equestrian objects	Tack	Bridle Fitting	E. Sax	M	M	AB
104	BM1 3		A	Rivet	323	Cast	Equestrian objects	Tack	Bridle Fitting	E. Sax	M	M	AB

Site	SF no.	SF sub div.	Ana l. area	XRF Location	Grave no.	Manuf. method	Category	Class	Sub class	Cultural period	Ost. Sex	Assigned Gender	Grave Phase
104	BM18		C	Arm (no plate)	323	Cast	Equestrian objects	Tack	Bridle Fitting	E. Sax	M	M	AB
104	BM18		D	Reverse (stud)	323	Cast	Equestrian objects	Tack	Bridle Fitting	E. Sax	M	M	AB
104	BM18		E	Reverse (arm)	323	Cast	Equestrian objects	Tack	Bridle Fitting	E. Sax	M	M	AB
104	BM19		D	Rivet	323	Cast	Equestrian objects	Tack	Bridle Fitting	E. Sax	M	M	AB
104	BM19		E	Reverse	323	Cast	Equestrian objects	Tack	Bridle Fitting	E. Sax	M	M	AB
104	BM20		B	Front (concave face)	323	Sheet	Equestrian objects	Tack	Bridle Fitting	E. Sax	M	M	AB
104	BM21		A	Front	323	Sheet	Equestrian objects	Tack	Bridle Fitting	E. Sax	M	M	AB
104	BM3		D	Reverse	323	Cast	Equestrian objects	Tack	Bridle Fitting	E. Sax	M	M	AB
104	BM33		C	Reverse (base metal)	323	Cast	Equestrian objects	Tack	Bridle Fitting	E. Sax	M	M	AB
104	BM5		F	Reverse (arm)	323	Cast	Equestrian objects	Tack	Bridle Fitting	E. Sax	M	M	AB
104	BM5		G	Central stud	323	Cast	Equestrian objects	Tack	Bridle Fitting	E. Sax	M	M	AB
104	BM6	7A	B	Rivet	323	Cast	Equestrian objects	Tack	Bit	E. Sax	M	M	AB
104	BM6	7A	C	Rivet	323	Cast	Equestrian objects	Tack	Bit	E. Sax	M	M	AB
104	BM6	7A	F	Brass strip	323	Sheet	Equestrian objects	Tack	Bit	E. Sax	M	M	AB
104	BM6	7A	G	Brass strip	323	Sheet	Equestrian objects	Tack	Bit	E. Sax	M	M	AB
114	1000		A	Head side		Struck	Coins, Tokens and Jettons	Coin	Undefined Coin	Roman			
114	1001		A	Rear		Cast	Dress Accessories	Brooch	Annular	E. Sax			
114	1004		A	foot	423	Cast	Dress Accessories	Brooch	Small-Long	E. Sax	N/A	F	A(2)
114	1005		A	Front	423	Cast	Dress Accessories	Brooch	Annular	E. Sax	N/A	F	A(2)
114	1007		B	Reverse	432	Cast	Military and weaponry	Shield	Misc. Shield Fragment	E. Sax	N/A	M	BC
114	1034		A	Front	423	Cast	Dress Accessories	Brooch	Annular	E. Sax	N/A	F	A(2)
114	1036		A		432	Cast	Military and weaponry	Shield	Misc. Shield Fragment	E. Sax	N/A	M	BC

Site	SF no.	SF sub div.	Ana l. area	XRF Location	Grave no.	Manuf. method	Category	Class	Sub class	Cultural period	Ost. Sex	Assigned Gender	Grave Phase
114	1037		B	Reverse	432	Cast	Military and weaponry	Shield	Misc. Shield Fragment	E. Sax	N/A	M	BC
114	1039		B	Reverse	432	Cast	Military and weaponry	Shield	Misc. Shield Fragment	E. Sax	N/A	M	BC
114	1040		A	Outer		Melted	Unknown	Unknown	Unknown	E. Sax			
114	1044		B	Reverse	432	Cast	Military and weaponry	Shield	Misc. Shield Fragment	E. Sax	N/A	M	BC
114	1048		A	Hook piece (front)	443	Cast	Dress Accessories	Wrist Clasp	Undefined Wrist Clasp	E. Sax	N/A	M	AB
114	1048		B	Bar (rear)	443	Cast	Dress Accessories	Wrist Clasp	Undefined Wrist Clasp	E. Sax	N/A	M	AB
114	1050		A	Outer		Sheet	Unknown	Unknown	Unknown	E. Sax			
114	1051		A	Hook piece (front)	443	Cast	Dress Accessories	Wrist Clasp	Undefined Wrist Clasp	E. Sax	N/A	M	AB
114	1051		B	Bar (reverse)	443	Cast	Dress Accessories	Wrist Clasp	Undefined Wrist Clasp	E. Sax	N/A	M	AB
114	1055		A	Reverse	465	Sheet	Dress Accessories	Brooch	Annular	E. Sax			
114	1055		B	Pin	465	Wire	Dress Accessories	Brooch	Annular	E. Sax			
114	1058		A		447	Cast	Dress Accessories	Brooch	Applied disc	E. Sax	N/A	F	A(2)
114	1059		A		447	Cast	Dress Accessories	Brooch	Applied disc	E. Sax	N/A	F	A(2)
114	1060		A		447	Cast	Dress Accessories	Brooch	Applied disc	E. Sax	N/A	F	A(2)
114	1061	A	A	Distal Terminal (rear)	447	Cast	Dress Accessories	Belt Fitting	Girdle-hanger	E. Sax	N/A	F	A(2)
114	1061	B	A	Distal Terminal (rear)	447	Cast	Dress Accessories	Belt Fitting	Girdle-hanger	E. Sax	N/A	F	A(2)
114	1061	C	A	Rounded Proximal Terminal (right, front)	447	Cast	Dress Accessories	Belt Fitting	Girdle-hanger	E. Sax	N/A	F	A(2)
114	1061	C	B	Upper Shaft front (two sheets joining the Distal Terminal and Central Shaft together)	447	Sheet	Dress Accessories	Belt Fitting	Girdle-hanger	E. Sax	N/A	F	A(2)
114	1061	C	C	Central Shaft (front)	447	Cast	Dress Accessories	Belt Fitting	Girdle-hanger	E. Sax	N/A	F	A(2)
114	1062		A		447	Cast	Dress Accessories	Brooch	Applied disc	E. Sax	N/A	F	A(2)
114	1064		A	Bow front	429	Cast	Dress Accessories	Brooch	Small-Long	E. Sax	N/A	F	A(2)

Site	SF no.	SF sub div.	Ana l. area	XRF Location	Grave no.	Manuf. method	Category	Class	Sub class	Cultural period	Ost. Sex	Assigned Gender	Grave Phase
114	1064		B	Catch	429	Cast	Dress Accessories	Brooch	Small-Long	E. Sax	N/A	F	A(2)
114	1065		A		429	Cast	Dress Accessories	Brooch	Small-Long	E. Sax	N/A	F	A(2)
114	1066		A	Hook piece front	429	Cast	Dress Accessories	Wrist Clasp	Undefined Wrist Clasp	E. Sax	N/A	F	A(2)
114	1066		B	Eye piece front	429	Cast	Dress Accessories	Wrist Clasp	Undefined Wrist Clasp	E. Sax	N/A	F	A(2)
114	1067		A	Hook piece front	429	Cast	Dress Accessories	Wrist Clasp	Undefined Wrist Clasp	E. Sax	N/A	F	A(2)
114	1067		B	Eye piece front	429	Cast	Dress Accessories	Wrist Clasp	Undefined Wrist Clasp	E. Sax	N/A	F	A(2)
114	1069		A		447	Cast	Dress Accessories	Brooch	Applied disc	E. Sax	N/A	F	A(2)
114	1070		A		447	Cast	Dress Accessories	Brooch	Applied disc	E. Sax	N/A	F	A(2)
114	1075		A		447	Cast	Dress Accessories	Brooch	Applied disc	E. Sax	N/A	F	A(2)
114	1094		A	Bow (front)	450	Cast	Dress Accessories	Brooch	Cruciform	E. Sax	N/A	F	A(2)
114	1148		A	Foot front	456	Cast	Dress Accessories	Buckle	Undefined Buckle	E. Sax	M	M	B
114	1159		A		434	Cast	Personal equipment	Implement	Awl	Bronze Age?			
114	1161		A	Front	450	Cast	Dress Accessories	Brooch	Annular	E. Sax	N/A	F	A(2)
114	1162		A	Front	450	Cast	Dress Accessories	Wrist Clasp	Undefined Wrist Clasp	E. Sax	N/A	F	A(2)
114	1162		B	Loose sheet	450	Sheet	Dress Accessories	Wrist Clasp	Undefined Wrist Clasp	E. Sax	N/A	F	A(2)
114	1163		A	Eye piece (reverse)	450	Cast	Dress Accessories	Wrist Clasp	Undefined Wrist Clasp	E. Sax	N/A	F	A(2)
114	1163		B	Hook piece (front)	450	Sheet	Dress Accessories	Wrist Clasp	Undefined Wrist Clasp	E. Sax	N/A	F	A(2)
114	1175		A	Outer crossover	450	Wire	Dress Accessories	Necklace	Necklace Ring	E. Sax	N/A	F	A(2)
114	1227		A	Bow (front)	458	Cast	Dress Accessories	Brooch	Cruciform	E. Sax	c	F	A(2)
114	1227		B	Catch	458	Cast	Dress Accessories	Brooch	Cruciform	E. Sax	c	F	A(2)
114	1228		A		458	Sheet	Dress Accessories	Brooch	Annular	E. Sax	c	F	A(2)
114	1242		A	Front	450	Cast	Dress Accessories	Brooch	Annular	E. Sax	N/A	F	A(2)

Site	SF no.	SF sub div.	Ana l. area	XRF Location	Grave no.	Manuf. method	Category	Class	Sub class	Cultural period	Ost. Sex	Assigned Gender	Grave Phase
114	1243		A	Hoop	458	Sheet	Dress Accessories	Bead	Undefined Bead	E. Sax	c	F	A(2)
114	1244		A	Hoop	458	Sheet	Dress Accessories	Bead	Undefined Bead	E. Sax	c	F	A(2)
114	1244		B	Disc	458	Sheet	Dress Accessories	Bead	Undefined Bead	E. Sax	c	F	A(2)
114	1245		A	Hoop	458	Sheet	Dress Accessories	Bead	Undefined Bead	E. Sax	c	F	A(2)
114	1245		B	Disc	458	Sheet	Dress Accessories	Bead	Undefined Bead	E. Sax	c	F	A(2)
114	1246		A	Hoop	458	Sheet	Dress Accessories	Bead	Undefined Bead	E. Sax	c	F	A(2)
114	1246		B	Disc	458	Sheet	Dress Accessories	Bead	Undefined Bead	E. Sax	c	F	A(2)
114	1247		A	Hoop	458	Sheet	Dress Accessories	Bead	Undefined Bead	E. Sax	c	F	A(2)
114	1248		A	Hoop	458	Sheet	Dress Accessories	Bead	Undefined Bead	E. Sax	c	F	A(2)
114	1248		B	Disc	458	Sheet	Dress Accessories	Bead	Undefined Bead	E. Sax	c	F	A(2)
114	1249		A	Hoop	458	Sheet	Dress Accessories	Bead	Undefined Bead	E. Sax	c	F	A(2)
114	1249		B	Disc	458	Sheet	Dress Accessories	Bead	Undefined Bead	E. Sax	c	F	A(2)
114	1250		A		458	Sheet	Dress Accessories	Bead	Undefined Bead	E. Sax	c	F	A(2)
114	1251		A	Hoop	458	Sheet	Dress Accessories	Bead	Undefined Bead	E. Sax	c	F	A(2)
114	1254		A		467	Cast	Dress Accessories	Brooch	Annular	E. Sax	N/A	F	A(2)
114	1255		A		467	Cast	Dress Accessories	Brooch	Annular	E. Sax	N/A	F	A(2)
114	1292		A		458	Sheet	Dress Accessories	Brooch	Annular	E. Sax	c	F	A(2)
114	1296		A	Front	445	Cast	Dress Accessories	Brooch	Annular	E. Sax	N/A	F	A(2)
114	1297		A	Front	445	Cast	Dress Accessories	Brooch	Annular	E. Sax	N/A	F	A(2)
114	1298		A	Bow (front)	445	Cast	Dress Accessories	Brooch	Cruciform	E. Sax	N/A	F	A(2)
114	1298		C	Small sheet bracket	445	Sheet	Dress Accessories	Brooch	Cruciform	E. Sax	N/A	F	A(2)
114	1319		A	Front	459	Cast	Dress Accessories	Brooch	Annular	E. Sax	F	F	A(2)
114	1319		B	Pin	459	Cast	Dress Accessories	Brooch	Annular	E. Sax	F	F	A(2)
114	1321		A		459	Cast	Dress Accessories	Belt Fitting	Belt ring	E. Sax	F	F	A(2)

Site	SF no.	SF sub div.	Ana l. area	XRF Location	Grave no.	Manuf. method	Category	Class	Sub class	Cultural period	Ost. Sex	Assigned Gender	Grave Phase
114	1322		A		459	Cast	Dress Accessories	Wrist Clasp	Undefined Wrist Clasp	E. Sax	F	F	A(2)
114	1341		A	Reverse	409	Cast	Dress Accessories	Wrist Clasp	Undefined Wrist Clasp	E. Sax	N/A	F	A
114	1342		A	Reverse	409	Cast	Dress Accessories	Wrist Clasp	Undefined Wrist Clasp	E. Sax	N/A	F	A
114	1343		A	Front	409	Cast	Dress Accessories	Wrist Clasp	Undefined Wrist Clasp	E. Sax	N/A	F	A
114	1344		A	Front	409	Cast	Dress Accessories	Wrist Clasp	Undefined Wrist Clasp	E. Sax	N/A	F	A
114	1347		A	Front	421	Cast	Dress Accessories	Buckle	Undefined Buckle	E. Sax	N/A	F	A(2)
114	1348		A		421	Cast	Dress Accessories	Brooch	Small-Long	E. Sax	N/A	F	A(2)
114	1349		A	Bow front	421	Cast	Dress Accessories	Brooch	Small-Long	E. Sax	N/A	F	A(2)
114	1370		A		422	Sheet	Dress Accessories	Bead	Undefined Bead	E. Sax	N/A	F	A(2)
114	1374		A	Tag	422	Sheet	Dress Accessories	Necklace	Pendant	E. Sax	N/A	F	A(2)
114	1374		B	Ring	422	Wire	Dress Accessories	Necklace	Pendant	E. Sax	N/A	F	A(2)
114	1375		A	Front of first (smaller) piece	422	Cast	Dress Accessories	Brooch	Annular	E. Sax	N/A	F	A(2)
114	1378		A	Tag	422	Sheet	Dress Accessories	Bead	Undefined Buckle	E. Sax	N/A	F	A(2)
114	1378		B	Ring	422	Cast	Dress Accessories	Bead	Undefined Buckle	E. Sax	N/A	F	A(2)
114	1380		A		422	Sheet	Dress Accessories	Bead	Undefined Bead	E. Sax	N/A	F	A(2)
114	1383		A	Eye piece	422	Cast	Dress Accessories	Wrist Clasp	Undefined Wrist Clasp	E. Sax	N/A	F	A(2)
114	1383		B	Hook piece	422	Cast	Dress Accessories	Wrist Clasp	Undefined Wrist Clasp	E. Sax	N/A	F	A(2)
114	1384		A	Eye piece front	422	Cast	Dress Accessories	Wrist Clasp	Undefined Wrist Clasp	E. Sax	N/A	F	A(2)
114	1384		B	Hook piece front	422	Cast	Dress Accessories	Wrist Clasp	Undefined Wrist Clasp	E. Sax	N/A	F	A(2)
114	1385		A	Large fragment	422	Cast	Dress Accessories	Belt Fitting	Strap-end	E. Sax	N/A	F	A(2)
114	1386		A	Reverse of small piece	422	Sheet	Dress Accessories	Belt Fitting	Strap-mount	E. Sax	N/A	F	A(2)
114	1387		A		422	Sheet	Dress Accessories	Belt Fitting	Strap-mount	E. Sax	N/A	F	A(2)

Site	SF no.	SF sub div.	Ana l. area	XRF Location	Grave no.	Manuf. method	Category	Class	Sub class	Cultural period	Ost. Sex	Assigned Gender	Grave Phase
114	1388		A		422	Sheet	Dress Accessories	Belt Fitting	Strap-mount	E. Sax	N/A	F	A(2)
114	1389		A		422	Sheet	Dress Accessories	Belt Fitting	Strap-mount	E. Sax	N/A	F	A(2)
114	1392		A	Small disc	422	Sheet	Dress Accessories	Bead	Undefined Bead	E. Sax	N/A	F	A(2)
114	1392		B	Small fragment.	422	Sheet	Dress Accessories	Bead	Undefined Bead	E. Sax	N/A	F	A(2)
114	1393		A		422	Sheet	Dress Accessories	Bead	Undefined Bead	E. Sax	N/A	F	A(2)
114	1394		A		422	Sheet	Dress Accessories	Bead	Undefined Bead	E. Sax	N/A	F	A(2)
114	1395		A	Disc	422	Sheet	Dress Accessories	Bead	Undefined Bead	E. Sax	N/A	F	A(2)
114	1398		A		422	Sheet	Dress Accessories	Belt Fitting	Strap-mount	E. Sax	N/A	F	A(2)
114	1399		A		422	Sheet	Dress Accessories	Belt Fitting	Strap-mount	E. Sax	N/A	F	A(2)
114	1400		A	Front		Cast	Dress Accessories	Wrist Clasp	Undefined Wrist Clasp	E. Sax			
114	1401		A		422	Sheet	Miscellaneous Fittings	Miscellaneous	Sheet	E. Sax	N/A	F	A(2)
114	1402		A	Distal Terminal (front)	422	Cast	Dress Accessories	Belt Fitting	Girdle-hanger	E. Sax	N/A	F	A(2)
114	1405		A	Reverse	422	Cast	Dress Accessories	Belt Fitting	Girdle-hanger	E. Sax	N/A	F	A(2)
114	1408		A	Front	422	Sheet	Miscellaneous Fittings	Miscellaneous	Sheet	E. Sax	N/A	F	A(2)
114	1414		A		419	Sheet	Miscellaneous Fittings	Miscellaneous	Sheet	E. Sax			
114	1430		A		422	Sheet	Dress Accessories	Bead	Undefined Bead	E. Sax	N/A	F	A(2)
114	1431		A	Only big enough for one analysis	422	Sheet	Dress Accessories	Bead	Undefined Bead	E. Sax	N/A	F	A(2)
114	1432		A		422	Sheet	Dress Accessories	Bead	Undefined Bead	E. Sax	N/A	F	A(2)
114	1433		A		422	Sheet	Dress Accessories	Bead	Undefined Bead	E. Sax	N/A	F	A(2)
114	1434		A		422	Sheet	Dress Accessories	Bead	Undefined Bead	E. Sax	N/A	F	A(2)
114	1435		A	Tag	422	Sheet	Dress Accessories	Necklace	Pendant	E. Sax	N/A	F	A(2)
114	1435		B	Ring	422	Wire	Dress Accessories	Necklace	Pendant	E. Sax	N/A	F	A(2)
114	1436		A		422	Sheet	Dress Accessories	Bead	Undefined Bead	E. Sax	N/A	F	A(2)

Site	SF no.	SF sub div.	Ana l. area	XRF Location	Grave no.	Manuf. method	Category	Class	Sub class	Cultural period	Ost. Sex	Assigned Gender	Grave Phase
114	1437		A	Tag	422	Sheet	Dress Accessories	Necklace	Pendant	E. Sax	N/A	F	A(2)
114	1437		B	Ring	422	Wire	Dress Accessories	Necklace	Pendant	E. Sax	N/A	F	A(2)
114	1438		A	Tag	422	Sheet	Dress Accessories	Necklace	Pendant	E. Sax	N/A	F	A(2)
114	1438		B	Ring	422	Wire	Dress Accessories	Necklace	Pendant	E. Sax	N/A	F	A(2)
114	1439		A	Tag	422	Sheet	Dress Accessories	Necklace	Pendant	E. Sax	N/A	F	A(2)
114	1439		B	Ring	422	Wire	Dress Accessories	Necklace	Pendant	E. Sax	N/A	F	A(2)
114	1440		A	Tag	422	Sheet	Dress Accessories	Necklace	Pendant	E. Sax	N/A	F	A(2)
114	1442		A		422	Sheet	Dress Accessories	Bead	Undefined Bead	E. Sax	N/A	F	A(2)
114	1450		A	Front	422	Cast	Dress Accessories	Brooch	Annular	E. Sax	N/A	F	A(2)
114	1452		A	Front	422	Sheet	Dress Accessories	Bead	Undefined Bead	E. Sax	N/A	F	A(2)
114	1458		A	Hoop	422	Sheet	Dress Accessories	Bead	Undefined Bead	E. Sax	N/A	F	A(2)
114	1460		A		422	Sheet	Dress Accessories	Bead	Undefined Bead	E. Sax	N/A	F	A(2)
114	1461		A		422	Sheet	Dress Accessories	Bead	Undefined Bead	E. Sax	N/A	F	A(2)
114	1464		B	Reverse	417	Cast	Dress Accessories	Necklace	Pendant	E. Sax	N/A	F	A(2)
114	1465		A		417	Cast	Dress Accessories	Brooch	Annular	E. Sax	N/A	F	A(2)
114	1479		A		405	Sheet	Dress Accessories	Wrist Clasp	Undefined Wrist Clasp	E. Sax	N/A	F	A(1)
114	1480		A	Bow	405	Cast	Dress Accessories	Brooch	Small-Long	E. Sax	N/A	F	A(1)
114	1481		A	Reverse (right)	405	Cast	Dress Accessories	Wrist Clasp	Undefined Wrist Clasp	E. Sax	N/A	F	A(1)
114	1483		A	Reverse (right)	405	Wire	Dress Accessories	Ring	Finger ring	E. Sax	N/A	F	A(1)
114	1484		A	Reverse (right)	405	Cast	Dress Accessories	Wrist Clasp	Undefined Wrist Clasp	E. Sax	N/A	F	A(1)
114	1484		B	Sheet Metal	405	Sheet	Dress Accessories	Wrist Clasp	Undefined Wrist Clasp	E. Sax	N/A	F	A(1)
114	1484		C	Frag	405	Sheet	Dress Accessories	Wrist Clasp	Undefined Wrist Clasp	E. Sax	N/A	F	A(1)
114	1486		A		413	Cast	Dress Accessories	Bead	Undefined Buckle	E. Sax	N/A	F	A(2)

Site	SF no.	SF sub div.	Ana l. area	XRF Location	Grave no.	Manuf. method	Category	Class	Sub class	Cultural period	Ost. Sex	Assigned Gender	Grave Phase
114	1487		A	Reverse	413	Cast	Dress Accessories	Brooch	Annular	E. Sax	N/A	F	A(2)
114	1488		A	Front	413	Cast	Dress Accessories	Brooch	Annular	E. Sax	N/A	F	A(2)
114	1491		A	Reverse	405	Cast	Dress Accessories	Wrist Clasp	Undefined Wrist Clasp	E. Sax	N/A	F	A(1)
114	1491		B	Sheet Metal	405	Sheet	Dress Accessories	Wrist Clasp	Undefined Wrist Clasp	E. Sax	N/A	F	A(1)
114	1491		C	Piece with two holes	405	Cast	Dress Accessories	Wrist Clasp	Undefined Wrist Clasp	E. Sax	N/A	F	A(1)
114	1491		D	Piece with one hole	405	Cast	Dress Accessories	Wrist Clasp	Undefined Wrist Clasp	E. Sax	N/A	F	A(1)
114	1501		A	Reverse		Struck	Coins, Tokens and Jettons	Coin	Undefined Coin	Roman			
114	1503		A	Reverse	462	Cast	Dress Accessories	Belt Fitting	Belt ring	E. Sax	F	F	A(2)
114	1504		A		462	Wire	Dress Accessories	Ring	Finger ring	E. Sax	F	F	A(2)
114	1505		A		462	Cast	Dress Accessories	Brooch	Annular	E. Sax	F	F	A(2)
114	1536		A		405	Cast	Dress Accessories	Wrist Clasp	Undefined Wrist Clasp	E. Sax	N/A	F	A(1)
114	1602		A	White layer	459	Sheet	Dress Accessories	Necklace	Pendant	E. Sax	F	F	A(2)
114	1603		A	White layer	459	Sheet	Dress Accessories	Necklace	Pendant	E. Sax	F	F	A(2)
114	1613		A	Bow (front)	443	Cast	Dress Accessories	Brooch	Cruciform	E. Sax	N/A	M	AB

Appendix XV. COPPER ALLOY NET PEAK AREA DATA

HHpXRF analytical data from Eriswell silver objects (sorted by small find number). The unshaded row shows the net peak areas (mean if more than one analysis taken) for each element, the second (shaded) row shows the coefficient of variation. The final column shows the number of analyses.

For the associated categorical variable data see Appendix XIV.

<i>Site</i>	SF no.	SF sub div.	Anal . area	XRF location	Manuf. method	Cu (K)	Pb (L)	Sn (K)	Ag (K)	As (K)	Ni (K)	Sb (K)	Au (L)	Bi (L)	Zn (K)	Co (K)	No. of analyses
<i>046</i>	1002		A	Reverse	Cast	1894892	121439	99241	4102	3838					68876		4
						<i>0.29</i>	<i>0.22</i>	<i>0.41</i>	<i>0.33</i>	<i>1.16</i>					<i>0.36</i>		
<i>046</i>	1006		A	Front	Cast	1387053	11771	204226	2889	1820		2273					4
						<i>0.25</i>	<i>0.20</i>	<i>0.19</i>	<i>0.18</i>	<i>0.68</i>		<i>0.13</i>					
<i>046</i>	1012		A	Front	Sheet	1471406	127503	207152	4048	1985		139			42902		2
						<i>0.02</i>	<i>0.48</i>	<i>0.49</i>	<i>1.41</i>	<i>1.41</i>		<i>1.41</i>			<i>0.03</i>		
<i>046</i>	1026		A	Pincer end	Sheet	684888	295888	318868	5226	12374	674		228		46322		4
						<i>0.25</i>	<i>0.18</i>	<i>0.16</i>	<i>0.71</i>	<i>0.69</i>	<i>1.16</i>		<i>2.00</i>		<i>0.13</i>		
<i>046</i>	1056		A	Central panel (front)	Cast	3788640	64715	72163	5650		7226				212236		3
						<i>0.11</i>	<i>0.33</i>	<i>0.09</i>	<i>0.12</i>		<i>0.06</i>				<i>0.08</i>		
<i>046</i>	1059		A	Front	Cast	2054097	156577	129850	5413			762			95692		4
						<i>0.17</i>	<i>0.62</i>	<i>0.14</i>	<i>0.14</i>			<i>0.25</i>			<i>0.33</i>		
<i>046</i>	1060		A	Front	Cast	1633676	148478	113496	14888						54071		3
						<i>0.27</i>	<i>0.21</i>	<i>0.30</i>	<i>0.37</i>						<i>0.30</i>		

<i>Site</i>	SF no.	SF sub div.	Anal . area	XRF location	Manuf. method	Cu (K)	Pb (L)	Sn (K)	Ag (K)	As (K)	Ni (K)	Sb (K)	Au (L)	Bi (L)	Zn (K)	Co (K)	No. of analyses
<i>046</i>	1068		A		Cast	2110134	212057	106177	11067	12668	1138	654			462131		5
						<i>0.18</i>	<i>0.42</i>	<i>0.28</i>	<i>0.40</i>	<i>0.56</i>	<i>1.37</i>	<i>0.94</i>			<i>0.55</i>		
<i>046</i>	1095		A		Cast	1686964	51025	159394	1788	4713	2152	871			47569		3
						<i>0.11</i>	<i>0.29</i>	<i>0.10</i>	<i>0.88</i>	<i>0.26</i>	<i>0.88</i>	<i>0.88</i>			<i>0.14</i>		
<i>046</i>	1097		A		Cast	789696	73981	117353	5962						13522		3
						<i>0.21</i>	<i>0.19</i>	<i>0.21</i>	<i>0.21</i>						<i>0.13</i>		
<i>046</i>	1098		A	Plate	Cast	1793466	296513	193330	4605						137275		3
						<i>0.14</i>	<i>0.13</i>	<i>0.07</i>	<i>0.06</i>						<i>0.13</i>		
<i>046</i>	1098		B	Bar	Cast	1113333	278611	165479	4495						26710		2
						<i>0.07</i>	<i>0.17</i>	<i>0.06</i>	<i>0.04</i>						<i>0.06</i>		
<i>046</i>	1099		A	Plate	Cast	2645839	119328	135280	1971						214950		4
						<i>0.13</i>	<i>0.31</i>	<i>0.14</i>	<i>0.20</i>						<i>0.31</i>		
<i>046</i>	1099		B	Bar	Cast	1141546	186025	165417	3122						34050		2
						<i>0.41</i>	<i>0.27</i>	<i>0.54</i>	<i>0.36</i>						<i>0.27</i>		
<i>046</i>	1100		A	Plate	Cast	1961434	212362	198259	5778						140685		4
						<i>0.27</i>	<i>0.29</i>	<i>0.16</i>	<i>0.58</i>						<i>0.41</i>		
<i>046</i>	1100		B	Bar	Cast	1043685	276726	172944							17497		2
						<i>0.26</i>	<i>0.01</i>	<i>0.09</i>							<i>0.18</i>		
<i>046</i>	1101		A	Plate	Cast	2673089	73824	162616	3310						195274		4
						<i>0.20</i>	<i>0.37</i>	<i>0.30</i>	<i>0.13</i>						<i>0.23</i>		
<i>046</i>	1101		B	Bar	Cast	1560780	67833	140439	4558						36252		2
						<i>0.12</i>	<i>0.07</i>	<i>0.38</i>	<i>0.21</i>						<i>0.17</i>		
<i>046</i>	1106		A	Distal Terminal (front)	Cast	2860611	146439	148017	13167			136			147074		6
						<i>0.19</i>	<i>0.40</i>	<i>0.21</i>	<i>0.21</i>			<i>2.45</i>			<i>0.28</i>		

<i>Site</i>	SF no.	SF sub div.	Anal. area	XRF location	Manuf. method	Cu (K)	Pb (L)	Sn (K)	Ag (K)	As (K)	Ni (K)	Sb (K)	Au (L)	Bi (L)	Zn (K)	Co (K)	No. of analyses
<i>046</i>	1107		A	Distal Terminal (front)	Cast	2751616	119128	92860	12492	1956					126781		6
						<i>0.15</i>	<i>0.46</i>	<i>0.30</i>	<i>0.31</i>	<i>2.45</i>					<i>0.39</i>		
<i>046</i>	1108		A	Central Shaft (front)	Cast	2169544	205925	198833	7046	19580	5088				234888		2
						<i>0.03</i>	<i>0.10</i>	<i>0.02</i>	<i>0.04</i>	<i>0.01</i>	<i>0.02</i>				<i>0.01</i>		
<i>046</i>	1140		A	Spiral (part of broken whole)	Wire	2077193	107954	55612	2723	6893	3444				687583		6
						<i>0.06</i>	<i>0.37</i>	<i>0.20</i>	<i>0.23</i>	<i>0.33</i>	<i>0.16</i>				<i>0.17</i>		
<i>046</i>	1140		B	Spiral, not attached to A	Wire	2194034	53957	62706	3190	4009					864169		1
<i>046</i>	1141		A	Spiral	Wire	2038070	95542	67046	3627	8279				818	332100		2
						<i>0.04</i>	<i>0.20</i>	<i>0.25</i>	<i>0.15</i>	<i>0.31</i>				<i>1.41</i>	<i>0.21</i>		
<i>046</i>	1141		B	Spiral	Wire	2601522	96602	58994	3016	7372					527094		2
						<i>0.12</i>	<i>0.42</i>	<i>0.24</i>	<i>0.16</i>	<i>0.39</i>					<i>0.10</i>		
<i>046</i>	1150		A		Cast	1119908	20754	135664	2403						40125		4
						<i>0.02</i>	<i>0.12</i>	<i>0.17</i>	<i>0.12</i>						<i>0.28</i>		
<i>046</i>	1160		A	Spiral	Cast	1848527	10341	6279	3705						116205		1
<i>046</i>	1160		B	Main bar	Cast	2706554	20444	14126	6456						71588		2
						<i>0.03</i>	<i>0.12</i>	<i>0.11</i>	<i>0.08</i>						<i>0.11</i>		
<i>046</i>	1160		C	Fragment with catch attached	Cast	3903010	15118	10625	5489						387725		1
<i>046</i>	1162		A		Cast	3419045	117163	120231	6687						59510		4
						<i>0.09</i>	<i>0.18</i>	<i>0.10</i>	<i>0.16</i>						<i>0.35</i>		
<i>046</i>	1163		A	Front	Cast	2184879	153765	194267	34116						198123		4

<i>Site</i>	SF no.	SF sub div.	Anal . area	XRF location	Manuf. method	Cu (K)	Pb (L)	Sn (K)	Ag (K)	As (K)	Ni (K)	Sb (K)	Au (L)	Bi (L)	Zn (K)	Co (K)	No. of analyses
						<i>0.35</i>	<i>0.63</i>	<i>0.31</i>	<i>0.36</i>						<i>0.38</i>		
<i>046</i>	1167		A	Front	Cast	1848170	196724	207467	45156						142887		4
						<i>0.17</i>	<i>0.35</i>	<i>0.07</i>	<i>0.17</i>						<i>0.26</i>		
<i>046</i>	1168		A	Foot (reverse)	Cast	2300365	235463	126074	6443	2907	576	415			81359		5
						<i>0.45</i>	<i>0.51</i>	<i>0.29</i>	<i>0.64</i>	<i>2.24</i>	<i>2.24</i>	<i>1.37</i>			<i>0.34</i>		
<i>046</i>	1176		A		Cast	2129563	162624	52999	3007						57004		5
						<i>0.08</i>	<i>0.38</i>	<i>0.28</i>	<i>0.38</i>						<i>0.44</i>		
<i>046</i>	1177		A		Cast	1953773	94590	46780	3748						63634		1
<i>046</i>	1182		A		Cast	3106809	140208	88760	4707						141402		5
						<i>0.11</i>	<i>0.31</i>	<i>0.17</i>	<i>0.14</i>						<i>0.30</i>		
<i>046</i>	1183		A		Cast	3769260	187070	140440	9374						151066		3
						<i>0.17</i>	<i>0.49</i>	<i>0.17</i>	<i>0.07</i>						<i>0.20</i>		
<i>046</i>	1184		A		Cast	3692925	275857	138642	9260						150519		5
						<i>0.16</i>	<i>0.59</i>	<i>0.12</i>	<i>0.09</i>						<i>0.17</i>		
<i>046</i>	1185		A		Sheet	2425805	234496	171648	9703						102868		3
						<i>0.38</i>	<i>0.34</i>	<i>0.15</i>	<i>0.05</i>						<i>0.41</i>		
<i>046</i>	1188		A		Sheet	4113305	160123	66210	3189	9573					551175		2
						<i>0.02</i>	<i>0.12</i>	<i>0.03</i>	<i>0.07</i>	<i>0.11</i>					<i>0.11</i>		
<i>046</i>	1192		A		Cast	2365527	90353	248854	6170	8058	5413	3364			33478		3
						<i>0.20</i>	<i>0.57</i>	<i>0.28</i>	<i>0.24</i>	<i>0.73</i>	<i>0.14</i>	<i>0.30</i>			<i>0.37</i>		
<i>046</i>	1193		A		Sheet	1930056	24788	53344	4183						76599		1
<i>046</i>	1194		A		Sheet	4361782	7472	110228		7677					628688		2

<i>Site</i>	SF no.	SF sub div.	Anal . area	XRF location	Manuf. method	Cu (K)	Pb (L)	Sn (K)	Ag (K)	As (K)	Ni (K)	Sb (K)	Au (L)	Bi (L)	Zn (K)	Co (K)	No. of analyses
						<i>0.03</i>	<i>0.23</i>	<i>0.13</i>		<i>0.26</i>					<i>0.00</i>		
<i>046</i>	1195		A		Sheet	3739412	159438	98303	7322						103828		5
						<i>0.11</i>	<i>0.67</i>	<i>0.13</i>	<i>0.10</i>						<i>0.45</i>		
<i>046</i>	1196		A		Sheet	4534062	51968	110650	4763	4257					353726		5
						<i>0.11</i>	<i>0.13</i>	<i>0.07</i>	<i>0.06</i>	<i>0.25</i>					<i>0.11</i>		
<i>046</i>	1197		A		Cast	4327368	71374	144170	3294	4280		601			58637		5
						<i>0.17</i>	<i>0.72</i>	<i>0.19</i>	<i>0.10</i>	<i>0.77</i>		<i>0.16</i>			<i>0.10</i>		
<i>046</i>	1200		A		Sheet	3396965	107880	95116	10453						239987		2
						<i>0.03</i>	<i>0.01</i>	<i>0.19</i>	<i>0.32</i>						<i>0.77</i>		
<i>046</i>	1202		A		Sheet	981208	208017	165467	11260			1245			37788		3
						<i>0.13</i>	<i>0.09</i>	<i>0.01</i>	<i>0.01</i>			<i>0.18</i>			<i>0.10</i>		
<i>046</i>	1203		A		Sheet	1985124	227575	252610	10595	21574		3525			22645		2
						<i>0.01</i>	<i>0.10</i>	<i>0.06</i>	<i>0.08</i>	<i>0.14</i>		<i>0.07</i>			<i>0.03</i>		
<i>046</i>	1225		A	Reverse	Sheet	3096122	67121	119823	1771		1850				276308		4
						<i>0.28</i>	<i>0.38</i>	<i>0.53</i>	<i>0.70</i>		<i>2.00</i>				<i>0.36</i>		
<i>046</i>	1306		A	Side E - top band	Sheet	2445736	238236	127035	9955	11731		951			65261		3
						<i>0.06</i>	<i>0.39</i>	<i>0.06</i>	<i>0.08</i>	<i>0.27</i>		<i>0.11</i>			<i>0.43</i>		
<i>046</i>	1306		B	Side N - bottom band	Sheet	2412608	200728	117818	9098	9942		882			74997		4
						<i>0.06</i>	<i>0.53</i>	<i>0.16</i>	<i>0.20</i>	<i>0.45</i>		<i>0.18</i>			<i>0.40</i>		
<i>046</i>	1306		C	Side N - middle band	Sheet	2624373	61533	106474	3352	3562		1339			187736		3
						<i>0.14</i>	<i>0.38</i>	<i>0.13</i>	<i>0.82</i>	<i>0.25</i>		<i>0.43</i>			<i>0.40</i>		
<i>046</i>	1306		D	Side N - top band	Sheet	2445736	238236	127035	9955	11731		951			65261		3
						<i>0.06</i>	<i>0.39</i>	<i>0.06</i>	<i>0.08</i>	<i>0.27</i>		<i>0.11</i>			<i>0.43</i>		
<i>046</i>	1306		E	Side S - top band	Sheet	2445736	238236	127035	9955	11731		951			65261		3

<i>Site</i>	SF no.	SF sub div.	Anal . area	XRF location	Manuf. method	Cu (K)	Pb (L)	Sn (K)	Ag (K)	As (K)	Ni (K)	Sb (K)	Au (L)	Bi (L)	Zn (K)	Co (K)	No. of analyses
						0.06	0.39	0.06	0.08	0.27		0.11			0.43		
046	1306		F	Side W - bottom band	Sheet	2587925	190545	123828	7881	9579		1150			111643		4
						0.12	0.64	0.07	0.53	0.53		0.35			0.86		
046	1306		G	Side W adjacent N - top band	Sheet	2445736	238236	127035	9955	11731		951			65261		3
						0.06	0.39	0.06	0.08	0.27		0.11			0.43		
046	1348		A		Wire	528468	100081	50349	5544	4892		722			63516		3
						0.29	0.13	0.14	0.18	0.19		0.14			0.13		
046	1352		A	Front	Cast	905144	336449	226697	18608	16417	2127	1584			211437		4
						0.66	0.27	0.17	0.19	0.33	0.40	0.19			0.20		
046	1353		A	Front	Cast	3350723	120345	65588	5248						67872		3
						0.17	0.35	0.17	0.17						0.35		
046	1355		A	Large fragment	Sheet	1366139	321424	248049	5268						75194		2
						0.31	0.73	0.10	0.10						0.28		
046	1355		B	Smaller Fragment	Sheet	1299800	372822	233106	5707						66020		2
						0.06	0.26	0.07	0.03						0.04		
046	1356		A	Large Fragment	Sheet	1725664	186927	213319	3939			594			90041		3
						0.60	0.70	0.60	0.13			0.30			0.51		
046	1356		B	Smaller Fragment	Sheet	1633045	255821	222445	4402			442			83741		2
						0.05	0.09	0.05	0.06			0.19			0.22		
046	1360		A	Front	Cast	1622441	260532	79672	3873			367			43322		4
						0.33	0.35	0.59	0.63			1.16			0.26		
046	1361		A	Front	Cast	986874	181501	111533	28916		238		308	1128	42559		4
						0.38	0.32	0.23	0.24		2.00		0.68	2.00	0.38		
046	1364		A		Wire	1555705	19370	197051	12037			348			96234		3

<i>Site</i>	SF no.	SF sub div.	Anal . area	XRF location	Manuf. method	Cu (K)	Pb (L)	Sn (K)	Ag (K)	As (K)	Ni (K)	Sb (K)	Au (L)	Bi (L)	Zn (K)	Co (K)	No. of analyses
						<i>0.11</i>	<i>0.08</i>	<i>0.12</i>	<i>0.03</i>			<i>0.46</i>			<i>0.11</i>		
<i>046</i>	1366		A		Cast	2984907	109740	92912	5297			611			74057		5
						<i>0.15</i>	<i>0.29</i>	<i>0.20</i>	<i>0.23</i>			<i>0.19</i>			<i>0.24</i>		
<i>046</i>	1370		A		Cast	3248695	146597	180829	8364	4320		681			188875		5
						<i>0.21</i>	<i>0.43</i>	<i>0.17</i>	<i>0.24</i>	<i>1.43</i>		<i>0.93</i>			<i>0.34</i>		
<i>046</i>	1371		A		Cast	3328191	92829	116525	17143		646	786			364714		5
						<i>0.26</i>	<i>0.40</i>	<i>0.26</i>	<i>0.23</i>	<i>2.24</i>		<i>0.57</i>			<i>0.33</i>		
<i>046</i>	1372		A		Cast	3829098	52426	49900	4734								4
						<i>0.04</i>	<i>0.19</i>	<i>0.12</i>	<i>0.14</i>								
<i>046</i>	1373		A		Cast	3882220	65945	56435	5602								4
						<i>0.06</i>	<i>0.49</i>	<i>0.08</i>	<i>0.04</i>								
<i>046</i>	1374		A		Cast	3618528	91672	59974	5591	4774		376					4
						<i>0.07</i>	<i>0.49</i>	<i>0.14</i>	<i>0.13</i>	<i>1.19</i>		<i>1.15</i>					
<i>046</i>	1519		A		Sheet	2232090	90655	39644	1306					667	414002		3
						<i>0.09</i>	<i>0.12</i>	<i>0.16</i>	<i>0.91</i>					<i>1.73</i>	<i>0.18</i>		
<i>046</i>	1520		A		Sheet	3790566	92546	21620	3600			653			664769		1
<i>046</i>	1521		A		Sheet	2648620	80508	22102	3498	8789					549712		3
						<i>0.03</i>	<i>0.31</i>	<i>0.07</i>	<i>0.01</i>	<i>0.21</i>					<i>0.14</i>		
<i>046</i>	1523		A		Sheet	3775496	114772	22292	4231			1052			564306		1
<i>046</i>	1524		A		Sheet	1754372	344242	116248	2300			255			495952		2
						<i>0.12</i>	<i>0.05</i>	<i>0.59</i>	<i>0.17</i>			<i>0.46</i>			<i>0.33</i>		
<i>046</i>	1525		A		Sheet	2477142	121981	22752	3213			319			493216		4

<i>Site</i>	SF no.	SF sub div.	Anal . area	XRF location	Manuf. method	Cu (K)	Pb (L)	Sn (K)	Ag (K)	As (K)	Ni (K)	Sb (K)	Au (L)	Bi (L)	Zn (K)	Co (K)	No. of analyses
						<i>0.17</i>	<i>0.30</i>	<i>0.13</i>	<i>0.06</i>			<i>1.16</i>			<i>0.19</i>		
<i>046</i>	1526		A		Sheet	2753796	107394	23201	2126			624			658255		2
						<i>0.07</i>	<i>0.06</i>	<i>0.13</i>	<i>0.05</i>			<i>0.04</i>			<i>0.16</i>		
<i>046</i>	1526		B		Sheet	2218683	178434	25818	2354			613			628899		2
						<i>0.03</i>	<i>0.06</i>	<i>0.00</i>	<i>0.02</i>			<i>0.14</i>			<i>0.01</i>		
<i>046</i>	1527		A		Sheet	3005864	90468	39984	2196	4651					711342		1
<i>046</i>	1528		A		Sheet	2437223	107182	36876	1748	6487					507617		3
						<i>0.15</i>	<i>0.14</i>	<i>0.13</i>	<i>0.05</i>	<i>0.17</i>					<i>0.15</i>		
<i>046</i>	1529		A		Sheet	3407823	81985	40323	1878	3718					490065		1
<i>046</i>	1531		A		Sheet	3257829	86148	34402	1225	5963					421356		1
<i>046</i>	1533		A		Sheet	3593978	107413	34489	1500	7989					421382		1
<i>046</i>	1534		A		Sheet	2090570	105753	33046	1734	7046					412499		4
						<i>0.11</i>	<i>0.20</i>	<i>0.11</i>	<i>0.05</i>	<i>0.18</i>					<i>0.20</i>		
<i>046</i>	1535		A		Sheet	2599035	93335	19809	3207	7202					466347		4
						<i>0.09</i>	<i>0.27</i>	<i>0.14</i>	<i>0.09</i>	<i>0.28</i>					<i>0.21</i>		
<i>046</i>	1536		A		Sheet	2305790	68422	17841	2879	5632					365499		3
						<i>0.04</i>	<i>0.08</i>	<i>0.02</i>	<i>0.06</i>	<i>0.23</i>					<i>0.27</i>		
<i>046</i>	1537		A		Sheet	3789140	86764	25453	4436	6819					717992		1
<i>046</i>	1538		A		Sheet	3629193	92686	22807	3714				294		584069		1

<i>Site</i>	SF no.	SF sub div.	Anal . area	XRF location	Manuf. method	Cu (K)	Pb (L)	Sn (K)	Ag (K)	As (K)	Ni (K)	Sb (K)	Au (L)	Bi (L)	Zn (K)	Co (K)	No. of analyses
<i>046</i>	1539		A		Sheet	3717373	58158	56516	2532	5003					413990		1
<i>046</i>	1540		A		Cast	3400230	139634	106505	3449	19729					598648		2
						<i>0.39</i>	<i>0.40</i>	<i>0.82</i>	<i>0.39</i>	<i>0.22</i>					<i>0.34</i>		
<i>046</i>	1605		A	Front	Cast	3891457	68962	57485	5358	3419					89489		4
						<i>0.03</i>	<i>0.11</i>	<i>0.13</i>	<i>0.19</i>	<i>0.32</i>					<i>0.32</i>		
<i>046</i>	1606		A	Smaller Fragment	Sheet	2753377	178731	90133	9538	5109	2372		373		121895		2
						<i>0.31</i>	<i>0.30</i>	<i>0.60</i>	<i>0.75</i>	<i>0.46</i>	<i>1.41</i>		<i>1.41</i>		<i>0.48</i>		
<i>046</i>	1606		B	Large Fragment	Sheet	2478388	115735	77644	9442	2768	1825				108912		2
						<i>0.16</i>	<i>0.10</i>	<i>0.12</i>	<i>0.17</i>	<i>1.41</i>	<i>1.41</i>				<i>0.00</i>		
<i>046</i>	1609		A		Sheet	2586890	118702	47871	2328	7938					434140		2
						<i>0.28</i>	<i>0.12</i>	<i>0.25</i>	<i>0.17</i>	<i>0.20</i>					<i>0.19</i>		
<i>046</i>	1636		A	Upper shaft (front)	Cast	3410104	99941	76313	3422	4577					249700		4
						<i>0.12</i>	<i>0.55</i>	<i>0.16</i>	<i>0.23</i>	<i>0.74</i>					<i>0.51</i>		
<i>046</i>	1638		A	Hoop (outer)	Sheet	1579130	257034	141931	2483	9185	2415				290397		2
						<i>0.80</i>	<i>0.62</i>	<i>0.85</i>	<i>0.21</i>	<i>1.41</i>	<i>1.41</i>				<i>0.76</i>		
<i>046</i>	1639		A		Sheet	885008	206007	108968	3663	14647	2640				157716		2
						<i>0.08</i>	<i>0.01</i>	<i>0.03</i>	<i>0.08</i>	<i>0.03</i>	<i>0.38</i>				<i>0.29</i>		
<i>046</i>	1647		A	Front	Cast	2118154	151120	86769	4998	8131	2935	874			353383		4
						<i>0.13</i>	<i>0.33</i>	<i>0.30</i>	<i>0.42</i>	<i>0.32</i>	<i>0.67</i>	<i>0.73</i>			<i>0.36</i>		
<i>046</i>	1648		A	Head (reverse)	Cast	3579151	18352	164115	1537						34604		4
						<i>0.09</i>	<i>0.88</i>	<i>0.09</i>	<i>0.21</i>						<i>0.19</i>		
<i>046</i>	1657		A	Hoop	Sheet	2350726	179068	60629	2431	11786					305500		3

<i>Site</i>	SF no.	SF sub div.	Anal . area	XRF location	Manuf. method	Cu (K)	Pb (L)	Sn (K)	Ag (K)	As (K)	Ni (K)	Sb (K)	Au (L)	Bi (L)	Zn (K)	Co (K)	No. of analyses
						<i>0.07</i>	<i>0.08</i>	<i>0.09</i>	<i>0.16</i>	<i>0.09</i>					<i>0.16</i>		
<i>046</i>	1657		B	Disc	Sheet	2487956	111866	75652	2690	8670					593475		2
						<i>0.34</i>	<i>0.55</i>	<i>0.89</i>	<i>0.18</i>	<i>0.54</i>					<i>0.30</i>		
<i>046</i>	1658		A	Hoop frag	Sheet	2551215	169066	144508	5134						109432		2
						<i>0.52</i>	<i>0.60</i>	<i>0.58</i>	<i>0.11</i>						<i>0.13</i>		
<i>046</i>	1658		B	Disc	Sheet	1879004	108667	88857	2559						381507		2
						<i>0.40</i>	<i>0.27</i>	<i>1.00</i>	<i>0.00</i>						<i>0.31</i>		
<i>046</i>	1661		A	Hoop	Sheet	2305669	119178	69956	3852						190404		3
						<i>0.03</i>	<i>0.18</i>	<i>0.03</i>	<i>0.13</i>						<i>0.20</i>		
<i>046</i>	1662		A	Hoop (outer)	Sheet	2194877	111896	56763	2224						544652		2
						<i>0.26</i>	<i>0.26</i>	<i>0.82</i>	<i>0.18</i>						<i>0.17</i>		
<i>046</i>	1671		A	Hoop (outer)	Sheet	2240081	118226	84358	2331						494101		2
						<i>0.47</i>	<i>0.10</i>	<i>0.60</i>	<i>0.06</i>						<i>0.34</i>		
<i>046</i>	1673		A	Front	Cast	3482207	69342	136852	1103			148			79552		4
						<i>0.24</i>	<i>0.34</i>	<i>0.29</i>	<i>1.17</i>			<i>1.27</i>			<i>0.37</i>		
<i>046</i>	1674		A	Sheet metal	Sheet	1733723	388509	139698	2545						418974		2
						<i>0.07</i>	<i>0.00</i>	<i>0.00</i>	<i>0.04</i>						<i>0.11</i>		
<i>046</i>	1674		B	Pin	Cast	1154901	70603	29731	1248						27979		1
<i>046</i>	1674		C	Sheet Fragment	Sheet	1975312	221777	139202	3912						78506		2
						<i>0.54</i>	<i>0.66</i>	<i>0.67</i>	<i>0.10</i>						<i>0.61</i>		
<i>046</i>	1682		A	Hoop	Sheet	2517809	196394	25417	1605						417522		2
						<i>0.07</i>	<i>0.51</i>	<i>0.19</i>	<i>0.04</i>						<i>0.12</i>		
<i>046</i>	1682		B	Disc	Sheet	3070721	104346	28911	2358						753356		1

<i>Site</i>	SF no.	SF sub div.	Anal. area	XRF location	Manuf. method	Cu (K)	Pb (L)	Sn (K)	Ag (K)	As (K)	Ni (K)	Sb (K)	Au (L)	Bi (L)	Zn (K)	Co (K)	No. of analyses
<i>046</i>	1713		A		Wire	770929	119180	80072	4927						67289		4
						<i>0.16</i>	<i>0.23</i>	<i>0.10</i>	<i>0.10</i>						<i>0.27</i>		
<i>046</i>	1715		A		Wire	753884	76450	81036	3152						57827		4
						<i>0.11</i>	<i>0.23</i>	<i>0.21</i>	<i>0.18</i>						<i>0.12</i>		
<i>046</i>	1727		A		Cast	3325540	24725	110714	2336								4
						<i>0.04</i>	<i>0.12</i>	<i>0.06</i>	<i>0.04</i>								
<i>046</i>	1729		A		Sheet	3272732	138387	89522	8854						280976		2
						<i>0.02</i>	<i>0.16</i>	<i>0.00</i>	<i>0.04</i>						<i>0.02</i>		
<i>046</i>	1735		A	Fragment 1 (eyes, one broken)	Cast	3205497	220281	154301	4834						81787		2
						<i>0.21</i>	<i>0.68</i>	<i>0.26</i>	<i>0.01</i>						<i>0.26</i>		
<i>046</i>	1735		B	Fragment 2 (eyes, both complete)	Cast	2434218	185312	179746	6593						61954		2
						<i>0.01</i>	<i>0.39</i>	<i>0.06</i>	<i>0.07</i>						<i>0.02</i>		
<i>046</i>	1735		C	Fragment 3 (no eyes)	Cast	2348849	205888	183754	5346						146055		2
						<i>0.16</i>	<i>0.16</i>	<i>0.03</i>	<i>0.06</i>						<i>0.23</i>		
<i>046</i>	1737		A	Spring	Cast	812769	186352	95767	1527						7433		1
<i>046</i>	1737		B	Bow (front)	Cast	539192	721482	93020				1549			23752		4
						<i>0.16</i>	<i>0.06</i>	<i>0.18</i>				<i>0.17</i>			<i>0.35</i>		
<i>046</i>	1737		C	Pin	Cast	280128	101667	71570	369			189			5228		2
						<i>0.29</i>	<i>0.33</i>	<i>0.24</i>	<i>1.41</i>			<i>1.41</i>			<i>0.01</i>		
<i>046</i>	1739		A		Sheet	2425440	85752	30220	2775						510767		2
						<i>0.05</i>	<i>0.09</i>	<i>0.17</i>	<i>0.21</i>						<i>0.17</i>		

<i>Site</i>	SF no.	SF sub div.	Anal . area	XRF location	Manuf. method	Cu (K)	Pb (L)	Sn (K)	Ag (K)	As (K)	Ni (K)	Sb (K)	Au (L)	Bi (L)	Zn (K)	Co (K)	No. of analyses
<i>046</i>	1750		A	Eye piece	Cast	2295232	278684	205130	5121						59699		2
						<i>0.14</i>	<i>0.40</i>	<i>0.03</i>	<i>0.01</i>						<i>0.17</i>		
<i>046</i>	1750		B	Bar	Cast	908889	302919	209953	3176						18726		2
						<i>0.09</i>	<i>0.38</i>	<i>0.20</i>	<i>0.21</i>						<i>0.14</i>		
<i>046</i>	1751		A		Cast	2127987				987							2
						<i>0.01</i>				<i>0.02</i>							
<i>046</i>	1774		A		Sheet	1408893	398198	177363	7117	26745	3224	1080			167470		2
						<i>0.18</i>	<i>0.12</i>	<i>0.10</i>	<i>0.06</i>	<i>0.13</i>	<i>0.24</i>	<i>0.03</i>			<i>0.26</i>		
<i>046</i>	1782		A		Cast	2280511	178924	42544	647						108580		4
						<i>0.17</i>	<i>0.16</i>	<i>0.07</i>	<i>1.16</i>						<i>0.15</i>		
<i>046</i>	1782		B		Cast	1306582	213194	46223	1836						76785		1
<i>046</i>	1792		A		Cast	3374356	125367	84333	7975						273815		2
						<i>0.07</i>	<i>0.68</i>	<i>0.13</i>	<i>0.12</i>						<i>0.15</i>		
<i>046</i>	1811		A	Foot (front)	Cast	1953440	187993	114139	13396						584517		6
						<i>0.31</i>	<i>0.32</i>	<i>0.66</i>	<i>0.64</i>						<i>0.74</i>		
<i>046</i>	1814		A		Cast	315882	645247	46723	1365						6961		4
						<i>0.36</i>	<i>0.07</i>	<i>0.16</i>	<i>0.22</i>						<i>0.22</i>		
<i>046</i>	1815		A		Cast	2629303	496135	76975	11971	32001		1601					2
						<i>0.17</i>	<i>0.06</i>	<i>0.13</i>	<i>0.22</i>	<i>0.05</i>		<i>0.11</i>					
<i>046</i>	1817		A	Reverse	Cast	1930438	251646	174181	8830	17555	4296	1515			398920		5
						<i>0.10</i>	<i>0.23</i>	<i>0.03</i>	<i>0.07</i>	<i>0.20</i>	<i>0.09</i>	<i>0.11</i>			<i>0.19</i>		
<i>046</i>	1818		A	Reverse	Cast	1521457	421242	172068	11438	5260	1976	1599			373057		4
						<i>0.40</i>	<i>0.16</i>	<i>0.26</i>	<i>0.31</i>	<i>2.00</i>	<i>0.67</i>	<i>0.21</i>			<i>0.42</i>		

<i>Site</i>	SF no.	SF sub div.	Anal . area	XRF location	Manuf. method	Cu (K)	Pb (L)	Sn (K)	Ag (K)	As (K)	Ni (K)	Sb (K)	Au (L)	Bi (L)	Zn (K)	Co (K)	No. of analyses
<i>046</i>	1819		A	Eye piece (outer)	Sheet	2428760	156178	175089	3051						62396		4
						<i>0.21</i>	<i>0.41</i>	<i>0.36</i>	<i>0.04</i>						<i>0.53</i>		
<i>046</i>	1819		B	Sheet with Repousse	Sheet	3044709	140750	109017	5593						126269		2
						<i>0.09</i>	<i>0.28</i>	<i>0.02</i>	<i>0.08</i>						<i>0.09</i>		
<i>046</i>	1820		A	Front	Cast	3031509	42691	129954	4553						44620		4
						<i>0.14</i>	<i>0.11</i>	<i>0.17</i>	<i>0.19</i>						<i>0.61</i>		
<i>046</i>	1820		B	Pin	Cast	1267560	43166	35103	4466						141140		2
						<i>0.22</i>	<i>0.51</i>	<i>0.18</i>	<i>0.22</i>						<i>0.32</i>		
<i>046</i>	1821		A	Front	Cast	3248307	19883	95978	1991								4
						<i>0.16</i>	<i>0.19</i>	<i>0.49</i>	<i>0.43</i>								
<i>046</i>	1822		A		Sheet	3622943	71307	30392	2761						794670		2
						<i>0.03</i>	<i>0.28</i>	<i>0.09</i>	<i>0.20</i>						<i>0.17</i>		
<i>046</i>	1824		A	Disc	Sheet	2482403	146623	51305	2658						460336		1
<i>104</i>	1000		A	Reverse	Cast	3330349	19920	1951	9620			762	3383				4
						<i>0.24</i>	<i>0.23</i>	<i>0.12</i>	<i>0.15</i>			<i>0.17</i>	<i>0.29</i>				
<i>104</i>	1001		A		Cast	675324	207308	77590	4791	12636		314			35655		5
						<i>0.22</i>	<i>0.17</i>	<i>0.11</i>	<i>0.19</i>	<i>0.16</i>		<i>0.92</i>			<i>0.11</i>		
<i>104</i>	1003		A		Cast	1968571	195582	169312	2884			418			72888		4
						<i>0.14</i>	<i>0.10</i>	<i>0.06</i>	<i>0.10</i>			<i>0.37</i>			<i>0.15</i>		
<i>104</i>	1004		A	Reverse	Melted	2350013	208659	97084	18346	12120		891			71878		3
						<i>0.06</i>	<i>0.14</i>	<i>0.14</i>	<i>0.17</i>	<i>0.13</i>		<i>0.87</i>			<i>0.38</i>		
<i>104</i>	1005		A		Melted	2152593	204327	110993	8070	11911					37695		4
						<i>0.13</i>	<i>0.26</i>	<i>0.13</i>	<i>0.17</i>	<i>0.24</i>					<i>0.18</i>		

<i>Site</i>	SF no.	SF sub div.	Anal . area	XRF location	Manuf. method	Cu (K)	Pb (L)	Sn (K)	Ag (K)	As (K)	Ni (K)	Sb (K)	Au (L)	Bi (L)	Zn (K)	Co (K)	No. of analyses
104	1006		A		Melted	1614208	153588	165552	10346	10757	678	705			35419		4
						<i>0.09</i>	<i>0.34</i>	<i>0.12</i>	<i>0.25</i>	<i>0.29</i>	<i>2.00</i>	<i>0.68</i>			<i>0.21</i>		
104	1026		A	Frame & prong	Cast	1400754	100294	21938	1960	16992		851			132799		2
						<i>0.11</i>	<i>0.73</i>	<i>0.86</i>	<i>0.53</i>	<i>0.95</i>		<i>0.10</i>			<i>0.12</i>		
104	1026		B	Buckle sheet	Sheet	2514674	81250	15329	1673	8505		512			822025		2
						<i>0.09</i>	<i>0.00</i>	<i>0.16</i>	<i>0.09</i>	<i>0.05</i>		<i>0.00</i>			<i>0.16</i>		
104	1026		C	Buckle sheet	Sheet	2512063	188069	16073	1643	16140		594			901664		2
						<i>0.14</i>	<i>0.64</i>	<i>0.04</i>	<i>0.03</i>	<i>0.42</i>		<i>0.28</i>			<i>0.16</i>		
104	1027		A	Reverse	Cast	2650407	109861	81885	5296	1434		650			63771		5
						<i>0.15</i>	<i>0.13</i>	<i>0.16</i>	<i>0.20</i>	<i>2.24</i>		<i>0.57</i>			<i>0.18</i>		
104	1033		A		Sheet	2549336	77350	222096	4876	10018		2511			53959		2
						<i>0.13</i>	<i>0.17</i>	<i>0.12</i>	<i>0.12</i>	<i>0.03</i>		<i>0.02</i>			<i>0.24</i>		
104	1035		A	Front	Cast	1338453	56968	250971	2337	4496							2
						<i>0.16</i>	<i>0.44</i>	<i>0.21</i>	<i>0.01</i>	<i>0.36</i>							
104	1038		A	Reverse	Melted	1885438	150449	90361	4490	14030		255			43468		4
						<i>0.14</i>	<i>0.29</i>	<i>0.08</i>	<i>0.09</i>	<i>0.05</i>		<i>1.18</i>			<i>0.21</i>		
104	1046		B	Reverse	Cast	1289850	295503	170345	11117	3468		344	402		51191		3
						<i>0.26</i>	<i>0.45</i>	<i>0.37</i>	<i>0.41</i>	<i>1.73</i>		<i>1.73</i>	<i>0.88</i>		<i>0.43</i>		
104	1047		A		Melted	1079198	110440	246831	8140			437					2
						<i>0.17</i>	<i>0.19</i>	<i>0.07</i>	<i>0.11</i>			<i>0.24</i>					
104	1048		A		Cast	1455768	109791	276593	11627			574					2
						<i>0.03</i>	<i>0.10</i>	<i>0.07</i>	<i>0.05</i>			<i>0.40</i>					
104	1049		A		Melted	1960367	152156	148280	4159			789			54152		4
						<i>0.23</i>	<i>0.26</i>	<i>0.05</i>	<i>0.09</i>			<i>0.23</i>			<i>0.29</i>		

<i>Site</i>	SF no.	SF sub div.	Anal . area	XRF location	Manuf. method	Cu (K)	Pb (L)	Sn (K)	Ag (K)	As (K)	Ni (K)	Sb (K)	Au (L)	Bi (L)	Zn (K)	Co (K)	No. of analyses
104	1057		A		Cast	924709	131803	102621	4404	13965	2524	924			229792		4
						<i>0.41</i>	<i>0.41</i>	<i>0.40</i>	<i>0.27</i>	<i>0.44</i>	<i>0.48</i>	<i>0.39</i>			<i>0.70</i>		
104	1058		A	Tweezers	Sheet	1996008	71295	222507	4282			348			22500		4
						<i>0.19</i>	<i>0.22</i>	<i>0.24</i>	<i>0.26</i>			<i>0.14</i>			<i>0.16</i>		
104	1058		B	Hoop	Cast	725346	30748	122195	2190	504		546			23193		3
						<i>0.42</i>	<i>0.48</i>	<i>0.40</i>	<i>0.37</i>	<i>1.73</i>		<i>0.14</i>			<i>0.21</i>		
104	1062		A	Bow (front)	Cast	1961234	163573	145617	5867	11760	2546	673			109734		5
						<i>0.05</i>	<i>0.20</i>	<i>0.15</i>	<i>0.19</i>	<i>0.25</i>	<i>0.97</i>	<i>0.57</i>			<i>0.29</i>		
104	1063		A		Cast	1856754	232789	141508	6926	16626	3170	843			216038		5
						<i>0.16</i>	<i>0.34</i>	<i>0.11</i>	<i>0.07</i>	<i>0.29</i>	<i>0.09</i>	<i>0.29</i>			<i>0.28</i>		
104	1074		A		Cast	1274064	527299	141433	8284	30066		1131			94826		4
						<i>0.12</i>	<i>0.11</i>	<i>0.10</i>	<i>0.23</i>	<i>0.08</i>		<i>0.14</i>			<i>0.30</i>		
104	1095		A		Wire	134488	3472	7300		565					18588		1
104	1098		A	Shiny area	Cast	1818648	163890	81915	5801	12177	1904	692			211427		6
						<i>0.08</i>	<i>0.42</i>	<i>0.13</i>	<i>0.07</i>	<i>0.38</i>	<i>0.78</i>	<i>0.40</i>			<i>0.34</i>		
104	1148		A		Sheet	2825225	139813	31693	3911			892			386062		5
						<i>0.03</i>	<i>0.27</i>	<i>0.07</i>	<i>0.05</i>			<i>0.15</i>			<i>0.06</i>		
104	1161		A	Reverse	Cast	1752135	112102	88396	4015	3983	628	618			64529		4
						<i>0.40</i>	<i>0.94</i>	<i>0.58</i>	<i>0.57</i>	<i>2.00</i>	<i>2.00</i>	<i>0.46</i>			<i>0.37</i>		
104	1162		A		Cast	2141600	149210	91978	4136			677			69265		5
						<i>0.14</i>	<i>0.11</i>	<i>0.09</i>	<i>0.19</i>			<i>0.11</i>			<i>0.35</i>		
104	1169		A	Front	Melted	2325406	107338	135339	1535		836						4
						<i>0.12</i>	<i>0.16</i>	<i>0.19</i>	<i>0.10</i>		<i>2.00</i>						

<i>Site</i>	SF no.	SF sub div.	Anal. area	XRF location	Manuf. method	Cu (K)	Pb (L)	Sn (K)	Ag (K)	As (K)	Ni (K)	Sb (K)	Au (L)	Bi (L)	Zn (K)	Co (K)	No. of analyses
104	1171		A	Front	Sheet	1703099	333889	179668	5183			661			64426		2
						<i>0.06</i>	<i>0.12</i>	<i>0.04</i>	<i>0.02</i>			<i>0.14</i>			<i>0.06</i>		
104	1173		A		Cast	1352992	107084	148600	5848			702			34655		4
						<i>0.19</i>	<i>0.11</i>	<i>0.10</i>	<i>0.10</i>			<i>0.16</i>			<i>0.29</i>		
104	1174		A	Reverse	Cast	1435075	437567	63590	3557			142			16627		4
						<i>0.17</i>	<i>0.18</i>	<i>0.16</i>	<i>0.27</i>			<i>2.00</i>			<i>0.27</i>		
104	1176		B	Non gilded area on front	Cast	2149388	160969	189670	16778		5825				575584		3
						<i>0.21</i>	<i>0.17</i>	<i>0.27</i>	<i>0.38</i>		<i>0.19</i>				<i>0.14</i>		
104	1176		C	Rivet on reverse	Cast	857303	13065	22485	497	3544	11985	98			821752		2
						<i>0.06</i>	<i>0.44</i>	<i>0.37</i>	<i>1.41</i>	<i>0.83</i>	<i>1.20</i>	<i>1.41</i>			<i>1.17</i>		
104	1178		A		Sheet	3313943	103766	37106	4565			700			480217		3
						<i>0.13</i>	<i>0.25</i>	<i>0.02</i>	<i>0.01</i>			<i>0.07</i>			<i>0.22</i>		
104	1182		A		Cast	2335755	66353	69448	5480			447			38986		3
						<i>0.61</i>	<i>0.46</i>	<i>0.64</i>	<i>0.63</i>			<i>1.11</i>			<i>0.58</i>		
104	1191		B	Non gilded area on front	Cast	2186573	213638	167425	56833	564			6053		141233		3
						<i>0.20</i>	<i>0.26</i>	<i>0.17</i>	<i>0.31</i>	<i>0.93</i>			<i>0.87</i>		<i>0.14</i>		
104	1191		C	Rivet on reverse	Cast	995559	40217	21193	6274	874			192		50642		2
						<i>0.25</i>	<i>0.34</i>	<i>0.03</i>	<i>0.06</i>	<i>0.34</i>			<i>0.73</i>		<i>0.15</i>		
104	1195		A		Sheet	2688695	192964	31375	3551			656			351856		3
						<i>0.07</i>	<i>0.48</i>	<i>0.06</i>	<i>0.17</i>			<i>0.13</i>			<i>0.16</i>		
104	1213		A	Large fragment	Cast	1817330	213508	74784	6153	3997			1101		295288		5
						<i>0.26</i>	<i>0.56</i>	<i>0.33</i>	<i>0.25</i>	<i>0.93</i>			<i>0.37</i>		<i>0.35</i>		
104	1227		A		Sheet	1195780	89890	100123	3557			375			58639		2
						<i>0.11</i>	<i>0.03</i>	<i>0.03</i>	<i>0.06</i>			<i>0.26</i>			<i>0.18</i>		

<i>Site</i>	SF no.	SF sub div.	Anal . area	XRF location	Manuf. method	Cu (K)	Pb (L)	Sn (K)	Ag (K)	As (K)	Ni (K)	Sb (K)	Au (L)	Bi (L)	Zn (K)	Co (K)	No. of analyses
<i>104</i>	1228		A		Sheet	2819788	113147	108847	3429	1566		530			189234		3
						<i>0.17</i>	<i>0.13</i>	<i>0.03</i>	<i>0.10</i>	<i>1.73</i>		<i>0.15</i>			<i>0.10</i>		
<i>104</i>	1239		A		Sheet	1963490	148432	105909	3109			760			65301		3
						<i>0.11</i>	<i>0.13</i>	<i>0.08</i>	<i>0.10</i>			<i>0.08</i>			<i>0.47</i>		
<i>104</i>	1248		A		Sheet	2363475	348216	92642	3728	1917		725			64015		4
						<i>0.15</i>	<i>0.63</i>	<i>0.06</i>	<i>0.13</i>	<i>2.00</i>		<i>0.14</i>			<i>0.20</i>		
<i>104</i>	1249		A		Sheet	2880143	97110	122129	5125	4969	1825	735			99646		3
						<i>0.15</i>	<i>0.04</i>	<i>0.06</i>	<i>0.06</i>	<i>0.87</i>	<i>1.73</i>	<i>0.07</i>			<i>0.13</i>		
<i>104</i>	1250		A		Sheet	2574780	173157	91201	4076			732			80078		3
						<i>0.03</i>	<i>0.42</i>	<i>0.10</i>	<i>0.13</i>			<i>0.17</i>			<i>0.05</i>		
<i>104</i>	1251		A		Sheet	4187083	98982	37737	3105			563			719968		3
						<i>0.01</i>	<i>0.31</i>	<i>0.05</i>	<i>0.08</i>			<i>0.27</i>			<i>0.03</i>		
<i>104</i>	1254		A		Sheet	2073137	590386	84652	3102			681			46393		3
						<i>0.07</i>	<i>0.18</i>	<i>0.03</i>	<i>0.11</i>			<i>0.22</i>			<i>0.08</i>		
<i>104</i>	1254		B		Sheet	1870935	209205	77143	3345			510			51701		3
						<i>0.42</i>	<i>0.49</i>	<i>0.48</i>	<i>0.33</i>			<i>0.37</i>			<i>0.37</i>		
<i>104</i>	1255		A		Sheet	1799175	56967	75689	3555			484			63844		2
						<i>0.24</i>	<i>0.29</i>	<i>0.28</i>	<i>0.27</i>			<i>0.25</i>			<i>0.30</i>		
<i>104</i>	1256		A		Sheet	3080058	161378	126604	5322			808			97457		4
						<i>0.04</i>	<i>0.11</i>	<i>0.08</i>	<i>0.10</i>			<i>0.31</i>			<i>0.07</i>		
<i>104</i>	1263		A	Sheet	Sheet	3070752	216109	124251	4856	9603	1398	858			102293		4
						<i>0.13</i>	<i>0.10</i>	<i>0.18</i>	<i>0.26</i>	<i>0.79</i>	<i>2.00</i>	<i>0.15</i>			<i>0.30</i>		
<i>104</i>	1263		B	Tube	Sheet	1418168	78120	54359	2700	3491	1582	434			46734		3
						<i>0.11</i>	<i>0.21</i>	<i>0.06</i>	<i>0.07</i>	<i>0.92</i>	<i>0.87</i>	<i>0.09</i>			<i>0.07</i>		

<i>Site</i>	SF no.	SF sub div.	Anal. area	XRF location	Manuf. method	Cu (K)	Pb (L)	Sn (K)	Ag (K)	As (K)	Ni (K)	Sb (K)	Au (L)	Bi (L)	Zn (K)	Co (K)	No. of analyses
<i>104</i>	1277		A		Cast	1495402	162682	41306	3332	8441	1930	622			1064058	466	4
						<i>0.43</i>	<i>0.22</i>	<i>0.63</i>	<i>0.37</i>	<i>0.36</i>	<i>1.20</i>	<i>0.15</i>			<i>0.90</i>	<i>0.51</i>	
<i>104</i>	1293		A		Melted	432781	57774	10969	39102	4028	557	154			39873		1
<i>104</i>	1296		A		Sheet	610761	202263	173784	11174	13382	693	803			95988		3
						<i>0.43</i>	<i>0.14</i>	<i>0.24</i>	<i>0.34</i>	<i>0.18</i>	<i>1.73</i>	<i>0.25</i>			<i>0.30</i>		
<i>104</i>	1317		A	Reverse	Cast	2533558	47902	63602	4307			2233			258751		4
						<i>0.11</i>	<i>0.16</i>	<i>0.16</i>	<i>0.37</i>			<i>0.17</i>			<i>0.26</i>		
<i>104</i>	1318		A		Cast	1669458	97299	228070	2650	3610		80					3
						<i>0.03</i>	<i>0.08</i>	<i>0.14</i>	<i>0.11</i>	<i>0.88</i>		<i>1.73</i>					
<i>104</i>	1323		A		Sheet	2477881	145755	74843	9939			357			324497		4
						<i>0.08</i>	<i>0.10</i>	<i>0.14</i>	<i>0.15</i>			<i>0.21</i>			<i>0.21</i>		
<i>104</i>	1324		A	Buckle sheet	Sheet	2768019	34550	8543	2149			1926			268865		2
						<i>0.05</i>	<i>0.10</i>	<i>0.13</i>	<i>0.08</i>			<i>0.29</i>			<i>0.29</i>		
<i>104</i>	1324		B	Buckle frame and tongue	Cast	1191464	33059	27289	1735			861			89621		2
						<i>0.16</i>	<i>0.09</i>	<i>0.15</i>	<i>0.19</i>			<i>0.12</i>			<i>0.24</i>		
<i>104</i>	1325		A		Cast	2898144	168915	72341	14298	14344		339			389186		4
						<i>0.10</i>	<i>0.26</i>	<i>0.17</i>	<i>0.18</i>	<i>0.49</i>		<i>1.16</i>			<i>0.16</i>		
<i>104</i>	1357		A	Folded sheet	Sheet	1707984	142933	146917	6115	9788		248			114365		3
						<i>0.06</i>	<i>0.08</i>	<i>0.03</i>	<i>0.09</i>	<i>0.16</i>		<i>1.73</i>			<i>0.13</i>		
<i>104</i>	1357		B	Cast rivet	Cast	342690	104658	92222	2568	5958	753	395			60970		1
<i>104</i>	1359		A	Bow (front)	Cast	2318950	235780	124492	5348	11234		452			85555		5
						<i>0.10</i>	<i>0.47</i>	<i>0.14</i>	<i>0.25</i>	<i>0.58</i>		<i>0.92</i>			<i>0.27</i>		

<i>Site</i>	SF no.	SF sub div.	Anal . area	XRF location	Manuf. method	Cu (K)	Pb (L)	Sn (K)	Ag (K)	As (K)	Ni (K)	Sb (K)	Au (L)	Bi (L)	Zn (K)	Co (K)	No. of analyses
104	1360		A		Sheet	1946303	105533	126815	3926	8101		171			39567		4
						<i>0.13</i>	<i>0.18</i>	<i>0.20</i>	<i>0.14</i>	<i>0.38</i>		<i>2.00</i>			<i>0.13</i>		
104	1362		B	Eye Piece (reverse)	Sheet	2370338	70691	41371	1696			304			342370		5
						<i>0.06</i>	<i>0.30</i>	<i>0.07</i>	<i>0.06</i>			<i>0.26</i>			<i>0.21</i>		
104	1363		A	Eye Piece (front)	Sheet	1871926	225391	105309	1945			393			332419		4
						<i>0.38</i>	<i>0.95</i>	<i>0.62</i>	<i>0.06</i>			<i>0.28</i>			<i>0.35</i>		
104	1363		B	Hook Piece (front)	Sheet	1384171	138379	172373	2000			413			270025		2
						<i>0.10</i>	<i>0.01</i>	<i>0.21</i>	<i>0.05</i>			<i>0.55</i>			<i>0.02</i>		
104	1364		A	Outer	Sheet	2671844	78546	165896	1873			1426			163786		4
						<i>0.06</i>	<i>0.09</i>	<i>0.03</i>	<i>0.07</i>			<i>0.07</i>			<i>0.11</i>		
104	1366		A	Bow (front)	Cast	2347582	159365	106064	4434	8872		276			73563		5
						<i>0.20</i>	<i>0.49</i>	<i>0.39</i>	<i>0.45</i>	<i>0.53</i>		<i>1.56</i>			<i>0.55</i>		
104	1368		A		Cast	1824710	125090	61135	3899	5572		397			77100		5
						<i>0.16</i>	<i>0.44</i>	<i>0.20</i>	<i>0.21</i>	<i>0.84</i>		<i>0.60</i>			<i>0.22</i>		
104	1413		A	Analysed in bag, only large enough for one reading	Sheet	1080265	145035	85760	6048			629			136981		1
104	1443		A		Sheet	2330483	113712	131338	18325	9481		778			248292		5
						<i>0.22</i>	<i>0.34</i>	<i>0.17</i>	<i>0.22</i>	<i>0.63</i>		<i>0.57</i>			<i>0.25</i>		
104	1444		A		Sheet	1504196	63216	164947	2951	7168							3
						<i>0.26</i>	<i>0.21</i>	<i>0.07</i>	<i>0.10</i>	<i>0.28</i>							
104	1445		A		Sheet	1951551	134558	100570	7872	7410		534			326842		4
						<i>0.25</i>	<i>0.17</i>	<i>0.02</i>	<i>0.09</i>	<i>0.68</i>		<i>0.69</i>			<i>0.06</i>		
104	1449		A		Sheet	3143430	19650	38215	2896	7718		506			361915		5

<i>Site</i>	SF no.	SF sub div.	Anal . area	XRF location	Manuf. method	Cu (K)	Pb (L)	Sn (K)	Ag (K)	As (K)	Ni (K)	Sb (K)	Au (L)	Bi (L)	Zn (K)	Co (K)	No. of analyses
						<i>0.10</i>	<i>0.89</i>	<i>0.13</i>	<i>0.31</i>	<i>0.50</i>		<i>0.14</i>			<i>0.45</i>		
104	1450	a	A	Front	Sheet	2425423	94835	125569	4905	6110		677			179267		4
						<i>0.08</i>	<i>0.25</i>	<i>0.19</i>	<i>0.15</i>	<i>0.34</i>		<i>0.73</i>			<i>0.20</i>		
104	1450	b	A	Front	Sheet	2676008	114820	113937	4014	6402	599	920			175689		4
						<i>0.39</i>	<i>1.12</i>	<i>0.35</i>	<i>0.41</i>	<i>1.43</i>	<i>2.00</i>	<i>0.34</i>			<i>0.18</i>		
104	1450	c	A	Front	Sheet	2709594	73061	120424	4670			871			148830		4
						<i>0.24</i>	<i>0.58</i>	<i>0.24</i>	<i>0.18</i>			<i>0.35</i>			<i>0.13</i>		
104	1450	d	A	Front	Sheet	1637077	163353	147916	5625	12528	2882	949			190272		3
						<i>0.16</i>	<i>0.25</i>	<i>0.18</i>	<i>0.10</i>	<i>0.23</i>	<i>0.11</i>	<i>0.21</i>			<i>0.11</i>		
104	1458		B	Reverse	Cast	1760888	183605	171504	6627	14034	1295	554			132128		4
						<i>0.37</i>	<i>0.43</i>	<i>0.18</i>	<i>0.18</i>	<i>0.27</i>	<i>1.16</i>	<i>1.16</i>			<i>0.06</i>		
104	1458		C	Catch	Cast	732308	187109	132239	7564		1367				66017		1
104	1458		E	Repousse sheet (front)	Sheet	1564771	286186	155067	5793			221					4
						<i>0.26</i>	<i>0.38</i>	<i>0.20</i>	<i>0.19</i>			<i>0.33</i>					
104	1458		F	Rivet	Cast	2943018	142783	160194	11865	7668		1550			113905		2
						<i>0.10</i>	<i>0.13</i>	<i>0.11</i>	<i>0.06</i>	<i>0.18</i>		<i>0.21</i>			<i>0.08</i>		
104	1461	a	A	Side	Sheet	1299532	341379	83938	1781	31823		218			120718		3
						<i>0.17</i>	<i>0.19</i>	<i>0.03</i>	<i>0.04</i>	<i>0.13</i>		<i>1.73</i>			<i>0.07</i>		
104	1461	b	A	Side	Sheet	1177804	277126	76274	2255	22198		141			111836		3
						<i>0.15</i>	<i>0.05</i>	<i>0.07</i>	<i>0.14</i>	<i>0.21</i>		<i>1.73</i>			<i>0.07</i>		
104	1461	c	A		Sheet	1194652	361815	93978	2025	31169		289			115810		4
						<i>0.42</i>	<i>0.25</i>	<i>0.29</i>	<i>0.18</i>	<i>0.12</i>		<i>1.16</i>			<i>0.48</i>		
104	1461	d	A	Side	Sheet	1391460	251237	90799	2233	21555	701	232			105010		4

<i>Site</i>	SF no.	SF sub div.	Anal . area	XRF location	Manuf. method	Cu (K)	Pb (L)	Sn (K)	Ag (K)	As (K)	Ni (K)	Sb (K)	Au (L)	Bi (L)	Zn (K)	Co (K)	No. of analyses
						<i>0.17</i>	<i>0.07</i>	<i>0.29</i>	<i>0.19</i>	<i>0.16</i>	<i>2.00</i>	<i>1.19</i>			<i>0.07</i>		
104	1461	e	A	Side	Sheet	1312100	314417	80174	2344	32371	2550	511			123000		3
						<i>0.17</i>	<i>0.07</i>	<i>0.15</i>	<i>0.26</i>	<i>0.06</i>	<i>0.08</i>	<i>0.16</i>			<i>0.12</i>		
104	1461	f	A	Side	Sheet	1329230	337513	86182	2514	37950	2651	713			140573		3
						<i>0.03</i>	<i>0.13</i>	<i>0.07</i>	<i>0.20</i>	<i>0.09</i>	<i>0.09</i>	<i>0.24</i>			<i>0.15</i>		
104	1466		A		Sheet	1608430	138628	55778	6380			682			68639		2
						<i>0.09</i>	<i>0.34</i>	<i>0.22</i>	<i>0.29</i>			<i>0.14</i>			<i>0.04</i>		
104	1476		A	Hook Piece (front)	Cast	2746497	226523	61622	4157	16577		745			266820		4
						<i>0.07</i>	<i>0.18</i>	<i>0.05</i>	<i>0.04</i>	<i>0.32</i>		<i>0.72</i>			<i>0.18</i>		
104	1476		B	Eye Piece (front)	Cast	2352330	325154	57817	3934			930			255886		4
						<i>0.08</i>	<i>0.45</i>	<i>0.15</i>	<i>0.11</i>			<i>0.17</i>			<i>0.14</i>		
104	1477		A	Eye Piece (front)	Cast	1964144	181827	94453	4353	15157		607			285011		4
						<i>0.05</i>	<i>0.22</i>	<i>0.19</i>	<i>0.16</i>	<i>0.25</i>		<i>0.67</i>			<i>0.05</i>		
104	1477		B	Hook Piece (front)	Cast	1733563	291142	101461	4806	23060		944			256936		4
						<i>0.17</i>	<i>0.33</i>	<i>0.12</i>	<i>0.17</i>	<i>0.24</i>		<i>0.15</i>			<i>0.18</i>		
104	1478		A		Sheet	2283097	95848	74132	3943	36698		813			233433		6
						<i>0.23</i>	<i>0.51</i>	<i>0.49</i>	<i>0.52</i>	<i>0.45</i>		<i>0.54</i>			<i>0.54</i>		
104	1509		A	Bow (front)	Cast	2260561	184288	173291	6839	6755		446			40473		5
						<i>0.08</i>	<i>0.45</i>	<i>0.35</i>	<i>0.43</i>	<i>0.80</i>		<i>1.38</i>			<i>0.28</i>		
104	1509		B	Sheet from soil block	Sheet	1493173	104253	283682	2846	4804					20193		2
						<i>0.39</i>	<i>0.14</i>	<i>0.18</i>	<i>0.49</i>	<i>0.02</i>					<i>0.62</i>		
104	1518		A	Reverse	Cast	1904628	8097	154367	1431			711			117037		6
						<i>0.06</i>	<i>0.29</i>	<i>0.19</i>	<i>0.21</i>			<i>0.25</i>			<i>0.26</i>		
104	1543		A	Bow (front)	Cast	1678019	249310	176302	20029	12500		1439			188414		5

<i>Site</i>	SF no.	SF sub div.	Anal . area	XRF location	Manuf. method	Cu (K)	Pb (L)	Sn (K)	Ag (K)	As (K)	Ni (K)	Sb (K)	Au (L)	Bi (L)	Zn (K)	Co (K)	No. of analyses
						<i>0.49</i>	<i>0.32</i>	<i>0.30</i>	<i>0.24</i>	<i>0.42</i>		<i>0.58</i>			<i>0.53</i>		
104	1545		A	Bow (front)	Cast	922229	300899	189994	16712	16257	1693	1735			214230		4
						<i>0.04</i>	<i>0.23</i>	<i>0.23</i>	<i>0.28</i>	<i>0.23</i>	<i>0.22</i>	<i>0.18</i>			<i>0.27</i>		
104	1546		A	Hook Piece (front)	Cast	1078051	338085	290248	11802	19286	637	1308			98831		6
						<i>0.33</i>	<i>0.14</i>	<i>0.07</i>	<i>0.14</i>	<i>0.16</i>	<i>1.58</i>	<i>0.52</i>			<i>0.16</i>		
104	1547		A	Hook Piece (front)	Cast	1019073	229610	197130	11911	13268	642	1675			147636		6
						<i>0.40</i>	<i>0.40</i>	<i>0.28</i>	<i>0.41</i>	<i>0.47</i>	<i>1.56</i>	<i>0.29</i>			<i>0.28</i>		
104	1547		B	Eye Piece (front)	Cast	1173374	308509	196447	26736	15427	1052	2069			105716		6
						<i>0.22</i>	<i>0.10</i>	<i>0.12</i>	<i>0.06</i>	<i>0.15</i>	<i>1.14</i>	<i>0.11</i>			<i>0.16</i>		
104	1563		A	Outer curve	Sheet	2390202	137073	111687	3181			423			111090		5
						<i>0.18</i>	<i>0.27</i>	<i>0.23</i>	<i>0.23</i>			<i>0.22</i>			<i>0.12</i>		
104	1568		A		Wire	621284	66499	64956	18056	4458					308387		1
104	1570		A		Sheet	1995201	142140	101061	6518	5615	3700	726			92741		3
						<i>0.22</i>	<i>0.14</i>	<i>0.14</i>	<i>0.20</i>	<i>0.17</i>	<i>0.32</i>	<i>0.19</i>			<i>0.38</i>		
104	1570		B		Sheet	1461859	216703	120985	7686	9658	2804	896			69461		3
						<i>0.17</i>	<i>0.23</i>	<i>0.14</i>	<i>0.12</i>	<i>0.23</i>	<i>0.12</i>	<i>0.08</i>			<i>0.23</i>		
104	1589		A	Buckle plate	Sheet	1918194	240876	20746	1926	4312	654	401			444066		3
						<i>0.29</i>	<i>0.35</i>	<i>0.16</i>	<i>0.09</i>	<i>1.73</i>	<i>1.73</i>	<i>0.40</i>			<i>0.10</i>		
104	1589		B	Buckle frame and tongue	Cast	654254	157238	79714	2695	9878	1418	474			197156		3
						<i>0.13</i>	<i>0.11</i>	<i>0.17</i>	<i>0.17</i>	<i>0.14</i>	<i>0.13</i>	<i>0.10</i>			<i>0.60</i>		
104	1592	c	A	Strap end 1	Sheet	2522755	89143	184714	1546			23					4
						<i>0.27</i>	<i>1.26</i>	<i>0.16</i>	<i>0.22</i>			<i>2.00</i>					
104	1592	c	B	Strap end 2	Cast	1522024	101688	175032	1457								3

<i>Site</i>	SF no.	SF sub div.	Anal . area	XRF location	Manuf. method	Cu (K)	Pb (L)	Sn (K)	Ag (K)	As (K)	Ni (K)	Sb (K)	Au (L)	Bi (L)	Zn (K)	Co (K)	No. of analyses
						0.47	0.66	0.10	0.10								
104	1593		A		Sheet	3189108	59890	112825	5620			577			95908		5
						0.06	0.08	0.05	0.09			0.18			0.03		
104	1593	b	A		Sheet	1222610	60409	2119	2119								3
						0.27	0.08	0.08	0.08								
104	1605		A	Reverse	Cast	2222811	194004	49478	3774	5099		733			264343		4
						0.22	0.22	0.30	0.17	1.16		0.17			0.28		
104	1620		A		Melted	2186409	107988	113849	1655						33348		4
						0.16	0.36	0.21	0.21						0.36		
104	1621		A		Cast	1245907	420197	60540	1934	22788		256			27968		2
						0.27	0.25	0.08	0.07	0.26		0.38			0.24		
104	1622		A		Melted	1057869	344578	62303	3547	21861		1477			123727		3
						0.10	0.19	0.16	0.18	0.17		0.89			0.22		
104	1643		A	Front	Cast	2894320	166854	67533	3634			843			51921		4
						0.17	0.62	0.07	0.05			0.15			0.16		
104	1656		A		Cast	2461775	184616	104358	3129	9981		786			111379		4
						0.05	0.13	0.15	0.21	0.15		0.18			0.31		
104	1668		A		Sheet	1264912	80992	51441	2724			450			41302		3
						0.11	0.31	0.17	0.18			0.20			0.13		
104	1681		A		Cast	2307878	129650	50881	1718						121345		3
						0.12	0.15	0.08	0.17						0.09		
104	1691		A	Hook piece (reverse)	Cast	1637071	206471	218157	7554	10607		628			98267		4
						0.12	0.21	0.14	0.35	0.26		0.76			0.44		
104	1692		A		Melted	1267846	713315	62977	5104	9698		1117			1749		6

<i>Site</i>	SF no.	SF sub div.	Anal . area	XRF location	Manuf. method	Cu (K)	Pb (L)	Sn (K)	Ag (K)	As (K)	Ni (K)	Sb (K)	Au (L)	Bi (L)	Zn (K)	Co (K)	No. of analyses
						<i>0.36</i>	<i>0.29</i>	<i>0.19</i>	<i>0.26</i>	<i>1.57</i>		<i>0.40</i>			<i>1.57</i>		
104	1693		A		Cast	1708029	249914	304069	6050	12017		805			70887		2
						<i>0.11</i>	<i>0.19</i>	<i>0.03</i>	<i>0.24</i>	<i>0.18</i>		<i>1.41</i>			<i>0.09</i>		
104	1694		A		Melted	1449520	316276	11848	3987			512			37797		4
						<i>0.21</i>	<i>0.35</i>	<i>0.43</i>	<i>0.18</i>			<i>0.28</i>			<i>0.79</i>		
104	1695		A	Front	Cast	769517	215890	80195	2582	10178		238			20919		4
						<i>0.43</i>	<i>0.40</i>	<i>0.57</i>	<i>0.33</i>	<i>0.40</i>		<i>1.19</i>			<i>0.59</i>		
104	1696		A		Sheet	2561566	102424	71709	3989	16552		802			493012		4
						<i>0.05</i>	<i>0.11</i>	<i>0.06</i>	<i>0.08</i>	<i>0.10</i>		<i>0.67</i>			<i>0.08</i>		
104	1698		A		Cast	2424217	176440	135952	9190	12015					105207		4
						<i>0.47</i>	<i>0.32</i>	<i>0.50</i>	<i>0.69</i>	<i>0.32</i>					<i>0.34</i>		
104	1704		A	Adjacent break between main body and foot (reverse)	Cast	2095670	319456	196767	2920			467			45060		4
						<i>0.37</i>	<i>0.49</i>	<i>0.49</i>	<i>0.10</i>			<i>0.27</i>			<i>0.12</i>		
104	1704		C	Head panel (reverse)	Cast	2940848	106208	111854	2981			605			62417		4
						<i>0.14</i>	<i>0.53</i>	<i>0.23</i>	<i>0.32</i>			<i>0.16</i>			<i>0.39</i>		
104	1705		A		Sheet	1387310	449805	46065	1419	20148	1144	118			675173		4
						<i>0.13</i>	<i>0.40</i>	<i>0.17</i>	<i>0.25</i>	<i>1.32</i>	<i>1.19</i>	<i>1.16</i>			<i>0.26</i>		
104	1706		A		Sheet	2294189	354441	41078	3259	23508		460			286015		5
						<i>0.18</i>	<i>0.31</i>	<i>0.20</i>	<i>0.38</i>	<i>0.31</i>		<i>0.68</i>			<i>0.41</i>		
104	1713		A	Foot (front)	Cast	4014329	33012	3464	3022						820148		5
						<i>0.20</i>	<i>0.12</i>	<i>0.18</i>	<i>0.11</i>						<i>0.15</i>		
104	1752		A	Hook piece (front)	Cast	2600912	212321	69625	6075	10367		589			125776		4
						<i>0.18</i>	<i>0.38</i>	<i>0.13</i>	<i>0.24</i>	<i>0.36</i>		<i>0.68</i>			<i>0.24</i>		

<i>Site</i>	SF no.	SF sub div.	Anal. area	XRF location	Manuf. method	Cu (K)	Pb (L)	Sn (K)	Ag (K)	As (K)	Ni (K)	Sb (K)	Au (L)	Bi (L)	Zn (K)	Co (K)	No. of analyses
104	1752		B	Eye piece (reverse)	Cast	2436501	148285	92221	8122	8293		212			135777		4
						<i>0.11</i>	<i>0.76</i>	<i>0.19</i>	<i>0.18</i>	<i>0.71</i>		<i>2.00</i>			<i>0.20</i>		
104	1753		A	Hook piece (front)	Cast	1993575	200623	111059	9880	7084		727			147897		4
						<i>0.17</i>	<i>0.25</i>	<i>0.06</i>	<i>0.02</i>	<i>0.78</i>		<i>0.67</i>			<i>0.28</i>		
104	1753		B	Eye piece (front)	Cast	2752286	85470	73379	7051	2687		478			224041		4
						<i>0.17</i>	<i>0.26</i>	<i>0.08</i>	<i>0.07</i>	<i>0.75</i>		<i>1.24</i>			<i>0.12</i>		
104	1768		A	Buckle plate	Sheet	1681354	40252	84862	4458	4147		264			187761		2
						<i>0.71</i>	<i>0.56</i>	<i>0.17</i>	<i>0.20</i>	<i>0.64</i>		<i>1.41</i>			<i>0.06</i>		
104	1776		A	Reverse	Sheet	2287185	271216	140930	9659	16003	8813	1006			405466		5
						<i>0.18</i>	<i>0.36</i>	<i>0.19</i>	<i>0.40</i>	<i>0.40</i>	<i>0.12</i>	<i>0.20</i>			<i>0.18</i>		
104	1777		A		Sheet	2887309	297580	97575	4781	7811	4382	832			293858		6
						<i>0.23</i>	<i>0.22</i>	<i>0.39</i>	<i>0.52</i>	<i>1.56</i>	<i>1.55</i>	<i>0.28</i>			<i>0.64</i>		
104	1782		A		Cast	2597714	295546	30430	7586			827					3
						<i>0.08</i>	<i>0.33</i>	<i>0.20</i>	<i>0.21</i>			<i>0.29</i>					
104	1786		A		Sheet	2688803	93464	75893	9925	7962		183			494827		5
						<i>0.12</i>	<i>0.26</i>	<i>0.11</i>	<i>0.10</i>	<i>0.18</i>		<i>1.39</i>			<i>0.22</i>		
104	1887		A	Bow (front)	Cast	2115078	87381	133493	4755			710			86338		5
						<i>0.12</i>	<i>0.17</i>	<i>0.14</i>	<i>0.12</i>			<i>0.25</i>			<i>0.23</i>		
104	1888		A	Bow (front)	Cast	1328473	556849	67044	1495			393			36385		5
						<i>0.30</i>	<i>0.40</i>	<i>0.51</i>	<i>0.39</i>			<i>0.94</i>			<i>0.42</i>		
104	1900		A	Reverse	Melted	2086584	208406	173659	1832			1840			36725		4
						<i>0.06</i>	<i>0.17</i>	<i>0.14</i>	<i>0.14</i>			<i>0.11</i>			<i>0.07</i>		
104	1903		A		Cast	1556775	154785	164025	11465	10299		927			91453		4
						<i>0.39</i>	<i>0.60</i>	<i>0.44</i>	<i>0.45</i>	<i>0.72</i>		<i>0.73</i>			<i>0.38</i>		

<i>Site</i>	SF no.	SF sub div.	Anal. area	XRF location	Manuf. method	Cu (K)	Pb (L)	Sn (K)	Ag (K)	As (K)	Ni (K)	Sb (K)	Au (L)	Bi (L)	Zn (K)	Co (K)	No. of analyses
104	1942		A		Melted	2068589	292281	98194	4897	17244		222			40004		4
						<i>0.09</i>	<i>0.41</i>	<i>0.15</i>	<i>0.16</i>	<i>0.42</i>		<i>2.00</i>			<i>0.15</i>		
104	1947		A		Cast	2573550	122200	90572	5484			666			69407		4
						<i>0.09</i>	<i>0.31</i>	<i>0.14</i>	<i>0.09</i>			<i>0.16</i>			<i>0.36</i>		
104	1948		A	Bow (front)	Cast	1626937	386337	129404	3903			1962			219305		5
						<i>0.17</i>	<i>0.41</i>	<i>0.21</i>	<i>0.19</i>			<i>0.22</i>			<i>0.35</i>		
104	1948		C	Separate side knob (reverse). On plate used to attach it to main brooch body.	Cast	2065317	314067	95501	3552			898			81903		4
						<i>0.24</i>	<i>0.60</i>	<i>0.16</i>	<i>0.24</i>			<i>0.27</i>			<i>0.24</i>		
104	1949		A		Cast	405966	216739	54423	1111	11250		311			6746		4
						<i>0.22</i>	<i>0.15</i>	<i>0.13</i>	<i>0.06</i>	<i>0.17</i>		<i>1.16</i>			<i>0.15</i>		
104	1950		A	Front	Cast	2188621	153830	167692	7107	7504	519	481			90567		5
						<i>0.50</i>	<i>0.75</i>	<i>0.28</i>	<i>0.31</i>	<i>1.29</i>	<i>2.24</i>	<i>0.96</i>			<i>0.27</i>		
104	1952		A		Cast	492619	657457	119797	6361		997				105938		1
104	1952		B		Cast	584142	670611	117385	5850	27699	615	295			101440		5
						<i>0.27</i>	<i>0.08</i>	<i>0.13</i>	<i>0.16</i>	<i>0.56</i>	<i>1.38</i>	<i>0.96</i>			<i>0.23</i>		
104	1953		A	Eye piece (front)	Sheet	2261890	55593	170684	3289	4708		462			78349		4
						<i>0.13</i>	<i>0.43</i>	<i>0.19</i>	<i>0.18</i>	<i>0.32</i>		<i>1.16</i>			<i>0.05</i>		
104	1954		A	Hook piece (front)	Sheet	1893794	60713	191993	3610	5537		861			79505		4
						<i>0.36</i>	<i>0.44</i>	<i>0.25</i>	<i>0.23</i>	<i>0.77</i>		<i>0.12</i>			<i>0.11</i>		
104	1955		A	Hook piece (front)	Sheet	2645713	36826	136362	2778	622		748			77474		4
						<i>0.19</i>	<i>0.16</i>	<i>0.12</i>	<i>0.07</i>	<i>2.00</i>		<i>0.24</i>			<i>0.25</i>		

<i>Site</i>	SF no.	SF sub div.	Anal. area	XRF location	Manuf. method	Cu (K)	Pb (L)	Sn (K)	Ag (K)	As (K)	Ni (K)	Sb (K)	Au (L)	Bi (L)	Zn (K)	Co (K)	No. of analyses
104	1956		A	Eye piece (rear)	Sheet	2245641	57652	165441	3143			757			90497		4
						<i>0.20</i>	<i>0.23</i>	<i>0.11</i>	<i>0.14</i>			<i>0.14</i>			<i>0.09</i>		
104	1960		A	Bow (front)	Cast	2029026	303441	105974	7423	11170	550	622			45788		5
						<i>0.19</i>	<i>0.39</i>	<i>0.65</i>	<i>0.34</i>	<i>0.75</i>	<i>2.24</i>	<i>0.93</i>			<i>0.39</i>		
104	1960		B	Catch	Cast	1432928	275903	156940	8229	6495		937			37821		2
						<i>0.12</i>	<i>0.24</i>	<i>0.16</i>	<i>0.20</i>	<i>1.41</i>		<i>0.37</i>			<i>0.13</i>		
104	2028		A	Bow (front)	Cast	4057553	62458	108963	4601	2230		248			78432		4
						<i>0.16</i>	<i>0.70</i>	<i>0.15</i>	<i>0.26</i>	<i>0.95</i>		<i>2.00</i>			<i>0.11</i>		
104	2028		B	Separate side knob (front)	Cast	3979124	63570	125601	5898	3248		506			67922		2
						<i>0.13</i>	<i>0.48</i>	<i>0.17</i>	<i>0.15</i>	<i>0.50</i>		<i>1.41</i>			<i>0.39</i>		
104	2028		C	Second separate side knob (front)	Cast	2110209	78991	117236	6560			1044			116947		1
104	2029		A	Bow (front)	Cast	3055507	91483	93675	7926	3602		1122			191232		5
						<i>0.38</i>	<i>0.29</i>	<i>0.09</i>	<i>0.12</i>	<i>0.80</i>		<i>0.19</i>			<i>0.18</i>		
104	2030		A	Bow (front)	Cast	2865799	245910	92335	9547	11429		870			312254		5
						<i>0.17</i>	<i>0.40</i>	<i>0.32</i>	<i>0.40</i>	<i>0.66</i>		<i>0.93</i>			<i>0.22</i>		
104	2030		B	Catch	Cast	1448620	196069	76308	9319			865			295475		1
104	2031		A		Sheet	2387484	73845	140504	3677	4668		362			84449		5
						<i>0.19</i>	<i>0.22</i>	<i>0.17</i>	<i>0.14</i>	<i>0.17</i>		<i>1.08</i>			<i>0.32</i>		
104	2054		A	Bow (front)	Cast	1656571	390710	94312	4616	22415		323			58352		5
						<i>0.20</i>	<i>0.53</i>	<i>0.28</i>	<i>0.43</i>	<i>0.55</i>		<i>1.37</i>			<i>0.45</i>		
104	2057		A	Bow (front)	Cast	2564915	119366	183643	7024			716			128153		5

<i>Site</i>	SF no.	SF sub div.	Anal . area	XRF location	Manuf. method	Cu (K)	Pb (L)	Sn (K)	Ag (K)	As (K)	Ni (K)	Sb (K)	Au (L)	Bi (L)	Zn (K)	Co (K)	No. of analyses
						<i>0.18</i>	<i>0.15</i>	<i>0.10</i>	<i>0.09</i>			<i>0.15</i>			<i>0.13</i>		
104	2059		A	Bow (front)	Cast	2700404	113696	210581	7101			416			72179		4
						<i>0.23</i>	<i>0.51</i>	<i>0.31</i>	<i>0.28</i>			<i>0.48</i>			<i>0.27</i>		
104	2124		A	Knop	Cast	1533227	404346	115551	7451	15315		558			44408		6
						<i>0.31</i>	<i>0.22</i>	<i>0.45</i>	<i>0.60</i>	<i>0.86</i>		<i>0.79</i>			<i>0.28</i>		
104	2125		A		Wire	2106133	59038	32760	2825			1157			164789		3
						<i>0.33</i>	<i>0.23</i>	<i>0.23</i>	<i>0.21</i>			<i>0.42</i>			<i>0.28</i>		
104	2126		A		Sheet	3336902	13981	185	2529	3486					274612		4
						<i>0.09</i>	<i>0.29</i>	<i>2.00</i>	<i>0.31</i>	<i>0.69</i>					<i>0.16</i>		
104	2135		A		Cast	2334231	141262	126888	7289	7687		392			140315		5
						<i>0.29</i>	<i>0.49</i>	<i>0.37</i>	<i>0.36</i>	<i>0.57</i>		<i>1.38</i>			<i>0.34</i>		
104	2136		A	Bow (front)	Cast	2136299	443754	59949	1502			305			38394		5
						<i>0.21</i>	<i>0.93</i>	<i>0.31</i>	<i>0.73</i>			<i>0.63</i>			<i>0.26</i>		
104	2136		B	Catch	Cast	801116	340138	60882	1731			194			24195		1
104	2137		A	Bow (front)	Cast	2946557	64776	61785	3539			450			62847		4
						<i>0.21</i>	<i>0.27</i>	<i>0.24</i>	<i>0.37</i>			<i>0.45</i>			<i>0.27</i>		
104	2137		B	Catch	Cast	1645806	129704	118797	8741	7203					121784		1
104	2138		A		Sheet	2804167	102590	108437	3789			1071			140568		8
						<i>0.25</i>	<i>0.32</i>	<i>0.58</i>	<i>0.37</i>			<i>0.41</i>			<i>0.73</i>		
104	2139		A		Cast	1824665	201108	122392	7474	17015		706			161549		5
						<i>0.45</i>	<i>0.75</i>	<i>0.30</i>	<i>0.33</i>	<i>0.57</i>		<i>0.59</i>			<i>0.30</i>		
104	2140		A		Cast	2309652	149692	94079	6191	10646		281			171828		5

<i>Site</i>	SF no.	SF sub div.	Anal . area	XRF location	Manuf. method	Cu (K)	Pb (L)	Sn (K)	Ag (K)	As (K)	Ni (K)	Sb (K)	Au (L)	Bi (L)	Zn (K)	Co (K)	No. of analyses
						<i>0.39</i>	<i>0.49</i>	<i>0.21</i>	<i>0.18</i>	<i>0.59</i>		<i>1.37</i>			<i>0.23</i>		
104	2221		A		Sheet	2498406	81791	172082	3164			205					4
						<i>0.03</i>	<i>0.08</i>	<i>0.06</i>	<i>0.08</i>			<i>0.32</i>					
104	2276		A		Sheet	1640357	211622	96452	2363			319			52135		2
						<i>0.05</i>	<i>0.38</i>	<i>0.07</i>	<i>0.09</i>			<i>0.09</i>			<i>0.14</i>		
104	2289		A		Wire	143053	2513	50998	1042	590	234	371			2221		3
						<i>0.44</i>	<i>0.23</i>	<i>0.33</i>	<i>0.13</i>	<i>0.96</i>	<i>0.94</i>	<i>0.32</i>			<i>0.26</i>		
104	2294		A		Melted	2189145	65053	70551	3428			575			30159		4
						<i>0.09</i>	<i>0.31</i>	<i>0.19</i>	<i>0.15</i>			<i>0.30</i>			<i>0.35</i>		
104	2298		A	Bow (front)	Cast	1875802	152644	182969	5177	8666					54741		5
						<i>0.21</i>	<i>0.31</i>	<i>0.11</i>	<i>0.12</i>	<i>0.32</i>					<i>0.24</i>		
104	2299		A	Hook piece (front)	Cast	2482233	137197	158668	7129	8153		543			60216		4
						<i>0.13</i>	<i>0.35</i>	<i>0.13</i>	<i>0.16</i>	<i>0.40</i>		<i>0.67</i>			<i>0.15</i>		
104	2300		A		Sheet	817609	136847	147794	3164	9058					14083		4
						<i>0.07</i>	<i>0.13</i>	<i>0.05</i>	<i>0.15</i>	<i>0.11</i>					<i>0.04</i>		
104	2301		A		Sheet	1436410	195941	157156	2999			234			285812		2
						<i>0.41</i>	<i>0.19</i>	<i>0.59</i>	<i>0.35</i>			<i>0.22</i>			<i>0.77</i>		
104	2308		A	Front	Cast	1978051	126718	154087	6883	8831		500			121970		4
						<i>0.21</i>	<i>0.23</i>	<i>0.15</i>	<i>0.12</i>	<i>0.24</i>		<i>0.69</i>			<i>0.20</i>		
104	2311		B	Reverse	Sheet	4785356	42324	22581	13860	4332		1003					1
104	2312		A		Sheet	2544878	141608	107840	3855	5677					161336		5
						<i>0.45</i>	<i>0.52</i>	<i>0.96</i>	<i>0.36</i>	<i>1.24</i>					<i>0.52</i>		
104	2312		D	Clip	Sheet	1639671	79205	49760	2723			214			153657		1

<i>Site</i>	SF no.	SF sub div.	Anal . area	XRF location	Manuf. method	Cu (K)	Pb (L)	Sn (K)	Ag (K)	As (K)	Ni (K)	Sb (K)	Au (L)	Bi (L)	Zn (K)	Co (K)	No. of analyses
104	2317		A	Wire	Wire	918676	105879	96011	6763	3884		577	93		49424		2
						<i>0.05</i>	<i>0.19</i>	<i>0.38</i>	<i>0.44</i>	<i>1.22</i>		<i>1.41</i>	<i>1.41</i>		<i>0.08</i>		
104	2317		B	Sheet disc A	Sheet	4758745	44528	23405	7223			929					1
104	2344		A		Sheet	4334504	72106	80516	3556			718			197023		2
						<i>0.05</i>	<i>0.14</i>	<i>0.02</i>	<i>0.04</i>			<i>0.12</i>			<i>0.18</i>		
104	2352		A		Sheet	3205415	119770	61104	1163			258			420320		4
						<i>0.14</i>	<i>0.21</i>	<i>0.10</i>	<i>0.09</i>			<i>0.38</i>			<i>0.21</i>		
104	2364		A	Wire	Wire	1202839	20663	55631	1126			52			7462		3
						<i>0.01</i>	<i>0.56</i>	<i>0.14</i>	<i>0.05</i>			<i>1.73</i>			<i>0.87</i>		
104	2364		B	Sheet attachment	Sheet	4162835	15842	132276	2168			379			13832		2
						<i>0.05</i>	<i>0.12</i>	<i>0.19</i>	<i>0.27</i>			<i>1.41</i>			<i>1.41</i>		
104	2364		C	Cast attachment	Cast	1721932	154097	84730	3081			185			7663		2
						<i>0.08</i>	<i>0.59</i>	<i>0.08</i>	<i>0.08</i>			<i>1.41</i>			<i>1.41</i>		
104	2373		A	Hoop	Sheet	3132651	125630	40649	2597			252			245911		3
						<i>0.09</i>	<i>0.19</i>	<i>0.11</i>	<i>0.10</i>			<i>0.91</i>			<i>0.54</i>		
104	2373		B	Clip	Sheet	1587041	69102	62063	2581			255			91731		1
104	2374		B	Clip	Sheet	1492266	61520	57484	2711						92710		1
104	2377		A	Hoop A	Sheet	3232106	73030	46179	2589			280			279002		3
						<i>0.15</i>	<i>0.38</i>	<i>0.21</i>	<i>0.02</i>			<i>0.16</i>			<i>0.27</i>		
104	2377		B	Hoop B	Sheet	3078770	69131	46471	2447			252			226712		3

<i>Site</i>	SF no.	SF sub div.	Anal . area	XRF location	Manuf. method	Cu (K)	Pb (L)	Sn (K)	Ag (K)	As (K)	Ni (K)	Sb (K)	Au (L)	Bi (L)	Zn (K)	Co (K)	No. of analyses
						<i>0.11</i>	<i>0.47</i>	<i>0.22</i>	<i>0.18</i>			<i>0.11</i>			<i>0.14</i>		
104	2380		A	Hoop	Sheet	3104862	61932	43134	2666			330			391881		2
						<i>0.13</i>	<i>0.01</i>	<i>0.05</i>	<i>0.21</i>			<i>0.72</i>			<i>0.26</i>		
104	2381		A	Hoop	Sheet	3326459	77025	40008	2690			288			292719		2
						<i>0.06</i>	<i>0.15</i>	<i>0.02</i>	<i>0.02</i>			<i>0.25</i>			<i>0.10</i>		
104	2387		A	Hoop	Sheet	2981573	89898	42025	2793			272			349658		3
						<i>0.08</i>	<i>0.18</i>	<i>0.08</i>	<i>0.14</i>			<i>0.29</i>			<i>0.39</i>		
104	2387		B	Clip	Sheet	2061156	59539	50609	3329			235			339742		1
104	2398		A	Reverse	Cast	1159420	219249	145345	7299	11676		768			62233		5
						<i>0.68</i>	<i>0.51</i>	<i>0.39</i>	<i>0.37</i>	<i>0.48</i>		<i>0.31</i>			<i>0.41</i>		
104	2399		A		Sheet	3715778	59522	86653	2069	6290	7957	356			317317		5
						<i>0.24</i>	<i>0.74</i>	<i>0.16</i>	<i>0.13</i>	<i>0.53</i>	<i>0.28</i>	<i>0.61</i>			<i>0.35</i>		
104	2401		A		Sheet	2658952	88079	140771	3255	16483	9770	461			403463		4
						<i>0.14</i>	<i>0.04</i>	<i>0.11</i>	<i>0.15</i>	<i>0.14</i>	<i>0.10</i>	<i>0.36</i>			<i>0.10</i>		
104	2402		A	Buckle sheet	Sheet	1319932	156319	232133	5498	17230	7631	599			417483		6
						<i>0.16</i>	<i>0.05</i>	<i>0.10</i>	<i>0.10</i>	<i>0.10</i>	<i>0.36</i>	<i>0.26</i>			<i>0.33</i>		
104	2403		A	Strap end A	Sheet	2817992	185083	166518	5480	7976		480			171633		4
						<i>0.30</i>	<i>0.79</i>	<i>0.42</i>	<i>0.19</i>	<i>1.25</i>		<i>0.68</i>			<i>0.33</i>		
104	2403		B	Strap end B	Sheet	2751567	181936	167017	5185	8628		472			199209		4
						<i>0.37</i>	<i>0.84</i>	<i>0.53</i>	<i>0.11</i>	<i>1.15</i>		<i>0.12</i>			<i>0.46</i>		
104	2411		A		Melted	1596517	328513	89614	2390			563			34460		3
						<i>0.09</i>	<i>0.21</i>	<i>0.11</i>	<i>0.24</i>			<i>0.12</i>			<i>0.07</i>		
104	2413		A		Melted	2058182	89055	129028	3087	2989		388			43350		2

<i>Site</i>	SF no.	SF sub div.	Anal . area	XRF location	Manuf. method	Cu (K)	Pb (L)	Sn (K)	Ag (K)	As (K)	Ni (K)	Sb (K)	Au (L)	Bi (L)	Zn (K)	Co (K)	No. of analyses
						<i>0.04</i>	<i>0.19</i>	<i>0.14</i>	<i>0.11</i>	<i>1.41</i>		<i>0.05</i>			<i>0.09</i>		
104	2450		A		Cast	2518016	59041	114529	2697			290			51573		2
						<i>0.14</i>	<i>0.31</i>	<i>0.38</i>	<i>0.14</i>			<i>0.13</i>			<i>0.64</i>		
104	2456		A		Sheet	2115596	32073	169146	2605	4338							1
104	2462		A		Cast	3304288	246366	72068	3902			631			103114		4
						<i>0.05</i>	<i>0.22</i>	<i>0.18</i>	<i>0.14</i>			<i>0.10</i>			<i>0.32</i>		
104	2463		A		Cast	2545887	334929	94291	4614	3419	948	848			120433		4
						<i>0.20</i>	<i>0.27</i>	<i>0.45</i>	<i>0.50</i>	<i>2.00</i>	<i>2.00</i>	<i>0.13</i>			<i>0.72</i>		
104	2479		A		Sheet	5012401	6885	14911	1068	2997		1601			382479		6
						<i>0.03</i>	<i>0.24</i>	<i>0.49</i>	<i>0.52</i>	<i>0.52</i>		<i>0.50</i>			<i>0.15</i>		
104	2494		A	Bow (front)	Cast	2214638	35165	145359	3215	1082		310			30636		5
						<i>0.34</i>	<i>0.11</i>	<i>0.15</i>	<i>0.14</i>	<i>1.38</i>		<i>0.28</i>			<i>0.24</i>		
104	2494		B	Catch (loose sheet)	Sheet	1714721	281535	186750	4714			742			56598		2
						<i>0.15</i>	<i>0.25</i>	<i>0.06</i>	<i>0.08</i>			<i>0.42</i>			<i>0.11</i>		
104	2499		A		Melted	1636477	321696	117253	7456	19030		834			86213		1
104	2500		A	Hook piece (front)	Cast	3073345	135543	101294	3760			649			123594		5
						<i>0.07</i>	<i>0.13</i>	<i>0.10</i>	<i>0.09</i>			<i>0.28</i>			<i>0.17</i>		
104	2501		A	Front	Cast	1875565	147677	84025	8270	12536		801			390836		3
						<i>0.08</i>	<i>0.13</i>	<i>0.10</i>	<i>0.10</i>	<i>0.16</i>		<i>0.87</i>			<i>0.17</i>		
104	2502		A		Cast	3188742	28305	20601	366	1522	3576	189			849271		4
						<i>0.12</i>	<i>0.15</i>	<i>0.10</i>	<i>1.16</i>	<i>1.18</i>	<i>1.20</i>	<i>1.19</i>			<i>0.24</i>		
104	2503		A		Melted	1272719	505360	152554	1412			760			29634		2

<i>Site</i>	SF no.	SF sub div.	Anal. area	XRF location	Manuf. method	Cu (K)	Pb (L)	Sn (K)	Ag (K)	As (K)	Ni (K)	Sb (K)	Au (L)	Bi (L)	Zn (K)	Co (K)	No. of analyses
						0.08	0.14	0.39	0.51			1.41			0.23		
104	2507		A	Large fragment	Sheet	2269931	106660	109117	3834	4227		513			282730		4
						0.05	0.08	0.05	0.09	0.74		0.22			0.36		
104	2507		B	Small fragment	Sheet	2016474	73955	82702	3012	5448		127			304579		2
						0.36	0.03	0.19	0.16	0.11		1.41			0.39		
104	2510		A		Melted	692072	145819	49024	1777						7252		1
104	2524		A		Sheet	2337041	137900	93807	4276			491			209201		2
						0.19	0.20	0.06	0.03			0.14			0.06		
104	2525		A		Sheet	1950692	179381	92627	3277	9499		362			233826		2
						0.04	0.14	0.06	0.07	0.08		1.41			0.08		
104	2526		A		Sheet	2314451	27899	180585	2409	5118							3
						0.01	0.15	0.11	0.13	0.13							
104	2528		A		Melted	2474403	101238	72421	3811	5276		373			48922		3
						0.13	0.28	0.47	0.39	0.44		0.90			0.45		
104	2529		A	Buckle plate	Cast	2386845	118734	137934	3099	8698	6224	875			71907		2
						0.06	0.18	0.07	0.08	0.01	0.19	0.29			0.67		
104	2529		B	Buckle frame & prong	Cast	1204209	132241	36042	1524	5994		162			304561		2
						0.08	0.53	0.31	0.38	1.41		1.41			0.19		
104	2532		A		Sheet	3339333	47096	40292	1882	21057	8557	425			294853		4
						0.06	0.25	0.13	0.22	0.22	0.17	0.20			0.14		
104	2533		A		Melted	1519411	165096	69917	7908	6207		740			216046		2
						0.36	0.59	0.56	0.70	1.41		0.56			0.63		
104	2540		A	Shaft (reverse, base)	Cast	2714060	81309	141122	2733	2806		88			22231		3

<i>Site</i>	SF no.	SF sub div.	Anal . area	XRF location	Manuf. method	Cu (K)	Pb (L)	Sn (K)	Ag (K)	As (K)	Ni (K)	Sb (K)	Au (L)	Bi (L)	Zn (K)	Co (K)	No. of analyses
						<i>0.18</i>	<i>0.75</i>	<i>0.10</i>	<i>0.10</i>	<i>1.07</i>		<i>1.73</i>			<i>0.88</i>		
104	2540	b	A	Side knob for 2494	Cast	1890913	63843	178869	3959	3445					37812		1
104	2540	b	B	Side knob for 2494	Cast	897796	90423	261263	6960	6660	2072	561			30081		1
104	2541		A	Bow (front)	Cast	2448108	47399	177996	3803	3032		234			35104		4
						<i>0.11</i>	<i>0.35</i>	<i>0.18</i>	<i>0.18</i>	<i>0.25</i>		<i>1.15</i>			<i>0.24</i>		
104	2577		A	Front	Cast	2024233	168290	40611	6181	7737		383			613124		4
						<i>0.21</i>	<i>0.41</i>	<i>0.17</i>	<i>0.12</i>	<i>0.83</i>		<i>0.10</i>			<i>0.10</i>		
104	2587		A	Sheet front	Sheet	3615068	23405	50377	9596			775					3
						<i>0.02</i>	<i>0.33</i>	<i>0.21</i>	<i>0.19</i>			<i>0.35</i>					
104	2587		B	Cast rivet	Cast	1073889	11244	15899	2854			430					1
104	2588		A	Rivet head	Cast	937709	184035	171824	162121	11116		147	8888		66095		4
						<i>0.35</i>	<i>0.26</i>	<i>0.36</i>	<i>1.04</i>	<i>1.92</i>		<i>2.00</i>	<i>0.86</i>		<i>0.68</i>		
104	2589		A		Melted	1818676	61012	216844	2909			814					3
						<i>0.03</i>	<i>0.11</i>	<i>0.10</i>	<i>0.12</i>			<i>0.14</i>					
104	2590		A	Front	Cast	2052887	393251	136706	6003	28003		1314			343739		4
						<i>0.08</i>	<i>0.40</i>	<i>0.04</i>	<i>0.10</i>	<i>0.46</i>		<i>0.15</i>			<i>0.36</i>		
104	2590		B	Reverse	Cast	1502908	451797	132068	6629		1878	565			517484	582	1
104	2591		A	Sheet metal	Sheet	1281772	164410	119760	4852	10830	2396	909			301166		1
104	2591		B	Buckle' part	Cast	532095	296656	61512	2167	15741		517			39578		1

<i>Site</i>	SF no.	SF sub div.	Anal. area	XRF location	Manuf. method	Cu (K)	Pb (L)	Sn (K)	Ag (K)	As (K)	Ni (K)	Sb (K)	Au (L)	Bi (L)	Zn (K)	Co (K)	No. of analyses
104	2613		A	Buckle sheet	Sheet	2222003	158732	103433	1933	17467	5314	636			412463		3
						<i>0.23</i>	<i>0.44</i>	<i>0.22</i>	<i>0.22</i>	<i>0.12</i>	<i>0.21</i>	<i>0.26</i>			<i>0.27</i>		
104	2613		B	Buckle frame and tongue	Cast	1108463	141544	66526	1935	12238	2394	436			149995		2
						<i>0.37</i>	<i>0.36</i>	<i>0.14</i>	<i>0.02</i>	<i>0.21</i>	<i>0.10</i>	<i>0.32</i>			<i>0.08</i>		
104	2622		A	Front	Sheet	2401666	77430	125015	4329			618			93445		2
						<i>0.45</i>	<i>0.11</i>	<i>0.15</i>	<i>0.16</i>			<i>0.32</i>			<i>0.39</i>		
104	2623		C	Arm (no plate)	Cast	1844266	309195	194330	15937			315			104294		2
						<i>0.01</i>	<i>0.14</i>	<i>0.17</i>	<i>0.07</i>			<i>0.22</i>			<i>0.05</i>		
104	2623		D	Reverse (arm)	Cast	559265	26718	26837	1159			92			34988		3
						<i>1.49</i>	<i>0.88</i>	<i>0.94</i>	<i>1.73</i>			<i>1.73</i>			<i>1.25</i>		
104	2623		E	Rivet	Cast	1463421	174084	136047	10330	11306					162157		1
104	2624		A	Reverse (foot)	Cast	2526408	125919	145807	40135						55689		3
						<i>0.33</i>	<i>0.12</i>	<i>0.15</i>	<i>0.17</i>						<i>0.27</i>		
104	2624		D	Catch (reverse)	Cast	3911809	63964	148526	8531			507	523		33266		1
104	2624		E	Front	Cast	1525696	223824	301844	45049						29003		1
104	2626		B	Reverse	Cast	2132890	187440	261572	4282			601			55120		1
104	2626		D	Front	Cast	3314968	157115	151272	4944			904			117729		2
						<i>0.03</i>	<i>0.04</i>	<i>0.01</i>	<i>0.06</i>			<i>0.02</i>			<i>0.02</i>		
104	2626		E	Front	Cast	3251930	161302	152415	4735			914			119352		1

<i>Site</i>	SF no.	SF sub div.	Anal . area	XRF location	Manuf. method	Cu (K)	Pb (L)	Sn (K)	Ag (K)	As (K)	Ni (K)	Sb (K)	Au (L)	Bi (L)	Zn (K)	Co (K)	No. of analyses
104	2627		A	Front	Cast	2757614	144177	148358	4819	11259					93440		3
						<i>0.23</i>	<i>0.22</i>	<i>0.08</i>	<i>0.06</i>	<i>0.35</i>					<i>0.20</i>		
104	2627		C	Reverse	Cast	3415354	132744	145601	4846	10530					112553		1
104	2631		A		Sheet	1267916	119442	111260	2659	9920		510			21246		3
						<i>0.06</i>	<i>0.10</i>	<i>0.04</i>	<i>0.06</i>	<i>0.07</i>		<i>0.20</i>			<i>0.02</i>		
104	2633		A		Sheet	1340087	58830	118547	1546	2407	1571	454			47556		2
						<i>0.14</i>	<i>0.84</i>	<i>0.45</i>	<i>1.41</i>	<i>1.41</i>	<i>1.41</i>	<i>1.41</i>			<i>1.41</i>		
104	2634		A	Buckle sheet	Sheet	917636	26567	87669	1336	2613		617			19794		2
						<i>0.26</i>	<i>0.29</i>	<i>0.36</i>	<i>0.05</i>	<i>0.65</i>		<i>0.55</i>			<i>0.32</i>		
104	2634		B	Buckle frame and tongue	Cast	693591	78770	108365	3878	6942	2633	540			26535		3
						<i>0.32</i>	<i>0.10</i>	<i>0.12</i>	<i>0.12</i>	<i>0.05</i>	<i>0.23</i>	<i>0.39</i>			<i>0.38</i>		
104	2636		A	Reverse	Sheet	1508719	218225	213408	6877			675			91367		1
104	2646		A	Buckle sheet	Sheet	2158023	13678	130585	1459	1604		326					2
						<i>0.04</i>	<i>0.64</i>	<i>0.47</i>	<i>0.38</i>	<i>1.41</i>		<i>1.41</i>					
104	2646		B	Frame & Prong	Cast	715941	134466	94550	2511	5482	1069	384			29814		2
						<i>0.18</i>	<i>0.02</i>	<i>0.25</i>	<i>0.29</i>	<i>1.41</i>	<i>1.41</i>	<i>0.45</i>			<i>0.18</i>		
104	2646		C	Loose sheet	Sheet	3492423	15710	99958	1326	734		333			8571		2
						<i>0.25</i>	<i>0.27</i>	<i>0.03</i>	<i>0.01</i>	<i>1.41</i>		<i>1.41</i>			<i>1.41</i>		
104	2647		A	Frame & Prong	Cast	348757	297862	68169	3564	14631	476	798			116940		2
						<i>0.14</i>	<i>0.13</i>	<i>0.22</i>	<i>0.12</i>	<i>0.06</i>	<i>1.41</i>	<i>0.22</i>			<i>0.21</i>		
104	2647		B	Buckle sheet	Sheet	951924	249426	195140	3511	13998	3384	795			46781		2

<i>Site</i>	SF no.	SF sub div.	Anal . area	XRF location	Manuf. method	Cu (K)	Pb (L)	Sn (K)	Ag (K)	As (K)	Ni (K)	Sb (K)	Au (L)	Bi (L)	Zn (K)	Co (K)	No. of analyses
						0.02	0.12	0.15	0.09	0.08	0.00	0.33			0.36		
104	2648		A		Cast	2435237	146950	128281	12291	8492		1324			164281		4
						0.13	0.29	0.11	0.15	0.39		0.08			0.17		
104	2649		A		Cast	2330635	87683	117951	10397	5456		442			37035		4
						0.27	0.41	0.22	0.22	0.65		1.16			0.35		
104	2650		A	Rolled sheet	Sheet	773151	194135	178164	10560	11524		510			92551		2
						0.00	0.00	0.01	0.03	0.07		0.04			0.01		
104	2651		A		Sheet	452525	233801	209950	10381	12711	391	738			68738		2
						0.07	0.08	0.10	0.06	0.01	1.41	0.09			0.15		
104	2655		A		Sheet	2299737	77724	55656	2236	8843		401			626921		3
						0.17	0.31	0.25	0.02	0.15		1.73			0.07		
104	2657		A		Sheet	2110544	78298	73506	4753	24741		552			192949		3
						0.15	0.30	0.13	0.10	0.08		0.87			0.37		
104	2671		A		Sheet	1767376	100362	144535	4663	10242	4101	400			435280		4
						0.06	0.03	0.06	0.05	0.10	0.24	0.35			0.18		
104	2672		A		Sheet	2441884	78962	96903	3275	6636	1672	63			332382		4
						0.13	0.23	0.09	0.05	0.56	2.00	2.00			0.68		
104	2672		B	Pin	Sheet	1387315	4305	8700		571					112889		2
						0.11	0.36	0.08		0.17					0.28		
104	2679		A		Sheet	1501852	62742	127317	2029	2617							3
						0.22	0.15	0.21	0.26	1.01							
104	2681		A	Uncorroded area	Sheet	3018520	80552	65493	3824	13389		752			634925		5
						0.09	0.21	0.11	0.09	0.19		0.56			0.18		
104	2682		A		Sheet	3183686	134536	76205	4127			1004			676485		4

<i>Site</i>	SF no.	SF sub div.	Anal . area	XRF location	Manuf. method	Cu (K)	Pb (L)	Sn (K)	Ag (K)	As (K)	Ni (K)	Sb (K)	Au (L)	Bi (L)	Zn (K)	Co (K)	No. of analyses
						0.12	0.18	0.04	0.06			0.08			0.29		
104	2706		A		Sheet	645699	365908	259971	18324	20402	1185	770			97799		2
						0.12	0.04	0.05	0.03	0.04	0.01	0.16			0.10		
104	2714		A		Cast	2483574	144820	68593	3535	17431		317			411409		4
						0.15	0.34	0.18	0.19	0.30		1.16			0.12		
104	2715		A		Cast	2025860	312421	81088	4022			627			281373		4
						0.04	0.26	0.09	0.10			0.16			0.08		
104	2716		A		Sheet	3686467	75049	63271	4003			917			1033078		2
						0.03	0.08	0.08	0.11			0.28			0.01		
104	2717		A		Cast	336957	33094	90455	3631	2615		422			8150		3
						0.06	0.02	0.09	0.08	0.23		0.95			0.14		
104	2719		A		Sheet	2020749	185314	221571	8891	13475		1198			194300		2
						0.01	0.05	0.08	0.01	0.06		0.05			0.12		
104	2748		A		Sheet	2166365	138989	92516	1493	1661		1092			172317		4
						0.31	0.23	0.78	0.22	2.00		0.75			0.26		
104	2749		A		Sheet	2024610	128607	94323	1618			1201			228511		4
						0.34	0.14	0.85	0.10			0.14			0.37		
104	2750		A	Front	Cast	1115438	61782	73448	1883			264			40286		4
						0.31	0.43	0.41	0.35			0.26			0.24		
104	2757		A	Bow (front)	Cast	2403519	147189	86124	3293			839			34587		5
						0.41	0.50	0.42	0.33			0.33			0.50		
104	2757		B	Catch	Cast	2195670	110737	98426	3676			930			39607		1
104	2758		A	Front	Cast	2328547	185511	98453	5909	9620		440			145567		5

<i>Site</i>	SF no.	SF sub div.	Anal . area	XRF location	Manuf. method	Cu (K)	Pb (L)	Sn (K)	Ag (K)	As (K)	Ni (K)	Sb (K)	Au (L)	Bi (L)	Zn (K)	Co (K)	No. of analyses
						<i>0.18</i>	<i>0.19</i>	<i>0.21</i>	<i>0.24</i>	<i>0.34</i>		<i>0.96</i>			<i>0.33</i>		
104	2759		A		Cast	2502204	267076	80542	3342			543			79803		5
						<i>0.10</i>	<i>0.17</i>	<i>0.35</i>	<i>0.34</i>			<i>0.36</i>			<i>0.50</i>		
104	2760		A	Front	Cast	784350	511025	118656	8936			2242			5198		4
						<i>0.14</i>	<i>0.18</i>	<i>0.14</i>	<i>0.20</i>			<i>0.10</i>			<i>0.67</i>		
104	2760		B	Reverse	Cast	2464341	76247	41796	2849			686					3
						<i>0.28</i>	<i>0.99</i>	<i>0.14</i>	<i>0.22</i>			<i>0.93</i>					
104	2770		A	Large fragment	Sheet	1800584	130285	172533	11715			741			121114		3
						<i>0.07</i>	<i>0.08</i>	<i>0.25</i>	<i>0.17</i>			<i>0.34</i>			<i>0.40</i>		
104	2770		B	Rolled sheet	Sheet	764110	90381	105830	5390			622			39954		1
104	2780		A		Sheet	3664865	158661	64304	3991	14651		1054			848931		6
						<i>0.03</i>	<i>0.24</i>	<i>0.04</i>	<i>0.09</i>	<i>0.51</i>		<i>0.09</i>			<i>0.10</i>		
104	2781		A	Cast hoop	Cast	824721	116907	42798	8856			614			69756		3
						<i>0.32</i>	<i>0.21</i>	<i>0.06</i>	<i>0.28</i>			<i>0.26</i>			<i>0.18</i>		
104	2781		B	Sheet attached to ring	Sheet	1370740	126686	37074	6031			651			194274		2
						<i>0.45</i>	<i>0.68</i>	<i>0.40</i>	<i>0.41</i>			<i>0.43</i>			<i>0.42</i>		
104	2782		A		Cast	2681107	74950	64708	2205			281			331184		4
						<i>0.04</i>	<i>0.43</i>	<i>0.07</i>	<i>0.12</i>			<i>0.61</i>			<i>0.27</i>		
104	2783		A	Bow (front)	Cast	2206214	36488	192764	2125			144					5
						<i>0.15</i>	<i>0.20</i>	<i>0.11</i>	<i>0.11</i>			<i>0.86</i>					
104	2784		A	Front	Sheet	3962540	116845	84169	2708			527			269527		5
						<i>0.11</i>	<i>0.14</i>	<i>0.18</i>	<i>0.23</i>			<i>0.08</i>			<i>0.41</i>		
104	2785		A	Reverse	Cast	2406132	115273	94126	10558	15340	7102	840			228762		4

<i>Site</i>	SF no.	SF sub div.	Anal . area	XRF location	Manuf. method	Cu (K)	Pb (L)	Sn (K)	Ag (K)	As (K)	Ni (K)	Sb (K)	Au (L)	Bi (L)	Zn (K)	Co (K)	No. of analyses
						<i>0.16</i>	<i>0.35</i>	<i>0.22</i>	<i>0.26</i>	<i>0.34</i>	<i>0.22</i>	<i>0.31</i>			<i>0.24</i>		
104	2785		B	Pin	Cast	972959	50499	40706	4194	5747		250			117307		2
						<i>0.24</i>	<i>0.19</i>	<i>0.94</i>	<i>0.01</i>	<i>0.77</i>		<i>1.41</i>			<i>0.88</i>		
104	2786		A	Reverse	Cast	1869608	279635	88603	6738	15598	2701	569			188406		4
						<i>0.18</i>	<i>0.50</i>	<i>0.35</i>	<i>0.13</i>	<i>0.60</i>	<i>1.16</i>	<i>0.73</i>			<i>0.52</i>		
104	2786		B	Pin	Cast	698018	77643	21321	7761	14086					134351		1
104	2787	a	A		Cast	1570336	97781	95122	3047			633			86549		4
						<i>0.25</i>	<i>0.29</i>	<i>0.22</i>	<i>0.16</i>			<i>0.25</i>			<i>0.27</i>		
104	2787	b	A		Cast	2337629	65496	76626	13329			699			218631		6
						<i>0.47</i>	<i>0.41</i>	<i>0.15</i>	<i>0.16</i>			<i>0.29</i>			<i>0.53</i>		
104	2787	c	A		Cast	3079330	31819	45772	2624			293			139706		4
						<i>0.27</i>	<i>0.43</i>	<i>0.36</i>	<i>0.32</i>			<i>0.44</i>			<i>0.06</i>		
104	2788		A		Cast	2736058	233812	158291	3707			1239			291297		4
						<i>0.15</i>	<i>0.29</i>	<i>0.21</i>	<i>0.27</i>			<i>0.15</i>			<i>0.14</i>		
104	2789		A		Wire	1071676	96837	97766	2606	2989		332			117223		2
						<i>0.17</i>	<i>0.31</i>	<i>0.09</i>	<i>0.02</i>	<i>1.41</i>		<i>0.01</i>			<i>0.08</i>		
104	2798		A		Cast	1591569	175214	205784	14066	12067	967	478			225498		5
						<i>0.38</i>	<i>0.14</i>	<i>0.15</i>	<i>0.14</i>	<i>0.24</i>	<i>1.37</i>	<i>1.37</i>			<i>0.14</i>		
104	2799		A	Front	Cast	1423096	152924	253025	13341	9555		1059		1747	95026		5
						<i>0.10</i>	<i>0.10</i>	<i>0.08</i>	<i>0.07</i>	<i>0.15</i>		<i>0.15</i>		<i>0.12</i>	<i>0.07</i>		
104	2800		A		Sheet	1980568	215059	180788	9839			1232			157207		2
						<i>0.10</i>	<i>0.40</i>	<i>0.22</i>	<i>0.18</i>			<i>0.01</i>			<i>0.04</i>		
104	2821		A	Front	Sheet	1009094	876224	163048	7540			1581			135373		4

<i>Site</i>	SF no.	SF sub div.	Anal . area	XRF location	Manuf. method	Cu (K)	Pb (L)	Sn (K)	Ag (K)	As (K)	Ni (K)	Sb (K)	Au (L)	Bi (L)	Zn (K)	Co (K)	No. of analyses
						<i>0.24</i>	<i>0.12</i>	<i>0.21</i>	<i>0.33</i>			<i>0.15</i>			<i>0.18</i>		
104	2821		B	Reverse	Sheet	1299845	765296	128189	5524			1261			120231		3
						<i>0.44</i>	<i>0.23</i>	<i>0.21</i>	<i>0.40</i>			<i>0.12</i>			<i>0.36</i>		
104	2823		A		Cast	2107856	226467	114642	8983			905			135556		4
						<i>0.10</i>	<i>0.36</i>	<i>0.10</i>	<i>0.17</i>			<i>0.11</i>			<i>0.24</i>		
104	2825		A		Cast	2453927	91951	90771	8253			553			135903		5
						<i>0.37</i>	<i>0.51</i>	<i>0.48</i>	<i>0.50</i>			<i>0.35</i>			<i>0.42</i>		
104	2826		A		Sheet	877536	197218	188132	6418			1009			26844		3
						<i>0.03</i>	<i>0.20</i>	<i>0.12</i>	<i>0.16</i>			<i>0.13</i>			<i>0.04</i>		
104	2827		A		Sheet	728714	159091	153890	4609			704			25705		3
						<i>0.10</i>	<i>0.02</i>	<i>0.02</i>	<i>0.04</i>			<i>0.20</i>			<i>0.12</i>		
104	2863		A		Cast	2514349	45532	35811	2496			310			407600		1
104	2865		A	Rivet 1 (head)	Cast	1226218	238128	188664	647101						182901		1
104	2865		C	Rivet 2	Cast	4436866	44417	162003	7867						436591		1
104	2865		E	Rivet 4	Cast	2367870	62417	138941	6288						256907		1
104	2866		A	Bow (front)	Cast	2029590	383736	101853	10181	13785		488			87722		4
						<i>0.40</i>	<i>0.56</i>	<i>0.29</i>	<i>0.36</i>	<i>1.30</i>		<i>0.72</i>			<i>0.36</i>		
104	2867		A		Cast	1207657	158516	119245	4483			632			64674		4
						<i>0.31</i>	<i>0.24</i>	<i>0.20</i>	<i>0.25</i>			<i>0.22</i>			<i>0.14</i>		
104	2868		A	Piece A	Sheet	2462325	196408	38070	5595			720			398442		4

<i>Site</i>	SF no.	SF sub div.	Anal. area	XRF location	Manuf. method	Cu (K)	Pb (L)	Sn (K)	Ag (K)	As (K)	Ni (K)	Sb (K)	Au (L)	Bi (L)	Zn (K)	Co (K)	No. of analyses
						<i>0.13</i>	<i>0.27</i>	<i>0.21</i>	<i>0.12</i>			<i>0.68</i>			<i>0.09</i>		
104	2868		B	Piece B	Sheet	2941491	160046	37601	5644			891			470600		4
						<i>0.06</i>	<i>0.34</i>	<i>0.13</i>	<i>0.14</i>			<i>0.15</i>			<i>0.29</i>		
104	2869		A		Sheet	769517	508001	251389	18621	40872	5044	8050					4
						<i>0.12</i>	<i>0.09</i>	<i>0.12</i>	<i>0.12</i>	<i>0.08</i>	<i>0.07</i>	<i>0.13</i>					
104	2870		A		Sheet	1847104	119351	104435	10380	6591		480			141912		3
						<i>0.04</i>	<i>0.90</i>	<i>0.10</i>	<i>0.60</i>	<i>1.03</i>		<i>0.18</i>			<i>0.23</i>		
104	2870		B	Recorded as being a gilded in post ex. assessment. Analysis shows not gilded, simply uncorroded.	Sheet	1866697	38153	110318	2053	1286		457			47477		3
						<i>0.56</i>	<i>0.47</i>	<i>0.41</i>	<i>0.26</i>	<i>1.73</i>		<i>0.43</i>			<i>0.62</i>		
104	2879		A		Cast	1428829	69514	103280	3454			305			154954		1
104	2888		A	Front	Cast	217724	23593	22565							30177		1
104	2895		A	Bow (front)	Cast	2169367	140276	167982	8911	2705	567	896			75856		4
						<i>0.27</i>	<i>0.32</i>	<i>0.14</i>	<i>0.18</i>	<i>2.00</i>	<i>2.00</i>	<i>0.35</i>			<i>0.10</i>		
104	2897		A		Cast	2558312	50472	61951	6238			635			112414		4
						<i>0.10</i>	<i>0.18</i>	<i>0.18</i>	<i>0.26</i>			<i>0.22</i>			<i>0.40</i>		
104	2899		A		Cast	1155085	150378	192327	9052	9777	2238	230			198311		4
						<i>0.56</i>	<i>0.24</i>	<i>0.12</i>	<i>0.15</i>	<i>0.36</i>	<i>0.60</i>	<i>1.21</i>			<i>0.37</i>		
104	2902		A	Brooch	Cast	1073851	245767	140034	7830			864			68863		4
						<i>0.29</i>	<i>0.28</i>	<i>0.10</i>	<i>0.13</i>			<i>0.12</i>			<i>0.09</i>		
104	2902		B	Pin	Cast	827907	97939	24796	1206			611			84557		2

<i>Site</i>	SF no.	SF sub div.	Anal . area	XRF location	Manuf. method	Cu (K)	Pb (L)	Sn (K)	Ag (K)	As (K)	Ni (K)	Sb (K)	Au (L)	Bi (L)	Zn (K)	Co (K)	No. of analyses
						<i>0.16</i>	<i>0.17</i>	<i>0.05</i>	<i>0.02</i>			<i>0.31</i>			<i>0.07</i>		
104	2937		A		Sheet	3171667	36302	82793	3038	352		308			496257		10
						<i>0.11</i>	<i>0.41</i>	<i>0.80</i>	<i>0.24</i>	<i>3.16</i>		<i>0.99</i>			<i>1.01</i>		
104	2943		A		Sheet	1448975	245660	171893	13081	16327		1006			249284		4
						<i>0.16</i>	<i>0.19</i>	<i>0.21</i>	<i>0.31</i>	<i>0.11</i>		<i>0.74</i>			<i>0.11</i>		
104	2949		A		Sheet	1549740	131636	110561	6073			808			87760		3
						<i>0.17</i>	<i>0.56</i>	<i>0.37</i>	<i>0.38</i>			<i>0.27</i>			<i>0.56</i>		
104	2950		B	Reverse	Cast	981202	166688	136187	293522				2613		21344		2
						<i>0.70</i>	<i>0.35</i>	<i>0.25</i>	<i>1.38</i>				<i>1.29</i>		<i>0.16</i>		
104	2993		A		Cast	1657464	173585	93033	3928	7180		610			422923		4
						<i>0.35</i>	<i>0.26</i>	<i>1.00</i>	<i>0.32</i>	<i>0.71</i>		<i>0.41</i>			<i>0.54</i>		
104	2995		A	Large fragment	Sheet	2199143	188275	150996	10811			965			111086		4
						<i>0.07</i>	<i>0.11</i>	<i>0.07</i>	<i>0.14</i>			<i>0.29</i>			<i>0.13</i>		
104	2995		B	Small fragment	Sheet	2202348	199465	151640	13590			900			138316		3
						<i>0.04</i>	<i>0.06</i>	<i>0.18</i>	<i>0.31</i>			<i>0.13</i>			<i>0.19</i>		
104	3026		A	Curved sheet strip	Sheet	2420390	122199	96463	3961			592			431749		5
						<i>0.28</i>	<i>0.66</i>	<i>0.44</i>	<i>0.14</i>			<i>0.25</i>			<i>0.17</i>		
104	3026		B	Cast hoop	Cast	1490996	19205	35129	2679			257			89634		2
						<i>0.05</i>	<i>0.15</i>	<i>0.01</i>	<i>0.08</i>			<i>0.38</i>			<i>0.04</i>		
104	3045		A	Tube	Sheet	124543	8276								15467		2
						<i>0.99</i>	<i>1.03</i>								<i>0.30</i>		
104	3045		B	Sheet fragment	Sheet	1264022	94265	75640	1572			250			250613		2
						<i>0.27</i>	<i>0.07</i>	<i>0.04</i>	<i>0.23</i>			<i>0.08</i>			<i>0.04</i>		
104	3045		C	Sheet fragment	Sheet	1893424	94849	103561	2632						471309		2

<i>Site</i>	SF no.	SF sub div.	Anal. area	XRF location	Manuf. method	Cu (K)	Pb (L)	Sn (K)	Ag (K)	As (K)	Ni (K)	Sb (K)	Au (L)	Bi (L)	Zn (K)	Co (K)	No. of analyses
						<i>0.02</i>	<i>0.45</i>	<i>0.05</i>	<i>0.33</i>						<i>0.07</i>		
104	3048		A	Pin head	Cast	722545	48754	77335	1282			1062			23428		4
						<i>0.19</i>	<i>0.43</i>	<i>0.19</i>	<i>0.16</i>			<i>0.24</i>			<i>0.25</i>		
104	3051		A	Front	Cast	2290099	237537	76589	3937			467			40356		4
						<i>0.10</i>	<i>0.43</i>	<i>0.23</i>	<i>0.25</i>			<i>0.11</i>			<i>0.30</i>		
104	3052		A	Front	Sheet	2106264	137699	101884	5955			659			68805		4
						<i>0.40</i>	<i>0.16</i>	<i>0.27</i>	<i>0.28</i>			<i>0.18</i>			<i>0.30</i>		
104	3059		A		Melted	2843297	152186	81073	3887						19037		3
						<i>0.13</i>	<i>0.25</i>	<i>0.09</i>	<i>0.01</i>						<i>0.12</i>		
104	3064		A		Melted	1014391	64149	236592	6695			391					2
						<i>0.16</i>	<i>0.17</i>	<i>0.17</i>	<i>0.16</i>			<i>0.28</i>					
104	3077		A		Sheet	1967420	133266	38927	4656	658	374	312			810950		8
						<i>0.22</i>	<i>0.60</i>	<i>0.25</i>	<i>0.17</i>	<i>2.83</i>	<i>2.83</i>	<i>1.11</i>			<i>0.46</i>		
104	3078		A	Hook piece (front)	Sheet	2018546	110921	36058	4577			266			952073		4
						<i>0.20</i>	<i>0.20</i>	<i>0.16</i>	<i>0.15</i>			<i>1.19</i>			<i>0.38</i>		
104	3078		B	Eye piece (front)	Sheet	1914535	136112	42137	4903	4736	1634	467			108761 6		4
						<i>0.14</i>	<i>0.47</i>	<i>0.22</i>	<i>0.23</i>	<i>0.85</i>	<i>0.71</i>	<i>0.67</i>			<i>0.45</i>		
104	3088		A		Sheet	3343786	38207	29410	5052			820			106156 4		5
						<i>0.13</i>	<i>0.74</i>	<i>0.17</i>	<i>0.12</i>			<i>0.58</i>			<i>0.51</i>		
104	3089		A	Distal terminal (front right)	Cast	2702650	62576	111817	6242			233			540495		4
						<i>0.16</i>	<i>0.26</i>	<i>0.18</i>	<i>0.16</i>			<i>1.22</i>			<i>0.17</i>		
104	3090		B	Front	Cast	3293116	104158	137471	14061	4542		547			375057		5
						<i>0.21</i>	<i>0.47</i>	<i>0.27</i>	<i>0.30</i>	<i>0.61</i>		<i>0.93</i>			<i>0.14</i>		

<i>Site</i>	SF no.	SF sub div.	Anal . area	XRF location	Manuf. method	Cu (K)	Pb (L)	Sn (K)	Ag (K)	As (K)	Ni (K)	Sb (K)	Au (L)	Bi (L)	Zn (K)	Co (K)	No. of analyses
104	3091		A	Brooch	Sheet	1588702	428988	42385	2975	11963		668			401128		4
						<i>0.18</i>	<i>0.39</i>	<i>0.26</i>	<i>0.17</i>	<i>2.00</i>		<i>0.19</i>			<i>0.19</i>		
104	3091		B	Pin	Cast	518352	83946	46060	2955	1924		446			308711		2
						<i>0.08</i>	<i>0.41</i>	<i>0.12</i>	<i>0.11</i>	<i>1.41</i>		<i>0.18</i>			<i>0.16</i>		
104	3093		A	Brooch	Sheet	1494200	403652	49048	3183	28481		796			554137		4
						<i>0.19</i>	<i>0.25</i>	<i>0.17</i>	<i>0.12</i>	<i>0.19</i>		<i>0.11</i>			<i>0.04</i>		
104	3093		B	Pin	Sheet	509646	84762	47044	3382	5450	612	479			201247		2
						<i>0.01</i>	<i>0.33</i>	<i>0.24</i>	<i>0.20</i>	<i>0.44</i>	<i>1.41</i>	<i>0.43</i>			<i>0.00</i>		
104	3143		A		Sheet	131545	10669	991		17014					18846		1
104	3144		A		Sheet	2644575	139598	65277	6463	13304	4587	935			171118 1		3
						<i>0.09</i>	<i>0.13</i>	<i>0.10</i>	<i>0.26</i>	<i>0.30</i>	<i>0.22</i>	<i>0.14</i>			<i>0.29</i>		
104	3161		A		Sheet	1278663	228254	192902	10344	15689	2338	1186			277139		3
						<i>0.07</i>	<i>0.40</i>	<i>0.18</i>	<i>0.16</i>	<i>0.44</i>	<i>0.10</i>	<i>0.18</i>			<i>0.19</i>		
104	3165		A		Sheet	3898349	75381	52185	5167			638			487079		3
						<i>0.15</i>	<i>0.10</i>	<i>0.02</i>	<i>0.02</i>			<i>0.24</i>			<i>0.43</i>		
104	3169		A		Sheet	3567590	62000	32268	4252			434			516196		3
						<i>0.21</i>	<i>0.20</i>	<i>0.56</i>	<i>0.03</i>			<i>0.87</i>			<i>0.29</i>		
104	3170		A		Sheet	1013087	98715	111933	3494	9754		149			95859		3
						<i>0.24</i>	<i>0.14</i>	<i>0.01</i>	<i>0.04</i>	<i>0.10</i>		<i>1.73</i>			<i>0.26</i>		
104	3203		A		Sheet	3752954	85450	84515	25552			1124			355061		6
						<i>0.15</i>	<i>0.44</i>	<i>0.19</i>	<i>0.20</i>			<i>0.16</i>			<i>0.24</i>		
104	3206		A		Sheet	1860326	96041	27247	2363	8496					469226		5
						<i>0.06</i>	<i>0.40</i>	<i>0.08</i>	<i>0.13</i>	<i>0.29</i>					<i>0.27</i>		

<i>Site</i>	SF no.	SF sub div.	Anal. area	XRF location	Manuf. method	Cu (K)	Pb (L)	Sn (K)	Ag (K)	As (K)	Ni (K)	Sb (K)	Au (L)	Bi (L)	Zn (K)	Co (K)	No. of analyses
<i>104</i>	3209		A		Wire	984138	6419								275416		4
						<i>0.11</i>	<i>0.17</i>								<i>0.30</i>		
<i>104</i>	3210		A		Cast	1009207	230422	143815	3752	13418		725			13069		3
						<i>0.09</i>	<i>0.16</i>	<i>0.07</i>	<i>0.10</i>	<i>0.20</i>		<i>0.20</i>			<i>0.14</i>		
<i>104</i>	3223		A		Sheet	3136850	138472	55937	3546	20881		1314			603270		3
						<i>0.21</i>	<i>0.41</i>	<i>0.30</i>	<i>0.88</i>	<i>0.54</i>		<i>0.04</i>			<i>0.31</i>		
<i>104</i>	3232		B	Cast buckle frame & prong	Cast	942354	4867		567910				989		32414		1
<i>104</i>	3236		A		Melted	1467646	95054	48522	2061			459			280813		2
						<i>0.14</i>	<i>0.09</i>	<i>0.11</i>	<i>0.16</i>			<i>0.18</i>			<i>0.05</i>		
<i>104</i>	3249		A		Cast	199544	13392	211	1418			135			59623		2
						<i>0.02</i>	<i>0.80</i>	<i>0.18</i>	<i>0.14</i>			<i>0.17</i>			<i>0.31</i>		
<i>104</i>	3283		A		Cast	2104854	48923	23158	1972			1075			172415		4
						<i>0.22</i>	<i>0.13</i>	<i>0.12</i>	<i>0.16</i>			<i>0.17</i>			<i>0.33</i>		
<i>104</i>	3299		B	Reverse	Sheet	1424093	808182	67659	1993			947			23932		2
						<i>0.02</i>	<i>0.11</i>	<i>0.27</i>	<i>0.32</i>			<i>0.25</i>			<i>0.10</i>		
<i>104</i>	3299		C	Tube	Sheet	705459	69594	176391	2051			543			8200		2
						<i>0.48</i>	<i>0.37</i>	<i>0.25</i>	<i>0.15</i>			<i>0.23</i>			<i>0.05</i>		
<i>104</i>	3300		A		Sheet	1887157	184430	144555	4076	5804		298	380		149534		4
						<i>0.32</i>	<i>0.55</i>	<i>0.25</i>	<i>0.27</i>	<i>0.59</i>		<i>1.16</i>	<i>1.16</i>		<i>0.33</i>		
<i>104</i>	3313		A		Cast	2057283	218444	136010	26057			1100			86863		4
						<i>0.15</i>	<i>0.29</i>	<i>0.14</i>	<i>1.04</i>			<i>0.19</i>			<i>0.33</i>		
<i>104</i>	3314		A		Sheet	1920646	142426	159939	4032	17868	2958	471			254098		3
						<i>0.12</i>	<i>0.41</i>	<i>0.19</i>	<i>0.02</i>	<i>0.13</i>	<i>0.92</i>	<i>0.36</i>			<i>0.34</i>		

<i>Site</i>	SF no.	SF sub div.	Anal . area	XRF location	Manuf. method	Cu (K)	Pb (L)	Sn (K)	Ag (K)	As (K)	Ni (K)	Sb (K)	Au (L)	Bi (L)	Zn (K)	Co (K)	No. of analyses
104	3316		A	Buckle sheet	Sheet	1841254	170695	178662	5980			899			73625		3
						<i>0.15</i>	<i>0.35</i>	<i>0.18</i>	<i>0.19</i>			<i>0.30</i>			<i>0.12</i>		
104	3316		B	Frame and tongue	Cast	1103470	46609	113042	1996			108			156568		2
						<i>0.50</i>	<i>0.31</i>	<i>0.13</i>	<i>0.00</i>			<i>1.41</i>			<i>0.44</i>		
104	3316		C	Rolled sheet	Sheet	783749	160138	113299	6460			664			57305		2
						<i>0.09</i>	<i>0.04</i>	<i>0.01</i>	<i>0.06</i>			<i>0.07</i>			<i>0.01</i>		
104	3317		A		Sheet	682410	190410	169526	5454			716			42490		3
						<i>0.29</i>	<i>0.22</i>	<i>0.11</i>	<i>0.12</i>			<i>0.24</i>			<i>0.16</i>		
104	3318	a	A		Sheet	1296144	250799	176047	6482	10452		889			101266		3
						<i>0.67</i>	<i>0.24</i>	<i>0.27</i>	<i>0.35</i>	<i>0.90</i>		<i>0.40</i>			<i>0.22</i>		
104	3318	b	A		Sheet	1004706	262340	207740	6320	9185	346	875		1873	85092		4
						<i>0.52</i>	<i>0.39</i>	<i>0.19</i>	<i>0.43</i>	<i>0.72</i>	<i>2.00</i>	<i>0.42</i>		<i>0.72</i>	<i>0.45</i>		
104	3318	c	A		Sheet	2433990	155319	145858	3480			567			135291		4
						<i>0.30</i>	<i>0.45</i>	<i>0.36</i>	<i>0.24</i>			<i>0.30</i>			<i>0.36</i>		
104	3318	d	A		Sheet	1479974	202606	179407	4261						100653		3
						<i>0.34</i>	<i>0.21</i>	<i>0.37</i>	<i>0.35</i>						<i>0.40</i>		
104	3318	e	A		Sheet	2144785	146091	109416	3860			371			86786		3
						<i>0.21</i>	<i>0.33</i>	<i>0.19</i>	<i>0.10</i>			<i>0.87</i>			<i>0.12</i>		
104	3318	f	A		Sheet	2774029	91847	98186	3389			387			89330		3
						<i>0.08</i>	<i>0.37</i>	<i>0.18</i>	<i>0.19</i>			<i>0.28</i>			<i>0.17</i>		
104	3327		A		Struck	2556252	68677	54772	2077			477			161543		4
						<i>0.20</i>	<i>0.73</i>	<i>0.60</i>	<i>0.62</i>			<i>0.38</i>			<i>0.42</i>		
104	3328		A		Cast	1874317	231650	164191	18821	17938					65705		2
						<i>0.16</i>	<i>0.12</i>	<i>0.13</i>	<i>0.09</i>	<i>0.02</i>					<i>0.20</i>		

<i>Site</i>	SF no.	SF sub div.	Anal. area	XRF location	Manuf. method	Cu (K)	Pb (L)	Sn (K)	Ag (K)	As (K)	Ni (K)	Sb (K)	Au (L)	Bi (L)	Zn (K)	Co (K)	No. of analyses
104	3329		A		Cast	2276565	127886	106202	4673			861			95028		4
						<i>0.23</i>	<i>0.53</i>	<i>0.62</i>	<i>0.70</i>			<i>0.15</i>			<i>0.82</i>		
104	3332		A		Wire	1272837	96556	87837	4904			380			36556		5
						<i>0.25</i>	<i>0.47</i>	<i>0.13</i>	<i>0.25</i>			<i>0.57</i>			<i>0.36</i>		
104	3342		A	Front (wood on reverse). Fragment A.	Sheet	2702056	56005	99327	5975	14074					263373		2
						<i>0.08</i>	<i>0.02</i>	<i>0.02</i>	<i>0.03</i>	<i>0.27</i>					<i>0.11</i>		
104	3342		B	Front (wood on reverse). Fragment B.	Sheet	2473493	58577	104377	6533	23303	1638	263			258103		2
						<i>0.08</i>	<i>0.09</i>	<i>0.01</i>	<i>0.01</i>	<i>0.01</i>	<i>1.41</i>	<i>1.41</i>			<i>0.04</i>		
104	3342		C	Front (wood on reverse). Fragment C.	Sheet	2492458	54941	101197	5965	20177					326155		1
104	3348	b	A		Sheet	2837543	92195	124972	6192			825			195886		6
						<i>0.06</i>	<i>0.15</i>	<i>0.10</i>	<i>0.14</i>			<i>0.13</i>			<i>0.18</i>		
104	3349		A	Eye piece (front)	Sheet	1944938	202937	131359	6182	15115	4430	946			260662		4
						<i>0.42</i>	<i>0.47</i>	<i>0.06</i>	<i>0.13</i>	<i>0.59</i>	<i>0.16</i>	<i>0.09</i>			<i>0.17</i>		
104	3349		B	Hook piece (reverse)	Cast	2395068	69418	56453	1934			1436			488805		4
						<i>0.16</i>	<i>0.41</i>	<i>0.18</i>	<i>0.16</i>			<i>0.15</i>			<i>0.14</i>		
104	3349		C	Repousse sheet (front)	Sheet	2607307	198287	37846	1741			1653			781448		3
						<i>0.18</i>	<i>0.62</i>	<i>0.39</i>	<i>0.33</i>			<i>0.26</i>			<i>0.19</i>		
104	3349		E	Bar	Cast	1691850	329145	110272	5041			789			113796		4
						<i>0.29</i>	<i>0.39</i>	<i>0.39</i>	<i>0.24</i>			<i>0.33</i>			<i>0.38</i>		
104	3350		B	Hook piece (reverse)	Sheet	2587466	49496	58975	1612			1517			412546		2
						<i>0.02</i>	<i>0.10</i>	<i>0.07</i>	<i>0.13</i>			<i>0.09</i>			<i>0.02</i>		
104	3350		D	Eye piece (reverse)	Sheet	2872952	58846	59074	1894			1534			383654		3

<i>Site</i>	SF no.	SF sub div.	Anal. area	XRF location	Manuf. method	Cu (K)	Pb (L)	Sn (K)	Ag (K)	As (K)	Ni (K)	Sb (K)	Au (L)	Bi (L)	Zn (K)	Co (K)	No. of analyses
						<i>0.12</i>	<i>0.33</i>	<i>0.12</i>	<i>0.23</i>			<i>0.05</i>			<i>0.15</i>		
104	3350		F	Eye piece, repousse sheet (front)	Sheet	2408850	103480	17100	1629			1391			527968		2
						<i>0.02</i>	<i>0.15</i>	<i>0.02</i>	<i>0.02</i>			<i>0.10</i>			<i>0.11</i>		
104	3355		A	Bow (front)	Cast	2750556	98201	92923	4513			504			142810		5
						<i>0.21</i>	<i>0.66</i>	<i>0.38</i>	<i>0.46</i>			<i>0.59</i>			<i>0.54</i>		
104	3363		A	Large folded sheet with wood	Sheet	3057065	60336	87389	2162	12755	7429	374			300560		3
						<i>0.03</i>	<i>0.18</i>	<i>0.21</i>	<i>0.27</i>	<i>0.32</i>	<i>0.14</i>	<i>0.18</i>			<i>0.24</i>		
104	3363		B	Small fragment	Sheet	3399456	48936	79384	2017	10609	9443	502			371493		1
104	3363		C	Large sheet fragment (avoiding bar)	Sheet	3177867	42073	73551	2206	6569	2948				200276		2
						<i>0.04</i>	<i>0.17</i>	<i>0.10</i>	<i>0.05</i>	<i>0.28</i>	<i>1.41</i>				<i>0.23</i>		
104	3363		D	Loose sheet strip	Sheet	2471534	44895	52887	3186	8256					391542		3
						<i>0.03</i>	<i>0.12</i>	<i>0.04</i>	<i>0.05</i>	<i>0.17</i>					<i>0.07</i>		
104	3364		A		Sheet	2744276	55756	99075	2429	11400					294548		5
						<i>0.14</i>	<i>0.16</i>	<i>0.06</i>	<i>0.10</i>	<i>0.12</i>					<i>0.29</i>		
104	3372		A		Cast	1298341	186425	140802	6660			352			104252		3
						<i>0.24</i>	<i>0.26</i>	<i>0.16</i>	<i>0.21</i>			<i>0.90</i>			<i>0.14</i>		
104	3373		A	Reverse	Sheet	2707382	94713	144809	6153			1404			108713		4
						<i>0.14</i>	<i>0.28</i>	<i>0.11</i>	<i>0.08</i>			<i>0.18</i>			<i>0.04</i>		
104	3373		B	Whitish residue	Sheet	2557472	117039	130585	5249			1221			105147		2
						<i>0.00</i>	<i>0.03</i>	<i>0.01</i>	<i>0.01</i>			<i>0.07</i>			<i>0.00</i>		
104	3387		A	Knot'	Wire	606446	174212	27604	3394	7972		405			90582		5
						<i>0.45</i>	<i>0.47</i>	<i>0.28</i>	<i>0.23</i>	<i>0.97</i>		<i>1.04</i>			<i>0.33</i>		

<i>Site</i>	SF no.	SF sub div.	Anal. area	XRF location	Manuf. method	Cu (K)	Pb (L)	Sn (K)	Ag (K)	As (K)	Ni (K)	Sb (K)	Au (L)	Bi (L)	Zn (K)	Co (K)	No. of analyses
104	3389		A		Cast	817796	676012	93701	5247	29315	1369	924			248303		5
						0.12	0.21	0.12	0.15	0.61	0.57	0.57			0.07		
104	3391		A	Front	Cast	2027521	177154	104374	76858			152	37775				5
						0.13	0.31	0.34	0.41			2.24	1.12				
104	3393		A	Hook piece (front)	Cast	2656372	145329	82208	4723	13846		648			331418		4
						0.25	0.16	0.21	0.26	0.19		0.28			0.32		
104	3393		B	Eye piece (reverse)	Cast	2573266	121353	89030	5761	11989		862			533369		4
						0.06	0.16	0.20	0.25	0.17		0.21			0.10		
104	3394		A		Cast	3151484	142784	60803	3653			524			347916		3
						0.11	0.07	0.17	0.25			0.08			0.40		
104	3395		A	Front	Sheet	2516966	176193	152517	4968	14012	10026	817			436503		5
						0.22	0.38	0.25	0.24	0.42	0.34	0.31			0.12		
104	3396		A		Sheet	3985467	93345	29000	5455			1123			742575		8
						0.11	0.46	0.18	0.37			0.12			0.23		
104	3443		A		Sheet	1245692	369154	246673	9317			1899			46868		1
104	3444		A		Cast	1398370	357133	180808	33826			830					4
						0.45	0.26	0.23	0.31			0.11					
104	3453		B	Top	Cast	3392510	34084	76256	16855			484	10898		43644		1
104	3460		A		Sheet	1058449	270103	208750	36078	14576	2354	889			110950		4
						0.43	0.19	0.11	0.26	0.29	0.23	0.09			0.41		
104	3475		A		Cast	2610062	14901	24789	3546	4764					19126		2
						0.11	0.52	0.09	0.33	0.81					0.07		

<i>Site</i>	SF no.	SF sub div.	Anal. area	XRF location	Manuf. method	Cu (K)	Pb (L)	Sn (K)	Ag (K)	As (K)	Ni (K)	Sb (K)	Au (L)	Bi (L)	Zn (K)	Co (K)	No. of analyses
104	3482		A	Only large enough for one analysis	Cast	1330680	533990	37332	8453			1062			369073		1
104	3494		A		Sheet	1900443	128408	98297	2681			653			124634		2
						0.23	0.25	0.25	0.05			0.20			0.10		
104	3495		A		Sheet	3080235	119197	98081	4774			919			175770		4
						0.06	0.39	0.09	0.08			0.15			0.15		
104	3524		A	Front	Cast	2433084	182353	106518	3556			668			195641		4
						0.10	0.55	0.18	0.20			0.38			0.16		
104	3525		A		Sheet	2346988	98030	100516	5160			791			260264		4
						0.22	0.15	0.50	0.63			0.64			0.47		
104	3530		A		Sheet	952147	21123	115633	1562			602					3
						0.29	0.12	0.04	0.21			0.87					
104	3532	1	A		Cast	1681597	123466	116326	5015			683			62423		3
						0.22	0.25	0.08	0.15			0.36			0.22		
104	3532		A	Reverse	Cast	1568756	42283	113054	3578			790	34468		27180		3
						0.26	0.26	0.12	0.63			0.17	1.10		0.06		
104	3532	a	A		Cast	2226690	1837	145202	1621	13945	16713	666					2
						0.21	0.05	0.04	0.13	0.20	0.05	0.30					
104	3532		C	Reverse	Cast	1429669	43995	139186	2434			940			24887		1
104	3534		A	Front	Sheet	1453816	198589	224739	35504			519			110610		4
						0.18	0.26	0.19	0.28			0.15			0.38		
104	3573		A		Sheet	2004022	103776	119273	5912	8890		577			355658		3
						0.34	0.39	0.18	0.06	0.51		0.16			0.12		

<i>Site</i>	SF no.	SF sub div.	Anal. area	XRF location	Manuf. method	Cu (K)	Pb (L)	Sn (K)	Ag (K)	As (K)	Ni (K)	Sb (K)	Au (L)	Bi (L)	Zn (K)	Co (K)	No. of analyses
<i>104</i>	3577		A		Sheet	948875	43205	93668	2338	5621	3044	251			134353		2
						<i>0.01</i>	<i>0.10</i>	<i>0.06</i>	<i>0.04</i>	<i>0.15</i>	<i>0.11</i>	<i>0.35</i>			<i>0.15</i>		
<i>104</i>	3579		A		Cast	655595	37002	109543	1672	929							4
						<i>0.43</i>	<i>0.23</i>	<i>0.18</i>	<i>0.18</i>	<i>2.00</i>							
<i>104</i>	3580		A	Reverse	Cast	1789250	159293	164581	14832	9979	1995	931			199549		5
						<i>0.06</i>	<i>0.22</i>	<i>0.11</i>	<i>0.07</i>	<i>0.37</i>	<i>0.91</i>	<i>0.12</i>			<i>0.12</i>		
<i>104</i>	3581		A	Repousse sheet (small fragment, reverse)	Sheet	2490814	66033	42582	1672	8749	5586	563			110615		4
						<i>0.16</i>	<i>0.19</i>	<i>0.15</i>	<i>0.13</i>	<i>0.30</i>	<i>0.32</i>	<i>0.39</i>			<i>0.15</i>		
<i>104</i>	3582		A	Outer edge	Cast	2535661	140964	106587	1906			428			311455		5
						<i>0.20</i>	<i>0.25</i>	<i>0.23</i>	<i>0.32</i>			<i>0.58</i>			<i>0.18</i>		
<i>104</i>	3596		A		Cast	1288163	211479	181922	11259			1130			77634		4
						<i>0.22</i>	<i>0.30</i>	<i>0.22</i>	<i>0.13</i>			<i>0.23</i>			<i>0.44</i>		
<i>104</i>	3597		A		Sheet	1984641	151364	132612	6976	13772		1429					4
						<i>0.19</i>	<i>0.14</i>	<i>0.15</i>	<i>0.24</i>	<i>0.11</i>		<i>0.17</i>					
<i>104</i>	3616		A		Melted	1209528	417064	157359	2507			979			85000		2
						<i>0.06</i>	<i>0.20</i>	<i>0.02</i>	<i>0.25</i>			<i>0.09</i>			<i>0.25</i>		
<i>104</i>	3618		A	Drop A	Melted	1785019	88572	218342	5464			429					1
<i>104</i>	3618		C	Drop C	Melted	655526	307763	68322	93307			882	8947				3
						<i>0.47</i>	<i>0.30</i>	<i>0.16</i>	<i>0.04</i>			<i>0.24</i>	<i>0.33</i>				
<i>104</i>	3618		D	Drop D	Melted	1891037	107949	56303	4888				3567		234574		2
						<i>0.07</i>	<i>0.05</i>	<i>0.06</i>	<i>0.01</i>				<i>0.14</i>		<i>0.06</i>		
<i>104</i>	3674	1	A	Thin plate on front	Cast	11318	39289	94234	6287					711	1671		2
						<i>1.12</i>	<i>1.38</i>	<i>1.40</i>	<i>0.82</i>					<i>1.41</i>	<i>0.13</i>		

<i>Site</i>	SF no.	SF sub div.	Anal. area	XRF location	Manuf. method	Cu (K)	Pb (L)	Sn (K)	Ag (K)	As (K)	Ni (K)	Sb (K)	Au (L)	Bi (L)	Zn (K)	Co (K)	No. of analyses
104	3674	2	B	Reverse of Stud	Cast	1597	497		1076	316					499		2
						<i>1.41</i>	<i>1.41</i>		<i>1.41</i>	<i>1.41</i>					<i>1.41</i>		
104	3675	1	B	Reverse of Stud	Cast	47888	2821								4755		2
						<i>0.05</i>	<i>0.19</i>								<i>0.11</i>		
104	3675	3	B	Reverse	Sheet	1728667	37780	11266	4475				162		50379		2
						<i>0.27</i>	<i>0.10</i>	<i>0.95</i>	<i>0.28</i>				<i>0.21</i>		<i>0.06</i>		
104	3677		A	Front	Sheet	2457998	186115	47582	3116	12113		604			188088		2
						<i>0.41</i>	<i>0.16</i>	<i>0.02</i>	<i>0.16</i>	<i>0.05</i>		<i>0.37</i>			<i>0.03</i>		
104	3677		B	Front	Sheet	1967091	181493	47756	3416	11341		630			288468		2
						<i>0.19</i>	<i>0.61</i>	<i>0.14</i>	<i>0.18</i>	<i>0.30</i>		<i>0.04</i>			<i>0.30</i>		
104	4211		A	Bow (front)	Cast	2111995	113458	110038	20827			1108			118599		5
						<i>0.21</i>	<i>0.24</i>	<i>0.17</i>	<i>0.10</i>			<i>0.15</i>			<i>0.36</i>		
104	BM1 2		A	Reverse (foot)	Cast	3460897	124681	132342	8193	3279		548			230034		3
						<i>0.10</i>	<i>0.61</i>	<i>0.09</i>	<i>0.14</i>	<i>1.73</i>		<i>0.87</i>			<i>0.13</i>		
104	BM1 2		B	Reverse	Sheet	1617044	243438	212997	7286			831			104603		1
104	BM1 3		A	Rivet	Cast	963003	151515	76238	5443			428			32689		1
104	BM1 8		C	Arm (no plate)	Cast	1412134	144935	243368	21015			150			108429		2
						<i>0.15</i>	<i>0.48</i>	<i>0.06</i>	<i>0.17</i>			<i>1.41</i>			<i>0.02</i>		
104	BM1 8		D	Reverse (stud)	Cast	751773	87039	107356	8840						126517		1
104	BM1 8		E	Reverse (arm)	Cast	136232	5155	16618							14895		2

<i>Site</i>	SF no.	SF sub div.	Anal. area	XRF location	Manuf. method	Cu (K)	Pb (L)	Sn (K)	Ag (K)	As (K)	Ni (K)	Sb (K)	Au (L)	Bi (L)	Zn (K)	Co (K)	No. of analyses
						<i>0.95</i>	<i>0.43</i>	<i>0.57</i>							<i>0.99</i>		
104	BM19		D	Rivet	Cast	1917806	331753	173279	8930		4660	1112			212619		1
104	BM19		E	Reverse	Cast	2312260	174087	186960	13535			1094			148995		2
						<i>0.56</i>	<i>0.50</i>	<i>0.20</i>	<i>0.22</i>			<i>0.28</i>			<i>0.29</i>		
104	BM1		F	Reverse (arm)	Cast	129967	9155	11277							12603		3
						<i>1.52</i>	<i>1.36</i>	<i>1.18</i>							<i>1.48</i>		
104	BM1		G	Stud	Cast	615900	135190	95223	6455			461			46674		1
104	BM20		B	Front (concave face)	Sheet	1200045	274333	92367	12715	5184		799			350986		2
						<i>0.08</i>	<i>0.38</i>	<i>1.41</i>	<i>0.15</i>	<i>1.41</i>		<i>1.41</i>			<i>0.06</i>		
104	BM21		A	Front	Sheet	1884574	113264	143900	8797	4600		318			267596		3
						<i>0.30</i>	<i>0.52</i>	<i>0.19</i>	<i>0.20</i>	<i>1.13</i>		<i>1.73</i>			<i>0.29</i>		
104	BM33		C	Reverse (base metal)	Cast	1986704	148979	152358	12776			1147			152635		2
						<i>0.64</i>	<i>0.36</i>	<i>0.09</i>	<i>0.07</i>			<i>0.08</i>			<i>0.64</i>		
104	BM3		D	Reverse	Cast	2141561	247736	182351	15121			536			185292		2
						<i>0.02</i>	<i>0.27</i>	<i>0.05</i>	<i>0.03</i>			<i>1.41</i>			<i>0.17</i>		
104	BM5		F	Reverse (arm)	Cast	716231	40029	56786	4497				3495		4325		2
						<i>1.22</i>	<i>0.75</i>	<i>0.30</i>	<i>0.53</i>				<i>1.41</i>		<i>1.41</i>		
104	BM5		G	Central stud	Cast	552560	45438	39550	3327	2758		269			64545		1
104	BM6	7A	B	Rivet	Cast	758829	61400	165314	4334				104				1

<i>Site</i>	SF no.	SF sub div.	Anal. area	XRF location	Manuf. method	Cu (K)	Pb (L)	Sn (K)	Ag (K)	As (K)	Ni (K)	Sb (K)	Au (L)	Bi (L)	Zn (K)	Co (K)	No. of analyses
104	BM6	7A	C	Rivet	Cast	210984	5936	22111	793			105			1296		1
104	BM6	7A	F	Brass strip	Sheet	774175	14076	23079	1483			387			189175		1
104	BM6	7A	G	Brass strip	Sheet	730064	11066	13751	1604			388			177232		1
114	1000		A	Head side	Struck	1115027	124643 3	5973	9512			1160					4
						<i>0.10</i>	<i>0.05</i>	<i>0.60</i>	<i>0.11</i>			<i>0.16</i>					
114	1001		A	Rear	Cast	1006201	386888	237801	7921	22780	1758	1917			99981		5
						<i>0.32</i>	<i>0.06</i>	<i>0.19</i>	<i>0.19</i>	<i>0.08</i>	<i>0.15</i>	<i>0.12</i>			<i>0.15</i>		
114	1004		A	foot	Cast	1717283	459184	155833	5573			168			94969		7
						<i>0.28</i>	<i>0.82</i>	<i>0.37</i>	<i>0.43</i>			<i>1.78</i>			<i>0.51</i>		
114	1005		A	Front	Cast	1939479	118907	123688	12004	33790		476			346208		5
						<i>0.24</i>	<i>0.39</i>	<i>0.28</i>	<i>0.30</i>	<i>0.61</i>		<i>0.94</i>			<i>0.32</i>		
114	1007		B	Reverse	Cast	1475372	122461	76570	8615						42989		2
						<i>0.32</i>	<i>0.06</i>	<i>0.02</i>	<i>0.13</i>						<i>0.69</i>		
114	1034		A	Front	Cast	1856296	232325	136573	8369	10888	2719	836			183292		5
						<i>0.29</i>	<i>0.29</i>	<i>0.19</i>	<i>0.18</i>	<i>0.63</i>	<i>0.61</i>	<i>0.20</i>			<i>0.13</i>		
114	1036		A		Cast	1223528	33874	131234	3647	2973					25470		1
114	1037		B	Reverse	Cast	1422271	86455	64220	7661						43260		2
						<i>0.49</i>	<i>0.34</i>	<i>0.26</i>	<i>0.03</i>						<i>0.80</i>		
114	1039		B	Reverse	Cast	2033865	54390	79319	8258			662			88883		1

<i>Site</i>	SF no.	SF sub div.	Anal. area	XRF location	Manuf. method	Cu (K)	Pb (L)	Sn (K)	Ag (K)	As (K)	Ni (K)	Sb (K)	Au (L)	Bi (L)	Zn (K)	Co (K)	No. of analyses
114	1040		A	Outer	Melted	1043395	325934	272266	7677	16313	5642	4016					2
						<i>0.04</i>	<i>0.01</i>	<i>0.08</i>	<i>0.20</i>	<i>0.01</i>	<i>0.15</i>	<i>0.07</i>					
114	1044		B	Reverse	Cast	1586809	99400	51836	5057						95851		2
						<i>0.78</i>	<i>0.78</i>	<i>0.43</i>	<i>0.22</i>						<i>1.08</i>		
114	1048		A	Hook piece (front)	Cast	2108702	88650	215836	1532								4
						<i>0.44</i>	<i>0.25</i>	<i>0.07</i>	<i>0.10</i>								
114	1048		B	Bar (rear)	Cast	1338659	307974	177207	5024			483			37257		4
						<i>0.19</i>	<i>0.37</i>	<i>0.34</i>	<i>0.22</i>			<i>1.16</i>			<i>0.16</i>		
114	1050		A	Outer	Sheet	1238969	106405	253167	3546	45290	1278	541		1725			2
						<i>0.02</i>	<i>0.67</i>	<i>0.40</i>	<i>0.31</i>	<i>0.46</i>	<i>1.41</i>	<i>1.41</i>		<i>1.41</i>			
114	1051		A	Hook piece (front)	Cast	2204049	194519	216028	1424								4
						<i>0.03</i>	<i>0.78</i>	<i>0.07</i>	<i>0.28</i>								
114	1051		B	Bar (reverse)	Cast	1052326	439654	182952	5136						31933		3
						<i>0.39</i>	<i>0.31</i>	<i>0.25</i>	<i>0.39</i>						<i>0.53</i>		
114	1055		A	Reverse	Sheet	2205021	110949	170463	7129	13534					176162		6
						<i>0.19</i>	<i>0.34</i>	<i>0.19</i>	<i>0.16</i>	<i>0.21</i>					<i>0.12</i>		
114	1055		B	Pin	Wire	612911	56238	86924	4197	6136					45457		2
						<i>0.20</i>	<i>0.11</i>	<i>0.01</i>	<i>0.01</i>	<i>0.08</i>					<i>0.20</i>		
114	1058		A		Cast	1964821	400077	55602	7716	21966		1031			315235		4
						<i>0.23</i>	<i>0.39</i>	<i>0.34</i>	<i>0.13</i>	<i>0.78</i>		<i>0.12</i>			<i>0.27</i>		
114	1059		A		Cast	2463924	201421	110472	6178	17925		843			337053		4
						<i>0.33</i>	<i>0.45</i>	<i>0.73</i>	<i>0.21</i>	<i>0.60</i>		<i>0.44</i>			<i>0.12</i>		
114	1060		A		Cast	2689272	368731	42777	6775			844			533800		4
						<i>0.10</i>	<i>0.22</i>	<i>0.14</i>	<i>0.17</i>			<i>0.17</i>			<i>0.24</i>		

<i>Site</i>	SF no.	SF sub div.	Anal. area	XRF location	Manuf. method	Cu (K)	Pb (L)	Sn (K)	Ag (K)	As (K)	Ni (K)	Sb (K)	Au (L)	Bi (L)	Zn (K)	Co (K)	No. of analyses
114	1061	A	A	Distal Terminal (rear)	Cast	3688547	60712	55869	6760	3567		141			240807		5
						<i>0.06</i>	<i>0.20</i>	<i>0.13</i>	<i>0.09</i>	<i>0.93</i>		<i>2.24</i>			<i>0.12</i>		
114	1061	B	A	Distal Terminal (rear)	Cast	3391159	96282	60732	8085	8073		664			181578		5
						<i>0.17</i>	<i>0.63</i>	<i>0.15</i>	<i>0.09</i>	<i>0.57</i>		<i>0.65</i>			<i>0.47</i>		
114	1061	C	A	Rounded Proximal Terminal (right, front)	Cast	1595359	524463	132090	6652			374			51049		4
						<i>0.24</i>	<i>0.25</i>	<i>0.29</i>	<i>0.15</i>			<i>1.17</i>			<i>0.18</i>		
114	1061	C	B	Upper Shaft front (two sheets joining the Distal Terminal and Central Shaft together)	Sheet	2364904	100013	97898	3711	7123					328241		2
						<i>0.03</i>	<i>0.67</i>	<i>0.48</i>	<i>0.54</i>	<i>0.59</i>					<i>0.01</i>		
114	1061	C	C	Central Shaft (front)	Cast	3040499	121710	68036	8451						146830		3
						<i>0.18</i>	<i>0.51</i>	<i>0.11</i>	<i>0.15</i>						<i>0.22</i>		
114	1062		A		Cast	1989440	575357	70438	7255	40367		888			322932		4
						<i>0.19</i>	<i>0.19</i>	<i>0.13</i>	<i>0.12</i>	<i>0.11</i>		<i>0.22</i>			<i>0.22</i>		
114	1064		A	Bow front	Cast	1731635	183394	167552	8212	12381	3874	770			241894		4
						<i>0.38</i>	<i>0.23</i>	<i>0.21</i>	<i>0.18</i>	<i>0.36</i>	<i>0.36</i>	<i>0.28</i>			<i>0.40</i>		
114	1064		B	Catch	Cast	850397	239218	196111	10353	15060	2645	1018			228432		1
114	1065		A		Cast	2488250	283838	118214	4704	2841	842	683			149119		5
						<i>0.08</i>	<i>0.09</i>	<i>0.24</i>	<i>0.32</i>	<i>2.24</i>	<i>2.24</i>	<i>0.11</i>			<i>0.51</i>		
114	1066		A	Hook piece front	Cast	1406268	358048	212939	6379			696			75717		4
						<i>0.19</i>	<i>0.15</i>	<i>0.08</i>	<i>0.14</i>			<i>0.29</i>			<i>0.14</i>		
114	1066		B	Eye piece front	Cast	2473253	237156	149793	6112			771			133093		4
						<i>0.37</i>	<i>0.51</i>	<i>0.49</i>	<i>0.07</i>			<i>0.33</i>			<i>0.26</i>		

<i>Site</i>	SF no.	SF sub div.	Anal . area	XRF location	Manuf. method	Cu (K)	Pb (L)	Sn (K)	Ag (K)	As (K)	Ni (K)	Sb (K)	Au (L)	Bi (L)	Zn (K)	Co (K)	No. of analyses
114	1067		A	Hook piece front	Cast	1784596	290598	175869	6975	9066		846			98335		4
						<i>0.19</i>	<i>0.26</i>	<i>0.36</i>	<i>0.29</i>	<i>1.16</i>		<i>0.30</i>			<i>0.39</i>		
114	1067		B	Eye piece front	Cast	1584475	359123	209584	6268			733			66594		4
						<i>0.13</i>	<i>0.30</i>	<i>0.08</i>	<i>0.08</i>			<i>0.30</i>			<i>0.10</i>		
114	1069		A		Cast	1948569	287680	115667	1397	20828	3517				225015		4
						<i>0.16</i>	<i>0.42</i>	<i>0.18</i>	<i>0.17</i>	<i>0.34</i>	<i>0.13</i>				<i>0.15</i>		
114	1070		A		Cast	1730848	423768	132232	5584	10522		773			188765		4
						<i>0.58</i>	<i>0.49</i>	<i>0.67</i>	<i>0.50</i>	<i>1.16</i>		<i>0.69</i>			<i>0.51</i>		
114	1075		A		Cast	1091116	922863	71838	8189	23060	1020	775			366440		4
						<i>0.38</i>	<i>0.33</i>	<i>0.11</i>	<i>0.21</i>	<i>1.26</i>	<i>1.28</i>	<i>0.11</i>			<i>0.56</i>		
114	1094		A	Bow (front)	Cast	2584499	130991	159281	6155			890			61467		6
						<i>0.25</i>	<i>0.47</i>	<i>0.23</i>	<i>0.26</i>			<i>0.20</i>			<i>0.34</i>		
114	1148		A	Foot front	Cast	2621994	509951	83785	4963			669			87457		4
						<i>0.04</i>	<i>0.09</i>	<i>0.06</i>	<i>0.06</i>			<i>0.10</i>			<i>0.10</i>		
114	1159		A		Cast	1503593	2218	162183	5247	7482							5
						<i>0.22</i>	<i>0.08</i>	<i>0.24</i>	<i>0.41</i>	<i>0.42</i>							
114	1161		A	Front	Cast	2845606	178254	104972	5370	3961		830			152623		5
						<i>0.28</i>	<i>0.81</i>	<i>0.31</i>	<i>0.31</i>	<i>2.24</i>		<i>0.20</i>			<i>0.34</i>		
114	1162		A	Front	Cast	1608698	304921	137881	4948	12431		629			145980		6
						<i>0.20</i>	<i>0.43</i>	<i>0.47</i>	<i>0.22</i>	<i>0.80</i>		<i>0.56</i>			<i>0.29</i>		
114	1162		B	Loose sheet	Sheet	1681126	329374	198828	4762	13143	1967	508			157055		4
						<i>0.23</i>	<i>0.12</i>	<i>0.42</i>	<i>0.47</i>	<i>1.16</i>	<i>1.17</i>	<i>0.82</i>			<i>0.67</i>		
114	1163		A	Eye piece (reverse)	Cast	1874250	228143	210552	8026			346			194227		4
						<i>0.41</i>	<i>0.36</i>	<i>0.36</i>	<i>0.34</i>			<i>1.16</i>			<i>0.71</i>		

<i>Site</i>	SF no.	SF sub div.	Anal . area	XRF location	Manuf. method	Cu (K)	Pb (L)	Sn (K)	Ag (K)	As (K)	Ni (K)	Sb (K)	Au (L)	Bi (L)	Zn (K)	Co (K)	No. of analyses
114	1163		B	Hook piece (front)	Sheet	2398690	121534	115556	2585	31124	5488	527			311473		4
						<i>0.12</i>	<i>0.14</i>	<i>0.05</i>	<i>0.06</i>	<i>0.07</i>	<i>0.11</i>	<i>0.15</i>			<i>0.07</i>		
114	1175		A	Outer crossover	Wire	662321	97522	140059	2729						4900		2
						<i>0.33</i>	<i>0.53</i>	<i>0.56</i>	<i>0.14</i>						<i>0.01</i>		
114	1227		A	Bow (front)	Cast	2008352	380239	145448	4620			621			29697		4
						<i>0.36</i>	<i>0.59</i>	<i>0.37</i>	<i>0.46</i>			<i>0.41</i>			<i>0.34</i>		
114	1227		B	Catch	Cast	1338721	343011	99183	3931	37728	4789	699			462887		1
114	1228		A		Sheet	1658774	216592	127831	23924			893			166778		5
						<i>0.42</i>	<i>0.43</i>	<i>0.26</i>	<i>0.22</i>			<i>0.21</i>			<i>0.22</i>		
114	1242		A	Front	Cast	1964594	89675	104032	6520			423			96845		4
						<i>0.09</i>	<i>0.54</i>	<i>0.35</i>	<i>0.41</i>			<i>1.16</i>			<i>0.42</i>		
114	1243		A	Hoop	Sheet	1828037	246567	55295	1876						352841		3
						<i>0.10</i>	<i>0.22</i>	<i>0.17</i>	<i>0.27</i>						<i>0.24</i>		
114	1244		A	Hoop	Sheet	1617569	240138	45720	1703						319334		3
						<i>0.11</i>	<i>0.14</i>	<i>0.05</i>	<i>0.21</i>						<i>0.32</i>		
114	1244		B	Disc	Sheet	1739402	247444	71336	4129			629			298285		2
						<i>0.26</i>	<i>0.24</i>	<i>0.54</i>	<i>0.26</i>			<i>0.47</i>			<i>0.23</i>		
114	1245		A	Hoop	Sheet	1558657	366353	62964	1975			82			263506		3
						<i>0.09</i>	<i>0.28</i>	<i>0.37</i>	<i>0.45</i>			<i>1.73</i>			<i>0.17</i>		
114	1245		B	Disc	Sheet	1729276	353328	145024	2600						238966		2
						<i>0.28</i>	<i>0.13</i>	<i>0.43</i>	<i>0.34</i>						<i>0.51</i>		
114	1246		A	Hoop	Sheet	1265710	363241	52656	2099						209987		3
						<i>0.13</i>	<i>0.04</i>	<i>0.32</i>	<i>0.32</i>						<i>0.22</i>		

<i>Site</i>	SF no.	SF sub div.	Anal. area	XRF location	Manuf. method	Cu (K)	Pb (L)	Sn (K)	Ag (K)	As (K)	Ni (K)	Sb (K)	Au (L)	Bi (L)	Zn (K)	Co (K)	No. of analyses
114	1246		B	Disc	Sheet	1922306	228062	211366	5355						339264		2
						<i>0.12</i>	<i>0.04</i>	<i>0.39</i>	<i>0.46</i>						<i>0.32</i>		
114	1247		A	Hoop	Sheet	1634959	185344	78727	2686						244334		3
						<i>0.11</i>	<i>0.05</i>	<i>0.21</i>	<i>0.28</i>						<i>0.21</i>		
114	1248		A	Hoop	Sheet	1643215	273995	41504	3148			806			231728		3
						<i>0.05</i>	<i>0.18</i>	<i>0.34</i>	<i>0.31</i>			<i>0.28</i>			<i>0.36</i>		
114	1248		B	Disc	Sheet	1534827	524506	159082	3402			443			205004		2
						<i>0.08</i>	<i>0.51</i>	<i>0.28</i>	<i>0.40</i>			<i>0.51</i>			<i>0.43</i>		
114	1249		A	Hoop	Sheet	1374433	260211	86210	3279	9698					243584		3
						<i>0.08</i>	<i>0.08</i>	<i>0.25</i>	<i>0.22</i>	<i>0.87</i>					<i>0.11</i>		
114	1249		B	Disc	Sheet	1781206	434642	130124	3628						282051		1
114	1250		A		Sheet	844944	657661	128029	2950	27841					161877		3
						<i>0.06</i>	<i>0.12</i>	<i>0.10</i>	<i>0.27</i>	<i>0.89</i>					<i>0.13</i>		
114	1251		A	Hoop	Sheet	1664780	309895	55882	4567	17898		1147			243392		3
						<i>0.15</i>	<i>0.25</i>	<i>0.15</i>	<i>0.23</i>	<i>0.25</i>		<i>0.11</i>			<i>0.42</i>		
114	1254		A		Cast	2211727	121084	163212	2043			1173					5
						<i>0.18</i>	<i>0.24</i>	<i>0.23</i>	<i>0.18</i>			<i>0.18</i>					
114	1255		A		Cast	1192077	257370	238425	2690			1304					5
						<i>0.42</i>	<i>0.39</i>	<i>0.34</i>	<i>0.28</i>			<i>0.56</i>					
114	1292		A		Sheet	1713085	128325	122330	26236			892			184734		5
						<i>0.35</i>	<i>0.37</i>	<i>0.16</i>	<i>0.31</i>			<i>0.17</i>			<i>0.25</i>		
114	1296		A	Front	Cast	2912013	345602	66165	2460	14036		1087			101411		5
						<i>0.08</i>	<i>0.33</i>	<i>0.32</i>	<i>0.25</i>	<i>1.01</i>		<i>0.34</i>			<i>0.40</i>		

<i>Site</i>	SF no.	SF sub div.	Anal . area	XRF location	Manuf. method	Cu (K)	Pb (L)	Sn (K)	Ag (K)	As (K)	Ni (K)	Sb (K)	Au (L)	Bi (L)	Zn (K)	Co (K)	No. of analyses
114	1297		A	Front	Cast	3106581	334533	77319	4437	19439	829	1144			124270		5
						<i>0.24</i>	<i>0.50</i>	<i>0.17</i>	<i>0.26</i>	<i>1.02</i>	<i>2.24</i>	<i>0.16</i>			<i>0.68</i>		
114	1298		A	Bow (front)	Cast	3273607	146509	24376	6554			651			152920		5
						<i>0.17</i>	<i>0.56</i>	<i>0.19</i>	<i>0.19</i>			<i>0.93</i>			<i>0.16</i>		
114	1298		C	Small sheet bracket	Sheet	1022360	498761	212700	2224			198			39756		2
						<i>0.10</i>	<i>0.26</i>	<i>0.29</i>	<i>0.15</i>			<i>1.41</i>			<i>0.22</i>		
114	1319		A	Front	Cast	959301	286285	217647	14002	11276	2457	811			181651		5
						<i>0.27</i>	<i>0.19</i>	<i>0.10</i>	<i>0.12</i>	<i>0.60</i>	<i>0.34</i>	<i>0.59</i>			<i>0.46</i>		
114	1319		B	Pin	Cast	201176	109503	64471	3380						18508		2
						<i>0.07</i>	<i>0.15</i>	<i>0.19</i>	<i>0.04</i>						<i>0.36</i>		
114	1321		A		Cast	802031	131546	264888	1740	10428	694				3462		4
						<i>0.55</i>	<i>0.27</i>	<i>0.11</i>	<i>0.12</i>	<i>0.27</i>	<i>1.15</i>				<i>1.16</i>		
114	1322		A		Cast	1659061	293554	94721	11118	15884	1014	843			745366		7
						<i>0.17</i>	<i>0.30</i>	<i>0.45</i>	<i>0.45</i>	<i>0.72</i>	<i>1.52</i>	<i>0.68</i>			<i>0.36</i>		
114	1341		A	Reverse	Cast	1946101	138097	206062	5948	6348		1318			153901		4
						<i>0.10</i>	<i>0.20</i>	<i>0.10</i>	<i>0.15</i>	<i>1.16</i>		<i>0.08</i>			<i>0.06</i>		
114	1342		A	Reverse	Cast	2282298	106807	206435	5844	5137		1262			150941		4
						<i>0.26</i>	<i>0.21</i>	<i>0.13</i>	<i>0.14</i>	<i>1.19</i>		<i>0.17</i>			<i>0.06</i>		
114	1343		A	Front	Cast	1686067	131238	254212	7701	1892		1418			172698		5
						<i>0.51</i>	<i>0.39</i>	<i>0.21</i>	<i>0.31</i>	<i>2.24</i>		<i>0.17</i>			<i>0.16</i>		
114	1344		A	Front	Cast	1609416	297103	239921	6556	16995		1307			156343		5
						<i>0.70</i>	<i>0.86</i>	<i>0.26</i>	<i>0.28</i>	<i>0.80</i>		<i>0.17</i>			<i>0.23</i>		
114	1347		A	Front	Cast	2541595	159137	105801	4536						103227		4
						<i>0.15</i>	<i>0.20</i>	<i>0.10</i>	<i>0.10</i>						<i>0.13</i>		

<i>Site</i>	SF no.	SF sub div.	Anal . area	XRF location	Manuf. method	Cu (K)	Pb (L)	Sn (K)	Ag (K)	As (K)	Ni (K)	Sb (K)	Au (L)	Bi (L)	Zn (K)	Co (K)	No. of analyses
114	1348		A		Cast	2782641	281228	78080	4544						81405		1
114	1349		A	Bow front	Cast	2245677	174135	173754	5346						55655		4
						<i>0.10</i>	<i>0.09</i>	<i>0.05</i>	<i>0.04</i>						<i>0.16</i>		
114	1370		A		Sheet	1514931	64721	65188	5003						111233		2
						<i>0.02</i>	<i>0.01</i>	<i>0.00</i>	<i>0.23</i>						<i>0.02</i>		
114	1374		A	Tag	Sheet	2027465	186538	95735	3619	5843	3101				182326		2
						<i>0.22</i>	<i>0.53</i>	<i>0.31</i>	<i>0.08</i>	<i>1.41</i>	<i>0.27</i>				<i>0.18</i>		
114	1374		B	Ring	Wire	704575	106698	47766	2505						70891		2
						<i>0.01</i>	<i>0.07</i>	<i>0.04</i>	<i>0.03</i>						<i>0.09</i>		
114	1375		A	Front of first (smaller) piece	Cast	1863212	62075	39406	3453	7071	389				158567 1	394	6
						<i>0.27</i>	<i>0.11</i>	<i>0.18</i>	<i>0.15</i>	<i>0.76</i>	<i>1.79</i>				<i>0.22</i>	<i>1.55</i>	
114	1378		A	Tag	Sheet	1770721	384397	157050	8033						169853		2
						<i>0.03</i>	<i>0.14</i>	<i>0.04</i>	<i>0.06</i>						<i>0.11</i>		
114	1378		B	Ring	Cast	529100	129992	47295	2595						70070		2
						<i>0.12</i>	<i>0.12</i>	<i>0.11</i>	<i>0.09</i>						<i>1.41</i>		
114	1380		A		Sheet	1728847	169167	68252	8286						238544		6
						<i>0.30</i>	<i>0.56</i>	<i>0.55</i>	<i>0.66</i>						<i>1.13</i>		
114	1383		A	Eye piece	Cast	2726444	323577	50924	5856	25324					574691	231	4
						<i>0.07</i>	<i>0.22</i>	<i>0.06</i>	<i>0.05</i>	<i>0.24</i>					<i>0.24</i>	<i>2.00</i>	
114	1383		B	Hook piece	Cast	3199397	238274	58113	6103	20766					470476		4
						<i>0.09</i>	<i>0.17</i>	<i>0.07</i>	<i>0.07</i>	<i>0.15</i>					<i>0.09</i>		
114	1384		A	Eye piece front	Cast	3111993	236529	51912	6465	11946					499804		4
						<i>0.10</i>	<i>0.33</i>	<i>0.08</i>	<i>0.27</i>	<i>0.90</i>					<i>0.06</i>		

<i>Site</i>	SF no.	SF sub div.	Anal . area	XRF location	Manuf. method	Cu (K)	Pb (L)	Sn (K)	Ag (K)	As (K)	Ni (K)	Sb (K)	Au (L)	Bi (L)	Zn (K)	Co (K)	No. of analyses
114	1384		B	Hook piece front	Cast	3388578	185911	58728	6089	11946					461767		3
						<i>0.01</i>	<i>0.09</i>	<i>0.09</i>	<i>0.11</i>	<i>0.88</i>					<i>0.03</i>		
114	1385		A	Green corosion, large frag	Cast	2591052	233665	97399	4198	3737	777	162			648276		5
						<i>0.23</i>	<i>0.45</i>	<i>0.31</i>	<i>0.16</i>	<i>2.24</i>	<i>2.24</i>	<i>2.24</i>			<i>0.46</i>		
114	1386		A	Reverse of small piece	Sheet	2069260	209510	114189	4638	4657	449	1316			265897		4
						<i>0.33</i>	<i>0.54</i>	<i>0.26</i>	<i>0.23</i>	<i>2.00</i>	<i>2.00</i>	<i>0.29</i>			<i>0.31</i>		
114	1387		A		Sheet	2264280	272530	110128	4725	2581		1125			304445		5
						<i>0.21</i>	<i>0.27</i>	<i>0.28</i>	<i>0.27</i>	<i>2.24</i>		<i>0.40</i>			<i>0.30</i>		
114	1388		A		Sheet	1486586	396575	231315	6146	8558	1151	860			74308		3
						<i>0.18</i>	<i>0.06</i>	<i>0.05</i>	<i>0.50</i>	<i>1.73</i>	<i>1.73</i>	<i>0.24</i>			<i>0.80</i>		
114	1389		A		Sheet	2320977	176174	105820	3833			1246			243043		4
						<i>0.20</i>	<i>0.25</i>	<i>0.17</i>	<i>0.16</i>			<i>0.16</i>			<i>0.10</i>		
114	1392		A	Small disc	Sheet	1953879	245926	111969	2812			595			75653		2
						<i>0.18</i>	<i>0.35</i>	<i>0.40</i>	<i>0.08</i>			<i>0.12</i>			<i>0.14</i>		
114	1392		B	TWO SMALL FRAGS	Sheet	2677601	163337	30683	4989			1104			430609		1
114	1393		A		Sheet	2004597	216549	57477	4391			741			371747		2
						<i>0.53</i>	<i>0.50</i>	<i>0.73</i>	<i>0.20</i>			<i>0.21</i>			<i>0.48</i>		
114	1394		A		Sheet	2060720	318155	124979	2715						80154		2
						<i>0.25</i>	<i>0.17</i>	<i>0.23</i>	<i>0.14</i>						<i>0.31</i>		
114	1395		A	Disc	Sheet	1476993	257409	92929	4262	4749		235			217016		6
						<i>0.55</i>	<i>0.52</i>	<i>0.55</i>	<i>0.61</i>	<i>1.69</i>		<i>1.59</i>			<i>1.27</i>		
114	1398		A		Sheet	1232583	286392	213303	7084	14832	1482	846			74448		4
						<i>0.42</i>	<i>0.22</i>	<i>0.20</i>	<i>0.33</i>	<i>0.74</i>	<i>1.16</i>	<i>0.50</i>			<i>0.67</i>		

<i>Site</i>	SF no.	SF sub div.	Anal . area	XRF location	Manuf. method	Cu (K)	Pb (L)	Sn (K)	Ag (K)	As (K)	Ni (K)	Sb (K)	Au (L)	Bi (L)	Zn (K)	Co (K)	No. of analyses
114	1399		A		Sheet	1882872	277435	134520	3536			1075			232504		4
						<i>0.10</i>	<i>0.36</i>	<i>0.46</i>	<i>0.27</i>			<i>0.21</i>			<i>0.34</i>		
114	1400		A	Front	Cast	2443874	81281	156757	3735	4710	1759				407114		5
						<i>0.24</i>	<i>0.16</i>	<i>0.29</i>	<i>0.28</i>	<i>1.03</i>	<i>1.37</i>				<i>0.32</i>		
114	1401		A		Sheet	2190900	198276	128612	5763	9919	1140	886			123687		5
						<i>0.25</i>	<i>0.33</i>	<i>0.23</i>	<i>0.26</i>	<i>0.68</i>	<i>1.37</i>	<i>0.17</i>			<i>0.12</i>		
114	1402		A	Distal Terminal (front)	Cast	962341	702156	187022	6872	26720	1470	943			152485		6
						<i>0.34</i>	<i>0.19</i>	<i>0.14</i>	<i>0.14</i>	<i>0.80</i>	<i>0.79</i>	<i>0.19</i>			<i>0.21</i>		
114	1405		A	Reverse	Cast	2728592	111598	144534	9439	3343	1299	398			201952		5
						<i>0.44</i>	<i>0.66</i>	<i>0.29</i>	<i>0.37</i>	<i>1.37</i>	<i>1.37</i>	<i>1.37</i>			<i>0.14</i>		
114	1408		A	Front	Sheet	2758736	91270	74419	3951						126768		4
						<i>0.06</i>	<i>0.32</i>	<i>0.05</i>	<i>0.08</i>						<i>0.18</i>		
114	1414		A		Sheet	2213576	42467	201929	3626						14578		4
						<i>0.23</i>	<i>0.28</i>	<i>0.15</i>	<i>0.37</i>						<i>0.12</i>		
114	1430		A		Sheet	1855786	197383	68109	4481						270357		6
						<i>0.35</i>	<i>0.55</i>	<i>0.70</i>	<i>0.43</i>						<i>0.33</i>		
114	1431		A	Only big enough for one analysis	Sheet	2711767	99665	33477	6579						380417		1
114	1432		A		Sheet	2208125	317690	144365	2887						53599		2
						<i>0.25</i>	<i>0.14</i>	<i>0.47</i>	<i>0.09</i>						<i>0.08</i>		
114	1433		A		Sheet	1708891	218994	53696	14840						255116		2
						<i>0.45</i>	<i>0.59</i>	<i>0.55</i>	<i>0.15</i>						<i>0.30</i>		
114	1434		A		Sheet	1810066	341376	147244	2898						57522		2
						<i>0.42</i>	<i>0.27</i>	<i>0.43</i>	<i>0.31</i>						<i>0.24</i>		

<i>Site</i>	SF no.	SF sub div.	Anal . area	XRF location	Manuf. method	Cu (K)	Pb (L)	Sn (K)	Ag (K)	As (K)	Ni (K)	Sb (K)	Au (L)	Bi (L)	Zn (K)	Co (K)	No. of analyses
114	1435		A	Tag	Sheet	1904213	244828	100760	5096						111884		2
						<i>0.13</i>	<i>0.35</i>	<i>0.09</i>	<i>0.07</i>						<i>0.05</i>		
114	1435		B	Ring	Wire	655794	51769	47254	1978						86547		2
						<i>0.01</i>	<i>0.04</i>	<i>0.04</i>	<i>0.11</i>						<i>0.04</i>		
114	1436		A		Sheet	1565855	106778	80269	3450						152983		2
						<i>0.01</i>	<i>0.01</i>	<i>0.00</i>	<i>0.10</i>						<i>0.00</i>		
114	1437		A	Tag	Sheet	2256467	86311	90074	3709						218286		2
						<i>0.17</i>	<i>0.26</i>	<i>0.14</i>	<i>0.23</i>						<i>0.27</i>		
114	1437		B	Ring	Wire	1290872	47844	40634	2106						83000		2
						<i>0.23</i>	<i>0.25</i>	<i>0.31</i>	<i>0.07</i>						<i>0.42</i>		
114	1438		A	Tag	Sheet	1741676	201240	125181	3693						168835		2
						<i>0.26</i>	<i>0.12</i>	<i>0.68</i>	<i>0.08</i>						<i>0.43</i>		
114	1438		B	Ring	Wire	1091071	96889	30790	2523						43069		2
						<i>0.01</i>	<i>0.44</i>	<i>0.10</i>	<i>0.02</i>						<i>0.15</i>		
114	1439		A	Tag	Sheet	1754395	278794	102030	2920		1755				180554		2
						<i>0.23</i>	<i>0.10</i>	<i>0.62</i>	<i>0.13</i>		<i>1.41</i>				<i>0.42</i>		
114	1439		B	Ring	Wire	543196	91392	41722	2823		484				50654		2
						<i>0.07</i>	<i>0.21</i>	<i>0.07</i>	<i>0.07</i>		<i>1.41</i>				<i>0.04</i>		
114	1440		A	Tag	Sheet	2265827	203667	117093	6427			900			135378		2
						<i>0.13</i>	<i>0.28</i>	<i>0.09</i>	<i>0.10</i>			<i>0.41</i>			<i>0.10</i>		
114	1442		A		Sheet	2161126	229241	150383	2666						52022		2
						<i>0.48</i>	<i>0.54</i>	<i>0.59</i>	<i>0.08</i>						<i>0.31</i>		
114	1450		A	Front	Cast	2646591	58572	36384	2825	8138	2245	130			118313 4	411	5
						<i>0.26</i>	<i>0.09</i>	<i>0.12</i>	<i>0.07</i>	<i>0.23</i>	<i>0.88</i>	<i>1.39</i>			<i>0.23</i>	<i>1.44</i>	

<i>Site</i>	SF no.	SF sub div.	Anal . area	XRF location	Manuf. method	Cu (K)	Pb (L)	Sn (K)	Ag (K)	As (K)	Ni (K)	Sb (K)	Au (L)	Bi (L)	Zn (K)	Co (K)	No. of analyses
114	1452		A	Front	Sheet	2658473	178253	115633	8462			1907			316188		1
114	1458		A	Hoop	Sheet	2355952	143600	74989	5901	3721	1245	1293			209957		3
						<i>0.16</i>	<i>0.15</i>	<i>0.08</i>	<i>0.08</i>	<i>1.73</i>	<i>1.73</i>	<i>0.12</i>			<i>0.27</i>		
114	1460		A		Sheet	2087383	311962	138277	3984						107985		2
						<i>0.43</i>	<i>0.55</i>	<i>0.30</i>	<i>0.24</i>						<i>0.48</i>		
114	1461		A		Sheet	1703481	116333	41257	13616			295			691692		2
						<i>0.18</i>	<i>0.15</i>	<i>0.17</i>	<i>0.26</i>			<i>1.41</i>			<i>0.31</i>		
114	1464		B	Reverse	Cast	1678016	86723	74220	12428						153648		2
						<i>0.32</i>	<i>0.08</i>	<i>0.16</i>	<i>0.25</i>						<i>0.34</i>		
114	1465		A		Cast	2658913	91530	109841	2920	12727	12004	265			361606		5
						<i>0.21</i>	<i>0.19</i>	<i>0.17</i>	<i>0.09</i>	<i>0.04</i>	<i>0.29</i>	<i>1.37</i>			<i>0.22</i>		
114	1479		A		Sheet	1505219	278546	291367	5862	11026		938			108811		2
						<i>0.30</i>	<i>0.53</i>	<i>0.45</i>	<i>0.49</i>	<i>1.41</i>		<i>0.66</i>			<i>0.80</i>		
114	1480		A	Bow	Cast	2945113	91585	86435	4591			550			134810		6
						<i>0.20</i>	<i>0.30</i>	<i>0.45</i>	<i>0.35</i>			<i>0.86</i>			<i>0.26</i>		
114	1481		A	Reverse (right)	Cast	1572018	199905	239932	78401						60897		5
						<i>0.40</i>	<i>0.33</i>	<i>0.77</i>	<i>1.79</i>						<i>0.27</i>		
114	1483		A	Reverse (right)	Wire	1703122	174587	157060	53036			93			84564		6
						<i>0.18</i>	<i>0.37</i>	<i>0.54</i>	<i>1.46</i>			<i>2.45</i>			<i>0.15</i>		
114	1484		A	Reverse (right)	Cast	1595059	301772	215615	19990						96915		4
						<i>0.21</i>	<i>0.38</i>	<i>0.36</i>	<i>1.52</i>						<i>0.14</i>		
114	1484		B	Sheet Metal	Sheet	2126287	297074	150115	6836						286316		5
						<i>0.31</i>	<i>0.30</i>	<i>0.46</i>	<i>0.13</i>						<i>0.23</i>		

<i>Site</i>	SF no.	SF sub div.	Anal . area	XRF location	Manuf. method	Cu (K)	Pb (L)	Sn (K)	Ag (K)	As (K)	Ni (K)	Sb (K)	Au (L)	Bi (L)	Zn (K)	Co (K)	No. of analyses
114	1484		C	Frag	Sheet	1945759	330639	156592	3600	3766					170095		4
						0.22	0.44	0.50	0.29	2.00					0.59		
114	1486		A		Cast	1361272	162598	119620	10719						70176		2
						0.03	0.28	0.08	0.10						0.11		
114	1487		A	Reverse	Cast	2185950	185667	125599	10008		661				141113		3
						0.57	0.19	0.30	0.33		1.73				0.53		
114	1488		A	Front	Cast	1490599	141549	124359	9726	5567	1424	626			129842		5
						0.17	0.21	0.11	0.13	0.98	0.92	0.15			0.21		
114	1491		A	Reverse	Cast	1739579	226243	226320	10839			597			75321		4
						0.14	0.33	0.16	0.65			0.07			0.19		
114	1491		B	Sheet Metal	Sheet	1952601	220898	183617	8859			191			294641		6
						0.29	0.35	0.49	0.17			1.11			0.27		
114	1491		C	Piece with two holes	Cast	2962313	200128	143695	4350	8495	5075				192454		2
						0.31	0.36	0.42	0.08	1.41	0.46				0.50		
114	1491		D	Piece with one hole	Cast	3262088	177670	119718	1843		2986				125121		2
						0.45	0.74	0.52	0.60		1.41				0.24		
114	1501		A	Reverse	Struck	2124690	307344	115025	118338	5184		1813	561		12889		4
						0.05	0.10	0.04	0.09	1.91		0.05	0.72		0.67		
114	1503		A	Reverse	Cast	1446661	205905	123760	2514			339			22340		5
						0.09	0.16	0.04	0.13			0.67			0.07		
114	1504		A		Wire	1791374	129964	56757	3012	14495	3000				263711		2
						0.07	0.10	0.10	0.00	0.16	0.14				0.08		
114	1505		A		Cast	1617982	309617	196457	8499	21117	1479	946			111877		6
						0.18	0.12	0.10	0.10	0.18	1.12	0.20			0.09		

<i>Site</i>	SF no.	SF sub div.	Anal . area	XRF location	Manuf. method	Cu (K)	Pb (L)	Sn (K)	Ag (K)	As (K)	Ni (K)	Sb (K)	Au (L)	Bi (L)	Zn (K)	Co (K)	No. of analyses
114	1536		A		Cast	1905827	7878	2519		2560		1097			333184		5
						<i>0.16</i>	<i>0.19</i>	<i>0.10</i>		<i>0.33</i>		<i>0.38</i>			<i>0.20</i>		
114	1602		A	White layer	Sheet	732528	250432	120995	11215	14691		1513			141305 5	883	2
						<i>0.03</i>	<i>0.20</i>	<i>0.04</i>	<i>0.14</i>	<i>0.18</i>		<i>0.23</i>			<i>0.04</i>	<i>0.12</i>	
114	1603		A	White layer	Sheet	1018411	213030	70533	7399	20852	676	1967			146452 4	691	4
						<i>0.42</i>	<i>0.48</i>	<i>0.35</i>	<i>0.25</i>	<i>0.49</i>	<i>1.52</i>	<i>0.35</i>			<i>0.36</i>	<i>0.46</i>	
114	1613		A	Bow (front)	Cast	2317140	134466	151624	7115			983			123805		6
						<i>0.17</i>	<i>0.18</i>	<i>0.27</i>	<i>0.12</i>			<i>0.13</i>			<i>0.31</i>		

Appendix XVI. COPPER ALLOY OUTLIERS

Outliers identified using the R package ‘mvoutlier’ (Filzmoser and Gschwandtner 2015). The untransformed column shows analyses determined to be outliers using the ‘aq.plot’ function. The logarithmic column shows outliers identified using a compositional data approach (involving an isometric log-ratio transformation of the data) using the routine ‘mvoutlier.CoDa’. See page 330 for a discussion of the outliers.

ID	Untrans.	ilr trans. (ex. As)	ilr trans. (inc. As)	XRF Location	Additional Notes	Grave No.	Manufacture method	Category	Class	Sub Class	Cultural Period
046-1821-A		Y	Y	Front		015	Cast	Dress Accessories	Brooch	Annular	E. Sax
046-1815-A	Y	Y	Y			018	Cast	Dress Accessories	Brooch	Undefined Brooch	E. Sax
046-1814-A	Y	Y	Y			018	Cast	Dress Accessories	Necklace	Necklace Ring	E. Sax
046-1811-A	Y			Foot (front)		018	Cast	Dress Accessories	Brooch	Great square- headed	E. Sax
046-1751-A		Y	Y				Cast	Dress Accessories	Pin	Undefined Pin	Undated
046-1737-B	Y	Y	Y	Bow (front)		043	Cast	Dress Accessories	Brooch	Roman	Roman
046-1727-A		Y	Y				Cast	Dress Accessories	Wrist Clasp	Form B 18	E. Sax
046-1648-A		Y	Y	Head (reverse)		025	Cast	Dress Accessories	Brooch	Fish	E. Sax
046-1374-A		Y	Y			005	Cast	Dress Accessories	Wrist Clasp	Form C 1	E. Sax
046-1373-A		Y	Y			005	Cast	Dress Accessories	Wrist Clasp	Form C 1	E. Sax
046-1372-A		Y	Y			005	Cast	Dress Accessories	Wrist Clasp	Form C 1	E. Sax
046-1371-A	Y					005	Cast	Dress Accessories	Brooch	Annular	E. Sax

ID	Untrans.	ilr trans. (ex. As)	ilr trans. (inc. As)	XRF Location	Additional Notes	Grave No.	Manufacture method	Category	Class	Sub Class	Cultural Period
046-1361-A	Y			Front		007	Cast	Dress Accessories	Brooch	Annular	E. Sax
046-1352-A	Y			Front		045	Cast	Dress Accessories	Brooch	Annular	E. Sax
046-1203-A	Y					024	Sheet	Equestrian objects	Tack	Mount Strip	E. Sax
046-1194-A		Y	Y			024	Sheet	Dress Accessories	Wrist Clasp	Form B 7	E. Sax
046-1192-A	Y					024	Cast	Dress Accessories	Necklace	Pendant	Roman
046-1167-A	Y			Front		040	Cast	Dress Accessories	Brooch	Annular	E. Sax
046-1163-A	Y			Front		040	Cast	Dress Accessories	Brooch	Annular	E. Sax
046-1160-C		Y	Y	Fragment with catch attached			Cast	Dress Accessories	Brooch	Colchester	Roman
046-1160-B		Y	Y	Main bar			Cast	Dress Accessories	Brooch	Colchester	Roman
046-1160-A		Y	Y	Spiral			Cast	Dress Accessories	Brooch	Colchester	Roman
046-1140-B	Y			Spiral, not attached to 046-1140-B		042	Wire	Dress Accessories	Wrist Clasp	Form A	E. Sax
046-1100-B		Y	Y	Bar		038	Cast	Dress Accessories	Wrist Clasp	Form B 13 a	E. Sax
046-1060-A	Y			Front		038	Cast	Dress Accessories	Brooch	Annular	E. Sax
046-1026-A	Y			Pincer end		053	Sheet	Toilet and surgical objects	Cosmetic Implements	Tweezers	Undated
046-1006-A	Y	Y	Y	Front		044	Cast	Dress Accessories	Brooch	Annular	E. Sax
114-1603-A	Y			White layer		459	Sheet	Dress Accessories	Necklace	Pendant	E. Sax
114-1602-A	Y	Y		White layer		459	Sheet	Dress Accessories	Necklace	Pendant	E. Sax
114-1536-A		Y	Y			405	Cast	Dress Accessories	Wrist Clasp	Undefined Wrist Clasp	E. Sax

ID	Untrans.	ilr trans. (ex. As)	ilr trans. (inc. As)	XRF Location	Additional Notes	Grave No.	Manufacture method	Category	Class	Sub Class	Cultural Period
114-1501-A	Y	Y	Y	Reverse			Struck	Coins, Tokens and Jettons	Coin	Undefined Coin	Roman
114-1484-A	Y			Reverse (right)		405	Cast	Dress Accessories	Wrist Clasp	Undefined Wrist Clasp	E. Sax
114-1483-A	Y			Reverse (right)		405	Wire	Dress Accessories	Ring	Finger ring	E. Sax
114-1481-A	Y	Y	Y	Reverse (right)		405	Cast	Dress Accessories	Wrist Clasp	Undefined Wrist Clasp	E. Sax
114-1464-B	Y			Reverse		417	Cast	Dress Accessories	Necklace	Pendant	E. Sax
114-1461-A	Y					422	Sheet	Dress Accessories	Bead	Undefined Bead	E. Sax
114-1450-A	Y			Front		422	Cast	Dress Accessories	Brooch	Annular	E. Sax
114-1433-A	Y					422	Sheet	Dress Accessories	Bead	Undefined Bead	E. Sax
114-1402-A	Y			Distal Terminal (front)		422	Cast	Dress Accessories	Belt Fitting	Girdle-hanger	E. Sax
114-1375-A	Y			Front of first (smaller) piece		422	Cast	Dress Accessories	Brooch	Annular	E. Sax
114-1322-A	Y					459	Cast	Dress Accessories	Wrist Clasp	Undefined Wrist Clasp	E. Sax
114-1321-A			Y			459	Cast	Dress Accessories	Belt Fitting	Belt ring	E. Sax
114-1298-C	Y			Small sheet bracket		445	Sheet	Dress Accessories	Brooch	Cruciform	E. Sax
114-1292-A	Y					458	Sheet	Dress Accessories	Brooch	Annular	E. Sax
114-1255-A		Y	Y			467	Cast	Dress Accessories	Brooch	Annular	E. Sax
114-1254-A		Y	Y			467	Cast	Dress Accessories	Brooch	Annular	E. Sax
114-1250-A	Y					458	Sheet	Dress Accessories	Bead	Undefined Bead	E. Sax
114-1228-A	Y					458	Sheet	Dress Accessories	Brooch	Annular	E. Sax

ID	Untrans.	ilr trans. (ex. As)	ilr trans. (inc. As)	XRF Location	Additional Notes	Grave No.	Manufacture method	Category	Class	Sub Class	Cultural Period
114-1159-A		Y	Y			434	Cast	Personal equipment	Implement	Awl	Bronze Age?
114-1148-A	Y			Foot front		456	Cast	Dress Accessories	Buckle	Undefined Buckle	E. Sax
114-1075-A	Y					447	Cast	Dress Accessories	Brooch	Applied disc	E. Sax
114-1062-A	Y					447	Cast	Dress Accessories	Brooch	Applied disc	E. Sax
114-1051-A		Y	Y	Hook piece (front)		443	Cast	Dress Accessories	Wrist Clasp	Undefined Wrist Clasp	E. Sax
114-1050-A		Y	Y	Outer			Sheet	Unknown	Unknown	Unknown	E. Sax
114-1048-A		Y	Y	Hook piece (front)		443	Cast	Dress Accessories	Wrist Clasp	Undefined Wrist Clasp	E. Sax
114-1040-A	Y	Y	Y	Outer			Melted	Unknown	Unknown	Unknown	E. Sax
114-1000-A	Y	Y	Y	Head side			Struck	Coins, Tokens and Jettons	Coin	Undefined Coin	Roman
104-BM6-7A-B		Y	Y	Rivet	Cu alloy	323	Cast	Equestrian objects	Tack	Bit	E. Sax
104-BM3-D	Y			Reverse	Base' metal	323	Cast	Equestrian objects	Tack	Bridle Fitting	E. Sax
104-BM1-F		Y	Y	Reverse (arm)		323	Cast	Equestrian objects	Tack	Bridle Fitting	E. Sax
104-BM18-E		Y	Y	Reverse (arm)		323	Cast	Equestrian objects	Tack	Bridle Fitting	E. Sax
104-BM18-C	Y			Arm (no plate)	Numbered arm 2 on on reverse	323	Cast	Equestrian objects	Tack	Bridle Fitting	E. Sax
104-4211-A	Y			Bow (front)		Unknown	Cast	Unknown	Unknown	Unknown	Unknown
104-3675-1-B		Y	Y	Reverse of Stud	Large amount of ferrous corrosion.	168	Cast	Military and weaponry	Shield	Shield Mount	E. Sax
104-3674-2-B		Y	Y	Reverse of Stud	<i>Small Cu peak but large amount of ferrous corrosion and mineralised wood.</i>	168	Cast	<i>Military and weaponry</i>	<i>Shield</i>	<i>Shield Mount</i>	<i>E. Sax</i>

ID	Untrans.	ilr trans. (ex. As)	ilr trans. (inc. As)	XRF Location	Additional Notes	Grave No.	Manufacture method	Category	Class	Sub Class	Cultural Period
104-3674-1-A		Y	Y	Thin plate on front	To see if any traces of plating remain...yes, but not silver.	168	Cast	Military and weaponry	Shield	Shield Mount	E. Sax
104-3618-C	Y	Y	Y	Drop C			Melted	Unknown	Unknown	Unknown	E. Sax
104-3618-A		Y	Y	Drop A			Melted	Unknown	Unknown	Unknown	E. Sax
104-3597-A		Y	Y		Sheet	350	Sheet	Miscellaneous Fittings	Miscellaneous	Sheet	E. Sax
104-3581-A	Y			Repousse sheet (small fragment, reverse)	Sheet	221	Sheet	Miscellaneous Fittings	Miscellaneous	Sheet	E. Sax
104-3579-A		Y	Y			268	Cast	Dress Accessories	Brooch	Penannular	E. Sax
104-3534-A	Y			Front		182	Sheet	Miscellaneous Fittings	Miscellaneous	Box Fitting	E. Sax
104-3532-a-A		Y	Y		Avoiding Fe rivet	206	Cast	Personal equipment	Purse	Purse Fitting	E. Sax
104-3530-A		Y	Y			206	Sheet	Dress Accessories	Pin	Undefined Pin	E. Sax
104-3482-A	Y			Only large enough for one analysis		116	Cast	Dress Accessories	Ring	Finger ring	E. Sax
104-3475-A		Y	Y		Pure Cu. Rounded 'blob'	171	Cast	Unknown	Unknown	Unknown	E. Sax
104-3460-A	Y				Sheet	166	Sheet	Dress Accessories	Brooch	Annular	E. Sax
104-3444-A	Y	Y	Y		Cu>Pb then Sn & Zn	166	Cast	Dress Accessories	Brooch	Annular	E. Sax
104-3391-A	Y	Y	Y	Front		286	Cast	Dress Accessories	Wrist Clasp	Undefined Wrist Clasp	E. Sax
104-3389-A	Y					286	Cast	Dress Accessories	Brooch	Annular	E. Sax
104-3349-C	Y			Repousse sheet (front)		292	Sheet	Dress Accessories	Wrist Clasp	Form B 13 a	E. Sax
104-3328-A	Y				Cast		Cast	Miscellaneous Fittings	Nails and Bolts	Stud	E. Sax

ID	Untrans.	ilr trans. (ex. As)	ilr trans. (inc. As)	XRF Location	Additional Notes	Grave No.	Manufacture method	Category	Class	Sub Class	Cultural Period
104-3313-A	Y					263	Cast	Dress Accessories	Belt Fitting	Latch-lifter	E. Sax
104-3299-B	Y			Reverse		359	Sheet	Miscellaneous Fittings	Fragment	Sheet	E. Sax
104-3249-A		Y	Y			221	Cast	Dress Accessories	Pin	Undefined Pin	E. Sax
104-3232-B	Y	Y	Y	Cast buckle frame & prong		139	Cast	Dress Accessories	Buckle	Undefined Buckle	E. Sax
104-3209-A		Y	Y		Wire		Wire	Miscellaneous Fittings	Fragment	Wire	E. Sax
104-3203-A	Y				Sheet	302	Sheet	Dress Accessories	Ring	Bracelet	E. Sax
104-3144-A	Y				Sheet	172	Sheet	Miscellaneous Fittings	Miscellaneous	Binding Ring	E. Sax
104-3143-A		Y	Y		Notes say "Not Non Ferrous!"	172	Sheet	Unknown	Unknown	Unknown	E. Sax
104-3090-B	Y			Front		172	Cast	Dress Accessories	Belt Fitting	Girdle-banger	E. Sax
104-3088-A	Y				Sheet	175	Sheet	Unknown	Unknown	Unknown	E. Sax
104-3078-B	Y			Eye piece (front)		172	Sheet	Dress Accessories	Wrist Clasp	Form B 7	E. Sax
104-3078-A	Y			Hook piece (front)		172	Sheet	Dress Accessories	Wrist Clasp	Form B 7	E. Sax
104-3077-A	Y					172	Sheet	Dress Accessories	Wrist Clasp	Form B 7	E. Sax
104-3064-A		Y	Y		Melted blob	Melted	Unknown	Unknown	Unknown	Unknown	E. Sax
104-3045-A		Y	Y	Tube	Sheet	176	Sheet	Dress Accessories	Bead	Undefined Bead	E. Sax
104-2950-B	Y	Y	Y	Reverse		357	Cast	Miscellaneous Fittings	Nails and Bolts	Stud	E. Sax
104-2869-A	Y	Y	Y			180	Sheet	Unknown	Unknown	Unknown	E. Sax
104-2865-A	Y	Y	Y	Rivet 1 (head)		323	Cast	Equestrian objects	Tack	Undefined Equestrian	E. Sax
104-2821-B	Y			Reverse	Sheet	185	Sheet	Dress Accessories	Brooch	Annular	E. Sax
104-2821-A	Y			Front	Sheet	185	Sheet	Dress	Brooch	Annular	E. Sax

ID	Untrans.	ilr trans. (ex. As)	ilr trans. (inc. As)	XRF Location	Additional Notes	Grave No.	Manufacture method	Category	Class	Sub Class	Cultural Period
								Accessories			
104-2783-A		Y	Y	Bow (front)	Cast	190	Cast	Dress Accessories	Brooch	Cruciform	E. Sax
104-2780-A	Y				Sheet	190	Sheet	Unknown	Unknown	Unknown	E. Sax
104-2760-B		Y	Y	Reverse	The front has a deformed to destroyed surface, pulvaresent corrosion. The reverse is hard, smooth and shiny.	358	Cast	Dress Accessories	Belt Fitting	Belt ring	E. Sax
104-2760-A	Y			Front	The front has a deformed to destroyed surface, pulvaresent corrosion. The reverse is hard, smooth and shiny.	358	Cast	Dress Accessories	Belt Fitting	Belt ring	E. Sax
104-2716-A	Y				Sheet	190	Sheet	Unknown	Unknown	Unknown	E. Sax
104-2706-A	Y				Sheet	205	Sheet	Dress Accessories	Bead	Undefined Bead	E. Sax
104-2679-A		Y	Y		Sheet		Sheet	Miscellaneous Fittings	Miscellaneous	Sheet	E. Sax
104-2672-B		Y	Y	Pin		214	Sheet	Dress Accessories	Brooch	Annular	E. Sax
104-2646-C		Y	Y	Loose sheet	Sheet	146	Sheet	Dress Accessories	Buckle	Undefined Buckle	E. Sax
104-2646-A		Y	Y	Buckle sheet	Sheet	146	Sheet	Dress Accessories	Buckle	Undefined Buckle	E. Sax
104-2624-E	Y		Y	Front	Above head, possible area of solder.	323	Cast	Equestrian objects	Tack	Bridle Fitting	E. Sax

ID	Untrans.	ilr trans. (ex. As)	ilr trans. (inc. As)	XRF Location	Additional Notes	Grave No.	Manufacture method	Category	Class	Sub Class	Cultural Period
104-2624-A	Y			Reverse (foot)	Cu cast alloy 'base' metal	323	Cast	Equestrian objects	Tack	Bridle Fitting	E. Sax
104-2623-C	Y			Arm (no plate)		323	Cast	Equestrian objects	Tack	Bridle mount	E. Sax
104-2589-A		Y	Y				Melted	Dress Accessories	Brooch	Undefined Brooch	E. Sax
104-2588-A	Y	Y	Y	Rivet head	Cast		Cast	Miscellaneous Fittings	Nails and Bolts	Stud	E. Sax
104-2587-B		Y	Y	Cast rivet	Geometry mean there is likely to be some contribution from the disc	Cast	Miscellaneous Fittings	Nails and Bolts		Stud	E. Sax
104-2587-A		Y	Y	Sheet front			Sheet	Miscellaneous Fittings	Nails and Bolts	Stud	E. Sax
104-2526-A		Y	Y			323	Sheet	Miscellaneous Fittings	Miscellaneous	Sheet	E. Sax
104-2503-A	Y				Cast		Melted	Dress Accessories	Brooch	Undefined Brooch	E. Sax
104-2502-A	Y	Y	Y		Cast spoon fragment	Cast	Unknown	Unknown		Unknown	E. Sax
104-2479-A	Y	Y	Y		Sheet	197	Sheet	Dress Accessories	Necklace	Pendant	E. Sax
104-2456-A		Y	Y				Sheet	Dress Accessories	Wrist Clasp	Form B	E. Sax
104-2364-B		Y	Y	Sheet attachmen t	Sheet	315	Sheet	Toilet and surgical objects	Cosmetic Implements	Brush fittings	E. Sax
104-2317-G	Y	Y	Y	Sheet disc B		315	Sheet	Dress Accessories	Ring	Ear Ring	E. Sax
104-2317-B	Y	Y	Y	Sheet disc A	Sheet	315	Sheet	Dress Accessories	Ring	Ear Ring	E. Sax
104-2311-B	Y	Y	Y	Reverse	Sheet	315	Sheet	Dress Accessories	Necklace	Pendant	E. Sax
104-2289-A		Y	Y			242	Wire	Dress Accessories	Ring	Ear Ring	E. Sax
104-2221-A		Y	Y		Not possible to avoid patina or rivets.	242	Sheet	Miscellaneous Fittings	Miscellaneous	Sheet	E. Sax

ID	Untrans.	ilr trans. (ex. As)	ilr trans. (inc. As)	XRF Location	Additional Notes	Grave No.	Manufacture method	Category	Class	Sub Class	Cultural Period
104-2136-A	Y			Bow (front)		242	Cast	Dress Accessories	Brooch	Cruciform	E. Sax
104-2126-A		Y	Y		Sheet	364	Sheet	Dress Accessories	Ring	Finger ring	E. Sax
104-1952-B	Y					362	Cast	Dress Accessories	Brooch	Annular	E. Sax
104-1952-A	Y					362	Cast	Dress Accessories	Brooch	Annular	E. Sax
104-1948-A	Y			Bow (front)		362	Cast	Dress Accessories	Brooch	Cruciform	E. Sax
104-1900-A	Y			Reverse			Melted	Dress Accessories	Brooch	Undefined Brooch	E. Sax
104-1888-A	Y			Bow (front)		363	Cast	Dress Accessories	Brooch	Cruciform	E. Sax
104-1782-A		Y	Y			305	Cast	Miscellaneous Fittings	Miscellaneous	Ring	E. Sax
104-1713-A		Y	Y	Foot (front)		290	Cast	Dress Accessories	Brooch	Radiate-head	E. Sax
104-1705-A	Y				Sheet	322	Sheet	Dress Accessories	Brooch	Annular	E. Sax
104-1704-D	Y			Separate joining sheet (reverse - side without solder)	Cast	322	Cast	Dress Accessories	Brooch	Great square- headed	E. Sax
104-1692-A	Y	Y	Y				Melted	Unknown	Unknown	Unknown	E. Sax
104-1593-b-A		Y	Y		Sheet	277	Sheet	Toilet and surgical objects	Cosmetic Implements	Brush fittings	E. Sax
104-1592-c-B		Y	Y	Strap end 2	Only 3 analyses possible on second strap end because of Fe rivet.	277	Cast	Dress Accessories	Belt Fitting	Strap-end	E. Sax
104-1592-c-A		Y	Y	Strap end	Shiny tarnished	277	Sheet	Dress	Belt Fitting	Strap-end	E. Sax

ID	Untrans.	ilr trans. (ex. As)	ilr trans. (inc. As)	XRF Location	Additional Notes	Grave No.	Manufacture method	Category	Class	Sub Class	Cultural Period
				1	but otherwise uncorroded area.			Accessories			
104-1568-A	Y	Y	Y	Only large enough for one analysis		266	Wire	Miscellaneous Fittings	Miscellaneous	Ring	E. Sax
104-1547-B	Y			Eye Piece (front)		258	Cast	Dress Accessories	Wrist Clasp	Form B 12	E. Sax
104-1545-A	Y			Bow (front)	Cast	258	Cast	Dress Accessories	Brooch	Cruciform	E. Sax
104-1543-A	Y			Bow (front)	Cast	258	Cast	Dress Accessories	Brooch	Cruciform	E. Sax
104-1518-A		Y	Y	Reverse	smooth and shiny	350	Cast	Dress Accessories	Brooch	Annular	E. Sax
104-1458-E		Y	Y	Repousse sheet (front)		341	Sheet	Dress Accessories	Brooch	Applied disc	E. Sax
104-1444-A		Y	Y			334	Sheet	Dress Accessories	Ring	Finger ring	E. Sax
104-1443-A	Y				Sheet	334	Sheet	Dress Accessories	Ring	Bracelet	E. Sax
104-1325-A	Y				Cast	268	Cast	Dress Accessories	Brooch	Annular	E. Sax
104-1324-A	Y			Buckle sheet		208	Sheet	Dress Accessories	Buckle	Undefined Buckle	E. Sax
104-1318-A		Y	Y		Cast		Cast	Dress Accessories	Brooch	Cruciform	E. Sax
104-1317-A	Y			Reverse			Cast	Dress Accessories	Brooch	Undefined Brooch	E. Sax
104-1293-A	Y	Y	Y		Only large enough for one reading.	252	Melted	Dress Accessories	Pin	Undefined Pin	E. Sax
104-1277-A	Y					221	Cast	Dress Accessories	Buckle	Undefined Buckle	E. Sax
104-1254-A	Y				Sheet	255	Sheet	Miscellaneous Fittings	Miscellaneous	Sheet	E. Sax
104-1191-B	Y	Y		Non gilded area on front	Pb & Sn could be contribution from solder (no	245	Cast	Military and weaponry	Shield	Shield Mount	E. Sax

ID	Untrans.	ilr trans. (ex. As)	ilr trans. (inc. As)	XRF Location	Additional Notes	Grave No.	Manufacture method	Category	Class	Sub Class	Cultural Period
104-1176-C	Y	Y		Rivet on reverse	other areas of the 'base' alloy are accessible)	245	Cast	Military and weaponry	Shield	Shield Mount	E. Sax
104-1176-B	Y			Non gilded area on front	Pb & Sn could be contribution from solder (no other areas of the 'base' alloy are accessible)	245	Cast	Military and weaponry	Shield	Shield Mount	E. Sax
104-1169-A		Y	Y	Front			Melted	Dress Accessories	Brooch	Cruciform	E. Sax
104-1095-A		Y	Y			232	Wire	Dress Accessories	Ring	Ear Ring	E. Sax
104-1048-A		Y	Y				Cast	Dress Accessories	Brooch	Cruciform	E. Sax
104-1047-A		Y	Y				Melted	Unknown	Unknown	Unknown	E. Sax
104-1035-A		Y	Y	Front			Cast	Dress Accessories	Brooch	Cruciform	E. Sax
104-1033-A	Y				Sheet	118	Sheet	Dress Accessories	Buckle	Buckle Plate	E. Sax
104-1026-C	Y			Buckle sheet		115	Sheet	Dress Accessories	Buckle	Undefined Buckle	E. Sax
104-1004-A	Y			Reverse			Melted	Dress Accessories	Brooch	Cruciform	E. Sax
104-1000-A	Y	Y	Y	Reverse			Cast	Miscellaneous Fittings	Miscellaneous	Sheet	E. Sax

Appendix XVII. COPPER ALLOY CLUSTER GROUPS

The table below sets out the clusters derived from hierarchical clustering on the PCA results. Four sets are provided: those derived from untransformed robust PCA, transformed PCA, untransformed PCA and transformed robust PCA. Of these four the last was considered most effective and carried forward for further assessment (column highlighted in grey).

Site	Small Find No.	SF Sub Division	Analysis Area	CLUSTER GROUPS			
				Untransformed Robust	Transformed Robust	Transformed	Untransformed
046	1002		A	UR 1	TR 3	T 3	U 2
046	1006		A	UR 3	TR 1	T 1	U 2
046	1012		A	UR 3	TR 2	T 2	U 2
046	1026		A	UR 3	TR 2	T 3	U 2
046	1056		A	UR 1	TR 3	T 3	U 1
046	1059		A	UR 3	TR 2	T 2	U 2
046	1060		A	UR 1	TR 2	T 3	U 2
046	1068		A	UR 1	TR 3	T 2	U 1
046	1095		A	UR 3	TR 2	T 2	U 2
046	1097		A	UR 2	TR 2	T 3	U 2
046	1098		A	UR 3	TR 3	T 3	U 2
046	1098		B	UR 3	TR 2	T 3	U 2
046	1099		A	UR 1	TR 3	T 3	U 1
046	1099		B	UR 3	TR 2	T 3	U 2
046	1100		A	UR 3	TR 3	T 3	U 2
046	1100		B	UR 3	TR 2	T 2	U 2

CLUSTER GROUPS							
Site	Small Find No.	SF Sub Division	Analysis Area	Untransformed Robust	Transformed Robust	Transformed	Untransformed
046	1101		A	UR 1	TR 3	T 3	U 2
046	1101		B	UR 3	TR 2	T 3	U 2
046	1106		A	UR 1	TR 2	T 2	U 1
046	1107		A	UR 1	TR 3	T 3	U 1
046	1108		A	UR 3	TR 3	T 3	U 2
046	1140		A	UR 1	TR 3	T 3	U 1
046	1140		B	UR 1	TR 3	T 3	U 1
046	1141		A	UR 2	TR 3	T 3	U 1
046	1141		B	UR 1	TR 3	T 3	U 1
046	1150		A	UR 2	TR 2	T 3	U 2
046	1162		A	UR 1	TR 2	T 3	U 1
046	1163		A	UR 3	TR 3	T 3	U 2
046	1167		A	UR 3	TR 2	T 3	U 2
046	1168		A	UR 3	TR 2	T 2	U 2
046	1176		A	UR 1	TR 3	T 3	U 2
046	1177		A	UR 2	TR 3	T 3	U 1
046	1182		A	UR 1	TR 3	T 3	U 1
046	1183		A	UR 1	TR 3	T 3	U 1
046	1184		A	UR 1	TR 3	T 3	U 1
046	1185		A	UR 3	TR 3	T 3	U 2
046	1188		A	UR 1	TR 3	T 3	U 1
046	1192		A	UR 3	TR 2	T 2	U 2
046	1193		A	UR 2	TR 3	T 3	U 1
046	1194		A	UR 1	TR 3	T 2	U 1

CLUSTER GROUPS							
Site	Small Find No.	SF Sub Division	Analysis Area	Untransformed Robust	Transformed Robust	Transformed	Untransformed
046	1195		A	UR 1	TR 3	T 3	U 1
046	1196		A	UR 1	TR 3	T 3	U 1
046	1197		A	UR 1	TR 2	T 2	U 1
046	1200		A	UR 1	TR 3	T 3	U 1
046	1202		A	UR 3	TR 2	T 2	U 2
046	1203		A	UR 3	TR 2	T 2	U 2
046	1225		A	UR 1	TR 3	T 3	U 1
046	1306		A	UR 3	TR 2	T 2	U 2
046	1306		B	UR 3	TR 2	T 2	U 2
046	1306		C	UR 1	TR 2	T 2	U 1
046	1306		D	UR 3	TR 2	T 2	U 2
046	1306		E	UR 3	TR 2	T 2	U 2
046	1306		F	UR 1	TR 2	T 2	U 2
046	1306		G	UR 3	TR 2	T 2	U 2
046	1348		A	UR 2	TR 2	T 2	U 2
046	1352		A	UR 3	TR 2	T 2	U 2
046	1353		A	UR 1	TR 3	T 3	U 1
046	1355		A	UR 3	TR 3	T 3	U 2
046	1355		B	UR 3	TR 3	T 3	U 2
046	1356		A	UR 3	TR 2	T 2	U 2
046	1356		B	UR 3	TR 2	T 2	U 2
046	1360		A	UR 2	TR 2	T 2	U 2
046	1361		A	UR 2	TR 2	T 3	U 2
046	1364		A	UR 3	TR 2	T 2	U 2

CLUSTER GROUPS							
Site	Small Find No.	SF Sub Division	Analysis Area	Untransformed Robust	Transformed Robust	Transformed	Untransformed
046	1366		A	UR 1	TR 2	T 2	U 1
046	1370		A	UR 1	TR 2	T 2	U 1
046	1371		A	UR 1	TR 2	T 2	U 1
046	1372		A	UR 1	TR 1	T 1	U 1
046	1373		A	UR 1	TR 1	T 1	U 1
046	1374		A	UR 1	TR 1	T 1	U 1
046	1519		A	UR 1	TR 3	T 3	U 1
046	1520		A	UR 1	TR 3	T 2	U 1
046	1521		A	UR 1	TR 3	T 3	U 1
046	1523		A	UR 1	TR 3	T 2	U 1
046	1524		A	UR 1	TR 3	T 2	U 2
046	1525		A	UR 1	TR 3	T 2	U 1
046	1526		A	UR 1	TR 3	T 2	U 1
046	1526		B	UR 1	TR 3	T 2	U 1
046	1527		A	UR 1	TR 3	T 3	U 1
046	1528		A	UR 1	TR 3	T 3	U 1
046	1529		A	UR 1	TR 3	T 3	U 1
046	1531		A	UR 1	TR 3	T 3	U 1
046	1533		A	UR 1	TR 3	T 3	U 1
046	1534		A	UR 1	TR 3	T 3	U 1
046	1535		A	UR 1	TR 3	T 3	U 1
046	1536		A	UR 1	TR 3	T 3	U 1
046	1537		A	UR 1	TR 3	T 3	U 1
046	1538		A	UR 1	TR 3	T 3	U 1

CLUSTER GROUPS							
Site	Small Find No.	SF Sub Division	Analysis Area	Untransformed Robust	Transformed Robust	Transformed	Untransformed
046	1539		A	UR 1	TR 3	T 3	U 1
046	1540		A	UR 1	TR 3	T 3	U 1
046	1605		A	UR 1	TR 2	T 3	U 1
046	1606		A	UR 1	TR 3	T 3	U 1
046	1606		B	UR 1	TR 3	T 3	U 1
046	1609		A	UR 1	TR 3	T 3	U 1
046	1636		A	UR 1	TR 3	T 3	U 1
046	1638		A	UR 3	TR 3	T 3	U 2
046	1639		A	UR 2	TR 3	T 3	U 2
046	1647		A	UR 1	TR 3	T 2	U 1
046	1648		A	UR 1	TR 2	T 3	U 1
046	1657		A	UR 1	TR 3	T 3	U 1
046	1657		B	UR 1	TR 3	T 3	U 1
046	1658		A	UR 3	TR 3	T 3	U 2
046	1658		B	UR 2	TR 3	T 3	U 1
046	1661		A	UR 1	TR 3	T 3	U 1
046	1662		A	UR 1	TR 3	T 3	U 1
046	1671		A	UR 1	TR 3	T 3	U 1
046	1673		A	UR 1	TR 2	T 2	U 1
046	1674		A	UR 1	TR 3	T 3	U 2
046	1674		B	UR 2	TR 3	T 3	U 2
046	1674		C	UR 3	TR 3	T 3	U 2
046	1682		A	UR 1	TR 3	T 3	U 1
046	1682		B	UR 1	TR 3	T 3	U 1

CLUSTER GROUPS							
Site	Small Find No.	SF Sub Division	Analysis Area	Untransformed Robust	Transformed Robust	Transformed	Untransformed
046	1713		A	UR 2	TR 3	T 3	U 2
046	1715		A	UR 2	TR 3	T 3	U 2
046	1727		A	UR 1	TR 1	T 1	U 1
046	1729		A	UR 1	TR 3	T 3	U 1
046	1735		A	UR 1	TR 3	T 3	U 2
046	1735		B	UR 3	TR 2	T 3	U 2
046	1735		C	UR 3	TR 3	T 3	U 2
046	1737		A	UR 2	TR 2	T 3	U 2
046	1737		B	UR 3	TR 2	T 2	U 2
046	1737		C	UR 2	TR 2	T 2	U 2
046	1739		A	UR 1	TR 3	T 3	U 1
046	1750		A	UR 3	TR 2	T 3	U 2
046	1750		B	UR 3	TR 2	T 3	U 2
046	1774		A	UR 3	TR 2	T 2	U 2
046	1782		A	UR 2	TR 3	T 3	U 1
046	1782		B	UR 2	TR 3	T 3	U 2
046	1792		A	UR 1	TR 3	T 3	U 1
046	1811		A	UR 1	TR 3	T 3	U 1
046	1814		A	UR 3	TR 2	T 3	U 2
046	1815		A	UR 1	TR 1	T 1	U 2
046	1817		A	UR 3	TR 3	T 2	U 2
046	1818		A	UR 3	TR 3	T 2	U 2
046	1819		A	UR 3	TR 2	T 3	U 2
046	1819		B	UR 1	TR 3	T 3	U 1

CLUSTER GROUPS							
Site	Small Find No.	SF Sub Division	Analysis Area	Untransformed Robust	Transformed Robust	Transformed	Untransformed
046	1820		A	UR 1	TR 2	T 3	U 1
046	1820		B	UR 2	TR 3	T 3	U 2
046	1821		A	UR 1	TR 1	T 1	U 1
046	1822		A	UR 1	TR 3	T 3	U 1
046	1824		A	UR 1	TR 3	T 3	U 1
104	1000		A	UR 1	TR 1	T 1	U 1
104	1001		A	UR 2	TR 2	T 2	U 2
104	1003		A	UR 3	TR 2	T 2	U 2
104	1004		A	UR 1	TR 2	T 2	U 2
104	1005		A	UR 3	TR 2	T 3	U 2
104	1006		A	UR 3	TR 2	T 2	U 2
104	1026		A	UR 2	TR 3	T 2	U 2
104	1026		B	UR 1	TR 3	T 2	U 1
104	1026		C	UR 1	TR 3	T 2	U 1
104	1027		A	UR 1	TR 2	T 2	U 1
104	1033		A	UR 3	TR 2	T 2	U 2
104	1035		A	UR 3	TR 1	T 1	U 2
104	1038		A	UR 1	TR 2	T 2	U 2
104	1046		B	UR 3	TR 2	T 2	U 2
104	1047		A	UR 3	TR 1	T 1	U 2
104	1048		A	UR 3	TR 1	T 1	U 2
104	1049		A	UR 3	TR 2	T 2	U 2
104	1057		A	UR 2	TR 3	T 2	U 2
104	1058		A	UR 3	TR 2	T 2	U 2

CLUSTER GROUPS							
Site	Small Find No.	SF Sub Division	Analysis Area	Untransformed Robust	Transformed Robust	Transformed	Untransformed
104	1058		B	UR 2	TR 2	T 2	U 2
104	1062		A	UR 3	TR 2	T 2	U 2
104	1063		A	UR 3	TR 2	T 2	U 2
104	1074		A	UR 3	TR 2	T 2	U 2
104	1095		A	UR 2	TR 3	T 2	U 2
104	1098		A	UR 2	TR 3	T 2	U 2
104	1148		A	UR 1	TR 3	T 2	U 1
104	1161		A	UR 1	TR 2	T 2	U 2
104	1162		A	UR 1	TR 2	T 2	U 2
104	1169		A	UR 1	TR 1	T 1	U 2
104	1171		A	UR 3	TR 2	T 2	U 2
104	1173		A	UR 3	TR 2	T 2	U 2
104	1174		A	UR 2	TR 2	T 2	U 2
104	1176		C	UR 1	TR 3	T 2	U 1
104	1178		A	UR 1	TR 3	T 2	U 1
104	1182		A	UR 1	TR 2	T 2	U 1
104	1191		C	UR 2	TR 3	T 3	U 2
104	1195		A	UR 1	TR 3	T 2	U 1
104	1213		A	UR 1	TR 3	T 2	U 2
104	1227		A	UR 2	TR 2	T 2	U 2
104	1228		A	UR 1	TR 2	T 2	U 1
104	1239		A	UR 1	TR 2	T 2	U 2
104	1248		A	UR 3	TR 2	T 2	U 2
104	1249		A	UR 1	TR 2	T 2	U 1

CLUSTER GROUPS							
Site	Small Find No.	SF Sub Division	Analysis Area	Untransformed Robust	Transformed Robust	Transformed	Untransformed
104	1250		A	UR 1	TR 2	T 2	U 2
104	1251		A	UR 1	TR 3	T 2	U 1
104	1254		A	UR 3	TR 2	T 2	U 2
104	1254		B	UR 1	TR 2	T 2	U 2
104	1255		A	UR 2	TR 2	T 2	U 2
104	1256		A	UR 1	TR 2	T 2	U 1
104	1263		A	UR 1	TR 2	T 2	U 2
104	1263		B	UR 2	TR 2	T 2	U 2
104	1277		A	UR 1	TR 3	T 2	U 1
104	1293		A	UR 2	TR 2	T 2	U 2
104	1296		A	UR 3	TR 2	T 2	U 2
104	1317		A	UR 1	TR 2	T 2	U 1
104	1318		A	UR 3	TR 1	T 1	U 2
104	1323		A	UR 1	TR 3	T 2	U 1
104	1324		A	UR 1	TR 3	T 2	U 1
104	1324		B	UR 2	TR 2	T 2	U 2
104	1325		A	UR 1	TR 3	T 2	U 1
104	1357		A	UR 3	TR 2	T 2	U 2
104	1357		B	UR 2	TR 2	T 2	U 2
104	1359		A	UR 3	TR 2	T 2	U 2
104	1360		A	UR 1	TR 2	T 2	U 2
104	1362		B	UR 1	TR 3	T 2	U 1
104	1363		A	UR 2	TR 3	T 2	U 2
104	1363		B	UR 3	TR 3	T 2	U 2

CLUSTER GROUPS							
Site	Small Find No.	SF Sub Division	Analysis Area	Untransformed Robust	Transformed Robust	Transformed	Untransformed
104	1364		A	UR 1	TR 2	T 2	U 2
104	1366		A	UR 1	TR 2	T 2	U 2
104	1368		A	UR 2	TR 2	T 2	U 2
104	1413		A	UR 2	TR 2	T 2	U 2
104	1443		A	UR 1	TR 2	T 2	U 2
104	1444		A	UR 3	TR 1	T 1	U 2
104	1445		A	UR 1	TR 3	T 2	U 1
104	1449		A	UR 1	TR 3	T 2	U 1
104	1450	a	B	UR 1	TR 2	T 2	U 1
104	1450	b	C	UR 1	TR 2	T 2	U 1
104	1450	c	E	UR 1	TR 2	T 2	U 1
104	1450	d	F	UR 3	TR 2	T 2	U 2
104	1458		A	UR 3	TR 2	T 2	U 2
104	1458		A	UR 3	TR 3	T 3	U 2
104	1458		B	UR 3	TR 1	T 1	U 2
104	1458		A	UR 1	TR 2	T 2	U 2
104	1461	a	B	UR 2	TR 3	T 2	U 2
104	1461	b	A	UR 2	TR 3	T 2	U 2
104	1461	c	A	UR 2	TR 3	T 2	U 2
104	1461	d	B	UR 2	TR 3	T 2	U 2
104	1461	e	A	UR 2	TR 3	T 2	U 2
104	1461	f	A	UR 2	TR 3	T 2	U 2
104	1466		A	UR 2	TR 2	T 2	U 2
104	1476		A	UR 1	TR 3	T 2	U 1

CLUSTER GROUPS							
Site	Small Find No.	SF Sub Division	Analysis Area	Untransformed Robust	Transformed Robust	Transformed	Untransformed
104	1476		A	UR 1	TR 3	T 2	U 1
104	1477		B	UR 1	TR 3	T 2	U 2
104	1477		A	UR 1	TR 3	T 2	U 2
104	1478		A	UR 1	TR 2	T 2	U 1
104	1509		A	UR 3	TR 2	T 2	U 2
104	1509		B	UR 3	TR 2	T 3	U 2
104	1518		A	UR 3	TR 2	T 2	U 2
104	1543		B	UR 3	TR 2	T 2	U 2
104	1545		A	UR 3	TR 2	T 2	U 2
104	1546		A	UR 3	TR 2	T 2	U 2
104	1547		A	UR 3	TR 2	T 2	U 2
104	1547		A	UR 3	TR 2	T 2	U 2
104	1563		A	UR 1	TR 2	T 2	U 2
104	1568		A	UR 2	TR 3	T 3	U 2
104	1570		A	UR 1	TR 2	T 2	U 2
104	1570		A	UR 3	TR 2	T 2	U 2
104	1589		A	UR 1	TR 3	T 2	U 1
104	1589		A	UR 2	TR 3	T 2	U 2
104	1592	c	A	UR 3	TR 1	T 1	U 2
104	1592	c	A	UR 3	TR 1	T 1	U 2
104	1593		A	UR 1	TR 2	T 2	U 1
104	1593	b	A	UR 2	TR 1	T 1	U 1
104	1605		A	UR 1	TR 3	T 2	U 1
104	1620		A	UR 1	TR 2	T 3	U 2

CLUSTER GROUPS							
Site	Small Find No.	SF Sub Division	Analysis Area	Untransformed Robust	Transformed Robust	Transformed	Untransformed
104	1621		A	UR 2	TR 2	T 2	U 2
104	1622		C	UR 2	TR 3	T 2	U 2
104	1643		D	UR 1	TR 2	T 2	U 1
104	1656		A	UR 1	TR 2	T 2	U 2
104	1668		A	UR 2	TR 2	T 2	U 2
104	1681		A	UR 1	TR 3	T 3	U 1
104	1691		A	UR 3	TR 2	T 2	U 2
104	1692		B	UR 3	TR 2	T 2	U 2
104	1693		A	UR 3	TR 2	T 2	U 2
104	1694		B	UR 2	TR 2	T 2	U 2
104	1695		A	UR 2	TR 2	T 2	U 2
104	1696		A	UR 1	TR 3	T 2	U 1
104	1698		A	UR 3	TR 3	T 3	U 2
104	1704		A	UR 3	TR 2	T 2	U 2
104	1704		A	UR 1	TR 2	T 2	U 1
104	1704		A	UR 3	TR 2	T 2	U 2
104	1705		A	UR 2	TR 3	T 2	U 1
104	1706		A	UR 2	TR 3	T 2	U 1
104	1713		A	UR 1	TR 3	T 3	U 1
104	1752		A	UR 1	TR 2	T 2	U 1
104	1752		A	UR 1	TR 2	T 2	U 1
104	1753		A	UR 1	TR 2	T 2	U 2
104	1753		C	UR 1	TR 2	T 2	U 1
104	1768		A	UR 2	TR 2	T 2	U 1

CLUSTER GROUPS							
Site	Small Find No.	SF Sub Division	Analysis Area	Untransformed Robust	Transformed Robust	Transformed	Untransformed
104	1776		A	UR 3	TR 3	T 2	U 2
104	1777		A	UR 1	TR 3	T 2	U 1
104	1782		B	UR 1	TR 1	T 1	U 1
104	1786		A	UR 1	TR 3	T 2	U 1
104	1887		A	UR 3	TR 2	T 2	U 2
104	1888		A	UR 2	TR 2	T 2	U 2
104	1900		A	UR 3	TR 2	T 2	U 2
104	1903		A	UR 3	TR 2	T 2	U 2
104	1942		B	UR 1	TR 2	T 2	U 2
104	1947		A	UR 1	TR 2	T 2	U 1
104	1948		B	UR 3	TR 3	T 2	U 2
104	1948		C	UR 1	TR 2	T 2	U 2
104	1949		A	UR 2	TR 2	T 2	U 2
104	1950		A	UR 3	TR 2	T 2	U 2
104	1952		B	UR 3	TR 2	T 3	U 2
104	1952		A	UR 3	TR 2	T 2	U 2
104	1953		A	UR 3	TR 2	T 2	U 2
104	1954		A	UR 3	TR 2	T 2	U 2
104	1955		A	UR 1	TR 2	T 2	U 2
104	1956		A	UR 3	TR 2	T 2	U 2
104	1960		A	UR 1	TR 2	T 2	U 2
104	1960		A	UR 3	TR 2	T 2	U 2
104	2028		A	UR 1	TR 2	T 2	U 1
104	2028		A	UR 1	TR 2	T 2	U 1

CLUSTER GROUPS							
Site	Small Find No.	SF Sub Division	Analysis Area	Untransformed Robust	Transformed Robust	Transformed	Untransformed
104	2028		B	UR 1	TR 2	T 2	U 2
104	2029		A	UR 1	TR 2	T 2	U 1
104	2030		B	UR 1	TR 3	T 2	U 1
104	2030		A	UR 2	TR 3	T 2	U 2
104	2031		A	UR 3	TR 2	T 2	U 2
104	2054		A	UR 2	TR 2	T 2	U 2
104	2057		A	UR 3	TR 2	T 2	U 2
104	2059		A	UR 3	TR 2	T 2	U 2
104	2124		A	UR 3	TR 2	T 2	U 2
104	2125		A	UR 1	TR 2	T 2	U 1
104	2126		A	UR 1	TR 3	T 2	U 1
104	2135		A	UR 1	TR 2	T 2	U 2
104	2136		A	UR 1	TR 2	T 2	U 2
104	2136		A	UR 2	TR 2	T 2	U 2
104	2137		A	UR 1	TR 2	T 2	U 1
104	2137		B	UR 1	TR 3	T 3	U 2
104	2138		A	UR 1	TR 2	T 2	U 1
104	2139		D	UR 1	TR 2	T 2	U 2
104	2140		A	UR 1	TR 3	T 2	U 1
104	2221		B	UR 3	TR 1	T 1	U 2
104	2276		G	UR 2	TR 2	T 2	U 2
104	2289		A	UR 2	TR 2	T 2	U 2
104	2294		A	UR 1	TR 2	T 2	U 2
104	2298		A	UR 3	TR 2	T 3	U 2

CLUSTER GROUPS							
Site	Small Find No.	SF Sub Division	Analysis Area	Untransformed Robust	Transformed Robust	Transformed	Untransformed
104	2299		B	UR 3	TR 2	T 2	U 2
104	2300		C	UR 3	TR 2	T 3	U 2
104	2301		A	UR 2	TR 3	T 2	U 2
104	2308		B	UR 3	TR 2	T 2	U 2
104	2311		B	UR 1	TR 1	T 1	U 1
104	2312		A	UR 1	TR 3	T 3	U 1
104	2312		B	UR 2	TR 3	T 2	U 1
104	2317		A	UR 2	TR 2	T 2	U 2
104	2317		A	UR 1	TR 1	T 1	U 1
104	2317		A	UR 1	TR 1	T 1	U 1
104	2344		B	UR 1	TR 2	T 2	U 1
104	2352		A	UR 1	TR 3	T 2	U 1
104	2364		A	UR 2	TR 2	T 2	U 2
104	2364		A	UR 1	TR 2	T 2	U 1
104	2364		A	UR 2	TR 2	T 2	U 2
104	2373		A	UR 1	TR 3	T 2	U 1
104	2373		B	UR 2	TR 2	T 2	U 2
104	2374		A	UR 2	TR 3	T 3	U 2
104	2377		A	UR 1	TR 3	T 2	U 1
104	2377		A	UR 1	TR 3	T 2	U 1
104	2380		A	UR 1	TR 3	T 2	U 1
104	2381		A	UR 1	TR 3	T 2	U 1
104	2387		A	UR 1	TR 3	T 2	U 1
104	2387		A	UR 1	TR 3	T 2	U 1

CLUSTER GROUPS							
Site	Small Find No.	SF Sub Division	Analysis Area	Untransformed Robust	Transformed Robust	Transformed	Untransformed
104	2398		A	UR 3	TR 2	T 2	U 2
104	2399		B	UR 1	TR 3	T 2	U 1
104	2401		A	UR 1	TR 2	T 2	U 1
104	2402		A	UR 3	TR 3	T 2	U 2
104	2403		A	UR 3	TR 2	T 2	U 2
104	2403		A	UR 3	TR 2	T 2	U 2
104	2411		A	UR 2	TR 2	T 2	U 2
104	2413		B	UR 1	TR 2	T 2	U 2
104	2450		A	UR 1	TR 2	T 2	U 1
104	2456		A	UR 3	TR 1	T 1	U 2
104	2462		A	UR 1	TR 2	T 2	U 1
104	2463		A	UR 3	TR 2	T 2	U 2
104	2479		A	UR 1	TR 3	T 2	U 1
104	2494		A	UR 3	TR 2	T 2	U 2
104	2494		B	UR 3	TR 2	T 2	U 2
104	2499		A	UR 3	TR 2	T 2	U 2
104	2500		A	UR 1	TR 2	T 2	U 1
104	2501		A	UR 2	TR 3	T 2	U 1
104	2503		A	UR 3	TR 2	T 2	U 2
104	2507		A	UR 1	TR 2	T 2	U 1
104	2507		A	UR 2	TR 3	T 2	U 1
104	2510		B	UR 2	TR 2	T 3	U 2
104	2524		A	UR 1	TR 3	T 2	U 1
104	2525		A	UR 2	TR 3	T 2	U 2

CLUSTER GROUPS							
Site	Small Find No.	SF Sub Division	Analysis Area	Untransformed Robust	Transformed Robust	Transformed	Untransformed
104	2526		A	UR 3	TR 1	T 1	U 2
104	2528		B	UR 1	TR 2	T 2	U 1
104	2529		A	UR 3	TR 2	T 2	U 2
104	2529		B	UR 2	TR 3	T 2	U 1
104	2532		A	UR 1	TR 3	T 2	U 1
104	2533		B	UR 2	TR 3	T 2	U 2
104	2540		A	UR 3	TR 2	T 2	U 2
104	2540	b	C	UR 3	TR 2	T 3	U 2
104	2540	b	D	UR 3	TR 2	T 2	U 2
104	2541		E	UR 3	TR 2	T 2	U 2
104	2577		A	UR 1	TR 3	T 2	U 1
104	2587		D	UR 1	TR 1	T 1	U 1
104	2587		B	UR 2	TR 1	T 1	U 1
104	2588		D	UR 3	TR 2	T 2	U 2
104	2589		E	UR 3	TR 1	T 1	U 2
104	2590		A	UR 3	TR 3	T 2	U 2
104	2590		C	UR 2	TR 3	T 2	U 2
104	2591		A	UR 2	TR 2	T 2	U 2
104	2613		A	UR 1	TR 3	T 2	U 1
104	2613		A	UR 2	TR 3	T 2	U 2
104	2622		B	UR 1	TR 2	T 2	U 2
104	2623		A	UR 3	TR 2	T 2	U 2
104	2623		A	UR 2	TR 2	T 2	U 2
104	2623		B	UR 3	TR 3	T 3	U 2

CLUSTER GROUPS							
Site	Small Find No.	SF Sub Division	Analysis Area	Untransformed Robust	Transformed Robust	Transformed	Untransformed
104	2624		C	UR 3	TR 2	T 3	U 2
104	2624		A	UR 1	TR 2	T 2	U 1
104	2626		B	UR 3	TR 2	T 2	U 2
104	2626		A	UR 1	TR 2	T 2	U 1
104	2626		A	UR 1	TR 2	T 2	U 1
104	2627		A	UR 3	TR 3	T 3	U 2
104	2627		A	UR 1	TR 3	T 3	U 1
104	2627		A	UR 1	TR 3	T 3	U 1
104	2631		A	UR 2	TR 2	T 2	U 2
104	2633		A	UR 2	TR 2	T 2	U 2
104	2634		A	UR 2	TR 2	T 2	U 2
104	2634		B	UR 2	TR 2	T 2	U 2
104	2636		A	UR 3	TR 2	T 2	U 2
104	2646		A	UR 1	TR 1	T 1	U 1
104	2646		A	UR 2	TR 2	T 2	U 2
104	2646		A	UR 1	TR 2	T 2	U 1
104	2647		A	UR 2	TR 2	T 2	U 2
104	2647		A	UR 3	TR 2	T 2	U 2
104	2648		A	UR 1	TR 2	T 2	U 2
104	2649		A	UR 1	TR 2	T 2	U 2
104	2650		A	UR 3	TR 2	T 2	U 2
104	2651		A	UR 3	TR 2	T 2	U 2
104	2655		A	UR 1	TR 3	T 2	U 1
104	2657		A	UR 2	TR 2	T 2	U 1

CLUSTER GROUPS							
Site	Small Find No.	SF Sub Division	Analysis Area	Untransformed Robust	Transformed Robust	Transformed	Untransformed
104	2671		A	UR 1	TR 2	T 2	U 1
104	2672		B	UR 1	TR 3	T 2	U 1
104	2672		A	UR 2	TR 3	T 2	U 1
104	2679		A	UR 1	TR 1	T 1	U 2
104	2681		A	UR 1	TR 3	T 2	U 1
104	2682		B	UR 1	TR 3	T 2	U 1
104	2706		A	UR 3	TR 2	T 2	U 2
104	2714		B	UR 1	TR 3	T 2	U 1
104	2715		A	UR 1	TR 3	T 2	U 2
104	2716		A	UR 1	TR 3	T 2	U 1
104	2717		B	UR 2	TR 2	T 2	U 2
104	2719		A	UR 3	TR 2	T 2	U 2
104	2748		A	UR 1	TR 3	T 2	U 2
104	2749		A	UR 1	TR 3	T 2	U 2
104	2750		A	UR 2	TR 2	T 2	U 2
104	2757		B	UR 1	TR 2	T 2	U 2
104	2757		A	UR 1	TR 2	T 2	U 2
104	2758		B	UR 1	TR 2	T 2	U 2
104	2759		A	UR 1	TR 2	T 2	U 2
104	2760		A	UR 1	TR 1	T 1	U 1
104	2770		A	UR 3	TR 2	T 2	U 2
104	2770		B	UR 2	TR 2	T 2	U 2
104	2780		A	UR 1	TR 3	T 2	U 1
104	2781		B	UR 2	TR 2	T 2	U 2

CLUSTER GROUPS							
Site	Small Find No.	SF Sub Division	Analysis Area	Untransformed Robust	Transformed Robust	Transformed	Untransformed
104	2781		A	UR 2	TR 3	T 2	U 2
104	2782		A	UR 1	TR 3	T 2	U 1
104	2783		A	UR 3	TR 1	T 1	U 2
104	2784		A	UR 1	TR 2	T 2	U 1
104	2785		A	UR 1	TR 2	T 2	U 1
104	2785		A	UR 2	TR 2	T 2	U 2
104	2786		A	UR 1	TR 3	T 2	U 2
104	2786		A	UR 2	TR 3	T 3	U 2
104	2787	a	B	UR 1	TR 2	T 2	U 2
104	2787	b	A	UR 1	TR 2	T 2	U 1
104	2787	c	A	UR 1	TR 2	T 2	U 1
104	2788		B	UR 1	TR 3	T 2	U 2
104	2789		A	UR 2	TR 2	T 2	U 2
104	2798		A	UR 3	TR 2	T 2	U 2
104	2799		A	UR 3	TR 2	T 2	U 2
104	2800		A	UR 3	TR 2	T 2	U 2
104	2821		A	UR 3	TR 2	T 2	U 2
104	2821		A	UR 3	TR 2	T 2	U 2
104	2823		B	UR 3	TR 2	T 2	U 2
104	2825		A	UR 1	TR 2	T 2	U 1
104	2826		A	UR 3	TR 2	T 2	U 2
104	2827		A	UR 3	TR 2	T 2	U 2
104	2863		B	UR 1	TR 3	T 2	U 1
104	2866		A	UR 1	TR 2	T 2	U 2

CLUSTER GROUPS							
Site	Small Find No.	SF Sub Division	Analysis Area	Untransformed Robust	Transformed Robust	Transformed	Untransformed
104	2867		A	UR 2	TR 2	T 2	U 2
104	2868		B	UR 1	TR 3	T 2	U 1
104	2868		A	UR 1	TR 3	T 2	U 1
104	2869		B	UR 3	TR 1	T 1	U 2
104	2870		A	UR 1	TR 2	T 2	U 2
104	2870		B	UR 1	TR 2	T 2	U 2
104	2879		C	UR 2	TR 2	T 2	U 2
104	2888		A	UR 2	TR 3	T 2	U 2
104	2895		A	UR 3	TR 2	T 2	U 2
104	2897		A	UR 1	TR 2	T 2	U 1
104	2899		A	UR 3	TR 2	T 2	U 2
104	2902		A	UR 3	TR 2	T 2	U 2
104	2902		A	UR 2	TR 3	T 2	U 2
104	2937		B	UR 1	TR 3	T 2	U 1
104	2943		A	UR 3	TR 2	T 2	U 2
104	2949		A	UR 1	TR 2	T 2	U 2
104	2950		B	UR 3	TR 2	T 3	U 3
104	2993		A	UR 2	TR 3	T 2	U 1
104	2995		B	UR 3	TR 2	T 2	U 2
104	2995		A	UR 3	TR 2	T 2	U 2
104	3026		B	UR 1	TR 3	T 2	U 1
104	3026		A	UR 2	TR 2	T 2	U 1
104	3045		A	UR 3	TR 3	T 2	U 2
104	3045		A	UR 2	TR 3	T 2	U 2

CLUSTER GROUPS							
Site	Small Find No.	SF Sub Division	Analysis Area	Untransformed Robust	Transformed Robust	Transformed	Untransformed
104	3045		A	UR 2	TR 3	T 3	U 1
104	3048		A	UR 2	TR 2	T 2	U 2
104	3051		A	UR 1	TR 2	T 2	U 2
104	3052		A	UR 1	TR 2	T 2	U 2
104	3059		A	UR 1	TR 2	T 3	U 1
104	3077		A	UR 1	TR 3	T 2	U 1
104	3078		A	UR 1	TR 3	T 2	U 1
104	3078		A	UR 1	TR 3	T 2	U 1
104	3088		B	UR 1	TR 3	T 2	U 1
104	3089		A	UR 1	TR 3	T 2	U 1
104	3090		A	UR 1	TR 2	T 2	U 1
104	3091		A	UR 2	TR 3	T 2	U 2
104	3091		B	UR 2	TR 3	T 2	U 2
104	3093		C	UR 2	TR 3	T 2	U 1
104	3093		A	UR 2	TR 3	T 2	U 2
104	3143		A	UR 2	TR 3	T 2	U 2
104	3144		A	UR 1	TR 3	T 2	U 1
104	3161		A	UR 3	TR 2	T 2	U 2
104	3165		B	UR 1	TR 3	T 2	U 1
104	3169		C	UR 1	TR 3	T 2	U 1
104	3170		A	UR 2	TR 2	T 2	U 2
104	3203		A	UR 1	TR 2	T 2	U 1
104	3206		A	UR 1	TR 3	T 3	U 1
104	3209		A	UR 2	TR 3	T 2	U 2

CLUSTER GROUPS							
Site	Small Find No.	SF Sub Division	Analysis Area	Untransformed Robust	Transformed Robust	Transformed	Untransformed
104	3210		A	UR 3	TR 2	T 2	U 2
104	3223		A	UR 1	TR 3	T 2	U 1
104	3232		B	UR 2	TR 3	T 2	U 3
104	3236		C	UR 2	TR 3	T 2	U 1
104	3249		A	UR 2	TR 3	T 2	U 2
104	3283		B	UR 1	TR 3	T 2	U 1
104	3299		C	UR 3	TR 2	T 2	U 2
104	3299		E	UR 3	TR 2	T 2	U 2
104	3300		B	UR 1	TR 2	T 2	U 2
104	3313		D	UR 3	TR 2	T 2	U 2
104	3314		F	UR 1	TR 3	T 2	U 2
104	3316		A	UR 3	TR 2	T 2	U 2
104	3316		A	UR 2	TR 2	T 2	U 2
104	3316		B	UR 2	TR 2	T 2	U 2
104	3317		C	UR 3	TR 2	T 2	U 2
104	3318	a	D	UR 3	TR 2	T 2	U 2
104	3318	b	A	UR 3	TR 2	T 2	U 2
104	3318	c	A	UR 3	TR 2	T 2	U 2
104	3318	d	A	UR 3	TR 3	T 3	U 2
104	3318	e	B	UR 1	TR 2	T 2	U 2
104	3318	f	A	UR 1	TR 2	T 2	U 1
104	3328		A	UR 3	TR 2	T 3	U 2
104	3329		A	UR 1	TR 2	T 2	U 2
104	3332		B	UR 2	TR 2	T 2	U 2

CLUSTER GROUPS							
Site	Small Find No.	SF Sub Division	Analysis Area	Untransformed Robust	Transformed Robust	Transformed	Untransformed
104	3342		A	UR 1	TR 3	T 3	U 1
104	3342		A	UR 1	TR 2	T 2	U 1
104	3342		A	UR 1	TR 3	T 3	U 1
104	3348	b	A	UR 1	TR 2	T 2	U 1
104	3349		A	UR 3	TR 3	T 2	U 2
104	3349		B	UR 1	TR 3	T 2	U 1
104	3349		A	UR 1	TR 3	T 2	U 1
104	3349		A	UR 3	TR 2	T 2	U 2
104	3350		A	UR 1	TR 3	T 2	U 1
104	3350		A	UR 1	TR 3	T 2	U 1
104	3350		A	UR 1	TR 3	T 2	U 1
104	3355		A	UR 1	TR 2	T 2	U 1
104	3363		A	UR 1	TR 3	T 2	U 1
104	3363		A	UR 1	TR 3	T 2	U 1
104	3363		A	UR 1	TR 3	T 3	U 1
104	3363		C	UR 1	TR 3	T 3	U 1
104	3364		A	UR 1	TR 3	T 3	U 1
104	3372		A	UR 2	TR 2	T 2	U 2
104	3373		A	UR 1	TR 2	T 2	U 2
104	3373		A	UR 1	TR 2	T 2	U 2
104	3387		A	UR 2	TR 3	T 2	U 2
104	3389		A	UR 3	TR 2	T 2	U 2
104	3391		A	UR 1	TR 1	T 1	U 2
104	3393		A	UR 1	TR 3	T 2	U 1

CLUSTER GROUPS							
Site	Small Find No.	SF Sub Division	Analysis Area	Untransformed Robust	Transformed Robust	Transformed	Untransformed
104	3393		A	UR 1	TR 3	T 2	U 1
104	3394		A	UR 1	TR 3	T 2	U 1
104	3395		A	UR 1	TR 3	T 2	U 1
104	3396		C	UR 1	TR 3	T 2	U 1
104	3443		D	UR 3	TR 2	T 2	U 2
104	3444		A	UR 3	TR 1	T 1	U 2
104	3453		B	UR 1	TR 2	T 2	U 1
104	3460		A	UR 3	TR 2	T 2	U 2
104	3475		B	UR 1	TR 2	T 3	U 1
104	3482		A	UR 2	TR 3	T 2	U 2
104	3494		C	UR 1	TR 2	T 2	U 2
104	3495		D	UR 1	TR 2	T 2	U 1
104	3524		E	UR 1	TR 3	T 2	U 2
104	3525		D	UR 1	TR 2	T 2	U 1
104	3530		E	UR 2	TR 1	T 1	U 2
104	3532	1	F	UR 1	TR 2	T 2	U 2
104	3532		G	UR 1	TR 2	T 2	U 2
104	3532	a	B	UR 1	TR 1	T 1	U 1
104	3532		A	UR 3	TR 2	T 2	U 2
104	3534		C	UR 3	TR 2	T 2	U 2
104	3573		D	UR 1	TR 2	T 2	U 1
104	3577		F	UR 2	TR 2	T 2	U 2
104	3579		G	UR 2	TR 1	T 1	U 2
104	3580		A	UR 3	TR 2	T 2	U 2

CLUSTER GROUPS							
Site	Small Find No.	SF Sub Division	Analysis Area	Untransformed Robust	Transformed Robust	Transformed	Untransformed
104	3581		A	UR 1	TR 3	T 2	U 1
104	3582		A	UR 1	TR 3	T 2	U 1
104	3596		B	UR 3	TR 2	T 2	U 2
104	3597		A	UR 3	TR 1	T 1	U 2
104	3616		A	UR 3	TR 2	T 2	U 2
104	3618		B	UR 3	TR 1	T 1	U 2
104	3618		B	UR 2	TR 1	T 1	U 2
104	3618		A	UR 2	TR 3	T 3	U 1
104	3674	1	B	UR 2	TR 2	T 3	U 2
104	3675	3	A	UR 1	TR 3	T 3	U 1
104	3677		B	UR 1	TR 3	T 2	U 1
104	3677		A	UR 2	TR 3	T 2	U 1
104	BM12		A	UR 1	TR 2	T 2	U 1
104	BM12		B	UR 3	TR 2	T 2	U 2
104	BM13		A	UR 2	TR 2	T 2	U 2
104	BM18		B	UR 3	TR 2	T 2	U 2
104	BM18		A	UR 2	TR 3	T 3	U 2
104	BM18		A	UR 2	TR 3	T 2	U 2
104	BM19		A	UR 3	TR 2	T 2	U 2
104	BM19		A	UR 3	TR 2	T 2	U 2
104	BM1		A	UR 2	TR 3	T 2	U 2
104	BM1		B	UR 2	TR 2	T 2	U 2
104	BM20		A	UR 2	TR 3	T 2	U 2
104	BM21		A	UR 1	TR 2	T 2	U 2

CLUSTER GROUPS							
Site	Small Find No.	SF Sub Division	Analysis Area	Untransformed Robust	Transformed Robust	Transformed	Untransformed
104	BM33		B	UR 3	TR 2	T 2	U 2
104	BM3		A	UR 3	TR 2	T 2	U 2
104	BM5		B	UR 2	TR 2	T 3	U 2
104	BM5		A	UR 2	TR 2	T 2	U 2
104	BM6	7A	A	UR 3	TR 1	T 1	U 2
104	BM6	7A	A	UR 2	TR 2	T 2	U 2
104	BM6	7A	A	UR 2	TR 3	T 2	U 2
104	BM6	7A	A	UR 2	TR 3	T 2	U 2
114	1001		A	UR 3	TR 2	T 2	U 2
114	1004		A	UR 3	TR 2	T 2	U 2
114	1005		A	UR 1	TR 2	T 2	U 1
114	1007		B	UR 2	TR 2	T 3	U 2
114	1034		A	UR 3	TR 2	T 2	U 2
114	1036		B	UR 2	TR 2	T 3	U 2
114	1037		A	UR 2	TR 2	T 3	U 2
114	1039		A	UR 1	TR 2	T 2	U 2
114	1040		B	UR 3	TR 1	T 1	U 2
114	1044		A	UR 2	TR 3	T 3	U 2
114	1048		A	UR 3	TR 1	T 1	U 2
114	1048		A	UR 3	TR 2	T 2	U 2
114	1050		A	UR 3	TR 1	T 1	U 2
114	1051		B	UR 3	TR 1	T 1	U 2
114	1051		A	UR 3	TR 2	T 3	U 2
114	1055		B	UR 3	TR 3	T 3	U 2

CLUSTER GROUPS							
Site	Small Find No.	SF Sub Division	Analysis Area	Untransformed Robust	Transformed Robust	Transformed	Untransformed
114	1055		A	UR 2	TR 2	T 3	U 2
114	1058		B	UR 1	TR 3	T 2	U 2
114	1059		A	UR 1	TR 3	T 2	U 1
114	1060		A	UR 1	TR 3	T 2	U 1
114	1061	A	B	UR 1	TR 3	T 2	U 1
114	1061	B	A	UR 1	TR 2	T 2	U 1
114	1061	C	B	UR 3	TR 2	T 2	U 2
114	1061	C	A	UR 1	TR 3	T 3	U 1
114	1061	C	A	UR 1	TR 3	T 3	U 1
114	1062		A	UR 1	TR 3	T 2	U 2
114	1064		A	UR 3	TR 2	T 2	U 2
114	1064		A	UR 3	TR 2	T 2	U 2
114	1065		A	UR 3	TR 2	T 2	U 2
114	1066		A	UR 3	TR 2	T 2	U 2
114	1066		A	UR 3	TR 2	T 2	U 2
114	1067		C	UR 3	TR 2	T 2	U 2
114	1067		A	UR 3	TR 2	T 2	U 2
114	1069		B	UR 1	TR 3	T 3	U 2
114	1070		A	UR 3	TR 3	T 2	U 2
114	1075		A	UR 3	TR 2	T 2	U 2
114	1094		A	UR 3	TR 2	T 2	U 2
114	1148		A	UR 3	TR 2	T 2	U 2
114	1159		A	UR 3	TR 2	T 3	U 2
114	1161		A	UR 1	TR 2	T 2	U 1

CLUSTER GROUPS							
Site	Small Find No.	SF Sub Division	Analysis Area	Untransformed Robust	Transformed Robust	Transformed	Untransformed
114	1162		A	UR 3	TR 2	T 2	U 2
114	1162		A	UR 3	TR 2	T 2	U 2
114	1163		A	UR 3	TR 2	T 2	U 2
114	1163		A	UR 1	TR 3	T 2	U 1
114	1175		A	UR 3	TR 2	T 3	U 2
114	1227		B	UR 3	TR 2	T 2	U 2
114	1227		A	UR 2	TR 3	T 2	U 2
114	1228		A	UR 1	TR 2	T 2	U 2
114	1242		B	UR 1	TR 2	T 2	U 2
114	1243		A	UR 2	TR 3	T 3	U 1
114	1244		A	UR 2	TR 3	T 3	U 1
114	1244		B	UR 2	TR 3	T 2	U 2
114	1245		A	UR 2	TR 3	T 2	U 2
114	1245		B	UR 3	TR 3	T 3	U 2
114	1246		A	UR 2	TR 3	T 3	U 2
114	1246		A	UR 3	TR 3	T 3	U 2
114	1247		A	UR 2	TR 3	T 3	U 2
114	1248		A	UR 2	TR 3	T 2	U 2
114	1248		A	UR 3	TR 3	T 2	U 2
114	1249		A	UR 2	TR 3	T 3	U 2
114	1249		B	UR 3	TR 3	T 3	U 2
114	1250		A	UR 3	TR 2	T 3	U 2
114	1251		A	UR 2	TR 3	T 2	U 2
114	1254		A	UR 3	TR 1	T 1	U 2

CLUSTER GROUPS							
Site	Small Find No.	SF Sub Division	Analysis Area	Untransformed Robust	Transformed Robust	Transformed	Untransformed
114	1255		A	UR 3	TR 1	T 1	U 2
114	1292		A	UR 1	TR 2	T 2	U 2
114	1296		A	UR 1	TR 2	T 2	U 2
114	1297		A	UR 1	TR 2	T 2	U 1
114	1298		A	UR 1	TR 3	T 2	U 1
114	1298		A	UR 3	TR 2	T 2	U 2
114	1319		A	UR 3	TR 2	T 2	U 2
114	1319		A	UR 2	TR 2	T 3	U 2
114	1321		A	UR 3	TR 2	T 3	U 2
114	1322		A	UR 2	TR 3	T 2	U 1
114	1341		A	UR 3	TR 2	T 2	U 2
114	1342		A	UR 3	TR 2	T 2	U 2
114	1343		A	UR 3	TR 2	T 2	U 2
114	1344		A	UR 3	TR 2	T 2	U 2
114	1347		B	UR 1	TR 3	T 3	U 2
114	1348		A	UR 1	TR 3	T 3	U 2
114	1349		A	UR 3	TR 2	T 3	U 2
114	1370		B	UR 2	TR 3	T 3	U 2
114	1374		A	UR 1	TR 3	T 3	U 2
114	1374		B	UR 2	TR 3	T 3	U 2
114	1375		A	UR 1	TR 3	T 3	U 1
114	1378		B	UR 3	TR 2	T 2	U 2
114	1378		A	UR 2	TR 3	T 2	U 2
114	1380		A	UR 2	TR 3	T 2	U 2

CLUSTER GROUPS							
Site	Small Find No.	SF Sub Division	Analysis Area	Untransformed Robust	Transformed Robust	Transformed	Untransformed
114	1383		A	UR 1	TR 3	T 2	U 1
114	1383		A	UR 1	TR 3	T 3	U 1
114	1384		A	UR 1	TR 3	T 3	U 1
114	1384		A	UR 1	TR 3	T 3	U 1
114	1385		A	UR 1	TR 3	T 2	U 1
114	1386		B	UR 1	TR 3	T 2	U 2
114	1387		A	UR 1	TR 3	T 2	U 2
114	1388		A	UR 3	TR 2	T 2	U 2
114	1389		A	UR 1	TR 3	T 2	U 2
114	1392		A	UR 1	TR 2	T 2	U 2
114	1392		A	UR 1	TR 3	T 2	U 1
114	1393		A	UR 2	TR 3	T 2	U 1
114	1394		B	UR 3	TR 3	T 3	U 2
114	1395		C	UR 2	TR 3	T 2	U 2
114	1398		A	UR 3	TR 2	T 2	U 2
114	1399		A	UR 3	TR 3	T 2	U 2
114	1400		A	UR 1	TR 3	T 3	U 1
114	1401		A	UR 3	TR 2	T 2	U 2
114	1402		B	UR 3	TR 2	T 2	U 2
114	1405		C	UR 1	TR 2	T 2	U 1
114	1408		D	UR 1	TR 3	T 3	U 1
114	1414		A	UR 3	TR 2	T 3	U 2
114	1430		A	UR 2	TR 3	T 3	U 1
114	1431		A	UR 1	TR 3	T 3	U 1

CLUSTER GROUPS							
Site	Small Find No.	SF Sub Division	Analysis Area	Untransformed Robust	Transformed Robust	Transformed	Untransformed
114	1432		A	UR 3	TR 3	T 3	U 2
114	1433		A	UR 2	TR 3	T 3	U 2
114	1434		A	UR 3	TR 3	T 3	U 2
114	1435		A	UR 1	TR 3	T 3	U 2
114	1435		B	UR 2	TR 3	T 3	U 2
114	1436		A	UR 2	TR 3	T 3	U 2
114	1437		A	UR 1	TR 3	T 3	U 1
114	1437		B	UR 2	TR 3	T 3	U 2
114	1438		A	UR 1	TR 3	T 3	U 2
114	1438		B	UR 2	TR 3	T 3	U 2
114	1439		A	UR 1	TR 3	T 3	U 2
114	1439		B	UR 2	TR 3	T 3	U 2
114	1440		A	UR 3	TR 2	T 2	U 2
114	1442		A	UR 3	TR 2	T 3	U 2
114	1450		A	UR 1	TR 3	T 2	U 1
114	1452		A	UR 1	TR 3	T 2	U 1
114	1458		A	UR 1	TR 3	T 2	U 1
114	1460		A	UR 3	TR 3	T 3	U 2
114	1461		A	UR 1	TR 3	T 2	U 1
114	1464		B	UR 2	TR 3	T 3	U 2
114	1465		A	UR 1	TR 3	T 2	U 1
114	1479		A	UR 3	TR 2	T 2	U 2
114	1480		A	UR 1	TR 2	T 2	U 1
114	1481		A	UR 3	TR 2	T 3	U 2

CLUSTER GROUPS							
Site	Small Find No.	SF Sub Division	Analysis Area	Untransformed Robust	Transformed Robust	Transformed	Untransformed
114	1483		A	UR 3	TR 2	T 2	U 2
114	1484		A	UR 3	TR 2	T 3	U 2
114	1484		B	UR 3	TR 3	T 3	U 2
114	1484		C	UR 3	TR 3	T 3	U 2
114	1486		A	UR 2	TR 3	T 3	U 2
114	1487		A	UR 3	TR 3	T 3	U 2
114	1488		A	UR 2	TR 2	T 2	U 2
114	1491		A	UR 3	TR 2	T 2	U 2
114	1491		B	UR 3	TR 3	T 2	U 2
114	1491		C	UR 1	TR 3	T 3	U 2
114	1491		D	UR 1	TR 3	T 3	U 1
114	1503		A	UR 2	TR 2	T 2	U 2
114	1504		A	UR 2	TR 3	T 3	U 1
114	1505		A	UR 3	TR 2	T 2	U 2
114	1536		A	UR 1	TR 3	T 2	U 1
114	1602		A	UR 1	TR 3	T 2	U 1
114	1603		A	UR 1	TR 3	T 2	U 1
114	1613		A	UR 3	TR 2	T 2	U 2

Appendix XVIII. BLADES COPPER ALLOY GROUPS

This table presents the categorical variables from Nigel Blades analysis of Early Saxon alloys (1995, 86–97). Blades did not include his individual alloy categorisations and so these are recreated here (as calculated by the author). For comparison Pollard et al.'s (2015) groupings are reproduced (as calculated by the author) and transformed robust clusters. Blades analytical results are not reproduced here as they are available in his thesis, which is publicly (and freely) available from the British Library EThOS service (<http://ethos.bl.uk/>).

Blades Anal. No.	Site Name	Description	Context	Find	Blades (1995) alloy group	Pollard et al. (2015) alloy group	TR clusters
166	West Heslerton	tweezers	12	AA	Gunmetal	Leaded Gunmetal	TR 3
167	West Heslerton	annular brooch	17	AA	Leaded Bronze	Leaded Gunmetal	TR 2
168	West Heslerton	cruciform-headed pin	31	CS	Bronze	Leaded Gunmetal	TR 2
169	West Heslerton	brooch, flat	34	AC	Bronze	Leaded Gunmetal	TR 2
170	West Heslerton	brooch, flat	34	AC	Bronze	Leaded Gunmetal	TR 2
173	West Heslerton	brooch, fibula	50	AB	Leaded Bronze	Leaded Bronze	TR 2
175	West Heslerton	brooch, small-long	50	AD	Bronze	Leaded Bronze	TR 2
179	West Heslerton	annular brooch	8	AC	Bronze	Bronze	TR 1
181	West Heslerton	annular brooch	10	AC	Gunmetal	Leaded Gunmetal	TR 2
182	West Heslerton	bangle	10	AE-F	Gunmetal	Leaded Gunmetal	TR 3
183	West Heslerton	annular brooch	10	AK	Gunmetal	Leaded Gunmetal	TR 2
185	West Heslerton	annular brooch	15	AA	Gunmetal	Leaded Gunmetal	TR 3
186	West Heslerton	wristclasp (cast bar)	17	AN	Gunmetal	Leaded Gunmetal	TR 3
187	West Heslerton	annular brooch	101	AX	Gunmetal	Leaded Gunmetal	TR 2
188	West Heslerton	annular brooch	101		Gunmetal	Leaded Gunmetal	TR 2
189	West Heslerton	annular brooch	104	AW	Gunmetal	Leaded Gunmetal	TR 2

Blades Anal. No.	Site Name	Description	Context	Find	Blades (1995) alloy group	Pollard et al. (2015) alloy group	TR clusters
190	West Heslerton	brooch, cruciform	105	BB	Bronze	Leaded Gunmetal	TR 2
192	West Heslerton	annular brooch	26	F	Bronze	Leaded Gunmetal	TR 2
193	West Heslerton	annular brooch	27	G	Gunmetal	Leaded Gunmetal	TR 3
195	West Heslerton	sheet fragment	42	AX	Bronze	Leaded Bronze	TR 1
203	West Heslerton	bangle	91	EG	Bronze	Leaded Gunmetal	TR 2
204	West Heslerton	ring-headed pin	91	EL	Bronze	Leaded Gunmetal	TR 2
205	West Heslerton	annular brooch	91	GW	Leaded Bronze	Leaded Bronze	TR 1
206	West Heslerton	annular brooch	91	GT	Leaded Bronze	Leaded Bronze	TR 1
206	West Heslerton	annular brooch	91	GT	Leaded Bronze	Leaded Bronze	TR 1
207	West Heslerton	bucket binding			Bronze	Gunmetal	TR 2
209	West Heslerton	brooch, cruciform	13	AA	Gunmetal	Leaded Gunmetal	TR 3
211	West Heslerton	annular brooch	13	DA	Bronze	Leaded Bronze	TR 2
212	West Heslerton	annular brooch	13	AD	Bronze	Leaded Bronze	TR 2
213	West Heslerton	annular brooch pin	13	AD	Gunmetal	Gunmetal	TR 3
214	West Heslerton	wristclasp (m)	13	AE	Gunmetal	Gunmetal	TR 3
215	West Heslerton	wristclasp (t)	13	AE	Gunmetal	Gunmetal	TR 3
216	West Heslerton	wristclasp (m)	13	DD	Gunmetal	Gunmetal	TR 3
217	West Heslerton	wristclasp (t)	13	DD	Gunmetal	Gunmetal	TR 3
219	West Heslerton	annular brooch	105		Gunmetal	Leaded Gunmetal	TR 2
234	West Heslerton	ring	46	GX	Bronze	Leaded Gunmetal	TR 2
235	West Heslerton	ring	12	CA	Bronze	Leaded Gunmetal	TR 2
236	West Heslerton	ring	12	CC	Gunmetal	Leaded Gunmetal	TR 3
237	West Heslerton	buckle	16	DL(b)	Gunmetal	Leaded Gunmetal	TR 3
238	West Heslerton	buckle pin	16	DL(a)	Gunmetal	Leaded Gunmetal	TR 3
239	West Heslerton	buckle	22	EE	Bronze	Leaded Bronze	TR 2

Blades Anal. No.	Site Name	Description	Context	Find	Blades (1995) alloy group	Pollard et al. (2015) alloy group	TR clusters
240	West Heslerton	rivet		CW	Gunmetal	Leaded Gunmetal	TR 3
241	West Heslerton	annular brooch	14	CR	Leaded Gunmetal	Leaded Gunmetal	TR 2
242	West Heslerton	annular brooch	14	CQ	Leaded Gunmetal	Leaded Gunmetal	TR 2
243	West Heslerton	annular brooch	12	CI	Gunmetal	Leaded Gunmetal	TR 3
244	West Heslerton	annular brooch	12	CE	Gunmetal	Leaded Gunmetal	TR 3
245	West Heslerton	annular brooch	11	BX	Leaded Gunmetal	Leaded Gunmetal	TR 2
246	West Heslerton	annular brooch	11	BY	Leaded Gunmetal	Leaded Gunmetal	TR 2
247	West Heslerton	annular brooch	43	FS	Bronze	Leaded Gunmetal	TR 2
248	West Heslerton	annular brooch	43	FT	Gunmetal	Leaded Gunmetal	TR 2
249	West Heslerton	annular brooch	24	EL	Gunmetal	Leaded Gunmetal	TR 3
250	West Heslerton	annular brooch	16	DP	Gunmetal	Leaded Gunmetal	TR 3
251	West Heslerton	annular brooch	16	DN	Gunmetal	Leaded Gunmetal	TR 2
252	West Heslerton	annular brooch	26	FA	Gunmetal	Leaded Gunmetal	TR 3
253	West Heslerton	annular brooch	11	FB	Gunmetal	Leaded Gunmetal	TR 3
254	West Heslerton	pin	43	FU	Bronze	Leaded Gunmetal	TR 2
255	West Heslerton	wristclasp (m)	43	FO	Impure Copper	FALSE	TR 1
256	West Heslerton	wristclasp (f)	43	FO	Impure Copper	Copper	TR 1
257	West Heslerton	wristclasp (m)	43	FP	Impure Copper	Bronze	TR 1
258	West Heslerton	wristclasp (f)	43	FP	Impure Copper	Bronze	TR 1
259	West Heslerton	wristclasp	20	EH	Bronze	Bronze	TR 2
260	West Heslerton	wristclasp	46	GR	Leaded Bronze	Leaded Bronze	TR 2
261	West Heslerton	slip-loop	46	GY	Leaded Gunmetal	Leaded Gunmetal	TR 2
262	West Heslerton	annular brooch		FD	Leaded Bronze	Leaded Bronze	TR 1
263	Morning Thorpe	Girdlehanger	393	B	Leaded Gunmetal	Leaded Gunmetal	TR 3
264	Morning Thorpe	Girdlehanger	393	E	Gunmetal	Leaded Gunmetal	TR 3

Blades Anal. No.	Site Name	Description	Context	Find	Blades (1995) alloy group	Pollard et al. (2015) alloy group	TR clusters
265	Morning Thorpe	Decorated ring	407	D	Gunmetal	Leaded Gunmetal	TR 2
266	Morning Thorpe	Annular brooch	3W	K	Leaded Bronze	Leaded Gunmetal	TR 2
267	Morning Thorpe	Ring	360	K	Bronze	Leaded Bronze	TR 2
268	Morning Thorpe	Wristclasp (f)	392	C(ii)	Leaded Bronze	Leaded Gunmetal	TR 2
269	Morning Thorpe	Cruciform small long brooch	370	H	Gunmetal	Leaded Gunmetal	TR 2
270	Morning Thorpe		370	ACiii)	Leaded Bronze	Leaded Bronze	TR 2
271	Morning Thorpe	Wristclasp	392	C(i)	Gunmetal	Leaded Gunmetal	TR 2
272	Morning Thorpe	Wristclasp (m)	392	8	Gunmetal	Leaded Gunmetal	TR 2
273	Morning Thorpe	Cruciform small long brooch	370	J	FALSE	Leaded Gunmetal	TR 2
274	Morning Thorpe	Cruciform small long brooch	358	Q(I)	Gunmetal	Leaded Gunmetal	TR 2
275	Morning Thorpe	Ring	374	A	Bronze	Gunmetal	TR 2
276	Morning Thorpe	Annular brooch	359	C	Gunmetal	Leaded Gunmetal	TR 2
277	Morning Thorpe	Annular brooch	396	G	Leaded Bronze	Leaded Gunmetal	TR 2
278	Morning Thorpe	Annular brooch	378	M	Gunmetal	Leaded Gunmetal	TR 3
279	Morning Thorpe	Annular brooch	362	K	Gunmetal	Leaded Gunmetal	TR 2
280	Morning Thorpe	Annular brooch	397	F	Gunmetal	Leaded Gunmetal	TR 2
281	Morning Thorpe	Annular brooch	374	B	Gunmetal	Leaded Gunmetal	TR 3
282	Morning Thorpe	Annular brooch	397	B	Gunmetal	Leaded Gunmetal	TR 2
283	Morning Thorpe	Annular brooch	378	L	Gunmetal	Leaded Gunmetal	TR 3
284	Morning Thorpe	Annular brooch	410	B	Gunmetal	Leaded Gunmetal	TR 3
285	Morning Thorpe	Annular brooch	371	D	Leaded Bronze	Leaded Gunmetal	TR 2
286	Morning Thorpe	Annular brooch	393	N	Gunmetal	Leaded Gunmetal	TR 3
287	Morning Thorpe	Girdlehanger	396	D	Gunmetal	Leaded Gunmetal	TR 2
288	Morning Thorpe	Annular brooch	359	B	Bronze	Leaded Gunmetal	TR 2
289	Morning Thorpe	Girdlehanger	396	C	Gunmetal	Leaded Gunmetal	TR 2

Blades Anal. No.	Site Name	Description	Context	Find	Blades (1995) alloy group	Pollard et al. (2015) alloy group	TR clusters
290	Morning Thorpe	Bucket binding	200		Bronze	Leaded Gunmetal	TR 2
291	Morning Thorpe	Cruciform brooch	353	R	Leaded Bronze	Leaded Gunmetal	TR 2
292	Morning Thorpe	Cruciform brooch	353	S	Leaded Bronze	Leaded Gunmetal	TR 2
293	Morning Thorpe	Ring	333	A(ii)	Leaded Bronze	Leaded Bronze	TR 2
294	Morning Thorpe	Small-long brooch	316	H(I)	Bronze	Leaded Gunmetal	TR 2
295	Morning Thorpe	Annular brooch	333	A(i)	Bronze	Leaded Gunmetal	TR 2
296	Morning Thorpe	Annular brooch	342	N	Bronze	Leaded Gunmetal	TR 2
298	Morning Thorpe	Wristclasp (f)	351	F	Gunmetal	Leaded Gunmetal	TR 2
299	Morning Thorpe	Wristclasp (m)	303	A(ii)	Gunmetal	Leaded Gunmetal	TR 2
300	Morning Thorpe	Annular brooch	334	C	Bronze	Leaded Gunmetal	TR 2
301	Morning Thorpe	Small-long brooch	328	B	Bronze	Leaded Gunmetal	TR 2
302	Morning Thorpe	Small-long brooch	328	D	Bronze	Leaded Gunmetal	TR 2
303	Morning Thorpe	Annular brooch	331	A	Gunmetal	Leaded Gunmetal	TR 3
304	Morning Thorpe	Annular brooch	331	B	Gunmetal	Leaded Gunmetal	TR 3
305	Morning Thorpe	Annular brooch	334	B	Bronze	Leaded Gunmetal	TR 2
306	Morning Thorpe	Small-long brooch	337	N(i)	Bronze	Leaded Gunmetal	TR 2
307	Morning Thorpe	Wristclasp (f)	312	E	Bronze	Leaded Gunmetal	TR 2
308	Morning Thorpe	Cruciform brooch foot	318	B	Leaded Gunmetal	Leaded Gunmetal	TR 3
309	Morning Thorpe	Small-long brooch	337	M	Bronze	Leaded Gunmetal	TR 2
310	Morning Thorpe	Small-long brooch	342	G	Leaded Bronze	Leaded Bronze	TR 1
311	Morning Thorpe	Small-long brooch	346	A	Bronze	Leaded Gunmetal	TR 2
312	Morning Thorpe	Annular brooch	299	0	Bronze	Leaded Gunmetal	TR 2
313	Morning Thorpe	Small-long brooch	316	F	Bronze	Leaded Gunmetal	TR 2
314	Morning Thorpe	Annular brooch	299	A	Bronze	Leaded Gunmetal	TR 2
315	Morning Thorpe	Wristclasp	312	0	Bronze	Leaded Gunmetal	TR 2

Blades Anal. No.	Site Name	Description	Context	Find	Blades (1995) alloy group	Pollard et al. (2015) alloy group	TR clusters
316	Morning Thorpe	Annular brooch	293	A	Gunmetal	Leaded Gunmetal	TR 2
317	Morning Thorpe	Annular brooch	293	E	Gunmetal	Leaded Gunmetal	TR 2
319	Morning Thorpe	Annular brooch	251	A(i)	Leaded Gunmetal	Leaded Gunmetal	TR 2
320	Morning Thorpe	Annular brooch	207	E	Bronze	Leaded Bronze	TR 2
321	Morning Thorpe	Annular brooch	207	B	Bronze	Leaded Bronze	TR 2
322	Morning Thorpe	Annular brooch	216	B	Bronze	Bronze	TR 2
323	Morning Thorpe	Annular brooch	221	A	Bronze	Leaded Gunmetal	TR 2
324	Morning Thorpe	Annular brooch	251	F	Gunmetal	Leaded Gunmetal	TR 2
325	Morning Thorpe	Annular brooch	216	A	Bronze	Leaded Gunmetal	TR 2
326	Morning Thorpe	Wristclasp (m)	208	J(i)	Bronze	Leaded Gunmetal	TR 2
327	Morning Thorpe	Wristclasp (f)	208	J(ii)	Bronze	Leaded Gunmetal	TR 2
328	Morning Thorpe	Annular brooch	208	B	Leaded Bronze	Leaded Gunmetal	TR 2
329	Morning Thorpe	Small-long brooch	231	A	Bronze	Leaded Gunmetal	TR 2
330	Morning Thorpe	Annular brooch	256	A(i)	Bronze	Leaded Gunmetal	TR 2
331	Morning Thorpe	Inlaid ring	153	A	Brass	Brass	TR 3
332	Morning Thorpe	Ring	178	F	Bronze	Bronze	TR 1
333	Morning Thorpe	Small-long brooch	148	L	Bronze	Leaded Bronze	TR 2
334	Morning Thorpe	Annular brooch	173	B	Bronze	Leaded Gunmetal	TR 2
335	Morning Thorpe	Buckle	115	H(i)	Leaded Bronze	Leaded Bronze	TR 2
336	Morning Thorpe	Annular brooch	140	J	Gunmetal	Leaded Gunmetal	TR 2
337	Morning Thorpe	Annular brooch	140	H	Gunmetal	Leaded Gunmetal	TR 2
338	Morning Thorpe	Annular brooch	185	A(i)	Gunmetal	Leaded Gunmetal	TR 3
339	Morning Thorpe	Annular brooch	133	E	Bronze	Leaded Gunmetal	TR 2
340	Morning Thorpe	Wristclasp (bar only)	133	L	Leaded Gunmetal	Leaded Gunmetal	TR 3
341	Morning Thorpe	Small-long brooch	141	C	Gunmetal	Leaded Gunmetal	TR 2

Blades Anal. No.	Site Name	Description	Context	Find	Blades (1995) alloy group	Pollard et al. (2015) alloy group	TR clusters
342	Morning Thorpe	Small-long brooch	153	H(i)	Gunmetal	Leaded Gunmetal	TR 2
343	Morning Thorpe	Small-long brooch	148	K	Bronze	Leaded Gunmetal	TR 2
344	Morning Thorpe	Annular brooch	131	B	Bronze	Leaded Bronze	TR 2
345	Morning Thorpe	Cruciform brooch	112	B	Bronze	Leaded Gunmetal	TR 2
346	Morning Thorpe	Buckle attachment plate	115	H(ii)	Bronze	Leaded Bronze	TR 1
347	Morning Thorpe	Annular brooch	114	B	Bronze	Leaded Bronze	TR 2
348	Morning Thorpe	Small-long brooch	153	F	Gunmetal	Leaded Gunmetal	TR 2
349	Morning Thorpe	Girdlehanger	108	V	Bronze	Leaded Gunmetal	TR 2
350	Morning Thorpe	Ring	66	E	Leaded Bronze	Leaded Bronze	TR 2
351	Morning Thorpe	Wristclasp	96	C(ii)	Gunmetal	Leaded Gunmetal	TR 2
352	Morning Thorpe	Wristclasp (f)	96	A(ii)	Bronze	Leaded Gunmetal	TR 2
353	Morning Thorpe	Wristclasp (m)	96	C(i)	Gunmetal	Leaded Gunmetal	TR 2
354	Morning Thorpe	Wristclasp (m)	96	A(i)	Gunmetal	Leaded Gunmetal	TR 2
355	Morning Thorpe	Annular brooch	86	A	Bronze	Leaded Gunmetal	TR 2
356	Morning Thorpe	Annular brooch	76	C	Bronze	Leaded Gunmetal	TR 2
357	Morning Thorpe	Annular brooch	76	B	Bronze	Leaded Bronze	TR 2
358	Morning Thorpe	Small-long brooch	96	E	Bronze	Leaded Gunmetal	TR 2
359	Morning Thorpe	Small-long brooch	96	D	Bronze	Leaded Gunmetal	TR 2
360	Morning Thorpe	Annular brooch	86	B	Bronze	Leaded Gunmetal	TR 2
361	Morning Thorpe	Annular brooch	80	I	Leaded Bronze	Leaded Gunmetal	TR 2
362	Morning Thorpe	Annular brooch	64	C(i)	Gunmetal	Leaded Gunmetal	TR 2
364	Morning Thorpe	Annular brooch	108	P	Gunmetal	Leaded Gunmetal	TR 2
365	Morning Thorpe	Annular brooch	108	M	Gunmetal	Leaded Gunmetal	TR 2
366	Morning Thorpe	Brooch pin of 76C	76	C(p)	Bronze	Leaded Bronze	TR 2
367	Morning Thorpe	Brooch pin of 76B	76	B(p)	Gunmetal	Leaded Gunmetal	TR 2

Blades Anal. No.	Site Name	Description	Context	Find	Blades (1995) alloy group	Pollard et al. (2015) alloy group	TR clusters
368	Morning Thorpe	Ring	30	E	Leaded Bronze	Leaded Bronze	TR 1
369	Morning Thorpe	Ring fragment	17	C	Leaded Bronze	Leaded Bronze	TR 1
370	Morning Thorpe	Annular brooch	30	O	Leaded Gunmetal	Leaded Gunmetal	TR 2
371	Morning Thorpe	Annular brooch	30	L	Leaded Gunmetal	Leaded Gunmetal	TR 2
372	Morning Thorpe	Annular brooch	50	D	Bronze	Leaded Gunmetal	TR 2
373	Morning Thorpe	Annular brooch	44	A	Leaded Bronze	Leaded Gunmetal	TR 2
374	Morning Thorpe	Wristclasp bar	35	T	Brass	Leaded Gunmetal	TR 3
375	Morning Thorpe	Small-long brooch	35	D(i)	Bronze	Leaded Gunmetal	TR 2
376	Morning Thorpe	Annular brooch	20	G	Gunmetal	Leaded Gunmetal	TR 2
377	Morning Thorpe	Annular brooch	18	B(i)	Bronze	Leaded Gunmetal	TR 2
378	Morning Thorpe	Annular brooch	51	E	Gunmetal	Leaded Gunmetal	TR 2
379	Morning Thorpe	Annular brooch	51	A	Leaded Bronze	Leaded Gunmetal	TR 2
380	Morning Thorpe	Annular brooch	18	B	Bronze	Leaded Gunmetal	TR 2
381	Spong Hill	brooch fragment	1956	1	Bronze	Leaded Bronze	TR 2
382	Spong Hill	wristclasp	1921	1	Bronze	Leaded Bronze	TR 2
383	Spong Hill	brooch fragment	1976	1	Brass	Leaded Gunmetal	TR 3
384	Spong Hill	square-headed brooch	2087	1	Leaded Bronze	Leaded Gunmetal	TR 2
385	Spong Hill	brooch fragment	2063	1	Leaded Bronze	Leaded Bronze	TR 2
386	Spong Hill	brooch fragment	2042	1	Leaded Bronze	Leaded Gunmetal	TR 2
387	Spong Hill	brooch fragment	2057	1	Bronze	Leaded Bronze	TR 2
388	Spong Hill	tweezers	1961	2	Bronze	Leaded Bronze	TR 1
389	Spong Hill	tweezers	2032	1	Leaded Gunmetal	Leaded Gunmetal	TR 3
390	Spong Hill	tweezers	1983	1	Leaded Bronze	Leaded Bronze	TR 2
391	Spong Hill	tweezers	3188	1	Leaded Brass	Leaded Brass	TR 3
392	Spong Hill	stutzarm brooch	3091	1	Leaded Bronze	Leaded Bronze	TR 2

Blades Anal. No.	Site Name	Description	Context	Find	Blades (1995) alloy group	Pollard et al. (2015) alloy group	TR clusters
393	Spong Hill	brooch	3095	1	Bronze	Leaded Bronze	TR 2
394	Spong Hill	brooch	3019	1	Bronze	Leaded Gunmetal	TR 2
395	Spong Hill	ring	3254	1	Bronze	Leaded Bronze	TR 2
396	Spong Hill	square-headed brooch	1719	1	Leaded Bronze	Leaded Gunmetal	TR 2
397	Spong Hill	square-headed brooch	1730	1	Bronze	Leaded Bronze	TR 2
398	Spong Hill	tweezers	1783	2	Gunmetal	Leaded Gunmetal	TR 2
399	Spong Hill	tweezers	1647	1	Bronze	Leaded Gunmetal	TR 2
400	Spong Hill	tweezers	1672	2	Bronze	Leaded Gunmetal	TR 2
401	Spong Hill	annular brooch	1571	1	Bronze	Leaded Gunmetal	TR 2
402	Spong Hill	square-headed brooch	1689	1	Leaded Bronze	Leaded Bronze	TR 2
403	Spong Hill	strap-end	2835	1	Gunmetal	Leaded Gunmetal	TR 2
404	Spong Hill	square-headed brooch	2796	1	Leaded Bronze	Leaded Gunmetal	TR 2
405	Spong Hill	wristclasp	2765	2	Leaded Bronze	Leaded Gunmetal	TR 2
406	Spong Hill	brooch knob	2982	1	Leaded Brass	Leaded Gunmetal	TR 3
407	Spong Hill	ring	2970	2	Bronze	Leaded Gunmetal	TR 2
408	Spong Hill	tweezers	2776	1	Gunmetal	Leaded Gunmetal	TR 2
409	Spong Hill	girdlehanger	2758	1	Gunmetal	Leaded Gunmetal	TR 2
410	Spong Hill	bowl fragment	2351	2	Leaded Bronze	FALSE	TR 2
411	Spong Hill	bucket fitting	2704	1	Leaded Bronze	Leaded Gunmetal	TR 2
412	Spong Hill	tweezers	2925	1	Leaded Bronze	Leaded Bronze	TR 2
413	Spong Hill	tweezers	2898	1	Bronze	Leaded Bronze	TR 2
414	Spong Hill	tweezers	2850	1	Bronze	Leaded Bronze	TR 2
415	Spong Hill	square-headed brooch	2208	1	Bronze	Leaded Bronze	TR 2
416	Spong Hill	girdlehanger	2346	1	Bronze	Leaded Gunmetal	TR 2
418	Spong Hill	annular brooch ring	2656	2	Brass	Leaded Brass	TR 3

Blades Anal. No.	Site Name	Description	Context	Find	Blades (1995) alloy group	Pollard et al. (2015) alloy group	TR clusters
419	Spong Hill	square-headed brooch	2324	1	Brass	Leaded Gunmetal	TR 3
420	Spong Hill	tweezers	2453	1	Brass	Brass	TR 3
421	Spong Hill	tweezers	2404	1	Gunmetal	Leaded Gunmetal	TR 3
422	Spong Hill	saucer brooch (a)	2376	4	Gunmetal	Gunmetal	TR 3
423	Spong Hill	saucer brooch (b)	2376	4	Gunmetal	Leaded Gunmetal	TR 3
424	Spong Hill	square-headed brooch	2208	1	Bronze	Leaded Gunmetal	TR 2
425	Spong Hill	wristclasp	1323	1	Bronze	Leaded Bronze	TR 2
426	Spong Hill	tweezers	1460	1	Brass	Leaded Gunmetal	TR 3
427	Spong Hill	tweezers	1336	1	Leaded Brass	Leaded Gunmetal	TR 3
428	Spong Hill	wire loop from tweezers	1336	1	Gunmetal	Gunmetal	TR 3
429	Spong Hill	bell	1281	1	Leaded Bronze	Leaded Bronze	TR 1
430	Spong Hill	square-headed brooch	1211	1	Bronze	Leaded Bronze	TR 1
431	Spong Hill	unknown	1724	2	Brass	Leaded Gunmetal	TR 3
432	Spong Hill	unknown	1168	3	Bronze	Leaded Gunmetal	TR 2
605	Empingham	annular brooch	98A		Gunmetal	Leaded Gunmetal	TR 3
606	Empingham	annular brooch	37		Leaded Gunmetal	Leaded Gunmetal	TR 3
607	Empingham	girdlehanger	98		Gunmetal	Leaded Gunmetal	TR 2
608	Empingham	girdlehanger	98		Bronze	Leaded Gunmetal	TR 2
609	Empingham	dress-pin	48		Brass	Leaded Gunmetal	TR 3
610	Empingham	florid cruciform brooch	73		Bronze	Leaded Bronze	TR 2
611	Empingham	cruciform brooch	50		Leaded Gunmetal	Leaded Gunmetal	TR 3
612	Empingham	small-long brooch	50		Bronze	Leaded Gunmetal	TR 2
613	Empingham	small-long brooch	50		Bronze	Leaded Gunmetal	TR 2
614	Empingham	large ring	41		Leaded Bronze	Leaded Bronze	TR 2
615	Empingham	wristclasp	85A		Leaded Gunmetal	Leaded Gunmetal	TR 2

Blades Anal. No.	Site Name	Description	Context	Find	Blades (1995) alloy group	Pollard et al. (2015) alloy group	TR clusters
616	Empingham	wristclasp	85A		Gunmetal	Leaded Gunmetal	TR 3
617	Empingham	florid cruciform brooch	81		Gunmetal	Leaded Gunmetal	TR 3
618	Empingham	cruciform brooch	85A		Gunmetal	Leaded Gunmetal	TR 2
619	Empingham	florid cruciform brooch	100		Gunmetal	Leaded Gunmetal	TR 2
620	Empingham	annular brooch	91		Bronze	Leaded Gunmetal	TR 2
621	Empingham	girdlehanger	40		Gunmetal	Leaded Gunmetal	TR 2
622	Empingham	girdlehanger	40		Gunmetal	Leaded Gunmetal	TR 2
623	Empingham	annular brooch	40		Leaded Gunmetal	Leaded Gunmetal	TR 3
624	Empingham	cognate brooch	90		Bronze	Leaded Gunmetal	TR 2
625	Empingham	cognate brooch	90		Bronze	Leaded Gunmetal	TR 2
626	Empingham	cognate brooch	17		Bronze	Leaded Gunmetal	TR 2
627	Empingham	cognate brooch	17		Gunmetal	Leaded Gunmetal	TR 2
628	Empingham	swastika/cognate brooch	27		Gunmetal	Leaded Gunmetal	TR 3
629	Empingham	swastika/oognate brooch	27		Gunmetal	Leaded Gunmetal	TR 3
630	Empingham	annular brooch	98B		Gunmetal	Leaded Gunmetal	TR 3
631	Empingham	annular brooch	22		Bronze	Leaded Gunmetal	TR 2
632	Empingham	girdlehanger	22		Gunmetal	Leaded Gunmetal	TR 2
635	Sancton	cruciform brooch fragment	S76		Bronze	Bronze	TR 2
636	Sancton	bow of cruciform brooch	S76		Bronze	Leaded Gunmetal	TR 2
637	Sancton	cruciform brooch fragment	S77		Gunmetal	Leaded Gunmetal	TR 2
638	Sancton	ringed tweezers			Bronze	Leaded Bronze	TR 2
640	West Garth Gardens	fragment	10		Gunmetal	Leaded Gunmetal	TR 3
641	West Garth Gardens	small-long brooch	7		Bronze	Leaded Gunmetal	TR 2
642	West Garth Gardens	small-long brooch	7		Gunmetal	Leaded Gunmetal	TR 2
643	West Garth Gardens	cruciform brooch	55		Bronze	Leaded Bronze	TR 1

Blades Anal. No.	Site Name	Description	Context	Find	Blades (1995) alloy group	Pollard et al. (2015) alloy group	TR clusters
644	West Garth Gardens	small-long brooch	55		Gunmetal	Leaded Gunmetal	TR 2
645	West Garth Gardens	wristclasp (f)	48		Bronze	Leaded Gunmetal	TR 2
646	West Garth Gardens	wristelasp (m)	48		Bronze	Leaded Gunmetal	TR 2
647	West Garth Gardens	wristolasp (m)	48		Bronze	Leaded Gunmetal	TR 2
648	West Garth Gardens	wristclasp (f)	48		Bronze	Leaded Gunmetal	TR 2
649	West Garth Gardens	small-long brooch	48		Leaded Bronze	Leaded Gunmetal	TR 2
650	West Garth Gardens	small-long brooch	48		Bronze	Leaded Gunmetal	TR 2
651	West Garth Gardens	equal-arm brooch	55		Gunmetal	Gunmetal	TR 3
652	West Garth Gardens	square-headod brooch	27		Gunmetal	Leaded Gunmetal	TR 3
653	West Garth Gardens	annular brooch (pin absent)	13		Bronze	Leaded Gunmetal	TR 2
654	West Garth Gardens	annular brooch (with pin)	13		Bronze	Leaded Gunmetal	TR 2
655	West Garth Gardens	annular brooch (pin absent)	52		Leaded Gunmetal	Leaded Gunmetal	TR 2
656	West Garth Gardens	annular brooch (with pin)	52		Leaded Bronze	Leaded Gunmetal	TR 2
657	West Garth Gardens	small-long brooch	16		Leaded Bronze	Leaded Bronze	TR 2
658	West Garth Gardens	small-long brooch	16		Leaded Bronze	Leaded Bronze	TR 2
659	West Garth Gardens	equal-arm brooch (pin absent)	36		Gunmetal	Leaded Gunmetal	TR 2
660	West Garth Gardens	equal arm brooch (with pin)	36		Bronze	Leaded Gunmetal	TR 2
661	West Garth Gardens	cruciform brooch	52		Bronze	Leaded Bronze	TR 1
662	West Garth Gardens	girdlehanger	19		Gunmetal	Leaded Gunmetal	TR 2
663	West Garth Gardens	cruciform brooch	61		Gunmetal	Leaded Gunmetal	TR 2
664	West Garth Gardens	cruciform brooch	61		Bronze	Leaded Bronze	TR 2
665	West Garth Gardens	cruciform brooch	61		Leaded Bronze	Leaded Gunmetal	TR 2
666	West Garth Gardens	buckle pin	30		Impure Copper	Leaded Brass	TR 2
667	West Garth Gardens	buckle	30		Bronze	Leaded Gunmetal	TR 2
670	Bergh Apton	ring	29	G	Leaded Bronze	Leaded Bronze	TR 2

Blades Anal. No.	Site Name	Description	Context	Find	Blades (1995) alloy group	Pollard et al. (2015) alloy group	TR clusters
671	Bergh Apton	ring	29	H	Bronze	Bronze	TR 1
672	Bergh Apton	buckle	22	A	Gunmetal	Leaded Gunmetal	TR 3
673	Bergh Apton	small-long brooch	6	A	Bronze	Leaded Bronze	TR 2
674	Bergh Apton	small-long brooch	5	A	Bronze	Leaded Bronze	TR 2
675	Bergh Apton	ring (rolled sheet)	7	E	Leaded Gunmetal	Leaded Gunmetal	TR 3
676	Bergh Apton	ring (rolled sheet)	37	J	Brass	Brass	TR 3
677	Bergh Apton	girdlehanger	29	H	Gunmetal	Leaded Gunmetal	TR 3
678	Bergh Apton	girdlehanger	29	H	Gunmetal	Leaded Gunmetal	TR 3
679	Bergh Apton	annular brooch	3	A	Gunmetal	Leaded Gunmetal	TR 2
680	Bergh Apton	annular brooch	21	8	Bronze	Leaded Bronze	TR 2
681	Bergh Apton	annular brooch	15	A	Bronze	Leaded Gunmetal	TR 2
682	Bergh Apton	annular brooch	9	C	Gunmetal	Leaded Gunmetal	TR 2
683	Bergh Apton	cast ring	21	Gi	Leaded Gunmetal	Leaded Gunmetal	TR 3
684	Bergh Apton	tinned stud	44	A	Gunmetal	Leaded Gunmetal	TR 3
685	Bergh Apton	annular brooch	70	A	Gunmetal	Leaded Gunmetal	TR 2
686	Bergh Apton	annular brooch	55	A	Bronze	Leaded Bronze	TR 1
687	Bergh Apton	annular brooch	65	C	Bronze	Leaded Gunmetal	TR 2
688	Bergh Apton	annular brooch	65	B	Bronze	Leaded Gunmetal	TR 2
689	Bergh Apton	annular brooch	45	C	Gunmetal	Leaded Gunmetal	TR 2
690	Bergh Apton	girdlehanger	45	G	Bronze	Leaded Gunmetal	TR 2
691	Bergh Apton	wristclasp (l)	65	F	Bronze	Leaded Bronze	TR 1
692	Bergh Apton	wristclasp (l)	65	E	Bronze	Leaded Bronze	TR 1
693	Bergh Apton	wristclasp (h)	65	E	Bronze	Leaded Bronze	TR 1
694	Bergh Apton	wristclasp (h)	65	G	Bronze	Leaded Bronze	TR 1
695	Bergh Apton	annular brooch	54	D	Bronze	Leaded Gunmetal	TR 2

Blades Anal. No.	Site Name	Description	Context	Find	Blades (1995) alloy group	Pollard et al. (2015) alloy group	TR clusters
696	Bergh Apton	Ring fragment	45	C	Leaded Gunmetal	Leaded Gunmetal	TR 3
697	Bergh Apton	Ring	54	L	Leaded Bronze	Leaded Bronze	TR 1
698	Bergh Apton	Ring	9	E	Gunmetal	Leaded Gunmetal	TR 3
699	Bergh Apton	Wristclasp (m)	64	H	Gunmetal	Leaded Gunmetal	TR 3
700	Bergh Apton	Wristclasp (m)	64	Fi	Gunmetal	Leaded Gunmetal	TR 3
701	Bergh Apton	Wristclasp (f)	37	Eii	Bronze	Leaded Gunmetal	TR 2
702	Bergh Apton	Wristclasp (m)	37	Fi	Bronze	Leaded Gunmetal	TR 2
703	Bergh Apton	Wristclasp (f)	37	Fii	Bronze	Leaded Gunmetal	TR 2
720	Spong Hill	annular brooch	56	5	Gunmetal	Leaded Gunmetal	TR 2
721	Spong Hill	annular brooch	58	6	Bronze	Leaded Bronze	TR 2
722	Spong Hill	small-long brooch	42	5	Gunmetal	Leaded Gunmetal	TR 3
723	Spong Hill	annular brooch	56	6	Gunmetal	Leaded Gunmetal	TR 3
724	Spong Hill	annular brooch	45	2	Gunmetal	Leaded Gunmetal	TR 2
725	Spong Hill	annular brooch	45	1	Leaded Bronze	Leaded Gunmetal	TR 2
726	Spong Hill	ring	46	6	Bronze	Leaded Gunmetal	TR 2
729	Spong Hill	ring	57	8	Gunmetal	Leaded Gunmetal	TR 3
731	Spong Hill	girdlehanger	38	1b	Gunmetal	Leaded Gunmetal	TR 2
732	Spong Hill	girdlehanger	38	1a	Bronze	Leaded Gunmetal	TR 2
733	Spong Hill	small-long brooch	14	4a	Bronze	Leaded Gunmetal	TR 2
734	Spong Hill	annular brooch	19	2	Bronze	Leaded Gunmetal	TR 2
735	Spong Hill	small-long brooch	5	6a	Bronze	Leaded Gunmetal	TR 2
736	Spong Hill	annular brooch	3	2	Bronze	Leaded Gunmetal	TR 2
737	Spong Hill	annular brooch	12	6	Bronze	Leaded Gunmetal	TR 2
738	Spong Hill	wristclasp	38	11	Gunmetal	Leaded Gunmetal	TR 2
739	Spong Hill	wristclasp	38	11	Gunmetal	Gunmetal	TR 3

Blades Anal. No.	Site Name	Description	Context	Find	Blades (1995) alloy group	Pollard et al. (2015) alloy group	TR clusters
740	Spong Hill	wristclasp	38	11	Bronze	Leaded Gunmetal	TR 2
741	Spong Hill	wristclasp	38	11	Gunmetal	Leaded Gunmetal	TR 2
742	Spong Hill	annular brooch	38	8	Bronze	Leaded Gunmetal	TR 2
743	Spong Hill	wristclasp	29	4	Bronze	Leaded Gunmetal	TR 2
744	Spong Hill	wristclasp	29	5	Bronze	Leaded Bronze	TR 2
745	Spong Hill	wristclasp	29	3	Bronze	Leaded Gunmetal	TR 2
746	Spong Hill	wristclasp	29	3	Gunmetal	Leaded Gunmetal	TR 2
747	Spong Hill	annular brooch	14	4	Bronze	Leaded Gunmetal	TR 2
748	Bergh Apton	gt square-headed brooch	64	a	Gunmetal	Leaded Gunmetal	TR 3
749	Bergh Apton	gt square-headed brooch	7	h	Gunmetal	Leaded Gunmetal	TR 3
750	Spong Hill	small-long brooch	18	6	Leaded Bronze	Leaded Bronze	TR 2
751	Spong Hill	square-headed brooch	38	7a	Gunmetal	Leaded Gunmetal	TR 3
752	Spong Hill	gt square-headed brooch	24	5a	Bronze	Leaded Gunmetal	TR 2
753	Spong Hill	small-long brooch	2	2	Bronze	Leaded Bronze	TR 2
754	Spong Hill	annular brooch	39	2a	Bronze	Leaded Gunmetal	TR 2
755	Spong Hill	annular brooch	39	7	Gunmetal	Leaded Gunmetal	TR 2
756	Spong Hill	annular brooch	29	2	Bronze	Gunmetal	TR 2
757	Spong Hill	equal-arm brooch	46	1	Gunmetal	Leaded Gunmetal	TR 2
758	Spong Hill	equal-arm brooch	46	2	Gunmetal	Leaded Gunmetal	TR 3
759	Spong Hill	shield applique	31	4	Bronze	Bronze	TR 1
760	Spong Hill	girdlehanger	24	4b	Gunmetal	Leaded Gunmetal	TR 2
761	Spong Hill	girdlehanger	24	4a	Gunmetal	Leaded Gunmetal	TR 2
763	Spong Hill	annular brooch	29	1	Bronze	Leaded Gunmetal	TR 2
764	Spong Hill	annular brooch	38	9	Bronze	Leaded Gunmetal	TR 2
765	Spong Hill	annular brooch	37	4	Bronze	Leaded Bronze	TR 2

Blades Anal. No.	Site Name	Description	Context	Find	Blades (1995) alloy group	Pollard et al. (2015) alloy group	TR clusters
770	Empingham	belt-fitting	50		Brass	Leaded Gunmetal	TR 3
771	Empingham	wristclasp	50		Leaded Bronze	Leaded Gunmetal	TR 2
772	Empingham	buckle	50		Gunmetal	Leaded Gunmetal	TR 3
773	Empingham	wristclasp (h)	98		Brass	Leaded Gunmetal	TR 3
774	Empingham	wristclasp (h)	98		Brass	Leaded Gunmetal	TR 3
775	Empingham	wristclasp (l)	49		Bronze	Leaded Gunmetal	TR 2
776	Empingham	wristclasp (h)	37		Brass	Gunmetal	TR 3
964	Brandon	cruciform brooch	5548		Gunmetal	Leaded Gunmetal	TR 2

Remember
EVERYTHING

&

**KEEP
YOUR
HEAD**

(Heaney 1984, 66)